

**STUDIES IN CARBONYLATION AND SUZUKI COUPLING
REACTIONS USING IMMOBILIZED PALLADIUM COMPLEX
CATALYSTS**

THESIS SUBMITTED TO THE
UNIVERSITY OF PUNE FOR THE DEGREE OF

**DOCTOR OF PHILOSOPHY
IN
CHEMISTRY**

BY
BIBHAS RANJAN SARKAR

HOMOGENEOUS CATALYSIS DIVISION
NATIONAL CHEMICAL LABORATORY
PUNE 411 008, INDIA

APRIL 2007



राष्ट्रीय रासायनिक प्रयोगशाला

(वैज्ञानिक तथा औद्योगिक अनुसंधान परिषद)

डॉ. होमी भाभा मार्ग पुणे - 411 008. भारत

NATIONAL CHEMICAL LABORATORY

(Council of Scientific & Industrial Research)

Dr. Homi Bhabha Road, Pune - 411 008. India.



CERTIFICATE

This is to certify that the work incorporated in the thesis, “**Studies in Carbonylation and Suzuki Coupling Reactions using Immobilized Palladium Complex Catalysts**” submitted by Mr. Bibhas Ranjan Sarkar, for the degree of Doctor of Philosophy, was carried out by the candidate under my supervision at the Homogeneous Catalysis Division, National Chemical Laboratory, Pune 411 008, India. Such material as has been obtained from other sources has been duly acknowledged in the thesis.

Dr. Raghunath V. Chaudhari

(Research Supervisor)

Declaration

I hereby declare that the thesis entitled “**Studies In Carbonylation And Suzuki Coupling Reactions Using Immobilized Palladium Complex Catalysts**”, submitted for the Degree of Doctor of Philosophy to the University of Pune, has been carried out by me at the National Chemical Laboratory, Pune under the supervision of Dr. R. V. Chaudhari. The work is original and has not been submitted in part or full by me for any other degree or diploma to this or any other University.

Date:

(Bibhas Ranjan Sarkar)

Place:

Dedicated to My Family

Acknowledgements

I find it difficult to acknowledge my research supervisor, Dr. Raghunath V. Chaudhari so briefly, though I feel deeply indebted to his immense contribution in the making of this thesis. I wish to express my sincere gratitude for his ceaseless inspiration, thoughtful guidance, constructive criticism and friendship to shape up the researcher in me. I take this opportunity to salute his supporting attitude that has always led me to think and work independently, and follow them in the proper perspectives. My deepest regards and reverence are always due for his wonderful personality.

I would like to thank the Council of Scientific and Industrial Research for awarding of research fellowship. I am thankful to Dr. S. Sivaram, Director, Dr. B. D. Kulkarni, Deputy Director, National Chemical Laboratory to carry out my research work and extending all possible infrastructural facilities for completion of my research work.

I sincerely acknowledge the invaluable interactions with all the scientific members of our Homogeneous Catalysis Division, especially, Dr. Jaganathan, Dr. Gupte, Dr. Kelkar, Dr. Deshpande, Dr. Rode, Dr. Grover, Dr. Ranade, Dr. Rane, Mr. Joshi, Mr. Jadkar and lastly Dr. Sengupta in several capacities for my build-up. I need to express my thanks to the support group (David, Subbi & associates) and all the staff members of our division, especially Mr. Raheja for his valuable cooperation and help and an exceptionally healthy working atmosphere. I shall also acknowledge the help from our NMR group - Deepak & Dr. Ajith; Dr. Selvaraj & Mr. Gaikwad - Centre for Materials characterization, Dr. Lakshmikantam and Dr. Sridhar from IICT Hyderabad, for their help in characterizations of catalysts.

I would like to express my gratitude to all my teachers with special reference to Professors Sachin Kumar Ghosh, Dhananjay Chatterjee, Bijoy Prasad Ghosh, Gurunath Mukherjee, Chaitali Mukhopadhyay & Ashutosh Ghosh, for giving me the vision of scientific endeavor.

I would like to thank all my colleagues and labmates (past and present) for their helpful hand and cheerful attitude that had made my working very easy and enjoyable. I should mention my seniors Seayad, Jayasree, Suju, Srikant, Kausik, Yogesh, Sunil (Sr.), Charu; and friends Anand, Nandu, Lalita, Rashmi, Ajay, Mohan, Ranjit, Madhavi, JP, Vikas, Ajit, Abhishek, Nitin, Shinde, Pippalad, Kausik (Bhatu), Sangeeta, Savita, Makarand, Mahesh, Kapil (Motu) and for their support and help. I shall specially thank our PP-I labmates Debu, Shashi, Amit and Malvi for their presence in all aspects of my Ph.D. career. I would like to acknowledge the friendship of Suman, Divya, Manaswini, Shraeddha, Tanpreet, Gitali, Samruddhi, Amit Deshmukh, Mahesh and many more in NCL, who made my stay more colorful.

It would be impossible to forget our Bangla Bhaat group with Ramuda, Dadu, Kamuda, Saotal, Ravan, Jamu, Ghotu, Debu, Chumku, Godai & Major - such a pleasure to be with you folks. My life during these days have been made fun-filled and lively in the association of friends like Probhas, Soumitra, Science, Saikat, Debashis, Sujit, Mama, Rahul , Debu (forsha), Chaitali, Candela, Chinmoy. My special thanks to Somnathda, Sujatadi & Diya; Prabalda; Nimu & Boudi; Tikla, Anamitra, Pallavi, Moitri, Amrita and many others. It brings to me great pleasure to thank my old friends Angshuman & Sagarika, Chiradip, Susmita, Nilanjana, Abhijit, Sarita for their loving support for all these years since college days in their very own ways.

This thesis would not have been complete without the heartfelt wishes, blessings and love of my parents - Mamoni & Baba. All that I have known, understood & acquired today is the result of your upbringing. I miss the ever-enthusiastic supportive pat from Baba today. No words would be sufficient in describing the affection and support of Bhai throughout my life in all aspects. I find this excellent opportunity to appreciate and acknowledge the immense support of Ma & Baba (my in-laws) and their unparallel belief and affection in me that has driven me to excel even under difficult situations. I am indebted with the pristine love of Deepa (my cute Bunu) that always brings the sparkle of joy in my life.

Nothing appropriate can describe the love and support of Roopa, my dearest wife, whose constant encouragement and admiration sets new horizons for me to reach, in every facet of my life. It's being the most colorful and glorious time of my life ever since our relation bloomed and that strengthens me everyday to achieve any goal with better ease and confidence.

Bibhas Ranjan Sarkar

Contents

List of Figures	vii
List of Schemes	xii
List of Tables	xiii
Abstract of Thesis	xv

Chapter 1: Introduction and Literature Report

1.1	Introduction	1
1.2	Carbonylation	3
1.2.1	Carbonylation of Olefins	5
1.2.1.1	Hydrocarboxylation and Hydroesterification	6
1.2.2	Carbonylation of Alcohols	18
1.2.3	Kinetics of Carbonylation Reactions	23
1.3	Suzuki Cross Coupling Reactions	24
1.3.1	Homogeneous Catalysts for Suzuki Coupling	24
1.3.2	Suzuki Coupling using Immobilized Catalysts	34
1.4	Catalyst – Product Separation	40
1.5	Immobilization of Metal Complex Catalysts	41
1.5.1	Anchored Catalysts	43
1.6	Immobilization in Mesoporous Matrices	44
1.6.1	Post-Synthesis Grafting Method	45
1.6.1.1	Grafting with Passive Surface Groups	45
1.6.1.2	Grafting with Reactive Surface Groups	45
1.6.1.3	Site – Selective Grafting	46
1.6.2	Coating Method	47
1.6.3	Co-condensation Method	47
1.7	Scope and Objective of Present Work	49
	References	51

Chapter 2: Anchored Pd–Complexes in Mesoporous Matrices: Novel Catalysts for Carbonylation of Olefins and Alcohols

2.1	Introduction	62
2.2	Experimental Section	64
2.2.1	Approach and Strategy of Immobilization	64
2.2.2	Materials	67
2.2.3	Syntheses	67
2.2.3.1	Synthesis of Pd(pyca)(PPh ₃)(OTs)	67
2.2.3.2	Synthesis of Mesoporous Matrices	68
2.2.3.2.1	Synthesis of MCM-41	68
2.2.3.2.2	Synthesis of MCM-48	68
2.2.3.2.3	Synthesis of SBA-15	69
2.2.3.3	Functionalization of Mesoporous Matrices	69
2.2.3.3.1	Post-synthesis Grafting	70
2.2.3.3.2	One-pot Co-condensation	71
2.2.3.4	Immobilization of Pd-complex Inside the Functionalized Mesoporous Matrices	71
2.2.3.4.1	MCM-41 and MCM-48 [using <i>M41-NH₂</i> & <i>M48-NH₂</i>]	71
2.2.3.4.2	SBA-15 [using <i>S15-NH₂-(G)</i> & <i>S15-NH₂-(C)</i>]	72
2.2.3.5	Syntheses of Supported Catalysts	72
2.2.3.5.1	Synthesis of SiO ₂ Supported Catalyst	72
2.2.3.5.2	Synthesis of NaY Zeolite Supported Catalyst	72
2.2.4	Carbonylation Procedure	73
2.2.5	Recycle Studies and Leaching Experiments	74
2.2.6	Analytical and Characterization Methods	75
2.3	Results and Discussions	76
2.3.1	Characterizations of Solid Catalysts	77
2.3.1.1	Powder X-Ray Diffraction	77
2.3.1.2	Adsorption-Desorption Studies	82

2.3.1.3	Scanning Electron Microscopy	86
2.3.1.4	Transmission Electron Microscopy	89
2.3.1.5	X-Ray Photoelectron Spectroscopy	91
2.3.1.6	Solid State CP-MAS NMR Spectroscopy	92
2.3.1.6.1	²⁹ Si CP-MAS NMR Studies	93
2.3.1.6.2	¹³ C CP-MAS NMR Studies	97
2.3.1.6.3	³¹ P CP-MAS NMR Studies	102
2.3.1.7	Fourier Transform Infra Red Spectroscopy	103
2.3.1.8	Palladium Content Analysis	105
2.3.2	Catalytic Reactions	106
2.3.2.1	Carbonylation of Olefins and Alcohols	106
2.3.2.2	Recycle and Stability Aspects	109
2.3.2.3	Parametric Variations	111
2.3.2.3.1	Effect of Substrate Concentration	111
2.3.2.3.2	Effect of Catalyst Loading	113
2.3.2.3.3	Effect of CO Partial Pressure	114
2.3.2.3.4	Effect of Promoters	115
2.3.2.3.5	Effect of Triphenylphosphine Concentration	118
2.3.2.3.6	Effect of Water	119
2.3.2.4	Different Substrates	120
2.3.2.5	Comparative Advancement Studies	123
2.4	Conclusions	125
2.5	Scope and Future Directions	126
	References	127

Chapter 3: Ossification – A Novel Immobilization Approach: Application in Carbonylation Reactions

3.1	Introduction	128
3.2	Experimental Section	130
3.2.1	Materials	130

3.2.2	Syntheses	131
3.2.2.1	Synthesis of IBPE	131
3.2.2.2	Synthesis of TPPTS	132
3.2.2.3	Synthesis of Palladium complexes	133
3.2.2.3.1	Pd(pyca)(PPh₃)(OTs) complex	133
3.2.2.3.2	Pd(acpy)(PPh₃)(OTs) complex	133
3.2.2.3.3	Pd(pycald)(PPh₃)(OTs) complex	134
3.2.2.3.4	Pd(bipy)(PPh₃)(OTs) complex	134
3.2.2.3.5	Synthesis of aqueous-soluble complexes	134
3.2.2.3.6	Ossification of Palladium Complexes	136
3.2.3	Carbonylation Procedure	136
3.2.4	Recycle Studies and Leaching Experiments	137
3.2.5	Analytical and Characterization Methods	137
3.3	Results and Discussions	139
3.3.1	Characterization of Catalysts	139
3.3.1.1	³¹P CP MAS NMR Spectroscopy	139
3.3.1.2	Powder X-Ray Diffraction	142
3.3.1.3	X-Ray Photoelectron Spectroscopy	145
3.3.1.4	Scanning Electron Microscopy	149
3.3.1.5	Surface Area Measurements	151
3.3.1.6	Palladium Content Analysis	152
3.3.2	Carbonylation Reactions	152
3.3.2.1	Carbonylation of Olefins and Alcohols	153
3.3.2.2	Recycle Studies and Stability Aspects	154
3.3.2.3	Parametric Variations	156
3.3.2.3.1	Effect of Substrate Concentration	156
3.3.2.3.2	Effect of Catalyst Loading	158
3.3.2.3.3	Effect of CO Partial Pressure	159
3.3.2.3.4	Effect of Promoters	160
3.3.2.3.5	Effect of Triphenylphosphine Concentration	161
3.3.2.3.6	Effect of Concentration of Water	162

3.3.2.3.7	Effect of Temperature	163
3.3.2.4	Different Catalysts	164
3.3.2.5	Different Substrates	166
3.3.2.6	Comparative Advancement Study	167
3.4	Conclusions	169
3.5	Future Directions and Scope	169
	References	170

Chapter 4: Kinetic modeling of Carbonylation of 4-Isobutylstyrene using Homogeneous and Ossified Pd(pyca)(PPh₃)(OTs)

4.1	Introduction	171
4.2	Experimental Section	172
4.2.1	Materials	172
4.2.2	Synthesis of 4-Isobutylstyrene, IBS	172
4.2.3	Carbonylation Reactions	173
4.2.4	Calculation of Initial Rates	173
4.3	Results and Discussions	173
4.3.1	Solubility Data	177
4.3.2	Analysis of Mass Transfer Effects	177
4.3.3	Kinetics of Carbonylation of IBS using Homogeneous Catalyst	179
4.3.3.1	Initial Rate Data	179
4.3.3.2	Kinetic Modeling	182
4.3.4	Kinetics of Carbonylation of IBS using Ossified Pd-complex Catalyst	190
4.3.4.1	Initial Rate Data	190
4.3.4.2	Kinetic Modeling	194
4.4	Comparison of Homogeneous and Heterogeneous Carbonylation	203
4.5	Conclusions	204
	References	204

Chapter 5: Suzuki Coupling Studies using Ossified Pd-Complex Catalysts

5.1	Introduction	205
5.2	Experimental Section	208
5.2.1	Materials	208
5.2.2	Reaction Methodology – Suzuki Reaction	209
5.2.3	Recycle and Leaching Studies	210
5.2.4	Analytical Methods	210
5.3	Results and Discussions	212
5.3.1	The Standard Reaction	212
5.3.2	The Parametric Variations	213
5.3.2.1	Effect off Mutual Ratio of Substrates	213
5.3.2.2	Effect of Catalyst Charge	214
5.3.2.3	Effect of Base	218
5.3.2.3.1	Choice of Base	218
5.3.2.3.2	Quantity of Base	220
5.3.2.4	Role of Solvent	221
5.3.3	Different Catalysts	225
5.3.4	Different Substrates	226
5.3.5	Recycle Studies	232
5.3.6	Conclusions	233
5.4	Scope and Future Directions	233
	Reference	234
	Appendix I	235
	Appendix II	242
	Publications/ Symposia	291

List of Figures

Number	Description	Page No.
1.1	Comparison of operating conditions for different carbonylation catalyst systems	7
2.1	Schematic of Carbonylation reaction setup	73
2.2	Powder XRD patterns of <i>M-41</i> and <i>M-48</i>	78
2.3	Comparative powder XRD patterns of <i>M-41</i> (Part A) and <i>M-48</i> (Part B)	79
2.4	Powder XRD patterns of as-synthesized and calcined SBA-15	80
2.5	Comparative powder XRD data of different SBA-15 materials	81
2.6	N ₂ adsorption-desorption isotherm and BJH pore size distribution of calcined MCM-41	83
2.7	N ₂ adsorption-desorption isotherm and BJH pore size distribution of calcined MCM-48	83
2.8	N ₂ adsorption-desorption isotherm of calcined SBA-15 at 77.35 K	84
2.9	SEM images of different MCM-41 and MCM-48 based catalysts	86
2.10	SEM micrographs of the different SBA-15 samples	88
2.11	TEM images of different MCM-41 and MCM-48 materials	89
2.12	XPS data for <i>M41-NH₂-Pd</i>	91
2.13	²⁹ Si CP MAS NMR spectra of <i>S15-NH₂-(G)-Pd</i> material	94
2.14	²⁹ Si CP MAS NMR spectra of <i>S15-NH₂-(C)-Pd</i> material	96
2.15	¹³ C CP MAS NMR spectra of <i>S15-NH₂-(G)-Pd</i> material	99
2.16	¹³ C CP MAS spectra of <i>S-15-NH₂-(C)-Pd</i> material	101
2.17	³¹ P CP MAS NMR spectra of various anchored Pd-complexes	102
2.18	Comparative FT-IR spectra of MCM-41 based catalyst (<i>M41-NH₂-Pd</i>)	104
2.19	A typical concentration-Time profile of carbonylation of styrene using <i>M41-NH₂-Pd</i> as catalyst	107
2.20	Major Product (2-PPA) concentration-Time profile for different anchored catalysts	109
2.21	Recycle studies using different anchored Pd-complex catalysts	110
2.22	Effect of substrate concentration on styrene carbonylation	112
2.23	Effect of catalyst charge on styrene concentration	113

2.24	Effect of CO partial pressure on styrene carbonylation	115
2.25	Effect of promoter amount on carbonylation of styrene	117
2.26	Effect of PPh ₃ concentration on styrene carbonylation	118
2.27	Effect of water on styrene carbonylation	120
3.1	Schematic representation of <i>Ossification of metal complexes</i>	129
3.2	Synthesis of aqueous soluble Pd(pyca)(TPPTS)(H ₂ O) complex	134
3.3	³¹ P CP MAS NMR spectra of catalysts	139
3.4	³¹ P CP-MAS NMR Spectra of the ossified catalysts using Ba ²⁺ ions, (A) Ossified Pd(pyca)(TPPTS) complex, (B) Ossified Pd(Acpy)(TPPTS) complex, (C) Ossified Pd(Pycald)(TPPTS) complex, (D) Ossified Pd(Bipy)(TPPTS) complex. . in the spectra indicate the side bands at 7kHz	141
3.5	Powder XRD pattern of ossified Pd(pyca)(TPPTS) complex using Ba ²⁺ cations. Numbers in the plot denote the different Miller indices for the respective Bragg's planes. Powder XRD patterns of different ossified Pd-complexes using Ba ²⁺ ions;	143
3.6	(A) Pd(acpy)(TPPTS) complex, (B) Pd(pycald)(TPPTS) complex, (C) Pd(bipy)(TPPTS) complex	144
3.7	XPS data of ossified Pd(pyca)(TPPTS) complex i.e. Catalyst 1A	147
3.8	SEM images of the different ossified Pd-complex catalysts	150
3.9	Concentration-time profile styrene carbonylation using Catalyst 1A	153
3.10	Recycle Studies for styrene carbonylation using Catalyst 1A	154
3.11	³¹ P CPMAS NMR of [A] virgin and [B] spent (after 4 th recycle) Catalyst 1A, for carbonylation of styrene used in the recycle studies, in spectra represents sidebands at 7kHz	155
3.12	Effect of substrate concentration on styrene carbonylation	157
3.13	Effect of Catalyst concentration on styrene carbonylation	158
3.14	Effect of CO partial pressure on styrene carbonylation	159
3.15	Effect of promoter concentration on styrene carbonylation	161
3.16	Effect of PPh ₃ concentration on styrene carbonylation	162
3.17	Effect of H ₂ O concentration on styrene carbonylation	163
3.18	Effect of temperature on styrene carbonylation	164

3.19	Comparison of different ossified Pd-complexes for carbonylation of styrene	165
4.1	(A) Concentration-Time profile (B) CO Absorption data for carbonylation of 4-Isobutylstyrene using homogeneous Pd(pyca)(PPh ₃)(OTs) complex catalyst	175
4.2	(A) Concentration-Time profile, (B) for carbonylation of 4-Isobutylstyrene using ossified Pd(pyca)(TPPTS) complex catalyst [Catalyst 1A]	176
4.3	Effect of agitation speed on IBS carbonylation using homogeneous	178
4.4	Effect of agitation speed on IBS carbonylation using Ossified Pd(pyca)(TPPTS) complex catalyst	178
4.5	Effect of concentration of IBS on initial rate of carbonylation	179
4.6	Effect of concentration of catalyst on initial rate of carbonylation	180
4.7	Effect of concentration of CO on initial rate of carbonylation	180
4.8	Effect of concentration of promoters on initial rate of carbonylation	181
4.9	Effect of concentration of water on initial rate of carbonylation	181
4.10	Standard carbonylation reaction at 388 K	183
4.11	Effect of IBS concentration at 388 K	184
4.12	Effect of IBS concentration at 388 K	184
4.13	Effect of catalyst concentration at 388 K	185
4.14	Effect of promoter concentration at 388 K	185
4.15	Effect of promoter concentration at 388 K	186
4.16	Effect of promoter concentration at 388 K	186
4.17	Effect of H ₂ O concentration at 388 K	187
4.18	Effect of H ₂ O concentration at 388 K	187
4.19	Effect of CO partial pressure at 388 K	188
4.20	Effect of CO partial pressure at 388 K	188
4.21	Standard carbonylation reaction at 378 K	189
4.22	Standard carbonylation reaction at 368 K	189
4.23	Arrhenius plot: Temperature dependence of rate constant k_1	190
4.24	Effect of concentration of IBS on rate of carbonylation	191
4.25	Effect of concentration of catalyst on initial rate of carbonylation	192

4.26	Effect of concentration of CO on initial rate of carbonylation	192
4.27	Effect of concentration of promoters on initial rate of carbonylation	193
4.28	Effect of concentration of water on initial rate of carbonylation	193
4.29	Effect of concentration of PPh ₃ on initial rate of carbonylation	194
4.30	Standard carbonylation reaction at 388 K	195
4.31	Effect of catalyst loading at 388 K	196
4.32	Effect of catalyst loading at 388 K	196
4.33	Effect of catalyst loading at 388 K	197
4.34	Effect of partial pressure of CO at 388 K	197
4.35	Effect of partial pressure of CO at 388 K	198
4.36	Effect of promoter at 388 K	198
4.37	Effect of promoter concentration at 388 K	199
4.38	Effect of water concentration at 388 K	199
4.39	Effect of water concentration at 388 K	200
4.40	Effect of concentration of IBS at 388 K	200
4.41	Effect of concentration of IBS at 388 K	201
4.42	Effect of concentration of IBS at 388 K	201
4.43	Standard reaction at 373 K	202
4.44	Standard reaction at 398 K	202
4.45	Arrhenius plot: Temperature dependence of rate constant k_3	203
5.1	Schematic diagram setup for Suzuki coupling reaction	209
5.2	A typical Concentration – Time profile of the Suzuki coupling of iodobenzene and phenylboronic acid using ossified Pd-pyca complex catalyst	212
5.3	Variation of iodobenzene conversion with molar ratio of iodobenzene to phenylboronic acid in Suzuki coupling reaction	214
5.4	Variation of conversion and chemoselectivity with catalyst charge for Suzuki coupling of iodobenzene and phenylboronic acid	215
5.5	Variation of conversion with the amount of K ₂ CO ₃ relative to iodobenzene in Suzuki coupling of iodobenzene and phenylboronic acid	220

5.6	Comparison of conversions and selectivity for Suzuki coupling reaction of iodobenzene and phenylboronic acid in different solvent	222
5.7	Comparison of conversions and selectivity for Suzuki coupling reaction of iodobenzene and phenylboronic acid in different alcohols as solvents	223
5.8	Performance of different ossified Pd-complex catalysts in Suzuki coupling reaction of iodobenzene and phenylboronic acid	225
5.9	Recycle studies of Suzuki coupling of iodobenzene and phenylboronic acid using Catalyst 1A	232

List of Schemes

Number	Description	Page No.
1.1	Olefin carbonylation	6
1.2	Schematic for carbonylation of olefins	7
1.3	Suzuki Cross -coupling	24
2.1	Hydrocarboxylation of alkenes or alcohols to acids with heterogeneous catalysts	66
4.1	Carbonylation of IBS	177
5.1	Suzuki Cross -coupling	205

List of Tables

Number	Description	Page No.
1.1	Industrial examples of processes using carbonylation technology	5
1.2	Literature report on carbonylation of olefins to acids or esters	14
1.3	Literature report on carbonylation of alcohols to acids or esters	20
1.4	Literature reports on homogeneous Suzuki cross coupling catalyst systems	27
1.5	Literature survey on immobilized catalysts for Suzuki cross-coupling reactions	36
2.1	Operation parameters of the method for GC analysis	76
2.2	Comparative physical characteristics of the different surface modified MCM-41, MCM-48, SBA-15 matrices	85
2.3	XPS data for different anchored and supported catalysts (values in eV)	92
2.4	FT-IR data of different anchored Pd-complex catalysts (values in cm^{-1})	105
2.5	Pd-content of different anchored and supported Pd-complex catalysts	106
2.6	Effect of mutual ratio of promoters on styrene carbonylation for different anchored Pd-complex catalysts	116
2.7	Carbonylation of different substrates using different anchored Pd-complex catalysts	121
2.8	Comparative study of Anchored Pd-complex catalysts with principle examples from literature for carbonylation of olefins and alcohols	124
3.1	Operation parameters of the method for GC analysis	137
3.2	XPS data for Catalyst 1B, 1C and 1D (values in eV)	148
3.3	BET surface area data for the ossified palladium complexes	151
3.4	Pd-content of different ossified Pd-complexes	152
3.5	Effect of Promoters on carbonylation of styrene	160
3.6	Carbonylation of different substituted olefins and alcohols	166
3.7	Comparative study of Ossified Pd-complexes with other heterogeneous Pd-Catalysts from literature for carbonylation of olefins and alcohols	168
4.1	Range of Parameters for Kinetic Studies	174
4.2	Henry's constants (H_e) of CO in a mixture of IBS in MEK at 388 K	177
5.1	Operation parameters of the method for GC/ GC-MS analysis	211
5.2	Comparative study of a few heterogeneous Pd catalysts for Suzuki coupling reactions	217

5.3	Comparative results of Suzuki coupling of iodobenzene and phenylboronic acid using different bases in presence of ossified Pd-pyca catalyst	218
5.4	Suzuki coupling reactions of different substituted aryl halides with phenylboronic acid using ossified Pd-pyca catalyst (Catalyst 1A)	227
5.5	Suzuki coupling reactions of different arylboronic acids with iodobenzene using ossified Pd-pyca catalyst (Catalyst 1A)	229
5.6	Suzuki coupling reactions of different arylboronic acids with miscellaneous aryl/ alkyl halides using ossified Pd-pyca catalyst (Catalyst 1A)	231

Abstract of Thesis

Catalysis has played an important role in the development of chemical industry during the last century. The applications of catalytic processes have been in diverse fields, which include petrochemicals agrochemicals, pharmaceuticals, polymers, fine and specialty chemicals. Particularly, the application in the development of environmentally benign processes and innovations in the pharmaceutical products have been highly significant. The catalytic materials used are generally classified as homogeneous or heterogeneous catalysts. While, most of the industrial processes employ heterogeneous solid-state catalysts, the homogeneous catalysis by soluble metal complexes have some unique features in providing high activity and selectivity under mild operating conditions. Several innovations using homogeneous catalysis have been recognized as *landmarks* in chemical technology. Some examples are Carbonylation of methanol to acetic acid, low-pressure hydroformylation process for oxo-alcohols, synthesis of L-dopa by asymmetric catalysis, hydrocyanation of butadiene to adiponitrile, Asymmetric hydrogenation in Metolachlor (an agrochemical) process, oxidation of p-xylene to terephthalic acid etc. The potential of designing new ligands and catalytic complexes is believed to be highly significant and hence, further research in this area is considered rewarding. Development of environmentally benign and economically viable catalytic routes for synthesis of useful products is of prime importance. In this context, reactions like carbonylation of olefins and Suzuki coupling reactions are chosen for investigation in this thesis. Catalyst-product separation is an important issue in these industrially important reactions considering high cost of the catalysts. Several different immobilization approaches have been investigated to achieve the advantages of both homogeneous and heterogeneous catalysts. However, demands of non-leaching heterogeneous catalysts with improved activity & selectivity is still a major challenge.

Carbonylation reactions are important in the manufacture of a variety of industrial products such as carboxylic acids, esters, aldehydes, alcohols etc. Typically, carbonylation of olefins/ alcohols using metal complex catalysts has emerged as an important tool for synthesis of a variety of drug intermediates and specialty products. Reviews in this subject are presented in textbooks^{1,2} and articles³. It is understood that this reaction uses mostly Pd-complexes as most active catalysts. Carbonylation route to Ibuprofen® is an example of use of homogeneous catalysis to develop clean atom-

efficient chemical technology. Recent developments in the carbonylation of arylolefins/ aryl alcohols to arylpropionic acids had seen the use of homogeneous Pd(pyca)(PPh₃)(OTs) complex catalyst by Jayasree et al⁴ showed the highest ever active and selective catalyst operating under mild conditions. However, the drawbacks of catalyst separation for homogeneous reaction mixture, motivated the studies to heterogenize them. The efficient and easy catalyst-product separation and reuse of these homogeneous Pd-complex catalysts is necessary. Attempts were made using aqueous biphasic catalysis⁵ to address the issue of easy catalyst-product separation but with less success,⁶ and further studies using solid catalysts did not yield much success as they suffered from drawbacks of Pd-leaching under the reaction conditions.⁷ So, the search for truly heterogeneous carbonylation catalyst working under mild reaction conditions having good activity and selectivity is still an important issue. Hence, the focus of research in this thesis has been the investigations on methods of immobilization of Pd-complex catalysts, with the aim of active, selective and stable catalysts.

Another interesting application of homogeneous catalysis is the C-C bond formation by the Suzuki Cross coupling reaction to generate biaryls. This reaction has emerged as an epoch-making discovery whereby ideally any arylboronic acid may be coupled to an aryl halide to obtain the desired biaryl with good selectivities. Since the pioneering works of Suzuki et al⁸, this reaction has been explored in all possible directions of novel homogeneous catalysis, to achieve improved catalysts. In spite of the different immobilized Pd-catalysts proposed for this reaction,⁹ the true heterogeneous catalyst with high activity, biaryl selectivity and efficient recyclability are required to be developed in the view of the leaching and low activity in most of the cases.

Considering the status of developments discussed above, the following problems were chosen for detailed studying this thesis.

- ✓ Immobilization of palladium complexes inside mesoporous materials to obtain novel, highly stable, carbonylation catalysts
- ✓ Investigations on the novel immobilization approach of “Ossification” for carbonylation reactions
- ✓ Kinetic modeling of carbonylation of 4-isobutylstyrene using homogeneous and immobilized catalysts

- ✓ Application of the Ossified Pd-complex catalysts to Suzuki coupling reactions

The thesis is presented in five distinguished chapters, the brief details of each of which is presented hereafter

CHAPTER 1

Introduction and Literature Survey

In this chapter, thorough literature review on the immobilization of Pd-complexes for (i) carbonylation of olefins/ alcohols and (ii) Suzuki coupling reactions, will be discussed. Carbonylation of olefins and alcohols using homogeneous and heterogeneous catalysts has been reviewed. Extensive survey on the Suzuki Coupling reaction of aryl halides and arylboronic acids using heterogeneous Pd-catalysts is also presented. The different catalyst systems reported in literature have been reviewed in detail to understand the activity and selectivity behavior. Based on the review, the following observations were made

- Carbonylation of olefins and alcohols are facilitated under a wide range of reactions conditions, using a variety of different transition metal complexes as catalysts. Of these, palladium complexes operate under milder conditions as compared to the others. Using Pd-complexes, numerous attempts have been made to enhance activity and selectivity for these reactions. Immobilizations of the Pd-complexes are also well studied using different strategies in the form of supported catalysts, aqueous biphasic catalysts, SAPC, tethered catalysts, encapsulated catalysts etc., but activity and selectivity are poor.
- Carbonylation of olefins and alcohols occur under high temperature, in the presence of protic acid and alkali metal halides as promoters. So, under such stringent reaction conditions, nearly all of the presently known immobilized Pd-complex catalysts succumb to leaching, the degree of which however vary. Thus, heterogeneity and effective recycle and reuse become important issues to study.
- The kinetics of carbonylation of aryl olefins/alcohols has been studied previously using $\text{PdCl}_2(\text{PPh}_3)_2$ complex catalyst. A detailed analysis of the rate models and mechanism has been discussed. However, no previous studies on the kinetics using the highly active $\text{Pd}(\text{pyca})(\text{PPh}_3)(\text{OTs})$ complex catalyst has been reported.

- Suzuki cross-coupling reactions occur using different transition metal catalysts (either in pure metallic/ metal complex form) of which Pd was the best with highest activity and selectivity. The base-promoted Suzuki coupling reaction poses problems of degradation of the solid Pd-catalysts either by agglomeration (for nano-sized cluster catalysts), or decomposition to Pd-black (for many Pd-complex catalysts, homogeneous and heterogeneous) for high temperature reactions, while the activities are quite low for reactions at room temperatures.

On the basis of these observations, the scope of work was defined as mentioned before. The description of the work is presented in the respective chapters

CHAPTER 2

Anchored Pd-Complexes in Mesoporous Matrices: Novel Catalysts for Carbonylation of Olefins and Alcohols

This chapter describes the anchoring of Pd-complexes in mesoporous matrices such as MCM-41, MCM-48 and SBA-15, followed by applications in carbonylation reactions. Owing to the larger size of the substrate molecules than the pore-sizes of most microporous matrices, mesoporous supports were chosen. For this purpose, a molecular anchor molecule is attached to the matrices followed by towing the catalytic complex to it. 3-aminopropyltrimethoxy silane (APTS) has been used here as an anchor. Two different synthesis methods were used to synthesize the NH₂-functionalized MCM-41, MCM-48 and SBA-15. In the post-synthesis grafting method, passivation of the external surface is followed by the grafting of the aminopropyl moiety onto the internal surface following the procedure described by Shephard et al¹⁰. While for SBA-15 only, co-condensation method was followed to comparatively study the grafting of the -NH₂ groups inside the channels of SBA-15 due to its larger channel diameter of ~100Å. These synthesized materials were characterized thoroughly using different techniques such as ³¹P CP-MAS NMR, powder XRD, XPS, SEM, TEM, AAS etc. to establish the immobilization methodology as well as to understand the nature of the complex after immobilization. The support matrices retained their original morphological constitution, but changes were observed in the pore volume, surface area etc., after the anchoring procedure. These materials were tested as catalysts for carbonylation of olefins and alcohols. All the catalysts showed high activities with turnover frequencies TOF ranging from from 300 to 700 h⁻¹, operating at 115°C, and 5.4 MPa CO pressure for styrene carbonylation. The catalysts were extremely stable

under such reaction conditions and showed almost negligible leaching of Pd in the reaction media and recycled efficiently with negligible changes in activity and selectivity. Thus, the anchored Pd-complexes inside mesoporous matrices were found to be superior compared to the previous reports in terms of activity, selectivity and stability.

CHAPTER 3

Ossification – A Novel Immobilization Approach: Application in Carbonylation Reactions

The difficulties in multi-step synthesis of the anchored Pd-complex catalysts in spite of their high activity, selectivity and stability demanded a search for an easy immobilization technique. The novel approach, termed *ossification* is illustrated in this chapter for the first time. "Ossification" is based on the natural phenomenon of slow deposition of osseous materials (bones, coral reefs etc.) from aqueous soluble precursor molecules and ions. The Pd(pyca)(PPh₃)(OTs) complex was converted to its water-soluble analog by exchange of PPh₃ ligand with its aqueous soluble counterpart (e.g. TPPTS) by known techniques.¹¹ Then the aqueous solution of metal complex is subjected to treatment with heavier group IIA cations resulting in the precipitation of the insoluble solid Pd-complex catalysts. These *ossified* complexes were characterized thoroughly using powder XRD, ³¹P CP-MAS NMR, SEM, AAS etc. to know the status of the Pd-complex after the ossification process. Interpretation of the characterizations confirmed the formation of the ossified complexes as proposed. These materials were expected to be intrinsically insoluble due to the formation of the Ba-sulphonate ion-pair, which is well known. Carbonylation of arylelefins and alcohols was studied using the ossified Pd catalysts using a stirred autoclave reactor. The catalysts showed excellent performance with respect to activity (TOF ~200-300 h⁻¹) and selectivity to the desired regioisomer (>99.5%). The catalysts recycled very efficiently with consistent activity and selectivity profiles for each recycle run.

CHAPTER 4

Kinetic Modeling of Carbonylation of 4-Isobutylstyrene using homogeneous and ossified Pd(pyca)(PPh₃)(OTs) complex

In this chapter the kinetics of carbonylation of 4-isobutylstyrene using homogeneous and ossified Pd(pyca)(PPh₃)(OTs) complex is presented. For this purpose the reactions were carried out in a stirred autoclave to investigate the effect of the different

parameters such as CO partial pressure, substrate concentration, promoters, temperature, etc. In all the experiments the C-T profiles were obtained. Initial rates were used to understand the order of dependence on each of the reaction parameters. Empirical models were proposed based on the initial trends for both the homogeneous and heterogeneous systems. The model predictions for the integral concentration-time profiles were in good parity with the experimental data. Activation energies were calculated from the temperature dependence of the rate constants for both the homogeneous and heterogeneous catalysts, employing the Arrhenius plots.

CHAPTER 5

Suzuki Coupling Studies using Ossified Pd-Complex Catalysts

The ossified palladium complex catalysts were investigated for the Suzuki cross coupling reactions as described in this chapter. The Suzuki coupling reactions were carried out using ethanol as solvent under reflux conditions and potassium carbonate as a base. The reaction of iodobenzene and phenyl boronic acid was used to study the effect of the various reaction parameters. The typical concentration-time profile showed that the reaction was a highly selective one without any byproducts at any point of reaction. The ossified Pd-pyca complex catalyst showed highest activity among all the four ossified catalysts. It was observed that the ossified catalyst had a high activity at very high substrate-to-catalyst ratios of $\sim 10,00,000$ yielding a TON of $> 11,00,000$ in a reaction time of 3 h, for iodobenzene substrate. The observed TOF $> 3,40,000 \text{ h}^{-1}$ of the Suzuki coupling was higher than the previously reported highest by Yamada et al¹². The catalyst showed no leaching under such conditions. The ossified catalyst was recycled 5 times without change in its activity and selectivity. The catalyst's applicability was tested for over 50 substrates having varied functional groups both on the aryl halides as well as on the arylboronic acids. The detailed parametric variation of the Suzuki coupling reaction was studied using the ossified Pd-pyca catalyst and iodobenzene and phenylboronic acid as substrates.

Key References

1. (a) Colquhoun, H M, Thompson D J, Twigg M V, *Carbonylation-Direct Synthesis of Carbonyl Compounds*, Plenum Press, New York **1991** (b) Falbe J (Ed.), *New Synthesis with Carbon Monoxide*, Springer-Verlag, Berlin **1980** (c) Lapidus A L, Pirozhkov S D, *Russ. Chem. Rev.*, **1989** 58 117 (d) Weisse L, *Specialty Chemicals Magazine*, **2002** 22(3) 36
2. Cornils B, Herrman W A, (Eds.), *Applied Homogeneous Catalysis with Organometallic Compounds (2nd Ed.)*, VCH, Weinheim, **2002** Vol 1 and 2
3. Van Leeuwen P W N M, Claver C, *Comprehensive Coordination Chemistry II*, **2004** 9 141
4. Jayasree S, Seayad A, Chaudhari R V, *Org. Lett.*, **2000** 2(2) 203
5. Cornils B, Herrman W A, (Eds.), *Aqueous-Phase Organometallic Catalysis*, (2nd Ed.) VCH, Weinheim, **2004**
6. Jayasree S, Seayad A, Chaudhari R V, *Chem. Commun.*, **2000** 14 1239
7. Jayasree S, Seayad A, Chaudhari R V, *Chem. Commun.*, **1999** 12 1067
8. (a) Miyaura N, Yamada Y, Suzuki A, *Tetrahedron Lett.*, **1979** 20 3437 (b) Miyaura N, Sugimoto H, Suzuki A, *Tetrahedron Lett.*, **1981** 22 127 (c) Miyaura N, Yamada K, Sugimoto H, Suzuki A, *J. Am. Chem. Soc.*, **1985** 107 972
9. a) Choudary B M, Madhi S, Chowdari N S, Kantam M L, Sreedhar B, *J. Am. Chem. Soc.*, **2002** 124(47) 14127 (b) Choudary B M, Madhi S, Kantam M L, Sreedhar B, *J. Am. Chem. Soc.*, **2004** 126(8) 2292 (c) Choudary B M, Madhi S, Chowdari N S, Kantam M L, Sreedhar B, (CSIR, India), US Pat. Appl. No. US 2004192542 A1, Sept **2004** (d) Baleizao C, Corma A, Garcia H, Levya A, *J. Org. Chem.*, **2004** 69(2) 439 (e) Corma A, Das D, Garcia H, Levya A, *J. Catal.*, **2005** 229(2) 322 (f) Shimizu K, Maruyama R, Komai S, Kodama T, Kitayama Y, *J. Catal.*, **2004** 227(1) 202 (g) Shimizu K, Koizumi S, Hatamachi T, Yoshida H, Komai S, Kodama T, Kitayama Y, *J. Catal.*, **2004** 228(1) 141 (h) Corma A, Garcia H, Levya A, *Appl. Catal. A Gen.*, **2002** 236(1-2) 179 (i) Corma A, Garcia H, Levya A, Primo A, *Appl. Catal. A: Gen.*, **2004** 257(1) 77
10. Shephard, D. S.; Zhou, W.; Maschmeyer, T.; Matters, J. M.; Caroline L., Roper, C. L.; Parsons, S.; Johnson, B. F. G.; Duer, M. J. *Angew. Chem., Int. Ed.* **1998** 37 2719
11. Jayasree S, Seayad A, Sarkar B. R., Chaudhari R V, *J. Mol. Catal. A: Chem* **2002** 181 221
12. Yamada Y M A, Takeda K, Takahashi H, Ikegami S, *J. Org. Chem.*, **2003** 68(20) 7733

Chapter **1**

Introduction And Literature Survey

This chapter presents a survey of the literature relevant to the subject area of investigation reported in this thesis. The gradual build-up of the problems around certain issues of current economic and environmental concern for the present day technology of carbonylation & C-C coupling reactions has been presented. The development of the homogeneous carbonylation & Suzuki coupling catalysts and the different immobilization strategies & techniques to facilitate effective catalyst-product separation and reuse has been described in this chapter. Moreover, applications of these for the respective reactions from literature have been reviewed to identify & choose the most effective one for the studies. The thorough discussion of the different aspects of the existing state-of-the-art, and the understanding gained from this review has evolved into a well-defined objective to work with.

1.1 Introduction

The advancement of science and technology has left indelible impressions in every aspect of present day human civilization. More remarkably, the innumerable applications of the chemical know-how into almost each and every commodity of daily use have been the revolutionary examples of the technological progress of the modern age, be it foodstuff, drugs & therapeutics, fabrics, agriculture, architecture, entertainment etc. The terminology “catalysis” has become synonymous with the chemical revolution since the last half of the twentieth century. Catalysis, since its origin, had an allure due to the inherent aspects of maximized output via energy and time-efficient alternative pathways and the use of non-conventional and eco-friendly resources. Thus, it has been the backbone to support the entire growth and development of the chemical industry and hence being the subject of focus of applied chemistry research over these years, in all the avenues of its cross-linked niche. The broad classification into the homogeneous and heterogeneous catalysis was based on the distribution of the components of the system viz. substrate, product(s), catalyst, and promoters & co-catalysts etc., into one or more phases of physical occurrence respectively, during the catalytic reaction. The high activity & product-specificity (chemo-, regio- or enantioselectivity) and convenient characterization of the actual intermediate species in a catalytic cycle, etc. are the characteristics of the homogeneous organo-transition metal complex catalysts. These aspects make them more understandable and thus tunable to the specific necessity. The heterogeneous catalysts on the other hand, have the facile catalyst-product separation advantage coupled with the lesser activity and specificity at times, either due to the transport limitations across the phases involved, or the catalyst morphology. The unambiguous structure-reactivity correlation, and reaction mechanism, established for some of the homogeneous catalysts had led to proper understanding and paved their way for successful commercialization. However, for heterogeneous catalysts, the high efficiency and economical separation issues had made them commercially viable in spite of the absence of thorough knowledge of the exact surface-speciation and *in situ* characterizations and mechanistic insights in many cases. Although, each class is characterized by specific advantages and drawbacks respectively, the intercalation of these fields has opened up new horizons in catalysis research in recent times. The

homogeneous-heterogeneous interface has emerged as the new dimension of catalysis research with immense possibilities of new and exciting findings.

Of the myriads of catalytic reactions envisaged so far, such as carbonylation, hydroformylation, hydrogenation, silylation, oligomerization, isomerization, condensation, polymerization, oxidation, epoxidation etc.^{1,2}, the carbonylation reaction is one of the important classes of step-up reactions. The C1 chemistry, as it bloomed during the World War II was mostly targeted towards the production of fuels by alternative routes of Fischer-Tropsch synthesis, synthesis-gas transformations etc., gradually diversified to innumerable product ranges in the later years by simple derivatizations. The importance of the carbonyl compounds as the main source of different fine and specialty chemicals³ such as, carboxylic acids, esters, lactones, ketones, anhydrides, amides, carbamates, polyketones, isocyanates, amino acids etc., was envisioned in the forthcoming years. The carbonylation reaction involves the insertion of a CO moiety in an organic molecule, in the presence or absence of an auxiliary molecule so as to derivatize it further. Organometallic complexes of various transition metals such as Ni, Pd, Pt, Rh and Ir etc. can catalyze these reactions. In the last few decades, enormous research attention was focused on this reaction class and development of novel catalysts, elucidation of intermediates and reaction pathways, and technology enhancement possibilities were investigated thereby highlighting this reaction as a potential candidate of alternate eco-friendly technology for various industrially important products.

Another important class of reactions namely, the C-C bond forming reactions have gained importance in the last half-a-century. Different coupling reactions were invented as in the development of the C-C coupling reactions with impacts having their inventors' names coined with them such as, Heck reaction, Suzuki coupling, Stille coupling, Sonogashira coupling reactions etc. These catalytic reactions have made the synthetic approach to complex organic molecules with remote functionalities extremely easy, which were otherwise very difficult. Different transition metals (in atomic state as well as metal complexes) have been used in these reactions as catalysts.

One of the most important and discussed issues concerning homogeneous catalysis is the catalyst-product separation and effective reuse. The stability of the transition metal complex catalysts under the recovery conditions is also questioned due to the thermal sensitivity of the ligands involved, along with the issues of byproduct

generation and their disposal. For complete removal of the soluble metal complex catalysts, the downstream processes are generally cumbersome and expensive while the environmental demands are also growing more stringent. These led to the necessity of modified homogeneous catalysts coupled with the facile separation advantages of the heterogeneous ones. Immobilization of transition metal complexes has been considered as the most fruitful option, whereby the soluble complex catalyst is immobilized into a phase, different from that of the substrate and product(s) providing easy separability. The other phase may be another immiscible liquid, a solid support, or even be a physically maneuverable medium of reaction.

The aim of this thesis was to investigate the carbonylation of olefins and alcohols producing carboxylic acids and esters, and Suzuki coupling reactions of different substrates which are of fine chemical and pharmaceutical importance, using novel immobilized organo-palladium complexes of different types, and drawing a comparative conclusion on the respective methodologies of heterogenization with respect to the activity, selectivity, recyclability, stability etc, and many related issues. The detailed study of the kinetics of carbonylation of these compounds using homogeneous and heterogenized homogeneous catalysts have also been explored. This chapter presents a review of literature on the carbonylation reactions, Suzuki Coupling reactions, techniques for immobilization of transition metal complexes and their application areas; and specifically the application of immobilized palladium catalysts for carbonylation and Suzuki coupling reactions.

1.2 Carbonylation

Carbonylation reaction is one of the most studied organic transformations catalyzed by the organometallic complexes for synthesis of a variety of industrially important products. In this reaction, a CO moiety is inserted into an organic substrate⁴,⁵ forming a carbonyl compound such as aldehyde, ketone, acid, amide, lactone, anhydride etc. In the presence of any auxiliary compound (if required), a derivative may be formed as the product. The range of functionalities that can be carbonylated may vary within acetylenes, mono- and di-olefins, alcohols, nitro compounds, amines, organic halides, etc. for both aliphatic and aromatic analogs.

Reppe⁶ initially investigated the metal carbonyl catalyzed carbonylations and this showed the path for investigations of varied types considering the economic and environmental advantages of carbonylation reaction, such as,

- (i) Easily available and cheaper feedstock like carbon monoxide
- (ii) High atom efficiency with minimum by-products
- (iii) More benign than the clandestine hazardous phosgenation route

Later advancements were shown as landmark works of Wilkinson⁷ using Rh-complexes, and of Heck⁸ and Tsuji⁹ using palladium-complexes respectively, which illustrated that, the reaction could be operated under milder reaction conditions. On the basis of further modifications and developments, a number of commercial processes were established successfully, e.g. carbonylation route to acetic acid from methanol, acetic anhydride, propanoic acid etc. (see Table 1.1) These were the best examples of the wider applicability of the carbonylation reactions as alternative eco-friendly routes to the conventional stoichiometric syntheses. In almost all of these processes the homogeneous metal complex catalysts, with or without the promoters/ co-catalysts provide good activity and selectivity to the desired products. Along with these existing industrial processes, large numbers of new processes have shown promises for synthesis of complex organic molecule with possible applications in the fine chemicals and pharmaceuticals. The most recent example being, the carbonylation route for arylpropionic acids synthesis (Ibuprofen in particular). One of the important emerging processes was the outcome of Shell's research for the carbonylation of propyne to methyl methacrylate¹⁰ using Pd(OAc)₂/2-PyPPh₂/H⁺ catalyst system operating at mild conditions (333K, 3-6 MPa) and thus competing with the Acetone Cyanohydrin (ACH) process in terms of the greener approach. Another advancement of the carbonylation technology can be evident from the co-polymerization of ethylene-CO yielding high performance polymers as polyketones, polyamides and polyesters.¹¹ The catalyst used for the polyketone synthesis was Pd(II) precursor in addition with a bidentate phosphine ligand as dppp at 358K and 4.5 MPa. The cis-mode of ligation of the bis-phosphine in the square planar transition state resulted in the very high cis-selectivity for the product. This illustrated the advantageous tuning of homogeneous catalysts to maximize desired yield, very well.

Since most of these products are difficult to distill and are also thermally sensitive, the catalyst-product separation issue becomes even more critical for the

commercial success of these chemistries. Therefore, in most of the cases further research is presently targeted in the areas of catalyst product separation, development of enantioselective catalysis, and better efficient catalyst design in terms of the activity and milder operating conditions.

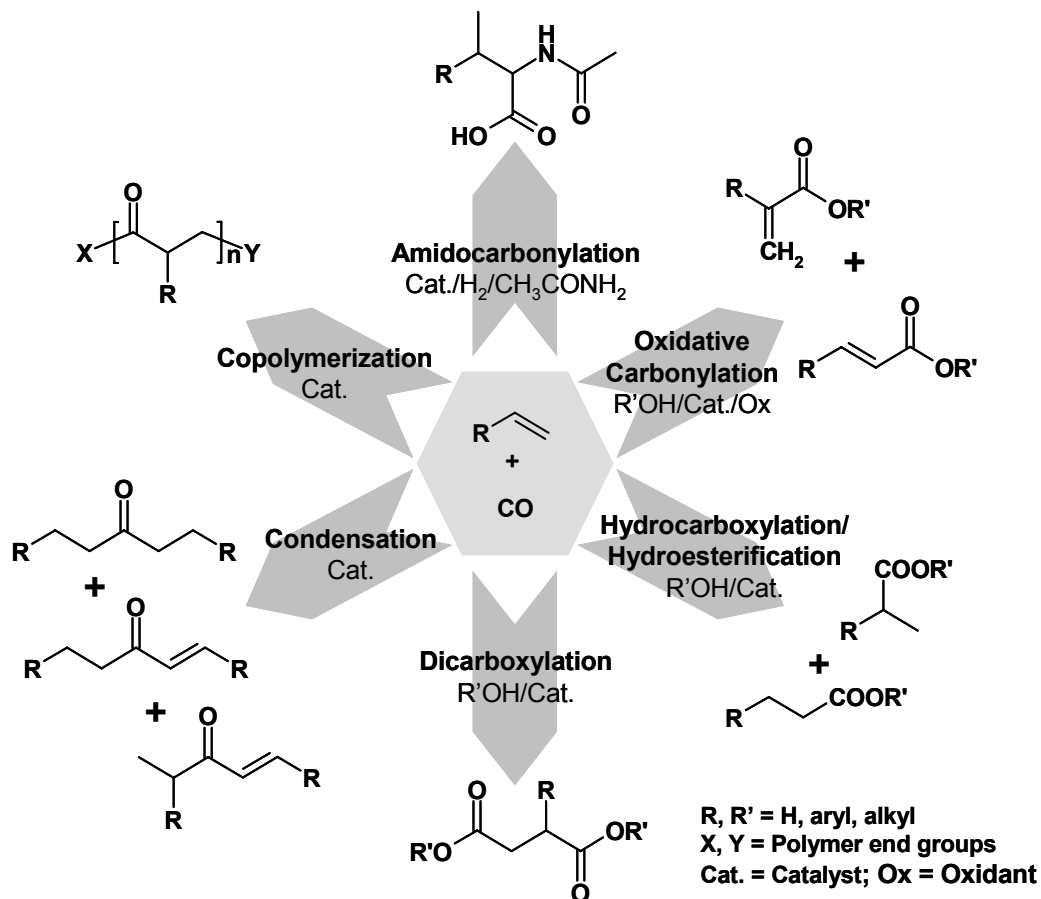
Table 1.1: Industrial examples of processes using carbonylation technology.

Entry	Process	Catalyst used	Company	Ref
<i>Commercial Processes</i>				
		$\text{Co}_2(\text{CO})_8$	BASF	12
1	Methanol to Acetic acid	RhCl ₃ / Iodide	Monsanto	13
		IrCl ₃ / Iodide	BP Chemicals	14
2	Methyl acetate to Acetic anhydride	RhCl ₃ / MeI	Halcon	15
		Rh/ MeI	Eastman Chemicals	16
3	Ethylene to Propionic acid	Ni(OCOC ₂ H ₅) ₂	BASF	17
4	Acetylene to Acrylic acid	Ni-salts/ carbonyls	BASF	18
5	Benzyl chloride to Phenylacetic acid	$\text{Co}_2(\text{CO})_8$	Montedison	19
6	Isobutylphenylethanol to Ibuprofen	PdCl ₂ (PPh ₃) ₂ /aq. HCl	Hoechst-Celanese	20
7	Methanol to Dimethyl carbonate	PdCl ₂ -CuCl ₂	Assoreni	21
<i>Emerging Processes</i>				
8	Propyne to Methyl methacrylate	Pd/2-Pyridylphosphine	Shell	22
9	Ethylene-CO copolymerization	Pd(OAc) ₂ /dppp/TsOH	Shell	23
10	4-Isobutylstyrene to S-Ibuprofen	PdCl ₂ /CuCl ₂ /BNPPA	-	24
11	Phenol to Diphenyl carbonate	Pd ^{II} /NH ₄ ⁺ salt/co-catalysts	GE	25
12	Nitro-compounds to Isocyanates	Pd ^{II} / Phenanthroline	-	26

1.2.1 Carbonylation of Olefins

Catalytic carbonylation of olefins end up to a number of classes of organic compounds, both saturated and unsaturated, namely simple carboxylic acids, esters,

ketones and polyketones, unsaturated acids and esters, amino acid derivatives etc. depending on the reactants, catalysts and reaction conditions. A schematic of the different products arising from carbonylation of olefins is shown in Scheme 1.1

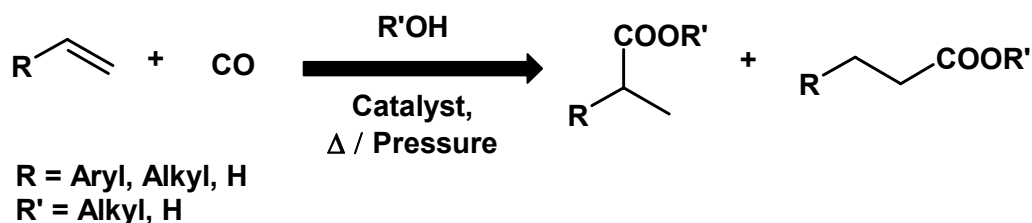


Scheme 1.1: Olefin carbonylation

As this thesis is focused on the hydrocarboxylation reaction, a detailed discussion on catalytic chemistry is presented below with relevant literature references.

1.2.1.1 Hydrocarboxylation and Hydroesterification

The hydrocarboxylation and hydroesterification of the olefins is one of the most important and oldest applications of transition metal complex catalyzed carbonylation reaction. A schematic representation of the reactions is illustrated in Scheme 1.2



Scheme 1.2 Schematic for carbonylation of olefins

As per the literature reports in earlier years, the carbonylation reactions were conducted at high pressure and temperature using Ni or Co carbonyl complexes as catalysts²⁷. In the later years, many other transition metal complex catalysts based on Pt, Pd, Rh, Ir, and Ru etc. were found to be effective at milder reaction conditions^{8,9,28}.

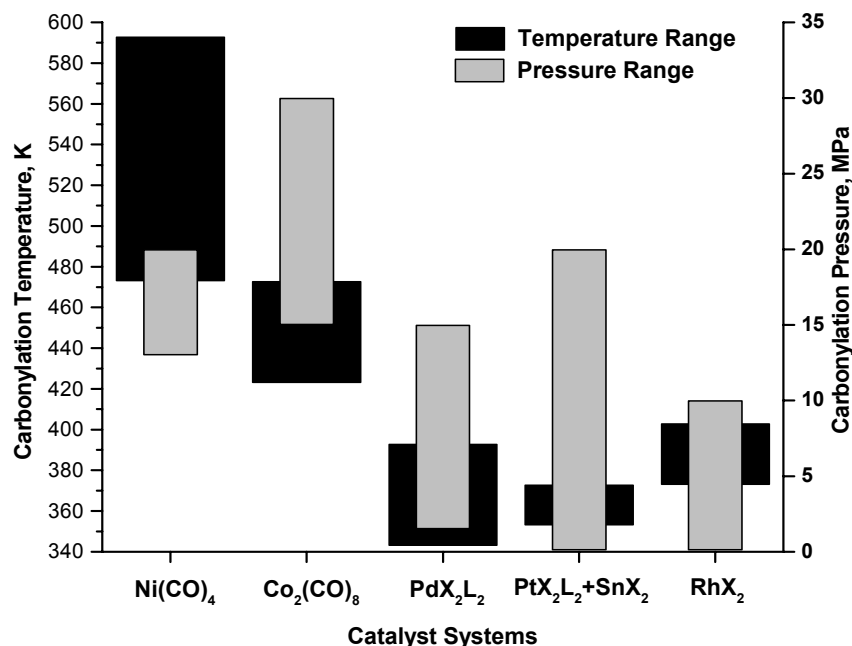


Figure 1.1: Comparison of operating conditions for different carbonylation catalyst systems

A comparative representation of the operating conditions for the different carbonylation catalyst systems is given in Figure 1.1 (based on the data of Beller and Tafesh^{1d [pg 188]}) showing the gradual advantageous-development of the low-pressure carbonylation technology. In these reactions, generally a mixture of linear and branched isomeric

products is obtained as products. So, selectivity, more precisely regioselectivity to the desired one, is one of the issues of interest for carbonylation of olefins. It was observed that with the classical nickel-based catalyst systems, moderately high regioselectivity (60-70%) to the branched isomer was obtained while that with the cobalt-based systems was reverse for the hydrocarboxylation reactions. Furthermore, the chemoselectivity to the acids itself was important, as under the higher operating conditions ($> 523\text{K}$) side-reactions such as isomerization, oligomerization etc. were prominent. Using the platinum, palladium and rhodium based catalyst systems; however the selectivity issues (both chemo- and regioselectivity) were improved to the desired level. Early reports by Tsuji et al²⁹ and Bittler et al³⁰ showed the use of PdCl_2 and $\text{PdCl}_2(\text{PPh}_3)_2$ with 10% HCl in ethanol as solvent respectively, whereby the reactions were carried out at around 368K and 30 – 70 MPa pressure. For ethylene and styrene as substrates 90% and 95% yields of ethyl propionate and ethyl-2-phenylpropionate were obtained respectively. The influence of the phosphine ligand was investigated by Sugi et al³¹ using a bidentate phosphine ligand as $\text{Ph}_2\text{P}(\text{CH}_2)_n\text{PPh}_2$, where $0 < n < 10$, which showed a complete reversal of the selectivity for hydroesterification. For the carbonylation of styrene using the $\text{PdCl}_2/\text{Ph}_2\text{P}(\text{CH}_2)_4\text{PPh}_2$ (diphenylphosphinobutane, dppb) catalyst system gave high selectivity (87%) to the linear ethyl-3-phenylpropionate product with turnover frequencies (TOF) of $\sim 10\text{-}20\text{ h}^{-1}$, at a maximum yield of 38.1%³². So it was almost confirmed that the monophosphines were more efficient in producing the branched products. However, monophosphine and arsine ligands stabilized palladium and platinum complexes in the presence of group IV B metal halides (SnCl_2 , GeCl_2 , PbCl_2 etc.) as promoters produced upto 98% selectivity to linear isomeric product for the hydroesterification of α -olefins.^{33,34} $\text{PdCl}_2(\text{PPh}_3)_2$ and $\text{PtCl}_2(\text{AsPh}_3)_2$ were used here as catalysts under mild operating conditions of 353 K and 30 MPa pressure. These observations indicate that the activity as well as the selectivity (both chemo- and regioselectivity) varies independently with the reaction parameters (temperature, pressure etc.) and catalyst properties (transition metal involved, ligands' stereo-electronic environments, promoters, co-catalysts etc.), for the carbonylation of olefins. Palladium complexes were found to be the best catalyst for the hydrocarboxylation and the hydroesterification of the olefins compared to other metals. The regioselectivity was also observed to be a function of the substituents on the

olefin. The aryl-substituted branched acids/ esters have applications as a class of non-steroidal anti-inflammatory drugs, as ibuprofen, naproxen, ketoprofen etc.

To achieve catalytic carbonylation at room temperature and atmospheric pressure was an interesting challenge. In one of the reports, Alper et al³⁵ demonstrated this idea, using PdCl₂ as a catalyst in the presence of molecular O₂ with CuCl₂, HCl and as catalysts. Later, this catalyst system was reported to be very active for the synthesis of the branched acids with a variety of aliphatic and aromatic terminal olefins as reported by Toda et al³⁶. For hydroesterification reaction also, the same catalyst system produced good selectivity to the branched ester (> 95%) with propene³⁷ as substrate. The role of CuCl₂ and O₂ was proved to re-oxidize the Pd(0) species, formed intermediately during reaction in the catalytic cycle, to the Pd(II) species. More studies were reported by Alper et al^{38, 39} using a Pd-source [either Pd(II) or Pd(0)] and formate ester in presence of CuCl₂, HCl and O₂ revealing that the carbonyl moiety of the esters formed were derived from CO but not from the formate ester. The activity of the catalyst system was found to be high, retaining the high linear-ester regioselectivity too. It was concluded that the Pd(0) catalyst systems such as Pd(PPh₃)₄ or Pd₂(dba)₃ in presence of dppb, catalyzed the hydroesterification of alkenes in presence of formates forming linear isomer predominantly, while use of PdCl₂(PPh₃)₂ under similar conditions yielded the branched chain isomer. Following this, many other catalyst systems were investigated, such as Pd(OAc)₂/ dppb/ formic or oxalic acid (working at 423K and 0.6-2 MPa)⁴⁰; PdCl₂/ CuCl₂/ HCl in presence of free PPh₃ ligand (working at 373K and 4.1 MPa)⁴¹ for olefin carbonylation. In a later report, ~93% regioselectivity to the branched product was obtained along with a TOF of ~25 h⁻¹ for the carbonylation of 4-methylstyrene. Interestingly enough, the introduction of molecular O₂ in the same system actually reduced the catalytic activity significantly pointing towards the formation of inactive Ph₃P=O from PPh₃ and O₂, as the probable reason. In some of the later reports, the carbonylation of *p*-isobutylstyrene to ibuprofen and that of 6-methoxy-2-vinylnaphthalene to naproxen were disclosed and the processes were patented by various companies such as, Nippon Petrochemical Company Ltd.⁴², Ethyl Corporation⁴³, Montedison⁴⁴ keeping an eye on the economical importance of these products. In one of the Nippon Petrochemical Corporation's patents^{42c} carbonylation of *p*-isobutylstyrene was reported in a biphasic catalyst system of PdCl₂(PPh₃)₂ (in toluene)/ 10% aq. HCl at 393K and 30 MPa pressure producing 100% conversion and

89% branched acid selectivity, but the rate of reaction was very poor ($\text{TOF} < 2 \text{ h}^{-1}$). In the next few years, emphasis of research was focused on the development of more active catalysts, and it was proposed that the cationic palladium complexes were efficient for hydroesterification reaction under mild conditions. The enhanced activity might be attributed to the availability of the vacant coordination site for easier activation of the reactant moieties. Different cationic palladium complexes as $[\text{Pd}(\text{MeCN})_2(\text{PPh}_3)_2][\text{BF}_4]_2$ ⁴⁵ and $[(\text{Cy}_3\text{P})_2\text{Pd}(\text{H})(\text{H}_2\text{O})][\text{BF}_4]$ ⁴⁶ were tested for hydroesterification of styrene. The former catalyst gave 96% selectivity to the branched product but again with a poor activity ($\text{TOF} \sim 3 \text{ h}^{-1}$) at room temperature and 2 MPa pressure. Seayad et al⁴⁷ made another important development using $\text{Pd}(\text{OTs})_2(\text{PPh}_3)_2$ catalyst for the hydroesterification of styrene. This complex was generated *in situ* from $\text{Pd}(\text{OAc})_2/\text{PPh}_3/\text{TsOH}$ mixture under the reaction conditions. High catalytic activity ($\text{TOF} \sim 411 \text{ h}^{-1}$) was obtained using this catalyst operating at mild conditions of 348K and 3.4 MPa. A number of different phosphine ligands were tested to understand the stereo-electronic effect of the phosphine on the activity. They also observed that the high activity was retained at high substrate concentrations, and the selectivity to the desired branched ester increases with decrease in the basicity of phosphine ligands as well as steric bulk around the palladium centre and also on the polarity of the reaction medium. The importance of the promoter ions for the reaction was also understood here. A detailed kinetic study was also reported where, an unusual trend of an increase in activity was observed beyond a styrene concentration of 3.84, kmol/m^3 . The rate also increased with an increase in the partial pressure of CO initially and was independent beyond 3.4 MPa. Various empirical rate models were chosen and tested to fit the rate data. Hydroesterification of styrene using the same catalyst system was also investigated in depth providing some mechanistic insights of the reaction.⁴⁸ Based on the NMR studies it was proposed that the reaction passes through a palladium hydride intermediate, and Pd-hydridocarbonyl and Pd-acyl complexes were isolated from the reaction medium. Since the complex $\text{PdCl}_2(\text{PPh}_3)_2$ was also found to be catalytically active, but the rate of reaction was considerably low in the biphasic system, this was used in the homogeneous mode by introducing two different promoters supplying the ions H^+ and Cl^- , as TsOH and LiCl by Seayad et al⁴⁹. This catalyst system proved to be a very active ($\text{TOF} \sim 2255 \text{ h}^{-1}$,) and regioselective (> 99.8 %) for styrene carbonylation to 2-phenylpropionic acid under mild operating conditions

of 388K and 5.4 MPa, thus setting a landmark advancement in carbonylation technology. A detailed study on the various reaction parameters and their effect on the activity and selectivity were also studied by Seayad et al⁵⁰. Jayasree et al⁵¹ investigated a class of novel cationic palladium complexes containing hemi-labile N-O, and N-N chelating ligands for the carbonylation reactions. Of the various complexes investigated hereby, the Pd(pyca)(PPh₃)(OTs) complex showed excellent activity and > 99.8% selectivity to the desired branched-carboxylic acid isomer in the presence of TsOH and LiCl promoters, under milder reaction conditions for the carbonylation of different alkenes. TOF's of 2600 h⁻¹ and ~1300 h⁻¹ were obtained for styrene and *p*-isobutylstyrene carbonylation respectively, which set new benchmark for homogeneous carbonylation of olefins. To facilitate easy separation of the catalyst from the products, Pd(TPPTS)₃ generated *in situ* from PdCl₂ and the water soluble ligand TPPTS (triphenylphosphine trisulfonate), along with TsOH as a promoter was used as the catalyst by Sheldon et al⁵², for hydrocarboxylation of *p*-isobutyl styrene (IBS) at 338 K and 5 MPa pressure without any organic solvent. The catalyst showed a selectivity of 74 % to the branched isomer (Ibuprofen), but activity was very low (TOF = 3 h⁻¹). For styrene as the substrate, TOF up to 49 h⁻¹ was observed with a maximum regioselectivity of 90 %, with a TPPTS/ Pd molar ratio of 4, at 14 MPa CO pressure and 338K. One of the disadvantages of the biphasic catalytic reaction was the very low reaction rate, due to the lower solubility of the organic reactants in the aqueous catalytic phase. To overcome this, agents such as co-solvents, cyclodextrins were used as exemplified in the hydrocarboxylation of higher α -olefins such as 1-decene.⁵³ In a recent report, Jayasree et al have described a novel water-soluble catalyst system for the hydrocarboxylation of olefins, producing excellent activity and selectivity⁵⁴. A detailed study⁵⁵ on the parametric effects and proposed mechanism using the aforesaid catalyst had also been discussed. The novel biphasic catalyst system consisted of Pd(pyca)(TPPTS)(OTs) with LiCl and TsOH as promoters. The aqueous soluble complex was prepared by simple partition technique of the exchange of the PPh₃ ligand with TPPTS, which actually brings the complex to the aqueous phase. Styrene was considered as the model substrate and the catalyst system showed good catalytic activity (TOF ~ 281 h⁻¹, for styrene), and selectivity (~ 91% branched product) patterns. The system was very stable under CO atmosphere, and recycled very efficiently, but when exposed to air, decomposed to palladium black gradually. This

drawback of the catalyst system was considered as the main motivation for further research in this area involving the exploration of immobilized metal complexes as catalysts for application in carbonylation chemistry. Jayasree et al⁵⁶ had reported a supported Pd-catalyst for the carbonylation reaction. A number of inorganic support materials were used, and the metallic Pd was stabilized by the use of free PPh₃ in the reaction mixture along with TsOH/ LiCl as promoters. This catalyst system was very efficient and gave very high TOF and selectivity to the desired products for a number of different substrates. An interesting point about this system was that the metal leached out of the catalyst during reactions and after reaction was ceased (on cooling), it went back to the support. This kind of thermo-regulated catalytic activity was proposed as the reason behind the high activity and selectivity. In the recent years, a number of different new catalyst systems were reported for the carbonylation of olefins, which may be described as follows. Various groups reinvestigated the importance of diphosphine ligands recently. Drent et al⁵⁷ had disclosed the carbonylation of conjugated dienes (e.g. 1,3-butadiene) using a Pd-source and a novel diphosphine ligand. Slany et al^{58,59} reported a novel *in situ* developed catalyst system comprising of Pd(OAc)₂/ diphosphine [e.g. 1,2-bis(4-phosphorinone)ethane], for the carbonylation of simple and functionalized alkenes (e.g. ethene, pentenoic acid etc.). The use of different novel diphosphine ligands, containing substituted 2-phosphatrimethylsilyloxyethyl group attached to the P-atom, were reported by Sava et al⁶⁰, for the carbonylation of conjugated dienes. The mechanistic insights into the influence of the electronic aspects of the spacer alkyl group in a diphosphine ligand were studied by Pugh et al⁶¹, for the hydroesterification reaction taking ethene as a typical substrate. Similar catalysis studies using novel bidentate phosphine ligands having a substituted adamantyl group attached to the P-atom by any of its tertiary C-atom were reported very recently by Eastham et al⁶². Gold-complex catalyzed carbonylation of olefins has been reported by Nkosi et al⁶³ for the first time for these classes of reactions. In a recent article, palladium-catalyzed carbonylation reactions and more precisely, the hydroesterification reactions were reviewed in details with respect to the catalysts, kinetic and the selectivity issues related to the reagents and promoters used, mechanism and reaction pathways, and catalyst stability etc. by Kiss⁶⁴. Zhou et al⁶⁵ recently reported carbonylation of allenes to methacrylates using a ruthenium carbonyl catalyst under mild operating conditions and 100% atom economy. Union Carbide

scientists⁶⁶ reported synthesis of some novel bis-chelating ligands, having biaryl rings and Rh complexes thereof for the carbonylation of alkenes very recently. Pt-complex catalyzed carbonylation of functional alkenes in the presence of bidentate ligands [e.g. 1,2-P,P'bis(9-phosphabicyclo[3.3.1]nonyl)ethane], SnCl₂, HCl etc. was recently reported by Drent et al⁶⁷.

Table 1.2: Literature report on carbonylation of olefins to acids* or esters*

Sl. No.	Catalyst system	Substrate	Reaction conditions			Conv. %	Selectivity, %		Reference
			T, K	P _{CO} , MPa	Miscellany		Iso	n	
1.	PdCl ₂ (PPh ₃) ₂ /HCl	Styrene	363	30–70	EtOH	–	65–95*	–	Bittler et al ³⁰
2.	PdPPh ₂ (CH ₂) ₄ PPh ₂ Cl ₂	Styrene	373	10–50	EtOH; 16 h	30–100	9–88*	7–65*	Sugi et al
3.	PdPPh ₂ (CH ₂) _n PPh ₂ Cl ₂ n = 1–6, 10	Styrene	398	20	EtOH-C ₆ H ₆ ; 16h	45–100	12–88*	5–67*	Sugi et al ³²
4.	PdCl ₂ +PPh ₃ /DIOP/ PPh ₂ (neomenthyl)	Styrene, $\bar{\alpha}$ -methyl styrene	373	38–72	ROH-C ₆ H ₆	–	1–100*	1–100*	Consiglio & Marchetti ⁶⁸
5.	PdCl ₂ (PPh ₃) ₂ /Ph ₂ NNO	2-vinyl-6-methoxy- naphthalene	–	–	EtOH/BF ₃ - Et ₂ O	–	69*	–	Takeda et al ⁶⁹
6.	Pd(dba) ₂ / (+)neomenthyldiphenyl Phosphine	Styrene; 2-vinyl-6- methoxy- naphthalene	293– 353	0.1–0.2	CF ₃ COOH- MeOH; 4h	–	94* (42–52% S)	6*	Cometti & Chiusoli
7.	PdCl ₂ (PPh ₃) ₂ /SnCl ₂	Pentafluoro styrene	373– 398	7–12	MeOH- Me ₂ CO; 24–60 h	9–92	22–79*	21–78*	Fuchikami et al ⁷⁰
8.	PdCl ₂ (PPh ₃) ₂ / HCl/ MCPBA	<i>p</i> -IBS	358	2–4	H ₂ O-dioxane; 6 h	–	90*	–	Mitsubishi Petrochem 71
9.	Co ₂ (CO) ₈ /pyridine	Styrene	373– 423	5	MeOH	40–100	–	25–79*	Zhigao & Zilin ⁷²
10.	Pd(II)complex/HCl	<i>p</i> -IBS	373	30	C ₆ H ₆	–	78*	–	Shimizu et al
11.	PdCl ₂ /HCl/CuCl ₂ /O ₂	<i>p</i> -Methyl styrene	RT	0.1	Dioxane; 24–95 h	–	90–92*	7*	Mlekuz et al

Table 1.2: Continued

12.	PdCl ₂	Styrene	313	0.1	MeOH/LiCl; 16-20 h	75	67*	33*	Wayner & Hartstock ⁷³
13.	PdO/HCl/PPh ₃ /ZnO	Arylethylenes	363	7.5	MeOH	93	98*	2*	Shimizu and Nomura ⁷⁴
14.	Pd(PPh ₃) ₄ or Pd(dba) ₂ /dppb	Substituted styrenes	423	8.2	48-72 h		6.6-96*	5-96*	Lin and Alper
15.	PdCl ₂ /CuCl ₂ /HCl/ BNPPA	<i>p</i> -IBS, 2-vinyl-6-methoxy naphthalene	RT	0.1	H ₂ O-THF; 18 h	–	46-89* (55-91% S)	–	Alper and Hamel
16.	PdCl ₂ (PPh ₃) ₂ / SnCl ₂	Styrene	368- 393	2	Dioxane	Kinetic and mechanistic studies			Noskov et al ⁷⁵
17.	PdCl ₂ (PPh ₃) ₂	<i>p</i> -IBS	393	30	Toluene- 10% aq. HCl	100	89*	–	Shimizu et al ⁷⁶
18.	PdCl ₂ (<i>c</i> -C ₆ H ₁₁ PPh ₂) ₂	2-vinyl-6-methoxy naphthalene	373	2-6	ROH-Me ₂ CO/ THF	73-100	64-95*	1.6-5*	Hiyama et al ⁷⁷
19.	Fe(CO) ₅ /OH ⁻	Styrene	328	0.1	H ₂ O <i>i</i> -prOH; 96h		>96*	2-3*	Brunet et al ⁷⁸
20.	Pd(OAc) ₂ /dppb/PPh ₃ / oxalic acid	Substituted styrenes	423	2	DME	35-90	12-24*	78-86*	El Ali and Alper
21.	Pd-C/dppb/PPh ₃ /formic acid or oxalic acid	Substituted styrenes	423	0.68-4	DME; 24 h	65-80	10-24*	68-90*	El Ali et al ⁷⁹
22.	PdCl ₂ /CuCl ₂ /PPh ₃ /HCl	<i>p</i> -IBS	323	3.4	H ₂ O-THF; 10 h	90-95	96*	–	Wu ^{43a,b}
23.	PdCl ₂ /CuCl ₂ /(+) <i>neomenth</i> <i>yl</i> diphenylphosphine/HCl	<i>p</i> -IBS	373	4.8	H ₂ O-THF; 10 h	100	100*	–	Wu ^{43c}
24.	(Cy ₃ P)Pd(H)(H ₂ O)]BF ₄ ⁻ /dppb/TsOH	Substituted styrenes	373	2	MeOH -THF; 48h	–	12-23*	77-88*	Huh & Alper
25.	Pd(OAc) ₂ - Montmorillonite-PPh ₃ /HCl	Substituted styrenes	398	4	MeOH-C ₆ H ₆ ; 24 h	88-100	100*	–	Lee & Alper ⁸⁰

Table 1.2: Continued

26.	Pd(OAc) ₂ /PPH ₂ CH ₂ COOH /TsOH	Styrene	403	4	EtOH; 6 h	53	7.6*	38*	Hongying et al ⁸¹
27.	Montmorillonite-diphenylphosphine PdCl ₂ /Ligand/HCl	Styrene	393	4.5	MeOH-C ₆ H ₆ ; 24 h		50–100*	2–50*	Nozaki et al ⁸²
28.	PdCl ₂ /TPPTS/TsOH	Styrene & <i>p</i> -IBS	338	5–14	H ₂ O; 6 h	62–100	56–90*	10–33*	Papadogianakis et al
29.	Pd(MeCN) ₂ (PPh ₃) ₂ (BF ₄) ₂	Styrene	303–353	0.5 to 2	MeOH; 4 h	21–94	27–83*	17–74*	Oi et al
30.	Pd(OAc) ₂ / PPh ₃ /TsOH or CF ₃ SO ₃ H	Styrene & <i>p</i> -IBS	RT–323	2	MeOH; 4 h	19–95	75–96*	4–25*	Oi et al
31.	Pd(OAc) ₂ / Chiral phosphine/TsOH	Styrene, 2-vinyl-6-MeO-naphthalene	RT	1	MeOH; 20h	17–42	31–44* (10–86 S)	40–70*	Oi et al
32.	PdCl ₂ /TPPTS/HCl, H ₂ SO ₄ or CH ₃ SO ₃ H	Substituted styrenes	373	5	Toluene - H ₂ O; 6 h	15–98	50–60*	40–50*	Tilloy et al ^{53b} Bertoux et al ⁸³
33.	[Pd(2,7-bis(SO ₃ Na)-Xanthos)]. (CH ₃ CN) _x (OTs) ₂ / TsOH	Styrene	343–368	3	H ₂ O; 3 h	-	35*	65*	Goedheijt et al ⁸⁴
34.	PdCl ₂ /CuCl ₂ /PPh ₃ / HCl	4-methylstyrene	373	4	H ₂ O-THF; 6 h	29	85*	–	Yoon et al
35.	PVP-PdCl ₂ -NiCl ₂ -PPh ₃	Styrene	353	2	MeOH – C ₆ H ₆ ; 10–36 h	79–100	91–99*	1–8*	Wan et al ⁸⁵
36.	PdCl ₂ (PhCN) ₂ / <i>p</i> -tert-butyl-calix[4]arene based phosphines/ phosphinite	Styrene	403	14	MeOH-toluene; 48–140 h	39–70	47–62*	–	Csok et al ⁸⁶
37.	PdCl ₂ -ferrocene based catalysts	Styrene	383	13	MeOH-toluene; 180–450 h	50–100	28*	–	Jedlicka et al ⁸⁷
38.	PdCl(Mebinas)(PPh ₃) or [PdCl(Mebinas)] ₂ / <i>n</i> PR ₃ /oxalic acid	Styrene	373	3	DME	25–90	74–97*	3–26*	Ruiz et al ⁸⁸

Table 1.2: Continued

39.	PdCl ₂ (PPh ₃) ₂ /SnCl ₂	Styrene, α -methyl styrene	403	4	ROH-toluene	Mechanistic studies			Benedek et al ⁸⁹
40.	Pd/ C with Bu ₃ N	3-bromo-2-(4-fluorophenyl)-2-cyclopentene-1-one	-	-	MeOH, DMA	-	-	-	Davis et al ⁹⁰
41.	Pd(OAc) ₂ /PPh ₃ /TsOH	Styrene	348	3.4	MeOH	Kinetic studies			Seayad et al
42.	Pd(OAc) ₂ /PPh ₃ /TsOH	Styrene	348	3.4	MeOH	Mechanistic studies			Seayad et al
43.	PdCl ₂ (PPh ₃) ₂ /TsOH/LiCl	Substituted styrenes	388	5.4	Methyl ethyl ketone-H ₂ O	90-100	95-99.5	-	Seayad et al ^{49,50}
44.	Pd-C/PPh ₃ /TsOH/LiCl	IBS	388	5.4	MEK	93	99.1*	0.9*	Jayasree et al
45.	Pd(pyca)(PPh ₃)(OTs)/TsOH/LiCl	Substituted styrenes	388	5.4	Methyl ethyl ketone-H ₂ O	>97%	>98.5*	1.0*	Jayasree et al
46.	RhCl ₃ / Cab-O-Sil	MeOH, Ethylene	-	-	Vap. Phase rxn,	Detailed kinetic study, for a tube reactor			Bodis ⁹¹
47.	Silica supported-Chitosan-Pd complex, Ni-Pd bimetallic cat.	6-methoxy-2-vinylnaphthalene	378	4-6	In MeOH, 10 h	<95%	90-95	-	Zhang et al ⁹²
48.	Co-Rh bimetallic nanoparticles	1,6-enynes	-	0.1	HSiR ₃ reqd. for silylation	-	-	-	Park et al ⁹³
49.	Pd/[BMIm] [BF ₄],	Aminocarbonylation of 17-iodo-5 α -androst-16-ene	-	0.1	Efficient recycles	94	-	-	Skoda-Foeldes et al ⁹⁴

1.2.2 Carbonylation of Alcohols

One of the best examples of the applications of the carbonylation reaction that has been implemented commercially is the carbonylation of alcohols. This application of organo-transition-metal complex catalysis has drawn immense research attention since the advent of carbonylation technology. Of the different alcohols carbonylated, the carbonylation of 1-aryl alcohols was viewed with special interest, as it was a proposed alternative catalytic route to 2-aryl propionic acids. The transition metal complexes of Co, Rh, Ir, Pd, and Pt etc. have been extensively used for this reaction. A detailed discussion is as follows.

Carbonylation of 1-aryl alcohols is an important topic considering the commercial interest associated with the 2-arylpropionic acids – a class of non-steroidal anti-inflammatory drugs. The synthesis of ibuprofen by catalytic carbonylation of 1-(4-isobutylphenyl)ethanol (IBPE)⁹⁵ had been a trendsetter in the use of organometallic catalysis by Hoechst-Celanese Corporation in developing an atom efficient alternative to stoichiometric synthesis. A biphasic catalyst system consisting of $\text{PdCl}_2(\text{PPh}_3)_2$ in methyl ethyl ketone and 10% aqueous HCl solution as promoter under 5-35 MPa pressure and 403K was used in this process. Allied reports earlier illustrated that the reaction gave low selectivity to the desired branched product (~ 69%) and lower activity (TOF ~ 45 h^{-1}) under moderate pressures (6 – 8 MPa).⁹⁶ The pressure-dependent variation of selectivity was observed, but the activity varied nominally with pressure. However, the variation of substrate/Pd ratio in the region of 15,000 to 30,000 under 10–16 MPa pressure showed a higher reaction rate (TOF ~75–125 h^{-1}).⁹⁷ The catalyst could be separated from the organic phase by the use of non-coordinating solvent.⁹⁸ Besides palladium complexes, several other metal complexes such as Rh-⁹⁹ and Ni-¹⁰⁰ complexes were also tested for this reaction. Few years later, further improvements were reported by Jang et al¹⁰¹, whereby $\text{PdCl}_2/\text{PPh}_3$ was used as the catalyst working at 6.8 MPa and 403K in presence of CuCl_2 and acidic promoters HCl/ H_2SO_4 respectively, for the ibuprofen synthesis from IBPE. This system gave nearly 90% selectivity to ibuprofen but also with lower reaction rates (TOF ~ 25 h^{-1}). Naproxen synthesis using similar catalyst system was demonstrated at 6 MPa and 373K via hydroesterification of 1-(6-methoxy-2-naphthyl)ethanol using TsOH as acid promoter.¹⁰² Nearly 100% regioselectivity to naproxen was reported at TsOH/Pd ratio of 13.1:1 but with low TOF (~ 2.1 h^{-1}) with this system. $\text{PdCl}_2(\text{PPh}_3)_2$ complex was

reported to be a highly active catalyst for the synthesis of 2-arylpropionic acids, along with TsOH and LiCl as promoters via carbonylation of 1-arylethanol by Seayad et al¹⁰³. Mild reaction conditions (388K and 5.4 MPa) were required for this catalyst system, and very high activity (TOF ~ 1200 h⁻¹) and regioselectivity (> 95%) were reported for the carbonylation of IBPE to ibuprofen. Recently, by the use of cationic palladium complexes having hemilabile chelating ligands, efficient carbonylation of aryl alcohols were reported by Jayasree et al. Typically, using the Pd(pyca)(PPh₃)(OTs) complex, very high TOF (~ 804 h⁻¹) were obtained for IBPE carbonylation to ibuprofen, working under milder operating conditions of 388K and 5.4 MPa. The issues like catalyst-product separation and recyclability, for these reactions are discussed in a later section. Biphasic carbonylation of IBPE using water soluble Pd(TPPTS)₃ complex in the presence of acidic and halide promoters were reported by Sheldon et al¹⁰⁴. In these reports, ibuprofen selectivity of 52–62% was observed at 5 MPa and 363K, but increasing the pressure to ~ 10–15 MPa, 89% regioselectivity was obtained with poor TOF of ~3 h⁻¹. Another heterogeneous catalyst system was reported by Jang et al¹⁰⁵, where a supported Pd catalyst in presence of phosphine ligands and HCl as promoter were used at 4 MPa and 398K. The ibuprofen selectivity obtained was 20–77% and it further increased to 97% if a silyl ligand was used along with montmorillonite as catalyst support. A supported Pd-catalyst for the carbonylation of alcohols was reported by Jayasree et al⁵⁶ as discussed before. This catalyst efficiently converted IBPE and 1-(6-methoxy-2-naphthyl)ethanol to the desired 2-arylpropionic acids respectively. Recently, reports by Xia et al¹⁰⁶ illustrated the synthesis of α -arylpropionic acids by the carbonylation of α -aryl alcohols, by Pd-catalyzed reaction in presence of PAr₃ ligand (Ar = Phenyl, Naphthyl). The catalyst comprised of PdCl₂-PVP and Fe/ Ni/ Cu-halides etc. in acidic medium, reacting at 80–120°C, 3–6 MPa for 12–28h and produced good yields. The salts of cationic metal complexes such as [Pd(CO)₄][Sb₂F₁₁]₂, [Pt(CO)₄][Sb₂F₁₁]₂ etc. were found to promote the carbonylation of alcohols catalyzed by [Cu(CO)_n]⁺.¹⁰⁷ Tsai et al¹⁰⁸ described Rh-based catalyst system for the carbonylation of different aryl alcohols, where an acid or ester was produced in the presence of a hydrohalic acid promoter and water (optionally). The brief description of the different catalysts used for the different substrates is presented in the Table 1.3.

Table 1.3: Literature report on carbonylation of alcohols to acids* or esters*

Sl. No.	Catalyst system	Substrate	Reaction conditions			Conv. %	Selectivity, %		Reference
			T, K	P _{CO} MPa	Miscellaneous		iso	n	
1.	RhX ₂ /I ₂	IBPE	403–453	3–6	H ₂ O-Dioxane	–	86	14	Tanaka et al
2.	PdCl ₂ (PPh ₃) ₂	IBPE	373–473	3.4–30	Aq. HCl-MEK	90–100	40–100*	10–60*	Elango et al ^{20,96}
3.	PdCl ₂ (PPh ₃) ₂	IBPCI, 1-(6-methoxy-2-naphthyl)ethyl chloride	373–473	3.4–30	Aq. HCl AcPh-MEK	99	25–72*		Elango
4.	PdCl ₂ (PPh ₃) ₂	IBPE	373–473	3.4–30	Aq. HCl-MEK	Catalyst recovery studies			Mott et al
5.	Ni-complex/PR ₃ /I ₂	IBPE	443	10	AcPh; 2 h	90–99	79–82*	–	Tanaka & Shima
6.	PdCl ₂ (PPh ₃) ₂	IBPE		3.4–30	Aq. HCl-MEK		-		Hendricks & Mott ^{96b}
7.	PdCl ₂ /TPPTS/TsOH	IBPE	363	3	De-aerated water; 20 h	49	62*	38*	Sheldon et al ^{104a} Papadagianakis et al ^{104b}
8.	PdCl ₂ /CuCl ₂ /PPh ₃ /TsOH	1-(6-methoxy-2-naphthyl)ethanol	373	6	MeOH-Dioxane; 24 h	96–100	67–100	0–16	Zhou et al
9.	PdCl ₂ /CuCl ₂ /chiral phosphine (DDPPI)	1-(6-methoxy-2-naphthyl)ethanol	373	8	MEK; 24-48h	–	90 ^b (S-81% ee)	–	Xie et al ¹⁰⁹
10.	PdCl ₂ /PPh ₃ /CuCl ₂ /H ₂ SO ₄ /HCl	IBPE	398	5	3-pentanone/MEK; 13 h	97–100	66–98*	0–7*	Jang et al

Table 1.3: Continued

11.	Pd-Montmorillonite /PPh ₃ /HCl	IBPE	398	4	3-pentanone; 13 h	90-99	59-96	1–5	Jang et al
12.	PdCl ₂ (PPh ₃) ₂ /TsOH/LiCl	1-arylethanol	388	5.4	In MEK-H ₂ O, 0.75 h	95-100	> 95	<5	Seayad et al
13.	PdCl ₂ (PPh ₃) ₂ /TsOH/LiCl	1-arylethanol	388	5.4	In MEK-H ₂ O, 0.75 h	Kinetic modeling			Seayad et al
14.	Pd-C/PPh ₃ /TsOH/LiCl	1-arylethanol	388	5.4	MEK	96	99.2*	0.8*	Jayasree et al
15.	Pd(pyca)(PPh ₃)(OTs)/TsOH/LiCl	1-arylethanol	388	5.4	MEK-H ₂ O	>97%	>98.5*	1.0*	Jayasree et al
16.	Rh-catalyst/RI	Aryl alcohols	-	-	in presence of H ₂ O-HX/ NR ₃	-	-	-	Tsai et al
17.	Nafion-H	ROH	433	9	In C ₆ H ₁₂ , DCM	79.6	-	-	Tsumori et al ¹¹⁰
18.	Pd(II)/ 2-PyPPh ₂ / [BMIm] [BF ₄], or [BMIm] [PF ₆]	Terminal alkynols	-	-	γ,δ-lactones formed	-	-	-	Consorti et al ¹¹¹
19.	PdCl ₂ -CuCl ₂ / Charcoal	EtOH	-	-	DEC formed	10	-	-	Dunn et al ¹¹²
20.	Cu+X zeolite	MeOH	373-513	0.1	DMC formed	Kinetic studies			Anderson et al ¹¹³
21.	Group VIII metals/ NAILs	MeOH	573	-	MeI promoter added	Gas phase formation of AcOH, in presence of a halide			Charles et al ¹¹⁴
22.	Mo/ γ-Al ₂ O ₃ or SiO ₂ or C, Sulphided Mo/ C	MeOH	-	-	-	50	80	-	Peng ¹¹⁵
23.	RhCl ₃ · 3H ₂ O in [BMIm][CF ₃ SO ₃]	Alcohol/ MeOH	-	-	-	Efficient recycle of catalyst performed			Magna et al ¹¹⁶
24.	CuCl on diamide functionalized SBA 15	MeOH	-	-	-	Dimethyl carbonate is formed as major pdt			Cao et al ¹¹⁷
25.	PdCl ₂ -CuCl ₂ –HMS Or other mesoporous matrices	MeOH	-	0.1	Flow reactor	DMC formed			Yang et al ¹¹⁸

Table 1.3: Continued

26.	Pd/ Gr VIII -porous C beads	MeOH	-	-	Vap. Phase;	-	-	-	Li et al ¹¹⁹
27.	Gr. VIII-carbonaceous Matrix	CH ₄ , MeOH	-	-	Temperature Programmed. pulse rxn.	-	-	-	Song et al ¹²⁰
28.	Ir & Sn on different solid supports	Lower ROH	-	-	Gas phase rxn	Esters & ester deriv. Formed			Zoeller et al ¹²¹
29.	H-ZSM 5 catalysts	t-BuOH	-	-	No deactivation after 120 h	80	Koch type rxn.		Tao et al ¹²²
30.	Au-C or SiO ₂ , Al ₂ O ₃ , MgO, TiO ₂ , clay, ceramics	Lower ROH, ROR', RCOOR'	-	-	Halide promoter added	Screening test rxns.			Zoeller et al ¹²³
31.	Pd/ Charcoal	Aryl iodides + aliph. ROH or PhOH	513	1.0		Polycondensation pdts obtained			Yoshihiro et al ¹²⁴
32.	Rh dispersed on nanoporous C	MeOH	-	-	New process for nano C prep.	AcOH formed			Li et al ¹²⁵
33.	CuCl ₂ -APTS-MCM41 or MCM48	MeOH	-	-	Vap. Phase rxn.	DMC formed in good selectivity			Cao et al ¹²⁶

1.2.3 Kinetics of Carbonylation Reactions

Kinetics of carbonylation reactions is important in providing in-depth knowledge of the interdependence of the various reaction parameters and also some insight into the reaction mechanism. Noskov and co-workers¹²⁷ have reported the kinetics of hydrocarboxylation of styrene using $\text{PdCl}_2(\text{PPh}_3)_2$ as a catalyst precursor system. They studied the mechanism of reaction, based on which, they developed rate models to explain the effect of different reaction parameters on the rates of formation of branched as well as linear acid isomers. It was observed that the rate of formation of the linear isomer had only a slight dependence on P_{CO} , whereas the order for formation of the branched isomer with respect to P_{CO} was nearly two.¹²⁸ However, both rates were increased as concentration of water increased upto 2 mol/L, above which the rate of formation of the linear isomer became virtually constant while that of the branched isomer decreased. Rate equations were proposed for the formation of individual isomers.

Ercoli et al¹²⁹ have reported the kinetics of carbonylation of cyclohexene using dicobalt octacarbonyl $[\text{Co}_2(\text{CO})_8]$ as the catalyst precursor. The rate was found to be proportional the concentration of water and half power of olefin concentration. At lower pressures (<21 MPa), the rate was directly proportional to the carbon monoxide pressure and decreased proportionately becoming inversely proportional above 34 MPa. Takezaki et al¹³⁰ have also reported a kinetic study on the hydroesterification of cyclohexene using of $\text{PdCl}_2/\text{PPh}_3$ as a catalyst. A first order dependence with respect to concentration of cyclohexene and zero order dependence with methanol were observed and empirical rate equation was proposed. No other detailed kinetic study was found in the literature for the kinetics of this important class of reaction.

The kinetic modeling of the carbonylation of 1-(4-isobutylphenyl)ethanol, [IBPE] was illustrated by Seayad et al¹³¹ using a $\text{PdCl}_2(\text{PPh}_3)_2/\text{TsOH}/\text{LiCl}$ catalyst system. They illustrated that the reaction followed in three steps and the actual active substrate was the halide derivative of the alcohol. The effect of the various reaction parameters, such as the CO partial pressure, temperature, substrate concentrations, catalyst loading, etc. on the rate of the reaction were studied over a temperature range of 378–398 K. An empirical semi-batch reactor model was also derived and the kinetic parameters were evaluated.

1.3 Suzuki Cross Coupling Reactions

The C-C bond formation is another important class of reactions emphasizing the importance of catalysis for the development of alternate route to classical multi-step stoichiometric organic syntheses. Among the different C-C bond formation reactions

Scheme 1.3: Suzuki Cross Coupling



involving two-component coupling, such as Heck, Stille, Sonogashira etc. Suzuki cross-coupling reaction is a very important and unique one. This involves coupling of an aryl/ vinyl halide and an aryl/ alkyl boronic acid leading to a variety of multi-functionalized biaryls, aryl-alkyl compounds etc. that are otherwise difficult to arrive synthetically. The relevant literature on this reaction is presented below:

1.3.1 Homogeneous Catalysts for Suzuki Coupling

Starting with the initial works of Miyaura and Suzuki¹³², where the regio- and stereo-selective formation of conjugated alkadienes and alkenynes were reported by the Pd-catalyzed cross-coupling of 1-alkenylboranes with bromoalkenes and bromoalkynes, this reaction has traveled a long way to its present day versatility in applications using a spectrum of functionalized compounds with unprecedented efficiency. Miyaura and Suzuki optimized a Pd(PPh₃)₄/ base (2 molar equiv.) catalyst system after trying out different combinations in different solvents. They also proposed a mechanism involving a transmetalation between 1-alkenylborane and an alkoypalladium(II) complex generated through the metathetical displacement of a halogen atom from RPd^{II}X with Na-alkoxide. Following Suzuki and coworkers, Soderquist et al¹³³ investigated formation of the substituted styrenes and 1,3-dienes via coupling route. The gradual development of the subject evolved into a wide spectrum of application areas using different palladium complex catalyst systems. A thorough literature survey of the different homogeneous metal complex catalyst systems for Suzuki coupling reactions has been presented in Table 1.4. Among the huge literature involving the palladium complex catalyst systems, a few examples of prime importance

are discussed as follows. Water-soluble Pd⁰ complexes were reported to be used for the synthesis of functionalized dienes via the coupling route by Genet et al¹³⁵, where organic bases were used to obtain 60-90% conversion of the substrate. Ligand-free Pd(OAc)₂ catalyst was used in the presence of tetrabutylammonium bromide, TBAB in aqueous medium without any organic co-solvent for the coupling reactions. Several attempts were made to use Pd⁰ complexes for the coupling reactions, but most of them had poor activity towards the coupling. Zakharin et al reported Pd(PPh₃)₄ complex, while Pd₂(dba)₃ was used as catalyst as well as catalyst precursor by several groups, e.g. Old et al, Bei et al, however the later got ~90 % conversion and 83-97 % selectivity to the desired product in the coupling of aryl chlorides. The reaction time was however very high. Use of Pd(PPh₃)₄ was reported by Haddach et al for the synthesis of ketones by coupling in presence of 5 eqv. of Cs₂CO₃ under anhydrous conditions. Allylpalladium complexes were used as catalysts for efficient C-C coupling in presence of refluxing xylene and K₂CO₃, whereby >95 % conversion was obtained in 1 h with a selectivity of >99% for the desired product, as reported by Tinkl et al. however the detailed information about the system is not presented in the patent. Pd^{II}-heterocyclic carbene complexes were used to obtain very high conversion (TON~1,27,500) as reported by McGuinness et al and following that, several other groups used heterocyclic carbenes as catalysts to obtain high activity (TOF~552 h⁻¹) for coupling of aryl chlorides. Insitu generated Pd-phosphite complexes were reported of exhibiting very high TONs (~8,20,000) for coupling aryl bromides, while phosphine free trifluoroacetyl cyclometallated imine complex of Pd was reported to give TON ~ 1,00,000 for coupling of bromides, but for most of the cases, the reaction time was quite high generating very low TOFs and hence the search was sustained for more better active catalyst. Bis(Octaethyldiphosphaferrocene) complex of Pd⁰ was reported by Sava et al for the coupling of bromides in refluxing toluene with a 98% conversion and a TON of 9,80,000. Oxime palladacycles were reported for the first time as efficient catalysts for Suzuki coupling by Alonso et al, who demonstrated very high activity for bromide and chlorides' coupling (TOF_{ArBr} 98,000 h⁻¹ and TOF_{ArCl} 4700 h⁻¹) under aerobic conditions. The bulky tetraphosphine ligands along with Pd^{II} precursor were also tried for obtaining high activity for the sterically hindered aryl bromides yielding TON of 97×10⁶ as reported by Feuerstein et al. Recently, Bedford et al reported very high TONs nearing 1,000,000 for the coupling of aryl chlorides using the mixed Pd-

complexes of tricyclohexylphosphane-triarylphosphite as catalysts and Cs_2CO_3 as base. Room temperature activation of the aryl halides, typically aryl bromides and aryl chlorides, is another direction of catalyst development, in which different groups of researchers made significant contributions. Oxime-derived palladacycles in presence of TBAB were reported as efficient catalysts for room temperature activation of aryl chlorides giving TON of ~9000 using aqueous methanol as solvent, by Botella et al. The use of DABCO in addition to $\text{Pd}(\text{OAc})_2$ in polyethylene glycol (PEG-400) as solvent, was reported by Li et al as a separable homogeneous catalyst yielding a TON of 950,000 for all types of aryl halides. This was another landmark development in the homogeneous Suzuki coupling catalysis. More later, Buchwald et al published a paper where they had used a novel ligand, XPhos for the coupling aryl halides that are generally hindered showing >96% conversion. Very recently, the successful coupling of the deactivated aryl chlorides were reported by using $\text{Pd}(\text{OAc})_2/1,3$ -dialkylbenzimidazoliumchloride as catalyst in the presence of Cs_2CO_3 as base, with a 100% selectivity to the desired product. Further increment in the performance of the catalyst by enhancement in the coupling rates and improving the selectivity, was visualized by the use of non-conventional sources of energy. Microwave assisted coupling reactions were reported by many research groups showing quantum leaps in activity and having good selectivity. Early reports of microwave assisted Suzuki coupling was disclosed by Larhed et al, who used the microwave radiation to enhance the rates in presence of Pd-complexes. The reactions took only 2.5 to 7 minutes to complete. Later on Leadbeater et al described ligand-free Pd-catalysts at extremely low loading for use under microwave irradiation at 423K in presence of Na_2CO_3 as the base. The reactions got over in 5-7 minutes showing excellent activity and selectivity. Activation of the aryl chlorides using microwave irradiation was reported by Whittall et al, requiring 30 h to completion working at 333K, and showing 100% selectivity to the desired product. In summary, the developments of homogeneous catalysts for Suzuki coupling reactions were focused on - new catalyst systems for better activity and selectivity, activation of hindered substrates (such as chlorides) and lowering the reaction conditions. However issues like separation of the catalyst and practical reuse are still pertinent issues and hence scope for development heterogeneous catalyst is still challenging.

Table 1.4: Literature reports on homogeneous Suzuki cross-coupling catalyst systems

Sl. No.	Catalyst system	Applied for	Reaction conditions			Conv., %	Sel., %		Reference
			Base	Solvent	Time		Desired	Others	
1.	Pd(PPh ₃) ₄ / PdCl ₂ (PPh ₃) ₂	Syntheses of alkadienes & alkenynes	NaOH/ NaOR - ROH	THF/ C ₆ H ₆	2-6 h	30-90	25-86	0-4	Miyaura et al
2.	Pd(PPh ₃) ₄ complex	Methylation and Synthesis of dienes & substituted Z-styrenes	NaOH	H ₂ O-THF	-	90	88	-	Soderquist et al
3.	Pd(PPh ₃) ₄ complex	Mechanism elucidation by electrospray MS analysis	-	-	-	-	-	-	Aliprantis et al ¹³⁴
4.	Water soluble Pd ⁰ - catalyst	Synthesis of functionalized dienes	Organic bases	H ₂ O		60-90			Genet et al ¹³⁵
5.	Pd(dba) _n , [n = 1.5 – 2]	Synthesis of 1,3-diarylpropenes	Suspended K ₂ CO ₃	C ₆ H ₆					Moreno-Manas et al ¹³⁶
6.	Ni ⁰ catalyst, formed <i>insitu</i> from NiCl ₂ (dppf) & Zn	Homo- and cross-coupling reactions	K ₃ PO ₄						Percec et al ¹³⁷
7.		Unsymmetrical biaryl coupling	Aqueous Ti(OH) ₃	DMAC, r.t.					Anderson et al ¹³⁸
8.	Pd-complexes	Use of MW irradiation as rate enhancer			2.5-7.0 mins.				Larhed et al ¹³⁹
9.	Ligand-free Pd(OAc) ₂	Coupling in presence of TBAB but without organic co-solvent		H ₂ O					Badone et al ¹⁴⁰
10.	**Cl ₂ (dppf)	Heteroarylation of anthraquinone-triflates in the presence of a O ₂ -scavenger	Anhy. K ₃ PO ₄	Anaerobic conditions					Coudret et al ¹⁴¹
11.	Ni-complexes especially NiCl ₂ (dppf)	Coupling of chloroarenes	K ₃ PO ₄	Dioxane, 95°C					Indolese ¹⁴²
12.	Pd-complexes using P(Cy) ₃ or dppp ligands	Coupling of chloroarenes				94.0			Shen ¹⁴³

Table 1.4: Continued

13.	Pd-complexes	D-labeling experiments to establish retention of configuration during trans-metalation step							Ridgway et al ¹⁴⁴
14.	Pd-catalysts	Synthesis of heterocycles via 2-nitrobiphenyls							Holzappel et al ¹⁴⁵
15.	Pd-catalysts	Study of base & cation effects on coupling of bulky boronic acids	KOBu ^t	DME					Zhang et al ¹⁴⁶
16.	Ligand-free Pd catalysts	Coupling of Na-tetraphenylborates & Ar-X	Na ₂ CO ₃ / NaOH	H ₂ O					Bumagin et al ¹⁴⁷
17.	Pd ₂ (dba) ₃ / Pd(OAc) ₂ & ligands	coupling of Ar-Br & ArCl with boronic acids		Room temp.					Old et al. ¹⁴⁸
18.	Pd-(dba) ₂ / Ph-backbone derived P,O- ligands	Coupling of aryl chlorides							Bei et al ¹⁴⁹
19.	Pd ⁰ and Ni ⁰ complexes of heterocyclic carbenes	Synthesis of biaryls via with full characterization		Organic solvents					McGuinness et al ¹⁵⁰
20.	Pd(PPh ₃) ₄ complex	Coupling of carboranes with phenyl boric acid	Na ₂ CO ₃ / NaOH	THF					Zakharin et al ¹⁵¹
21.	Pd-carbene complexes e.g. Pd(NHC)(PR ₃) ₂	Activation of all aryl halides							Wedkamp et al ¹⁵²
22.	Pd/ 2- <i>t</i> -Butyl phosphane based ligands	Tailored the C-C coupling reactions							Wolfe et al ¹⁵³
23.	Novel Pd-complexes	Ullmann-type reductive coupling of aryl halides		Aqueous acetone					Venkatraman et al ¹⁵⁴
24.	Pd(dba) ₂ / ligand	Coupling of aryl chlorides				~ 90	83-97		Bei et al ¹⁵⁵
25.	Pd/ imidazole-2-ylidene complexes	Activation of chloroarenes							Zhang et al ¹⁵⁶
26.	Dimeric Pd- complex <i>o</i> -metalated Ar ₃ -phosphite	C-C coupling reactions							Albisson et al ¹⁵⁷
27.	Pd(PPh ₃) ₄ – anhydrous conditions	Synthesis of ketones by coupling of acid-chlorides	Cs ₂ CO ₃ (5 eqv.)			60-70			Haddach et al ¹⁵⁸

Table 1.4: Continued

28.	Allylpalladium complexes	C-C coupling reactions	K ₂ CO ₃	Xylene, reflux	~ 1 h	> 95	>99	Tinkl et al ¹⁵⁹
29.	PdCl ₂ [Ph ₂ P(CH ₂) ₄ SO ₃ Na] - CTAB	Surfactant assisted enhanced coupling		H ₂ O/ EtOH/ PhMe		< 99	99	Oehme et al ¹⁶⁰
30.	Pd ^{II} – heterocyclic carbene complexes	Highly efficient coupling				TON ~ 1,27,500		McGuinness et al ¹⁶¹
31.	Pd(OAc) ₂ / <i>o,o'</i> -bis-(<i>t</i> -Bu ₂ P)biphenyl etc.	Coupling of arylchlorides						Wolfe et al ¹⁶²
32.	Pd ₂ (dba) ₃ / Ligands	Coupling of various substituted aryl halides	NaOBu ^t / CsF	PhMe		~ 95		Guram et al ¹⁶³
33.	Pd ₂ (dba) ₃ or Pd(OAc) ₂ with P(<i>t</i> -Bu) ₃ or PCy ₃ etc.	Coupling of Ar-X, Ar-OTf & mechanistic insights		Room temp.				Littke et al ¹⁶⁴
34.	Pd ^{II} -complexes	Coupling of halophenyl-guanidines to phosphines						Machinitzki et al ¹⁶⁵
35.	Pd-(Bu ^t -thioether) & PdCl ₂ (SEt ₂) ₂	Coupling reactions involving Ar-Br & Ar-Cl		Room temp.				Zim et al ¹⁶⁶
36.	<i>In situ</i> generated Pd-phosphite complexes	Coupling of Ar-Br				TON ~ 8,20,000		Zapf et al ¹⁶⁷
37.	Pd ⁰ -heterocyclic carbene complexes	Coupling of chloroarenes		Dioxane,		TOF~552 h ⁻¹		Bohm et al ¹⁶⁸
38.	Pd ^{II} & Ni complexes of biphenyl-2-yl-phosphines	Different C-C coupling reactions		THF		93		Haber et al ¹⁶⁹
39.	(CF ₃ CO ₂) ₂ Pd-cyclo-metallated Imine complex	Phosphine-free coupling of Ar-Br				TON > 10 ⁵		Weissman et al ¹⁷⁰
40.		Coupling of cyclopropyl boronic acids	Ag ₂ O & KOH					Chen et al ¹⁷¹
41.	Pd-complexes	Coupling of β-(perfluoroalkyl)ethyl iodides & boronic acids	NaHCO ₃	H ₂ O –DME		High		Yang et al ¹⁷²
42.	NiCl ₂ (NEt ₃) ₂ or NiCl ₂ (bipy) complexes	Phosphine free coupling of aryl halides						Leadbeater et al ¹⁷³
43.	NiCl ₂ (PCy ₃) ₂ / PCy ₃	Coupling of aryl tosylates with arylboronic acids	K ₃ PO ₄	Dioxane, 130°C		~ 94		Zim et al ¹⁷⁴

Table 1.4: Continued

44.	Bis(Octaethylidiphosphaferrrocene)Pd ⁰ complex	Coupling using bromoarenes		PhMe, reflux		TON~ 9,80,000	98	Sava et al ¹⁷⁵
45.	Pd ^{II} -carbene complexes	C-C coupling reactions				TON ~ 1,77,500		Magill et al ¹⁷⁶
46.	Oxopalladacycles	Coupling in presence of hydroquinone	Na ₂ CO ₃	NMP			99	Munoz et al ¹⁷⁷
47.	Pd ₂ (dba) ₃ & chiral binaphthyl ligands	Synthesis of axially chiral biaryl compounds/ chiral ligand synthesis				86	86 ee	Yin et al ¹⁷⁸
48.	Aq. sol. Pd-bulky alkylphosphine complex	Coupling of aryl bromides				TON ~ 7,34,000		Shaughnessey et al ¹⁷⁹
49.	Pd-[bis(oxazoliny)pyrrole] complex	Coupling of activated & non-activated Ar-Br		70°C		TON ~ 1,00,000		Mazet et al ¹⁸⁰
50.	Pd ⁰ – monophosphine/ 1,6-diene complexes	Coupling of chloroarenes						Andreu et al ¹⁸¹
51.	Pd(PPh ₃) ₄ complex	Coupling of substituted alkenyl triflates & cyclopropyl boronic acids	Cs ₂ CO ₃ or K ₃ PO ₄				83	Yao et al ¹⁸²
52.	Pd(OAc) ₂ /imidazolium ion	Coupling of chloroarenes	KOMe					Fustner et al ¹⁸³
53.	Pd(OAc) ₂ / di-adamentyl-n-butylphosphane	Coupling of chloroarenes						Zapf et al ¹⁸⁴
54.	Pd ^{II} / Pd ⁰ complexes of substd. imidazolium salts	Coupling of halo-arenes	Cs ₂ CO ₃	Dioxane, 80°C			99	Grasa et al ¹⁸⁵
55.	NiCl ₂ dppf complex	Coupling using Ar-Cl	K ₃ PO ₄			80		Indolese et al ¹⁸⁶
56.	Pd-piperazine complexes	Coupling of chloroarenes		PhMe		100		Clarke et al ¹⁸⁷
57.	Pd-catalyst/ Aliquat 336	Low temperature coupling of aryl halides		DME/ PhMe				Castanet et al ¹⁸⁸
58.	<i>In situ</i> generated Pd(PPh ₃) ₂ X ₂ in IL media	Coupling of aryl halides		[bmim][BF ₄] room temp.				Smith et al ¹⁸⁹
59.								

Table 1.4: Continued

60.										
61.	Oxime palladacycles	Coupling of aryl bromides and chlorides		Aerobic conditions					TOF _(ArBr) ~ 98,000h ⁻¹ , TOF _(ArCl) ~ 4,700h ⁻¹	Alonso et al ¹⁹⁰
62.	Pd(OAc) ₂ / 2-aryl-2-oxazoline	Coupling of aryl bromides								Tao et al ¹⁹¹
63.	Pd ⁰ – TPPTS complex	Coupling of Bromoarenes		H ₂ O						Dupuis et al ¹⁹²
64.	Pt-complexes/ N-donating o-metallated Pd complex	Coupling of PhB(OH) ₂ & 4-BrPhCOCH ₃ , others	K ₃ PO ₄	Dioxane,				100		Bedford et al ¹⁹³
65.	PdCl(C ₃ H ₅) ₂ /bulky tetraphosphine ligand	Coupling of sterically hindered aryl bromides						TON ~ 97 x 10 ⁶		Feuerstein et al ¹⁹⁴
66.	Ligand-free Pd complex or PdCl ₂ (dppf)/ CH ₂ Cl ₂	Aerobic coupling of aryltrifluoroborates	K ₂ CO ₃ / Cs ₂ CO ₃	MeOH or THF/ H ₂ O						Molander et al ¹⁹⁵
67.	Pd-catalysts/ triaryl phosphines	Reactions of activated/ de-activated substrates								Liu et al ¹⁹⁶
68.	Ligand-free Pd-catalysts	MW assisted coupling using very low Pd-loading	Na ₂ CO ₃ / Bu ⁿ ₄ NBr	H ₂ O, 150°C	5-10 min					Leadbeater et al ¹⁹⁷
69.	Ni, Pd or Pt – diene phosphine catalysts	Coupling of all types of Ar-X in a sealed tube	K ₃ PO ₄	THF, 100°C	~ 22 h			~ 97		Beller et al ¹⁹⁸
70.	Pd- complexes of fluororous dialkyl sulfides	Coupling of aryl bromides with boronic acids	K ₃ PO ₄	CF ₃ C ₆ F ₁₁ / DMF/ H ₂ O, r.t						Rocoboy et al ¹⁹⁹
71.	Pd-catalysts & Cu ₂ O co-catalysts	Use of cheap & less toxic Cu as co-catalysts								Liu et al ²⁰⁰
72.	Pd(imidazolium)(carbene) complex	Coupling of different types of substrates		0°C to r.t.	2-4 h			80-90		Andrus et al ²⁰¹
73.	Pd ^{II} / Re-complexes with P-donor ligands	Coupling reactions using various substrates	K ₃ PO ₄	PhMe, 60 – 100 °C						Eichenseher et al ²⁰²
74.	Pd(dba) ₂ .CHCl ₃ / R-BINAP	Coupling route to cyclic compounds	Ba(OH) ₂	Dioxane/ H ₂ O (9:1)				40 % ee		Herrbach et al ²⁰³

Table 1.4: Continued

75.	Pd complexes of mixed tricyclohexylphosphane-triarylphosphite	Coupling of aryl chlorides	Cs ₂ CO ₃			TON ~ 1,000,000			Bedford et al ²⁰⁴
76.	Pd ₂ (dba) ₃ -phosphadamentane based ligand	Reactions involving all the halides		Room temp.					Adjabeng et al ²⁰⁵
77.	Oxime derived palladacycles/ TBAB	Coupling of aryl bromides and chlorides		H ₂ O reflux/ aq. MeOH at r.t.		TONs ~ 10 ⁵ (Ar-Br); 9000(Ar-Cl)			Botella et al ²⁰⁶
78.	Pd-phosphine system	Carbonylative cross-coupling reactions				80-95			Couve-Bonnaire et al ²⁰⁷
79.	Pd(OAc) ₂ / aq. TBAB	Simple coupling reactions	K ₃ PO ₄	H ₂ O		65	3		Bedford et al ²⁰⁸
80.	PdCl ₂ / Diphosphane ligand	Different coupling reactions	aq. NaOH 3(M)	THF-H ₂ O (5:1), 65°C	~16 h	> 99	100	-	Hong et al ²⁰⁹
81.	Pd/ NCP-pincer palladacycle	Coupling involving Ar-Cl, e ⁻ -rich/ e ⁻ -poor							Rosa et al ²¹⁰
82.	Pd ⁰ -Iminophosphine complex	Syntheses of corroles		110°C	~ 2 h	TON ~ 200,000			Scivanti et al ²¹¹
83.	Pd-glucosamine based phosphine complex	Coupling reactions involving all halides				TON ~ 97,000			Kolodziuk et al ²¹²
84.	Phosphine-free Pd(OAc) ₂ in boiling H ₂ O	Coupling of quinoline derivatives		H ₂ O		98	78-98	12-2	Friesen et al ²¹³
85.	Ligand-free PdCl ₂	Coupling of Ar-Br	K ₂ CO ₃	Pyridine			>90		Tao et al ²¹⁴
86.	Pd(OAc) ₂ – DABCO	Coupling of most Ar-X, recyclable catalyst		PEG-400		TON ~ 950,000			Li et al ²¹⁵
87.	Pd-benzamide derived P,O-ligand	Coupling of sterically hindered substrates		80-110°C					Dai et al ²¹⁶
88.	Pd ₂ (dba) ₃ / (XPhos) i.e. 2-Me ₂ NC ₆ H ₄ C ₆ H ₄ PCy ₃	Reaction of all types of halides	NaOBu ^t	PhMe, 80°C		96			Buchwald et al ²¹⁷
89.	Re complex of P-donor ligands	Ar-Br coupling	K ₃ PO ₄	PhMe, 60-100°C		TON ~ 1000			Eichenseher et al ²¹⁸
90.	Pd(OAc) ₂ / bulky NHC ligand	Cl-arene coupling	K ₃ PO ₄	PhMe, 100°C	16 h		96		Altenhoff et al ²¹⁹

Table 1.4: Continued

91.	<i>In situ</i> formed Pd-bulky thiourea complexes	Coupling of PhI	K ₂ CO ₃	<i>i</i> -PrOH/ H ₂ O, 80°C	5 h		97	Dai et al ²²⁰
92.	Pd-Dialkylphosphino-imidazole complex	Coupling reaction of Ar-Cl				TON ~ 1900 to 8500	85- 99	Harkal et al ²²¹
93.	Pd/dibutyl ¹ (ferrocenylmethyl)phosphine complex	Coupling of Ar-Br		100°C				Sliger et al ²²²
94.	Planar chiral Pd-complex of ferrocenylphosphine	MW assisted coupling involving Ar-Cl		60°C	30 h		100	Whittall et al ²²³
95.	Pd(OAc) ₂ /1,3-dialkyl benzimidazolium chloride	Reaction of deactivated Ar-Cl	Cs ₂ CO ₃				100	Oezdemir et al ²²⁴
96.	Pd-Chugaev carbene complex	Coupling involving functionalized Ar-Br in air				99		Moncada et al ²²⁵
97.	PCy ₃ adducts of cyclopalladated ferrocenylimines	Reactions of deactivated/non-activated Ar-Cl	Cs ₂ CO ₃ (2 eqv.)	Dioxane, 100°C			> 90	Gong et al ²²⁶
98.	Di(2-pyridyl)methylamine-PdCl ₂ complex	Coupling in aq. solvents, aerobic conditions	K ₂ CO ₃ /KOH	H ₂ O-100°C MeOH, r.t.			>95	Najera et al ²²⁷
99.	PdCl ₂ -EDTA complex	Coupling of Ar-X		H ₂ O, 20 to 100°C		TON~97,000		Korolev et al ²²⁸
100.	Ni ⁰ PCy ₃ complex	Coupling of alkenyl tosylates						Tang et al ²²⁹
101.	Pd(OAc) ₂ /Co-containing monodentate phosphine ligand	Coupling of Ar-Br using very low catalyst loading						Hong et al ²³⁰
102.	Ni(NO ₃) ₂ - PPh ₃	Coupling of Ar-X	K ₃ PO ₄	Diglyme, 80°C	3 h		91	Itabashi et al ²³¹

1.3.2 Suzuki Coupling using Immobilized Catalysts

The most promising applications of Suzuki coupling reaction have been for synthesis of organic compounds with complex structures, which are often non-volatile in nature. Therefore, the issue of catalyst-product separation is at forefront in this case like most other homogeneous catalytic reactions. Obviously, efforts have been made to immobilize the homogeneous catalyst to facilitate the practical applications of Suzuki coupling reaction. The crucial points to be considered for a heterogeneous catalyst for the Suzuki coupling reaction are as follows,

- ✓ The catalyst should be stable (chemically non-degrading and physically robust) under the highly basic environment required for the coupling reaction
- ✓ Should be non-interacting (non-coalescing) with the reaction products enabling easy separation
- ✓ Should sustain under higher temperatures (~80-150°C)

A number of heterogeneous catalyst systems have been reported for the Suzuki coupling reactions. A detailed literature survey is presented in the Table 1.5. It is observed that for Suzuki coupling reactions two types of heterogeneous palladium catalysts are used, which may be categorized broadly as

- (i) Nano-sized Pd-cluster catalysts stabilized by using different materials were most extensively studied systems
- (ii) Immobilized Pd-complex catalysts.

For the immobilized Pd-complex catalysts for Suzuki coupling, different kinds of supports matrices may be used. As in the reports Pd-complexes are mostly supported onto different polymeric matrices (such as different types of gels, fibers, polymers etc.). However, the ordered molecular matrices, mostly siliceous (such as Zeolites, Mesoporous matrices, clays etc.) were also tested as scaffolds for the immobilization of the Pd-complexes. Of the numerous examples from literature, a few of prime importance are discussed here. Early reports involved the use of Merrifield resin-bound Pd(PPh₃)₄ for the coupling reactions which took 24 h to complete with 90-94% conversion. However, 0.6% loss of Pd was reported during the reaction. Use of supercritical CO₂ as reaction medium was reported by Shezad et al for the coupling of aryl iodides, where fluorous complex of Pd was used as the catalyst, giving 94% conversion in 24 h. Bergbrieter et al reported the Pd^{II}-SCS complex bound to the PNIPAM/ PEG as liquid supports, for the coupling reactions under thermo-morphic reactions producing 32-56 % of the desired product in 20 h. Biphasic

Pd-complex catalysts under the influence of phase transfer agents were reported by Paetzold et al showing 99% conversion. A comparative study of the different Pd-complex catalysts supported on MCM-41 and other siliceous matrices was reported by Kosslick et al, bringing out the probable effects of the supports' properties on the rates of the coupling reactions. Ligand-free coupling involving aryl chlorides was demonstrated while using Pd-C catalyst to get 37-100% conversions in 24 h as reported by LeBlond et al. Different supports such as FibreCat® or TunaCat® etc were also tested as supports for solid catalysts for the coupling of different aryl halides in ethanol-water solvent by Colacot et al. Mechanistic details of coupling reactions using heterogeneous ligand-free nanosized Pd⁰ clusters in layered double hydroxides were studied by Choudary et al, and this is the only authentic report on the mechanism of heterogeneous Suzuki coupling reactions. Pd^{II}-exchanged NaY zeolite was also reported to be a ligand free catalyst system for the coupling of different aryl halides, giving 77-92 % conversion in as low as 1 h of reaction time at a low reaction temperature of 323 K by Bulut et al. Use of zeolites was also reported by Corma et al, where they used basic zeolites/ alkali sepiolites for the coupling of all aryl halides, and interestingly they reported that the catalyst regained the lost reactivity on further reuse. Following the use of palladacycles as homogeneous catalysts, their immobilized counterparts – supported on MCM-41, SiO₂ or polymers was used by Baleizao et al for coupling of aryl halides in water-dioxane solvent. SiO₂ was reported to be the best support to stabilize the catalyst. Superparamagnetic nanoparticles were used as novel supports for attaching N-heterocyclic amine complexes of Pd to catalyze the coupling of aryl iodides and aryl bromides with ~93 % conversions in 20 h in a recent report by Stevens et al. Cravotto et al used microwave heating for a ligand-free Pd-C catalyzed coupling, yielding 19-97 % conversion only. As observed from the survey, even though the separation of the catalyst and product was addressed well, the activities of the catalysts were quite low requiring long duration of reactions except for the cases where non-conventional sources of energy (microwave or ultrasonic irradiation etc.) were used. Also, the stability and recyclability are still critical issues to attend to. In view of the above observations, the necessity of a true heterogeneous catalyst having a high activity, stability and reusability as criteria, is still alive and quite an exciting idea to search for.

Table 1.5: Literature survey on immobilized catalysts for Suzuki cross-coupling reactions

Sl. No.	Catalyst System	Applied for	Reaction Conditions			Conv., %	Sel., %	Key Features	Reference
			Base	Solvent	Time				
1.	Polymer bound Pd catalyst	Coupling of triflates for 10 recycles	K ₃ PO ₄	Dioxane, 85°C	5-11 h	88-96		Cumulative TON ~ 500	Jang ²³²
2.	Pd-catalysts anchored to Tenta Gel S RAM	MW assisted coupling of heteroarylboronic acids & X-benzoic acids	Na ₂ CO ₃	H ₂ O-EtOH-DME	3.8 min	84-98		Resin regenerated with TFA	Larhed et al ²³³
3.	Pd(PPh ₃) ₄ bound to Merrifield polymer	Coupling of Ar-Br	Na ₂ CO ₃	H ₂ O-EtOH-PhMe, 80°C	24 h	90-94		0.6% Pd lost in reaction	Fenger et al ²³⁴
4.	Pd-doped KF/Al ₂ O ₃	Coupling of Ar-X/ MW assisted coupling	K ₂ CO ₃ , NaF, etc.	Solvent-less	3 min (MW)	74-98		Alkyl-X, Vinyl-X couplings failed	Kabalka et al ²³⁵
5.	Pd(CF ₃ CO ₂) ₂ / Pd(F ₆ -acac) ₂ in scCO ₂	Coupling of Ar-I	DIPEA	85°C	24 h	> 95		scCO ₂ , 1800 psi	Shezad et al ²³⁶
6.	Pd-thiourea resin - Deloxan THP	Coupling of all Ar-X	K ₂ CO ₃	Pr'OH- H ₂ O	3-4 h	27-96		Air-stable catalyst	Zhang et al ²³⁷
7.	Clay-PdCl ₂ / P(Ph ₃) ₄ Br	Coupling of Ar-X	K ₂ CO ₃	DMF, 80°C	0.5-12 h	100	51-95	2 recycles shown	Verma et al ²³⁸
8.	Pd-nanoparticles-PVP/PAMAM	Coupling rates & nano-Pd stability evaluated	Na ₃ PO ₄	EtOH-H ₂ O, 100°C	12-48 h	30-90		Stability-activity relation studied	Li et al ²³⁹
9.	Pd(PPh ₃) ₄ -glycol	Coupling of resin bound Ar-X & Ar'-B(OH) ₂	Et ₃ N	DMF, 105°C		100	100	Resin bound product easily released by TFA	Gravel et al ²⁴⁰

10.	Pd ^{II} -SCS bound to PNIPAM/ PEG	Thermomorphic reaction conditions	Et ₃ N	C ₇ H ₁₆ / 90% Aq. EtOH, ~ 95°C	20 h	32-56	-	Facile product separation (L-L)	Bergbreiter et al ²⁴¹
11.	Aq.-soluble Pd complexes	Coupling in presence of Phase transfer agents	Na ₂ CO ₃	H ₂ O, 30-78°C		99		Very low catalyst charge, ~ ppm	Paetzold et al ²⁴²
12.	Ni-C & LiBr/ phosphines	Coupling of Ar-Cl	Anhy K ₃ PO ₄	Dioxane, 135°C	18-24 h	71-92		Anhy. conditions required	Lipshutz et al ²⁴³
13.	Nano-PVP coated with Pd	All coupling reactions							Pathak et al ²⁴⁴
14.	Pd ⁰ -trimeric olefinic macrocycle/ polystyrene, nano-Pd-fluorous phase	Coupling in biphasic/ fluorous biphasic media	K ₂ CO ₃	C ₆ H ₆ / perfluoro-Octyl-Br		~90		No catalyst loss	Cortes et al ²⁴⁵
15.	Pd-complex-Al-MCM-41/ other Si-matrices	Comparative study of the supports' effect	Na ₂ CO ₃	PhMe/ H ₂ O EtOH, 78°C					Kosslick et al ²⁴⁶
16.	Pd-C	Ligand-free coupling of Ar-Cl	K ₂ CO ₃	DMA- H ₂ O, 80°C	24 h	37-100			LeBlond et al ²⁴⁷
17.	Aq. soluble (GCLAphos) ₂ PdCl ₂	Coupling of Ar-Br	NaOH	H ₂ O, 80°C	16 h	~ 95			Miyaura et al ²⁴⁸
18.	Pd nanoparticles in Keggin anions/ Al ₂ O ₃	Coupling of all Ar-X	KF					15-20 nm Pd clusters used	Kogan et al ²⁴⁹
19.	(NH ₄) ₂ PdCl ₄ -polymer	Coupling of Ar-X & Ar-OTf with Ar-B(OH) ₂	Na ₂ CO ₃	H ₂ O, Ar-blanket		84-98	91-96	Catalyst reused 10 times	Yamada et al ²⁵⁰
20.	FiberCat-Pd, Pd-C, TunaCat (FiberCat+Bu ^t ₃ P)	Coupling of all Ar-X		EtOH-H ₂ O				Air-stable catalyst	Colacot et al ²⁵¹

21.	(ArgoGel-PPh ₃ -HCHO)-Pd ^{II} (allyl) complex	Coupling of Ar-X, allyl-X	K ₂ CO ₃	H ₂ O		94-99		3-recycles shown	Uozumi et al ²⁵²
22.	Pd(PPh ₃) ₄ / dendrimer-bound Ar-X	Coupling with mobile Ar-B(OH) ₂	Na ₂ CO ₃	DMF	8-10 h	59-99		Dendrimer-pdt adduct formed	Zhang et al ²⁵³
23.	10% Pd-C or Pd ⁰ -cyclodextrins (α, β, γ)	Coupling of halophenols	K ₂ CO ₃	H ₂ O		99	100	Mechanism proposed	Sakurai et al ²⁵⁴
24.	Polyurea-Pd(OAc) ₂	PPh ₃ -free coupling in/without scCO ₂						4 recycles reported	Ley et al ²⁵⁵
25.	Pd hollow spheres	Coupling of Ar-X	K ₂ PO ₄	EtOH	24 h	98	~95	Recyclable catalyst	Kim et al ²⁵⁶
26.	nano- Pd ⁰ supported on layered double hydroxides	Ligand-free coupling reactions						Mechanistic studies	Choudary et al ²⁵⁷
27.	Pd ^{II} -exchanged NaY	Ligand-free reaction	Na ₂ CO ₃	DMF-H ₂ O, 50°C	1 h	77-92		Rxn ceased with added Ph ₂ MeP	Bulut et al ²⁵⁸
28.	Poly(amidoamine) dendrimer-Pd ⁰	Coupling of Ar-I & Ar-Br	K ₂ CO ₃	Solvent-H ₂ O, reflux				Pd-black formed after rxn.	Pittelkow et al ²⁵⁹
29.	Pd ₂ (dba) ₃ / PBU ^t ₃	Coupling of resin bound chloropyrimidines	Spray-dried KF	THF, 50°C	~8 h			Resin cleaved to get product	Wade et al ²⁶⁰
30.	Pd(PPh ₃) ₄ / Pd(dba) ₂	Coupling of polyglycerol bound Ar-B(OH) ₂	K ₂ CO ₃	DMF				Homogeneous reaction	Hebel et al ²⁶¹
31.	Pd ^{II} -basic zeolites/ Alkali-Sapiolites	Coupling of Ar-X		PhMe				Regenerates lost activity in reuse	Corma et al ²⁶²

32.	Oxime palladacycle-MCM41/ SiO ₂ / polymers	Coupling of all Ar-X		H ₂ O-Dioxane				MCM-41, SiO ₂ tested best	Baleizao et al ²⁶³
33.	Pd ^{II} exchanged Sepiolite/ Pd ^{II} -anchored FSM-16	Coupling of bromophenols	Na ₂ CO ₃	H ₂ O, reflux	24 h	TON~940000	94	Results are specific for 4-Br-phenol only	Shimizu et al ²⁶⁴
34.	SiO ₂ -supported Pd catalysts	Coupling of Ar-Br	K ₂ CO ₃	<i>o</i> -Xylene		100		Recycled for 7 times	Paul et al ²⁶⁵
35.	Pd ^{II} -pyridinecarboimine anchored to FSM-16	Coupling involving Ar-I & Ar-Br			1.5 h	50-100		Recyclable catalyst	Horniakova et al ²⁶⁶
36.	Polystyrene-bound palladacycles	Reaction of Ar-Cl						Leaching seen in extracted catalyst	Bedford et al ²⁶⁷
37.	Pd ^{II} -functionalized SBA-15	Coupling of 4-Br-acetophenone							Crudden et al ²⁶⁸
38.	Superparamagnetic nanoparticle-supported Pd-NHC complex	Coupling of Ar-I & Ar-Br	Na ₂ CO ₃	DMF, 50°C	20 h	~93		Nanoparticles used as novel supports	Stevens et al ²⁶⁹
39.	Pd-C or Aq. PdCl ₂ -TEBA	Sonochemical coupling of Ar-X	KF, K ₂ CO ₃	MeOH-H ₂ O				Ultrasound used	Polackova et al ²⁷⁰
40.	Pd-C	Coupling under dual effect of US & MW	Cs ₂ CO ₃	H ₂ O or DME, 45-48°C		19-97		Ligand free coupling shown	Cravotto et al ²⁷¹
41.	Commercial 10% Pd-C	Coupling of Ar-Br	Na ₂ CO ₃	EtOH-H ₂ O (1:1), r.t.		94-100		Phosphine-free coupling	Zhang ²⁷²

The literature review on both carbonylation and Suzuki cross coupling reactions indicates that the issues related to catalyst-product separation are as much important as the overall activity and selectivity of the metal complex catalysts. Clearly, the performance of the immobilized catalysts is not very satisfactory though a number of approaches and concepts have been demonstrated using these reactions. There is a need for developing new catalytic materials with significant improvements in activity, selectivity and more importantly the stability during such reactions. Equally, important aspects would be the characterization of catalysts and understanding the mechanistic pathways of the catalytic cycles for the lead catalyst systems.

1.4 Catalyst-Product Separation

One of the driving issues in the development of the metal-complex catalyzed reactions is the separation of the soluble catalysts from the reaction mixture and its efficient re-use. The drawbacks of the soluble metal complex catalysis are well known and can be summed up as follows:

- Transition metals being used as catalysts need to be separated for the prevention of environmental hazards and economic utilization
- Catalysts being precious and costly, need to be re-used
- Complex energy-intensive separation processes for the catalyst from the reaction mixture often required
- Deactivation/ transformation of the active complexes into catalytically inactive forms during most of the catalyst recovery processes
- Stability of the product(s) may be affected under catalyst-separation conditions

One of the most important issues related to the development of the organometallic catalysis is the catalyst – product separation. However, the main advantages of the organometallic complex catalysis viz. the high activity and selectivity by tuning of the stereo-electronic environment of the coordination zone, possibility of unambiguous characterization of the intermediates providing better understanding of the system, are made to look diminutive in front of the disadvantages associated.

Thus, the commercial application prospects of homogeneous catalytic processes are reduced to a good extent with respect to its actual potential. Hence, the homogeneous catalysts need to rise above these shortfalls and add some attributes on

these issues. The heterogeneous catalysts however are advantageous on the facile separation and consequently on the other aspects of stability, in spite of the lower activities in many cases due to the transport barriers. The catalyst–product separation has been the interest for the catalysis research since start but has gained good impetus in the last few decades with the goal of developing sustainable technology. Consequently, numerous strategies have been adopted to facilitate the separation in energy-efficient and cost effective manner. The idea of immobilization/heterogenization of homogeneous complex catalysts is thus the obvious tool for achieving the target of making catalysts with combined advantages of both the homogeneous and heterogeneous catalysts. The *expected* advantages envisioned by using the immobilized organometallic catalysts are enlisted as follows,

- Easy separation of catalyst from the reaction mixture
- High activity analogous to the homogeneous counterpart
- Chances of deactivation of catalyst during to the separation procedures are reduced
- Efficient recycle of the precious metals, contributing to the production economy
- Environmentally benign processes evolved

Thus, the catalyst – product separation is a challenging area of research for all branches of the homogeneously catalyzed organic transformations.

1.5 Immobilization of Metal Complex Catalysts

The immobilization of the transition metal complex catalysts, to reap advantages of the homogeneous as well as the heterogeneous catalysis, has well been a case beyond debate a potential solution to the catalyst – product separation and catalyst recycle issue. Immobilization of the homogeneous catalysts can be defined as the *restricting the mobility of the organometallic complex catalyst to mix with the reaction mixture, thus affecting an easier separation but preserving the identity and characteristic properties of the active catalytic entity in its original form*. Ideally, a perfectly immobilized homogeneous complex catalyst should show all the properties of the homogeneous counterpart in terms of its activity, selectivity etc. in addition to the ease of separation and re-use with retention of the stability during these operations. *The immobilization of the soluble catalysts in general is achieved by the introduction of a phase differentiation between the catalyst and the other components*. The other

phase may be either a different immiscible liquid phase (e.g. biphasic catalysis) or a separable solid phase (e.g. supported, anchored, encapsulated etc. catalysts). Phase differentiation may be generated by the manipulation of some physical parameters as temperature (thermo-regulated catalysis), solubility (soluble supports as dendrimers, phase transfer catalysis), pressure & temperature (e.g. supercritical medium catalysis) etc. The transition metal complexes however should be transformed accordingly by the numerous strategies to achieve these, and each of these strategies employs at least one physical/ chemical interactive force. The judicious application of a particular force of interaction and the ease of operation actually determines the impact/ credit of the heterogenization approach. The immobilization processes can be classified into different groups depending on the nature of the interactive force employed for the generation of the phase differentiation, which are presented as follows,

- *Liquid – Liquid Phase Differentiation*
 - ↪ Biphasic catalysis – Aqueous, Non-aqueous, Fluorous (*Solvation forces*)
 - ↪ Supported Liquid Phase (*Solvation forces associated with surface interactions*)
 - ↪ Reverse Biphasic and Phase Transfer Catalysis (*Solvation forces*)
- *Solid – Liquid Phase Differentiation*
 - ↪ Supporting onto solid matrices (*Non-bonding molecular forces as physisorption, van der Waals forces etc.*)
 - ↪ Encapsulation of metal complexes (*Physical conformational constraints*)
 - ↪ Anchoring to the solid surfaces (*Covalent interactive forces*)
 - ↪ Tethering onto support materials (*Ionic interactive forces*)
- *Manipulation of Physical Parameters*
 - ↪ Xerothermal catalysis (*Temperature dependent solvation*)
 - ↪ Supercritical media (*Temperature and pressure dependent phase transitions*)

A detailed description of each of these is beyond the scope of this thesis, but discussions on the topics such as anchored catalysts using different kinds of support is presented hereafter. A brief categorical description of the different strategies of anchoring in different kinds of supports is presented here to have a general understanding of the state-of-the-art.

1.5.1 Anchored Catalysts

Covalently bonded soluble complexes to the matrices may be formed in two different methodologies. Either the *support possesses relevant groups* to anchor the complex, *or a molecular linker is attached between the support & the complex* to hold it to the surface.

The use of functional organic polymers, e.g. polystyrene, styrene-divinylbenzene co-polymer, modified with $-\text{PPh}_2$ & $-\text{NRR}$ ²⁷³, $-\text{CH}_3\text{CN}$ ²⁷⁴, $-\text{SH}$ ²⁷⁵, etc. groups which can bind to the complex were employed for the purpose. The unmodified polymers are subjected to these functionalizations to get the anchors. Different other polymers as polyvinyls²⁷⁶ polyacrylates²⁷⁷, cellulose²⁷⁸ etc. were also used as support matrices. Of these materials, the phosphinated polystyrenes were found to perform the best for the anchoring of catalysts. Use of crosslinking agent was discussed for the increase in the flexibility of the polymer backbone. Different groups²⁷⁹ studied the optimization of the amount of crosslinking in the polymeric support. Grubbs²⁸⁰ and Collman²⁸¹ had immobilized different types of Rh and Ir catalysts with varying degree of crosslinking in the polymeric support. A number of catalytic transformations such as hydrogenation, hydroformylation, hydrosilylation, oligomerization, acetoxylation, polymerization, cyclo-oligomerization etc. were investigated using these polymer-anchored catalysts.²⁸²

The use of a covalently bonded “molecular anchor” to the surface of the support matrix may be considered as one of the very important method of immobilization of the homogeneous catalysts onto insoluble supports. The support materials generally contain certain surface groups, which may be easily bonded to a bifunctional molecule having one end capable of holding to the complex, while the other end can be attached to the surface of the support via a permanent covalent bonding. For the siliceous matrices, the surface contains $-\text{OH}$ groups, which may be used to attach a linker having at least one reactive silyl group to combine with, at one end while another end holds the ligating functional group to bind to the complex. Using molecular anchors to bind complexes was applied initially to the mesoporous materials; a detailed discussion on the strategies and applications will be presented in the next section.

1.6 Immobilization in Mesoporous Matrices

Among the different solid matrices already dealt with, in context with the immobilization of the homogeneous catalysts, mesoporous materials have also been seen as potential candidates. These materials are generally categorized by their medium sized pore dimensions ranging from 20 to 100Å. They may have long tubular or zigzag or cross-linked etc. types of channel structures with highly regular long-range periodicity and very high surface areas. The bigger pore-dimensions in comparison to the microporous materials make them unique in respect of their properties and likewise in the approaches to immobilize the homogeneous complex catalysts also. The discovery of numerous classes of materials such as the M-41S²⁸³, FSMs²⁸⁴, SBAs²⁸⁵, etc. with distinctive properties, has opened access to these new candidates as hosts for the immobilization of metal complexes. The pore size of these materials are so high that the encapsulation of the complexes by simply trapping inside the cage is not viable, and hence it needs 'chemical appendages' to hold them to the support matrices. In most of the cases, the *covalent linkage* of the 'molecular tether' between itself and support matrix is used for immobilization. This is similar to the anchoring technique as described in the Section 1.5.5. This sort of surface organo-functionalization of the inorganic silicate materials actually imparts a dual property to the material. The inorganic support matrix provides mechanical strength and thermal stability while the organic dangling groups are flexible enough to permit any further transformations. Thus, the tunability factor is the main attraction of this class of organic-inorganic hybrid materials, and can be tailor-made for any particular function. Depending on the approach of inclusion of the organo-functional moiety into/ onto the mesoporous silicates, a number of categories can be described for the pathway for preparation of the hybrid mesoporous silicates and immobilization of metal complexes thereof. Stein et al²⁸⁶ have reviewed a vivid description of all the strategies, and results. The preparation methods of the hybrid materials may be categorized as follows,

- ✓ Post-synthesis grafting method
- ✓ Coating method
- ✓ Co-condensation method

A brief description of each of the above-mentioned classes may be presented as follows,

1.6.1 Post-Synthesis Grafting Method

The surface modification of a pre-fabricated mesoporous matrix by covalent fixation of a functional molecule to its surface may be termed as post synthetic grafting. The term grafting or anchoring may be synonymously used for these processes. Generally, the silylation of the surface is done involving the surface silanol group(s) and a functionalized silane molecule. An optimized amount of the surface silanol groups and surface adsorbed water is needed for the efficient silylation, as excess of water may result in the hydrolysis of the functional siloxy compound and subsequent self-condensation may occur. The generality of the idea of grafting may be extended to the *three* different classes based on the nature of the organic functional groups, as

1.6.1.1 Grafting with passive surface groups

This involves the grafting of the mesoporous surfaces with *low-reactive groups*. Mostly, these may include alkyl chains, phenyl rings etc., which are used to manipulate the surface hydrophobicity, passivate silanol groups, engineer pore wall thickness etc. as per necessity. This kind of grafting is actually necessary for the cosmetic manipulation of the mesoporous supports, and do not participate in the chemical reaction directly, but assist the course of a transformation indirectly. Examples of the tuning of the pore sizes of various supports (e.g. MCM-41, FSM-16 etc.) were reported by several groups²⁸⁷, applying grafting with passive groups. Zhao et al²⁸⁸ reported a detailed study of the surface coverage of MCM-41 using trimethylchlorosilane (TMCS) as graft, whereby ~85% coverage was obtained maximally. Properties as hydrophobicity, hydration and mechanical stability were enhanced along with. It was observed by Anwender et al²⁸⁹, that the surface coverage was most efficient when the silylating agent has less sterically demanding groups. Multiple functionalization of the surface was also obtained by consecutive or competitive silylation. It was observed from the competitive silylation reactions that the grafting reaction rate was guided by the steric factors of the silyl groups.

1.6.1.2 Grafting with reactive surface groups

This approach is a tool for the surface-modification of the mesoporous silicates to get functionalized organo-hybrid materials, which may be addressed to further transformations if required. The functional end-groups obtained by the grafting of the reactive groups to the surface are capable of performing either further *functional transformation* or *coordination to metal ions/ complexes*, depending on its nature. A

number of end-groups such as olefins, nitriles, alkyl thiols, alkyl amines, alkyl halides, epoxides etc. may be grafted onto the siliceous matrices. The wide applicability of the reactive grafts can be understood as the following,

Functional transformation of the organo-hybrid matrices is possible for a number of end-groups attached to the mesoporous matrices. For example,

- ⌘ Olefins i.e. the vinyl-functionalized mesoporous materials may be subjected to bromination²⁹⁰ or hydroboration^{289b} to form bromo- and hydroborate functionalized matrices respectively.
- ⌘ Nitrile end groups may be hydrolyzed to carboxylic acid²⁹¹, while thiol functionality may be oxidized to sulphonic acid²⁹² end groups. Acidic functions can be used further to attach to amino acids by electrostatic interactions.²⁹³
- ⌘ Derivatization of the amine function on the hybrid materials may lead to the formation of amides, imides etc. and also may undergo alkylation or nucleophilic substitution.²⁹⁴
- ⌘ Alkyl halides may undergo nucleophilic substitution of the halogen atom.²⁹⁵

Coordination to metal ions/ complexes may also be performed by the organo-grafted mesoporous matrices. Certain functionalities already bound to the support matrices may coordinate to the transition-metal centres, thus immobilizing the complex. For example,

- ⌘ Amine-ligand-functionalized MCM-41 matrices (e.g. ethylenediamine, EDTA, diethylenetriamine, etc.) bind to the cobalt-centres immobilizing the complex.²⁹⁶
- ⌘ Amine-functionalized MCM-41 & MCM-48 coordinate directly to HRh(CO)(PPh₃)₃ complex for immobilization and use in hydroformylation reactions.²⁹⁷

Thus, a large number of reactive functional groups may be either incorporated or derived at, into the mesoporous matrices, with wide-ranging applications.

1.5.1.3 Site-selective grafting

This approach of the use of multiple grafts on the siliceous support materials, with proper selectivity to the specific sites, has been practiced in recent years. Depending on the necessity of the catalyst system, the multiple/ differential grafting of the interior and exterior mesoporous surfaces can be obtained, e.g. uncovered surface after silylation may be re-silylated for passivation.²⁹⁸

The exterior surface is more easily accessible and thus functionalized before the interior surface, preferentially.²⁹⁹ Also, the accessibility is the same for the

catalytic reactions, and hence, strategic blocking (passivation) of the exterior surface is done before the functionalization of the internal silanol groups. Shephard et al³⁰⁰ demonstrated the passivation of the external surface of MCM-41, using Ph_2SiCl_2 , followed by the functionalization of the internal surface using 3-aminopropyltrimethoxysilane (APTS) to anchor redox-active Ru-cluster. In another approach by de Juan et al³⁰¹, the as-synthesized material (MCM-41) is subjected to grafting of the external surface (the surfactant-filled internal channels do not allow grafting internally due to steric reasons), followed by the removal of the templates to get an exteriorly passivated mesoporous material. Functionalization of the same on the interior surface in subsequent steps gave a diverse-functionalized matrix on interior and exterior surfaces appropriate for particular application.

1.6.2 Coating Method

The uniform availability of the surface silanol groups if obtained, will ensure a continuous coating of the functional group, and consequently the immobilization of the metal complex may be attached to the surface with better concentration. This can be achieved by hydrating the surface of the siliceous material to regenerate more surface silanol groups and we may get more surface concentration of the organics. Such water-controlled coating of mercaptopropyl functionality over MCM-41 and HMS materials were reported recently.³⁰² Another imprint coating method was reported by Dai et al³⁰³, where a metal complex was directly grafted to MCM-41, after which the metal was removed to get a 'metal-imprinted' grafted ligand, which can catch any other similar metal atom. This type of imprinting coating was observed with mesoporous silica only. The higher concentration of the grafted organo-functions makes this method useful for the preparation of purification catalysts.

1.6.3 Co-condensation Method

Co-condensation or 'one-pot' synthesis of the organic-inorganic hybrid materials is another convenient route to these materials. Co-condensation occurs between a tetra-alkoxy silane (precursor of the siliceous framework) and one or more organo-alkoxy silane (precursor of the functional group) forming the organic-inorganic hybrid networks via a sol-gel process.³⁰⁴ Co-condensation was attempted to couple with surfactant-template-mediated synthesis process for these materials by many groups under a wide range of synthesis conditions.³⁰⁵ Several mechanistic classes have been proposed for the surfactant-mediated co-condensation of these precursors

based on the diverse ionic/ polar nature of the surfactant source and the silica precursors. Each of these classes operates within a different set of reaction conditions.

S^+I^- pathway involves a cationic surfactant, S^+ (mostly 4° alkylammonium ions) and an anionic silica precursor I^- , which are obtained under basic conditions. Surfactants may be removed by HCl/ alcohol treatment or by calcination at ~350°C. Reports by Mann et al³⁰⁶ presented such a methodology using cetyltrimethylammonium bromide (CTAB), and a host of organo-silica sources for functionalized MCM-41 preparation, was an early example.

Key Features: Higher mesopore wall thickness; Dependable synthesis methodology

$S^+X^-I^+$ pathway employs both cationic surfactant S^+ , and silica precursor I^+ , along with certain anions X^- , under acidic conditions, for co-condensation. Stucky et al^{305d}, described a lamellar mesoporous matrix functionalization, using a C_{16} anchor. Recently, Babonneau et al³⁰⁷ reported alkyl-grafted mesoporous silicates, and phenyl-grafted hexagonally ordered mesoporous matrix syntheses using the aforesaid strategy.

Key Features: Acidic conditions allow formation of films and meso-structured monoliths

S^0I^0 pathway involves the uncharged silica precursors S^0 , along with neutral amine surfactant micelles I^0 . In this type of synthesis, due to the weak interactions between the neutral surfactants and the mesopore walls, the removal of the surfactants can be done by extraction with ethanol simple. The first report of such type of synthesis by Macquarrie^{305c} was followed by inclusion of vinyl and 3-chloropropyl³⁰⁸, mercaptopropyl³⁰⁹ grafts by other groups.

Key Features: Smaller pore sizes obtained; Order or porosity may be lost due to trapping of small alkyl groups

N⁰P pathway makes use of a nonionic surfactant *N⁰*, & a neutral silica precursor *P⁰*. Generally, alkylpoly(ethylene oxide) materials (e.g. Triton-X100, Tergitol 15-S-12 etc.) are used as structure-directing agents.³¹⁰ The syntheses are done at neutral pH and easy removal of surfactant by extraction with EtOH was possible for this synthesis strategy.

Key Features: Smaller lattice space; Convenient method

Random multifunctional surfaces may be generated by the one-pot co-condensation of silica precursor with the different functional organosilanes. Reports by Mann et al³¹¹ and Macquarrie³¹² described the anchoring of phenyl & aminopropyl; phenyl & mercaptopropyl; phenyl & allyl groups respectively onto the mesoporous matrices.

Key Features: Randomly distributed functional groups available

The co-condensation method may thus be applied to a spectrum of precursor types according to the specific requirement.

1.7 Scope and Objective of Present Work

In view of the literature survey, it is evident that the carbonylation of olefins and alcohols represent important classes of industrially important transition metal catalyzed reactions, which proceed through a cleaner, cheaper and eco-friendly alternate route than the conventional pathways. Although, considerable advancement have been made since the first examples of homogeneous catalysts, for the development of a better-active catalyst, it is observable that the homogeneous catalysts still possess the challenge of efficient catalyst-product separation and reuse. The benchmark homogeneous catalysts being already been established, the target is now set for developing truly immobilized catalyst systems for the carbonylation reaction. Suzuki coupling reactions as described already, has emerged as a potent tool for obtaining C-C coupled products bearing diverse functionalities. Following the survey presented here, this reaction also needs similar robust, recyclable active heterogeneous catalysts for being industrially viable/ acceptable. Concerning the immobilization of the homogeneous catalysts, innumerable strategies have been designed, and applied for different classes of reactions. However, for the carbonylation

reactions, the use of immobilized catalysts has been limited due to the severity of the reaction parameters involved, such as high temperature, high pressure, presence of acids and salts as promoters etc., which renders the immobilization vulnerable to metal-leaching and catalyst degradation and also provides a scope for effective research in the area. For Suzuki coupling reactions, the existing heterogeneous catalysts may be showing good results in terms of activity and selectivity; however, there is further scope for enhancement in reaction rates.

The objective of this thesis is to present the works oriented towards the design of true and easy-to-make immobilized homogeneous catalysts for carbonylation reactions and Suzuki coupling reactions, combining the advantageous aspects of both homogeneous and heterogeneous catalysis. Since these two reactions occur under utterly different reaction conditions, achieving a successful immobilization of Pd-complexes that makes catalysts stable to sustain such diverse conditions is a highly promising target. The issues like synthesis and characterization of the catalyst systems and correlating these with the enhanced activity and stability may be the milestones to the conceived goal. Also, the basic understanding of the intrinsic reaction kinetics of carbonylation may provide insight to develop/ fine-tune the catalyst system. Proper understanding of all of these may lead to further advancement of the catalysis technology of the present age.

Keeping these objectives in the background, the specific targets have been chosen for the present work as follows,

- Synthesis, characterization and catalytic studies using novel anchored palladium complex catalysts for carbonylation of alcohols and alkenes
- Ossification of metal complex catalysts – a novel process for immobilization of homogeneous catalysts and application for the carbonylation of alkenes and alcohols
- Comparative kinetic studies on the carbonylation of IBS, using the homogeneous and immobilized palladium complex
- Studies in the Suzuki Cross Coupling reactions for the syntheses of functionalized bi-aryls using the novel ossified palladium complex catalysts

Each of these topics will be discussed in details in a separate detailed chapter keeping parity with the necessity and targets as visualized here.

References

- 1 (a) Parshall G W, *Homogeneous Catalysis*, Wiley-InterScience, New York, **1980** (b) Masters C, *Homogeneous Transition-Metal Catalysis*, Chapman & Hall, London, **1981** (c) Weisseimel K and Arpe H J, *Industrial Organic Chemistry*, 2nd Ed., VCH Press, Weinheim, **1993** (d) Cornils B, Herrman W A, (Eds.), *Applied Homogeneous Catalysis with Organometallic Compounds* (2nd Ed.), VCH, Weinheim, , **2002** Vol 1 and 2 (e) Cornils B, Herrman W A, (Eds.), *Aqueous-Phase Organometallic Catalysis*, (2nd Ed.) VCH, Weinheim, **2004** (f) Beller M, Bolm C (Eds.), *Transition Metals for Organic Synthesis: Building Blocks and Fine Chemicals*, VCH, Weinheim, **1998** Vol 1 and 2
- 2 (a) Genet J P, *Actualite Chimique*, **2003** 4 25 (b) Fairlamb I J S, *Annual Reports on the Progress of Chemistry, Section B: Organic Chemistry*, **2003** 99 104
- 3 (a) Metivier P, *Spl Publication (Clean Technology for the Manufacture of Specialty Chemicals)* -RSC, **2001** 260 68 (b) Zapf A, Beller M, *Topics in Catalysis*, **2002** 19(1) 101
- 4 (a) Colquhoun, H M, Thompson D J, Twigg M V, *Carbonylation-Direct Synthesis of Carbonyl Compounds*, Plenum Press, New York **1991** (b) Falbe J (Ed.), *New Synthesis with Carbon Monoxide*, Springer-Verlag, Berlin **1980** (c) Lapidus A L, Pirozhkov S D, *Russ. Chem. Rev.*, **1989** 58 117 (d) Weisse L, *Specialty Chemicals Magazine*, **2002** 22(3) 36
- 5 Van Leeuwen P W N M, Claver C, *Comprehensive Coordination Chemistry II*, **2004** 9 141
- 6 (a) Reppe W (IG Farbers) DE 855110 **1939** (b) Reppe W, Liebig, *Ann. Chem.* **1953** 582 1
- 7 (a) Osborn J A, Young J F, Wilkinson G, *J. Chem. Soc. Chem. Commun.*, **1965** 17 (b) Evans D, Osborn J A, Wilkinson G, *J. Chem. Soc. A.*, **1968** 3133 (c) Evans D, Yagupski G, Wilkinson G, *J. Chem. Soc. A.*, **1968** 2660
- 8 Heck R F, *Palladium Reagents in Organic Synthesis*, Academic Press, New York, **1985**
- 9 (a) Tsuji J, *Organic Synthesis with Palladium Compounds*, Springer-Verlag, Berlin, **1980** (b) Tsuji J, *Palladium Reagents and Catalysis: Innovations in Organic Catalysis*, John-Wiley & Sons, New York, **1997** (c) Tsuji J, *New J. Chem.*, **2000** 24 127
- 10 (a) Drent E, Arnoldy P, Budzelaar P H M, *J. Orgnomet. Chem.*, **1994** 475 57 (b) Drent E, (Shell Research BV) EP 271145 A2 **1988** (c) Drent E, Budzelaar P H M, Jager W W, (Shell Oil Corp.) US 5099062 **1992**
- 11 (a) Drent E, Budzelaar P H M, *Chem. Rev.*, **1996** 96 663 (b) Sen A, *CHEMTECH*, **1986** 48 (c) Sen A, *Adv. Poly. Sci.*, **1986** 73-74 125 (d) Sen A, *Acc. Chem. Res.*, **1993** 26 303
- 12 (a) Hohenshutz H, von Kutepow N, Himmele W, *Hydrocarbon Process*, 45 **1966** 141 (b) Falbe J, *J. Organomet. Chem.*, **1975** 94 213
- 13 (a) Roth J F, Craddock J H, Hershmann A, Paulik F E, *CHEMTECH*, **1971** 1 600 (b) Roth J.F., *Platinum Met. Rev.*, **1975** 19 12
- 14 Watson D J, Herkes F E, Heinemann H (Eds.), *Catalysis of Organic Reactions*, Marcell Decker Inc. **1998** 369
- 15 Coover H W, Hart R C, *Chem. Eng. Prog.* **1982** 72
- 16 Agreda V H , Pond D M, Zoeller J R , *CHEMTECH*, **1992** 172
- 17 Hohenschutz H, Franz D, Bulow H, Dinkhauser G, (BASF AG) DE 2133349 **1973**
- 18 Blumenberg B, *Nahr. Chem. Tech. Lab.*, **1984** 480
- 19 (a) Cassar L, *Chem. Ind.* **1985** 67 256 (b) Parshall G W, Nugent W A, *CHEMTECH*, **1988** 314
- 20 Elango V, Murphy M A, Mott G N, Zey E G, Smith B L, Moss G L, EP 400892 **1990**
- 21 Ugo R, Renato T, Marcello M M, Pierluigi R, *Ind. Eng. Chem. Prod. Res. Dev.*, **1980** 19 396
- 22 Schwaar R H, *Methacrylic Acid and Esters*, Report No. 11D, SRI International **1994**
- 23 Ash C E, *J. Mater. Edu.*, **1994** 16 1
- 24 Alper H, Hamel H, *J. Am. Chem. Soc.*, **1990** 112 2803

- 25 Hallgren J E, Mathews R O, *J. Organomet. Chem.*, **1979** 175 135
- 26 Leconte P, Metz F, Mortreux A, Osborn J.A, Paul F, Petit F, Pillot A, *J. Chem. Soc. Chem. Commun.*, **1990** 1616
- 27 (a) Germain J E, *Catalytic Conversions of Hydrocarbons*, Academic Press, New York **1969** 278 (b) Levering D R, Glasebrook A R, *J. Org. Chem.*, **1975** 23 1836
- 28 Beller M, Cornils B, Frohning C D, Kohlpaitner C W, *J. Mol. Catal. A: Chem.*, **1995** 104 17
- 29 (a) Tsuji J, *Adv. Org. Chem.*, (Eds. Taylor E, Winberg C), Wiley, New York, **1969** 6 150
(b) Tsuji J, *Acc. Chem. Res.*, **1969** 2 144 (c) Tsuji J, Morikawa M, Kiji J, *Tetrahedron Lett.*, **1963** 1437
- 30 Bittler K, Kutepow N V, Neubauer D, Reis H, *Angew. Chem. Int. Ed. Engl.*, **1968** 7 329
- 31 Sugi Y, Bando K, Shin S, *Chem. Ind.*, **1975** 397
- 32 Sugi Y, Bando K, *Chem. Lett.*, **1976** 727
- 33 Knifton J F, *J. Org. Chem.*, **1976** 41 2885
- 34 (a) Kehoe L J, Schell R A, *J. Org. Chem.*, **1970** 35 2846 (b) Knifton J F, *J. Org. Chem.*, **1976** 41 793
- 35 Alper H, Woell J B, Despeyroux B, Smith D J H, *J. Chem. Soc., Chem. Commun.*, **1983** 1270
- 36 Toda S, Miyamoto M, Kinoshita H, Inomata K, *Bull. Chem. Soc. Jpn.*, **1991** 64 3600
- 37 Bertoux F, Castanet Y, Civade E, Monflier E, Mortreux A, *Catal. Lett.*, **1998** 54 199
- 38 Mlekuz M, Joo F, Alper H, *Organometallics*, **1987** 6 1591
- 39 Lin I J B, Alper H, *J. Chem. Soc. Chem. Commun.*, **1989** 248
- 40 El Ali B., Alper H., *J. Mol. Catal.* **1992** 77 71
- 41 Yoon Je Y, Jang E J, Lee K H, Lee J S, *J. Mol. Catal. A: Chem.*, **1997** 118 181
- 42 (a) Shimizu I, Hirano R, Matsumura Y, Nomura H, Uchida K, Sato A, US 4694100 **1987**
(b) Shimizu I, Matsumura Y, Tokumoto Y, Uchida K, (Nippon) US 5097061 **1992** (c)
Shimizu I, Matsumura Y, Tokumoto Y, Uchida K, (Nippon) US 5260477 **1993**
- 43 (a) Wu Tse-C, (Ethyl Corp.) US 5254720 **1992** (b) Wu Tse-C, (Ethyl Corp.) US 5315026
1994 (c) Wu Tse-C, (Ethyl Corp.) US 5315028 **1994**
- 44 (a) Cometti G, Chiusoli G P, US 4439618 **1984** (b) Cometti G, Chiusoli G P, EP 0074866
A1 **1983**
- 45 Oi S, Nomura M, Aiko T, Inoue Y, *J. Mol. Catal. A: Chem.*, **1997** 115 289
- 46 Huh K-Tae, Alper H, *Bull. Kor. Chem. Soc.* **1994** 15 304
- 47 (a) Seayad A, Kelkar A A, Toniolo L, Chaudhari R V, *J. Mol. Catal. A: Chem.*, **2000** 151
47 (b) Seayad A, Kelkar A A, Toniolo L, Chaudhari R V, *Ind. Eng. Chem. Res.*, **1998** 37
2180
- 48 Seayad A, Jayasree S, Damodaran K, Toniolo L, Chaudhari R V, *J. Organomet. Chem.*
2000 601(2) 100
- 49 Seayad A, Jayasree S, Chaudhari R V, *Org. Lett.*, **1999** 1 459
- 50 Seayad A, Jayasree S, Chaudhari R V, *J. Mol. Catal. A: Chem.*, **2001** 172(1-2) 151
- 51 Jayasree S, Seayad A, Chaudhari R V, *Org. Lett.*, **2000** 2(2) 203
- 52 Papadagianakis G, Verspui G, Matt L, Sheldon R A, *Catal. Lett.*, **1997** 47 43
- 53 (a) Monflier E, Tilloy S, Bertoux B, Castanet Y, Mortreux A, *New J. Chem.*, **1997** 21 857
(b) Tilloy S, Monflier E, Bertoux B, Castanet Y, Mortreux A, *New J. Chem.*, **1997** 21 529
- 54 Jayasree S, Seayad A, Chaudhari R V, *Chem. Commun.*, **2000** 14 1239
- 55 Jayasree S, Seayad A, Sarkar B R, Chaudhari R V, *J. Mol. Catal. A: Chem.*, **2002** 181(1-
2) 221
- 56 Jayasree S, Seayad A, Chaudhari R V, *Chem. Commun.*, **1999** 12 1067
- 57 Drent E, Jager W W, Sielken O E, Toth I, WO 2002026690 A1, Apr **2002**
- 58 Slany M, Schaefer M, Roeper M, (BASF AG) DE 10106348 A1 Aug **2002**
- 59 Slany M, Schaefer M, Roeper M, (BASF AG) PCT Appl. No. WO 2002046143, Jun **2002**
- 60 Sava X, Slany M, Roeper M, (BASF AG) PCT Appl. No. WO 2003031457 A1, Apr **2003**

- 61 (a) Pugh R I, Drent E, *Adv. Synth. & Catal.*, **2002** 344(8) 837 (b) Pugh R I, Drent E, *Catalysis by Metal Complexes*, Kluwer Academic Publishers, **2003** 27 9
- 62 (a) Eastham G R, Cameron P A, Tooze R P, Cavell K J, Edwards P G, Coleman D L, (Lucite Int. Ltd., UK) PCT Appl. No. WO 2004014552 A1, Feb **2004** (b) Eastham G R, Jimenez C, Cole-Hamilton D, (Lucite Int. Ltd., UK) PCT Appl. No. WO 2004014834 A1, Feb **2004**
- 63 Nkosi B S, Terblans Y M, (Sasol Tech. Pvt. Ltd.) PCT Appl. No. WO 2002018047 A2, Mar **2002**
- 64 Kiss G, *Chem. Rev.*, **2001** 101(11) 3435
- 65 Zhou D, Yoneda E, Onitsuka K, Takahashi S, *Chem. Commun.*, **2002** 23 2868
- 66 Peng W, Holloday J E, (Union Carbide USA), PCT Appl. No. WO 2004035595 A1, Apr **2004**
- 67 (a) Drent E, US Appl. No. US 2004024247 A1, Feb **2004** (b) Drent E, Eberhard M R, Pringle P G, US Appl. No. US 2004024258 A1, Feb **2004**
- 68 Consiglio G, Marchetti M, *Chimia*, **1976** 30 26
- 69 Takeda M, Uchide M, Iwane H, (Mitsubishi) DE 2646792 **1977**.
- 70 Fuchikami T, Ohishi K, Ojima I, *J. Org. Chem.*, **1983** 48 3803
- 71 Mitsubishi Petrochemical Co., JP 59010545 **1984**
- 72 Zhigao X, Zilin J, *Youji Huaxue.*, **1986** 3 216.
- 73 Wayner D D M, Hartstock F W, *J. Mol. Catal.*, **1988** 48 15
- 74 Shimizu I, Nomura H, (Nippon) JP 63287746 **1988**
- 75 (a) Noskov Y G, Terekhova M I, Petrov E S, *Kinetica Kataliz*, **1989** 30 234 (b) Noskov Y G, Novikov N A, Terekhova M I, Petrov E S, *Kinetica Kataliz*, **1991** 32 331
- 76 Shimizu I., Matsumura Y., Tokumoto Y., Uchida K., (Nippon) JP 02006431 **1990**
- 77 Hiyama T, Wakasa N, Kusumoto T, *Synlett*, **1991** 569
- 78 Brunet J J, Neibecker D, Srivastava R S, *Tet. Lett.*, **1993** 34 2759
- 79 El Ali B, Vasapollo G, Alper H, *J. Org. Chem.*, **1993** 58 47391
- 80 Lee C W, Alper H, *J. Org. Chem.*, **1995** 60 2501
- 81 Hongying Z B W, Shijie L, Jing C, Hongxiang F, *Mol. Catal. (China)*, **1996** 10 13
- 82 Nozaki K, Kantam M L, Horiuchi T, Takaya H, *J. Mol. Catal. A: Chem.*, **1997** 118 247
- 83 Bertoux F, Monflier E, Castanet Y, Mortreux A, *J. Mol. Catal. A: Chem.*, **1999** 143 23
- 84 Goedheijt M S, Reek J N H, Kamer P C J, van Leeuwen P W N M, *Chem. Commun.*, **1998** 2431
- 85 Wan B S, Liao S J, Xu Y, Yu D R, *J. Mol. Catal. A: Chem.*, **1998** 136 263
- 86 Csók Z, Szalontai G, Czira G, Kollár L, *J. Organomet. Chem.*, **1998** 570 23
- 87 Jedlicka B, Weissensteiner W, Kégl T, Kollár L, *J. Organomet. Chem.*, **1998** 563 37
- 88 Ruiz N, del Río I, Jiménez J L, Claver C, Forniés-Cámer J, Cardin C C J, Gladiali S, *J. Mol. Catal. A: Chem.*, **1999** 143 171
- 89 Benedek C, Törös S, Heil B, *J. Organomet. Chem.*, **1999** 586 85
- 90 Davis I W, Matty L, Hughes D L, Reider P J, *J. Am. Chem. Soc.*, **2001** 123(41) 10139
- 91 Bodis J, *In situ Spectroscopy of Monomer and Polymer Synthesis*, Puskas J E, Long T E, Storey R F, (Eds.) Kluwer Academic/ Inim Publishers, New York, **2003** 187
- 92 Zhang J, Xia C, *J. Mol. Catal. A: Chem.*, **2003** 206(1-2) 59
- 93 Park K H, Jung I G, Kim S Y, Chung Y K, *Org. Lett.*, **2003** 5(26) 4967
- 94 Skoda-Foeldes R, Takacs E, Horvath J, Tuba Z, Kollar L, *Green Chem.*, **2003** 5(5) 643
- 95 (a) Sheldon R A, *Chem. Ind.*, **1992** 903 (b) Dartt C B, Davis M E, *Ind. Eng. Chem. Res.*, **1994** 33 2887
- 96 (a) Elango V, Murphy M A, Smith B L, Davenport K G, Mott G N, Moss G L, (Hoechst Celanese Corp.) EP 284310 **1988** (b) Hendricks J D, Mott G N, (Hoechst Celanese Corp.) US 5166418 **1992**
- 97 Elango V, Murphy M A, Smith B L, Davenport K G, Mott G N, Zey E G, Moss G L, (Hoechst Celanese Corp.) US 4981995 **1991**

- 98 Mott G N, Zey E G, EP 337803 **1989**
- 99 (a) Tanaka Y, Kojima H, Tsuji Y, (Daicel Chem. Ind. Ltd.) UK Pat. Appl. GB 2199030 **1988** (b) Tanaka Y, Kojima H, Tsuji Y, (Daicel Chem. Ind. Ltd.) US 4843172 **1989**
- 100 Tanaka K, Shima Y, (Mitsubishi Gas Chem. Comp, Inc.) US 4937362 **1990**
- 101 Jang E J, Lee K H, Lee J S, Kim Y G, *J. Mol. Catal. A: Chem.*, **1999** 138 25
- 102 Zhou H, Cheng J, Lu S, Fu H, Wang H, *J. Organomet. Chem.*, **1998** 556 239
- 103 Seayad A, Jayasree S, Chaudhari R V, *Catal. Lett.*, **1999** 61 99
- 104 (a) Sheldon R A, Maat L, Papadogianakis G, (Hoechst Celanese Corp.) US 5536874 **1996**
(b) Papadogianakis G, Maat L, Sheldon R A, *J. Chem. Tech. Biotechnol.*, **1997** 70 83
- 105 Jang E J, Lee K H, Lee J S, Kim Y G, *J. Mol. Catal. A: Chem.*, **1999** 144 431
- 106 Xia C, Li Y, Xie B, Sun W, CN 1289759 A, Apr **2001**
- 107 Souma Y, Tsumori N, Wilner H, Xu Q, Mori H, Morisaki Y, *J. Mol. Catal. A: Chem.*, **2002** 189(1) 67
- 108 Tsai C J, Liu Y L, Tsai H C, US Appl. No. US 2003130540 A1, Jul **2003**
- 109 Xie B, Xia C, Lu S, Chen K, Kou Y, Yin Y, *Tet. Lett.*, **1998** 39 7365
- 110 Tsumori N, Xu Q, Souma Y, Mori H, *J. Mol. Catal. A: Chem.*, **2002** 179(1-2) 271
- 111 Consorti C S, Ebeling G, Dupont J, *Tet. Lett.*, **2002** 43(5) 753
- 112 Dunn B C, Guenneau C, Hilton S A, Pahnke J, Eyring E M, Dworzanski J, Meuzelaar H L C, Hu J Z, Soulm M S, Pugmire R J, *Energy & Fuels*, **2002** 16(1) 177
- 113 Anderson S A, Root T W, *J. Catal.*, **2003** 217(2) 396
- 114 Charles G, Michelle R, US Pat. Appl. No. US 2003212295 A1, Nov **2003**
- 115 Peng F, *J. Natural Gas Chem.*, **2003** 12(1) 31
- 116 Magna L, Oliver B H, Harry S, Commereuc D, Eur. Appl. No. EP 1364936 A1, Nov **2003**
- 117 Cao Y, Hu J, Yang O, Dai W, Fan K, *Chem. Commun.*, **2003** 7 908
- 118 Yang P, Cao Y, Hu J, Dai W, Fan K, *Appl. Catal. A: General*, **2003** 241(1-2) 363
- 119 Li F, Huang Z, Zou J, Pan P, Yuan G, *Appl. Catal. A: General*, **2003** 251(2) 295
- 120 Song L, Yan Z, Shen S, *Preprints of Symposia – ACS*, **2004** 49(1) 358
- 121 Zoeller J R, Singleton A H, Tsutin G C, Carver D L, PCT Appl. No. WO 2003000409 A1, Jan **2003**
- 122 Tao L, Tsumori N, Souma Y, Xu Q, *Chem. Commun.*, **2003** 16 2070
- 123 Zoeller J R, Singleton A H, Tustin G C, Carver D L, US 6509293 B1, Jan **2003**
- 124 Yoshihiro S, Chinnasamy R, Nakamura R, Kubota Y, Miwa M, *Synthesis*, **2003** 4 501
- 125 Li F, Zou J, Yuan G, *Catal. Lett.*, **2003** 89(1-2) 115
- 126 Cao W, Zhang H, Yuan Y, *Catal. Lett.*, **2003** 91(3-4) 243
- 127 Kron T E, Noskov Yu G, Terekhova M I, Petrov E S, *Russ. J. Phys. Chem.*, **1996** 70 76
(translated from *Zhurnal Fizicheskoi Khimii*, **1996** 70 82)
- 128 (a) Noskov Y G, Terekhova M I, Petrov E S, *Kinetika kataliz*, **1989** 30 234 (b) Noskov Y G, Novikov N A, Terekhova M I, Petrov E S, *Kinetika kataliz*, **1991** 32 331 (c) Noskov Y G, Terekhova M I, Petrov E S, *Kinetics and Catalysis*, **1993** 34 898 (d) Noskov Y G, Petrov E S, *Kinetics and Catalysis*, **1993** 34 902 (e) Noskov Y G, Petrov E S, *Kinetics and Catalysis*, **1994** 35 672 (translated from *Kinetika i Kataliz*, **1994** 35 728 (f) Noskov Y G, Petrov E S, *Kinetics and Catalysis*, **1997** 38 520 (translated from *Kinetika i Kataliz*, **1997** 38 568)
- 129 Ercoli R, Signorini G, Santambrogio E, *Chim. e ind. (Milan)*, **1960** 42 587
- 130 Yoshida H, Sugita N, Kudo K, Takezaki Y, *Bull. Chem. Soc. Jpn.*, **1976** 49 2245.
- 131 Seayad A M, Jayasree S, Mills P L, Chaudhari R V, *Ind. Eng. Chem. Res.*, **2003** 42(12) 2496
- 132 (a) Miyaura N, Yamada Y, Suzuki A, *Tetrahedron Lett.*, **1979** 20 3437 (b) Miyaura N, Suginome H, Suzuki A, *Tetrahedron Lett.*, **1981** 22 127 (c) Miyaura N, Yamada K, Suginome H, Suzuki A, *J. Am. Chem. Soc.*, **1985** 107 972

- 133 (a) Soderquist J A, Santiago B, *Tetrahedron Lett.*, **1990** 31(39) 5541 (b) Soderquist J A, Leon-Colon G, *Tetrahedron Lett.*, **1991** 32(1) 43
- 134 Aliprantis A O, Canary J W, *J. Am. Chem. Soc.*, **1994** 116(15) 6985
- 135 Genet J P, Linguist A, Blard E, Mouries V, Sabignac M, Vaultier M, *Tetrahedron Lett.*, **1995** 36(9) 1443
- 136 Moreno-Manas M, Pajuelo F, Pleixats R, *J. Org. Chem.*, **1995** 60(8) 2396
- 137 Percec V, Bae J Y, Hill D H, *J. Org. Chem.*, **1995** 60(4) 1060
- 138 Anderson J C, Namli H, Roberts C A, *Tetrahedron Lett.*, **1997** 53(44) 15123
- 139 Larhed M, Hallberg A, *J. Org. Chem.*, **1996** 61(26) 9584
- 140 Badone D, Baroni M, Cardamone R, Ielmini A, Guzzi U, *J. Org. Chem.*, **1997** 62(21) 7170
- 141 Coudret C, Mazenc V, *Tetrahedron Lett.*, **1997** 38(30) 5293
- 142 Indolese A F, *Tetrahedron Lett.*, **1997** 38(20) 3153
- 143 Shen W, *Tetrahedron Lett.*, **1997** 38(32) 5575
- 144 Ridgway B H, Woerpel K A, *J. Org. Chem.*, **1998** 63(3) 458
- 145 Holzapfel C W, Dwyer C, *Heterocycles* **1998** 48(8) 1513
- 146 Zhand H, Kwonf F Y, Tian Y, Chang K S, *J. Org. Chem.*, **1998** 63(20) 6886
- 147 Bumagin N A, Bykov V V, *Tetrahedron* **1997** 53(42) 14437
- 148 Old D W, Wolfe J P, Buchwald S L, *J. Am. Chem. Soc.*, **1998** 120(37) 9722
- 149 Bei X, Turner H W, Weinberg W H, Guram A S, Peterson J L, *J. Org. Chem.*, **1999** 64(18) 6797
- 150 McGuinness D S, Cavell K J, Skelton B W, White A H, *Organometallics*, **1999** 18(9) 1596
- 151 Zakharkin L I, Balaguroeva E V, Lebedev V N, *Russ. J. Gen. Chem.*, **1998** 68(6) 922
- 152 Weskamp T, Bohm V P W, Herrmann W A, *J. Organomet. Chem.*, **1999** 585(2) 348
- 153 Wolfe J P, Buchwald S L, *Angew. Chem.*, **1999** 38(16) 2413
- 154 Venkatraman S, Li C-J, *Org. Lett.*, **1999** 1(7) 1133
- 155 Bei X, Crevier T, Guram A S, Jandeleit B, Powers T S, Turner H W, Uno T, Weinberg W H, *Tetrahedron*, **1999** 40(20) 3855
- 156 Zhang C, Huang J, Trudell M L, Nolan S P, *J. Org. Chem.*, **1999** 64(11) 3804
- 157 Albisson D A, Bedford R B, Noelle S P, Lawrence S E, *Chem. Commun.*, **1998** 19 2095
- 158 Haddach M, McCarthy J R, *Tetrahedron Lett.*, **1999** 40(16) 3109
- 159 (a) Tinkl M, Hafner A, (Ciba Specialty Chemicals Holding Inc., Switzerland) PCT Intl. Appl. No. WO 9947474 A1, Sept **1999** (b) Tinkl M, Hafner A, (Ciba Specialty Chemicals Holding Inc., Switzerland) PCT Intl. Appl. No. WO 2001016057 A1, Mar **2001**
- 160 Oehme G, Paetzold E, Frank M, (iFOK, Germany) DE 19809166 A1, Sept **1999**
- 161 McGuinness D S, Cavell K J, *Organometallics* **2000** 19(5) 741
- 162 Wolfe J P, Singer R A, Yang B H, Buchwald S L, *J. Am. Chem. Soc.*, **1999** 121(41) 9550
- 163 (a) Guram A, Bei X, Powers T, Jandeleit B, Crevier T, (Symyx Technologies Inc., USA) PCT Intl. Appl. No. WO 2000008032 A1, Feb **2000** (b) Guram A, Bei X, Powers T, Jandeleit B, Crevier T, (Symyx Technologies Inc., USA) US 6124476 A, Sept **2000** (c) Guram A, Bei X, (Symyx Technologies Inc., USA) US 6268513 B1, Jul **2001**
- 164 Littke A F, Dai C, Fu G C, *J. Am. Chem. Soc.*, **2000** 122(17) 4020
- 165 Macnitzki P, Tepper M, Wenz K, Kirsten S, Othmer H, Herdtweck E, *J. Organomet. Chem.*, **2000** 602(1-2) 158
- 166 (a) Zim D, Gruber A S, Ebeling G, Dupont J, Momteiro A L, *Org. Lett.*, **2000** 2(18) 2881 (b) Zim D, Monteiro A L, Dupont J, *Tetrahedron Lett.*, **2001** 41(43) 8199
- 167 Zapf A, Beller M, *Chem. Eur. J.*, **2000** 6(10) 1830
- 168 (a) Bohm V P W, Gstottmayr C W K, Weskamp T, Herrmann W A, *J. Organomet. Chem.*, **2000** 595(2) 186 (b) Gstottmayr C W K, Bohm V P W, Herdtweck E, Grosche M, Herrmann W A, *Angew. Chem. Int. Ed.*, **2002** 41(8) 1363
- 169 Haber S, Meudt A, Norenberg A, Scherer S, Vollmueller F, (Clariant G. m. b. H. Germany) DE 19920847 A1, Nov **2000**
- 170 Weissman H, Milstein D, *Chem. Commun.*, **2000** 18 1901

- 171 Chen H, Deng M-Z, *Perkin 1*, **2000** 10 1609
- 172 Yang G-S, Xie X-J, Zhao G, Ding Y, *J. Fluorine Chem.*, **1999** 98(2) 159
- 173 Leadbeater N E, Resouly S M, *Tetrahedron*, **1999** 55(40) 11889
- 174 Zim D, Lando V R, Dupont J, Monteiro A L, *Org. Lett.*, **2001** 3(19) 3049
- 175 Sava X, Ricard L, Mahtey F, Le Foch P, *Organometallics*, **2000** 19(23) 4899
- 176 Magill A M, McGuinness D S, Cavell K J, Britovsek G J P, Gibson V C, White A J P, Williams D J, White A H, Skelton B W, *J. Organomet. Chem.*, **2001** 617-618 546
- 177 Munoz M P, Martin-Matute B, Fernandez-Rivas C, Cardenas D J, Echavarren A M, *Adv. Synth. Catal.*, **2001** 343(4) 338
- 178 Yin J, Buchwald S L, *J. Am. Chem. Soc.*, **2000** 122(48) 12051
- 179 Shaughnessey K H, Booth R S, *Org. Lett.*, **2001** 3(17) 2757
- 180 Mazet C, Gade L H, *Organometallics*, **2001** 20(20) 4144
- 181 Andreu M G, Zapf A, Beller M, *Chem. Commun.*, **2000** 24 2475
- 182 Yao M L, Deng M Z, *Tetrahedron Lett.*, **2000** 41(47) 9038
- 183 Fustner A, Leitner A, *Synlett*, **2001** 2 290
- 184 Zapf A, Ehrentraut A, Beller M, *Angew. Chem. Int. Ed.*, **2000** 39(22) 4153
- 185 Grasa G A, Viciu M S, *Organometallics*, **2002** 21(14) 2866
- 186 Indolese A F, Schnyder A, Aemmer T B, Nsenda T B, Portmann R B, Ubelhart M B, *Synthetic Methods of Organometallic and Inorganic Chemistry, Thieme, Stuttgart*, **2002** 10 105
- 187 Clarke M L, Cole-Hamilton D J, Woollins J D, *J. Chem. Soc. Dalton Trans.*, **2001** 19 2721
- 188 Castanet A S, Colober F, Desmurs J R, Schlama T, *J. Mol. Catal. A: Chemical*, **2002** 182-183 481
- 189 Smith P J, Welton T, *ACS Symposium Series USA*, **2002** 818 310
- 190 Alonso D A, Najers C, Pacheco M C, *J. Org. Chem.*, **2002** 67(16) 5588
- 191 Tao B, Boykin D W, *Tetrahedron Lett.*, **2002** 43(28) 4955
- 192 Dupuis C, Adiey K, Charruault L, Michelet V, Savignac M, Genet J P, *Tetrahedron Lett.*, **2001** 42(37) 6523
- 193 (a) Bedford R B, Hazelwood S L, Albisson D A, *Organometallics*, **2002** 21(13) 2599 (b) Bedford R B, Cazin C S J, *Chem. Commun.*, **2001** 17 1540 (c) Bedford R B, Hazelwood S L, Limmert M E, Albisson D A, Draper S M, Scully P N, Coles S J, Hursthouse M B, *Chem. Eur. J.*, **2003** 9(14) 3227 (d) Bedford R B, Hazelwood S L, Horton P N, Hursthouse M B, *Dalton Trans.*, **2003** 21 4164
- 194 (a) Feuerstein M, Duocet H, Santelli M, *Tetrahedron Lett.*, **2001** 42(38) 6667 (b) Feuerstein M, Laurenti D, Doucet H, Santelli M, *Synthesis*, **2001** 15 2320
- 195 (a) Molander G A, Biolatto B, *Org. Lett.*, **2002** 4(11) 1867 (b) Molander G A, Katona B W, Machrouhi F, *J. Org. Chem.*, **2002** 67(24) 8416
- 196 Liu S-Y, Choi M J, Fu G C, *Chem. Commun.*, **2001** 23 2408
- 197 (a) Leadbeater N E, Marco M, *Org. Lett.*, **2002** 4(17) 2973 (b) Leadbeater N E, Marco M, *J. Org. Chem.*, **2003** 68(3) 888 (c) Leadbeater N E, Marco M, *Angew. Chem. Int. Ed.* **2003** 42(12) 1407
- 198 Beller M, Gomez-Andreo M, Zapf A, Karch R, Kleinmaechter I, Briel O, (Omg Ag & Co. Kg, Germany) Eur. Pat. Appl. No. EP 1199292 A1, Apr **2002**
- 199 Rocaboy C, Gladysz J A, *Tetrahedron*, **2002** 58(20) 4007
- 200 Liu X, Dend M-Z, *Chem. Commun.*, **2002** 6 622
- 201 Andrus M B, Song C, *Org. Lett.*, **2001** 3(23) 3761
- 202 Eichenseher S, Kromm K, Delacroix O, Gladysz J A, *Chem. Commun.*, **2002** 10 1046
- 203 Herrbach A, Merinetti A, Baudoin O, Guenard D, Gueritte F, *J. Org. Chem.*, **2003** 68(12) 4897
- 204 Bedford R B, Cazin C S J, Hazelwood S L, *Angew. Chem. Int. Ed.* **2002** 41(21) 4120
- 205 Adjabeng G, Brenstrum T, Wilson J, Frampton C, Robertson A, Hiilhouse J, McNulty J, Capretta A, *Org. Lett.*, **2003** 5(6) 953

- 206 Botella L, Najera C, *J. Organomet. Chem.*, **2002** 663(1-2) 46
- 207 Couve-Bonnaire S, Carpentier J-F, Morteaux A, Castanet Y, *Tetrahedron*, **2003** 59(16) 2793
- 208 Bedford R B, Blake M E, Butts C P, Holder D, *Chem. Commun.*, **2003** 4 466
- 209 Hong F-E, Chang Y-C, Chang C-P, Huang Y-L, *Dalton Trans.*, **2004** 1 157
- 210 Rosa G R, Ebeling G, Dupont J, Monteiro A L, *Synthesis*, **2003** 18 2894
- 211 (a) Scivanti A, Baghetto V, Matteoli U, Antonaroli S, Marini A F, Paolesse R, *Tetrahedron Lett.*, **2004** 45(30) 5861 (b) Scivanti A, Baghetto V, Matteoli U, Antonaroli S, Marini A, Crociani B, *Tetrahedron*, **2005** 61(41) 9752
- 212 Kolodziuk R, Penciu A, Tollabi M, Framery E, Goux-Henry C, Iourtchenko A, Sinou D, *J. Organomet. Chem.*, **2003** 687(2) 384
- 213 Friesen R W, Trimble L A, *Can. J. Chem.*, **2004** 82(2) 206
- 214 tao X, Zhao Y, Shen D, *Synlett*, **2004** 2 359
- 215 (a) Li J-H, Liu W-J, *Org. Lett.*, **2004** 6(16) 2809 (b) Li J-H, Liu W-J, Xie Y-X, *J. Org. Chem.*, **2005** 70(14) 5409
- 216 (a) Dai W-M, Li Y, Zhang Y, Lai K W, Wu J, *Tetrahedron Lett.*, **2004** 45(9) 1999
- 217 Buchwald S L, Huang X, Zim D, (MIT, USA) WO 2004052939 A2, Jun **2004**
- 218 Eichenseher S, Delacroix O, Kromm K, Hampel F, Gladysz J A, *Organometallics*, **2005** 24(2) 245
- 219 Altenhoff G, Goddard R, Lehmann C W, Glorius F, *J. Am. Chem. Soc.*, **2004** 126(46) 15195
- 220 Dai M, Liang B, Wang C, You Z, Xiang J, Dong G, Chen J, Yang Z, *Adv. Synth. Catal.*, **2004** 346(13-15) 1669
- 221 Harkal S, Rataboul F, Zapf A, Fuhrmann C, Riermeier T, Monsees Axel, Beller M, *Adv. Synth. Catal.*, **2004** 346(13-15) 1742
- 222 Sliger M D, Broker G A, Griffin S T, Rogers R D, Shaughnessy K H, *J. Organomet. Chem.*, **2005** 690(6) 1478
- 223 Whittall J, Pickett T E, (Stylacats Limited, UK) UK Pat. Appl. No. GB 2410247 A1, Jul **2005**
- 224 (a) Oezdemir I, Goek Y, Guerbuez N, Cetinkaya E, Cetinkaya B, *Heteroatom Chem.*, **2004** 15(6) 419 (b) Oezdemir I, Demir S, Yasar S, Cetinkaya B, *Appl. Organomet. Chem.*, **2005** 19(1) 55
- 225 Moncada A I, Khan M A, Slaughter L M, *Tetrahedron Lett.*, **2005** 46(9) 1399
- 226 Gong J, Liu G, Du C, Zhu Y, Wu Y, *J. Organomet. Chem.*, **2005** 690(17) 3963
- 227 Najera C, Gil-Molto J, Karlstroem S, *Adv. Synth. Catal.*, **2004** 346(13-15) 1798
- 228 Korolev D N, Bumagin N A, *Tetrahedron Lett.*, **2005** 46(34) 5751
- 229 Tang Z-Y, Hu Q-S, *Adv. Synth. Catal.*, **2004** 346(13-15) 1635
- 230 Hong F-E, Ho Y-J, Chang -C, Huang Y-L, *J. Organomet. Chem.*, **2005** 690(5) 1249
- 231 Itabashi T, Kamikawa T, (Sumitomo Chemical Co. Ltd. Japan) Jpn. Kokkai Tokkyo Koho JP 2005008578 A2, Jan **2005**
- 232 Jang S-B, *Tetrahedron Lett.*, **1997** 38(10) 1793
- 233 Larhed M, Lindeberg G, Hallberg A, *Tetrahedron Lett.*, **1996** 37(45) 8219
- 234 Fenger I, Le Drian C, *Tetrahedron Lett.*, **1998** 39(24) 4287
- 235 (a) Kabalka G W, Pagni R M, Hair C M, *Org. Lett.*, **1999** 1(9) 1423 (b) Kabalka G W, Namboodiri V, Wang L, *Chem. Commun.*, **2001** 8 775 (c) Kabalka G W, Pagni R M, Wang L, Namboodiri V, Hair C M, *Green Chem.*, **2000** 2(3) 120 (d) Kabalka G W, Pagni R M, Hair C M, Norris J L, Wang L, Namboodiri V, *ACS Symposium Series* **2001** 783 148
- 236 (a) Shezad N, Oakes R S, Clifford A A, Rayner C M, *Tetrahedron Lett.*, **1999** 40(11) 2221 (b) Shezad N, Oakes R S, Clifford A A, Rayner C M, *Chemical Industries*, **2001** 82 459
- 237 Zhang T Y, Allen M J, *Tetrahedron Lett.*, **1999** 40(32) 5813
- 238 Verma R S, Naicker K P, *Tetrahedron Lett.*, **1999** 40(3) 439

- 239 (a) Li Y, Hong X M, Collard D M, El-Sayed M A, *Org. Lett.*, **2000** 2(15) 2385 (b) Li Y, El-Sayed M A, *J. Phys. Chem. B*, **2001** 105(37) 8938 (c) Li Y, Boone E, El-Sayed MA, *Langmuir*, **2002** 18(12) 4921
- 240 Gravel M, Berube C D, Hall D G, *J. Comb. Chem.*, **2000** 2(3) 228
- 241 Bergbreiter D E, Osburn P L, Wilson A, Sink E M, *J. Am. Chem. Soc.*, **2000** 122(38) 9058
- 242 Paetzold E, Oehme G, *J. Mol. Catal. A: Chem.*, **2000** 152(1) 69
- 243 Lipshutz B H, Sclafani J A, Blomgren P A, *Tetrahedron*, **2000** 56(15) 2139
- 244 Pathak S, Greci M T, Kwong R C, Mercado K, Prakash G K S, Olah G A, *Chem. Mater.*, **2000** 12(7) 1985
- 245 (a) Cortes J, Moreno-Manas M, Pleixats R, *Eur. J. Org. Chem.*, **2000** 2 239 (b) Moreno-Manas M, Pleixats R, Villaroya S, *Organometallics*, **2001** 20(22) 4524
- 246 (a) Kosslick H, Monnich I, Paetzold E, Fuhrmann H, Fricke R, Muller D, Oehme G, *Microporous Mesoporous Mater.*, **201** 44-45 537 (b) Paetzold E, Oehme G, Fuhrmann H, Richter M, Eckelt R, Pohl M-M, Kosslick H, *Microporous Mesoporous Mater.*, **2001** 44-45 517
- 247 LeBlond C R, Andrews A T, Sun Y, Sowa J R, *Org. Lett.*, **2001** 3(10) 1555
- 248 Miyaura N, (Mitsubishi Rayon Co. Ltd. Japan), PCT Appl. No WO2001068657 A1, Sept **2001**
- 249 Kogan V, Aizenshtat Z, Popovitz-Biro R, Neuman R, *Org. Lett.*, **2002** 4(20) 3529
- 250 (a) Yamada Y M A, Takeda K, Takahashi H, Ikegami S, *Org. Lett.*, **2002** 4(20) 3371 (b) Yamada Y M A, *Chemical Pharma. Bull.*, **2005** 53(7) 723
- 251 Colacot T J, Gore E S, Kuber A, *Organometallics*, **2002** 21(16) 3301
- 252 Uozumi Y, Nakai Y, *Org. Lett.*, **2002** 4(17) 2997
- 253 Zhang J, Aszodi J, Chartier C, L'hermite N, Weston j, *Tetrahedron Lett.*, **2001** 42(38) 6683
- 254 (a) Sakurai H, Tsukuda T, Hirao T, *J. Org. Chem.*, **2002** 67(8) 2721 (b) Sakurai H, Hirao T, Negishi Y, Tsunakawa H, Tsukuda T, *Transac. Mater. Res. Soc. Jpn.*, **2002** 27(1) 185
- 255 Ley S V, Ramarao C, Gordon R S, Holmes A B, Morrison A J, McConvey I F, Shirley I M, Smith S C, Smith M D, *Chem. Commun.*, **2002** 10 1134
- 256 Kim S-W, Kim M, Lee W Y, Hyeon T, *J. Am. Chem. Soc.*, **2002** 124(26) 7642
- 257 (a) Choudary B M, Madhi S, Chowdari N S, Kantam M L, Sreedhar B, *J. Am. Chem. Soc.*, **2002** 124(47) 14127 (b) Choudary B M, Madhi S, Kantam M L, Sreedhar B, *J. Am. Chem. Soc.*, **2004** 126(8) 2292 (c) Choudary B M, Madhi S, Chowdari N S, Kantam M L, Sreedhar B, (CSIR, India), US Pat. Appl. No. US 2004192542 A1, Sept **2004**
- 258 Bulut H, Artok L, Yilmazu S, *Tetrahedron Lett.*, **2002** 44(2) 289
- 259 Pittelkow M, Moth-Poulsen K, Boas U, Christensen J B, *Langmuir*, **2003** 19(18) 7682
- 260 Wade J V, Kruger C A, *J. Combi. Chem.*, **2003** 5(3) 267
- 261 Hebel A, Haag R, *J. Org. Chem.*, **2002** 67(26) 9452
- 262 (a) Corma A, Garcia H, Levya A, *Appl. Catal. A Gen.*, **2002** 236(1-2) 179 (b) Corma A, Garcia H, Levya A, Primo A, *Appl. Catal. A: Gen.*, **2004** 257(1) 77
- 263 (a) Baleizao C, Corma A, Garcia H, Levya A, *J. Org. Chem.*, **2004** 69(2) 439 (b) Corma A, Das D, Garcia H, Levya A, *J. Catal.*, **2005** 229(2) 322
- 264 (a) Shimizu K, Maruyama R, Komai S, Kodama T, Kitayama Y, *J. Catal.*, **2004** 227(1) 202 (b) Shimizu K, Koizumi S, Hatamachi T, Yoshida H, Komai S, Kodama T, Kitayama Y, *J. Catal.*, **2004** 228(1) 141
- 265 Paul S, Clark J H, *Green Chem.*, **2003** 5(5) 635
- 266 Horniakova J, Raja T, Kubota Y, Sugi Y, *J. Mol. Catal. A: Chem.*, **2004** 217(1-2) 73
- 267 Bedford R B, Coles S J, Hursthouse M B, Scordia V J M, *Dalton Transac.*, **2005** 5 991
- 268 Crudden C M, Sateesh M, Lewis R, *J. Am. Chem. Soc.*, **2005** 127(28) 10045
- 269 (a) Stevens P D, Li G, Fan J, Yen M, Gao Y, *Chem. Commun.*, **2005** 35 4435 (b) Stevens P D, Fan J, Gardimalla H M R, Yen M, Gao Y, *Org. Lett.*, **2005** 7(11) 2085
- 270 Polackova V, Hutka M, Toma S, *Ultrasonics Sonochemistry*, **2005** 12(1-2) 99

- 271 (a) Cravotto G, Beggiato M, Penoni A, Palmisano G, Tollari S, Leveque J-M, Bonrath W, *Tetrahedron Lett.*, **2005** 46(13) 2267 (b) Cravotto G, Palmisano G, Tollari S, Nano G M, Penoni A, *Ultrasonics Sonochemistry*, **2005** 12(1-2) 91
- 272 Zhang G, *Synthesis*, **2005** 4 537
- 273 Capka M, Svoboda P, Kraus M, Hetflejš J, *Chem. Ind.*, **1972** 650
- 274 Kraus M, *Collect. Czech. Chem. Commun.*, **1974** 39 1318
- 275 Rollmann L D, *Inorg. Chim. Acta*, **1972** 6 137
- 276 Allum K G, Hancock R D, Howell I V, Pitkethly R C, Robinson P J, *J. Organomet. Chem.*, **1975** 87 189
- 277 Takaishi N, Imai H, Bertelo C A, Stille J K, *J. Am. Chem. Soc.*, **1976** 98 5400
- 278 Kaneda K, Imanaka T, *Trends Org. Chem.*, **1991** 2 109
- 279 (a) Mitchell T D, Whitehurst D D, *3rd Am. Conf. Catal. Soc.*, San Francisco **1974** (b) Grubbs R H, Kroll L C, Sweet E M, *J. Makromol. Sci. Chem.*, **1973** 7 1047
- 280 Grubbs R H, Gibbons C, Kroll L C, Bonds W D, Brubaker C H, *J. Am. Chem. Soc.*, **1973** 95 2373
- 281 Collman J P, Hegedus L S, Cooke M P, Norton J R, Dolcetti G, Marquardt D N, *J. Am. Chem. Soc.*, **1972** 94 1789
- 282 Hartley F R, Vezey P N, *Adv. Organomet. Chem.*, **1977** 15 189
- 283 (a) Kresge C T, Leonowicz M E, Roth W J, Vartuli J C, Beck J S, *Nature*, **1992** 359 710 (b) Beck J S, Vartuli J C, Roth W J, Leonowicz M E, Kresge C T, Schmitt K D, Chu C T, Olson D H, Sheppard E W, McCullen S B, Higgins J B, Schlenker J L, *J. Am. Chem. Soc.*, **1992** 114 10834
- 284 (a) Yanagisawa T, Shimizu T, Kuroda K, Kato C, *Bull. Chem. Soc. Jpn.*, **1990** 63 988 (b) Inagaki S, Fukushima Y, Kuroda K, *J. Chem. Soc. Chem. Commun.*, **1993** 680
- 285 (a) Zhao D, Feng J, Huo Q, Melosh N, Fredrickson G H, Chmelka B F, Stucky G D, *Science*, **1998** 279 548 (b) Zhao D, Huo Q, Feng J, Chmelka B F, Stucky G D, *J. Am. Chem. Soc.*, **1998** 120 6024
- 286 Stein A, Melde B J, Schrodner R C, *Adv. Mater.*, **2000** 12(19) 1403
- 287 (a) Beck J S, Calabro D C, McCullen S B, Pelrine B P, Schmitt K D, Vartuli J C, *Method for Functionalising Synthetic Mesoporous Crystalline Material* (Mobil Oil Corp.), **1992** (b) Kimura T, Saeki S, Sugahara Y, Kuroda K, *Langmuir*, **1999** 15 2794
- 288 Zhao X S, Lu G Q, *J. Phys. Chem. B*, **1998** 102 1556
- 289 (a) Anwender R, Palm C, Stelzer J, Groeger O, Engelhardt G, *Stud. Surf. Sci. Catal.*, **1998** 117 135 (b) Anwender R, Nagl I, Widenmeyer M, Engelhardt G, Groeger O, Palm C, Röser T, *J. Phys. Chem. B*, **2000** 104 3532
- 290 Lim M H, Blanford C F, Stein A, *J. Am. Chem. Soc.*, **1997** 117 4090
- 291 Lim M H, Blanford C F, Stein A, *Chem. Mater.*, **1998** 10 467
- 292 van Rhijn W M, De Vos D E, Sels B F, Basaert W D, Jacobs P A, *Chem. Commun.*, **1998** 317
- 293 Lim M H, Stein A, unpublished results
- 294 Clark J H, Macquarrie D J, *Chem. Commun.*, **1998** 853
- 295 Brunel D, *Microporous Mesoporous Mater.*, **1999** 27 329
- 296 Díaz J F, Balkus Jr K J, Bedioui F, Kurshev V, Kevan L, *Chem. Mater.*, **1997** 9 61
- 297 Mukhopadhyay K, Mandale A B, Chaudhari R V, *Chem. Mater.*, **2003** 1766
- 298 Tatsumi T, Koyano K A, Tanaka Y, Nakata S, *Stud. Surf. Sci. Catal.*, **1998** 117 143
- 299 Lim M H, Stein A, *Chem. Mater.*, **1999** 11 3285
- 300 Shephard D S, Zhou W, Maschmeyer T, Matters J M, Roper C L, Parsons S, Johnson B F G, Duer M J, *Angew. Chem. Int. Ed. Engl.*, **1998** 37 2719
- 301 de Juan F, Ruiz-Hitzky E, *Adv. Mater.*, **2000** 12 430
- 302 (a) Feng X, Fryxell G E, Wang L, Kim A Y, Liu J, Kemner K M, *Science* **1997** 276 923 (b) van Rhijn W, DeVos D, Bossaert W, Bullen J, Wouters B, Grobet P, Jacobs P, *Stud. Surf. Sci. Catal.*, **1998** 117 183

- 303 Dai S, Burkeigh M C, Shin Y, Morrow C C, Barnes C E, Xue Z, *Angew. Chem. Int. Ed. Engl.*, **1999** 1999 1235
- 304 Sanchez C, Ribol F, *New J. Chem.*, **1994** 18 1007
- 305 (a) Burkett S L, Sims S D, Mann S, *Chem. Commun.*, **1996** 1367 (b) Sims S D, Burkett S L, Mann S, *Mater. Res. Soc. Symp. Proc.*, **1996** 431 77 (c) Macquarrie D J, *Chem. Commun.*, **1996** 1961 (d) Huo Q, Margolese D I, Stucky G D, *Chem. Mater.*, **1996** 8 1147
- 306 Fowler C E, Burkett S L, Mann S, *Chem. Commun.*, **1997** 1769
- 307 Babonneau F, Leite L, Fontlupt S, *J. Mater. Chem.*, **1999** 9 175
- 308 Macquarrie D J, Jackson D B, Mdoe J E G, Clark J H, *New J. Chem.*, **1999** 23 539
- 309 Bossaert W D, De Vos D E, Van Rhijn W M, Bullen J, Grobet P J, Jacobs P A, *J. Catal.*, **1999** 182 156
- 310 (a) Richer R, Mercier L, *Chem. Commun.*, **1998** 1775 (b) Brown J, Richer R, Mercier L, *Microporous Mesoporous Mater.*, **2000** 37 41
- 311 Hall S R, Fowler C E, Lebeau F, Mann S, *Chem. Commun.*, **1999** 201
- 312 Macquarrie D J, *Green Chem.*, **1999** 195

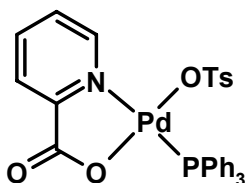
Chapter 2

Anchored Pd - Complexes in Mesoporous Matrices: Novel Catalysts for Carbonylation of Olefins and Alcohols

This chapter describes the synthesis of novel immobilized Pd-catalysts by anchoring inside the mesoporous materials, and thorough characterization thereafter, using powder XRD, multinuclear CPMAS NMR, XPS, SEM, TEM, ICP-AES etc. An improved technique for anchoring of the catalytically active palladium complexes to the interior walls of the mesoporous channels using a molecular anchor APTS, has been discussed, reducing the chance of leaching of the complexes thus, stabilizing the catalyst entity. The application of these catalysts for the carbonylation of olefins and alcohols has also been presented here. The different parametric studies on the activity and selectivity of the reaction have been performed for the proper understanding and optimization of the catalyst system. The anchored Pd-complexes were found to be highly active, selective, stable and recyclable, and thus were demonstrated to be efficient and truly heterogeneous carbonylation catalysts.

2.1 Introduction

Carbonylation of aryl olefins and alcohols is one of the promising and environmentally benign routes to a wide range of specialty products, of which the synthesis of aryl-propionic acids is an important application, as these form a useful class of non-steroidal anti-inflammatory agents.¹ This reaction is often considered as the best example of application of catalysis to develop “greener” routes for fine chemicals and pharmaceuticals, replacing stoichiometric organic synthesis routes, as established by the commercial success of the Hoechst-Celanese process for Ibuprofen². This involves the carbonylation route using a Pd-complex catalyst and 10% aqueous HCl as a promoter, where a very high regioselectivity to the branched isomeric product was obtained at fairly high pressures (16 – 35 MPa), which actually reduced to ~60% at lower pressures of ~ 6 – 7 MPa, even the activity was poor (TOF ~ 50 –70 h⁻¹) for the higher operating conditions. As already discussed in the previous chapter, i.e. Chapter 1, the later developments in the catalysts for minimizing the operating conditions have led to invention of different homogeneous Pd-complex catalysts. Recent developments have illustrated the necessity of an acid and an alkali-metal halide as the promoters for efficiently running of a low-pressure carbonylation process with very high TOF, and regioselectivity.³ The benchmark catalyst system has been recently described by Jayasree et al⁴ attaining significant enhancement in the activity (TOF = 800–2600 h⁻¹) and regioselectivity (> 99 %) for ibuprofen, at lower pressures (5 – 6 MPa) and temperature (388 K). They reported novel Pd-complexes consisting hemilabile N[∩]O chelating ligands as catalysts for the carbonylation reactions



**Pd(pyca)(PPh₃)(OTs)
complex**

of a variety of olefins and alcohols. A typical example being Pd(pyca)(PPh₃)(OTs) complex, [pyca=2-picolinate] as shown beside, which showed the breakthrough advancement in the low-pressure catalytic carbonylation. Even though considerable advancement in homogeneous carbonylation catalysis was achieved, the separation of the precious metal catalyst from the reaction mixture and its reuse has been intriguing issues from commercial viewpoint. Moreover, following this reasoning, immense research efforts have been targeted towards development of separable catalysts to avail the advantages of both homogeneous and heterogeneous catalysts i.e. high activity, high selectivity and stability with facile and efficient separability. The heterogenized

homogeneous complex catalysts are the nearest to this notion and are visualized as the ideal candidates to address this problem.

Developments of biphasic systems using water as the catalyst-bearing phase was an interesting idea and several groups had investigated the biphasic Pd-complex catalyzed carbonylation of olefins and alcohols, e.g. Sheldon et al⁵, Tilloy et al⁶, Bertoux et al⁷, Goedheijt et al⁸. For most of these aqueous biphasic systems, the separation was efficient but the low catalytic activity and selectivity were really the negative aspects, as 50-70 % conversions were only reported with TOFs in the range of 40 – 240 h⁻¹. Aqueous biphasic catalyst developed by Jayasree et al⁹ using the aqueous analog of the Pd(pyca)(PPh₃)(OTs) i.e. Pd(pyca)(TPPTS)(OTs) was also a partially successful immobilized catalyst, as the catalyst recycled only under CO atmosphere and also had a low activity (TOF ~ 280 h⁻¹). Later supported catalysts using different matrices such as montmorillonite, activated charcoal etc. were attempted to obtain stable catalysts for carbonylation. Lee et al¹⁰ and Jang et al¹¹ had reported the montmorillonite supported Pd-catalysts. In the formers' report, ~88% conversion was reported in a long reaction duration of 24 h and in the later, 23-77% selectivity to ibuprofen was obtained at 4 MPa pressure and 398 K. The selectivity increased to ~97 % by the use of silyl ligands, but with a poor activity only (TOF ~ 3-10 h⁻¹). Several research groups had reported heterogeneous catalysts using activated charcoal as catalyst support for carbonylation reactions. Jayasree et al¹² had used Pd/C catalyst, whereby very high activity (TOF ~ 1675 – 3375 h⁻¹) and regioselectivity (>99 %) were obtained, but considerable leaching of Pd was observed during the reaction, which on cooling was to found to be reabsorbed onto the solid matrix. The high activity was attributed to the homogeneous Pd-catalyzed reaction, rather than the heterogeneous catalyst itself. Therefore, the problem of developing a true heterogeneous Pd-catalyst for carbonylation reactions remained an open challenge.

With this background, it was proposed to anchor palladium complexes inside inorganic matrices for carbonylation reactions with the objective of developing active, selective and stable heterogeneous catalysts. Pd-complexes having N[∩]O chelating ligands, e.g. Pd(pyca)(PPh₃)(OTs), [already established for showing the highest catalytic activity and regioselectivity] were selected for anchoring. The detailed discussion of the different types and modes of immobilization in mesoporous matrices has already been presented in the previous chapter (Section 1.6). This chapter

describes the novel heterogeneous palladium complex catalysts having Pd-complexes anchored inside mesoporous support matrices MCM-41, MCM-48 and SBA-15. In the following sections, the syntheses, characterization of these hybrid organic-inorganic composites will be discussed followed by the catalytic performance of them for the hydrocarboxylation of olefins and alcohols.

The immobilized palladium complex catalysts thus conceptualized were characterized thoroughly to validate true heterogeneity and integrity of the structure of metal complexes. The anchored palladium complexes were characterized using numerous techniques such as, powder X-ray diffraction study (XRD) [low angle scanning required for the mesoporous matrices], ^1H - ^{31}P cross-polarized magic-angle spinning nuclear magnetic resonance spectroscopy (^{31}P CP-MAS NMR), X-ray photoelectron spectroscopy (XPS), X-ray fluorescence spectroscopy (XRF), Fourier-transform infra-red spectroscopy (FT-IR), scanning electron microscopy (SEM), transmission electron microscopy (TEM), thermo-gravimetric analysis (TGA), elemental analysis, BET-surface area analysis and N_2 -adsorption desorption studies etc.

2.2 Experimental Section

2.2.1 Approach and Strategy of Immobilization

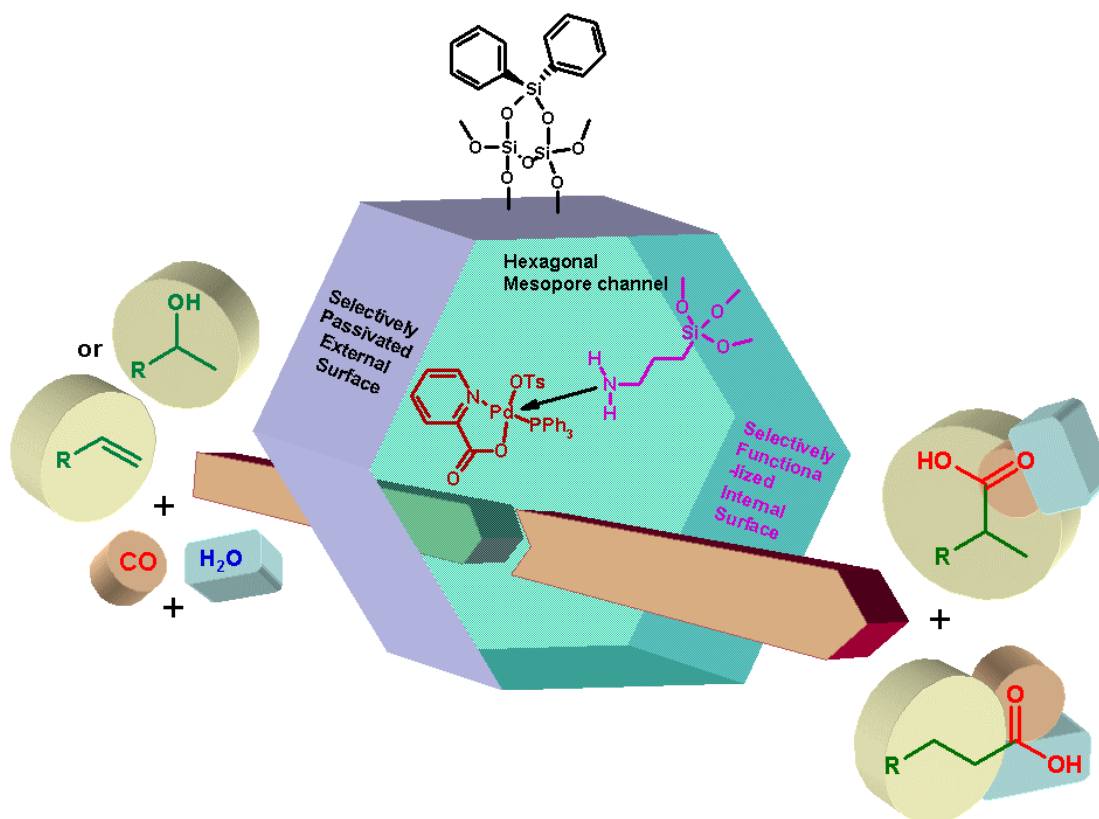
To select from a wide range of available support materials, a few criteria were employed, such as,

- (i) The matrix should be chemically non-invasive to the organometallic chemical environment of the anchored complex
- (ii) The matrix should accommodate the complex comfortably without distorting the conformational requirements for catalysis
- (iii) The matrix should be easy to synthesize and subsequently easy to functionalize using choice of functional materials for tailor-made purposes
- (iv) The matrix should have good stability to sustain the functionalization and application environments
- (v) The matrix should have distinguishable deterministic properties different from those of the complex, which could be used for characterization of the ensemble

A siliceous support matrix would be the most effective for the previously mentioned purpose, as it would not interfere with the palladium complex during synthesis as well as the carbonylation reactions. Microporous materials such as ZSM-5

etc. were handicapped of the smaller size of the 3-dimensional cavity in their framework to accommodate the relatively larger Pd-complexes, which might actually fit inside the cavity but with distortion, thus tampering the organometallic atmosphere conducive to catalysis. Therefore, mesoporous matrices appeared as the next option. Mesoporous materials have the characteristic pore dimensions of 20 to 300 Å, with very high surface areas and hydrothermal stability. These materials unlike simple silica are high surface area porous substances having long-range periodicity and tunable pore structures, e.g. MCM-41, MCM-48 etc.¹³ Also, the SBA class of materials have emerged lately as good candidates for support matrices. These SBAs are mesoporous materials with high porosity and surface areas, having larger pore-wall thickness than the MCM-41 and MCM-48 materials.¹⁴ Being larger than the microporous materials, these mesoporous materials might lose the organometallic complex if they are just entrapped physically. Therefore, the complexes need to be *chemically fixed* to the channel-walls to prevent leaching. The large pore dimensions (unit cell parameter, $a_0 \sim 35$ to 300 Å) would be expected to allow the easy access of the substrate(s) and reagent(s) to the catalytic sites and hence a good catalytic activity, along with the separation advantage by simple filtration, and reuse of the catalysts may be visualized. As discussed in the previous chapter (Section 1.7), the literature survey of the heterogeneously catalyzed carbonylation reactions presented the fact that the search for a truly heterogeneous carbonylation catalyst is still on, with issues like easy-to-make, non-leaching and recyclable catalyst with high catalytic activity etc. In case of MCM-41 & MCM-48, the selective passivation of the outer surface might work due to the smaller size of the channels (~ 35 Å), which enables kinetically rapid silylation (passivation) of the outer surface only. However, for SBA-15 materials, two different techniques of immobilization of the metal complex were undertaken, namely the post-synthesis grafting (different from that of M41s) and co-condensation techniques. This was primarily because of the larger pore size of the SBA-15 material (~ 80 -100 Å), where the access of the soluble graft molecule to the internal as well as the external surface is almost equal. Thus, if a selective passivation of the external surface is attempted, it may so happen that the graft molecule is distributed over the inner surface, in addition to the outer surface also resulting in a randomly passivated (rather randomly functionalized) support matrix. To immobilize Pd-complex catalysts 3-Aminopropyltrimethoxysilane (APTS) was used as the molecular graft to hold the metal

complex, while dichlorodiphenylsilane and hexamethyldisilazane (HMDS) were used as the passive graft to block the surface silanol groups on the external mesopore wall. A schematic representation of the novel anchored palladium complex catalysts for catalytic carbonylation is given in Scheme 2.1. To describe the general morphology of these hybrid composites a hexagonal motif of the support matrix has been chosen. The selectively passivated external surface ensures that the catalytically active palladium complex is anchored only to the internal wall of the mesoporous channels, thus minimizing the chances of the degradation and leaching of the palladium complex from the catalyst-composite under the stringent reaction conditions as required for the carbonylation reactions.



Scheme 2.1. Hydrocarboxylation of alkenes or alcohols to acids with heterogeneous catalysts

2.2.2 Materials

Styrene, substituted styrenes, *p*-toluenesulphonic acid monohydrate (TsOH), triphenyl phosphine (PPh₃), Palladium acetate Pd(OAc)₂, Picolinic acid (pycaH), fumed silica (high surface area ~380 m²g⁻¹), Cetyltrimethylammonium bromide, (CTABr), Dichlorodiphenylsilane (Ph₂SiCl₂), Hexamethyldisilazane (CH₃)₃Si-NH-Si(CH₃)₃, HMDS, 3-Aminopropyltrimethoxysilane (APTS), Phosphotungstic acid dodecahydrate, Pluronic P123 (nonionic block copolymer of ethylene oxide and propylene oxide, EO₂₀PO₇₀EO₂₀, M_{av}~ 5800), Tetraethyl orthosilicate (TEOS) were imported from Aldrich Chemicals, USA and were used as obtained. Reagents such as Lithium chloride (LiCl), Sodium hydroxide (NaOH), Sodium Chloride (NaCl), and acids such as Hydrochloric acid (HCl), Sulphuric Acid (H₂SO₄) were procured from Merck, India. Nitrogen (N₂) and Argon (Ar) were obtained from Indian Oxygen Limited, Mumbai, India while Carbon monoxide (CO, 99.9% purity) gas was imported from Matheson, USA. All solvents (Chloroform, CHCl₃; *n*-Hexane; Diethyl ether, Methyl ethyl ketone) were freshly distilled using known procedures and degassed using argon for 5-6 h, before use.

2.2.3 Syntheses

2.2.3.1 Synthesis of Pd(pyca)(PPh₃)(OTs) complex

The Pd(pyca)(PPh₃)(OTs) complex was prepared by the literature procedure^{4b}. In a typical synthesis 0.5g Pd(OAc)₂ (2.225 mmol), 0.274g pyridine-2-carboxylic acid (pycaH) (2.225 mmol), 0.846g *p*-toluenesulphonic acid (4.45 mmol) and 1.168g triphenylphosphine (4.45 mmol) were taken in minimum volume of chloroform in a round-bottomed flask and the mixture vigorously shaken at room temperature for a few minutes until all the components were completely dissolved and the solution turned bright yellow from the brownish yellow color of the Pd(OAc)₂ solution. The product was isolated as yellow oily mass by addition of *n*-hexane to the chloroform solution and vigorous shaking for 10 minutes. The oily material was washed with *n*-hexane and then with diethyl ether a number of times. Applying vacuum led to the formation of a yellow fluffy solid. For elemental and spectroscopic analysis, the complex was purified by re-precipitation from chloroform four times. The synthesized complex was preserved under argon and used hereafter as such.

2.2.3.2 Synthesis of Mesoporous Matrices

Three different mesoporous materials were synthesized keeping in mind their unique morphological characteristics. While the MCM-41 has hexagonal channel-like structures, MCM-48 has cubic structure and SBA-15 has hexagonal channel structure, they differ also in the dimension of their pores. MCM-41 and MCM-48 are medium-pore mesoporous matrices having d -values in the range of 35 to 50 Å, while SBA-15 is a large pore mesoporous matrix. The MCM-41, MCM-48 materials were synthesized using anionic surfactant micelles as templates, while for SBA-15 a nonionic block copolymer was used as the synthesis template. The detailed descriptions of the syntheses methods are described as follows.

2.2.3.2.1 Synthesis of MCM-41

MCM-41 was synthesized following the procedure as reported by Mukhopadhyay et al¹⁵ with slight modifications to obtain reproducible results. No promoters were used in the synthesis of MCM-41. The stoichiometric composition of the synthesis gel was $\text{SiO}_2\text{-}0.32 \text{ NaOH-}0.2 \text{ CTABr-}125 \text{ H}_2\text{O}$. For a typical synthesis batch, 3g of fumed silica was added to a solution of 0.64g NaOH in 50 mL H_2O , and stirred for 1 h. To this mixture, a solution of 3.64 g of CTABr in 50 mL H_2O was added drop wise under vigorous stirring. After this, 12 mL H_2O was also added drop wise, and the mixture was stirred vigorously for another 90 minutes, after which the gel was autoclaved at 373 K for 16 h. After cooling to ambient temperature, the white precipitate was filtered, washed with copious amount of water and was air-dried. The white solid was the calcined at 813 K for 6 h in air using a slow heating rate of 1 degree per minute. After cooling, the free flowing powder was preserved, sealed under argon atmosphere. This was designated as *M41* for further use.

2.2.3.2.2 Synthesis of MCM-48

MCM-48 was prepared following the literature procedure as reported by Mukhopadhyay et al using a promoter-mediated synthesis method. The initial stoichiometric composition of gel was as $\text{SiO}_2\text{-}0.4 \text{ NaOH-}0.21 \text{ CTAB-}120 \text{ H}_2\text{O-}0.0033 \text{ P}$. For a typical synthesis batch, 3g of fumed silica was added to a solution of 0.8 g of NaOH in 50 mL H_2O and stirred for 1 h. To this mixture, drop wise addition of a solution of 3.82 g CTABr in 50 mL H_2O was followed by the addition of a solution of 0.472 g

phosphotungstic acid in 8 mL H₂O with vigorous stirring. The mixture was then stirred for 90 minutes and then the gel was autoclaved at 423 K for 12 h. After cooling, the contents of the autoclave were filtered, washed thoroughly with generous amount water to remove any residual water-soluble promoter. The white residue was air-dried and then calcined at 813 K for 8 h in air following a very slow heating ramp of 1 degree per minute. After cooling, the free-flowing white powder was preserved under argon atmosphere for further use. This was designated as *M48* for all further use.

2.2.3.2.3 Synthesis of SBA-15

SBA-15 material was synthesized following the procedure as reported by Zhao et al, with slight modifications in the methodology as required to obtain reproducible results. In a typical batch synthesis, 8 g of the nonionic block copolymer Pluronic P123 were taken in a polypropylene beaker and 60 mL distilled deionized water was added to it. The mixture was stirred thoroughly using an overhead stirrer (with teflon blades) for 4h to dissolve the gel completely. To this solution, 240 mL of 2N HCl were added drop wise and was allowed to stir further for 1 h at ambient temperature (~301-303 K). The temperature of the mixture was then raised to 313 K and stirred for 1 h again. To this warm mixture, 18 g tetraethylorthosilicate (TEOS) were added drop wise with vigorous stirring. After the completion of addition, the mixture was allowed to stir for 24 h, maintaining the temperature at 313 K. The synthesis gel thus formed was then loaded in a 500 mL polypropylene bottle, sealed using teflon tape and kept at 373 K for 48 h under static condition. After this, the bottle was removed from oven and was allowed to cool to ambient temperature, then, the contents were filtered and residue was washed with copious amount of water. The white solid was allowed to dry in air, and then crushed in a mortar-pestle. Calcination of the as-synthesized solid material was done at 773 K for 6 h in air, using a slow heating ramp of 1 degree per minute. The sample was cooled to ambient temperature and preserved under argon atmosphere for further use. This was designated as *S15* for all future use.

2.2.3.3 Functionalization of Mesoporous Matrices

The mesoporous matrices were functionalized following different strategies as discussed in the Section 2.1. For MCM-41 and MCM-48, only post-synthesis

grafting method was applied but for SBA-15, both post-synthesis grafting and one-pot co-condensation methods were applied.

2.2.3.3.1 Post-synthesis grafting

Functionalization of MCM-41 and MCM-48 were done using the method described by Shephard et al¹⁶. In this method, consecutive application of an inert graft and an active graft molecule is used to obtain a material with a passivated outer surface and the active-functionalized inner one. In a typical preparation method, 1 g of calcined MCM-41/ 48 was taken in a round bottomed flask and stirred well with 30 mL dichloromethane under argon atmosphere to get a uniform slurry. To it, 0.03 mL of dichlorodiphenylsilane was added and stirred for 1 h. The reaction mixture was cooled to 195 K and 1 mL of 3-aminopropyl trimethoxysilane (APTS) was added to the slurry. The mixture was stirred for 24 h at 313 K, filtered. The residue was washed with DCM and dried in vacuo. This resulted in MCM-41/ 48 with passivated outer silanol groups by diphenylsilyl groups while the inner silanol groups were functionalized to 3-aminopropyl end-groups. The functionalized MCM-41 and MCM-48 samples were designated as *M41-NH₂* and *M48-NH₂* respectively.

Post-synthesis functionalization of SBA-15 was done following a method derived from that described by Asefa et al¹⁷. This method employed the strategic passivation of the external surface of the as-synthesized material using an inert graft before the removal of the template. Washing out the template revealed the inner surface which was functionalized using an active graft molecule. In a typical batch of preparation, 5 g of the as-synthesized SBA-15 was treated with 5 mL hexamethyldisilazane (HMDS) in 60 mL toluene under inert atmosphere. Filtering and washing the residue yielded a white powder. Removal of the template was done by stirring the passivated SBA-15 with 1:1 diethyl ether and ethanol (100 mL per 0.5 g of solid) at ambient temperature for 6 h. The solid was filtered, washed and dried. To introduce the dangling amine function onto the inner surface, 1 g of the dried solid suspended in 60 mL DCM was cooled to 250 K and to it 1 mL of APTS was added very slowly with vigorous stirring. After the completion of addition, the reaction mixture was brought to ambient temperature and then heated to 313 K and stirred for 24 h. The solid was filtered out and washed thoroughly using more DCM, and then dried. Thus, we obtained SBA-15 having external silanol groups passivated with trimethylsilyl

groups and inner ones functionalized with 3-aminopropyl end-groups. The material was designated as *S15-NH₂-(G)*.

2.2.3.3.2 One-pot Co-condensation

For the functionalization of SBA-15 using the one-pot co-condensation technique, the typical synthesis of SBA-15 as described previously (Section 2.2.2.2.3) was modified following the strategies described by Wang et al¹⁸. The synthesis was downscaled to half for this purpose. The molar recipe of the synthesis gel was (1-x) TEOS: x APTS: 6.1 HCl: 0.017 P123: 165 H₂O (where x = 0.05 to 0.2). In a typical synthesis batch, 4 g of Pluronic P123 was dissolved in 30 mL H₂O for 4 h, to this 120 mL of 2N HCl was added and stirred for 1 h at ambient temperature. The temperature was raised to 313 K and the mixture was stirred at 313 K for another 2 h and then 9(1-x) g TEOS was added drop wise. The mixture was allowed to prehydrolyze for 0-3 h before the addition of requisite amount of APTS, after which it was allowed to stir for a total of 24h (including prehydrolysis) at 313 K. The mixture was transferred to a 250 mL polypropylene vessel and heated at 373 K for 48 h under static conditions. The contents were cooled, filtered, and washed to water and dried. The white solid was then refluxed in EtOH for 24 h (200 mL EtOH per 1.5 g of solid), filtered and dried to get the amine-functionalized SBA-15. This functionalized SBA-15 was designated as *S15-NH₂-(C)*.

2.2.3.4 Immobilization of Pd-complex Inside the Functionalized Mesoporous Matrices

2.2.3.4.1 MCM-41 and MCM-48 [using *M41-NH₂* and *M48-NH₂*]

To immobilize the Pd-complexes inside the mesoporous channels of the functionalized MCM-41 and MCM-48, these materials were treated with the solutions of the metal complexes under inert atmosphere. For a typical synthesis batch, 1 g of the functionalized support matrix, namely *M41-NH₂* and *M48-NH₂*, was suspended in 30 mL dichloromethane (DCM). To it, a 50 mL solution containing 0.33 g of Pd(pyca)(PPh₃)(OTs) complex in dichloromethane, and was stirred for 24 h at room temperature. The pale yellow solid obtained after filtration, washing and subsequent drying in air was given a Soxhlet extraction in DCM for 10 h. the paler yellow solid was

preserved under argon for further use. The catalysts were designated as *M41-NH₂-Pd* and *M48-NH₂-Pd* respectively following the respective supports used.

2.2.3.4.2 SBA-15 [using *S15-NH₂-(G)* and *S15-NH₂-(C)*]

To a suspension of 1.5 g of the functionalized SBA-15 matrix in 100 mL dichloromethane, a solution of 100 mg of Pd(pyca)(PPh₃)(OTs) complex in 25 mL in DCM was added and stirred for 24 h at room temperature under argon atmosphere. The contents were filtered, washed with DCM and dried in air. The dried pale yellowish solid was given Soxhlet extraction with dichloromethane for 8 h, to obtain a faint yellow colored free-flowing solid. This process was used for both the amine – functionalized SBA-15 matrices, and the corresponding immobilized catalysts were designated as *S15-NH₂-(G)-Pd* and *S15-NH₂-(C)-Pd* respectively.

2.2.3.5 Syntheses of Supported Catalysts

Two different supported catalysts were prepared and used for the carbonylation reactions. The support matrix was varied in the two. An aluminosilicate material having a well-ordered definite structure was used i.e. NaY zeolite, and pure silica (catalyst grade from Davisil®) was used for supporting the Pd-complex to it by simple adsorption on the surface. Such choice was administered so as to understand the effect of structure on the nature of the supported catalysts, if any. The typical synthesis procedures are presented as follows.

2.2.3.5.1 Synthesis of SiO₂ supported Pd(pyca)(PPh₃)(OTs) catalyst

For this synthesis, 3 g of Davisil® silica, 100-200 mesh, was suspended in ethanol, and stirred for 15 minutes to obtain a uniform slurry, to it an ethanolic solution of 0.135 moles of Pd(pyca)(PPh₃)(OTs) complex was added and the moisture was refluxed for 18 h. The solid was filtered off and dried and 353 K. The faint yellow solid was stored under argon and was designated as *Pd-S*

2.2.3.5.2 Synthesis of NaY zeolite supported Pd(pyca)(PPh₃)(OTs) catalyst

To slurry of 3 g NaY zeolite in 30 mL ethanol, an ethanolic solution of Pd(pyca)(PPh₃)(OTs) complex was added and refluxed for 18 h. After bringing to the

ambient temperature, the contents were filtered, washed and dried at 353 K and was stored under argon as a free-flowing pale yellow solid. This was designated as Pd-Y.

2.2.4 Carbonylation Procedure[£]

The carbonylation reactions were carried out in batch reactor mode. Autoclave made of Hastelloy C-276 by Parr Instrument Co. USA, having a capacity of 50 ml (total dead volume including head-space and appendages was 72 mL) was used. The reactor had facilities for intermittent sampling, gas inlet & outlet, thermocouple, pressure transducer attachment (sensitivity of 0.1 psi), along with magnetically driven agitation impeller and temperature-controlled external heating device as shown in the schematic (Figure 2.1). As a safety precaution, a gold-faced rupture disc, capable of withstanding 14 MPa pressure was present with the reactor. In charged into the bomb. Then the liquid charge consisting of requisite amount of

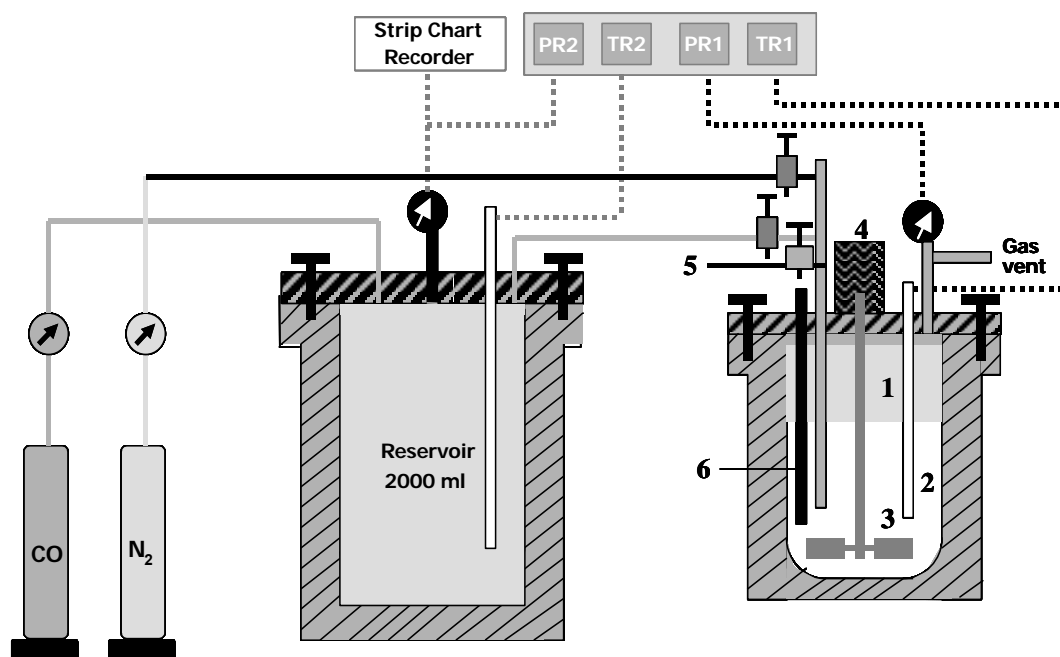


Figure 2.1: Schematic of Carbonylation Reaction Setup

1: Reactor; 2: Thermo well; 3: stirrer shaft with impeller; 4: magnetic stirrer; 5: sampling valve; 6: internal cooling tube; TR1: Reactor temperature indicator; PR1: Reactor pressure indicator; TR2: Reservoir temperature indicator; PR2: Reservoir pressure indicator; N₂ : Nitrogen cylinder CO: Carbon monoxide cylinder

[£] Hazardous carbon monoxide involved, safe handling is a pre-requisite

substrate, water and the solvent (MEK) were added into the autoclave, and closed. The contents were flushed four times with nitrogen followed by carbon monoxide thrice and heated to the desired temperature with very slow stirring for proper heat distribution. After attaining the temperature, the autoclave was pressurized with CO to the required level. The reaction was started by switching the agitation on (15-17 Hz). During the typical experiment, known quantities of the solid catalyst, and promoters were reaction progress, to maintain a constant pressure in the reactor, CO was fed through a constant-pressure regulator from a reservoir vessel (capacity 2.0 L) maintained at higher pressure than the reaction pressure. Another pressure transducer, attached to the reservoir, recorded the pressure drop in the reservoir. Intermediate liquid samples were also taken at regular intervals of time, if required. The reaction was continued for a specified time. After the reaction, the autoclave was brought to ambient temperature, CO de-pressurized, flushed with nitrogen and the reaction mixture was removed for further processing and analyses.

2.2.5 Recycle Studies and Leaching Experiments

For the recycle studies using the anchored catalysts, the following procedure was followed. After the carbonylation reaction run was complete, the reactor was allowed to rest, to settle the solid catalyst and the supernatant organic phase was decanted slowly to separate it from the solid catalyst. The solid residue was washed with the reaction solvent i.e. methyl ethyl ketone for a couple of times in the same manner. A fresh charge of reactants and promoters was introduced and the reaction was carried on in the same fashion as described previously, after withdrawing an initial sample before starting the recycle run. This was repeated for all the recycle reactions. The reaction mixture thus obtained was retained for further analyses.

Metal leaching experiments with the novel anchored Pd-complex catalysts were performed by filtration of the hot reaction mixture at 388K by stopping the reaction abruptly at ~30% conversion and subsequently, testing the catalytic activity of the filtrate for hydrocarboxylation without the addition of any fresh heterogeneous catalyst. The filtrate and the catalyst thus recovered were analyzed for Pd-content by ICP-AES (Inductively Coupled Plasma with Atomic Emission Spectroscopy) analyses to contemplate the palladium content in solution and loss of palladium from the parent catalyst during the reaction.

2.2.6 Analytical and Characterization Methods

For characterization of the synthesized materials at different stages of synthesis and after the reactions etc., numerous techniques have been employed to identify, understand and confirm our postulates. Powder XRD analysis of the mesoporous materials at room temperature were done using two instruments for different 2θ ranges. Philips XL machine was used for the low-angle scans (2θ range of 0.5 to 5.0 degrees) required for SBA-15 samples, while MCM-41, MCM-48 were analyzed using a Rigaku Miniflex instrument for 2θ range of 1.5 to 10 degrees at a slow scan rate of $1^\circ/\text{min}$ using $\text{Cu-K}\alpha$ ($\lambda = 1.5404 \text{ \AA}$) radiation. FT-IR spectra were obtained using a Perkin Elmer Spectrum-2000 in transmission mode using KBr pellets as well as in Shimadzu Hyper IR in DRS (Diffused Reflectance Spectroscopy) mode by mixing samples with KBr. NMR was obtained from a Bruker-MSL-300 and Bruker-DRX-500 spectrometers. The ^{31}P NMR spectra were recorded at 202.456 MHz by using 85% H_3PO_4 as an external standard and data were collected at spectral width of 20 kHz with a flip angle of 45° , with ~ 6000 actual data points and 5 s relaxation delay. Solid-state analyses were done using a 3 mm CP-MAS probe. X-ray photoelectron spectra (XPS) were recorded on a VG – Microtech ESCA 3000 spectrometer using the $\text{Mg-K}\alpha$ emission ($E = 1253 \text{ eV}$) under a vacuum of $\sim 10^{-9}$ torr. Scanning electron microscopy (SEM) were performed using a Philips XL 30 instrument – the catalyst materials were suspended in isopropanol, cast on gold plated discs followed by drying under vacuum and coating with a conducting material and then were imaged. For the catalytic carbonylation reactions, the reaction mixtures (liquids) were analyzed by gas chromatography, using a Hewlett-Packard 6890 Series GC instrument, controlled by *HP ChemStation* software, and HP-FFAP capillary column (25 m x 0.33 mm x 0.2 μm film-thickness, on a polyethylene glycol stationary phase). The typical set of parameters for the method developed for analysis of the reactants and products are in the following Table 2.1. Calibration of the method was performed using standard materials in the concentration range similar to that of the catalytic reactions for each component of substrate(s) and products in the reaction mixture.

Table 2.1 Operation parameters of the method for GC analysis

Injector (split) temperature	523K
Flame Ionization Detector temperature	523K
Column (Oven) temperature	423K to 483K (@ 35K/ min), hold 13 min.
Carrier gas (He) flow rate	2.5 ml/ min
Inlet Pressure (He)	25 psi
Split ratio	100:1
Injection volume (manual)	0.5 μl

For evaluating the performance of the solid catalysts and to explain them in terms of the observed properties, three important terminologies need to be defined first.

The conversion, selectivity and turnover frequency (TOF) for a typical catalytic reaction were calculated as follows,

$$\text{Conversion, \%} = \frac{\text{Initial concentration of substrate} - \text{Final concentration of substrate}}{\text{Initial concentration of substrate}} \times 100$$

$$\text{Selectivity, \%} = \frac{\text{No. of moles of the particular product formed}}{\text{No. of moles of substrate converted}} \times 100$$

$$\text{TOF, h}^{-1} = \frac{\text{No. of moles of carbonylation product formed}}{\text{No. of moles of catalyst used} \times \text{reaction time (in hours)}}$$

2.3 Results and Discussions

With the syntheses of the immobilized catalysts being described, the results on their characterization using numerous techniques and applications in the carbonylation will be presented in this section. This will be subsequently discussed under two subheadings illustrating the characterization of the solid catalysts and the results of catalytic application of these materials, respectively.

2.3.1 Characterizations of the solid catalysts

2.3.1.1 Powder X-Ray Diffraction

Powder X-ray diffraction is one of the most important tools for the determination of the phasic composition of the materials as well as some other derived aspects such as the size of the crystallites, their crystallographic properties etc. The mesoporous materials used in this work were supposed to have characteristic powder XRD fingerprints which were used to identify the materials synthesized, calculate the unit cell parameters, determining the thickness of the mesoporous channel-walls and above all comparative variation in each and every aspect as a function of any modification of the matrix, physical or chemical. The typical XRD patterns of the calcined pure MCM-41 and MCM-48 are presented in Figure 2.2. This represents the characteristic powder XRD patterns of MCM-41 and MCM-48. Curve (a) clearly describes the fingerprint pattern for the pristine mesoporous *M-41*, showing the four characteristic low angle reflections (strong 100 and much feeble 110, 200 and 210 peaks) at 2θ values of 2.08° , 3.67° , 4.27° and 5.57° respectively, while Curve (b) is the characteristic pattern for *M-48* showing eight fingerprint reflections (sharp 211, 220 and weak 321, 400, 420, 322, 422, 431 peaks) at 2θ values of 2.37° , 2.67° , 3.57° , 3.58° , 4.37° , 4.59° , 4.78° , 4.88° respectively, the latter five peaks being visible on a 10-fold magnification only. The peak identifier numbers are the Miller indices of the Bragg's planes of diffraction for the respective materials. The XRD patterns show that both the mesoporous matrices have highly ordered long-range mesoporosity and also a hexagonal ($p6mm$) and cubic ($la3d$) symmetric nature of the mesophases for MCM-41 and MCM-48 respectively. The d -spacings as calculated from the XRD patterns are 42.3 \AA (d_{100}) and 37.1 \AA (d_{211}) respectively for *M-41* and *M-48*. The highly ordered mesoporous matrices thus formed were used for further experiments as supports for anchoring the Pd-complex, as described later.

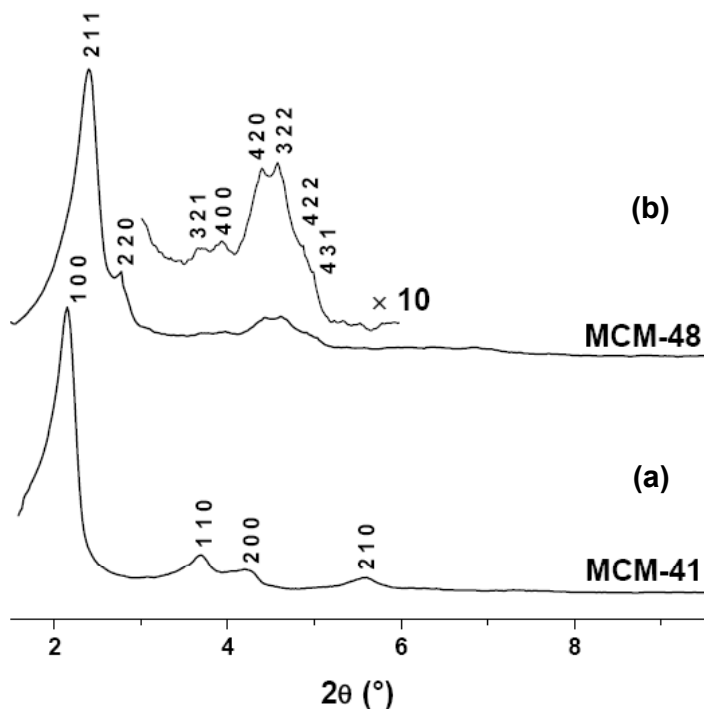


Figure 2.2: Powder XRD patterns of *M-41* and *M-48*

The next figure (Figure 2.3) presents the comparison of the powder XRD patterns at the different stages synthesis of the immobilized Pd(pyca)(PPh₃)(OTs) complex inside the mesoporous *M-41* (Part A) and *M-48* (Part B), respectively. For both the parts (A and B) in Figure 2.3, the powder XRD patterns of the sequential passivation of the exterior surface [(b)-Curves], amine-functionalization of the externally passivated mesoporous matrices [(c)-Curves], and Pd-complex anchored to the internal surfaces of the mesoporous matrices [(d)-Curves] have been described. It is clearly indicated from the observations that the characteristic diffraction peaks of the mesoporous matrices are present in all the samples. Interestingly, both the mesoporous matrices, MCM-41 and MCM-48 retain their respective characteristic properties during the process of anchoring of the Pd-complex to the interior surface of these matrices. Practically no changes in the peak positions were observed for the step of passivation of the exterior silanol groups [(b)-curves] for both the *M-41* and *M-48* matrices. A slight shifting of the principle peaks (100 for *M41-NH₂-Pd*, and 211 for *M48-NH₂-Pd*) to the higher 2θ values was observed indicating the incorporation of the Pd-complex inside the mesoporous cavity leading to the shrinkage of the unit cell dimension parameters (a_0) also. The detailed data of physical characteristics of the different MCMs at the different stages of immobilization of the Pd-complexes is provided in Table 2.2. It is

necessary to mention that the preferential passivation of the exterior silanol groups in both the MCM-41 and MCM-48 occurred by the relatively faster silylation kinetics to the most accessible external silanols only. However, it was observed elsewhere¹⁹ that when the treatment with Ph_2SiCl_2 was omitted, random uncontrollable amine-functionalization and subsequent anchoring of the Pd-complex was obtained, which consequently may weaken the orderedness of the matrices.

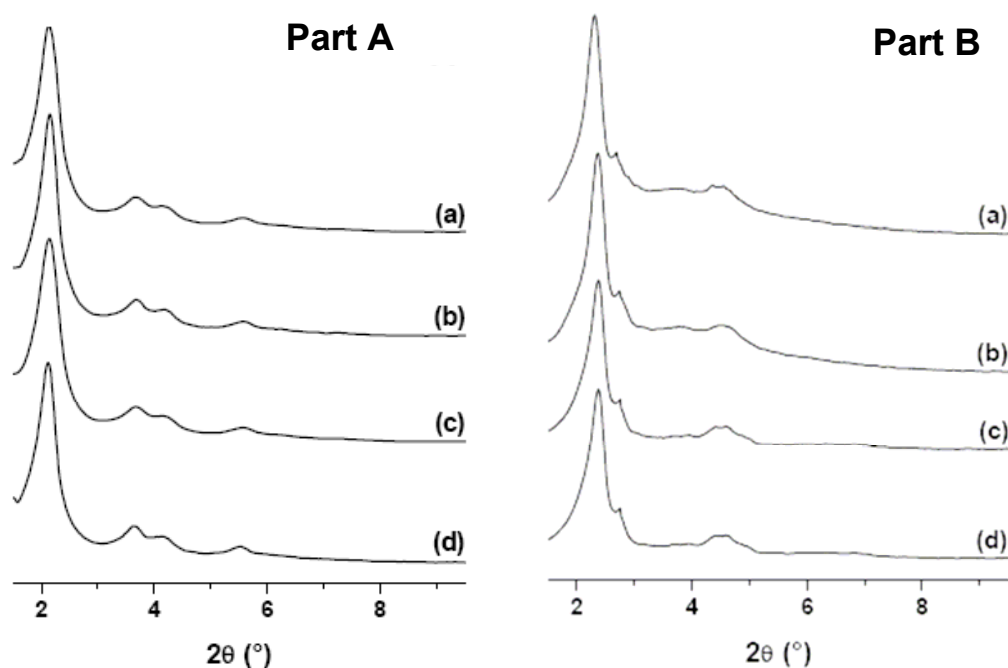


Figure 2.3: Comparative powder XRD patterns of *M-41* (Part A) and *M-48* (Part B)
(a)-Curves = Pristine mesoporous matrices [*M-41* & *M-48*]; (b)-Curves = Exterior surface-passivated mesoporous matrices using Ph_2SiCl_2 ; (c)-Curves = NH_2 functionalized mesoporous matrices [*M41-NH₂* & *M48-NH₂*]; (d)-Curves = $\text{Pd}(\text{pyca})(\text{PPh}_3)(\text{OTs})$ complex anchored inside mesoporous matrices [*M41-NH₂-Pd* & *M48-NH₂-Pd*] respectively

Figure 2.4 shows the powder XRD pattern for the as-synthesized and calcined SBA-15 material. The plots show that the characteristic reflections of the 100, 110, 200 peaks are clearly visible for both the as synthesized and the calcined samples at the 2θ values of 0.875° , 1.505° and 1.705° respectively. The peak intensity however changes and for the calcined SBA-15, the peaks become sharp and prominent than those of the as-synthesized sample. This might be attributed to the better-aligned diffraction planes due to the removal of the template. The d -spacing (d_{100}) and the unit

cell parameter (a_0) were calculated with respect to the (100) peak as 101 Å and 116.5 Å respectively. Thus, the powder XRD proved the formation of good quality SBA-15 as a large pore mesoporous matrix with highly ordered mesoporosity.

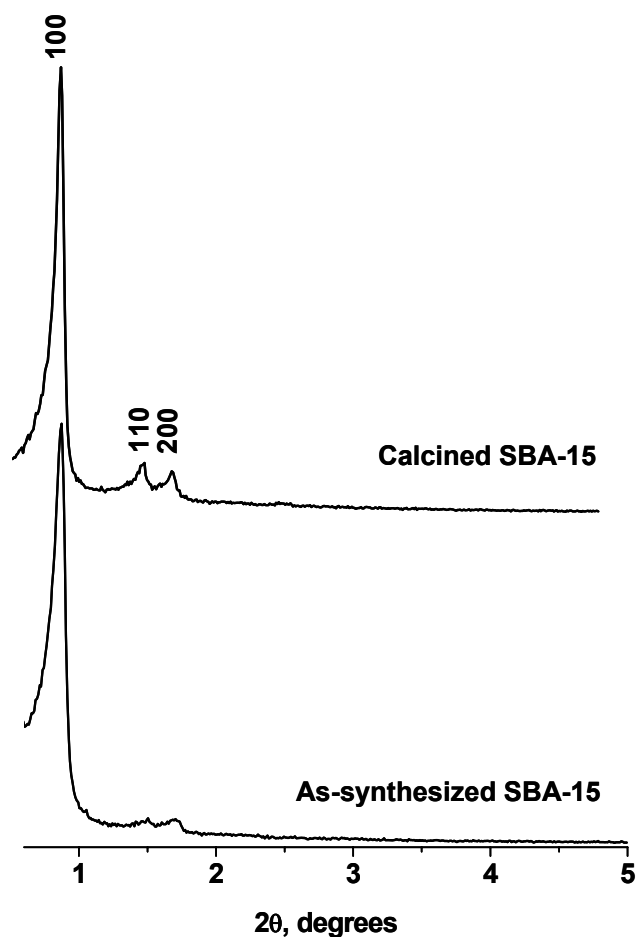


Figure 2.4: Powder XRD patterns of as-synthesized and calcined SBA-15

Sequential powder XRD experiments were carried out on different SBA-15 materials during the course of the immobilization of the Pd-complex and the results are presented in Figure 2.5. It was clear from the plot that the SBA-15 did not change during the process of anchoring of the Pd-complex. The principle peaks at 100, 110, 200 were clearly visible for all of the SBA-15 samples. The intensities of these peaks were almost equal. However, for the NH_2 -functionalized SBA-15, prepared by grafting method (*S15-NH₂-G*), and the subsequent Pd-complex anchored SBA-15 (*S15-NH₂-G-Pd*) showed shift of the (100) peak towards higher 2θ value. This decrease in the d -spacing might be due to the incorporation of the $-\text{NH}_2$ group and the Pd-complex

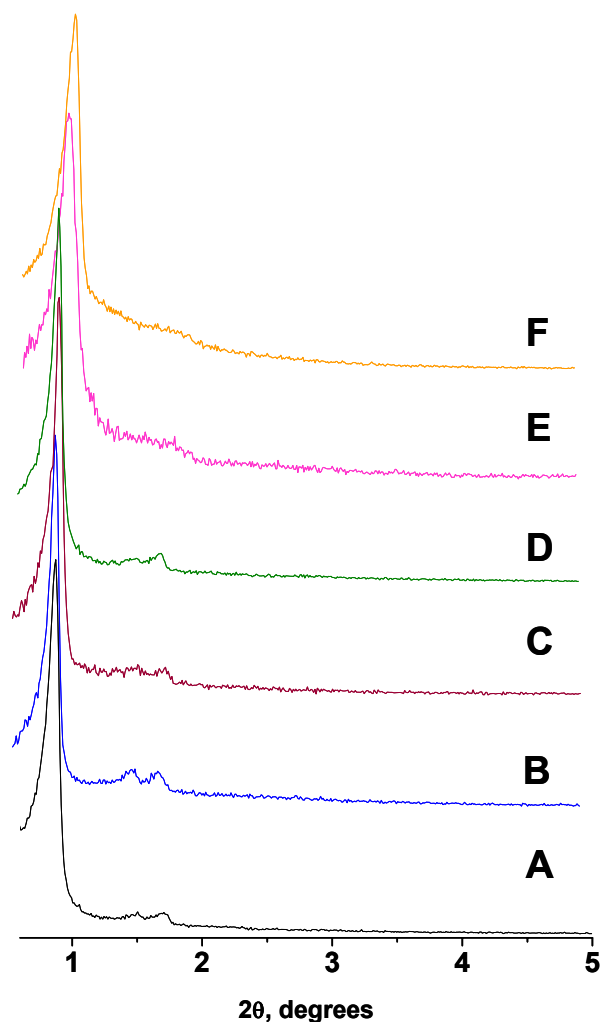


Figure 2.5: Comparative powder XRD data of different SBA-15 materials

A: As-synthesized SBA-15 (*S15*); B: Outer surface passivated SBA-15; C: NH_2 -functionalized on the internal surface of SBA-15 (*S15-NH₂-G*); D: Pd-complex anchored inside SBA-15 (*S15-NH₂-G-Pd*); E: *insitu* NH_2 -functionalized SBA-15 (*S15-NH₂-C*), F: Pd-complex anchored to *insitu* NH_2 -functionalized SBA-15 (*S15-NH₂-C-Pd*)

inside the mesopores. For the *insitu* functionalized SBA-15 (*S15-NH₂-C*), the (100) peak appeared at slightly higher 2θ than its grafted counterpart (*S15-NH₂-G*) as also for the Pd-complex anchored SBA-15 (*S15-NH₂-C-Pd*). This might be due to the initially larger number of the anchoring agent molecules (APTS) entering building units before the condensation of the SiO_4^{4-} monomers in the synthesis gel, during the *insitu* synthesis-cum-functionalization step. The resulting smaller d -values are self-implicative

of the space required by the larger number of the anchoring agent moieties, leaving out only a smaller void space. The d -spacing further decreased (d_{100} 92.4 Å) when the Pd-complex was incorporated into the channels. Thus, the powder XRD illustrates successfully, the incorporation of the graft moiety by both the methods, and the anchoring of the Pd(pyca)(PPh₃)(OTs) complex inside the mesoporous matrices.

2.3.1.2 Adsorption-Desorption Studies

The nitrogen adsorption-desorption isotherm along with the pore size distribution of calcined MCM-41 and MCM-48 are presented in the Figure 2.6 and 2.7 respectively. Both the isotherms show one sharp inflection point. For MCM-41 and MCM-48, the adsorption and desorption regions of the isotherms almost overlap each other except for a very narrow dissimilar region indicating a very narrow pore size distribution, and a slight capillary condensation. For MCM-41 and MCM-48, the adsorption isotherms were classified as Type IV of the IUPAC conventions²⁰ - characteristic of the M41S type materials;²¹ and the inflection point near $P/P_0 \sim 0.3-0.4$ indicated the sharp capillary condensation region, showing a very narrow pore size distribution. A very small hysteresis loop was observed for both the materials around $P/P_0 \sim 0.25$ to 0.4. However, for MCM-48 the pore-size distribution curve showed the maximum at a lower pore diameter (between 20 and 30 Å) than that for MCM-41 (between 30 and 40 Å) indicating smaller pores. The N₂ adsorption-desorption isotherm of calcined SBA-15 material is shown in the Figure 2.8. The adsorption arm of the plot clearly showed three distinguished regions corresponding to [a] Monolayer-multilayer adsorption, [b] Capillary condensation inside the porous cavities & walls, and [c] multilayer adsorption on the external surface of the material. A clear but small hysteresis loop of Type I is also observed in the adsorption-desorption isotherm, showing the occurrence of capillary condensation at higher relative pressures ($P/P_0 \sim 0.65$ to 0.8). The surface area obtained from single point calculations at $P/P_0 = 0.30318$ using the Brunauer Emmett Teller (BET) equation for adsorption isotherm was 871.25 m²/g. However, multi-point calculations and averaging at lower relative pressures ($P/P_0 < 0.31$, hence, considering monolayer formation only) gave us another surface area based on unimolecular layer formation during adsorption, as 885.94 m²/g. Further calculations using the BJH method gave us the pore dimensions from the same

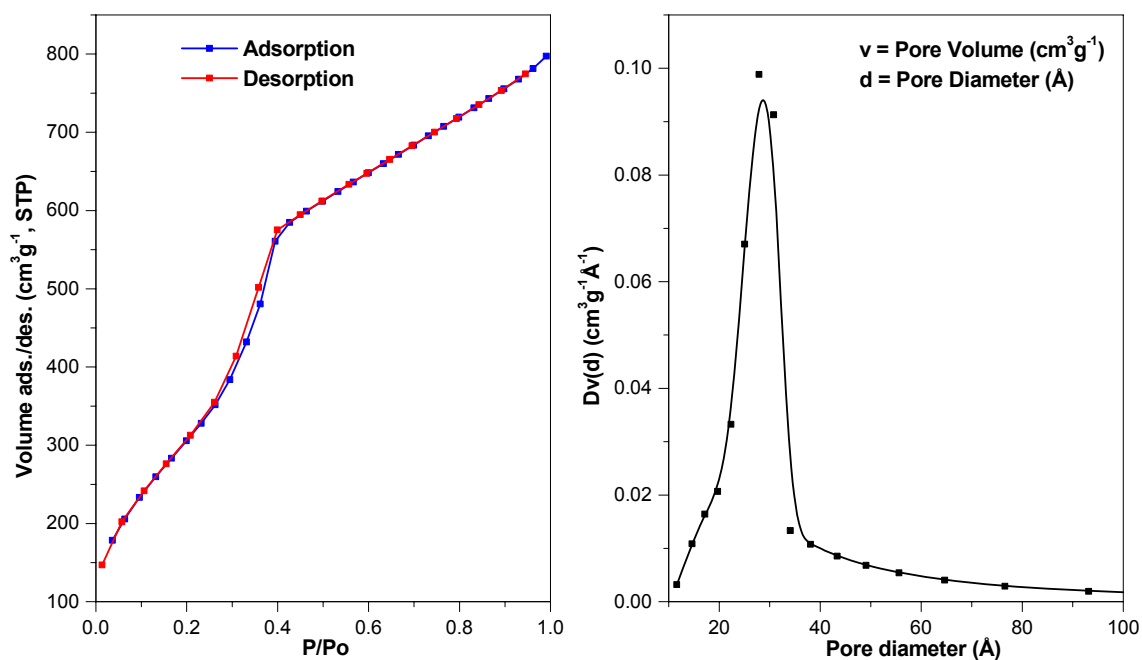


Figure 2.6: N_2 adsorption-desorption isotherm and BJH pore size distribution of calcined MCM-41

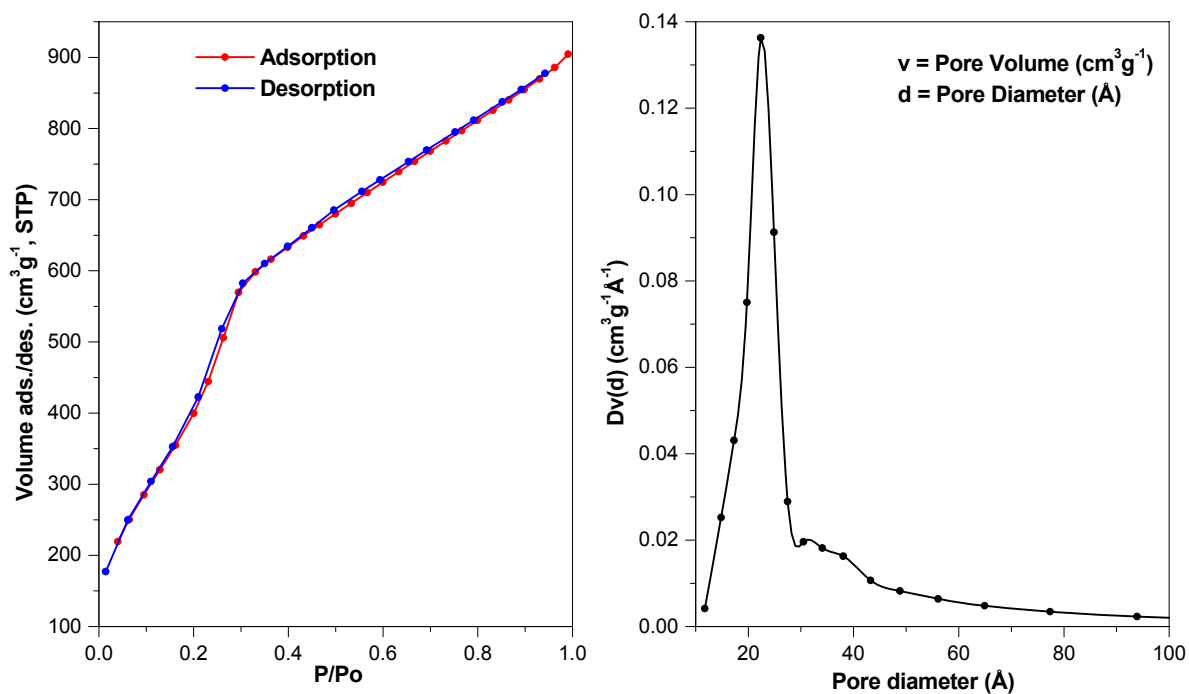


Figure 2.7: N_2 adsorption-desorption isotherm and BJH pore size distribution of calcined MCM-48

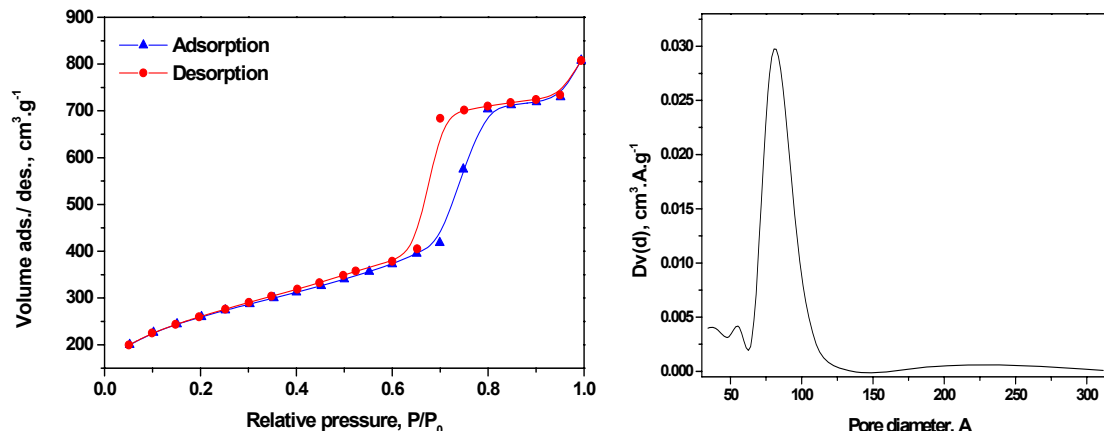


Figure 2.8: N₂ adsorption-desorption isotherm of calcined SBA-15 at 77.35 K

N₂-adsorption isotherm. Using the adsorption branch of the isotherm, the pore diameter was determined as 77.46 Å, having an average pore volume of 1.1892 cm³/g. The pore-size distribution curve showed a very narrow distribution pattern having a maximum at ~ 77.5 Å corresponding to the average pore size. Considering the d_{100} spacing from the powder XRD data (from Section 2.3.1.1) and the unit cell volume, a_0 , the pore wall thickness was found to be nearly 39 Å, which is almost the same as the pore size of the MCM-41 material. Thus, the SBA-15 was proved to be having very high surface area with larger pore size and thicker mesoporous frame-walls than MCM-41, which might be of better mechanical strength. A comparative presentation of the different surface parameters of all three mesoporous matrices as well as their functionalized and metal-complex loaded counterparts is given in Table 2.2.

From the data, it is observed that for all of the functionalized matrices and the Pd-complex loaded mesoporous materials, the long-range order is maintained along with the consistent variation of certain parameters. As observed from the powder XRD patterns already, the shifting of the position of the principle peak towards the higher 2θ values during the NH₂-functionalization and subsequent loading of the palladium complex is being reinforced by the surface analyses, which shows that such an argument is supported by the decrease in the pore volume (and pore diameter) and the surface areas of the support matrix. The N₂ adsorption-desorption data distinctly supports this kind of reasoning.

Table 2.2: Comparative physical characteristics of the different surface-modified MCM-41, MCM-48 and SBA-15 matrices

Sample designation	d_{hkl}^a , Å	a_0^b , Å	Pore volume, $\text{cm}^3 \cdot \text{g}^{-1}$	Pore diameter, Å	Wall thickness ^c , Å	Surface area, $\text{m}^2 \cdot \text{g}^{-1}$
M41	42.32 (100)	48.9	1.203	36.68	12.22	1322
M41-NH ₂	41.22 (100)	47.6	1.101	30.22	17.38	1152
M41-NH ₂ -Pd	41.64(100)	48.1	1.057	28.96	19.14	1035
M48	37.11 (211)	90.9	1.399	30.4	14.20	1632
M48-NH ₂	37.08 (211)	90.8	1.243	27.6	15.60	1510
M48-NH ₂ -Pd	36.81 (211)	89.6	1.176	25.3	16.32	1401
S15	101.00 (100)	116.5	1.189	77.46	39.04	886
S15-NH ₂ (G)	100.84 (100)	116.4	1.134	72.24	44.16	798
S15-NH ₂ (G)-Pd	93.46 (100)	107.8	0.976	62.51	45.29	734
S15-NH ₂ (C)	100.90 (100)	116.5	1.087	72.46	44.04	774
S15-NH ₂ (C)-Pd	92.42 (100)	106.7	1.002	61.51	45.19	721
Pd-S	-	-	-	-	-	189
Pd-Y	-	-	-	-	-	785

^a Calculated from powder XRD patterns, as $n\lambda=2d\sin\theta$, where, $n=1$, $\lambda=1.5404$ Å ; values in parentheses indicate the Miller indices

^b Calculated as $a_0=2d_{100}\sqrt{3}$ (for MCM-41 & SBA-15), $a_0=d_{211}\times\sqrt{6}$ (for MCM-48)

^c Calculated as a_0-PD (for MCM-41 & SBA-15), $a_0/3.092 - PD/2$ (for MCM-48), where PD = pore diameter

The surface area analyses were also carried out using the silica-supported and NaY zeolite supported Pd(pyca)(PPh₃)(OTs)catalysts, namely, *Pd-S* and *Pd-Y*. It was observed that the surface area of the silica changed from ~380 m²/g to 189 m²/g after the complex was supported upon the silica gel (Fumed silica). However, the surface area of the NaY supported Pd-complex also changed after supporting the palladium complex (from 840 m²/g to 785 m²/g).

In brief, the surface analyses and the adsorption-desorption studies along with the powder XRD analysis have confirmed the selective functionalization of the mesoporous matrix as desired, followed by the incorporation of the palladium complex by anchoring to the interior walls of the support matrix.

2.3.1.3 Scanning Electron Microscopy

Scanning electron microscopy provides us the sight of the morphological pattern of the synthesized materials in a sub-micron level. The SEM micrographs of the different samples of catalysts based on MCM-41 and MCM-48 are presented in Figure 2.9. For both MCM-41 and MCM-48 materials based catalysts, regular spherical morphology was observed for the pristine support matrices (i.e. *M41* and *M48*) and also for the Pd(pyca)(PPh₃)(OTs) complex anchored inside the mesoporous matrices (i.e. *M41-NH₂-Pd* and *M48-NH₂-Pd*). The anchored catalysts did not appear much different from the pristine support matrices in terms of the general morphology. The average sizes of the particles were around 500 nm in diameter, for all the samples. From the SEM images of the anchored palladium complex catalysts (*M41-NH₂-Pd* and

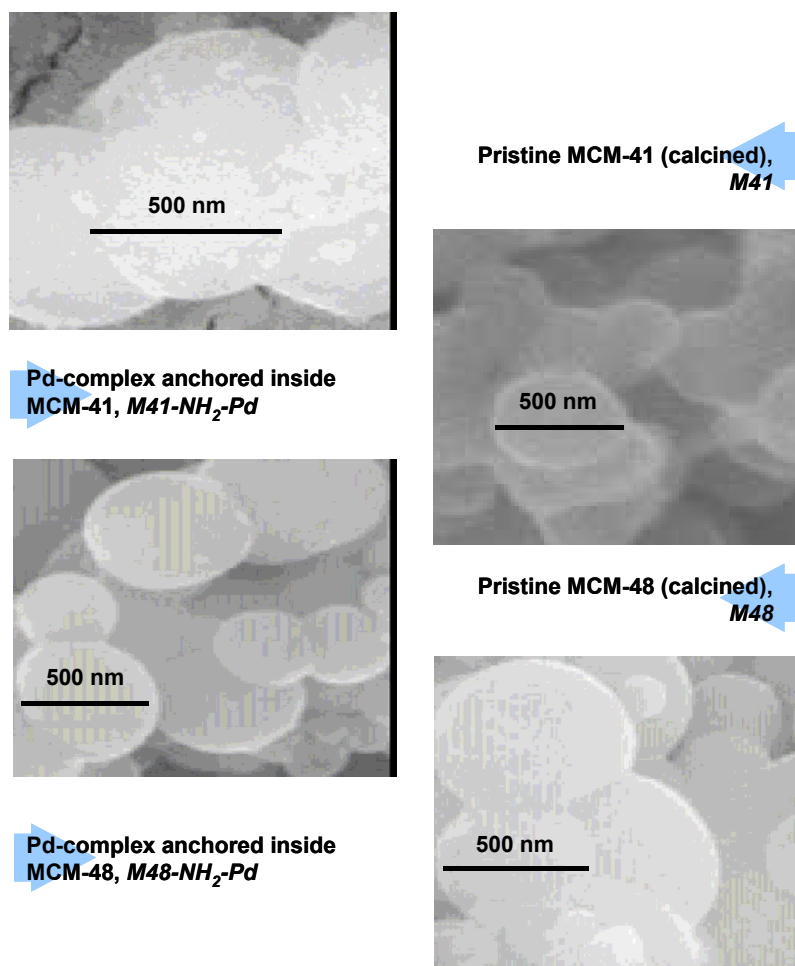


Figure 2.9: SEM images of different MCM-41 and MCM-48 based catalysts

M48-NH₂-Pd), it may be pointed that both the mesoporous matrices did not undergo any change in the morphological pattern while subjected to the multistep synthesis process. In addition, no physical degradation of the matrices was visible. Thus, the anchored palladium complexes in MCM-41 and MCM-48 were found to be robust and non-degrading in nature.

The SEM micrographs of the different samples of catalysts made using SBA-15 as the mesoporous support are presented in Figure 2.10. The characteristic worm-like entwined morphology is clearly evident from the SEM images of the as synthesized as well as the calcined SBA-15 samples. This shows that the external morphology of SBA-15 did not change upon calcination at 813 K, which removed the surfactant micelles from the internal channels of SBA-15. For all the samples of SBA-15 matrix at different stages of immobilization of the palladium complex inside the mesoporous channels, the similar worm-like morphology was observed. This stable morphological pattern as maintained throughout the immobilization process definitely refers to the stability and robust nature of the solid catalyst materials. Another important observation from the SEM was that the immobilized Pd-complex catalyst materials did not show any structural degradation (e.g. grinding or breaking into pieces) of the materials while immobilization process that involved the highly agitated slurry of the solids under moderately high temperatures. These infer about the mechanical stability of the SBA-15 support matrix and also for the synthesized catalysts.

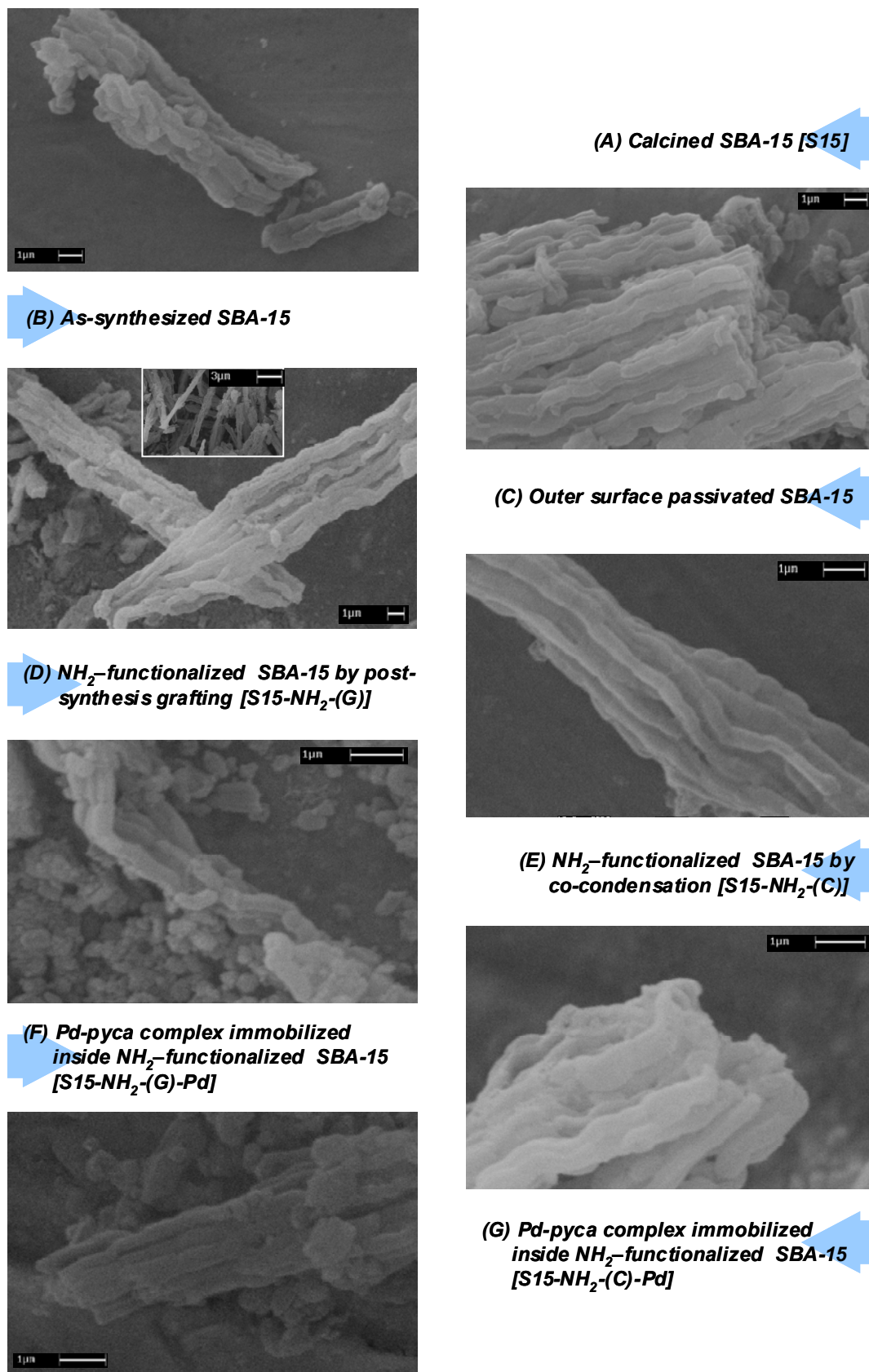


Figure 2.10: SEM micrographs of the different SBA-15 samples

2.3.1.4 Transmission Electron Microscopy

The transmission electron microscopy is one of the important tools for the analysis for the structure elucidation of mesoporous materials. In addition to its use to view metal nanoparticles, it has already been used to visualize the position of metal (complexes) inside the porous matrices. In a recent report by Shephard et al, the

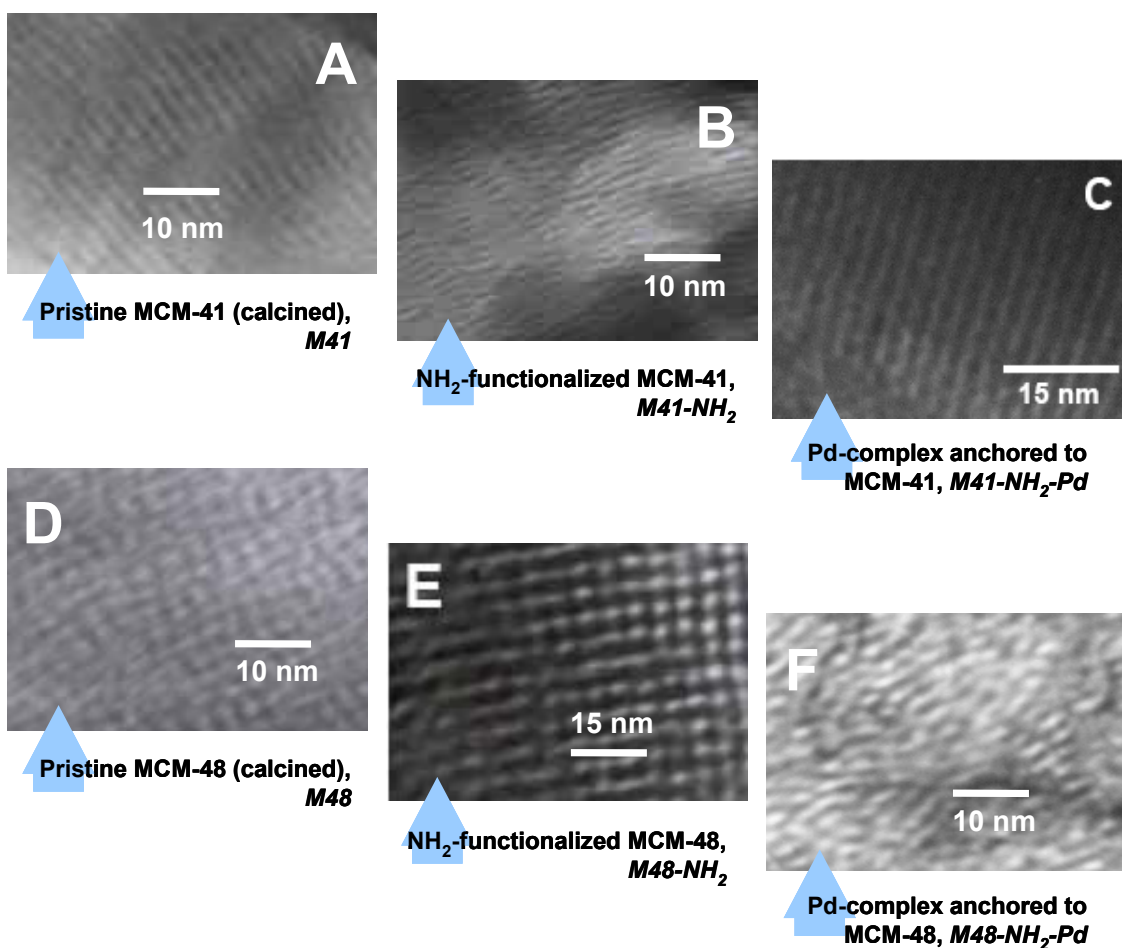


Figure 2.11: TEM images of different MCM-41 and MCM-48 materials

location of the metal complexes inside the mesoporous channels had been ascertained using TEM. Thus, by following a similar logic and understanding, the immobilization of the Pd-complex inside the MCM-41 and MCM-48 using the anchoring technique, has been assessed here. The pristine MCM-41 and MCM-48 were imaged beforehand and are shown in Figure 2.11 (images A and D). Distinct hexagonal and cubic mesophases were clearly visible for MCM-41 and MCM-48 respectively. After passivation of the exterior surface with Ph_2SiCl_2 and functionalization of the interior walls of the matrices

with an aminopropyl group, the materials (namely, *M41-NH₂* and *M48-NH₂* respectively) were also imaged using TEM (Images B and E in Figure 2.11). Not much difference of the patterns was observed in the images with the images A and D in Figure 2.11. However, after the anchoring of the Pd(pyca)(PPh₃)(OTs) complex inside the mesoporous channels (*M41-NH₂-Pd* and *M48-NH₂-Pd*), the images (C and F in Figure 2.11 respectively) showed distinct deep contrasting furrows with respect to the light shaded surface. This might be interpreted as due to the presence of the metal complexes inside the matrix, but not on the surface. If the Pd-complex was anchored on the surface of the functionalized matrices, then the high-contrast dark furrows would have appeared along the boundary of the visualized matrices and not inside the porous body as observed previously by Shephard et al. Thus, it may be concluded that the palladium complexes were immobilized inside the pores of the mesoporous matrices, by anchoring to the interior walls of these porous channels.

2.3.1.5 X-Ray Photoelectron Spectroscopy

The oxidation state of the elements present in the catalyst is typically analyzed using the X-ray photoelectron spectroscopy. The elements of major concern are Pd, N, C, P etc., which might prove decisive in the determination of the actual stereo-electronic conditions arising out of the anchoring process. For the MCM-41 based catalyst (*M41-NH₂-Pd*) the results are presented in Figure 2.12 which showed a full-scale binding energy data for the catalyst. The peaks in the spectra are typically identified as the different elements and the binding energies were used to assign the oxidation states of the respective elements. All the values were corrected to the standard carbon 1s peak arising out of the adventitious carbon at 285 eV. The data of the different other catalysts namely, *M48-NH₂-Pd*, *S15-NH₂-(G)-Pd*, *S15-NH₂-(C)-Pd*, *Pd-S* and *Pd-Y* are presented in Table 2.3. The analyses of the different oxidation states of the individual elements present in them are of prime importance for understanding of the nature of the synthesized catalysts.

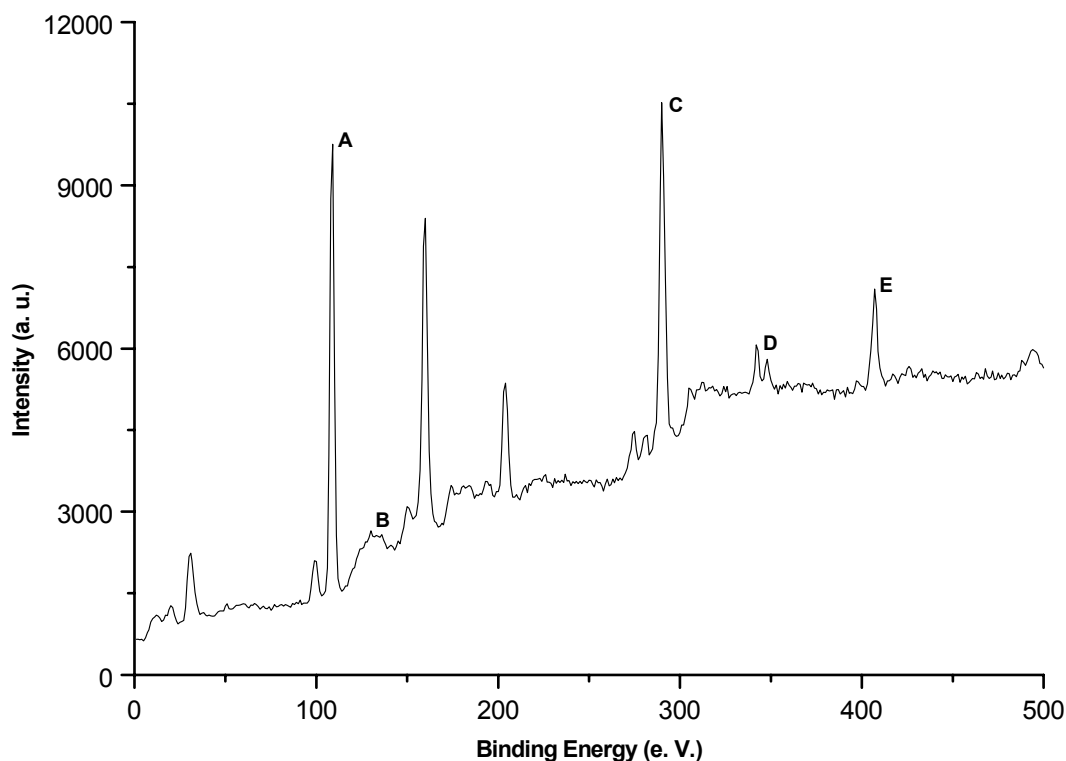


Figure 2.12: XPS data for *M41-NH₂-Pd*

Peaks as identified are, A: Silicon, B: Phosphorous, C: Carbon, D: Palladium, E: Nitrogen

As observed from the XPS data of the *M41-NH₂-Pd* sample, the binding energies of palladium was 337.3 eV and 342.5 eV respectively, which were assigned for its 3d_{5/2} and 3d_{3/2} states respectively of the Pd(II) oxidation states. The characteristic band gap of 5.2 eV was also indicating to the same conclusion. No peaks in the vicinity of 335 eV was observed confirming the absence of any Pd(0) state in the catalyst. The other elements were also complying with the expected oxidation states in the anchored catalyst, e.g. Si 2p (101.4 eV), N 1s (399.8 eV), P 2p(132.5 eV). The observed values were in good agreement with standard oxidation states as reported elsewhere.²² The *M48-NH₂-Pd*, *S15-NH₂-(G)-Pd* and *S15-NH₂-(C)-Pd* catalyst showed results similar to those of the *M41-NH₂-Pd* catalyst as seen from the data in Table 2.3. all these concluded that the Pd complex retained its original oxidation state of Pd(II) during the synthesis of the anchored catalysis each by using a different methodology and reagents as required by the different support matrix. Thus, the catalysts were stable and robust as far as the synthesis is concerned.

Table 2.3: XPS data for different anchored and supported catalysts (values in eV)

Elements Catalysts	Si 2p	Pd 3d _{5/2} ; 3d _{3/2}	N 1s	P 2p
<i>M41-NH₂-Pd</i>	103.8	337.3; 342.5	400	132.6
<i>M48-NH₂-Pd</i>	103.7	337.1; 342.3	399.9	132.6
<i>S15-NH₂-(G)-Pd</i>	103.7	337.1; 342.4	400.8	132.5
<i>S15-NH₂-(C)-Pd</i>	103.8	337.4; 342.8	400.6	132.4
<i>Pd-Y</i>	102.8	337.1; 342.4	400.3	132.5
<i>Pd-S</i>	102.8	337.4; 342.8	400.2	132.6

2.3.1.6 Solid State CP-MAS NMR Spectroscopy

Multi-nuclear NMR studies were used for the characterization of the anchored Pd-complex catalysts. To understand the changes occurring under the synthesis as well as during the course of reaction conditions, ¹³C, ²⁹Si and ³¹P solid-state CP MAS NMR experiments were performed at every step of synthesis of the SBA-15 based anchored catalysts (for both post-synthesis grafting and co-

condensation methods) and also after the carbonylation reactions as a test the stability of the catalysts. Results of the other catalysts (using MCM-41 and MCM-48) are also presented here. NMR experiments involving each of the three nuclei are discussed in details as follows.

2.3.1.6.1 ²⁹Si CP-MAS NMR studies

The SBA-15 material is mainly a siliceous support matrix and therefore, ²⁹Si NMR studies is an important tool to track and identify the structural and functional changes in the matrix during the various stages of anchoring process (e.g. selective surface functionalization, anchoring of Pd-complex) and carbonylation reaction, if any. Two different methodologies of catalyst preparation were utilized for the synthesis of catalysts, as mentioned earlier, leading to two different batches of the catalysts. The anchored catalyst prepared using the post-synthesis grafting method, i.e. *S15-NH₂-(G)-Pd* had the external surface passivated prior to the functionalization and anchoring, while for the material synthesized using the direct one-pot co-condensation method, i.e. *S15-NH₂-(C)-Pd* no passivation was required.

For the post synthesis grafted material [S15-NH₂-(G)-Pd]

The results of stepwise ²⁹Si CP-MAS NMR experiments of *S15-NH₂-(G)-Pd* sample are presented in Figure 2.13. The calcined SBA-15 and the as-synthesized sample (Curves i and ii respectively) showed almost identical chemical shift values, with peaks at $\delta = -93.14, -102.32, -112.33$ ppm. The occurrence of these multiple peaks is attributed to the different types of the Si-sites namely Q^2 [(SiO)₂Si(OH)₂], Q^3 [(SiO)₃Si(OH)] and Q^4 [(SiO)₄Si], based on the number of free silanol groups, Si-OH on the Si-atom - 2, 1, 0 respectively. The spectra clearly showed that the proportion of Q^3 was the highest in the SBA-15 sample as expected for a well-ordered siliceous matrix having a high degree of cross-linking in the silica.²³ The occurrence of identical peak patterns in the as-synthesized and the calcined samples conclude that the SBA-15 did not undergo any structural change due to the calcination, and the long-range mesoporosity order is maintained after the calcination process. The Curve iii of the Figure 2.13 presents the spectrum for the external surface passivated SBA-15, which shows an additional peak at δ 11.85 ppm and the disappearance of the Q^2 peak with respect to Curve ii. The peak at δ 11.85 ppm is attributed to the presence of the -SiMe₃ moiety as the passive graft onto the

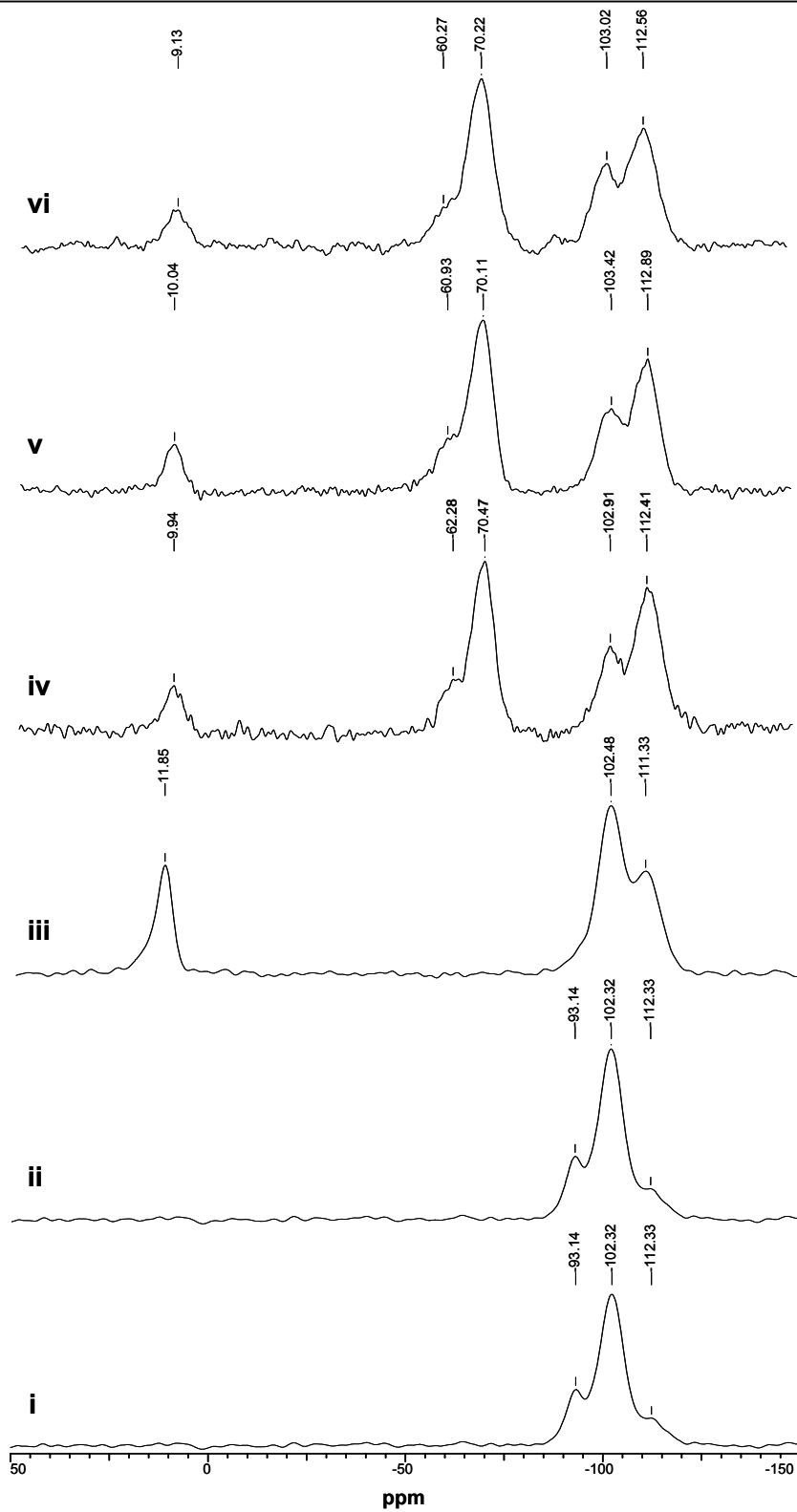


Figure 2.13: ^{29}Si CP MAS NMR spectra of S15-NH₂-(G)-Pd material
i- Calcined; *ii*- As-synthesized; *iii*- Outer silanol passivated; *iv*- NH₂-functionalized; *v*- Palladium-complex anchored; *vi*- After carbonylation reaction

surface of SBA-15. The disappearance of the Q^2 peak might be due to the absence of any dihydroxysilyl unit, in the matrix, as those might have been consumed in the silylation process using HMDS, leaving only monohydroxylated silyl moiety, Q^3 and non-hydroxylated silyl moiety, Q^4 in the matrix, with a higher proportion of the former. This might be the expected material having the outer surface passivated by $-\text{SiMe}_3$ groups and the internal silanol groups made available after the removal of the template. It may be mentioned here that the passivation using HMDS was performed before the template removal so that most of the external Si-OH groups are methylated, without affecting the internal silanol groups. The next spectrum, Curve iv represents the spectrum for the aminopropyl functionalized SBA-15, i.e. $S15-NH_2-(G)$, which shows appearance of two new peaks at $\delta -62.28$ ppm and $\delta -70.47$ ppm, along with the reversal of the proportions of the Q^3 and Q^4 peaks in comparison to Curve iii. The new peaks may be assigned to the T^2 [$-\text{SiR}(\text{OSi})_2(\text{OH})$] and T^3 [$-\text{SiR}(\text{OSi})_3$] moieties, in which R group is the 3-aminopropyl group, $\text{H}_2\text{N}-\text{CH}_2-\text{CH}_2-\text{CH}_2-$. These values of chemical shifts are in good agreement of the literature.²⁴ The other peaks due to Q^3 , Q^4 and $\delta 10$ ppm however remain unchanged in comparison to the previous spectrum i.e. Curve iii. The appearance of the T^m ($m = 2$ and 3) peaks confirm that the organosilyl graft moiety i.e. 3-aminopropylsilyl groups are incorporated as a part of the silica wall structure. It may be mentioned here that the proportion of the T^3 is higher than that of T^2 , which also indicates that after the incorporation of both the passive and the active graft, only a small amount of silanol groups are left free, and they occur only as single silanol groups on Si-centres in the functionalized SBA-15 matrix (as T^2 and Q^3 only). The next spectrum in Figure 2.13 i.e. Curve v, represents the spectrum of $\text{Pd}(\text{pyca})(\text{PPh}_3)(\text{OTs})$ complex anchored to the $-\text{NH}_2$ group of the aminopropyl moiety of the functionalized SBA-15, i.e. the $S15-NH_2-(G)-Pd$ material. This spectrum is very similar to the Curve iv with respect to the peak positions as well as the relative intensities. It may be concluded from this spectrum that, the incorporation of the Pd-complex does not affect the siliceous mesostructure of SBA-15 at all during the anchoring process. This is in agreement with the powder XRD patterns as seen previously (Section 2.3.1.1, Figure 2.5). The Curve vi represents the spectrum of the anchored Pd-complex material $S15-NH_2-(G)-Pd$ after carbonylation reaction. The spectrum shows no change in the characteristic peaks in position or intensity, reinstating the stability of the anchored Pd-complex catalyst for carbonylation.

For the one-pot co-condensed material [S15-NH₂(C)-Pd]

The results of the sequential ^{29}Si CP MAS NMR experiments of the catalyst material synthesized using the direct one-pot co-condensation method are presented in Figure 2.14. For this material, the matrix synthesis was performed in the presence of the precursor of the active graft molecule, and hence the as-synthesized material itself held the functional group in it, so calcination was not possible. The solvent extracted material was the first sample obtained. Curve i shows the spectrum of the solvent extracted material. The spectrum shows a bunch of three peaks around δ 93.6, 102.6 and 112.4 ppm, and another bunch at δ 64.07 and 71.6 ppm respectively. The first group of peaks is attributed to the Q², Q³ and Q⁴ species of the SBA-15 matrix respectively. It may be mentioned here that the relative proportion of Q³ is the highest

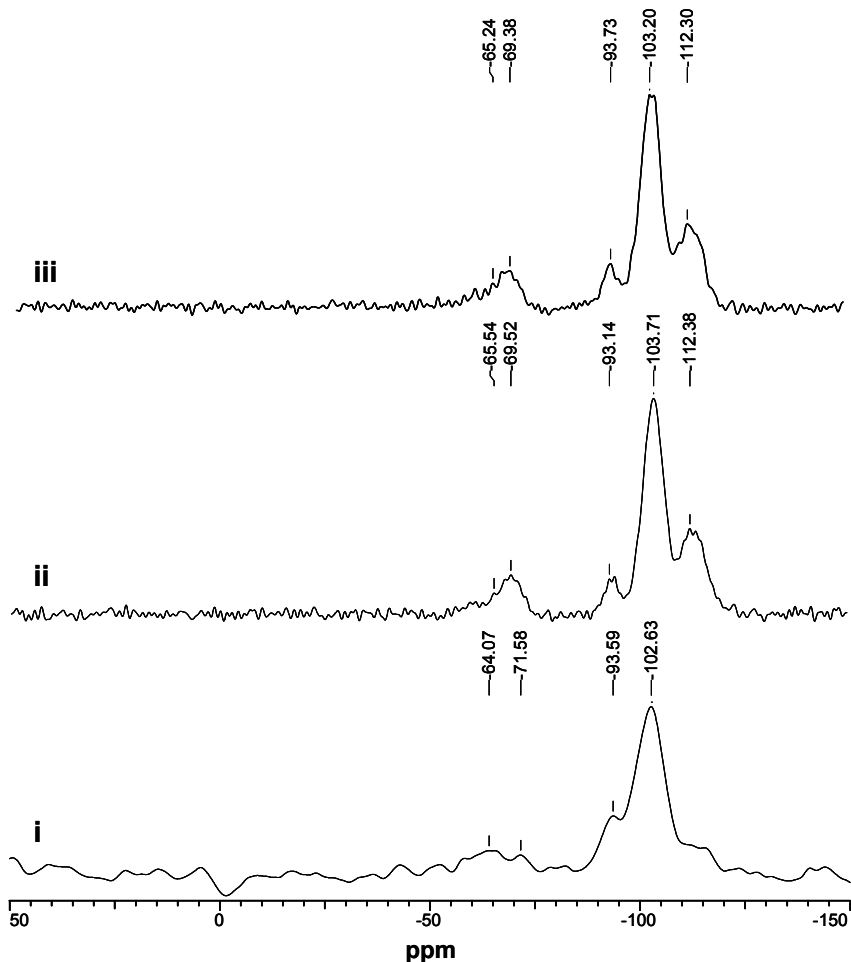


Figure 2.14: ^{29}Si CP MAS NMR spectra of S15-NH₂(C)-Pd material

i- Solvent extracted S15-NH₂(C); *ii*- Pd-complex loaded [S15-NH₂(C)-Pd], *iii*- After carbonylation reaction

for this material showing good cross-linking of siliceous matrix. The other two peaks at δ 64.07 and 71.6 ppm are assigned to the T^2 and T^3 moieties respectively. The occurrence of the T^m peaks in the NMR spectra again confirm that the functionalization of the mesoporous matrix was complete as speculated, by the one-pot *insitu* co-condensation of the precursors inside the synthesis gel, and as a result, the functional groups have been incorporated within the walls of the mesoporous matrix. Also, the removal of the template after the one-pot synthesis by solvent extraction method left the functionalized matrix *S15-NH₂-(C)* unchanged. The peaks resemble those of the material synthesized using the grafting method in position and intensity. The next spectrum, i.e. Curve ii represents the spectrum of the Pd(pyca)(PPh₃)(OTs) complex anchored inside the functionalized matrix, i.e. *S15-NH₂-(C)-Pd*. The peaks due to the Q^2 , Q^3 and Q^4 species appear at the same positions as that in Curve i, so also the peaks for T^2 and T^3 species of the functionalized SBA-15. These imply that the mesoporous matrix did not undergo any change in structure during the anchoring. The Curve iii in the Figure 2.14 represents the spectrum of the *S15-NH₂-(C)-Pd* after a carbonylation reaction. The observation of the peaks due to Q^2 , Q^3 and Q^4 as well as for the T^2 and T^3 in the same position with the same intensity reflected on the stability of the anchored catalyst even after treatment with strong acid promoter (TsOH) at high temperature (388 K) and pressures (~5.4 MPa).

Thus, ²⁹Si CP MAS NMR data gave important information regarding the nature of the anchored catalyst, its formation and stability during the synthesis as well as carbonylation reaction.

2.3.1.6.2 ¹³C CP-MAS NMR studies

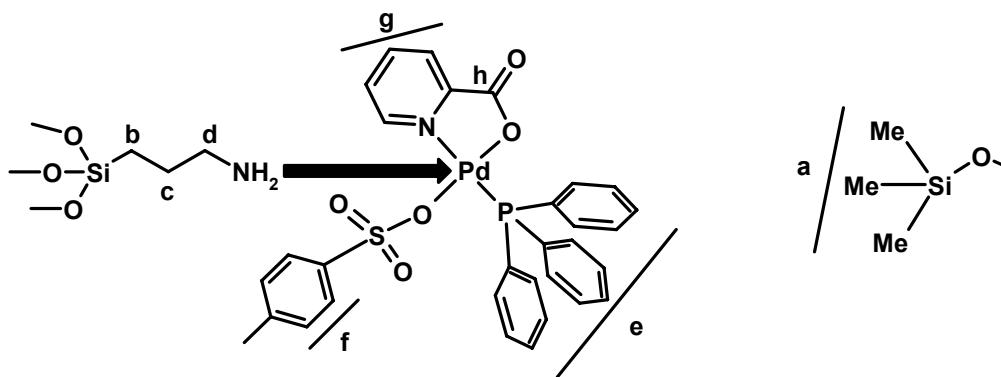
The anchored catalysts consist of a molecular anchor holding the catalyst molecule at one end and itself being attached to the support matrix. Essentially, these are organic molecules having desired functional groups. So ¹³C CP MAS NMR studies are important from viewpoint of understanding of the molecular environment of the anchored catalysts. With this target, sequential ¹³C CP MAS NMR experiments were carried out for all steps of synthesis of the anchored catalysts to learn about the chemical pathway of anchoring process, its stabilization and reactivity. Both the

pathways i.e. post- synthesis grafting and co-condensation as used for the anchoring of Pd complex, were investigated. The detailed reports are as follows.

For the post synthesis grafted material [S15-NH₂-(G)-Pd]

The ¹³C CP-MAS NMR experimental results are presented in Figure 2.15. The purely siliceous SBA-15 matrix used for anchoring the Pd-complex has no C-atoms in it, so the spectrum of calcined SBA-15 showed no ¹³C signals. However, for the post synthesis grafting method, the as-synthesized material was first treated with HMDS to ensure that all the exterior silanol groups were passivated by the –SiMe₃ moieties. This outer-surface passivated material was solvent extracted, and the NMR result is given in Curve i. The curve showed a single peak at δ 0.00 ppm, which is attributed to the three methyl carbons of the –SiMe₃ moiety. The absence of any resonance around δ 62-70 ppm confirmed that all the surfactants (Pluronic P123) were successfully removed during the template removal extraction step.²⁵ The next spectrum, Curve ii is the spectrum of the amine-functionalized SBA-15 i.e. [S15-NH₂-(G)]. It is notable that three distinct peaks at δ 42.7, 21.9 and 10.8 ppm are observed along with the 0 ppm peak for –SiMe₃. These correspond to the three C-atoms in the 3-aminopropyl group, H₂N-CH₂-CH₂-CH₂-Si of the molecular anchor, in the left-to-right order respectively, as similar to the literature data.²⁶ The presence of these peaks directly implied the incorporation of the 3-aminopropylsilyl anchor moiety in the walls of the SBA-15 matrix and also proved that the aminopropyl group was not decomposed under the preparation procedure. The Curve iii of the figure represents the spectrum of Pd(pyca)(PPh₃)(OTs) complex anchored to the NH₂-functionalized SBA-15 i.e. S15-NH₂-(G)-Pd material. The appearance of a number of peaks in the spectrum may be attributed to the different types of C-atoms present in the complex, in addition to those

Model of anchored Pd-complex



already in the solid matrix. The assignment of each of these peaks is given in the adjacent model, though the peaks of many C-atoms may easily overlap for some

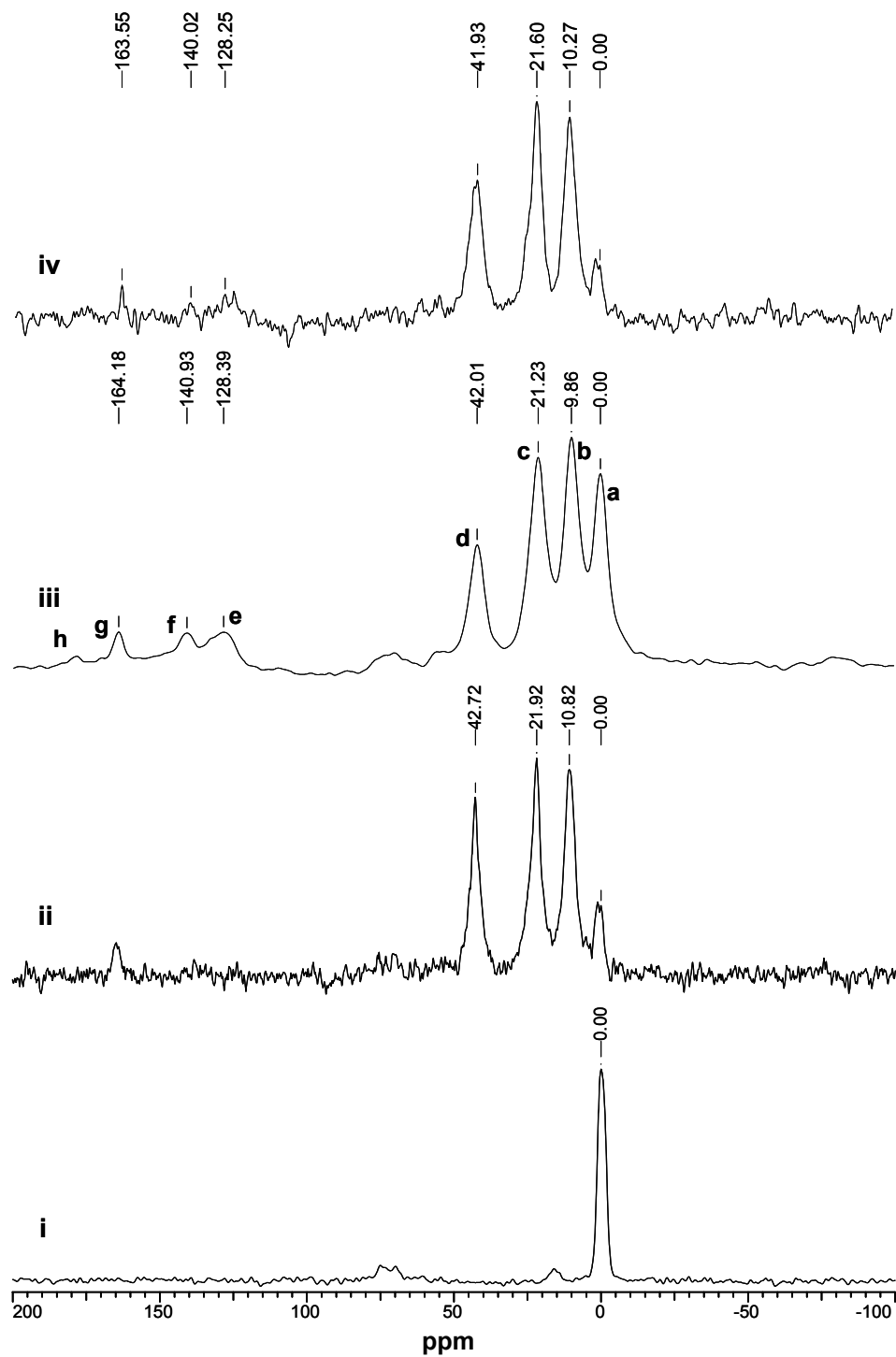


Figure 2.15: ^{13}C CP MAS NMR spectra of $\text{S15-NH}_2\text{-(G)-Pd}$ material

i- Exterior Si-OH passivated; ii- NH_2 -propyl-functionalized, iii- Pd-complex anchored, iv- After carbonylation reaction

of the atoms in the aromatic region i.e. ~130 to 170 ppm. However, the data are in satisfactory matching with those in the literature.²⁷ Thus, the Pd complex was proved to be chemically anchored to the functionalized walls of the SBA-15 matrix using an aminopropylsilyl bridge. The next spectrum, i.e. Curve iv represents the ¹³C spectrum of the used catalyst after a carbonylation reaction of styrene. The spectrum is almost similar to that of the fresh catalyst, (Curve iii) and all the principle peaks as marked are observed with negligible change in intensity and position, and hence it may be concluded from the comparison that the catalyst material did not change *chemically* during the carbonylation reaction. Furthermore, the Pd-complex and the other organic fragments were intact after the reaction, proving the stability of the catalyst under the stringent carbonylation conditions. Therefore, the post-synthetic grafting method proved to be a truly efficient methodology for the anchoring of Pd complexes to generate very stable heterogeneous catalysts.

For the one-pot co-condensed material [S15-NH₂-(C)-Pd]

The ¹³C CP MAS NMR experimental results of the anchored Pd-complex catalyst synthesized by the one-pot co-condensation method are presented in Figure 2.16. No passivation of the exterior silanol groups was necessary for the one-pot synthesis and hence this step was not present in the synthesis process. The first spectrum in this figure, i.e. Curve i showed three distinct peaks at δ 9.2, 21.1 and 42.7 ppm. These are attributed to the carbon atoms of the 3-aminopropyl group present in the molecular anchor as similar to the previously described material i.e. S15-NH₂-(G)-Pd. The designations of the three peaks are the same as for the Figure 2.15. The absence of the 0.0 ppm peak in the spectrum of S15-NH₂-(C)-Pd was also justified, as the material was synthesized using one-pot synthesis, without using any passivation step. The Curve ii of the Figure 2.16 represents the spectrum of the Pd-complex anchored material. The occurrence of the several peaks at $\sim \delta$ 128, 140, 167, 174 ppm in the spectrum indicate the presence of the Pd(pyca)(PPh₃)(OTs) complex attached to the walls of the functionalized SBA-15 solid matrix. The assigning of the peaks is similar to that of the spectra in Figure 2.15, which further confirms that the Pd-complex was attached to the NH₂-functionalized SBA-15 formed by the co-condensation method, in the same manner as the post synthetic grafted material. The next spectrum, i.e. Curve iii is of the used catalyst after a run of carbonylation of styrene. It is noticeable here that the principle peaks in the spectrum did not change at all (in

intensity or position) after the successful carbonylation run. Therefore, the anchored catalyst prepared by one-pot co-condensation method was equally stable as the previously described material.

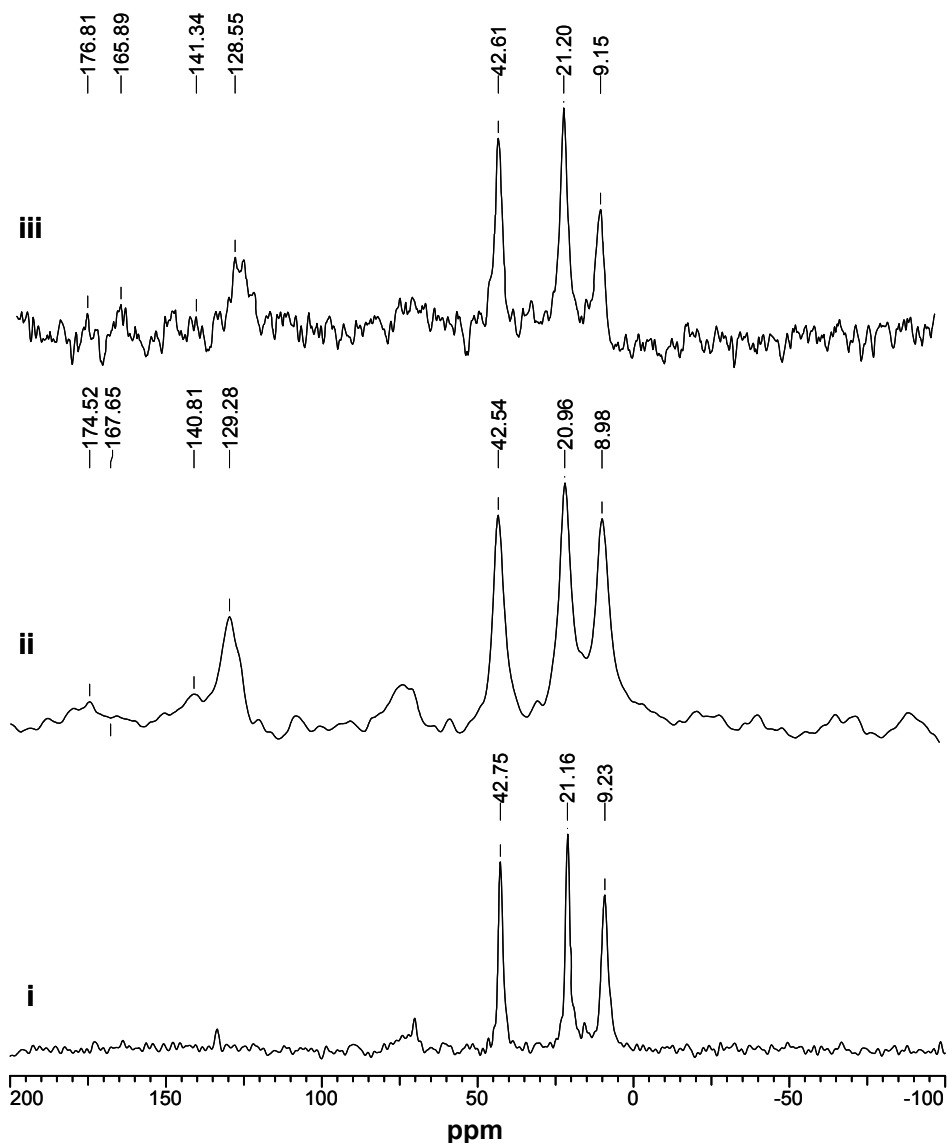


Figure 2.16: ^{13}C CP MAS spectra of S-15-NH₂-(C)-Pd material

i- NH₂-functionalized SBA-15 by co-condensation method; ii- Pd-complex anchored; iii- After carbonylation reaction

The characterization of the anchored Pd-complex catalysts using ^{13}C CP MAS NMR experiments was successful in understanding the nature of the support SBA-15, Pd-complex at different stages of immobilization as well as after reaction.

2.3.1.6.3 ^{31}P CP-MAS NMR studies

^{31}P CP MAS NMR experiments of the solid catalysts is essential to understand the coordination environment of the central Pd-atom in the anchored catalyst. This is necessary to explain the behavior of the anchored Pd-complex involved in catalysis in, light of the observed change in the stereo-electronic properties in the complex itself as a result of immobilization.

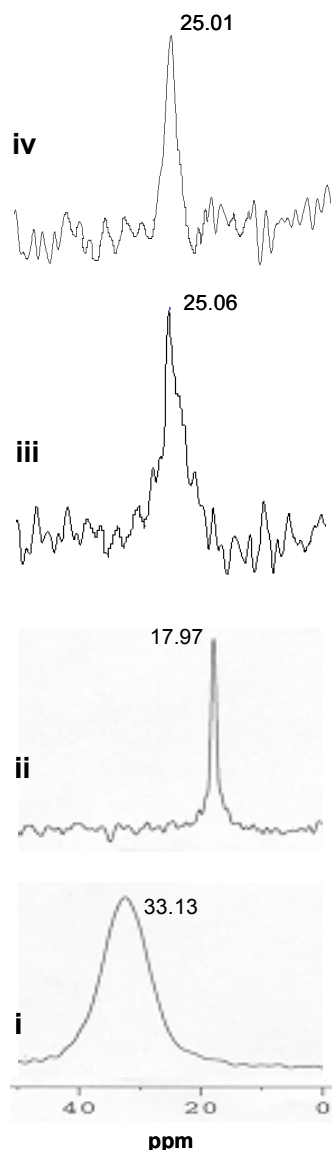


Figure 2.17: ^{31}P CPMAS spectra of various anchored Pd-complexes

i- Pd(pyca)(PPh₃)(OTs); *ii-* M41-NH₂-Pd, *iii-* S15-NH₂-(G)-Pd; *iv-* S15-NH₂-(C)-Pd

A comparison of the ^{31}P CP MAS NMR spectra of the different anchored catalysts, namely M41-NH₂-Pd, S15-NH₂-(G)-Pd and S15-NH₂-(C)-Pd along with that of the Pd(pyca)(PPh₃)(OTs) complex are presented in Figure 2.17. As observed from the spectra, there is considerable change in the peak positions in the different samples. The pure Pd-complex shows a signal at δ 33.13 ppm (Curve i). This value of the chemical shift is slightly different from the liquid state spectrum of the complex, which shows two signals at $\sim \delta$ 36.45 and 35 ppm respectively, corresponding to the *cis* and *trans* isomers existing in the solution phase. In the solid-state spectrum such isomerization equilibrium is not existent and also the width is much higher due to the anisotropic effects. Each of the anchored complexes showed a strong single peak (Curves ii, iii and iv) at an upfield position to the pure complex. The peaks for the M41-NH₂-Pd, M48-NH₂-Pd, S15-NH₂-(G)-Pd, and S15-NH₂-(C)-Pd occur at δ 17.97, 17.86 (not shown in Figure 2.17), 25.06, 25.01 ppm respectively. The occurrence of the single peaks in all the anchored complexes is

indicative of the stability and integrity of the Pd-complex after immobilization, as any degradation in the complex would have been reflected in the ³¹P NMR spectra. The shifting of the peaks to an upfield position definitely points to some sort of interaction of the complex with the functionalized support matrix. And a probable coordination of the N_{APTS} → Pd may be visualized as the cause of such shifts, which may be varying in magnitude for the different matrix environments. The N-atom of the 3-aminopropyl group attached to the walls of the siliceous matrices coordinates to the Pd-centre, which thus becomes more electron rich. This electron density may however be transferred to the P-atom of the triphenyl phosphine ligand via a probable dπ – dπ back-bonding interaction, as the PPh₃ possesses good π-acid properties. This enhancement in the electron density over the P-atom will cause the upfield shift of the resonance peaks as observed in the spectra. The degree of variation of this phenomenon may be different for the different matrices (MCM-41, SBA-15 etc.), which might depend on the unit cell dimensions and hence vary the molecular constraints and mobility of the Pd-complex inside the porous channels. For example, the narrower channels in MCM-41 (diameter ~3.5 nm) might have very different set of stereo-electronic constraints than for the larger pore SBA-15 matrix (diameter ~10 nm).

Therefore, ³¹P CP MAS NMR experiments validated the proposed chemical anchoring of the Pd-complexes to the solid matrices via a N_{APTS} → Pd coordination. The stability of the complexes during the immobilization process is successfully proven by these NMR studies. The stability of the anchored complexes under the carbonylation environment was also appreciable. Though primarily observed from the NMR studies this may be better understood after detailed leaching experiments, and will be described in a later section in this chapter.

2.3.1.7 Fourier Transform Infra Red Spectroscopy

The FT-IR spectroscopy was used to understand the nature of the different functional groups in the different anchored palladium complexes and analyze the change brought in by the process of anchoring to the different functional groups present in the complex and the interactions if any. The typical comparative FT-IR spectra of the pure Pd-complex, pristine support matrix and the anchored catalyst *M41-NH₂-Pd* is presented in Figure 2.18. It is clearly observed from the graph for the pristine MCM-41 (blue curve of *M41*) that the bands at 962 cm⁻¹ and 1090 cm⁻¹ are

characteristic of the $\nu(\text{Si-OH})$ and $\nu_{\text{asym}}(\text{Si-O-Si})$ vibrations respectively. It is noticeable that these bands are also clearly visible for the catalyst *M41-NH₂-Pd* showing that the support matrix, i.e. MCM-41 does not undergo any change during the anchoring process and all the Si-OH groups are not occupied totally by either the passive or the active graft molecule. The bands for the stretching vibrations at 1329 cm^{-1} ($\nu_{\text{O=C-O}}$), 1605 cm^{-1} ($\nu_{\text{C=C}}$, very weak band) and 1669 cm^{-1} ($\nu_{\text{C=O}}$), were observed for the anchored catalyst i.e. *M41-NH₂-Pd* catalyst as similar to those of Pd(pyca)(PPh₃)(OTs) complex at 1330 cm^{-1} , 1604 cm^{-1} and 1668 cm^{-1} respectively, as reported elsewhere.^{4b} One interesting observation might be mentioned here that a little variation in the stretching frequencies was found for the Pd-N bond. The *M41-NH₂-Pd* catalyst showed a peak at 563 cm^{-1} ($\nu_{\text{Pd-N}}$) which is different from that of the Pd(pyca)(PPh₃)(OTs) complex ($\nu_{\text{Pd-N}} = 569\text{ cm}^{-1}$)^{4b}. This shift of the stretching frequency to a lower wave number might be attributed to the possible N→Pd coordination by the dangling NH₂-group of the NH₂-functionalized MCM-41 (*M41-NH₂*). This interaction might increase the electron density on the Pd-atom and hence the Pd-N stretching frequency (N of pyridine moiety) decreases and consequently the red shift is observed. Thus, it might

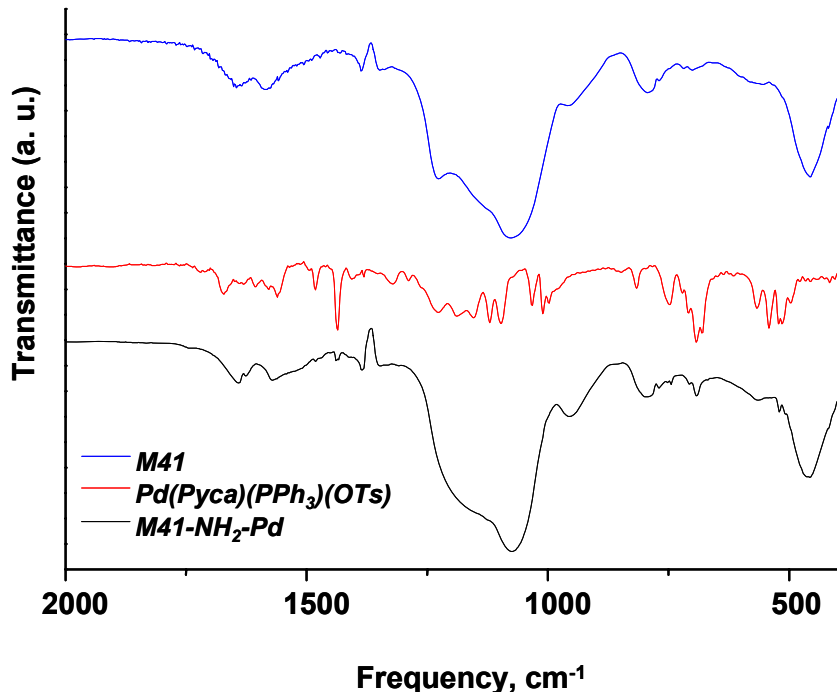


Figure 2.18: Comparative FT-IR spectra of MCM-41 based catalyst (*M41-NH₂-Pd*)

be consolidated that the Pd(pyca)(PPh₃)(OTs) complex did not show much change in the vibrational behavior, only except the Pd-N stretching vibration which actually otherwise confirmed the N_{APTS}→Pd coordination resulting the stabilization of the Pd-complex inside the mesoporous matrix. The different IR stretching bands for the different catalysts is presented in Table 2.4. The data in Table 2.4 also reflects the similar causes for the changes in the stretching bands for the different catalysts enlisted. The interaction of the N_{APTS} with the palladium centre is clearly visible for all of the catalysts and as a result the direct involvement of the stated interaction clearly confirmed the coordination of the N_{APTS} to the Pd-atom and hence an efficient anchoring of the Pd(pyca)(PPh₃)(OTs) complex inside the mesoporous matrices.

Table: 2.4: FT-IR data of different anchored Pd-complex catalysts (values in cm⁻¹)

Catalysts	IR Bands	V _{Si-OH}	V _{Si-O-Si}	V _{O=C-O}	V _{C=O}	V _{Pd-N}
<i>Pd(pyca)(PPh₃)(OTs)</i>		-	-	1330	1668	569
<i>M41-NH₂-Pd</i>		962	1090	1329	1669	563
<i>M48-NH₂-Pd</i>		963	1090	1329	1668	563
<i>S15-NH₂(G)-Pd</i>		962	1089	1329	1668	564
<i>S15-NH₂(C)-Pd</i>		962	1089	1330	1669	564

2.3.1.8 Palladium Content Analysis

All the four anchored palladium complexes were analyzed for Pd-content using the atomic absorption spectroscopic (AAS) method. The samples of a fixed weight were dissolved and digested in concentrated HNO₃ and were diluted to a fixed volume. AAS experiments were conducted using these solutions. The other supported Pd-complex catalysts i.e. Pd-S and Pd-Y were also analyzed similarly. The results of AAS analysis are presented in Table 2.5. It was generally observed that the palladium content of the different anchored Pd-complex catalysts were roughly in the range of 0.1 to 0.3 % by weight for the anchored catalysts while, the Pd-content was relatively higher for the supported catalysts. This may be due to the fact that for the supported catalysts the complex is simply adsorbed at random to the surface and voids, while for

the anchored catalysts, the complex are attached to only the specific anchoring sites, which are much less in number.

Table 2.5: Pd-content of different anchored and supported Pd-complex catalysts

Entry	Material	Pd-content, %
1	M41-NH ₂ -Pd	0.18
2	M48-NH ₂ -Pd	0.20
3	S15-NH ₂ -(G)-Pd	0.11
4	S15-NH ₂ -(C)-Pd	0.21
5	Pd-S	0.62
6	Pd-Y	0.81

2.3.2 Catalytic Reactions

Catalytic carbonylation reactions were performed using the novel anchored palladium complex catalysts to evaluate the efficiency of the catalyst comparative to the different other heterogeneous catalysts available for this reaction in terms of the activity, regioselectivity, stability and recyclability aspects. The carbonylation of alcohols and olefins as already been discussed in the previous chapter, Chapter 1), is one of the most important catalytic transformations yielding industrially important products. The importance of the 2-aryl propionic acids as the non-steroidal anti-inflammatory agents has boosted the research interest in this branch of the carbonylation reactions. With these as the important targets, the carbonylation of aryl olefins and alcohols were undertaken. Details of the studies are described categorically as follows.

2.3.2.1 Carbonylation of Olefins and Alcohols

Carbonylation of aryl olefins and alcohols were performed using the anchored Pd(pyca)(PPh₃)OTs) complex inside the mesoporous channels of MCM-41, MCM-48 and SBA-15. Following the homogeneous counterpart^{4b} as the standard benchmark, all the reactions were carried out in the presence of an acidic and an alkali metal halide promoter, with a little amount of free triphenyl phosphine (5-25 mg) with a

target to obtain highest catalytic activity, selectivity and a truly heterogeneous catalyst for the carbonylation reactions. Styrene was used as the model substrate for the standardization reactions, however, different substrates were also tried, the results of which will be discussed in a later section. The reactions using all the four anchored Pd-complex catalysts i.e. *M41-NH₂-Pd*, *M48-NH₂-Pd*, *S15-NH₂-(G)-Pd* and *S15-NH₂-(C)-Pd* required long durations of ~12 h to complete. >98% conversion was observed for all the catalysts with outstanding chemo- and regioselectivity of > 99 %. As similar to the homogeneous Pd(pyca)(PPh₃)OTs complex catalyst, the carbonylation of styrene proceeded via intermediate derivatization of the substrate to the chloro-derivative which might be the active substrate in the catalytic cycle. The amount of the chloro-derivative, i.e. 1-chloroethylbenzene (1-CEB) gradually increased, reached a maximum and then receded at the end of the reaction. A typical concentration-time profile for carbonylation of styrene using *M41-NH₂-Pd* is presented in Figure 2.19. It is noticeable that the reaction has an initial period of ~3 h as the induction period of the reaction. Moreover, after that, the reaction rate becomes really fast. There was 100% mass

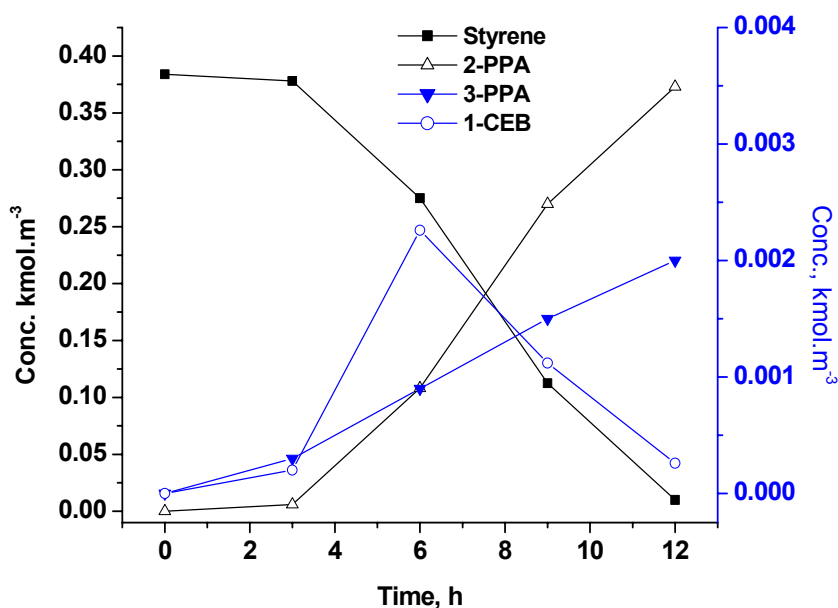


Figure 2.19: A typical concentration-Time profile of carbonylation of styrene using *M41-NH₂-Pd* as catalyst

Reaction conditions: Catalyst: 100 mg; Styrene: 9.6 mmol; LiCl: 0.5 mmol; TsOH: 0.5 mmol; PPh₃: 0.095 mmol; H₂O: 50 mmol; Solvent: MEK; P_{CO}: 5.4 MPa; Temperature: 388K

balance of the liquid reaction mixture. The C-T profile shows all the components of the reaction mixture. The substrate and the major product (2-phenylpropionic acid, 2-PPA) are plotted on the left Y-axis while the minor product (3-phenylpropionic acid, 3-PPA) and the chloro intermediate (1-chloroethylbenzene, 1-CEB) are plotted on the right Y-axis for better clarity. Upon completion of 12 h, a high conversion of 98.12% was observed. A turnover number of 5568 was obtained with a very high turnover frequency of 464 h^{-1} achieved. The regioselectivity of > 99.31% to the desired branched acid (2-PPA) was obtained.

To understand the leaching behavior of the novel anchored catalyst, a standard reaction was stopped abruptly at ~ 30 % conversion level and the reaction mixture were filtered hot to remove any solid catalyst. The pale yellow filtrate was charged in a reactor and reaction was conducted without any more of fresh catalyst. This reaction showed no further conversion and the Pd-content was analyzed to be only 3.5×10^{-4} % of the total Pd-charged in a reaction, which may be deemed negligible. Thus, the novel anchored Pd-complex catalyst showed good activity, selectivity and stability.

To compare the carbonylation activities of the other anchored catalysts, the standard reaction was repeated using them, namely *M48-NH₂-Pd*, *S15-NH₂-(G)-Pd* and *S15-NH₂-(C)-Pd*, and the product profiles for the major are presented in Figure 2.20. An important observation of these reactions was that the reaction using the SBA-15 based catalyst [*S15-NH₂-(G)-Pd*] was found to be the most active anchored Pd-complex catalyst. This reaction got over (98.25 % conversion) in 12 h with a very high regioselectivity (99.54%) to the branched-acid product. The TOFs were calculated to be 464, 417, 760 and 401 h^{-1} respectively for the catalysts *M41-NH₂-Pd*, *M48-NH₂-Pd*, *S15-NH₂-(G)-Pd* and *S15-NH₂-(C)-Pd*. Thus, the novel anchored Pd-complex catalysts proved to be efficient carbonylation catalysts.

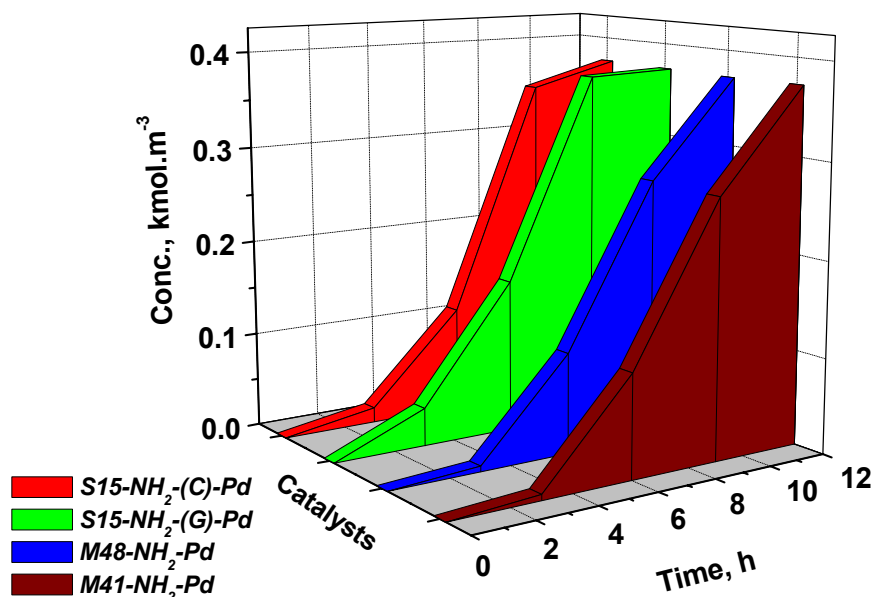


Figure 2.20: Major-product (2-PPA) concentration vs. Time profiles for different anchored catalysts

Reaction conditions: Catalyst: 100 mg; Styrene: 9.6 mmol; LiCl: 0.5 mmol; TsOH: 0.5 mmol; PPh₃: 0.095 mmol; H₂O: 50 mmol; Solvent: MEK; P_{CO}: 5.4 MPa; Temperature: 388K, Duration: 12 h

2.3.2.2 Recycle and Stability Aspects

With the demonstration of the high activity of the novel anchored catalysts, it was important to know the recyclability and stability of the anchored catalysts. The comparative recycle studies of the four novel anchored Pd-complex catalysts are presented in Figure 2.21. All the reactions were carried out upto a fixed duration of 12 h and each catalyst was recycled for three successive recycles following the standard reactions. It is clearly evident from the recycle studies that the anchored complex catalysts in mesoporous matrices recycled efficiently for at least three recycles, without any significant variation in the activity and regioselectivity. The efficient recycling of the catalysts also effectively increased the cumulative turnover numbers for the anchored catalysts ($>2.2 \times 10^4$ for all the catalysts), especially a cumulative TON of 36,500 was obtained while using the S15-NH₂-(G)-Pd catalyst, thus illustrating the high efficiency.

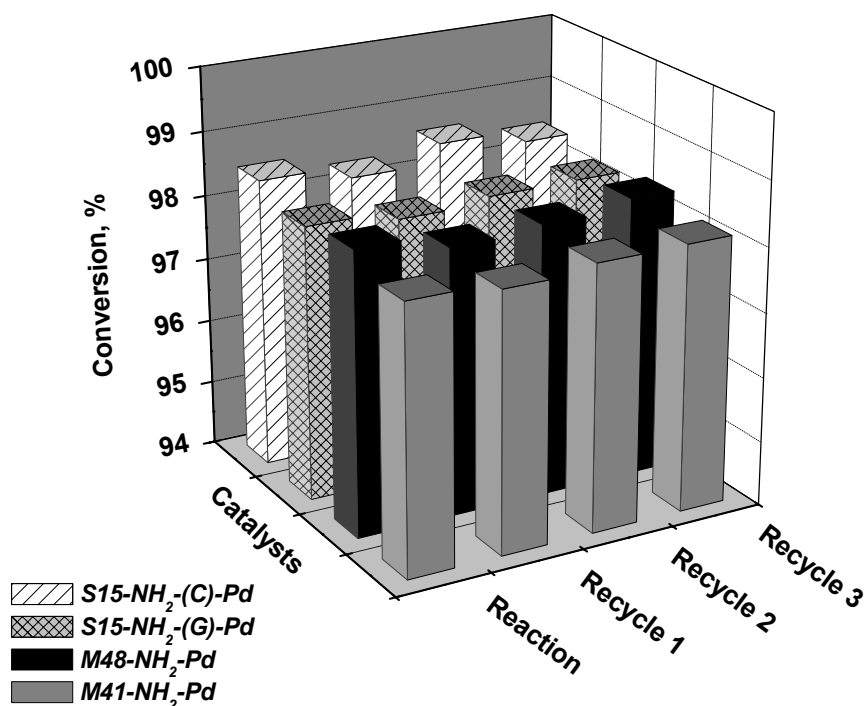


Figure 2.22: Recycle studies using different anchored Pd-complex catalysts

Reaction conditions: Catalyst: 100 mg; Styrene: 9.6 mmol; LiCl: 0.5 mmol; TsOH: 0.5 mmol; PPh₃: 0.095 mmol; H₂O: 50 mmol; Solvent: MEK; P_{CO}: 5.4 MPa; Temperature: 388K, Duration: 12 h

This is worth mentioning that the regioselectivity to the branched-acid product was maintained at >99.4% for all the recycle reactions. As previously mentioned in Section 2.3.2.1, the anchored catalysts showed extremely good stability and even though a very negligible amount of Pd ($\sim 3.5 \times 10^{-4}$ % for *M41-NH₂-Pd* and 2.16×10^{-4} % for *S15-NH₂(G)-Pd*) was lost during each run of the catalyst, the change in the TOF was quite insignificant. To understand the importance of “chemically” anchoring of the Pd(pyca)(PPh₃)(OTs) to the mesoporous matrices in the stability of the catalysts, the *Pd-Y* and *Pd-S* catalysts were employed for carbonylation of styrene. Both *Pd-Y* and *Pd-S* showed extensive leaching of Pd in the reaction mixture and as much as 20% of the Pd-loaded was lost during the first reactions only. Even if when NaY zeolite was used as a support matrix (in *Pd-Y*) having a regular defined structure, ~18% of the total

palladium charged in a particular reaction was leached out in to the organic reaction mixture. Also, the reaction mixtures turned blackish which gave minute black precipitates on standing – this might be due to the degradation of the detached Pd-complex under the reaction conditions to Pd(0). For the four anchored catalysts, no such degradation was observed and hence, the novel anchored Pd-complex catalysts were one of the best heterogenized/ immobilized Pd-complex catalysts for the carbonylation reactions. Therefore, the Pd-complex being chemically attached to the surface of the siliceous support matrices were observed to be stable and was less susceptible to leaching under the stringent carbonylation reaction conditions. Further, these results were reinforced by the CP MAS NMR and XPS studies as described before.

2.3.2.3 Parametric Variations

After optimizing the reaction using the anchored Pd-complex catalysts, a detailed parametric variation was important to study to understand the dependence of the catalyst performance on the different reaction parameters. Styrene was used as the substrate for these studies. The effect of variation of the reaction parameters such as substrate concentration, catalyst loading, promoter concentrations and ratios of H⁺ and Cl⁻, CO-partial pressure, temperature etc. were studied in details and the results are discussed under categorized heads as follows.

2.3.2.3.1 Effect of Substrate Concentration

The effect of the variation of the concentration of the substrate is an important issue for the proper understanding of the reaction. Substrate concentration effect was investigated using three different styrene concentrations as simple fraction/multiple of the standard conditions of 9.6×10^{-3} moles in 25 mL of solution (i.e. $0.384 \text{ kmol.m}^{-3}$) Keeping all other reaction conditions as constants, all the reactions were carried out for the same duration of 12 h to assess the results comparatively. The conversions of the reactions using the different catalysts i.e. *M41-NH₂-Pd*, *M48-NH₂-Pd*, *S15-NH₂-(G)-Pd* and *S15-NH₂-(C)-Pd* is presented in Figure 2.22. It is observed that the conversion of styrene was changing with its concentration for all the catalysts, with slight variations in the values. When the concentration was half of that of the standard charge, the reactions went to complete conversion (> 99%) for all the

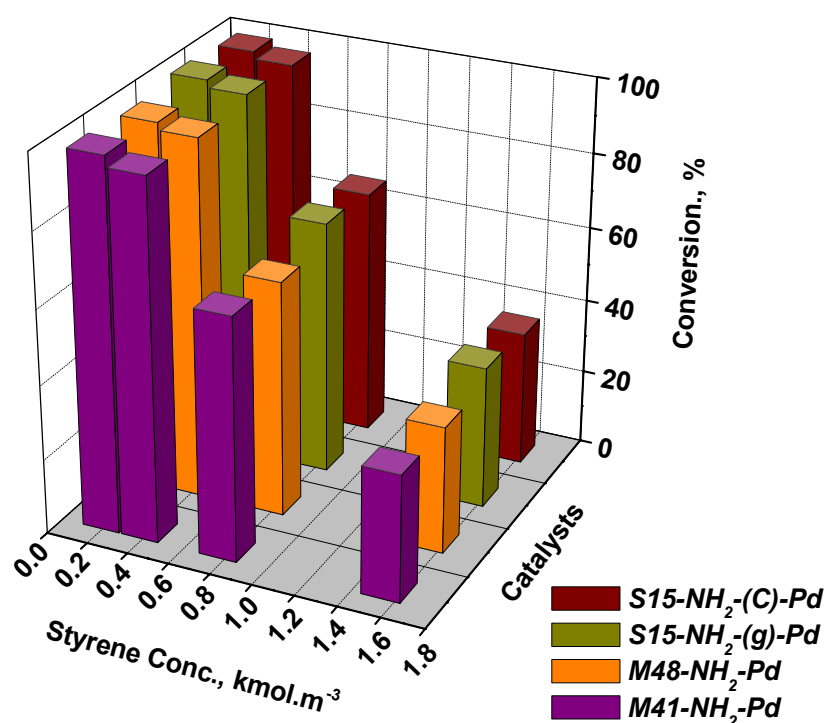


Figure 2.23: Effect of substrate concentration on styrene carbonylation

Reaction conditions: Catalyst: 100 mg; LiCl: 0.5 mmol; TsOH: 0.5 mmol; PPh₃: 0.095 mmol; H₂O: 50 mmol; Solvent: MEK; P_{CO}: 5.4 MPa; T: 388K, Duration: 12 h

catalysts. The regioselectivity to the branched acid product was maintained at >99.5% for all the catalysts. When the substrate concentration was doubled to 0.768 kmol.m⁻³ the reaction rate was almost similar and as a result, the conversion at the end of 12 h was much less (~63 %) than the standard reaction. On further increase of the substrate concentration to four times the standard (~1.536 kmol.m⁻³), the reaction conversion decreased showed only ~ 35 % conversion for all the catalysts. However, in all the cases, the regioselectivity to the 2-PPA was as high as the standard reaction, nearly 99.5% for all the catalysts. The reason behind this kind of a variation might be due to the accessibility of the active sites by the active substrate molecules. Since the catalyst and the promoter concentrations are the same in all the reactions, more number of the substrate molecules does not ensure that the catalyst sites and the promoters activate more molecules, hence in a particular duration of the reaction a definite amount of the substrate is only converted. Since the total charge of the substrate is high, the

conversion levels show a decrement. The constancy of the regioselectivity values prove that the catalytic chemistry is unhindered by the styrene concentrations.

2.3.2.3.2 Effect of Catalyst Loading

It is an important to investigate the effect of the catalyst concentration for the novel anchored Pd-complex catalysts. The variation of the catalyst charges were done in the range of 50 to 600 mg, in the standard charge of the reactions, for all the

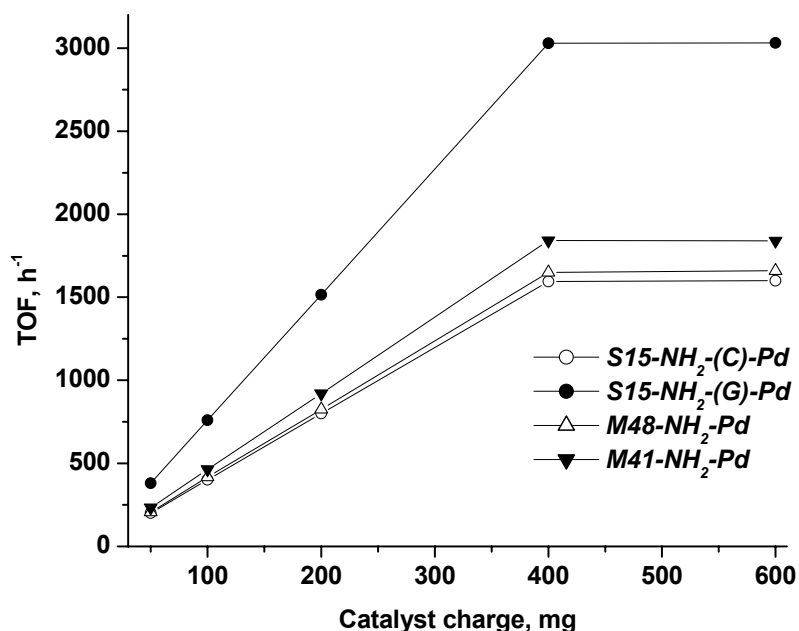


Figure 2.23: Effect of catalyst charge on styrene concentration

Reaction conditions: Styrene: 9.6 mmol; LiCl: 0.5 mmol; TsOH: 0.5 mmol; PPh₃: 0.095 mmol; H₂O: 50 mmol; Solvent: MEK; P_{CO}: 5.4 MPa; T: 388K

four novel anchored Pd-complex catalysts, namely, *M41-NH₂-Pd*, *M48-NH₂-Pd*, *S15-NH₂-(G)-Pd* and *S15-NH₂-(C)-Pd*. The variations in the catalyst activity for the different catalysts, with the varying catalyst charge are presented in Figure 2.23. The trends show that the activity/ reaction rate (expressed as the TOF) increased with the increase in the catalyst concentration almost linearly until a certain concentration, specifically upto four times the standard catalyst charge, but ceased to manifest any effect beyond that for all of the anchored catalysts. The *S15-NH₂-(G)-Pd* catalyst showed highest activity among the other catalysts for all the concentrations. The lowest

TOFs were obtained for the *S15-NH₂-(C)-Pd* catalyst due to the higher Pd-content in it. The catalyst concentration however did not have any effect on the regioselectivity of the reaction, and > 99% regioselectivity was obtained for the branched acid, 2-PPA for all of the reactions using the four anchored catalysts. These observations might be attributed to the nature of the catalysts and the number of accessible active sites on them. When the catalyst concentration was increased, the actual number of the active catalytic sites increased, which were manifested in the rise in the activity, quite proportionally until a certain concentration of the catalyst. Thereafter, the further increase in the catalyst concentration did not show any increment in activity. This may be explained as that the population of the active sites might be far in excess to that of the active substrate moiety beyond a certain catalyst concentration, therefore no change in catalyst activity was observed then. This logic seems to be universal for all the catalysts, all of which register a similar kind of variation. Also another reason might be due to the mass transfer parameters working under the reaction conditions mentioned. The further detailed evaluation of mass transfer resistances was not performed. Since the high regioselectivity to 2-PPA (>99.5%) did not alter due to the variation in the catalyst concentrations, it may be concluded that the catalytic cycle is independent of the catalyst concentration effect, for all the anchored catalysts.

2.3.2.3.3 Effect of CO Partial Pressure

The partial pressure of carbon monoxide is one of the influencing factors for the carbonylation activity of any catalyst, hence it is very important to study the effect of CO partial pressure on the carbonylation of styrene using the four novel anchored Pd-complex catalysts. Reactions were carried out using the four anchored catalysts for different carbon monoxide partial pressures. All the reactions were performed using the same catalyst charge and keeping the standard set of reaction conditions. The results are presented in the Figure 2.24. It is clearly noticeable from the graphs that the catalytic activity was influenced directly by the CO partial pressure. The rate of the reaction (expressed in terms of TOF of the reaction) seemed to vary almost linearly with respect to the partial pressure of carbon monoxide, in the range of the CO-pressures selected. The direct dependence of the activity of all the four anchored catalysts with the partial pressure of CO reflects the involvement of carbon monoxide in the catalytic cycle as the CO insertion step. As known commonly that the

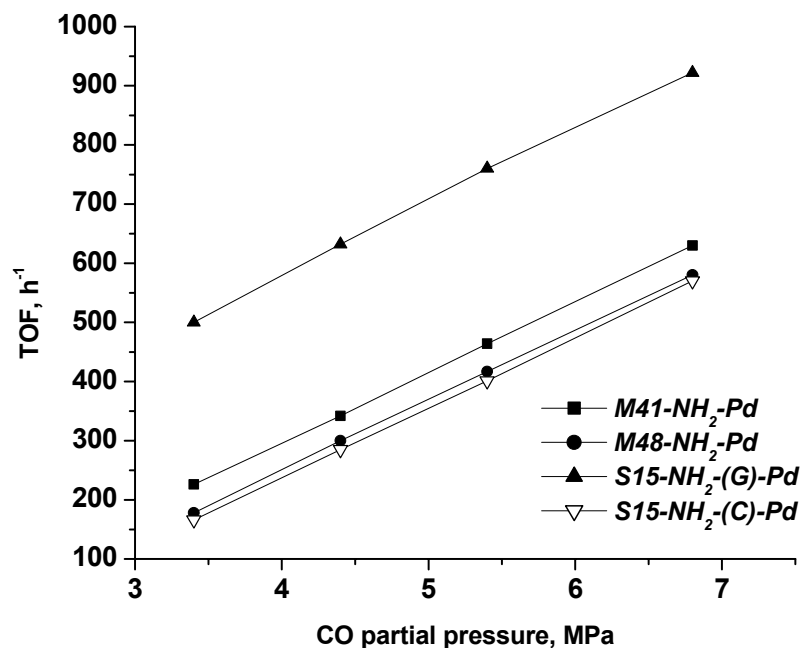


Figure 2.24: Effect of CO partial pressure on styrene carbonylation

Reaction Conditions: Catalyst: 100 mg; Styrene: 9.6 mmol; LiCl: 0.5 mmol; TsOH: 0.5 mmol; PPh₃: 0.095 mmol; H₂O: 50 mmol; Solvent: MEK; T: 388K

regioselectivity to the branched isomer is also dependent on the CO partial pressure, which is manifested as the rise in regioselectivity with rising CO partial pressure.²⁸ However, in contrary to the previous observations, no variation in the regioselectivities was observed for the anchored catalysts. The slower progress of the reactions using the anchored catalysts (reaction times ~10-12 h) might lead to the faster equilibration at the CO-insertion step, leading to no variation on the regioselectivity observed for the branched acid product 2-PPA. Thus, the partial pressure of carbon monoxide played an important role in the carbonylation of styrene as a direct dependence, in the range of partial pressures as shown.

2.3.2.3.4 Effect of Promoters

Promoters play a very important role in the carbonylation reactions of olefins and alcohols. As already demonstrated for the homogeneous catalysis using the Pd(pyca)(PPh₃)(OTs) complex, TsOH and LiCl have been used as the source of H⁺ and Cl⁻ ions, which promote the carbonylation reactions achieving the highest turnovers reported.^{1b} As a routine comparison and optimization study of the variation of

catalytic activity with the promoters, two different aspects were recognized, such as the mutual ratio of the promoters and the total quantity of the promoters used. The effect of the mutual ratio of promoters on the performance of the carbonylation is presented in Table 2.6.

Table 2.6: Effect of mutual ratio of promoters on styrene carbonylation for different anchored Pd-complex catalysts

Sl. No.	Catalyst	Ratio of promoters	Conv., %	Time, h	iso	n	TOF
1	M41-NH ₂ -Pd	2:1	96.55	12	99.23	0.1	456
2	M41-NH ₂ -Pd	1:1	98.12	12	99.31	0.68	464
3	M41-NH ₂ -Pd	1:2	97.50	12	99.32	0.6	461
4	M48-NH ₂ -Pd	2:1	97.21	12	99.10	0.1	412
5	M48-NH ₂ -Pd	1:1	98.37	12	99.10	0.1	417
6	M48-NH ₂ -Pd	1:2	97.60	12	99.20	0.1	414
7	S15-NH ₂ -(G)-Pd	2:1	97.61	12	99.40	0.50	755
8	S15-NH ₂ -(G)-Pd	1:1	98.25	12	99.54	0.44	760
9	S15-NH ₂ -(G)-Pd	1:2	98.23	12	99.50	0.46	758
10	S15-NH ₂ -(C)-Pd	2:1	96.80	12	99.21	0.76	395
11	S15-NH ₂ -(C)-Pd	1:1	98.19	12	99.46	0.52	401
12	S15-NH ₂ -(C)-Pd	1:2	97.60	12	99.35	0.64	398

Reaction conditions: Catalyst: 100 mg; Styrene: 9.6 mmol; LiCl: 0.5 mmol; TsOH: 0.5 mmol; PPh₃: 0.095 mmol; H₂O: 50 mmol; Solvent: MEK; P_{CO}: 5.4 MPa; Temperature: 388K, Duration: 12 h

The data as presented in the Table 2.5 represents that the reactions did not vary in great magnitude when the mutual ratio of the two promoters were changed. While using the 1:1 mutual ratio of TsOH to LiCl in the reaction mixture, the reactions showed slightly better performances for all the four anchored catalysts. Even though we had observed the involvement of the chloro-derivative (1-CEB) as the intermediate in the carbonylation of styrene, formed by the reaction of styrene and Cl⁻, the conversions and turnovers for the reactions using TsOH: LiCl as 1:2 were not higher than the

reactions using 1:1 ratio of the respective promoters. The reason behind this might be the balance between the optimum populations of the chloro-derivative as the active

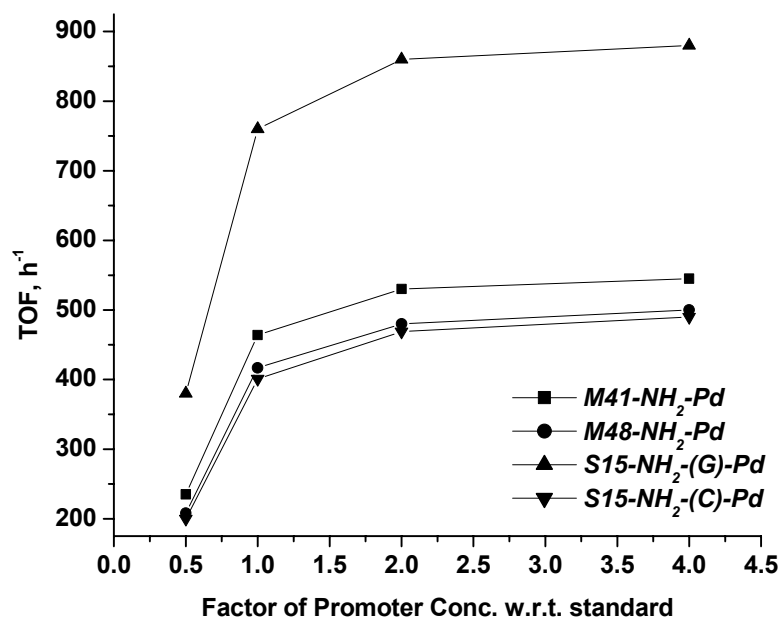


Figure 2.25: Effect of promoter amount on carbonylation of styrene

Reaction conditions: Catalyst: 100 mg; Styrene: 9.6 mmol; LiCl-to-TsOH ratio = 1:1 (standard amount: 0.5 mmol each); PPh₃: 0.095 mmol; H₂O: 50 mmol; Solvent: MEK; P_{co}: 5.4 MPa; Temperature: 388K

substrate and the faster protonation step in the catalytic cycle. A competitive outplay of these two effects is manifested in the results for all the four different anchored catalysts. The regioselectivity to the branched isomeric product did not alter at all due to such variations as mentioned for any of the four different anchored catalysts. Therefore, a mutual ratio of 1:1 proved to be the best for the carbonylation of styrene.

However, after fixing the ratio of TsOH and LiCl at 1:1 as optimum for the styrene carbonylation in the mentioned scale, the issue of quantity of the promoters becomes the most pertinent. The amount of the promoters was varied as factors with respect to the standard amount of 0.5 mmol each, and the results are presented in Figure 2.25. The graph shows that when the promoter amount was reduced to half, the TOF for all the four catalysts became nearly half as those of the standard runs. In

addition, when the promoter charge was doubled or quadrupled, increase in the TOF was not that much exfoliated. The reason behind this is however not clear at present.

2.3.2.3.5 Effect of Triphenylphosphine Concentration

The use of free triphenylphosphine was necessary for the carbonylation of styrene using the anchored Pd-complex catalysts. The homogeneous carbonylation of styrene however did not require any free phosphines to achieve good activity, but for the heterogenized catalyst, it was observed that the reaction did not proceed without any free triphenylphosphine. A speculative explanation can be presented as that, PPh_3 can stabilize the Pd(0) species which might be formed as an intermediate in the catalytic cycle. Therefore, we can expect the use of a catalytic amount of it for the proper

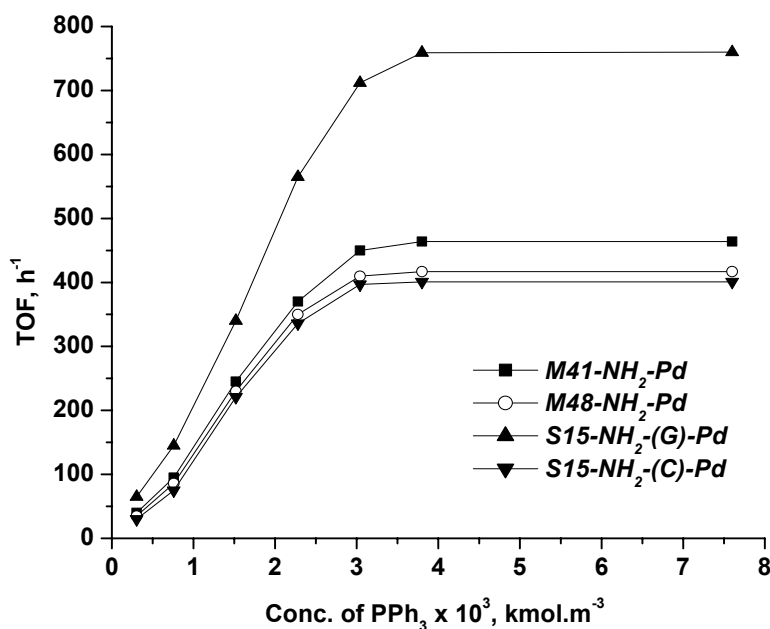


Figure 2.26: Effect of PPh_3 concentration on styrene carbonylation

Reaction conditions: Catalyst: 100 mg; Styrene: 9.6 mmol; LiCl: 0.5 mmol; TsOH: 0.5 mmol; PPh_3 : 0.095 mmol; H_2O : 50 mmol; Solvent: MEK; P_{CO} : 5.4 MPa; Temperature: 388K

functioning of the catalytic cycle, which otherwise may not operate at all, and hence the effect of PPh_3 concentration on the activity of the anchored catalysts needs to be investigated for the carbonylation of styrene. Different concentrations of PPh_3 were used to study this effect for all the four catalysts. The results of this variation studies are presented in Figure 2.26. It is clearly observed from the graphs that the reaction

progress is dependent upon the concentration of the excess triphenyl phosphine only at lower concentrations. The activity of the catalysts increase almost linearly with the concentration of PPh_3 until a specific quantity, and beyond that concentration, the reaction rates did not alter showing a plateau in the graph. The nature of variation of the catalytic activity was same for all the four anchored catalysts, but the turnover frequencies are different for each of them, due to their intrinsic different activity. This may be attributed to the total number of active sites present in the catalysts. The physical significance of the enhancement in the activity may be directly linked to the number of active sites, and in each case the PPh_3 present will just aggravate the activity until a certain concentration of it only. Further to this limiting value, the activity remains constant.

2.3.2.3.6 Effect of Water

The influence of water on the carbonylation of olefins is an important one to study. Water has multiple roles to play in the carbonylation of olefins and alcohols. It is not only an essential component reagent for the hydroxycarbonylation of olefins, but also helps to solubilize the polar promoters (LiCl particularly) in the reaction mixture (MEK solvent), during carbonylation. As because the miscibility of the water is ~15% in MEK, the variation in the quantity of water in the reaction mixture is important to avoid liquid-liquid phase separation and related added transport limitations. When within the singular phase also the concentration of water also changes the different properties and the activity of the same catalysts. The concentration of water was varied within the soluble range. The detailed results are presented in Figure 2.27. An important observation was that the activity of the catalyst showed had little variation in the lower concentration region of water, but this variation gradually diminished when larger amounts of water was used during the reaction. The reason of such an observation may be that the amount of water added was more than the stoichiometric amount as required for the chemical reaction, and the excess water might facilitate in the solvation and other similar phenomena, which indirectly vary the activity of the catalysts. Reactions were also carried out without any added water, but then the conversions were within only ~2.5 – 3.2% range. The water present in the solvent and the other reagents added during the reaction might be responsible for such an observation. The reactions testify that water is essential for the carbonylation of olefins and also imply

that the amount of added water is sufficiently higher than that exactly required for the reaction, and thus concentration effect of water is not much prominent.

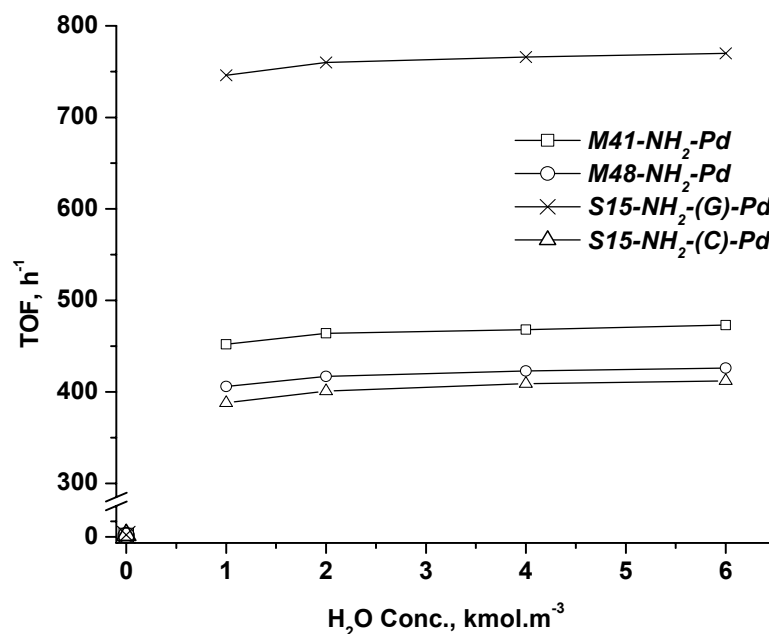


Figure 2.27: Effect of water on styrene carbonylation

Reaction conditions: Catalyst: 100 mg; Substrate: 9.6 mmol; LiCl: 0.5 mmol; TsOH: 0.5 mmol; PPh₃: 0.095 mmol; Solvent: MEK; P_{CO}: 5.4 MPa; Temp: 388K, Agitation: 16.7 Hz.

2.3.2.4 Different Substrates

After optimization of the reaction, and the thorough parametric studies, it is important to investigate the range of different types of substrates that may be activated for carbonylation reaction using the anchored Pd-complex catalysts, a series of reactions were carried out using different substrates, for each of the catalysts. The results of carbonylation of different substrates using the four different anchored Pd-complex catalysts is presented in Table 2.7

Table 2.7: Carbonylation of different substrates using different anchored Pd-complex catalysts

Sl. No.	Catalysts	Substrate	Conversion, %	Selectivity, %		TON	Time, h	TOF, h ⁻¹
				iso	n			
1	M41-NH ₂ -Pd	Styrene	98.12	99.31	0.68	5568	12	464
2	M41-NH ₂ -Pd	Styrene	98.37	99.10	0.90	5004	12	417
3	S15-NH ₂ -(G)-Pd	Styrene	98.25	99.54	0.44	9120	12	760
4	S15-NH ₂ -(C)-Pd	Styrene	98.19	99.46	0.52	4812	12	401
5	M41-NH ₂ -Pd	4-Methylstyrene	85.85	98.60	1.38	4872	12	406
6	M41-NH ₂ -Pd	4-Methylstyrene	86.19	99.10	0.88	4404	12	367
7	S15-NH ₂ -(G)-Pd	4-Methylstyrene	83.09	99.66	0.44	7716	12	643
8	S15-NH ₂ -(C)-Pd	4-Methylstyrene	87.33	99.53	0.46	4248	12	354
9	M41-NH ₂ -Pd	4- ^t Butylstyrene	93.40	99.31	0.67	5300	12	441
10	M41-NH ₂ -Pd	4- ^t Butylstyrene	95.10	99.23	0.75	4858	12	405
11	S15-NH ₂ -(G)-Pd	4- ^t Butylstyrene	95.00	99.32	0.67	8822	12	735
12	S15-NH ₂ -(C)-Pd	4- ^t Butylstyrene	94.80	99.29	0.68	4604	12	383
13	M41-NH ₂ -Pd	4-Acetylstyrene	91.35	98.27	1.71	5184	12	432
14	M41-NH ₂ -Pd	4-Acetylstyrene	94.41	98.33	1.65	4824	12	402
15	S15-NH ₂ -(G)-Pd	4-Acetylstyrene	94.07	98.65	1.12	8736	12	728
16	S15-NH ₂ -(C)-Pd	4-Acetylstyrene	93.99	98.47	0.68	4572	12	381
17	M41-NH ₂ -Pd	4-Methoxystyrene	90.50	99.01	0.90	5136	12	428
18	M41-NH ₂ -Pd	4-Methoxystyrene	93.95	98.86	0.12	4800	12	400
19	S15-NH ₂ -(G)-Pd	4-Methoxystyrene	93.55	99.03	0.95	8688	12	724
20	S15-NH ₂ -(C)-Pd	4-Methoxystyrene	93.50	99.10	0.86	4548	12	379

Sl. No.	Catalysts	Substrate	Conversion, %	Selectivity, %		TON	Time, h	TOF, h ⁻¹
				iso	n			
21	M41-NH ₂ -Pd	4-Chlorostyrene	94.73	98.42	1.55	5376	12	448
22	M41-NH ₂ -Pd	4-Chlorostyrene	92.77	98.16	1.82	4740	12	395
23	S15-NH ₂ -(G)-Pd	4-Chlorostyrene	95.23	99.06	0.82	8844	12	737
24	S15-NH ₂ -(C)-Pd	4-Chlorostyrene	91.60	98.89	1.10	4452	12	371
25	M41-NH ₂ -Pd	4-Isobutylstyrene [†]	97.27	98.35	1.56	5520	12	460
26	M41-NH ₂ -Pd	4-Isobutylstyrene	96.29	98.67	1.30	4920	12	410
27	S15-NH ₂ -(G)-Pd	4-Isobutylstyrene	97.43	99.06	0.91	9048	12	754
28	S15-NH ₂ -(C)-Pd	4-Isobutylstyrene	97.44	98.94	1.05	4740	12	395
29	M41-NH ₂ -Pd	1-Phenylethanol	96.42	99.60	0.38	5472	12	456
30	M41-NH ₂ -Pd	1-Phenylethanol	95.59	99.50	0.49	4884	12	407
31	S15-NH ₂ -(G)-Pd	1-Phenylethanol	96.27	99.60	0.40	8940	12	745
32	S15-NH ₂ -(C)-Pd	1-Phenylethanol	95.72	99.46	0.52	4656	12	388
33	M41-NH ₂ -Pd	IBPE [‡]	95.15	97.50	2.45	5400	12	450
34	M41-NH ₂ -Pd	IBPE	95.00	97.90	1.18	4853	12	405
35	S15-NH ₂ -(G)-Pd	IBPE	96.07	98.10	1.90	8928	12	744
36	S15-NH ₂ -(C)-Pd	IBPE	96.71	97.89	1.11	4704	12	392

Reaction conditions:

Catalyst: 100 mg; Substrate: 9.6 mmol; LiCl: 0.5 mmol; TsOH: 0.5 mmol; PPh₃: 0.095 mmol; H₂O: 50 mmol; Solvent: MEK; P_{CO}: 5.4 MPa; Temperature: 388K, Agitation: 16.7 Hz.

[†]10 ppm *t*-Butylcatechol was used as polymerization inhibitor for 4-isobutylstyrene

[‡]IBPE = 1-(4-Isobutylphenyl)ethanol

2.3.2.5 Comparative Advancement Studies

A comparative study of the novel anchored Pd(pyca)(PPh₃)(OTs) complex catalysts inside the channels of the mesoporous channels of MCM-41, MCM-48 and SBA-15, with the other heterogeneous Pd-based catalysts for the carbonylation of olefins and alcohols is essential to understand the advancement made in the development of these catalysts. While most of the previous literature reports of heterogeneous Pd-based catalysts for the carbonylation of alcohols and alkenes as described in Chapter 1 do not deal with the aryl substituted substrates, only a few of them are relevant for this comparison. The relevant reports are compared with the present data in the Table 2.8.

As clearly evident from the comparison table that the data of Lee and Alper²⁹ and Nozaki et al³⁰, using Montmorillonite as support gave high conversion and branched acid selectivity but the duration was too long and involved benzene as solvent. Biphasic systems developed by Papadogianakis et al^{5a}, Tilloy et al; Bertoux et al and Goedheijt et al were effective for styrene carbonylation but with only minimal conversion (~ 50%). The Biphasic catalyst system developed by Jayasree et al showed good conversions and selectivities but the catalyst recycled only under CO-atmosphere and lost activity after 2-3 recycles only. Pd-Charcoal catalyst as demonstrated by Jayasree et al showed extremely high TOFs for IBS carbonylation but high leaching of Pd under reaction conditions was also observed. Use of SiO₂-supported Chitosan-Pd complex catalyst³¹ showed poor selectivity; also the presence of another metal (Lewis acids) is another obstacle for making it a recyclable catalyst. In comparison to these literature results, the experimental data of the four anchored Pd-complex catalyst illustrate high activity and selectivity, high stability and good recyclability. The extremely low leaching and consequent negligible Pd-loss makes the anchored Pd(pyca)(PPh₃)(OTs) inside mesoporous channels, as one of the most effective heterogeneous catalyst for carbonylation reactions.

Table 2.8: Comparative study of Anchored Pd-complex catalysts with principle examples from literature for carbonylation of olefins and alcohols

Entry	Substrate	Catalyst system	Conv., %	Selectivity, %		TON	Time, h	TOF, h ⁻¹	Pd-loss in reaction	Remarks - Authors
				iso	n					
1	Styrene	Homogeneous Pd(pyca)(PPh ₃)(OTs) ^a	97	99.01	0.98	468	0.18	2600	-	Tedious catalyst-product separation and reuse
2	Substituted styrenes	Pd(OAc) ₂ -Montmorillonite-PPh ₃ /HCl	88-100	100	-	-	24	-	-	Long reaction duration, used C ₆ H ₆ -MeOH as solvent – Lee et al
3	Styrene & IBS	PdCl ₂ /TPPTS/TsOH and other biphasic systems	62-100	56-90	33-10	240-1200	6	40-200	-	Low activity ^{5,6,7,8}
4	Styrene	Montmorillonite-dipenyl phosphine-PdCl ₂ -HCl	-	50-100	-	-	24	-	-	Long reaction duration, used C ₆ H ₆ -MeOH as solvent – Nozaki et al
5	Styrene	Aq. biphasic Pd(pyca)(TPPTS) ^c	94.5	92	7.2	428	1.42	302	0.225 %	Catalyst deactivates in air, recycles only under CO atmosphere – Jayasree et al ⁹
6	Olefins & alcohols	Pd/C ^b	92	98	1.9	13340	4.6	2900	37.5 %	Heavy leaching obtained, high activity due to leached Pd – Jayasree et al ¹²
7	Substituted styrenes	Silica-Chitosan-Pd complex	-	-	-	-	-	-	-	Poor selectivity, use of hazardous co-catalysts – Zhang et al ³¹
8	Styrene	M41-NH ₂ -Pd	98.1	99.3	0.68	5568	12	464	3.5×10 ⁻⁴ %	Highly stable recyclable and truly heterogeneous catalyst with negligible leaching
9	Styrene	M48-NH ₂ -Pd	98.4	99.1	0.90	5004	12	417	-	
10	Styrene	S15-NH ₂ -(G)-Pd	98.2	99.5	0.44	9120	12	760	2.16×10 ⁻⁴ %	
11	Styrene	S15-NH ₂ -(C)-Pd	98.2	99.4	0.52	4812	12	401	-	

2.4 Conclusions

The anchoring of palladium complexes have been demonstrated successfully using the mesoporous siliceous materials such as MCM-41, MCM-48 and SBA-15 as the support matrices. All the synthesized materials were thoroughly characterized using the different techniques to understand the nature and state of the Pd-complex after the anchoring process and the stability of the heterogeneous catalysts obtained by this method of immobilization. In addition, these characterizations helped to establish the efficient anchoring of the Pd-complexes inside the mesopores by the help of the dangling -NH_2 functionality attached to the interior walls of the channels, quite successfully. The synthesized materials were studied as potential candidate catalysts for the carbonylation of olefins and alcohols. Of the different catalysts synthesized, the catalyst prepared using the SBA-15 as support and using the post-synthetic grafting methodology was found to be the best. This catalyst, namely, *S15-NH₂-(G)-Pd* showed outstanding turnover frequency of 760 h^{-1} , with $> 99.5 \%$ regioselectivity to the branched product isomer. The novel anchored Pd-complex catalysts were analyzed thoroughly for the variation in the different reaction parameters and were also applied to a series of different substrates to illustrate their wider range of applications. The anchored Pd-complex catalysts were found to be highly stable showing a negligible leaching of Pd into the reaction mixtures. In addition, the anchored catalysts were recycled for three times without any objectionable variation in the activity and selectivity of the catalysts. The reactions and recycles also helped establishing the unique stabilization provided to the Pd-complex by this anchoring technique. The identification of the exact reasoning behind such stabilization is still an important and relevant issue, even though the structural aspects have been studied using the different characterizations. Therefore, the anchored Pd-complex catalysts have been demonstrated as highly stable, highly selective and active catalysts for carbonylation reactions

2.5 Scope and Future Directions

The demonstration of the anchored Pd-complex catalysts as highly stable and recyclable catalyst with high activity and selectivity has evolved some directions for future research, which may be enlisted as follows,

- The enhancement in stability of the palladium complexes as a result of the anchoring may be studied in details using more insitu studies
- The roles of different reaction parameters haven been studied leaving the understanding of the mechanism of the working of the heterogeneous catalyst
- Anchoring of different other complexes may show immense possibilities of application to numerous other reactions
- Develop still better catalysts for carbonylation reaction

References

- 1 (a) Colquhoun, H M, Thompson D J, Twigg M V, *Carbonylation-Direct Synthesis of Carbonyl Compounds*, Plenum Press, New York **1991** (b) Weisse L, *Specialty Chemicals Magazine*, **2002** 22(3) 36
- 2 Elango V, Murphy M A, Mott G N, Zey E G, Smith B L, Moss G L, EP 400892 **1990**
- 3 a) Seayad A, Kelkar A A, Toniolo L, Chaudhari R V, *J. Mol. Catal. A: Chem.*, **2000** 151 47 (b) Seayad A, Kelkar A A, Toniolo L, Chaudhari R V, *Ind. Eng. Chem. Res.*, **1998** 37 2180 (c) Seayad A, Jayasree S, Damodaran K, Toniolo L, Chaudhari R V, *J. Organomet. Chem.* **2000** 601(2) 100 (d) Seayad A, Jayasree S, Chaudhari R V, *Org. Lett.*, **1999** 1 459 (e) Seayad A, Jayasree S, Chaudhari R V, *J. Mol. Catal. A: Chem.*, **2001** 172(1-2) 151
- 4 (a) Jayasree S, Seayad A, Chaudhari R V, *Org. Lett.*, **2000** 2 203 (b) Chaudhari R V, Jayasree S, Seayad A M, (CSIR, India) US Patent 6093,847 **2000**
- 5 (a) Sheldon R A, Maat L, Papadogianakis G, (Hoechst Celanese Corp.) US 5536874, **1996** (b) Papadogianakis G, Verspui G, Matt L, Sheldon R A, *Catal. Lett.*, **1997** 47 43
- 6 Tilloy S, Monflier E, Bertoux B, Castanet Y, Mortreux A, *New J. Chem.*, **1997** 21 529
- 7 Bertoux F, Monflier E, Castanet Y, Mortreux A, *J. Mol. Catal. A: Chem.*, **1999** 143 23
- 8 Goedheijt M S, Reek J N H, Kamer P C J, van Leeuwen P W N M, *Chem. Commun.*, **1998** 2431
- 9 Jayasree S, Seayad A, Chaudhari R V, *Chem. Commun.* **2000** 1239
- 10 Lee C W, Alper H, *J. Org. Chem.*, **1995** 60 2501
- 11 Jang E J, Lee K H, Lee J S, Kim Y G, *J. Mol. Catal. A: Chem.*, **1999** 144 431
- 12 Jayasree S, Seayad A, Chaudhari R V, *Chem. Commun.*, **1999** 12 1067
- 13 (a) Kresge C T, Leonowicz M E, Roth W J, Vertulli J C, Beck J S, *Nature*, **1992** 359 710 (b) Beck J S, Vertulli J C, Roth W J, Leonowicz M E, Kresge C T, Schmitt K D, Chu C T-W, Olson D H, Sheppard E W, McCullen S B, Higgins J B, Schlenker J L, *J. Am. Chem. Soc.*, **1992** 114 10834
- 14 (a) Zhao D, Feng J, Huo Q, Melosh N, Fredrickson G H, Chmelka B F, Stucky G D, *Science*, **1998** 279 548 (b) Zhao D, Huo Q, Feng J, Chmelka B F, Stucky G D, *J. Am. Chem. Soc.*, **1998** 120 6024
- 15 Mukhopadhyay K, Ghosh A, Kumar R, *Chem. Commun.*, **2002** 2404
- 16 Shephard D S, Zhou W, Maschmeyer T, Matters J M, Roper C L, Parsons S, Johnson B F G, Duer M J, *Angew. Chem. Int. Ed.*, **1998** 37(19) 2719
- 17 Asefa T, Lennox R B, *Chem. Mater.*, **2005** 17(10) 2483
- 18 Wang X, Lin K S K, Chen J C C, Cheng S, *J. Phys. Chem. B*, **2005** 109 1763
- 19 Ghosh A, *Ph.D. Thesis, University of Pune*, **2004**, Chapter 2, 63
- 20 Gregg S J, Sing K S W, *Adsorption, Surface Area and Porosity*, Academic Press, London, **1967** 121
- 21 Chen C-Y, Li H-X, Davis M E, *Microporous Mater.*, **1993** 2 17
- 22 Wagner C D, Riggs W M, Davis L E, Moulder J E, Muilenberg G E, (Editors), *Handbook of X-ray Photoelectron Spectroscopy*, Perkin-Elmer Corporation (USA). **1979**
- 23 (a) Chen C Y, Li H X, Davis M E, *Microporous Mater.*, **1993** 2 17 (b) Chen C Y, Li H X, Davis M E, *Microporous Mater.*, **1993** 2 27
- 24 (a) Llusar M, Monros G, Roux C, Pozzo J L, Sanchez C, *J. Mater. Chem.*, **2003** 13 2505, (b) Wang Y Q, Yang C M, Zibrowius B, Spliethoff B, Linden M. Schuth F, *Chem. Mater.*, **2003** 15 5029
- 25 Yang C, Zibrowius B, Schuth F, *Chem. Commun.*, **2003** 1772
- 26 Yiu H H P, Wright P A, Botting N P, *J. Mol. Catal. B: Enzym.*, **2001** 15 81
- 27 Zapilko C, Widenmeyer M, Nagl I, Estler F, Anwander R, Raudaschl-Sieber G, Groeger O, Engelhardt G, *J. Am. Chem. Soc.*, **2006** 128(50) 16266
- 28 Jayasree S, *Ph.D. Thesis, University of Pune*, **2000**
- 29 Lee C W, Alper H, *J. Org. Chem.*, **1995** 60 2501
- 30 Nozaki K, Kantam M L, Horiuchi T, Takaya H, *J. Mol. Catal. A: Chem.*, **1997** 118 247
- 31 Zhang J, Xia C, *J. Mol. Catal. A: Chem.*, **2003** 206(1-2) 59

Chapter 3

Ossification – A Novel Immobilization Approach: Application in Carbonylation Reactions

This chapter presents a novel approach for the immobilization of homogeneous catalysts we term as “Ossification”, which is transforming the metal complex into its intrinsically insoluble counterpart thus forming a molecularly heterogenized catalyst entity. The palladium complexes thus immobilized may form truly heterogenized homogeneous catalysts. These catalysts have been characterized by numerous techniques as powder XRD, ³¹P CP MAS NMR, XPS, SEM, ICP-AES etc. ensuring that the integrity of the complex is maintained during the immobilization process. The catalysts were tested for the carbonylation reactions of alkenes and alcohols. These catalysts had shown impressive activity and selectivity profiles for these reactions, along with efficient recycle with retention of catalytic performance and structural integrity.

3.1 Introduction

The numerous techniques of immobilization of homogeneous catalysts as already introduced in Chapter 1, have been practiced and evaluated for different reactions. The performances of these heterogenized catalysts however depend on the reactions themselves and also on the versatility of the approach. The different approaches as described by many, may be efficient, but their exotic synthetic procedures and applicability background deliver the hue of negativity for commercial implementation of such ideas. The multi-step syntheses and treatment procedures of immobilized catalysts are tedious and sometimes non-reproducible. Also, the time and efficacy of preparation of such catalysts are often considered as trivial issues in the laboratory-scale attempts during validation, but when tested for industrial-scale processes may show different results, thus eluding the industrial acceptability. Moreover, the catalytic reaction time for carbonylation using these catalysts were in the range of 10 to 12 hours due to the diffusion-related barriers of the reactant moieties, which are normal properties for the heterogenized catalysts. Also, since these materials have lesser number of active catalytic environments due to distribution of the active metal sites on the support matrices, the activity of these is lower in comparison to their homogeneous counterparts. Therefore, the overall potential of the “heterogenized of organometallic complexes” is yet to be harnessed completely. For attaining industrial relevance, the immobilization procedures require to be operationally easy, using cheaper and easily available materials and having advantages in environmental aspects too. The concept of a molecularly heterogenized organometallic catalyst can be thought of as a solution of to these problems. For such a target catalyst, an organometallic complex has to have an insoluble appendage attached to it – incorporating heterogeneity, and an intact flexible coordination environment to perform catalysis, in the same molecular entity. Using a similar approach, Lin and coworkers¹ recently have reported the synthesis and use of some heterogeneous catalysts for asymmetric hydrogenation reactions. They attached phosphonate functionality to the chiral ligand followed by the precipitation of the complex using Zr^{4+} cations. The main drawback of this system was the sensitive nature of the phosphates and also the handling of the air-sensitive reagents required for its synthesis. Moreover, the performance of these catalysts was poor (TOF $\sim 500\text{ h}^{-1}$) with respect to the standard hydrogenation reactions (TOF $>5000\text{ h}^{-1}$)

Keeping this as target, the idea of *ossification of homogeneous metal complex catalysts* has been proposed. Classically speaking, *ossification* is referred to the biological process of slow accumulation of osseous tissue from simple water-soluble precursors leading to the formation of robust insoluble biomaterial structures, such as bones in vertebrates, coral reefs, shells for molluscs, etc. which are well known for their natural strength and durability. Our novel immobilization approach involves the preparation of inherently insoluble catalytically active material by a process resembling the self-assembly of the aforesaid robust insoluble biomaterials, from simpler precursor molecules and ions. To attain this, a protocol is designed, whereby the organometallic complexes are made soluble in aqueous phase by insertion of any non-coordinating anionic functionality as sulfonate, $-\text{SO}_3^-$, carboxylate, $-\text{CO}_2^-$ etc. to any of the ligand/s of the complex. The insertion of anionic functional groups into a ligand is already established for the formation of aqueous-soluble catalysts.² This derivatization of the ligand and thus of the complex, is followed by their transformation to solid materials (precipitates) by treatment with the heavier group II-A cations. Strontium (Sr^{+2}), barium (Ba^{+2}) etc. are known to form sulphates and carbonates which are inherently insoluble in water, acids and most of the organic solvents, and are high-melting and non-subliming solids. Thus, we may visualize molecular solids having their catalytically active transition-metal-centered environments intact, in a novel procedure termed as *ossification of metal complexes*. For the proper growth and uniform dispersion of these precipitates, the mediation of another solid support matrix e.g. silica (SiO_2), Charcoal etc. may or may not be necessary. Thus we can think of a whole new world of molecularly heterogenized organometallic catalysts. A schematic representation of the *ossification of metal complexes* is given in Figure 3.1

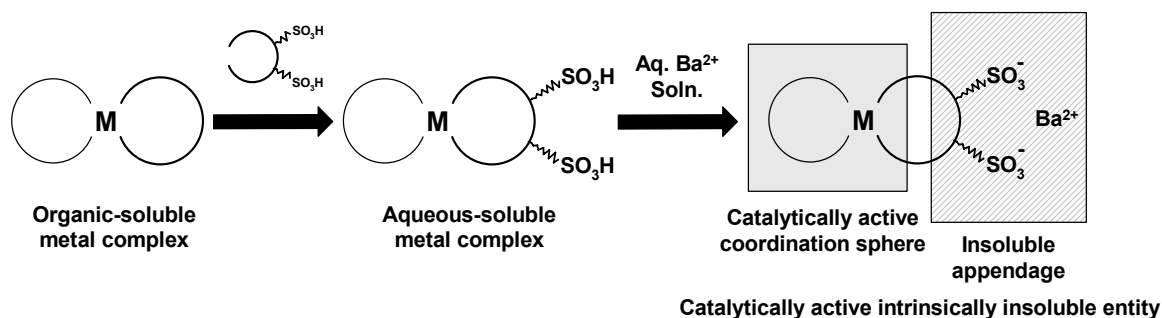


Figure 3.1: Schematic representation of *Ossification of metal complexes*

The carbonylation of olefins and alcohols, as also described in the previous chapter, is one of the most important reactions with applications in fine chemicals and pharmaceutical industry. The use of heterogenized catalysts for this reaction has been very limited due to the metal leaching observed under practical conditions in most cases. Thus, stability, high activity and regioselectivity are the prime targets for an immobilized metal-complex carbonylation catalyst.

In this chapter, this novel technique of immobilization of homogeneous catalysts, namely the *ossification* has been demonstrated. The heterogenization of a class of palladium complexes having a hemi-labile chelating N-N or N-O ligands, followed by their application as catalysts for hydroxycarbonylation of olefins and alcohols has been studied. A thorough characterization of the new catalyst materials using powder X-ray diffraction study (XRD), ^{31}P cross-polarized magic-angle spinning nuclear magnetic resonance spectroscopy (^{31}P CP-MAS NMR), X-ray photoelectron spectroscopy (XPS), Fourier-transform infra-red spectroscopy (FT-IR), scanning electron microscopy (SEM), elemental microanalysis, BET surface area analysis etc. has been presented. The effect of various reaction parameters on the activity and selectivity in carbonylation of styrene has been discussed. Recycle studies showing stability and true heterogeneity of the catalysts have also been demonstrated. The ossified catalysts were compared with the previously reported heterogeneous Pd-catalysts to bring out the advantages of the ossification approach for immobilization.

3.2 Experimental section

3.2.1 Materials

All the materials required for the experimental work in this chapter were procured from the following sources. Palladium acetate, $\text{Pd}(\text{OAc})_2$; Palladium chloride, PdCl_2 ; Triphenylphosphine, PPh_3 ; *p*-Toluenesulphonic acid monohydrate, TsOH ; Picolinic acid, pycaH ; 2-Acetylpyridine, acpy ; Pyridine-2-carboxyaldehyde, pycald ; Bipyridine, bipy ; Styrene were procured from Aldrich, USA, and used as obtained. *iso*-Butylbenzene, IBB ; Acetyl Chloride, AlCl_3 ; Lithium Chloride, LiCl ; Sodium Borohydride, NaBH_4 ; Barium nitrate, $\text{Ba}(\text{NO}_3)_2$; Strontium nitrate, $\text{Sr}(\text{NO}_3)_2$, were obtained from s.d. Fine Chemicals, India, Sulphuric acid, H_2SO_4 ; Phosphorous pentoxide, P_2O_5 ; Sodium hydroxide, NaOH ; Hydrochloric acid, HCl ; Sodium bicarbonate, NaHCO_3 ; Anhydrous Sodium sulphate, Na_2SO_4 ; Chloroform, CHCl_3 ; *n*-Hexane; Diethyl ether, Methyl ethyl

ketone etc. were procured from Merck, India. Nitrogen, N₂ and Argon, Ar gases were supplied from Indian Oxygen Limited, Mumbai and Carbon monoxide gas; CO (>99.8% pure) was obtained from Matheson Gas Company, USA.

3.2.2 Syntheses

Several different substrates, catalysts, and reagents, unavailable in the market, were prepared in the laboratory following the procedures from literature and the details are described below.

3.2.2.1 Synthesis of *p*-Isobutylphenylethanol (IBPE)

A two-step synthesis procedure was adopted for the synthesis of IBPE, consisting of (1) Acylation of *isobutylbenzene* (IBB) to *p*-isobutyl acetophenone (IBAP) and (2) Reduction of IBAP to IBPE.

In the acylation step, acetyl chloride (58.25 g) and anhydrous AlCl₃ (100g) were taken in dichloromethane (500 mL) at 273–278 K and mixed thoroughly. To it, 67 g IBB was slowly added under vigorous stirring, keeping the temperature constant. After 4–5 hours of stirring at 273–278 K, the reaction mixture was poured into crushed ice to quench the reaction. The organic layer was separated from the aqueous layer. The aqueous layer was re-extracted with CH₂Cl₂ and the combined organic layer was washed with saturated brine and then with saturated sodium bicarbonate. The washed dichloromethane layer was then dried over anhydrous sodium sulfate, concentrated and distilled under reduced pressure to yield (98%) *p*-isobutyl acetophenone (IBAP).

The reduction of IBAP was carried out using sodium borohydride. 1.4 g of NaBH₄ was added to a solution of 13 g IBAP in 75 ml methanol in an ice-bath. After one hour of continuous stirring at 273–283 K, the reaction mixture was treated with dilute HCl and extracted with dichloromethane. The CH₂Cl₂ layer was washed with brine and then with saturated sodium bicarbonate dried over anhydrous sodium sulfate, concentrated and distilled under vacuum to yield (98%) pure *p*-isobutyl phenyl ethanol.

3.2.2.2 Synthesis of Triphenylphosphine trisulphonate, sodium salt (TPPTS-Na)

TPPTS was prepared by sulphonation of Triphenylphosphine using oleum following the literature procedure by Bhanage et al³. Firstly, 66 % oleum was

synthesized by distillation of H_2SO_4 over anhydrous P_2O_5 . In a typical oleum synthesis[†] 500 g anhydrous P_2O_5 was taken in a round-bottomed flask, and 400 mL concentrated H_2SO_4 was added with stirring over a period of 2 hours. The mixture was heated till the solid dissolved and mixture started fuming. On further heating, oleum fumes emanated which were condensed by an air-condenser and collected in a jar already containing 45 mL concentrated H_2SO_4 , till the total volume was 148 mL (~ 66 % oleum) was obtained.

In the next step, 50 g PPh_3 was taken in the sulphonation vessel (a water-jacketed stirred glass reactor); to it 200 g (~100mL) concentrated H_2SO_4 was added slowly over a period of 2 h at 283 K To this solution, 280 g 65% oleum was added very cautiously maintaining constant temperature, with stirring for efficient mixing and heat dissipation. The mixture was stirred for 76 h after the completion of oleum addition at a constant temperature of 295 K. After completion of the reaction, the temperature was lowered to 273 K and the contents were diluted using 50 mL degassed distilled water slowly so that temperature does not exceed 278 K and then further another 500 mL distilled water was added. 50% NaOH solution was added with stirring to neutralize the mixture under a controlled temperature not exceeding 278 K. The pH of the solution was lowered to 6 using conc. H_2SO_4 . The solid Na_2SO_4 formed during neutralization was removed by filtration. After further concentration of the filtrate in a rotary evaporator, 2 liters of methanol was added to separate more Na_2SO_4 as white precipitate. The methanol-water solution was refluxed for two hours, when further precipitation of white Na_2SO_4 was observed, which was removed by filtration. Then, the supernatant liquor (after the removal of all solid Na_2SO_4) was evaporated to dryness to get sodium salt of TPPTS as a white powder. This white solid was dissolved in minimum volume water and re-precipitated by adding ethanol as pure TPPTS (> 99 %). This was dried under high vacuum and stored under argon.

3.2.2.3 Syntheses of Palladium complexes

A number of palladium complexes having hemi-labile N-O or N-N chelating ligands, known to show carbonylation activity, were synthesized as follows.

[†] **CAUTION:** Oleum is extremely corrosive & may cause dangerous outcome on exposure of any sort, so safe and protective handling is required.

3.2.2.3.1 Pd(pyca)(PPh₃)(OTs) complex

The Pd(pyca)(PPh₃)(OTs) complex was prepared by the literature procedure⁴. In a typical synthesis 0.5g Pd(OAc)₂ (2.225 mmol), 0.274g pyridine-2-carboxylic acid (pycaH) (2.225 mmol), 0.846g *p*-toluenesulphonic acid (4.45 mmol) and 1.168g triphenylphosphine (4.45 mmol) were taken in minimum volume of chloroform in a round-bottomed flask and were vigorously shaken at room temperature for few minutes until all the components were completely dissolved and the solution turned bright yellow from the brownish yellow colour of the Pd(OAc)₂ solution. The product was isolated as yellow oily mass by addition of *n*-hexane to the chloroform solution and vigorous shaking for 10 minutes. The oily material was washed with *n*-hexane and then with diethyl ether a number of times. Applying vacuum led to the formation of a yellow fluffy solid. For elemental and spectroscopic analysis, the complex was purified by re-precipitation from chloroform four times.

3.2.2.3.2 Pd(acpy)(PPh₃)(OTs) complex

A similar procedure as that described above in section 3.2.2.3.1 was used. 0.2g Pd(OAc)₂ (0.89 mmol), 0.108g 2-acetyl pyridine (acpy) (0.89 mmol), 0.338g *p*-toluenesulphonic acid (TsOH) (1.78 mmol) and 0.468g PPh₃ (1.78 mmol) in chloroform were vigorously stirred or shaken under room temperature for 30 minutes until all the components were completely dissolved and the solution turned yellow. The product complex was isolated as yellow oil by adding *n*-hexane. The oily product was washed several times with *n*-hexane and diethyl ether and was kept under vacuum forming a yellow fluffy solid, which was purified by re-precipitation from chloroform.

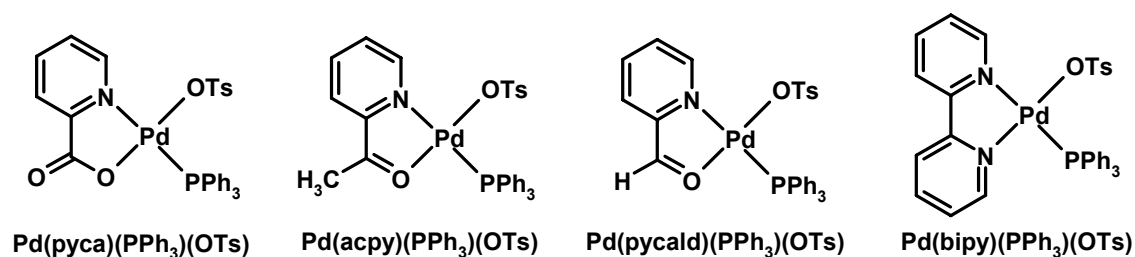
3.2.2.3.3 Pd(pycald)(PPh₃)(OTs) complex

A similar procedure as that described above in section 3.2.2.3.2 was used. 0.2g Pd(OAc)₂ (0.89 mmol), 0.095g pyridine-2-carboxaldehyde (pycald) (0.89 mmol), 0.338g *p*-toluenesulphonic acid (TsOH) (1.78 mmol) and 0.468g PPh₃ (1.78 mmol) in chloroform were vigorously shaken at room temperature for 30 minutes until all the components were completely dissolved and the solution turned yellow. The complex was isolated as yellow thick oil by adding *n*-hexane. The oily product was washed several times with *n*-hexane and diethyl ether and was kept under vacuum forming a yellow fluffy solid, which was purified by re-precipitation from chloroform.

3.2.2.3.4 Pd(bipy)(PPh₃)(OTs) complex

0.2g Pd(OAc)₂ (0.89 mmol), 0.139g 2,2'-Bipyridine, (bipy) (0.89 mmol), 0.338g *p*-toluenesulphonic acid (TsOH) (1.78 mmol) and 0.468g PPh₃ (1.78 mmol) in chloroform were vigorously stirred under room temperature for 30 minutes until all the components were completely dissolved and the solution turned yellow. The complex was isolated as yellow oil by addition of *n*-hexane. The oily product was washed several times with *n*-hexane and diethyl ether and was kept under vacuum forming a yellow fluffy solid, which was purified by re-precipitation from chloroform several times.

The structure of these four complexes may be represented as follows:



3.2.2.3.5 Synthesis of aqueous-soluble complexes

For complexes having N-N and N-O hemi-labile ligands (namely pyca, acpy, pycald and bipy), a common protocol was followed as similar to literature⁵. Since each of these complexes contain only one phosphine ligand coordinated to the palladium centre, only a very slight excess of the free TPPTS was added. The particular complex was dissolved in 10 ml chloroform, CHCl₃ and shaken vigorously with a solution of 1.1 equivalents of TPPTS in 6 ml distilled, degassed water in a separatory funnel. The yellow color of the CHCl₃ layer disappeared and the aqueous layer became yellow in color indicating the formation of the aqueous soluble complex by substitution of the

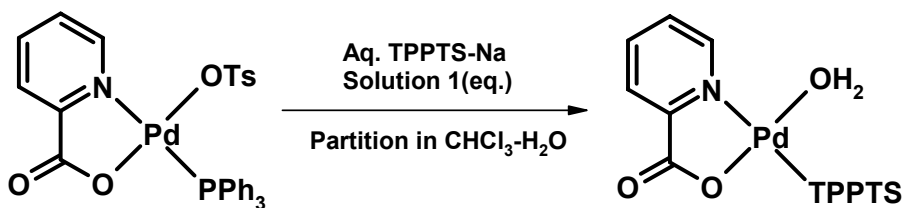
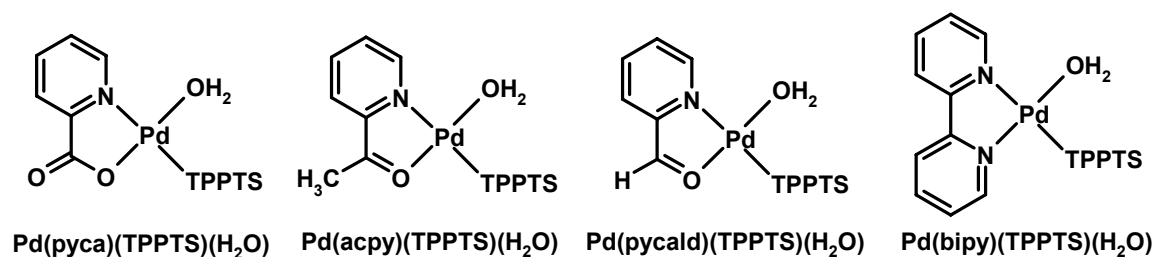


Figure 3.2: Synthesis of aqueous soluble Pd(pyca)(TPPTS)(H₂O) complex

PPh₃ by TPPTS at the Pd-centre. The aqueous layer was allowed to separate well and then removed, followed by washing with 5ml portions of fresh CHCl₃ thrice to remove any organic soluble precursor. The aqueous solution of the catalyst was flushed with

argon and preserved under argon. A typical scheme for the synthesis of Pd(pyca)(TPPTS)(H₂O) complex from its organic soluble counterpart Pd(pyca)(PPh₃)(OTs) is shown in Figure 3.2. The OTs⁻ being a more labile ligand gives place to H₂O during partition, and remains in CHCl₃ layer. The other three aqueous-soluble complexes were synthesized similarly. For the next step, i.e. ossification, the same solution was used. But the pure water-soluble complex can be obtained by precipitation, on the addition of methanol as faint yellow solid. The yellow fine powder was filtered under argon, washed with methanol and dried under vacuum to yield a yellow fine powder. However, for preparation of very pure aqueous soluble complexes, *exactly stoichiometric* amount of TPPTS was used for partition. This was done to prevent the occurrence of any free non-coordinated TPPTS, in the aqueous solution, which might generate the contaminants during *ossification*. However, this may result in loss of Pd due to incomplete partition (CHCl₃ layer remain slightly yellow, post-partition), but ensures the purity of the aqueous-soluble complex and hence the ossified Pd-catalyst in turn. The four different aqueous-soluble complexes may be represented as follows



3.2.2.3.6 Ossification of palladium complexes

The protocol adopted for ossification of the metal complexes is based on very simple approach of precipitation of insoluble salts of sulphonated-ligand coordinated to the transition metal centres. Since, BaSO₄ and SrSO₄ are most well-known as insoluble materials in water and almost all organic solvents, Ba²⁺ was used for ossification. To a sufficiently excess amount of a saturated solution of Ba(NO₃)₂ (15 ml) in degassed de-ionized water, taken in a double-necked round bottomed flask, the aqueous solution of the Pd-complex prepared as mentioned earlier was added dropwisely, with vigorous stirring of around 12 Hz, at ambient temperature (~298K). Inert atmosphere of argon was maintained in the whole procedure. Immediate appearance of pale yellow precipitate was observed on the addition. Slow addition of

the metal complex with good agitation was required to prevent rapid agglomeration of the precipitate. After completion of addition, the mixture was allowed to stir for 10 h at ambient temperature, to let all precipitation complete. Then the material was separated by filtration using Sartorius 393 quantitative filter paper as pale yellow solid. The solid was washed with copious amount of water to remove all Ba^{2+} adhering the solid (since Ba^{2+} was used in excess), till the washings were tested Ba-free. The solid was given a wash with acetone to remove any organic moieties. It was dried in air and then given Soxhlet extraction with water and acetone successively, for 16 hours each. The catalyst material was obtained as a free-flowing pale yellow powder after drying in air. This process of ossification was used for all the palladium complexes with no variations at all. The four different ossified palladium complexes were designated as ossified Pd(pyca)(TPPTS) – Catalyst 1A, ossified Pd(acpy)(TPPTS) – Catalyst 1B, ossified Pd(pycald)(TPPTS) – Catalyst 1C and Pd(bipy)(TPPTS) – Catalyst 1D respectively, and the catalysts will be henceforth referred to as mentioned above.

3.2.3 Carbonylation procedure[‡]

The carbonylation reactions were carried out in batch reactor in the same manner as described in Section 2.2.3 in a autoclave made of Hastelloy C–276 by Parr Instrument Co. USA, having a capacity of 50 ml (total dead volume including head-space and appendages was 72ml). The schematic of the setup is also shown previously in Figure 2.2.3. Post-reaction processing of the reaction mixture was followed-up similarly as before when the anchored catalysts were used, as described in the previous chapter. However, minor changes, e.g. in the reaction charges etc. were different in this case.

3.2.4 Recycle studies and leaching experiments

For the recycle studies using the ossified catalysts, after the carbonylation reaction run was complete, the reactor was allowed rest, to settle the solid catalyst and the supernatant organic phase was decanted slowly to separate it from the solid catalyst. The solid was washed with the reaction solvent for a couple of times in the same manner. A fresh charge of reactants and promoters was introduced and the reaction was carried on in the same fashion as described previously, after withdrawing

[‡] **CAUTION:** Carbonylation experiments involve hazardous carbon monoxide gas at high temperature and pressures; so safe expert handling is a compulsory pre-requisite.

an initial sample before starting the recycle run. This was repeated for all the recycle reactions. The reaction mixture thus obtained was retained for further analyses.

Metal leaching experiments were performed by filtration of the hot reaction mixture at 388K by stopping the reaction abruptly at ~30% conversion and subsequently, testing the catalytic activity of the filtrate for hydrocarboxylation without addition of the fresh heterogeneous catalyst. These filtrate and the catalysts thus recovered were also analyzed for Pd-content by ICP–AES (Inductively Coupled Plasma with Atomic Emission Spectroscopy) analyses to contemplate the palladium content in solution and loss of palladium from the parent catalyst during the reaction.

3.2.5 Analytical and characterization methods

Numerous analytical techniques were used for the characterization and proper analysis of the work. For the catalytic carbonylation reactions, the reaction mixtures (liquids) were analyzed by gas chromatography, using a Hewlett-Packard 6890 Series GC instrument, controlled by *HP ChemStation* software, and HP-FFAP capillary column (25 m x 0.33 mm x 0.2 μ m film-thickness, on a polyethylene glycol stationary phase having free fatty acid phase). The typical set of parameters for the method developed for analysis of the reactants and products in the samples of the actual reaction mixture are in the following Table 3.1. Calibration of the method was performed using standard materials in the concentration range similar to that of the catalytic reactions for each component of substrate(s) and products in the reaction mixture. The calibrated method gave the quantitative data for the analysis of the components of the reaction mixture.

Table 3.1 Operation parameters of the method for GC analysis

Injector (split) temperature	523K
Flame Ionization Detector temperature	523K
Column (Oven) temperature	423K to 483K (@ 35K/ min), hold 13 min
Carrier gas (He) flow rate	2.5 mL/ min
Inlet Pressure (He)	25 psi
Split ratio	100:1
Injection volume (manual)	0.5 μL

For the identification of the unknown compounds formed during the reaction, GC-MS was performed with the final reaction mixtures using HP-GCMS instrument with either of HP-5 and HP-FFAP capillary columns depending expected polarity/affinity of the components. NMR was obtained from a Bruker- MSL-300 and Bruker-DRX-500 spectrometers. The ^{31}P NMR spectra were recorded at 202.456 MHz by using 85% H_3PO_4 as an external standard and data were collected at spectral width of 20 kHz with a flip angle of 45° , with ~ 6000 actual data points and 5 s relaxation delay. Solid-state analyses were done using a 3mm CP-MAS probe. Elemental analysis of the complexes was carried out on a CHNS-O EA1108, Elemental analyzer of Carlo Erba Instruments, Italy. X-ray photoelectron spectra (XPS) were recorded on a VG – Microtech ESCA 3000 spectrometer using the Mg-K α emission ($E = 1253$ eV) under a vacuum of $\sim 10^{-9}$ torr. Scanning electron microscopy (SEM) were performed using a Philips XL 30 instrument – the catalyst materials were suspended in isopropanol, cast on gold plated discs followed by drying under vacuum and coating with a conducting material and then were imaged. The surface area measurements were performed using a Quantachrome C instrument with degassing and subsequent cooling of the samples at liquid nitrogen temperature. A mixture of argon and nitrogen was used for the adsorption-desorption at 77K.

The conversion, selectivity and turnover frequency (TOF) for a typical catalytic reaction were calculated as follows,

$$\text{Conversion, \%} = \frac{\text{Initial concentration of substrate} - \text{Final concentration of substrate}}{\text{Initial concentration of substrate}} \times 100$$

$$\text{Selectivity, \%} = \frac{\text{No. of moles of the particular product formed}}{\text{No. of moles of substrate converted}} \times 100$$

$$\text{TOF, h}^{-1} = \frac{\text{No. of moles of carbonylat ion product formed}}{\text{No. of moles of catalyst used} \times \text{reaction time (in hours)}}$$

3.3 Results and discussions

The results obtained from the characterizations as well as the various catalytic experiments are described in subsequent sections as follows. The catalyst entities, as visualized were characterized by using numerous techniques to establish the synthesis methodology undertaken, beyond ambiguity. Also, the results of these

characterizations were helpful in improving the synthesis strategy for the ossification methodology. The results of the catalytic tests are also important data to establish the activity of the ossified complexes and comparatively observe their performance in the light of the already existing heterogeneous Pd-complex catalysts for the carbonylation reactions.

3.3.1 Characterization of the Catalysts

3.3.1.1 ³¹P Cross-Polarized Magic Angle Spinning NMR Spectroscopy

The solid state NMR experiments were performed for establishing the novel concept of immobilization. In principle, the single phosphorous atom of the phosphine ligand present in the chosen Pd-complexes should show a definite chemical shift in the pure form. The existence of the *cis-trans* equilibrium between the isomers may not be visible in the solid state NMR spectra due to the partial quenching of the molecular dynamics and line-broadening in solid state due to static anisotropic interactions.

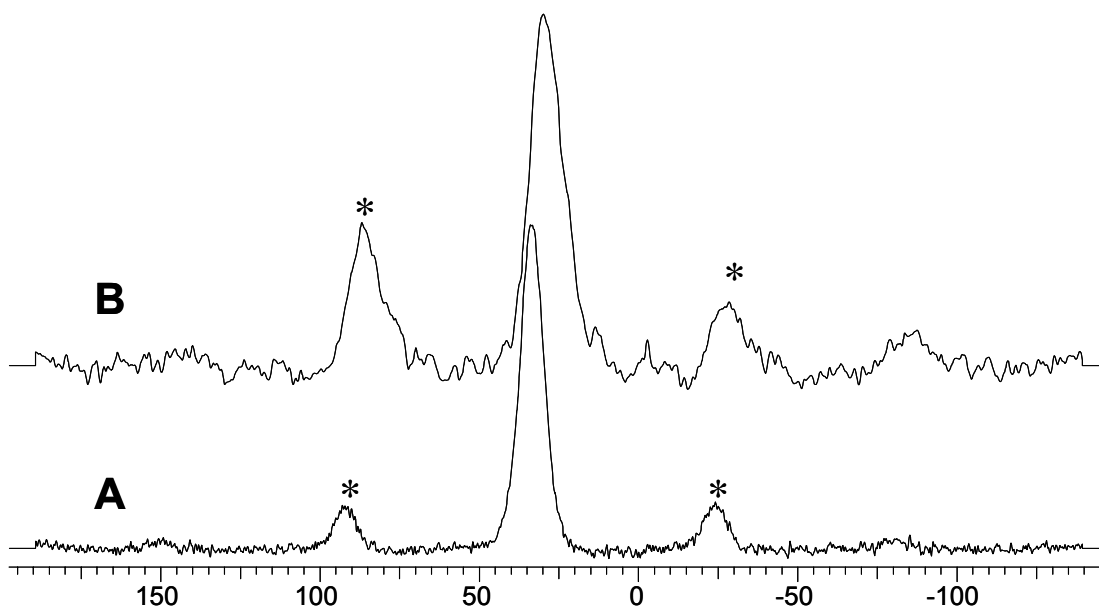


Figure 3.3: ³¹P CP MAS NMR Spectra of the catalysts, (A) Pd(pyca)(PPh₃)(OTs) complex, (B) Ossified Pd(pyca)(TPPTS)(H₂O) complex using Ba²⁺ ions. * in the spectra indicate the side bands at 7kHz

Variation of the position of the chemical shift is likely whenever electron-mobility is operating in the complex from any source, which may be due to the introduction of substituents in the present ligand, or a new ligand. The ³¹P signal for the pure

Pd(pyca)(PPh₃)(OTs) complex appears at δ_{iso} 33.44 ppm (Figure 3.3A) wherein, the anisotropic and dipolar coupling are averaged to zero by the magic-angle spinning. However, the ³¹P-NMR signal for the water-soluble complex Pd(pyca)(TPPTS)(H₂O) in D₂O appeared at 35.31 and 36.13 ppm respectively, which are justifiable by the fact that the presence of the electron-withdrawing sulfonate functionality, -SO₃H on the P-atom causes the change in its electronic environment and thus also the chemical shift position in the NMR spectrum, also the liquid phase spectrum demonstrated the presence of the *cis-trans* isomers in liquid phase. The ³¹P signal for the solid ossified Pd(pyca)(TPPTS)(H₂O) complex occurs at δ_{iso} 29.83 ppm as a single peak as shown in Figure 3.3. We observe an upfield shift of the position of the signal due to the P-atom in the ossified Pd(pyca)(TPPTS) complex. This upfield shift of the signal may be attributed to the formation of the Ba-sulphonate ion-pair by the ionic interaction of the SO₃⁻ with the Ba²⁺ cations. The ionic interaction of the anionic sulphonate moiety of the TPPTS coordinated to the Pd-centre, with the Ba²⁺ cation, quenches the electron withdrawing effect of the -SO₃⁻ on the phenyl rings and subsequently on the P-atom which thus appears at a lower ppm on the ³¹P NMR spectrum. Also, the formation of a Ba-sulphonate lattice may impart some environmental effect to this upfield shift. These spectra confirm the formation of the ossified complex with the retention of the structure of the parent coordination environment in the Pd-complex. Also, the integrity of the complex was maintained during the ossification process, which may be concluded from the absence of the peak at $\delta_{\text{iso}} - 4.3$ ppm which corresponds to the free Ba₃(TPPTS)₂ type species. This might have been observed from either in the case of disintegration of the Pd-complex during the ossification process, or if there was any free excess TPPTS in the aqueous solution of the complex prior to ossification, - giving rise to the free Ba₃(TPPTS)₂ peak. The ³¹P CP-MAS NMR spectra of the other Pd-complexes with different ligands (see Figure 3.4) show similar patterns of chemical shifts with slightly different δ -values. This variation of the chemical shift values may be attributed to the change in the stereo-electronic environments around the Pd-centre in the said complexes due to the different chelating ligands present in them. Of the ligands selected in the Pd-complexes for ossification, the order of nucleophilicity is Pyca > Acpy > Pycald > Bipy. Eventually, the ³¹P CP-MAS NMR chemical shift values (δ_{iso}) of their ossified Pd-complexes show a trend in the reverse order as 29.83, 30.23, 30.74 and 30.90 ppm respectively as shown in Figure 3.4 A to D. This order may be justified

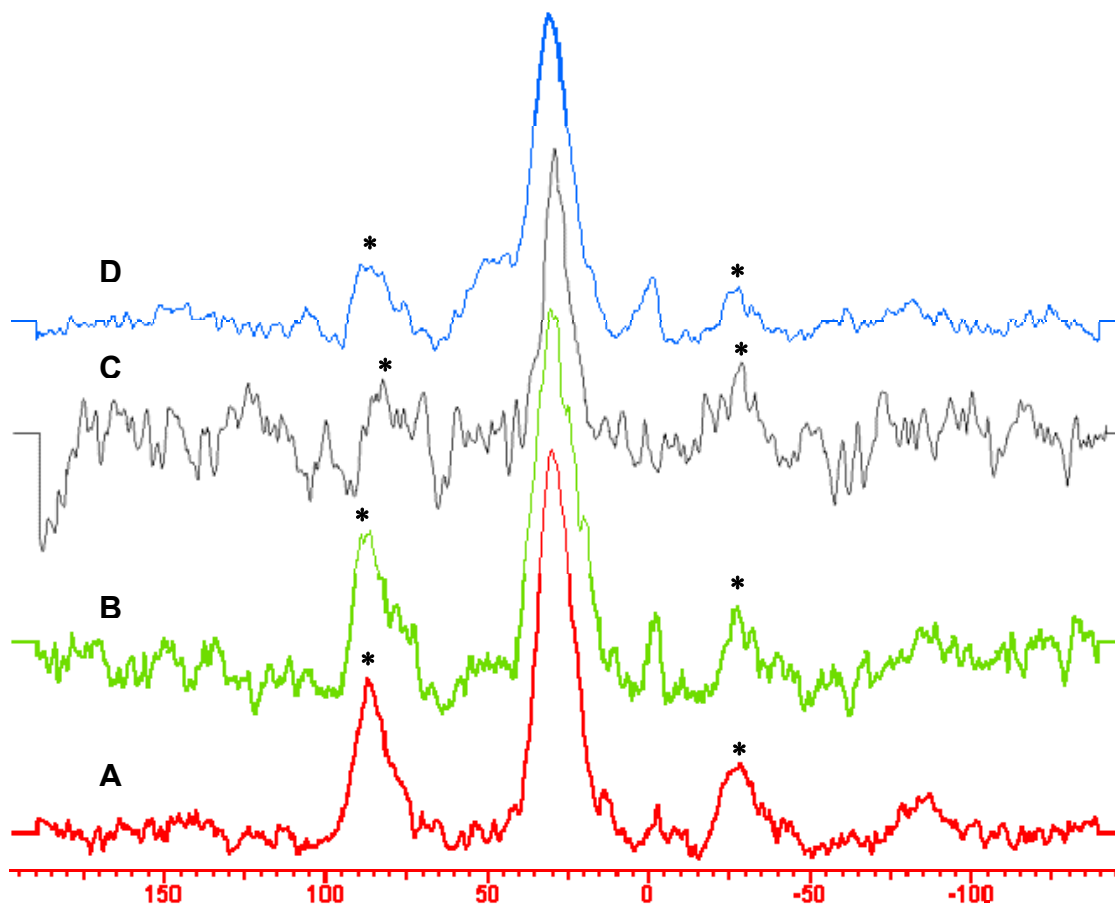


Figure 3.4: ³¹P CP-MAS NMR Spectra of the ossified catalysts using Ba²⁺ ions, (A) Ossified Pd(pyca)(TPPTS) complex, (B) Ossified Pd(Acpy)(TPPTS) complex, (C) Ossified Pd(Pycald)(TPPTS) complex, (D) Ossified Pd(Bipy)(TPPTS) complex. * in the spectra indicate the side bands at 7kHz.

as follows. The phosphine ligand being the same TPPTS in all the complexes, the effect of the nucleophilicity of the other ligands in the palladium complexes is reflected on the chemical shifts respectively. More nucleophilic is the ligand it transfers more electron density of the Pd-atom, and subsequently, more electron density is transmitted to the P-atom by the π -acceptor property of the triphenylphosphino ligand, using the $d\pi$ - $d\pi$ back bonding. Thus the P-atom of Ba-[Pd(Pyca)(TPPTS)] moiety will resonate at an upfield position in comparison to the Ba-[Pd(Bipy)(TPPTS)] species, which is exactly as observed in the spectra.

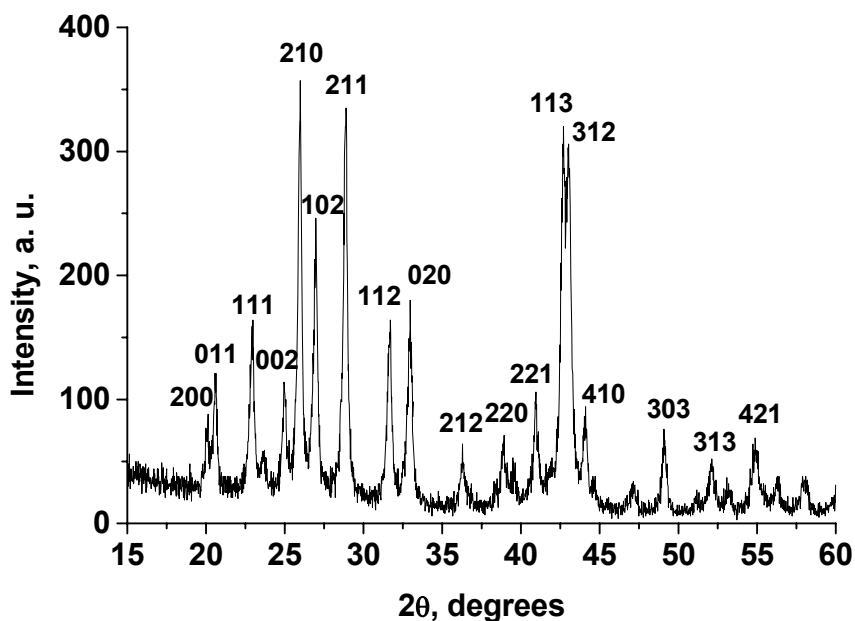
Thus, the ³¹P CPMAS NMR studies clearly illustrated that the ossified palladium complexes maintained the stereoelectronic orientation of the original Pd-

complexes throughout the ossification process and after ossification, the complexes retained their Pd-centres intact, as required for the catalytic cycle to operate. This also established our protocol of ossification, and further emphasized on the stability of the ossified Pd-complexes under aerial and moisture-laden conditions, in contrary to the pristine Pd-complexes which were quite air and moisture-sensitive, and decomposed to black mass on prolonged exposure to air or moisture.

3.3.1.2 Powder X-Ray Diffraction

The powder X-ray diffraction is another important tool for the characterization of the materials prepared by the ossification technique. The Ba-sulphonate formed may be anticipated of having similarity in the powder XRD pattern of that of the inorganic BaSO₄ salt, as the functionalities are same, but since the sulphonate ion concerned in the ossification methodology is a functionalized one (bearing phenyl rings attached to a P-atom, for TPPTS), the relative intensity of the principle peaks *may* differ from the pure inorganic salt, due to the variation in the unit cell dimensions caused by the difference in the size with the pure SO₄²⁻ anion. The powder XRD will also be instrumental in determining the nature of the solid as amorphous or crystalline.

With this logical background the ossified palladium complexes were recorded and the result for ossified Pd(pyca)(TPPTS) complex, using Ba²⁺ cations, i.e. Catalyst 1A is presented in Figure 3.5. The XRD pattern showed that the Ba-sulphonate ionic entity of the ossified complex (Catalyst 1A) had a similar constitution as that of the inorganic BaSO₄. The complete indexing of the pattern was performed for the ossified Pd-complex and it was observed that the Miller indices of all the peaks matched exactly with that of BaSO₄. However, the intensity of some peaks showed dissimilarity, which was as expected for the barium salt of a functionalized sulphonate moiety. The peak with highest intensity was assigned for the Bragg's plane of 210, which is different from that of pure BaSO₄, where, the principle peak (considered 100% intensity) occurs for the plane 211. The other peaks also were consistent with the diffraction planes of the inorganic BaSO₄ with respect to the peak positions. Hence, we can also speculate anrthorhombic unit cell for the ossified material by calculating the *d*-values of the Bragg's planes as in the case of pure BaSO₄. Thus, the ossified palladium complex resembled the pure BaSO₄ in X-ray diffraction pattern. This showed that the protocol



conceived for the formation of the Ba-sulphonate ion-pair by the reaction of a functionalized sulphonate moiety with Ba^{2+} cation was established, and thus the

Figure 3.5: Powder XRD pattern of ossified Pd(pyca)(TPPTS) complex using Ba^{2+} cations. Numbers in the plot denote the different Miller indices for the respective Bragg's planes.

o immobilization of the metal complex in the form of a solid molecule is rationalized. The powder XRD characterization was also used to characterize the other ossified Pd-metal complexes prepared using Ba^{2+} cations. These materials (Catalyst 1B, 1C and 1D) also had the characteristic peaks for the Ba-sulphonate ion-pair as similar to that of the ossified Pd-pyca complex (Catalyst 1A), as expected. The comparative results of the three different ossified palladium complexes, namely ossified Pd(acpy)(TPPTS) complex, ossified Pd(pycald)(TPPTS) complex and ossified Pd(bipy)(TPPTS) complex are presented in Figure 3.6. From the powder XRD data, it was clear that the postulated Ba-sulphonate ion pair was formed for all of the palladium complexes, while the differences in the relative intensities of the principle peaks in the spectra of the respective ossified complexes were also visible. This variation of the relative intensities of the principle peaks might be attributed to the difference in the nature of the different chelating ligand in each of them. The slight variation in the stereo-electronic contribution of the ligands was manifested in terms of the variation

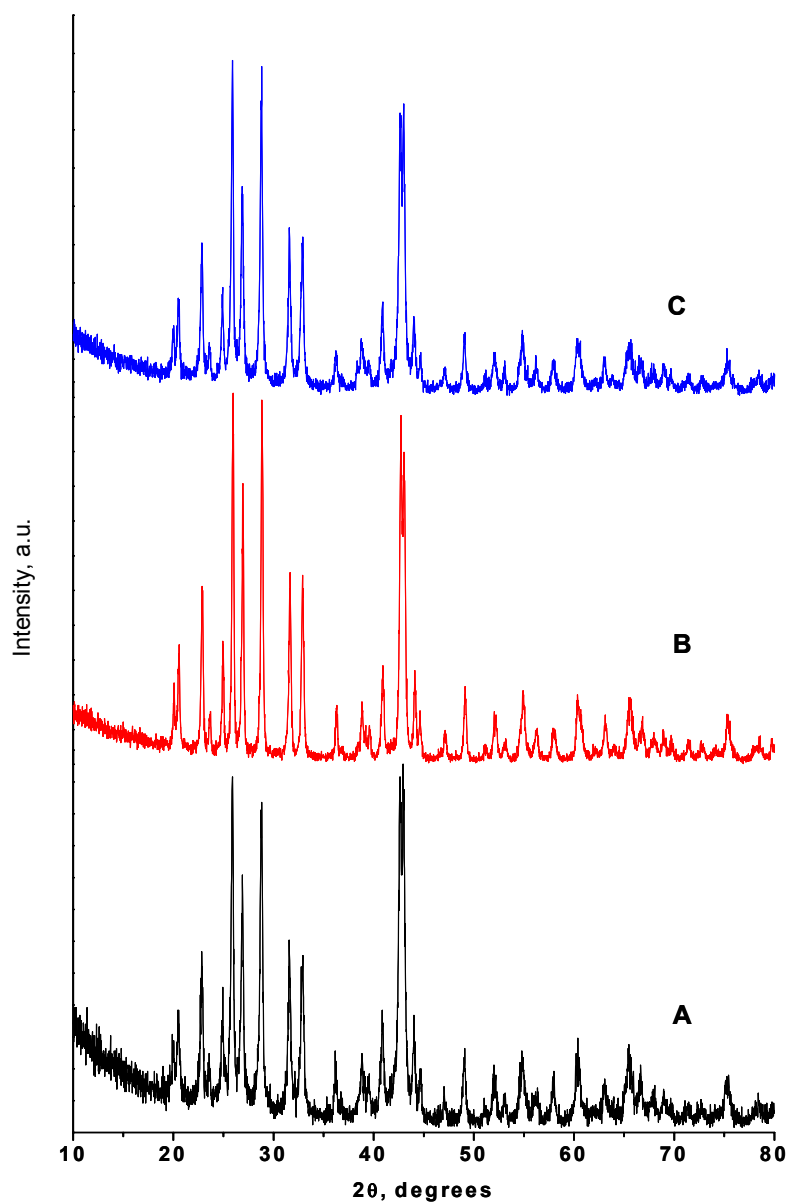


Figure 3.6: Powder XRD patterns of different ossified Pd-complexes using Ba^{2+} ions; (A) Pd(acpy)(TPPTS) complex, (B) Pd(pycald)(TPPTS) complex, (C) Pd(bipy)(TPPTS) complex

of the relative peak intensities. The steric as well as the electron-cloud environment of the different chelating ligands might influence the arrangements of the crystallographic planes of the Ba-sulphonate ion-pair, thus generating the dissimilarities in the intensities of the same peaks, for the four different ossified palladium complexes.

Thus, the powder XRD characterization of the ossified palladium complex catalysts had shown that the formation of the Ba-sulphonate ion-pair had occurred just as hypothesized, and the protocol of ossification is thus further consolidated.

3.3.1.3 X-Ray Photoelectron Spectroscopy

The X-ray photoelectron spectroscopy was used for the determination of the oxidation states of the respective elements present in the catalyst composites. The X-ray actually removes the core orbital electrons of the elements at specific binding energies, which are fingerprints for particular oxidation states of the element. The XPS data also delivers some information about the immediate local electronic environment of the selected element incorporating the perturbation of the electron density due to the neighboring functional groups and/or ligands. The XPS spectra of the different elements present in ossified Pd(pyca)(TPPTS) complex, Catalyst 1A using barium is presented in Figure 3.7. The data for each element is corrected with respect to signal of the adventitious carbon at 285 eV. Based on the binding energies of the observed signals the different peaks were assigned to the different elements with different oxidation states. The full-scale spectrum shows peaks for almost all of the elements present in the Catalyst 1A, but further intricate details are obtained by analyzing the individual peaks more precisely. The peaks at 796 and 780.7 eV correspond to the $3d_{3/2}$ and $3d_{5/2}$ states of Ba^{2+} oxidation state with the characteristic band gap of 15.3 eV. The absence of any further peaks for barium confirms its presence in +2 oxidation state as Ba^{2+} ions in the solid Catalyst 1A. The peaks at 341.3 and 336 eV are assigned to the $3d_{3/2}$ and $3d_{5/2}$ states of +2 oxidation state of palladium. A very interesting observation in this regard is that for pure $Pd(OAc)_2$ the $3d_{5/2}$ state occurs at around 338.5 eV, while the palladium is in the same +2 oxidation state. The soft and resonating character of the OAc^- anion imparts lesser electron density to the Pd centre and hence Pd binding energy is slightly higher for $Pd(OAc)_2$. For Catalyst 1A, the pyridine-2-carboxylate anionic ligand can impart its electron density better onto the Pd^{2+} centre along with the other ligands, thus increasing the electron-cloud density over the Pd-atom, consequently, palladium appears at a lower binding energy (336 eV), than that for $Pd(OAc)_2$. A characteristic band gap of 5.3 eV was also observed between the $3d_{5/2}$ and $3d_{3/2}$ signals of palladium for Catalyst 1A. The binding energies of the other elements however matched very nicely with the electronic condition of the

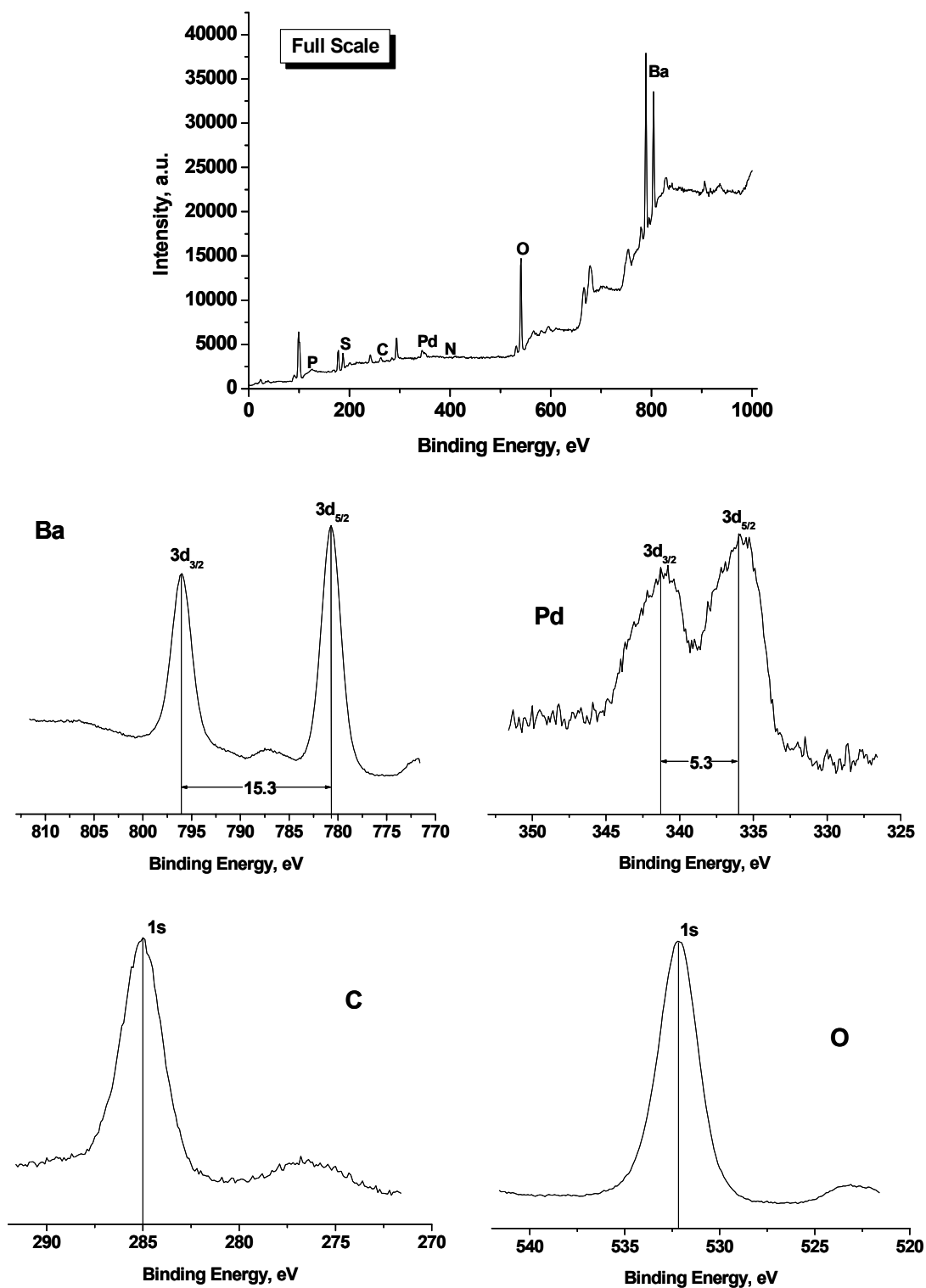


Figure 3.7: XPS data of ossified Pd(pyca)(TPPTS) complex i.e. Catalyst 1A

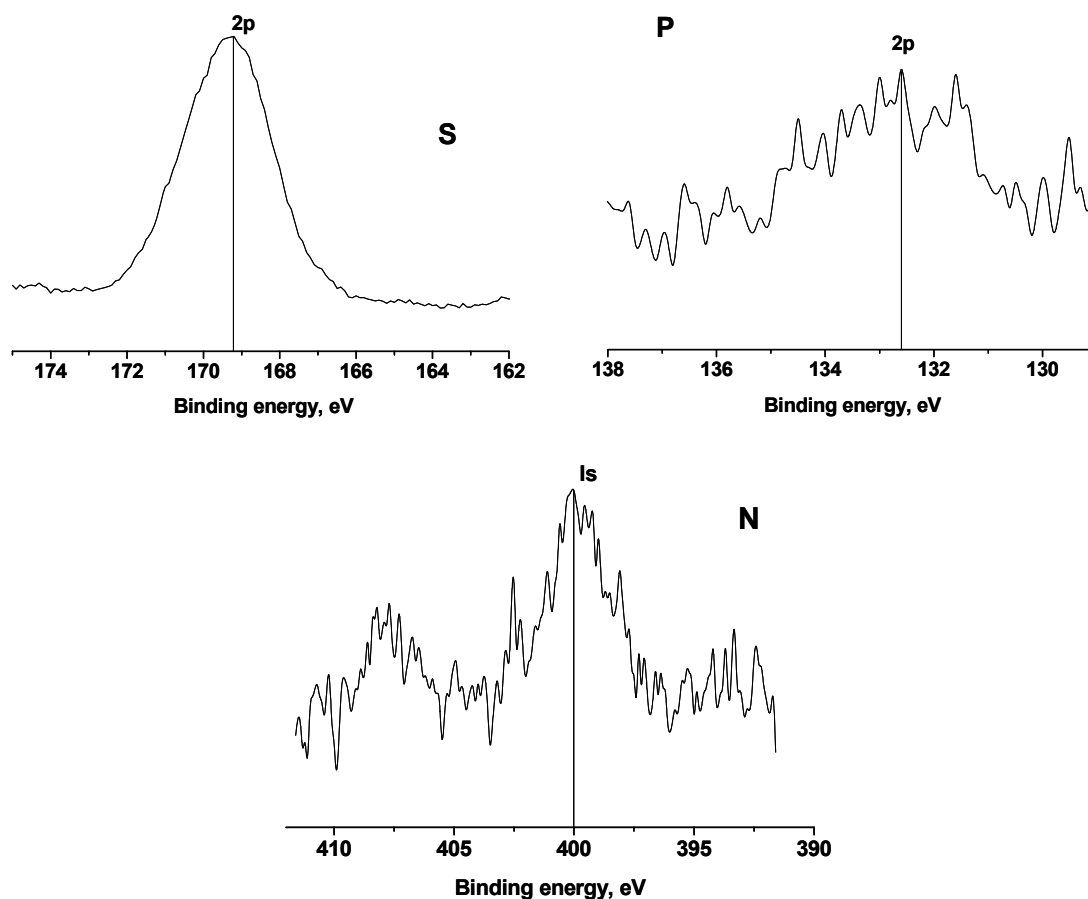


Figure 3.7 (continued): XPS data of ossified Pd(pyca)(TPPTS) complex i.e. Catalyst 1A ossified complex. For instance, O 1s state occurs at 532.1 eV, which is similar to the +2 oxidation state of oxygen in an anion, e.g. carboxylate, or sulphonate; binding energy value for N 1s in Catalyst 1A was 400 eV, which is slightly higher than the binding energy for N in pyridine (~398.7 eV) due to the chelation through the N-atom in the complex and consequent depletion of electron density. The binding energy values of sulphur 2p and phosphorous 2p were also observed to be matching with those of sulphonate group and coordinated phosphine moieties owing to the depletion of electron density while chelation to the metal centre. All these binding energy values indirectly confirm that the coordination pattern in the ossified Pd(pyca)(TPPTS) complex are intact as in the pure complex. Also, no degradation of the ligand/s was understandably detected during the ossification process, as if it were such, then the binding energies of the clue elements e.g. Pd, N, P etc would have been much different. The XPS data for the other three ossified complexes, namely Catalyst 1B,

1C, and 1D respectively, are presented in Table 3.2 which also consistently match with the stereo-electronic variation of the respective ligands in them. Interestingly, the variations are best manifested in the binding energies of the clue elements as N, O and Pd. For example, in Catalyst 1D, the presence of the bipyridyl ligand makes use of two N-atoms as highly electron-donating centres, which thus become electron-deficient thus increasing the binding energy value for N1s. Consequently, the Pd atom becomes little more electron rich thus decreasing the binding energy for Pd 3d_{5/2}.

Table 3.2: XPS data for Catalyst 1B, 1C and 1D (values in eV)

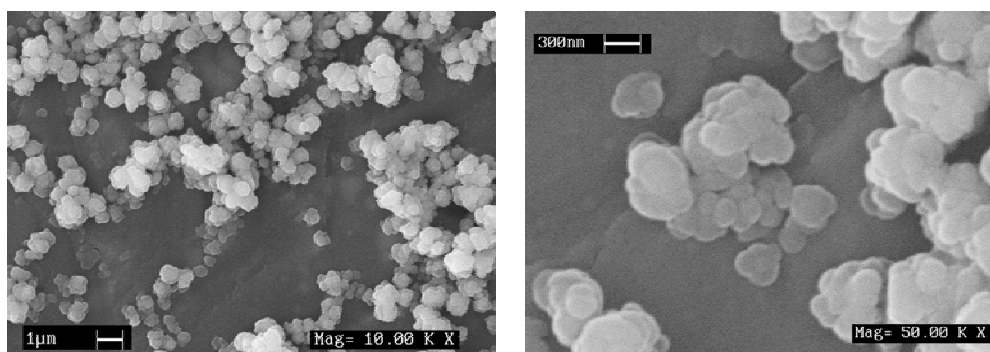
Elements Catalysts	Ba 3d _{5/2}	Pd 3d _{5/2}	O 1s	N 1s	P 2p	S 2p
Catalyst 1B	780.5	336	532	400	132.6	169.3
Catalyst 1C	780.5	336	531.8	399.9	132.6	169.2
Catalyst 1D	780.6	335.9	531.9	400.8	132.5	169.2

The x-ray photoelectronic spectra data thus delivers important evidence in support of the states of the individual atoms and stability of the complex during the course of the ossification process. The Pd-complexes were in the oxidation states as expected, and did not change during the synthesis of the catalyst materials.

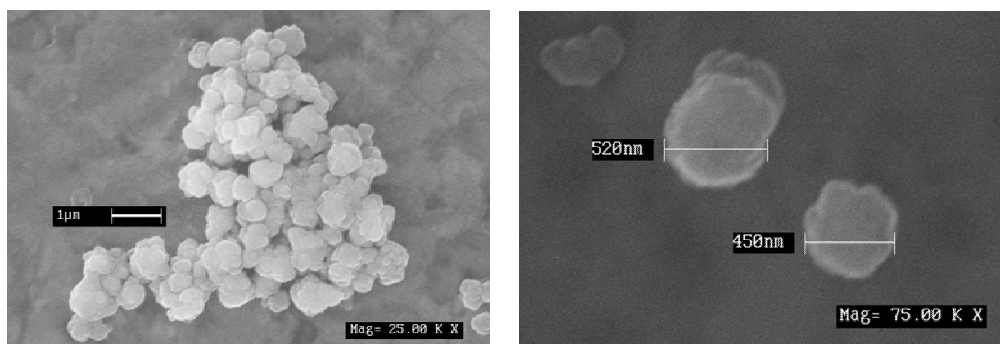
3.3.1.4 Scanning Electron Microscopy

The morphological characterization of the ossified Pd-complexes were done by scanning electron microscopy (SEM), in terms of the size and shape of the solid particles and their particulate distribution also. Taking ossified Pd(pyca)(TPPTS) complex i.e. Catalyst 1A material as the typical example for illustration of the characterization, it was observed that the material was in the form of irregular polyhedral particles of average diameter of about 450nm. These particles were discreet and non-cohesive with distinct borders/ boundaries with more or less uniform particles of the said size. On a closer look, by applying magnification to a small grain of the catalyst, the particles seem to be macro-clusters of the solid catalyst molecules with regular sizes. The SEM images of the different ossified palladium complex catalyst entities such as, Pd(acpy)(TPPTS), Pd(pycald)(TPPTS), Pd(bipy)(PPh₃)(OTs), using Ba²⁺ cations are presented in the Figure 3.8. All of the catalyst composites showed similar kind of evenly dispersed irregular polyhedral particulate materials, which area

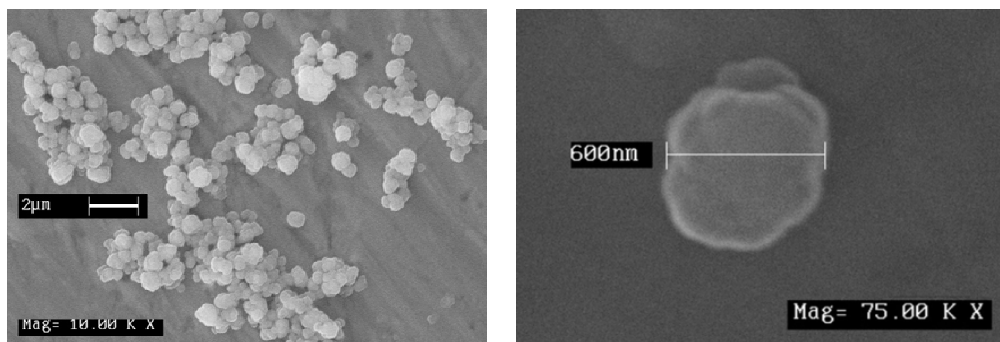
actually clusters of the heterogeneous catalyst molecules. On further magnification, all the catalysts revealed discrete clusters of irregular shapes and of sizes varying from 450 nm to 600 nm on an average was observed for the Catalyst 1A, 1B, 1C and 1D. However, the almost uniform size of the particles in each case may be attributed to the fact that the agitation of the synthesis mixture during the precipitation might be one of the size-dictating factors for the ossification procedure. The particles of average diameter ~450 to 600 nm was typically observed when the agitation of the synthesis mixture was around 600 rpm i.e. 10 Hz. However, when the agitation speed was lowered to 6.66 Hz, larger lumps of average particle diameter $\sim 1\mu\text{m}$ was obtained. This further confirmed that the occurrence of a particular particle size might be due to agitation effect of the reaction mixture at the time of precipitation from aqueous medium. The SEM micrographs also showed no existence of any smaller particles or fragments, which indicated that the clusters of the ossified complexes had grown uniformly during the synthesis procedure and also, they are resistant to the physical wear and tear they are subjected to, while under high agitation during their preparation.



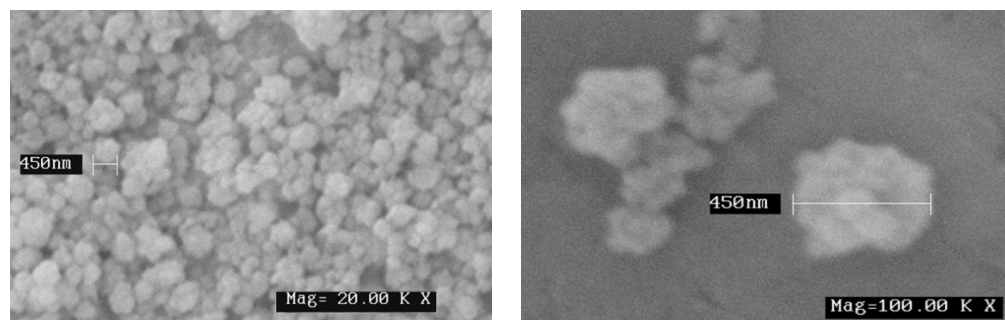
Ossified [Pd(pycald)(TPPTS)] complex



Ossified [Pd(bipy)(TPPTS)] complex



Ossified [Pd(acpy)(TPPTS)] complex



Ossified [Pd(pyca)(TPPTS)] complex

Figure 3.8: SEM images of the different ossified Pd-complex catalysts

3.3.1.5 Surface Area Measurements

The ossified palladium complexes were analyzed for the determination of the surface area of the composite matrices formed. It was important from the viewpoint of the activity of the catalyst, as the larger the surface area, greater is the accessibility of the reactants to the catalytic sites, and better is the activity. The surface area analyses of the ossified palladium complexes were done using N₂-physisorption-desorption technique, using the BET formula. The results are presented in Table 3.3. It is clearly observed from the data in Table 3.2 that the ossified Pd-complexes have quite low surface areas, not exceeding 20 m²g⁻¹. Such low surface areas might be justified from the fact that these materials were synthesized by simple precipitation technique, where the agglomeration might be a very common phenomenon. More importantly, the solubility of the Ba-sulphonates being very low (if considered similar to the sparingly soluble BaSO₄), might lead to ultra-fast formation of the ion-pair precipitate, leading to agglomeration and consequently a low surface area. This is in commensurate with the SEM data, which shows the irregular polyhedral clusters for all the four ossified complexes, with the average sizes of the particles ranging from 450 to 600 nm. The single-point adsorption-desorption studies also indicated that the particulate ossified materials Catalyst 1A, 1B, 1C and 1D were non-porous in nature, as in that case, the respective surface areas would have been much higher. This also matched with the SEM analyses and thus, it may be concluded that the ossified palladium complex catalysts were non-porous robust solid clusters of uniform average size ranging from 450 to 600 μm in diameter, having surface areas in the range of 11 to 20 m²g⁻¹.

Table 3.3: BET surface area data for the ossified palladium complexes

<i>Entry</i>	<i>Material</i>	<i>Surface area, m²g⁻¹</i>
1	Ossified Pd(pyca)(TPPTS) complex	18.6
2	Ossified Pd(acpy)(TPPTS) complex	17.1
3	Ossified Pd(pycald)(TPPTS) complex	11.9
4	Ossified Pd(bipy)(TPPTS) complex	18.7

3.3.1.6 Palladium Content Analysis

All the ossified palladium complexes were analyzed for Pd-content using the atomic absorption spectroscopic (AAS) method. The samples of fixed weight were digested and dissolved in concentrated HNO₃ and was diluted to a fixed volume. Further AAS experiments were conducted using these solutions. The results of AAS analysis are presented in Table 3.4

Table 3.4: Pd-content of different ossified Pd-complexes

<i>Entry</i>	<i>Material</i>	<i>Pd-content, %</i>
1	Ossified Pd(pyca)(TPPTS) complex	0.44
2	Ossified Pd(acpy)(TPPTS) complex	0.48
3	Ossified Pd(pycald)(TPPTS) complex	0.45
4	Ossified Pd(bipy)(TPPTS) complex	0.46

3.3.2 Catalytic Reactions

The carbonylation of olefins and alcohols were carried out using the ossified catalysts to investigate the performance of the palladium complexes after the ossification procedure and to analyze the merits/ demerits of this novel immobilization process in the light of the activity, selectivity and stability issues etc. The initial variations in the reactions parameters were performed to optimize the reaction conditions and to standardize the reaction protocol for the carbonylation reactions using the ossified catalysts. The importance of the 2-arylpropionic acids as efficient non-steroidal anti-inflammatory drugs, as mentioned in Chapter 1, was one of the motivations behind the study of carbonylation reactions using a heterogeneous catalyst to facilitate an easy separation and reuse of the catalyst with high turnovers. Also, the carbonylation reactions being carried out under stringent conditions of high temperature (~390K) and high pressures (~5-6 MPa) and in the presence of acidic and alkali metal salts as promoters, may be the perfect reaction to test the novel “ossified” complex catalysts from the stability perspective. Sustainability of any heterogenized metal complex catalyst under such reaction conditions, with proper recycle efficiency would ensure the success of the immobilization technique used to get the catalyst.

3.3.2.1 Carbonylation of olefins and alcohols

The carbonylation of both functionalized and terminal olefins and alcohols were performed using the ossified palladium complex catalysts. In all of the examples, hydrocarboxylation was carried on in the presence of a protic acid (*p*-toluenesulphonic acid) and alkali metal halide (lithium halides) promoters respectively, and also some excess phosphine (5-10 mg) was used in the reactions. Styrene was used as the model substrate for standardizing the reaction, using ossified Pd(pyca)(TPPTS) complex, i.e. Catalyst 1A as the catalyst, after which different substrates were investigated for carbonylation. It was observed that the carbonylation of styrene went to completion in only 6h with 99.9% regioselectivity to the branched-acid product. The reaction was monitored using intermediate sampling, and analyzing them using GC-MS and it was observed that no chloro-derivative was formed as intermediate from styrene at any point of the reaction progress. 100% mass balance of the reactants was obtained for carbonylation product i.e. 2-phenylpropionic acid. The reaction was slow in the first 30 minutes but progressed in a steady way till 96% conversion in 6 h, attaining a high TOF of 194 h^{-1} . The occurrence of the negligible amount of the linear regio-

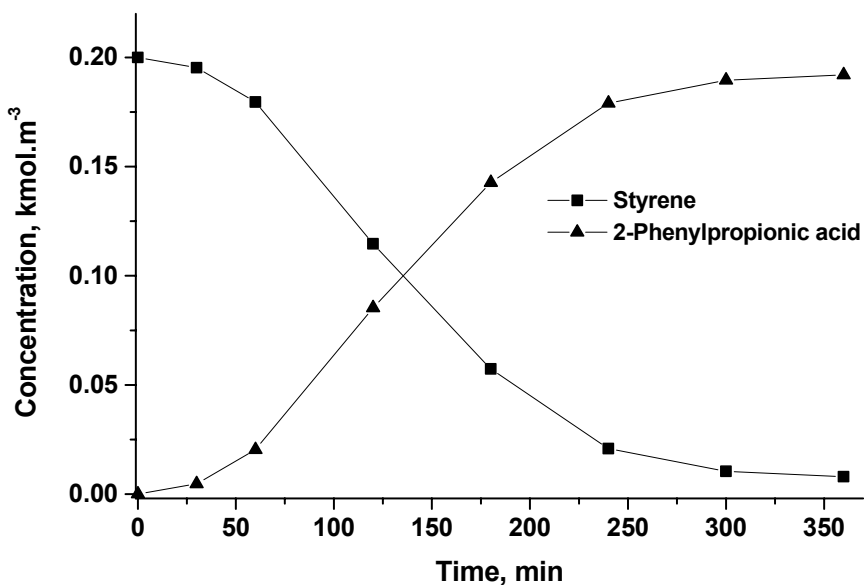


Figure 3.9: Concentration-time profile styrene carbonylation using Catalyst 1A

Reaction conditions: Styrene: 5 mmol; Catalyst: 100 mg; LiCl: 1.7 mmol; TsOH: 0.85 mmol; PPh₃: 0.019 mmol; H₂O: 27 mmol; Solvent: MEK; T: 388K; P_{CO}: 5.4 MPa

isomeric product (< 0.1%) is definitely an important observation and might be considered as advancement towards the regiospecific catalytic carbonylation of substituted olefins and alcohols where, the branched acid is the desired product. A typical concentration-time profile for the hydroxycarbonylation of styrene is presented in Figure 3.9.

The hot-filtered reaction mixture taken from the abruptly stopped reaction showed no carbonylation activity when reacted for a prolonged reaction time without any catalyst added further. However, the AAS analysis of this reaction mixture gave the Pd-content of this solution as negligibly low, corresponding to only $8.8 \times 10^{-5}\%$ loss of the total Pd charged in a single run. Thus, the ossified palladium catalyst was found to be highly stable and hence might be considered as an excellent palladium-based heterogenized/ immobilized complex catalyst.

3.3.2.2 Recycle Studies and Stability Aspects

The ossified palladium complex (Catalyst 1A) had exhibited its performance for the carbonylation of styrene, and it was important to investigate its activity under recycle conditions and also its stability after the recycle runs. The recycle studies were performed as described in early in Section 3.2.4. It was observed that the Catalyst 1A

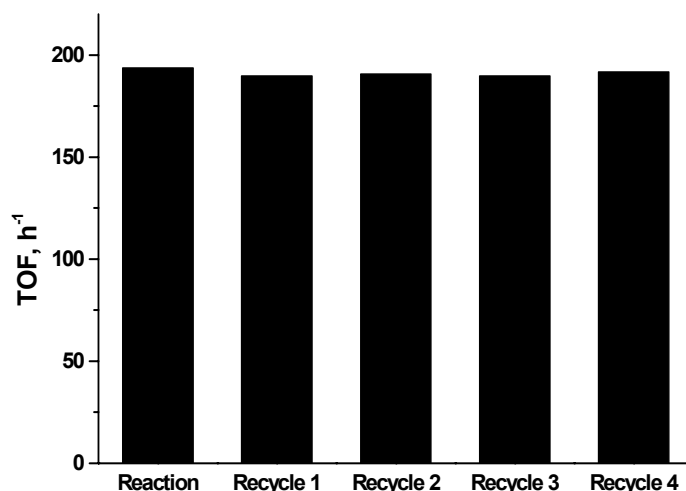


Figure 3.10: Recycle Studies for styrene carbonylation using Catalyst 1A

Reaction conditions: Styrene: 5 mmol; Catalyst: 100 mg; LiCl: 1.7 mmol; TsOH: 0.85 mmol; PPh₃: 0.038 mmol; H₂O: 27 mmol; Solvent: MEK; T: 388K; P_{CO}: 5.4 MPa

recycled four times continuously, with a nominal change in the activity (TOF of 4th recycle was 192 h⁻¹, compared to 194 h⁻¹ for the initial reaction). The regioselectivity for the branched acid product was also maintained at >99.4% for all of the recycle runs. Figure 3.10 presents the recycle studies of carbonylation of styrene using Catalyst 1A. As mentioned in Section 3.2.4, the stability of the ossified Pd-complex (Catalyst 1A) was tested by using the hot-filtered intermediate reaction mixture for carbonylation, and there was no residual carbonylation activity observed for this solution. This indicated that even if negligible amount of Pd was lost in the solution ($8.8 \times 10^{-5}\%$ of the total Pd charged), this was inactive for operating carbonylation. The catalyst activity (TOFs) differed for the successive recycle runs (194, 192, 193, 193 and 192 h⁻¹ respectively) might be due to the personal handling errors. The stability of the ossified Pd(pyca)(TPPTS) complex catalyst was further justified by ³¹P CPMAS NMR and XPS experiments of the used catalysts. The ³¹P CPMAS NMR data is presented in Figure 3.11, which shows that the chemical shift value for the P-atom in the used ossified Pd-complex (used Catalyst 1A) is seen at δ_{iso} 29.8 ppm. This is matching with the signal for the virgin catalyst (Catalyst 1A), which occurs at 29.83 ppm.

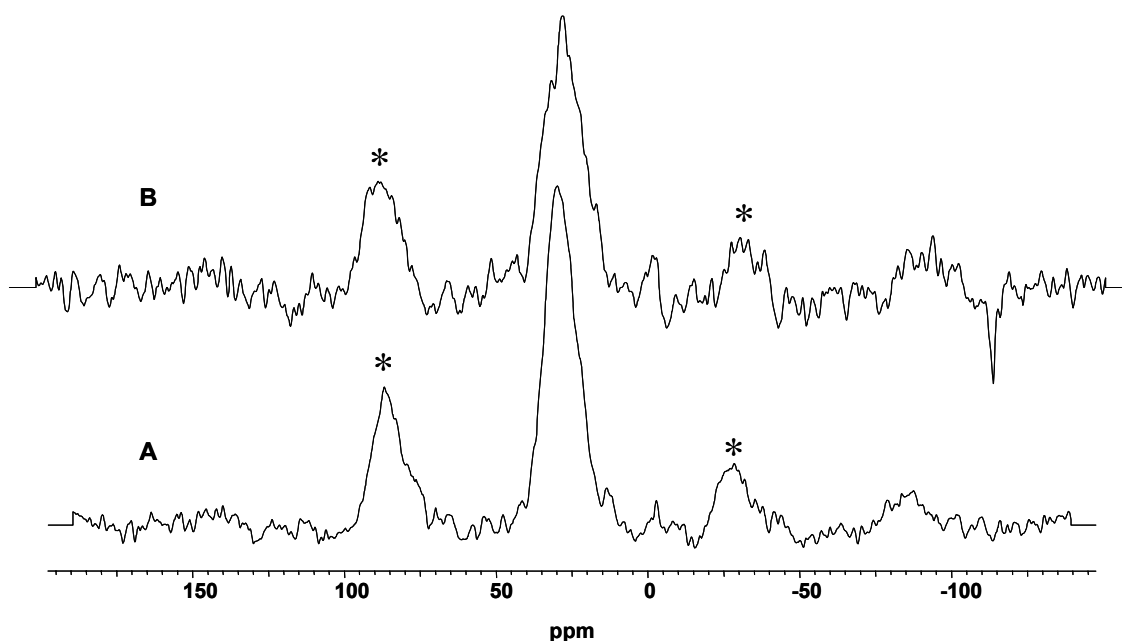


Figure 3.11: ³¹P CPMAS NMR of [A] virgin and [B] spent (after 4th recycle) Catalyst 1A, for carbonylation of styrene used in the recycle studies.* in spectra represents sidebands at 7kHz

A small protrusion around -5 ppm was observed for the recycled catalyst, this might be due to the presence of any free PPh_3 used during the reaction that had remained unwashed. The XPS of the used Catalyst 1A showed peaks at 336 eV, as the characteristic Pd $3d_{5/2}$ corresponding to Pd^{2+} oxidation state. These characterizations thus confirm that the ossified Pd-complex remained intact during the recycle runs and gave excellent activity and regioselectivity for carbonylation of styrene, and is thus a very stable, active and recyclable carbonylation catalyst.

3.3.2.3 Parametric Variations

After optimizing the reaction, the different reaction parameters were varied within a small range to understand the activity behavior of the reaction with variation in each parameter individually, for the hydrocarboxylation of styrene. The different parameters varied were, substrate loading, catalyst loading, CO partial pressure, promoter concentrations, water content, temperature etc. The detailed effect of variation of each parameter is presented under different heads as follows

3.3.2.3.1 Effect of Substrate Concentration

Substrate loading effect was investigated for the styrene carbonylation using the ossified $\text{Pd}(\text{pyca})(\text{TPPTS})$ complex (catalyst 1A) at three different substrate loading other than the standard charge of 5×10^{-3} mol in 25 mL total solution i.e. 0.2 kmol.m^{-3} . The different charges were selected as simple fraction or multiple of the standard charge. Keeping all the other reaction parameters as constant for a particular duration of the reaction progress, these reactions actually presented a varied substrate-to-catalyst ratio under the similar reaction conditions. The result is presented in Figure 3.12. It was observed that the degree of carbonylation of styrene was dependent on the substrate concentration for a particular charge of the catalyst. When the amount of substrate was reduced to half, the conversion in 6 h was same as our standard reaction. But, for the reactions using double and quadruple amount of the substrate in fixed duration, the conversions were decreased to 65% and 34% respectively. It may be remarked in this regard that, with the increase in concentration of the substrate, the rate of the carbonylation changed, but not proportionally. The TOF values as presented in the Figure 3.12 reveals that as the substrate-to-catalyst ratio changed to four-fold and eight-fold respectively, the TOF values increased, but

disproportionately. This might be due to the cause that the total number of active sites available for the reaction being fixed; the substrate concentration could not increase the turnover frequencies much. The constancy of the regioselectivity to the branched isomer at around ~99 % for all the concentrations of the substrates showed that the presence of the excess styrene did not influence the catalytic cycle in any form and

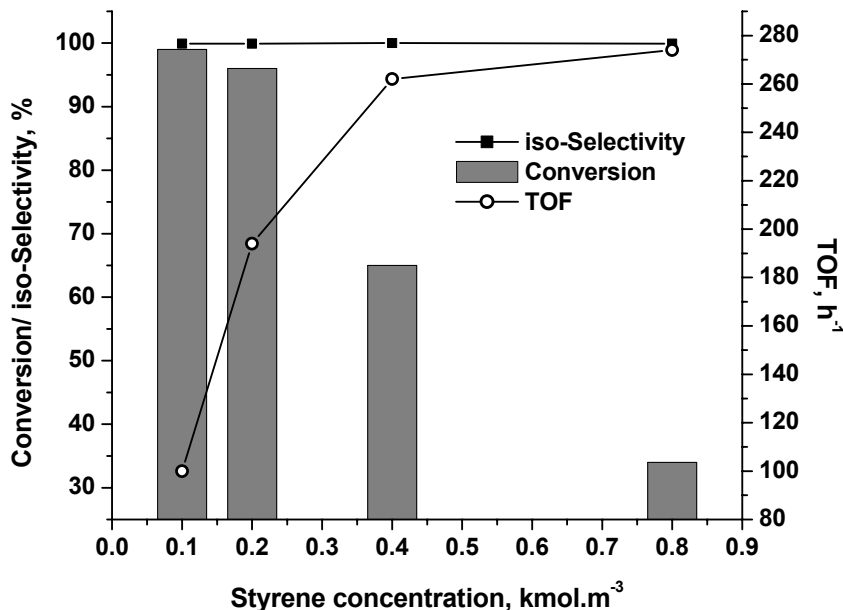


Figure 3.12: Effect of substrate concentration on styrene carbonylation

Reaction conditions: Catalyst: 100 mg; LiCl: 1.7 mmol; TsOH: 0.85 mmol; PPh₃: 0.038 mmol; H₂O: 27 mmol; Solvent: Methyl ethyl ketone (MEK); T: 388 K; P_{CO}: 5.4 MPa, Duration 6h

hence selectivity behavior was unaltered. The lowering down of the conversion levels for the individual reactions at higher substrate concentrations are actually in order with the efficiency of the catalyst. The lowest amount of the substrate was fully converted in 6h while for the higher ones, nearly equivalent amounts (to the standard run) of the substrates was only converted during the same duration of the reaction, as observed. The substrate concentration effect on the carbonylation of styrene thus may be specified as dependent but not linearly. The regioselectivity to the linear isomer of the carbonylation product was however almost negligible, as no detectable amount of it was formed in the reactions with the higher substrate loading. Rather, when at least < 0.1% of the n-isomer was observed for the standard run using 0.2 kmol.m⁻³ of styrene, for the higher concentrations of styrene no linear regioisomers were observed.

3.3.2.3.2 Effect of Catalyst Loading

The effect of the concentration of the catalyst was investigated for the carbonylation of styrene using Catalyst 1A. The results are presented in Figure 3.13. It was quite interesting to observe that the carbonylation reaction rate was doubled when double the amount was used but, when the catalyst charge was quadrupled the change in the reaction rate was not that much manifested as expected. A nonlinear enhancement in the activity and hence the reaction rate was observed for the range catalyst concentrations beyond three equivalents of the catalyst as that of the standard run. However, for still further increase in catalyst concentrations to six equivalents of the standard run, a plateau in rate was observed. The physical significance of such an observation is that the increase in catalyst concentration above four equivalents may lead to an excess of the catalytic sites than the population of the active substrate moieties, leading to no tangible change in TOF beyond that particular catalyst charge. The regioselectivity to

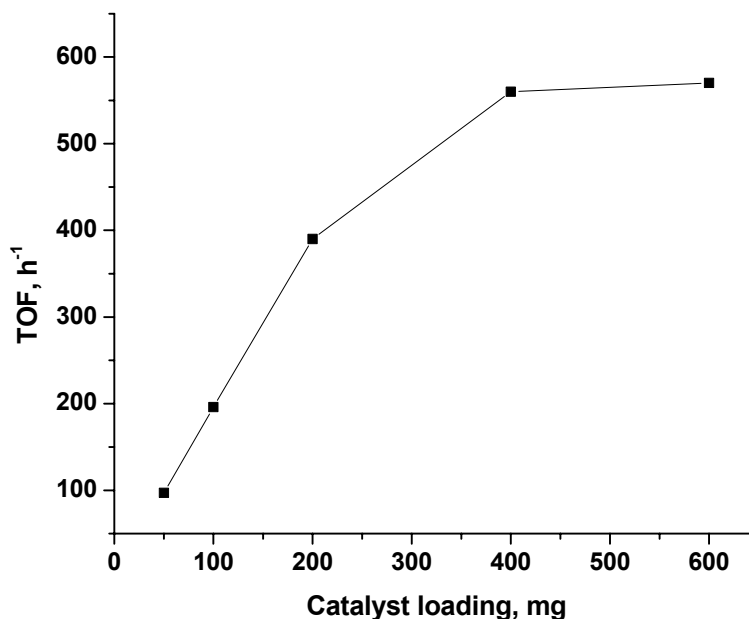


Figure 3.13: Effect of Catalyst concentration on styrene carbonylation

Reaction conditions: Substrate: 5 mmol; LiCl: 1.7 mmol; TsOH: 0.85 mmol; PPh₃: 0.038 mmol; H₂O: 27 mmol; Solvent: Methyl ethyl ketone (MEK); T: 388 K; P_{CO}: 5.4 MPa,

the branched acid product was however maintained at $\sim >99\%$ for all of these variation in catalyst concentrations

3.3.2.3.3 Effect of CO Partial Pressure

The partial pressure of carbon monoxide (CO) is one of the most important factors to assess the performance of a novel catalyst. The ossified Pd(pyca)(TPPTS) complex was also tested under different partial pressures of CO. for the four partial pressures tested, the reaction maintains a linear variation in the activity and hence in the reaction rate when carried out under different CO-partial pressures. The results are presented in Figure 3.14. An interesting observation was that under the lower partial pressures the regioselectivity to 2-phenylpropionic acid was a little bit less, $\sim 97.5\%$, while at higher CO-partial pressures, steady and increased regioselectivity of $> 99.5\%$ was observed for all of these runs. It is worth mentioning that while using the homogeneous catalyst Pd(pyca)(PPh₃)(OTs) a similar variation in regioselectivity was observed, which was attributed to the probable slow migratory insertion of the CO, forming the Pd-acyl species, which was CO-dependent.⁶ The dependence in this case may also be speculated as due to the same reason. Thus, the CO-partial pressure has important impact on the activity and selectivity of the ossified Pd-complex catalyst for the carbonylation of styrene.

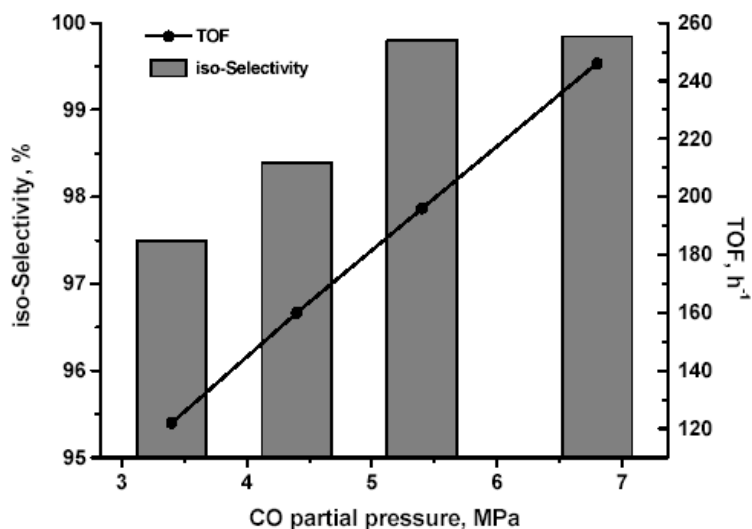


Figure 3.14: Effect of CO partial pressure on styrene carbonylation

Reaction conditions: Substrate: 5 mmol; LiCl: 1.7 mmol; TsOH: 0.85 mmol; PPh₃: 0.038 mmol; H₂O: 27 mmol; Solvent: Methyl ethyl ketone (MEK); T: 388 K; Duration: 6h

3.3.2.3.4 Effect of Promoters

The importance of the promoters for the carbonylation reaction is already well established and hence this needs to be studied while using the ossified Pd-complex as catalysts. The choice of LiCl and TsOH as the source of the Cl⁻ and H⁺ respectively has been considered as benchmarks after the works of Jayasree et al⁴, and in this study the variation of their mutual ratio as well as the quantity relative to the substrate are evaluated. The results in brief are presented in Table 3.5. From the data

Table 3.5: Effect of Promoters on carbonylation of styrene

Sl. No.	Promoter		Molar ratio of H ⁺ :Cl ⁻	Conv, %	Time, h	Selectivity, %		TOF, h ⁻¹
	Acid	Halide				iso	n	
1	TsOH	LiCl	0.85: 0.85	90.6	6	99.3	0.6	183
2	TsOH	LiCl	1.70: 0.85	91	6	99.2	0.8	184
3	TsOH	LiCl	0.85: 1.70	96	6	99.9	0.1	194
4	TsOH	LiCl	1.70: 3.40	98	5	99.9	0.1	238
5	TsOH	LiCl	3.40: 6.80	98	4.5	99.8	0.1	264
6	TsOH	LiCl	0.425: 0.85	98	11	99.8	0.1	106

Reaction conditions: Substrate: 5 mmol; Catalyst: 100 mg; PPh₃: 0.038 mmol; H₂O: 27 mmol; Solvent: Methyl ethyl ketone (MEK); T: 388 K; P_{CO}: 5.4 MPa

it may be inferred that using a mutual ratio of 2:1 ratio of Cl⁻ to H⁺ ions gives better results than the other ratios as 1:1 or 1:2 respectively. This might be due to the involvement of the Cl⁻ ion in the catalytic cycle concerning the activation of the substrate. But it is also worth mentioning that the concentration-time profile for styrene carbonylation using the ossified Pd-complex catalyst did not show the formation of the chloro-derivative of the substrate as the intermediate/ active substrate, hence a clear picture of the role of Cl⁻ is still to be known. So, using this ratio as constant different amounts of promoters were used for the carbonylation of styrene. It was observed that the activity of the catalyst increased by a fractional order with respect to the catalyst quantity and the variation in the activity of the catalyst i.e. the turnover frequency (TOF) is quite low. The variation in the carbonylation activity with respect to the amount of the promoter (LiCl: TsOH = 2:1) is presented in Figure 2.15. The flattening of the curve towards the higher promoter charge was prominent from the curve, which might be due

to the fact that even if the substrate activation is done involving the Cl^- ions showing rate enhancement at lower promoter concentrations, the catalytic cycle operates at the active sites which are not varied by the presence of excess of Cl^- ions. However, the promoters did not seem to be having any effect on the regioselectivity of the carbonylation, and unique and consistent regioselectivity of >99% was observed for all the experiments.

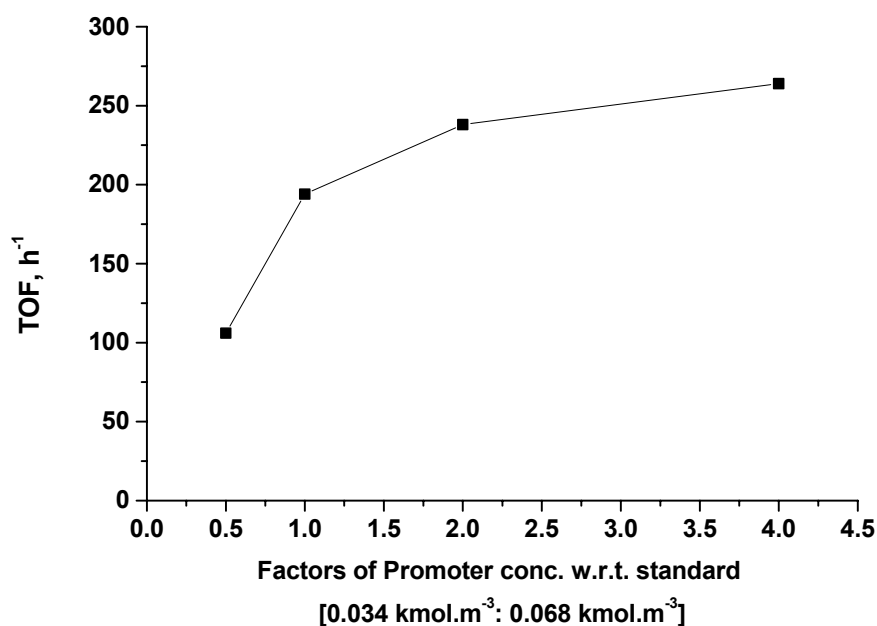


Figure 3.15: Effect of promoter concentration on styrene carbonylation

Reaction conditions: Substrate: 5 mmol; Catalyst: 100 mg; LiCl: TsOH: 2:1 (standard amount: LiCl 1.7mmol, TsOH 0.85 mmol); P_{CO} : 5.4 MPa PPh_3 : 0.038 mmol; H_2O : 27 mmol; Solvent: Methyl ethyl ketone (MEK); T: 388 K

3.3.2.3.5 Effect of Triphenylphosphine Concentration

The carbonylation of styrene using the ossified Pd-complex catalysts was carried out in the presence of a small quantity of triphenylphosphine, PPh_3 . The exact role of PPh_3 is still unknown, but it might be speculated that the stabilization of the intermediate Pd(0) species formed in the catalytic cycle is better obtained by the use of PPh_3 , as it can stabilize the lower oxidation states of Pd due to its good π -acid character. However, the concentration of PPh_3 is crucial for attaining good activity and regioselectivity to the branched isomeric product. The concentration of PPh_3 was varied from $3.8 \times 10^{-4} \text{ kmol.m}^{-3}$ to $3.8 \times 10^{-3} \text{ kmol.m}^{-3}$ and the activity (TOF) of the catalyst was

measured for all experiments. The data are presented in Figure 3.16 as follows. At lower concentrations of PPh_3 , the reaction rates are dependent directly on the PPh_3 -

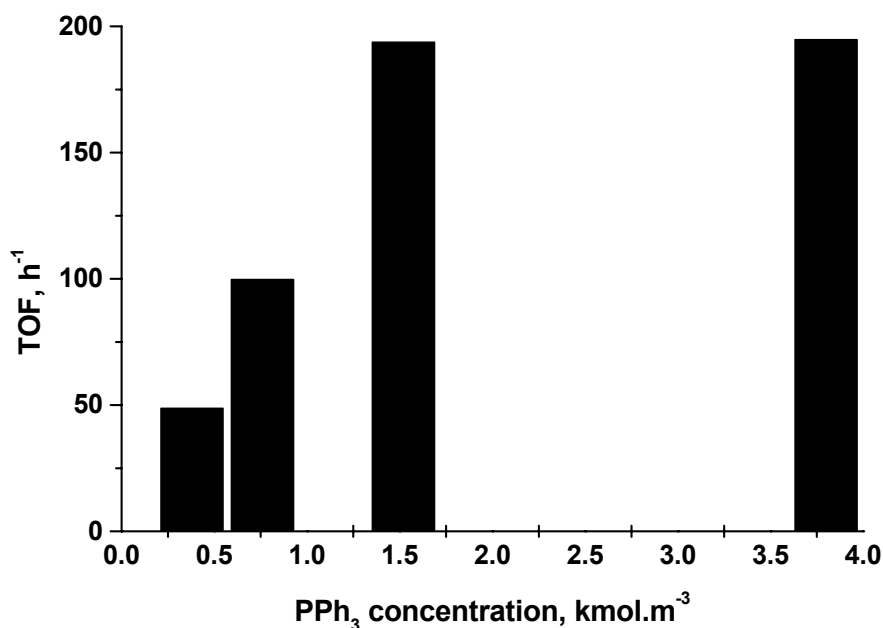


Figure 3.16: Effect of PPh_3 concentration on styrene carbonylation

Reaction conditions: Substrate: 5 mmol; Catalyst 100 mg; LiCl: 1.7 mmol; TsOH: 0.85 mmol; H_2O : 27 mmol; Solvent: Methyl ethyl ketone (MEK); T: 388 K; Duration: 6h

concentration, but beyond $1.52 \times 10^{-3} kmol.m^{-3}$ the reaction rates do not have any impact. This may be directly linked with the number of active sites present in the catalyst available for carbonylation. While using a particular charge of the catalyst, a further increase in the PPh_3 concentration will not enhance the reaction rates beyond a saturation limit. So, it may be concluded that the PPh_3 ligand has an enhancing effect within a range of concentration.

3.3.2.3.6 Effect of Concentration of Water

Water plays a very important role in the catalytic cycle for the carbonylation of olefins. The effect of added water into the reaction mixture is thus an important issue to investigate. Water not only is a requisite for the catalytic cycle, but also helps to solubilize the ionic components as TsOH and LiCl. It is well known that ~15% water is soluble in methyl ethyl ketone (MEK), and hence the addition of water may lead to

arising of different conditions (an immiscible liquid phase) under operating reaction conditions. But since we are dealing with much less quantity of water in the reaction mixture (mostly in the miscible range), we varied the water added to the reaction mixture. And the effect is presented in Figure 3.17. Reaction was also performed without water, but the reaction showed only 3% conversion. This may be due to the dissolved moisture in the solvent MEK and also in the reagents, which allow the reaction to run only to such an extent. The results clearly reveal that the activity of the ossified catalyst and hence the reaction rates are varying almost linearly with the concentration of water, within its range of miscibility with MEK.

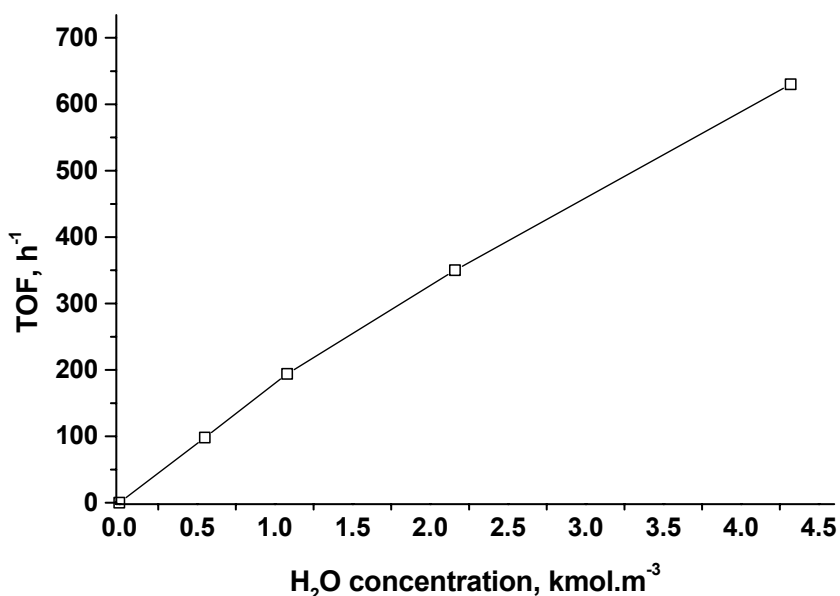


Figure 3.17: Effect of H₂O concentration on styrene carbonylation

Reaction conditions: Substrate: 5 mmol; Catalyst: 100 mg; LiCl: 1.7 mmol; TsOH: 0.85 mmol; PPh₃: 0.038 mmol; Solvent: Methyl ethyl ketone (MEK); T: 388 K; P_{CO}: 5.4 MPa; Duration: 6h

3.3.2.3.7 Effect of Temperature

Temperature plays a key role in the catalytic reactions as regard to the activation of the substrate and other kinetic issues. The effect of temperature on the carbonylation of styrene was studied to understand the reaction better. The reactions were carried out at three different reaction temperatures 378, 388 and 398K, for the same duration to bring out the impact of reaction temperature on the reaction.

The results are presented in Figure 3.18, where, the concentration of the major product i.e. 2-phenylpropionic acid (2-PPA) is plotted against reaction time for reactions at the three different reaction temperatures. As observed from the graph, the reaction at 378 K is quite slower than the standard reaction at 388K and proceeds only to 92% conversion in 6 h. Regioselectivity however is not influenced by temperature. While at 398 K, the reaction leads to ~96% conversion in 4.5 h compared to the standard 96% conversion in 6 h. thus, the effect of the reaction temperature is quite prominent for the carbonylation of styrene, using the ossified Pd-complex catalyst, Catalyst 1A.

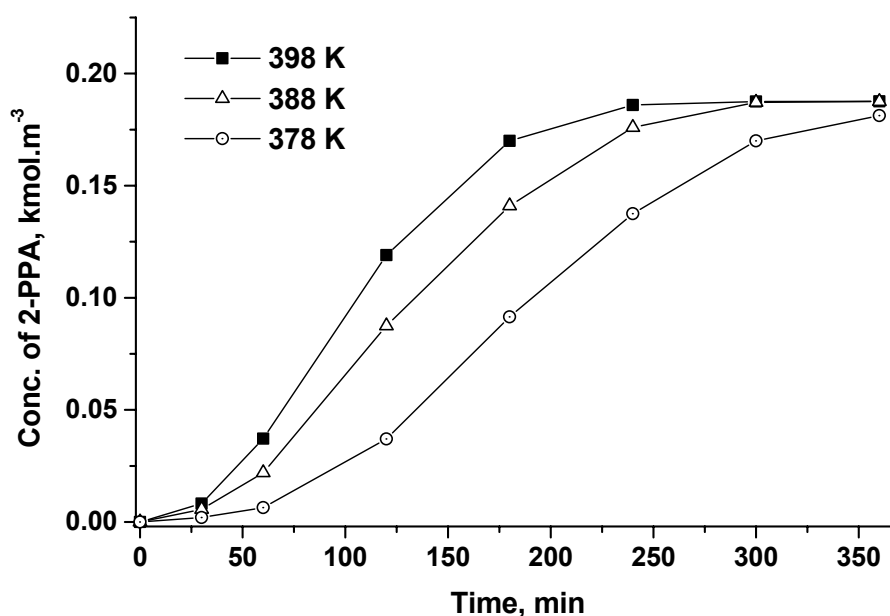


Figure 3.18: Effect of temperature on styrene carbonylation

Reaction conditions: Substrate: 5 mmol; Catalyst: 100 mg; LiCl: 1.7 mmol; TsOH: 0.85 mmol; PPh₃: 0.038 mmol; H₂O: 27 mmol; Solvent: Methyl ethyl ketone (MEK); P_{CO}: 5.4 MPa; Duration: 6h

This might be due to the thermal activation of the substrate or any of the active reaction intermediates during the catalytic cycle. Detailed mechanistic studies will be required for confirmation of such probability.

3.3.2.4 Different Catalysts

Having done the parametric variations the carbonylation reaction using styrene as the substrate and Catalyst 1A, all the four different ossified palladium complex catalysts were tested for the carbonylation of styrene and the results were

compared to screen out the most superior catalyst. All the reactions were carried out for the same duration of 6 h and the results are presented in Figure 3.19. It is clearly visible from the graph that the ossified Pd(pyca)(TPPTS) complex i.e. Catalyst 1A was the best in terms of the performance for the carbonylation of styrene, showing 96% conversion and 99.9% regioselectivity to the desired 2-phenylpropionic acid in 6 h. The ossified Pd(bipy)(TPPTS) complex i.e. Catalyst 1D showed the next highest activity with comparable conversion (95%) in 6h, while the regioselectivity to the branched acid product was 99%. The other two catalysts, namely ossified Pd(acpy)(TPPTS) complex

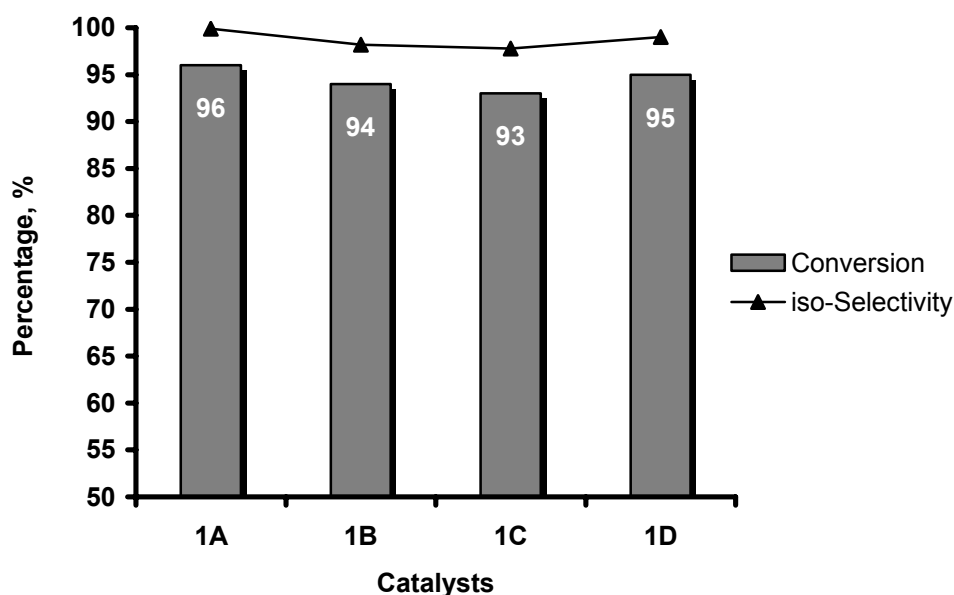


Figure 3.19: Comparison of different ossified Pd-complexes for carbonylation of styrene

Reaction conditions: Substrate: 5 mmol; Catalyst: 100 mg; LiCl: 1.7 mmol; TsOH: 0.85 mmol; PPh₃: 0.038 mmol; H₂O: 27 mmol; Solvent: Methyl ethyl ketone (MEK); T: 388 K; P_{CO}: 5.4 MPa, Pd-contents: Catalyst 1A = 0.44%, Catalyst 1B = 0.48%, Catalyst 1C = 0.45%, Catalyst 1D = 0.46%; Duration: 6h

and Pd(pycald)(TPPTS) complex i.e. Catalysts 1B and 1C respectively performed similarly but with slightly lower activity and regioselectivity. While using all of these catalysts, no side-product or intermediate chloro-derivative was observed for styrene carbonylation. However, it may be mentioned in this regard, that the homogeneous styrene carbonylation passed through an intermediate chloro-derivative, obtained from the reaction with LiCl, but for the heterogeneously catalyzed carbonylation of styrene was uniquely different in this aspect.

3.3.2.5 Different Substrates

The results of carbonylation of different substrates are presented in Table 3.6. The activity and selectivity aspects of the immobilized Pd-complexes were the

Table 3.6: Carbonylation of different substituted olefins and alcohols

Sl. No	Substrate	Product (major)	Conv., %	Sel., %		Time, h	TOF, h ⁻¹
				iso	n		
1			96	99.9	-	6	194
2			94	99.8	0.1	6	189
3			93	99.5	0.4	6	187
4			95	99.3	0.5	6	191
5			95	99.4	0.5	6	191
6			92	99.2	0.7	6	183
7			92	99.9	-	6	184
8			96	99.8	0.1	6	194
9			93	99.8	0.1	11	96

Reaction conditions: Substrate: 5 mmol; Catalyst: 100 mg; LiCl: 1.7 mmol; TsOH: 0.85 mmol; PPh₃: 0.038 mmol; H₂O: 27 mmol; Solvent: Methyl ethyl ketone (MEK); T: 388 K; P_{CO}: 5.4 MPa, Pd-contents: Catalyst 1A = 0.44%

important issues to observe in these tests. Using the ossified Pd(pyca)(TPPTS) complex (i.e. Catalyst 1A) along with TsOH and LiCl promoters, fairly high activity was obtained for almost all the substrates. The olefins used for the carbonylation reaction were chosen from different categories such as terminal aliphatic olefins, aryl olefins and olefins with other functional groups attached to the molecule. Among the aryl-substituted olefins, styrene showed highest activity (TOF $\sim 194 \text{ h}^{-1}$) followed by the *p*-methyl styrene and *p*-tert butyl styrene, which had almost comparable turnover frequencies (183 and 184 h^{-1} respectively). The reactions with other terminal olefins also showed that the ossified catalysts perform comparatively well (follow Table 3.2). One important observation regarding this is that in spite of the turnover frequencies of the catalysts being considerably lesser than those of the homogeneous catalysts, the turnover numbers are quite similar or higher in some reactions.

3.3.2.6 Comparative Advancement Study

A comparison of the carbonylation activity, regioselectivity, and stability aspects of the different heterogenized palladium complex catalyst as obtained from literature is presented in Table 3.7. Of the different heterogeneous Pd-catalysts presented^{7, 8, 9}, the ossified catalyst had some unique advantages. In spite of the slightly lower activity of the ossified Pd-complexes than the anchored Pd-complex catalysts, the ossified complexes have synthetic advantages. Where most of the immobilization processes involve exotic chemical reagents and cumbersome multi-step methodology, the ossification technique is relatively easiest of all involving commonly used reagents and easy-to-handle preparation method. The highly stable and non-leaching nature of the ossified catalysts adds to the merits along with the easy separation and reusability. Thus, ossified Pd-complexes have emerged as truly heterogeneous, active carbonylation catalysts.

Table 3.7: Comparative study of Ossified Pd-complexes with other heterogeneous Pd-Catalysts from literature for carbonylation of olefins and alcohols

Entry	Substrate	Catalyst system	Conv., %	Selectivity, %		TON	Time, h	TOF, h ⁻¹	Pd-loss in reaction	Remarks
				iso	n					
1	S	Homogeneous Pd(pyca)(PPh ₃)(OTs) ^a	97	99.01	0.98	468	0.18	2600	-	Tedious catalyst-product separation and reuse
2	S	Pd/C ^b	92	98	1.9	13340	4.6	2900	37.5 %	Heavy leaching obtained, activity might be due to leached Pd
3	S	Aq. biphasic Pd(pyca)(TPPTS) ^c	94.5	92	7.2	428	1.42	302	0.225 %	Catalyst deactivates in air, recycles active only under CO atmosphere
4	S	Pd(pyca)(PPh ₃)(OTs) anchored inside MCM-41 ^d	98.12	99.3	0.68	5556	12	463	3.5×10 ⁻⁴ %	Cumbersome multi-step catalyst synthesis involving sensitive/ exotic reagents
5	S	Catalyst 1A ^e	96	99.9	-	1160	6	194	8.8×10 ⁻⁵ %	Extremely easy catalyst synthesis method, Highly stable recyclable and truly heterogeneous catalyst with negligible leaching
6	S	Catalyst 1B ^e	94	98.2	1.78	1050	7	150	-	
7	S	Catalyst 1C ^e	93	97.8	2.09	1106	7	158	-	
8	S	Catalyst 1D ^e	95	99.0	0.88	1099	7	157	-	

^e Reaction conditions: Substrate: 5 mmol; Catalyst: 100 mg; LiCl: 1.7 mmol; TsOH: 0.85 mmol; PPh₃: 0.038 mmol; H₂O: 27 mmol; Solvent: Methyl ethyl ketone (MEK); T: 388 K; P_{CO}: 5.4 MPa, Pd-contents: Catalyst 1A = 0.44%, Catalyst 1B = 0.48%, Catalyst 1C = 0.45%, Catalyst 1D = 0.46%, S = Styrene

Reaction conditions: ^a as in reference [4]; ^b as in reference [7]; ^c as in reference [8]; ^d as in reference [9]

3.4 Conclusions

The novel method of immobilization namely, the ossification of metal complexes has been demonstrated to be a very efficient, easy and effective method for obtaining heterogeneous metal complex catalysts. The concept has been established in this chapter with ample evidence in form of numerous characterizations and experiments. As an application to evaluate the stability of the thus ossified Pd-complexes, carbonylation of different aryl olefins and alcohols has been undertaken. The ossified Pd-complexes have been found to be highly active, regioselective, and extremely stable under the stringent reactions conditions of the carbonylation reactions. The high stability and efficient recyclability of the catalyst for the carbonylation reactions have not only established the immobilization strategy as an immensely successful one, but also have marked the “ossification” methodology as the most promising approach for the immobilization of metal complex catalysts. A detailed parametric study of carbonylation of aryl olefins has been presented in this chapter using styrene as the model substrate to understand the performance matrix of the ossified Pd-complexes concerning the activity regime of the catalysts. The important applications of carbonylation as shown in this chapter clearly demonstrate ossified Pd-complex catalysts as truly heterogeneous, highly active, selective and extremely stable and recyclable catalysts.

3.5 Future Directions and Scope

Ossification of the metal complex catalysts has been demonstrated as the most efficient and easy immobilization strategy, and has been effectively used here for the carbonylation of olefins and alcohols. Based on the observations as illustrated in this chapter, a set of directives can be lined up for future research as follows,

- Ossification may be extended to different other ligand systems (other than phosphines) to expand the applicability to numerous other reactions
- Carbonylation of different other classes of compounds, e.g. halides, conjugated dienes, α,β -unsaturated compounds, intramolecular active-functional substrates etc. may be targeted as important application areas
- More detailed mechanistic insights of the ossified Pd-complex catalyzed carbonylation reactions need to be studied

References

- 1 (a) Hu A, Ngo H L, Lin W, *J. Am. Chem. Soc.*, **2003** 125 11490 (b) Hu A, Ngo H L, Lin W, *Angew. Chem. Int. Ed. Engl.*, **2003** 42 6000
- 2 Cornils, B. and Herrmann, W. A., Eds. *Aqueous Phase Organometallic Catalysis: Concepts and Applications*, Wiley-VCH, Weinheim, 2nd Edition, **2004**
- 3 Bhanage B. M., Divekar S. S., Deshpande R. M., Chaudhari R. V., *Org. Process Res. Dev.*, **2000**, 4(5), 342
- 4 Jayasree S., Seayad A., Chaudhari R. V., *Org. Lett.*, **2000**, 2(2), 203
- 5 Jayasree S., Seayad A., Chaudhari R. V., *Chem. Commun.*, **2000**, 1239
- 6 Jayasree S, *Ph.D. Thesis*, University of Pune, **2000**
- 7 Seayad A, Seayad J, Chaudhari R V, *Chem. Commun.*, **1999** 1067
- 8 Jayasree S, Seayad A, Chaudhari R V, *Chem. Commun.* **2000** 1239
- 9 Mukhopadhyay K, Sarkar B R, Chaudhari R V, *J. Am. Chem. Soc.* **2002** 124 9692

Chapter **4**

Kinetic Modeling of Carbonylation of 4-Isobutylstyrene Using Homogeneous and Ossified Pd(pyca)(PPh₃)(OTs) Complex

This chapter presents the kinetic studies of the carbonylation of 4-isobutylstyrene (IBS), using homogeneous Pd(pyca)(PPh₃)(OTs) complex and its ossified counterpart as heterogeneous catalyst. The kinetics of the reaction was studied in a semi batch stirred slurry reactor with parametric variations of catalyst loading, promoters, IBS, CO-partial pressure etc. at a temperature range of 368 - 388K. A reaction pathway involving the formation of the active catalytic Pd(0) species using substrate 4-isobutylstyrene in the catalytic cycle has been proposed. Empirical semi-batch models have been derived and found to predict the concentration-time profiles at all temperatures satisfactorily.

4.1 Introduction

Knowledge of kinetics is most essential to understand the mechanistic pathways of chemical reactions and the overall dependency of the rate of reaction on reaction parameters. In catalytic reactions, the kinetic studies often provide the best clues to the rate determining steps and the supporting evidence to the catalytic cycle. Hydroxycarbonylation of the aryl olefins and alcohols has been a prime area of research in the C1 chemistry and catalysis due to the immense economical importance of the products as already described in several previous sections. As evident from the literature review in Chapter 1, the majority of the previous studies involving the carbonylation of aryl olefins and alcohols were focused on development of catalysts for improving the catalytic performance and product regioselectivity, while only a few reports have described the kinetics of these important reactions. The detailed kinetic investigations reported by Seayad et al¹ described the use of 1-(4-Isobutylphenyl)ethanol, IBPE as the effective substrate using PdCl₂(PPh₃)₂/ TsOH/ LiCl as catalyst system, but no reports of the kinetic studies using IBS as a substrate had been published till date. Also, no reports on the kinetics are available using the most active Pd complex catalyst system (see Chapter 1, Section 1.2.3), Pd(pyca)(PPh₃)(OTs)/ TsOH/ LiCl [pyca = 2-picolinate]. The immobilization of this particular complex has already been described in Chapters 2 and 3 of this thesis in the form of anchored catalyst inside mesoporous silicas, and the *ossified* catalysts respectively, which illustrated successful heterogenization having excellent activity, regioselectivity and stability. And also, no reports on kinetics using a heterogenized Pd-complex have been published before.

The aim of this work was, therefore, to study the kinetics of carbonylation of 4-iso butylstyrene (IBS) using the homogeneous and immobilized (*ossified*) Pd(pyca)(PPh₃)(OTs) complex catalysts in the presence of TsOH and LiCl as promoters and methylethyl ketone (MEK) as a solvent. The effect of CO partial pressure, concentration of substrate, concentration of promoters, water etc. on the rate of carbonylation has been studied at 388 K and the results compared for both the homogeneous and heterogeneous catalyst systems. Based on these data, rate equations have been proposed and possible reaction pathway discussed.

4.2 Experimental Section

4.2.1 Materials

The materials required for this study were either procured from different sources or synthesized. The catalysts were synthesized as described earlier - Pd(pyca)(PPh₃)(OTs) (in Section 2.2.2.1) and ossified Pd-pyca complex (in Section 3.2.2.3.6). The materials required for synthesis of IBS such as Sodium borohydride, NaBH₄, anhydrous sodium sulphates, Na₂SO₄, Methanol, MeOH, Methyl ethyl ketone, MEK, Ethyl acetate, EtOAc were of AR grade and were procured from Merck India Ltd. The precursor 4-Isobutylacetophenone, IBAP obtained from Lancaster Chemicals, UK

4.2.2 Synthesis of 4-Isobutylstyrene, IBS

4-Isobutyl styrene was prepared by a two-step process starting from the precursor 4-isobutylacetophenone using hydrogenation – dehydration pathway. For the first step, i.e. hydrogenation step, in a typical batch 35.25 g (0.2 moles) of IBAP was mixed with 200 mL MeOH under ice cold condition and to it 15.18 g (0.4 moles) of NaBH₄ was added slowly in intervals under vigorous stirring so that the temperature did not rise abruptly. The mixture was brought to ambient temperature after the completion of addition, and was stirred overnight (~8 h). Later, the reaction mixture was concentrated (MeOH removed), quenched using dilute aqueous NaHCO₃ solution, and partitioned using ethyl acetate to retain the desired products 1-(4-isobutylphenyl)ethanol (IBPE) in the organic layer. This was dried using anhydrous Na₂SO₄ and then EtOAc was removed.

The IBPE thus obtained was dehydrated using acid catalyst TsOH in toluene-water azeotropic distillation in a Dean-Stark apparatus. In a particular batch, 0.11 g TsOH was added in to a 60 mL mixture of IBPE in toluene and refluxed for 3 h. A dab (~20 mg) of TBC was used to prevent polymerization of IBS occurring under the acidic conditions. After cooling to room temperature, the mixture was washed using water to remove all free acids (tested using a pH paper strip). Then toluene was removed in a rotary evaporator and the IBS was distilled out under reduced pressure using an ultra high vacuum (~10⁻⁵ bar) in presence of a little amount of TBC again. The distilled IBS was stored under argon.

4.2.3 Carbonylation Reactions

The carbonylation reactions of IBS were carried out in a 50 mL Parr autoclave reactor made of Hastelloy C-276 in the same manner as described in a previous section (Section 2.2.3).

4.2.4 Calculation of Initial Rates

The initial rate of the carbonylation reactions was calculated from the CO absorption data for the reactions. The consumption of CO (in moles) was observed as a function of time. The initial rate of carbonylation is defined as the number of moles of CO consumed per unit time, per unit volume of the reactants (reaction mixture).

$$r_A = \frac{\text{moles of CO consumed}}{\text{time} \times \text{volume of reactant}} \quad (4.1)$$

For the determination of the initial rates of carbonylation, the amount of CO consumed per unit volume was plotted against time, for an initial period of 10-15 minutes, and the slope was measured as the rate of carbonylation.

4.3 Results and Discussions

The work presented in this chapter is mainly focused to address the following issues on catalytic carbonylation of IBS,

- i) To study the effect of different reaction parameters on the rate of carbonylation of IBS using homogeneous Pd(pyca)(PPh₃)(OTs) /TsOH/ LiCl catalyst system and develop rate equations
- ii) To study the effect of different reaction parameters on the rate of carbonylation of IBS using heterogeneous ossified Pd(pyca)(TPPTS)/TsOH/LiCl/PPh₃ catalyst system and develop rate equations
- iii) To correlate the impact of homogeneous and heterogeneous catalysts on kinetics of carbonylation by comparison of data and physical interpretation

For the purpose of kinetic study, carbonylation reactions were carried out in a batch mode and the concentration-time data were obtained under a wide range of reaction conditions, which are summarized in Table 4.1.

Table 4.1: Range of Parameters for Kinetic Studies

	Parameters	Units	Range
Catalyst	Pd(pyca)(PPh ₃)(OTs)	kmol.m ⁻³	2.94×10 ⁻⁴ – 2.24×10 ⁻³
	Ossified Pd(pyca)(TPPTS)		0.05 – 0.3 g (0.47% Pd)
Substrate, IBS	Homogeneous	kmol.m ⁻³	0.313 – 2.5
	Heterogeneous		0.208 – 1.25
Promoters, TsOH/LiCl (1:1)	Homogeneous	kmol.m ⁻³	2.78×10 ⁻² – 2.34×10 ⁻¹
	Heterogeneous		5.87×10 ⁻² – 2.35×10 ⁻¹
PPh₃	Homogeneous	kmol.m ⁻³	0
	Heterogeneous		1.53×10 ⁻³ – 6.1×10 ⁻³
Partial pressure of CO		MPa	4.08 – 6.8
Temperature		K	378 – 398
Volume of liquid phase		m ³	2.5 × 10 ⁻⁵
Agitation speed		Hz	15 – 16.67

In all the experiments, isothermal conditions were maintained. Typical concentrations vs. time profiles for the homogeneous and heterogeneously catalyzed carbonylation reactions are presented in Figures 4.1(A) and 4.2(A) respectively, while the CO absorption data is presented in the Figures 4.1(B) and 4.2(B) for the homogeneous and the heterogeneously catalyzed reactions respectively. From the concentration-time and the CO-absorption profiles, some important observations may be marked as follows.

- ✓ A single product namely, 2-(4-isobutylphenyl)propionic acid, IBN, was obtained as the product. No linear isomer was observed in the product profile for both the homogeneously and heterogeneously catalyzed reactions, consistent with the results discussed in Chapter 3.
- ✓ No intermediate (as chloro-derivative of substrate) or any by-product was observed in the GC-MS analysis, which is markedly different from that in the carbonylation of IBPE

- ✓ Excellent mass balance (>98%) was observed between the IBS and CO consumed and the product i.e. IBN for both the cases.
- ✓ The reaction using heterogeneous catalyst was much slower than the homogeneous reaction.

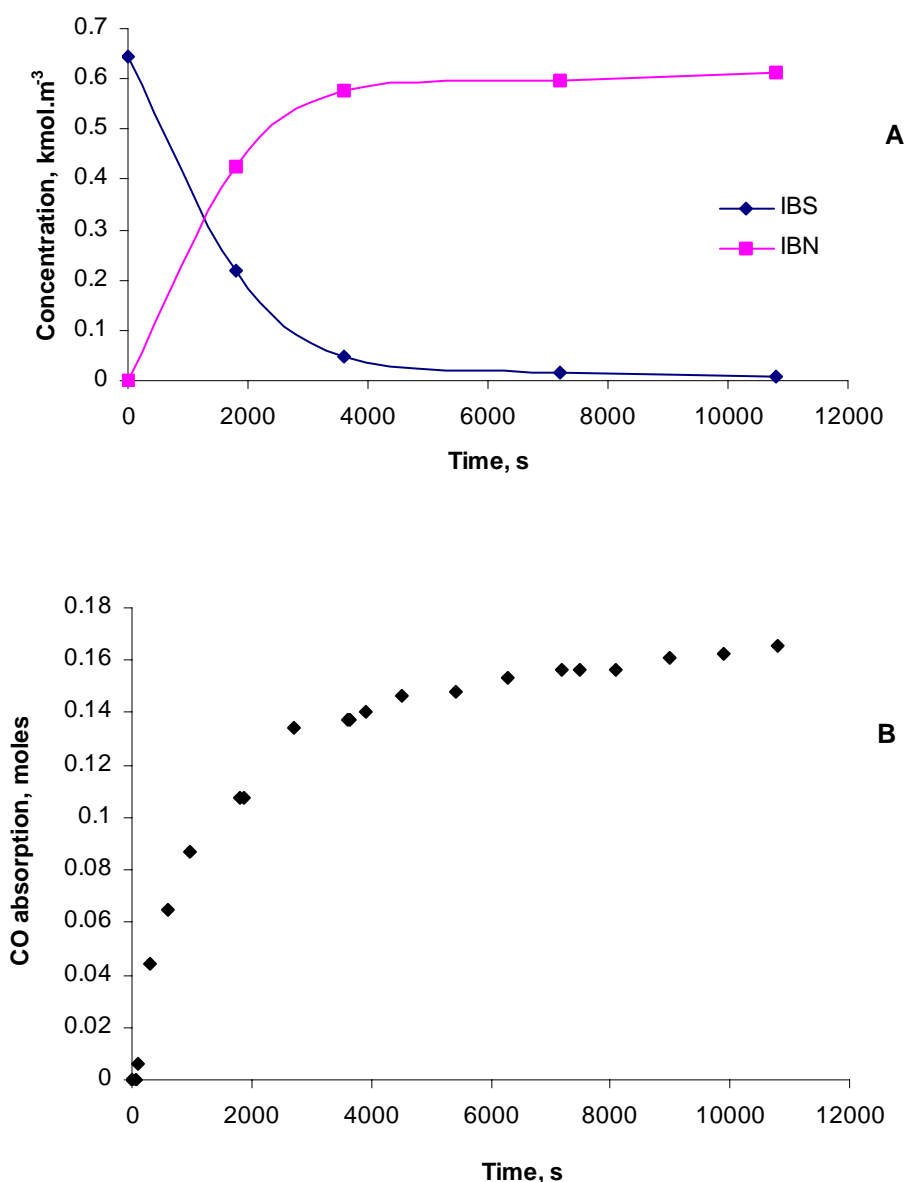


Figure 4.1: (A) Concentration-Time profile (B) CO Absorption data for carbonylation of 4-Isobutylstyrene using homogeneous $\text{Pd}(\text{pyca})(\text{PPh}_3)(\text{OTs})$ complex catalyst

Reaction conditions: IBS: $0.625 \text{ kmol.m}^{-3}$; $\text{Pd}(\text{pyca})(\text{PPh}_3)(\text{OTs})$: $1.1 \times 10^{-3} \text{ kmol.m}^{-3}$; TsOH/LiCl (1:1): $0.116 \text{ kmol.m}^{-3}$; H_2O : 1.56 kmol.m^{-3} ; P_{CO} : 5.4 MPa; Solvent: MEK; 9.5 kmol.m^{-3} ; Temp: 388 K, Agitation: 15 Hz, Total volume: $2.5 \times 10^{-5} \text{ m}^3$

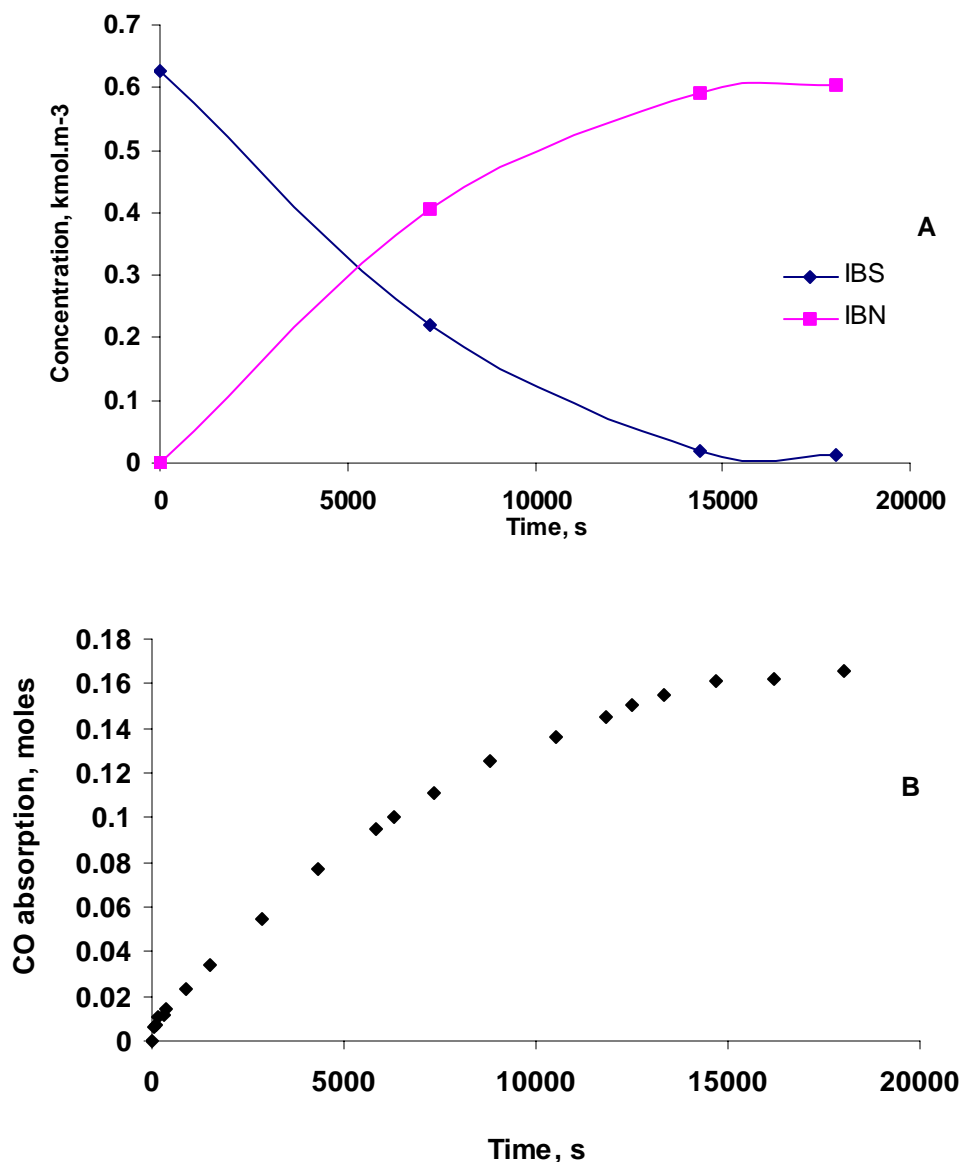
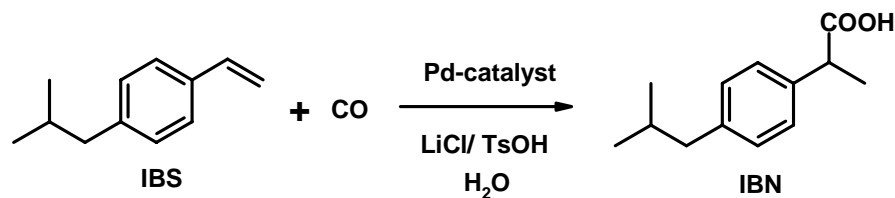


Figure 4.2: (A) Concentration-Time profile, (B) for carbonylation of 4-Isobutylstyrene using ossified Pd(pyca)(TPPTS) complex catalyst [Catalyst 1A]

Reaction conditions: IBS: $0.625 \text{ kmol.m}^{-3}$; Catalyst 1A: $0.1 \times 10^{-3} \text{ kg}$; TsOH/LiCl (1:1): $0.1175 \text{ kmol.m}^{-3}$; H_2O : 1.6 kmol.m^{-3} ; PPh_3 : $3.8 \times 10^{-3} \text{ kmol.m}^{-3}$; P_{CO} : 5.4 MPa ; Solvent: MEK; 9.5 kmol.m^{-3} ; Temp: 388 K , Agitation: 16.67 Hz ; Total volume: $2.5 \times 10^{-5} \text{ m}^3$

The absence of the chloro-derivative of the substrate as an intermediate was a very crucial observation for both the homogeneously and heterogeneously catalyzed reactions, as it was thus speculated that the substrate was directly involved into the catalytic reaction cycle. Based on these observations, the carbonylation of IBS may be represented as in Scheme 4.1



Scheme 4.1: Carbonylation of IBS

Following this scheme, the reaction was standardized for doing the kinetics study, with respect to each parameter and a set of standard reaction conditions were arrived at as described in Table 4.1.

4.3.1 Solubility Data

For the interpretation of kinetic data, the knowledge of the solubility of CO in MEK-IBS mixture was necessary. The solubility of CO in different mixtures of IBS and MEK containing 3% water at different IBS concentrations were *estimated* at 388 K, using the method described by Purwanto et al², and the solubility data are presented in Table 4.2

Table 4.2: Henry's constants (H_e) of CO in a mixture of IBS in MEK at 388 K

Entry	IBS in MEK, % w/w	$H_e \times 10^3, \text{ kmol.m}^{-3}.\text{MPa}^{-1}$
1	5	6.98
2	10	6.34
3	20	5.75

It was observed that the solubility of CO decreased with increasing concentration of IBS in the mixture. The concentration of the dissolved CO may be calculated as,

$$A^* = P_{\text{CO}} \cdot H_e \quad (4.2)$$

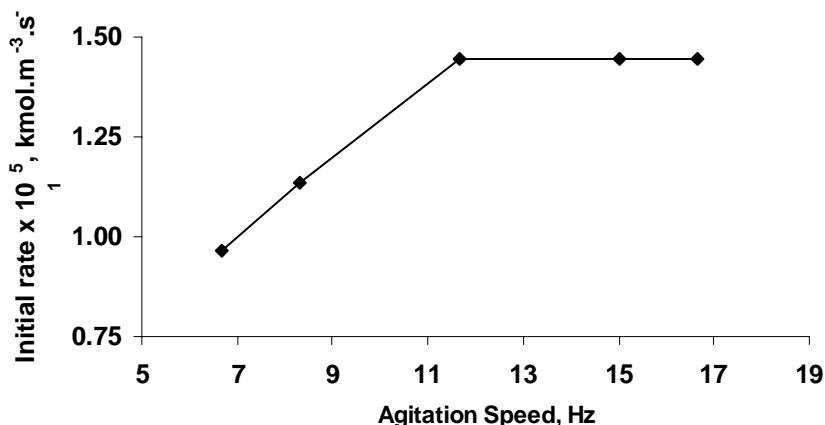
where, P_{CO} is the partial pressure of carbon monoxide

4.3.2 Analysis of Mass Transfer Effects

For the homogenous carbonylation reaction, the gas liquid mass-transfer effect is the only important restricting parameter, while for the heterogeneously catalyzed reaction, both gas-liquid and liquid-solid the mass transfer effects may come into play. The detailed calculations of mass transfer in the case of the homogeneous as well as

the heterogeneous catalyzed reactions are presented in Appendix 1. However, ensured that the mass transfer effects were absent for both the homogeneous and heterogeneous carbonylation reaction.

Figure 4.3: Effect of agitation speed on IBS carbonylation using



homogeneous Pd(pyca)(PPh₃)(OTs) complex catalyst

Reaction conditions: IBS: 0.625 kmol.m⁻³; Pd(pyca)(PPh₃)(OTs): 1.1×10⁻³ kmol.m⁻³; TsOH/LiCl (1:1): 0.116 kmol.m⁻³; H₂O: 1.56 kmol.m⁻³; P_{CO}: 5.4 MPa; Solvent: MEK; 9.5 kmol.m⁻³; Temp: 388 K, Total volume: 2.5×10⁻⁵ m³

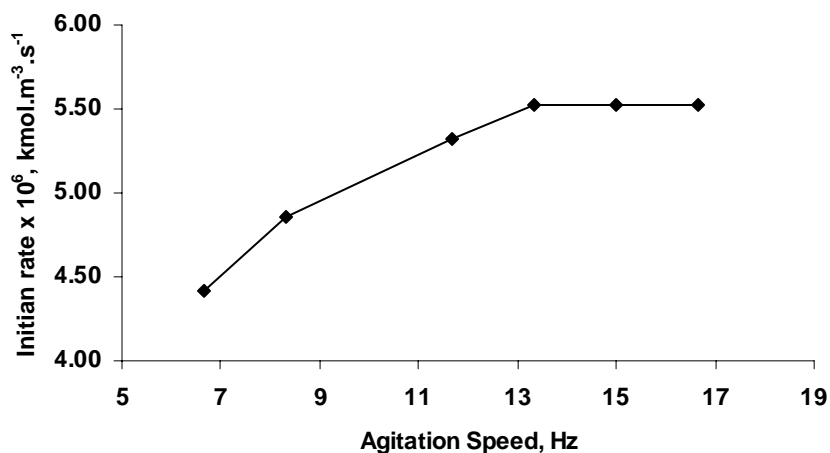


Figure 4.4: Effect of agitation speed on IBS carbonylation using Ossified Pd(pyca)(TPPTS) complex catalyst

Reaction conditions: IBS: 0.625 kmol.m⁻³; Catalyst 1A: 0.1×10⁻³ kg; TsOH/LiCl (1:1): 0.1175 kmol.m⁻³; H₂O: 1.6 kmol.m⁻³; PPh₃: 3.8×10⁻³ kmol.m⁻³; P_{CO}: 5.4 MPa; Solvent: MEK; 9.5 kmol.m⁻³; Temp: 388 K, Total volume: 2.5×10⁻⁵ m³

In addition to the mass-transfer parameters, the effect of the agitation speed was studied experimentally for both the homogeneous and heterogeneously catalyzed reactions to ensure that the reaction is in kinetic regime. The variations of the initial rates of IBS carbonylation with agitation speed for the homogeneous and heterogeneous reactions are presented in Figures 4.3 and 4.4 respectively. It was observed that for the homogeneous reaction, the rate did not vary beyond 11.66 Hz and remained constant for any higher speed of agitation. For the heterogeneous catalyzed reaction, the reaction rate became constant only beyond 13.33 Hz. Following these results, the homogeneous reactions were carried out at 15 Hz, while the heterogeneous reactions were carried out at 16.67 Hz.

4.3.3 Kinetics of Carbonylation of IBS using Homogeneous Catalyst

4.3.3.1 Initial Rate Data

The analysis of the initial rates was performed as mentioned before. The variations of the reaction rates due to the different reaction parameters are studied to analyze the contribution of each of the parameters in the kinetics.

For homogeneous catalyzed reactions, the variations of the initial rates with respect to the different reaction parameters are presented in Figures 4.5 to 4.9

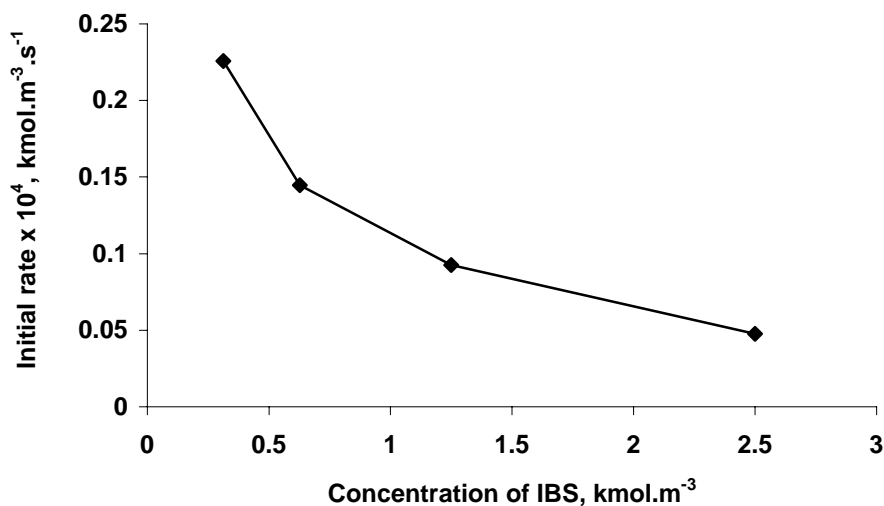


Figure 4.5: Effect of concentration of IBS on initial rate of carbonylation

Reaction conditions: Pd(pyca)(PPh₃)(OTs): 1.1×10^{-3} kmol.m⁻³; TsOH/LiCl (1:1): 0.116 kmol.m⁻³; H₂O: 1.56 kmol.m⁻³; P_{CO}: 5.4 MPa; Solvent: MEK; 9.5 kmol.m⁻³; Temp: 388 K, Agitation: 15 Hz, Total volume: 2.5×10^{-5} m³

From the Figure 4.5, it is clearly observed that the initial rate of the reaction decreases with the increase of the concentration of the substrate in a non-linear fashion. Therefore, this is an example of a substrate-inhibited kinetics.

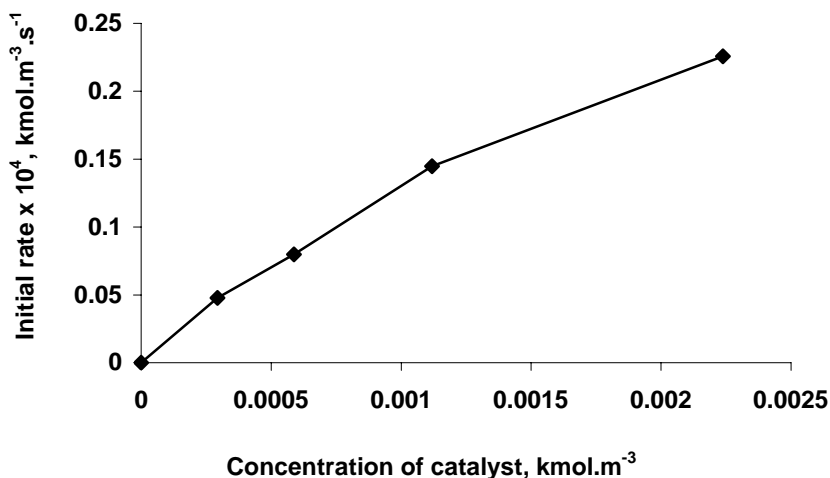


Figure 4.6: Effect of concentration of catalyst on initial rate of carbonylation

Reaction conditions: IBS: 0.625 kmol.m⁻³; TsOH/LiCl (1:1): 0.116 kmol.m⁻³; H₂O: 1.56 kmol.m⁻³; P_{CO}: 5.4 MPa; Solvent: MEK; 9.5 kmol.m⁻³; Temp: 388 K, Agitation: 15 Hz, Total volume: 2.5×10⁻⁵ m³

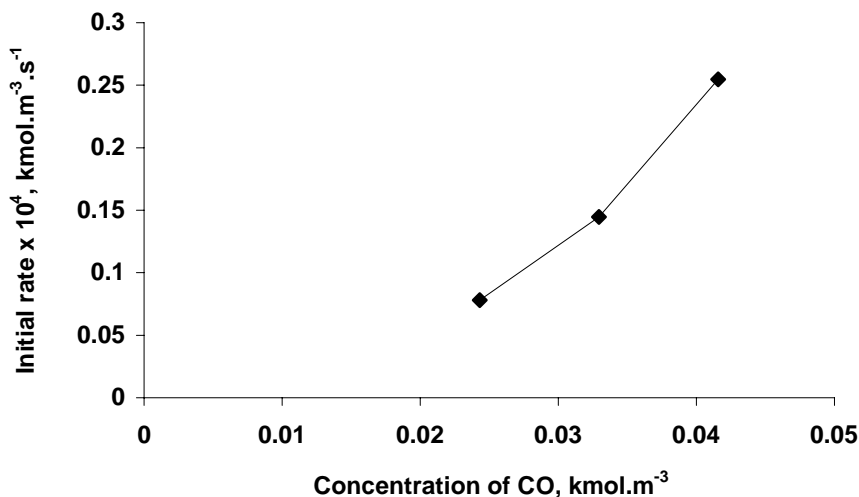


Figure 4.7: Effect of concentration of CO on initial rate of carbonylation

Reaction conditions: IBS: 0.625 kmol.m⁻³; Pd(pyca)(PPh₃)(OTs): 1.1×10⁻³ kmol.m⁻³; TsOH/LiCl (1:1): 0.116 kmol.m⁻³; H₂O: 1.56 kmol.m⁻³; Solvent: MEK; 9.5 kmol.m⁻³; Temp: 388 K, Agitation: 15 Hz, Total volume: 2.5×10⁻⁵ m³

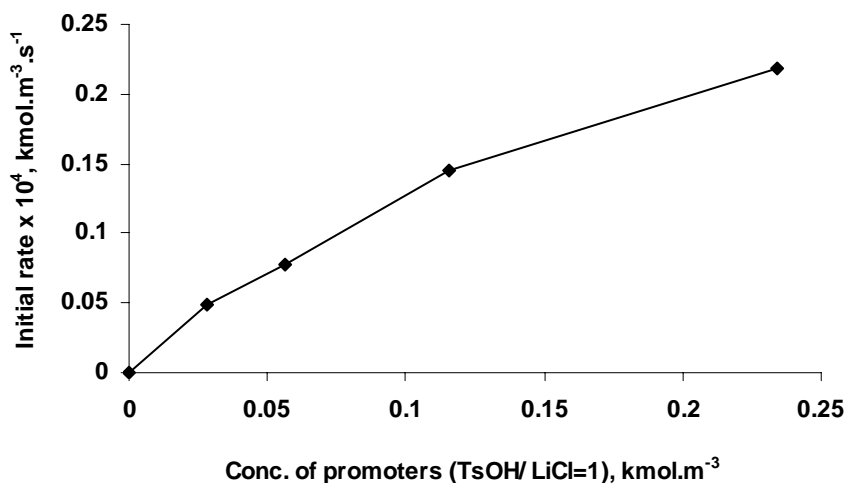


Figure 4.8: Effect of concentration of promoters on initial rate of carbonylation

Reaction conditions: IBS: $0.625 \text{ kmol.m}^{-3}$; Pd(pyca)(PPh₃)(OTs): $1.1 \times 10^{-3} \text{ kmol.m}^{-3}$; H₂O: 1.56 kmol.m^{-3} ; P_{CO}: 5.4 MPa ; Solvent: MEK; 9.5 kmol.m^{-3} ; Temp: 388 K , Agitation: 15 Hz , Total volume: $2.5 \times 10^{-5} \text{ m}^3$

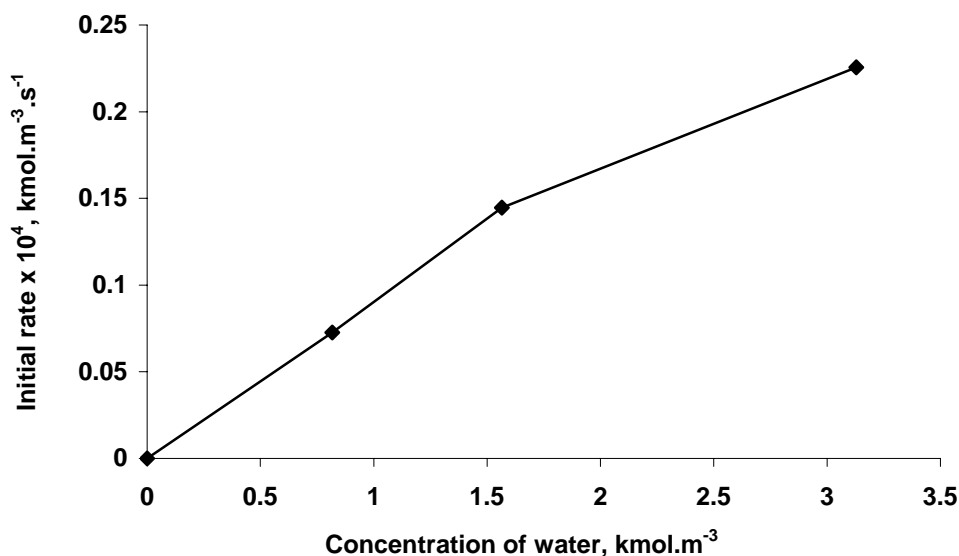


Figure 4.9: Effect of concentration of water on initial rate of carbonylation

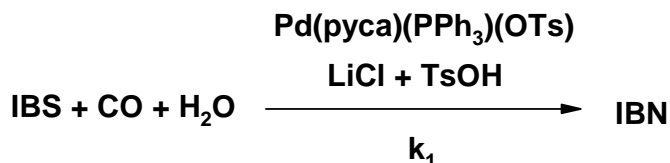
Reaction conditions: IBS: $0.625 \text{ kmol.m}^{-3}$; Pd(pyca)(PPh₃)(OTs): $1.1 \times 10^{-3} \text{ kmol.m}^{-3}$; TsOH/LiCl (1:1): $0.116 \text{ kmol.m}^{-3}$; H₂O: 1.56 kmol.m^{-3} ; P_{CO}: 5.4 MPa ; Solvent: MEK; 9.5 kmol.m^{-3} ; Temp: 388 K , Agitation: 15 Hz , Total volume: $2.5 \times 10^{-5} \text{ m}^3$

The Figure 4.6 presents the variation of the initial rate of carbonylation with the catalyst concentration. It shows that the reaction rate increases almost linearly with respect to the concentration of the catalyst indicating a first order with respect to

the catalyst concentration. The reaction was found to be second order with respect to CO concentration as obtained from the slope of the logarithmic plot of rate vs. concentration of CO in the liquid phase. Figure 4.8 presents the variation of initial rates with respect to the concentration of the promoters (TsOH and LiCl in 1:1 ratio). For this case also the order was calculated from the logarithmic plot of rate vs. concentration respectively and the order of reaction was found to be 0.5 with respect to the promoter concentration. The necessity of the promoters has already been described previously with a mutual ratio of 1:1 giving the best performance.³ Figure 4.9 presents the variation of the initial rates with respect to the concentration of added water in the reaction mixture. The rate seemed to vary almost linearly and hence the order of reaction was considered unity with respect to water concentration.

4.3.3.2 Kinetic Modeling

Based on the observed trends on the rates of carbonylation of IBS with different parameters using the homogeneous Pd(pyca)(PPh₃)(OTs) complex as catalyst, scheme as in Scheme 4.2



Scheme 4.2: Carbonylation of IBS using a homogeneous Pd-complex catalyst

The following empirical form of rate equation was proposed based on the initial rate data:

$$r_A = \frac{k_1 [\text{IBS}] [\text{Catalyst}] [\text{Promoter}]^{0.5} [\text{H}_2\text{O}] [\text{CO}]^2}{1 + K_2 [\text{IBS}]} \quad (4.3)$$

Considering the excellent mass balance obtained from the GC data, for the reactant (IBS) and the product (IBN), in the kinetic regime in a batch reactor under isothermal conditions, the following mass balance equations may be written, since no other product is formed

$$r_A = -\frac{d[\text{IBS}]}{dt} = \frac{d[\text{IBN}]}{dt} \quad (4.4)$$

Applying initial conditions, i.e. at $t=0$, $[\text{IBS}] = [\text{IBS}]_0$, and $[\text{IBN}] = 0$, where $[\text{IBS}]$ is the initial concentration of IBS in the reaction mixture, and r_A is the rate of the reaction. The

equations 4.3 and 4.4 represent the variation of concentrations of reactant IBS and the product IBN as a function of time, expressed in terms of all the different parameters of the reaction. Different guess values of k_1 and K_2 were calculated from the experimental data in certain regions of the concentration – time profile of the reactions for the variation of different parameters and these were used to predict and generate the data for the concentration – time patterns for all the parametric variations. In order to optimize the rate parameters, a computer programme based on Marquart's method combined with Runge-Kutta method for solving differential equations was used. The simulated concentration-time profiles were compared to the experimental data. A comparison of the of the experimental data with the model predictions is shown in the following Figures 4.10 to 4.22 for a few parameters, though the predictions agreed for all the reaction parameters over the entire range of investigation.

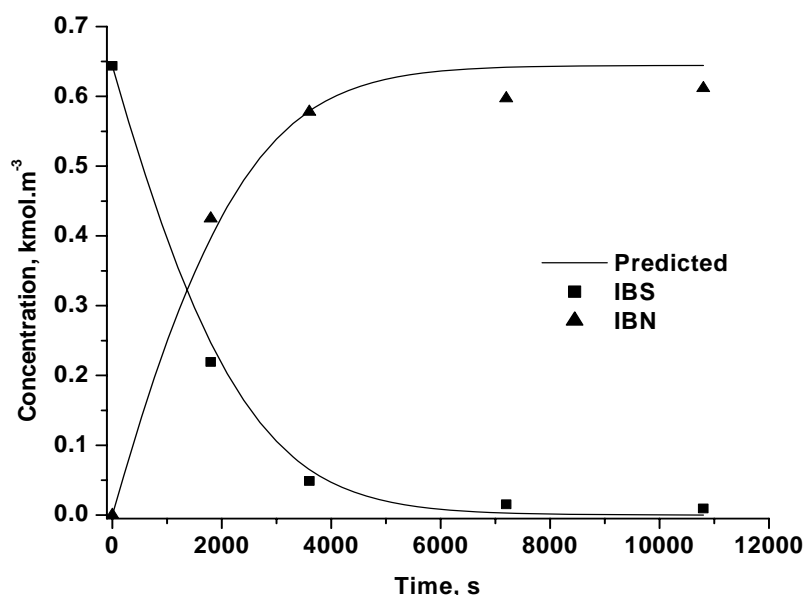


Figure 4.10: Standard carbonylation reaction at 388 K

Reaction conditions: IBS: $0.625 \text{ kmol.m}^{-3}$; $\text{Pd(pyca)}(\text{PPh}_3)(\text{OTs})$: $1.1 \times 10^{-3} \text{ kmol.m}^{-3}$; TsOH/LiCl (1:1): $0.116 \text{ kmol.m}^{-3}$; H_2O : 1.56 kmol.m^{-3} ; P_{CO} : 5.4 MPa ; Solvent: MEK; 9.5 kmol.m^{-3} ; Temp: 388 K , Agitation: 15 Hz , Total volume: $2.5 \times 10^{-5} \text{ m}^3$

The predicted curve matched with the experimental data points and therefore the model is appreciably good in predicting the concentration – time profiles for the variation of different reaction parameters within the range of investigation.

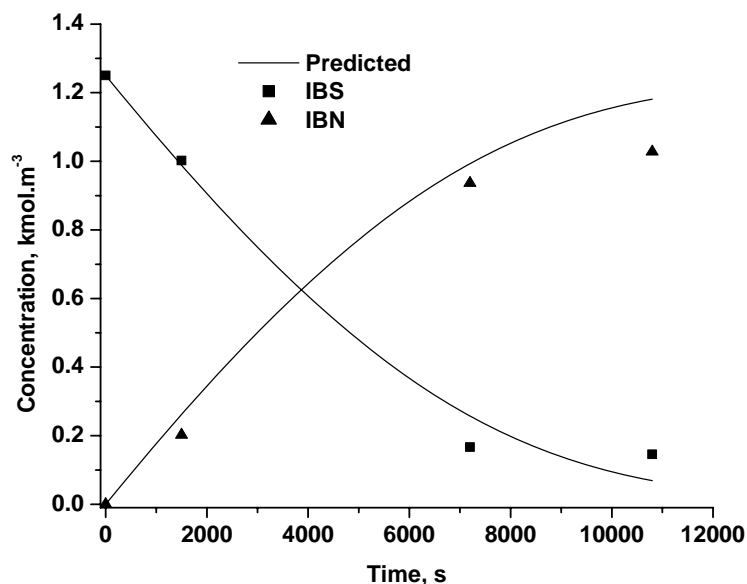


Figure 4.11: Effect of IBS concentration at 388 K

Reaction conditions: IBS: $1.2504 \text{ kmol.m}^{-3}$; $\text{Pd}(\text{pyca})(\text{PPh}_3)(\text{OTs})$: $1.1 \times 10^{-3} \text{ kmol.m}^{-3}$; TsOH/LiCl (1:1): $0.116 \text{ kmol.m}^{-3}$; H_2O : 1.56 kmol.m^{-3} ; P_{CO} : 5.4 MPa; Solvent: MEK; 9.5 kmol.m^{-3} ; Temp: 388 K, Agitation: 15 Hz, Total volume: $2.5 \times 10^{-5} \text{ m}^3$

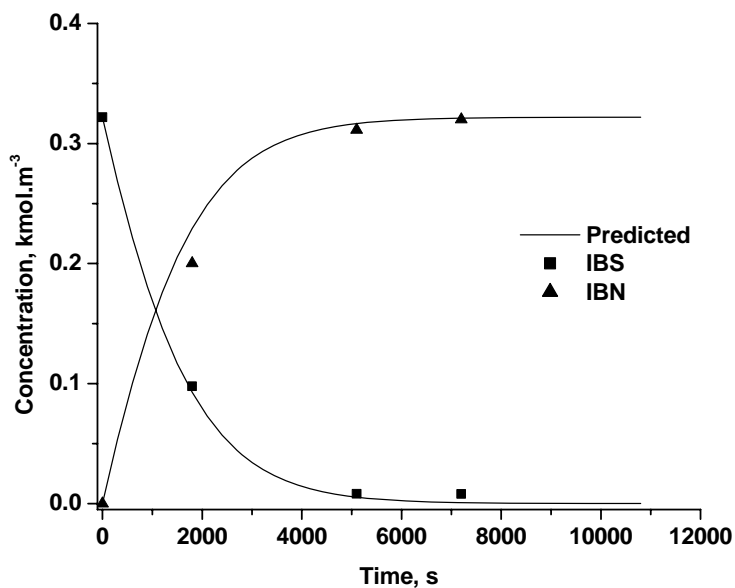


Figure 4.12: Effect of IBS concentration at 388 K

Reaction conditions: IBS: $0.322 \text{ kmol.m}^{-3}$; $\text{Pd}(\text{pyca})(\text{PPh}_3)(\text{OTs})$: $1.1 \times 10^{-3} \text{ kmol.m}^{-3}$; TsOH/LiCl (1:1): $0.116 \text{ kmol.m}^{-3}$; H_2O : 1.56 kmol.m^{-3} ; P_{CO} : 5.4 MPa; Solvent: MEK; 9.5 kmol.m^{-3} ; Temp: 388 K, Agitation: 15 Hz, Total volume: $2.5 \times 10^{-5} \text{ m}^3$

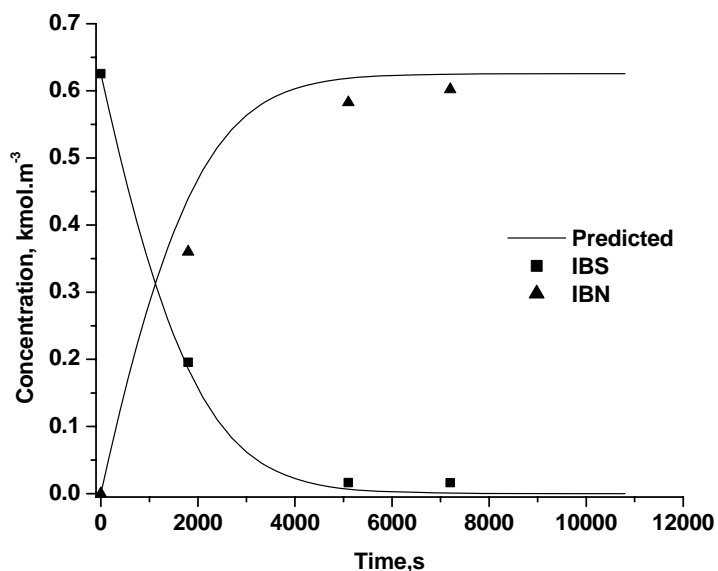


Figure 4.13: Effect of catalyst concentration at 388 K

Reaction conditions: IBS: $0.6255 \text{ kmol.m}^{-3}$; Pd(pyca)(PPh₃)(OTs): $2.2 \times 10^{-3} \text{ kmol.m}^{-3}$; TsOH/LiCl (1:1): $0.116 \text{ kmol.m}^{-3}$; H₂O: 1.56 kmol.m^{-3} ; P_{CO}: 5.4 MPa; Solvent: MEK; 9.5 kmol.m^{-3} ; Temp: 388 K, Agitation: 15 Hz, Total volume: $2.5 \times 10^{-5} \text{ m}^3$

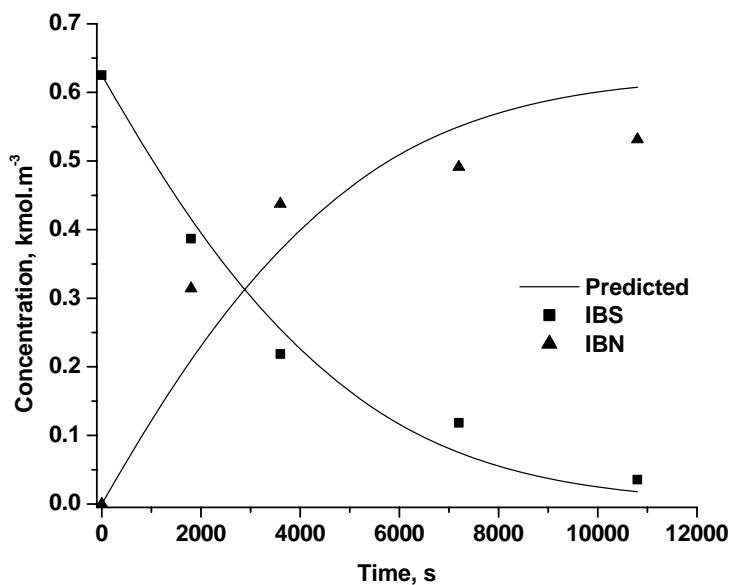


Figure 4.14: Effect of promoter concentration at 388 K

Reaction conditions: IBS: $0.6253 \text{ kmol.m}^{-3}$; Pd(pyca)(PPh₃)(OTs): $1.1 \times 10^{-3} \text{ kmol.m}^{-3}$; TsOH/LiCl (1:1): $0.02796 \text{ kmol.m}^{-3}$; H₂O: 1.56 kmol.m^{-3} ; P_{CO}: 5.4 MPa; Solvent: MEK; 9.5 kmol.m^{-3} ; Temp: 388 K, Agitation: 15 Hz, Total volume: $2.5 \times 10^{-5} \text{ m}^3$

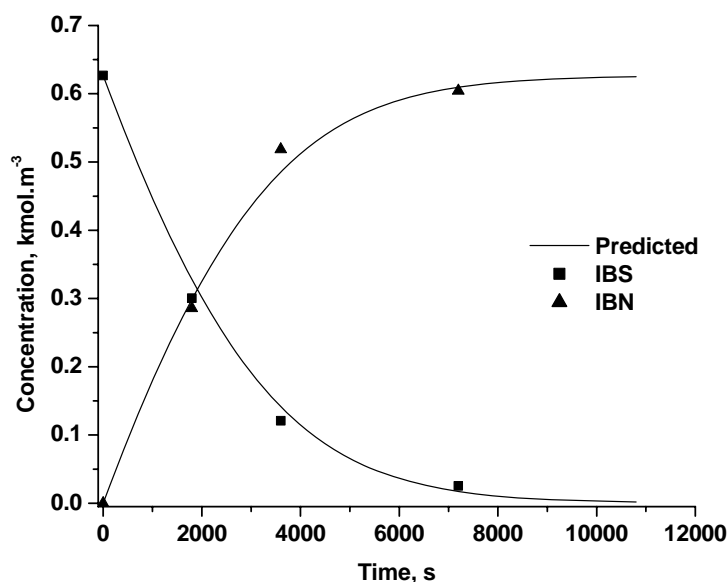


Figure 4.15: Effect of promoter concentration at 388 K

Reaction conditions: IBS: $0.6267 \text{ kmol.m}^{-3}$; $\text{Pd}(\text{pyca})(\text{PPh}_3)(\text{OTs})$: $1.1 \times 10^{-3} \text{ kmol.m}^{-3}$; TsOH/LiCl (1:1): $0.0578 \text{ kmol.m}^{-3}$; H_2O : 1.56 kmol.m^{-3} ; P_{CO} : 5.4 MPa; Solvent: MEK; 9.5 kmol.m^{-3} ; Temp: 388 K, Agitation: 15 Hz, Total volume: $2.5 \times 10^{-5} \text{ m}^3$

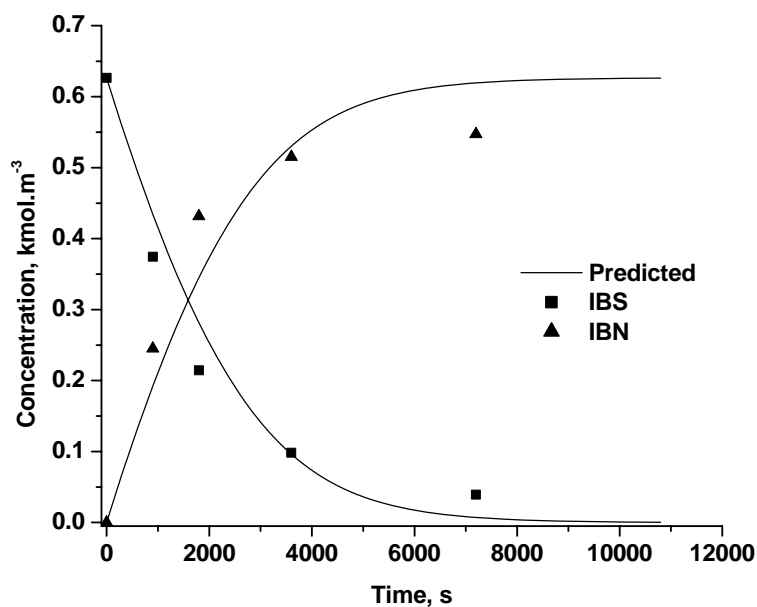


Figure 4.16: Effect of promoter concentration at 388 K

Reaction conditions: IBS: $0.6265 \text{ kmol.m}^{-3}$; $\text{Pd}(\text{pyca})(\text{PPh}_3)(\text{OTs})$: $1.1 \times 10^{-3} \text{ kmol.m}^{-3}$; TsOH/LiCl (1:1): $0.2312 \text{ kmol.m}^{-3}$; H_2O : 1.56 kmol.m^{-3} ; P_{CO} : 5.4 MPa; Solvent: MEK; 9.5 kmol.m^{-3} ; Temp: 388 K, Agitation: 15 Hz, Total volume: $2.5 \times 10^{-5} \text{ m}^3$

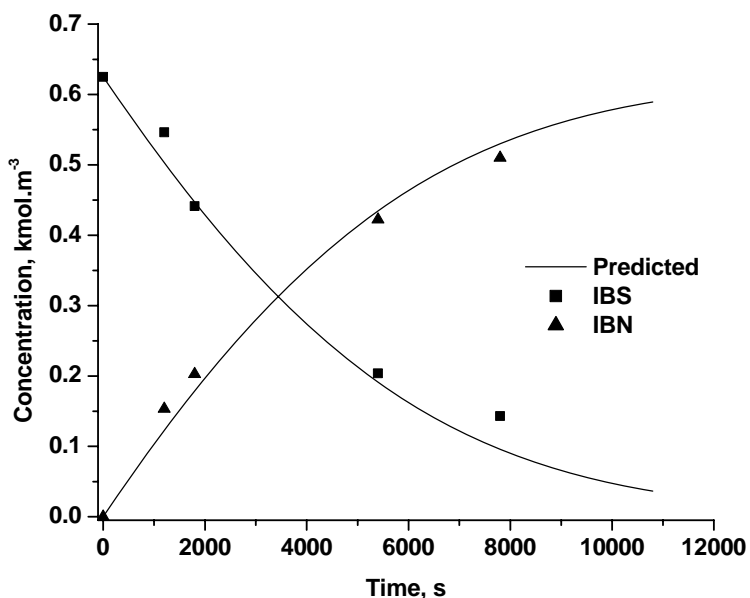


Figure 4.17: Effect of H₂O concentration at 388 K

Reaction conditions: IBS: $0.625 \text{ kmol.m}^{-3}$; Pd(pyca)(PPh₃)(OTs): $1.1 \times 10^{-3} \text{ kmol.m}^{-3}$; TsOH/LiCl (1:1): $0.1156 \text{ kmol.m}^{-3}$; H₂O: $0.8178 \text{ kmol.m}^{-3}$; P_{CO}: 5.4 MPa; Solvent: MEK; 9.5 kmol.m^{-3} ; Temp: 388 K, Agitation: 15 Hz, Total volume: $2.5 \times 10^{-5} \text{ m}^3$

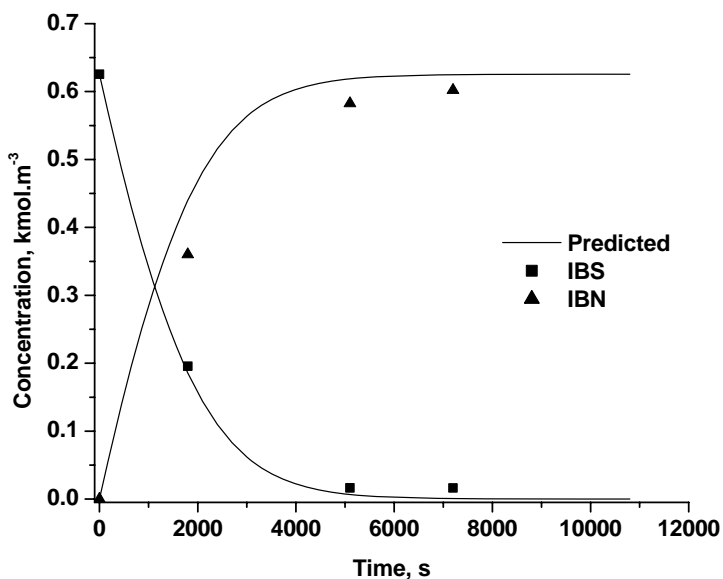


Figure 4.18: Effect of H₂O concentration at 388 K

Reaction conditions: IBS: $0.6255 \text{ kmol.m}^{-3}$; Pd(pyca)(PPh₃)(OTs): $1.1 \times 10^{-3} \text{ kmol.m}^{-3}$; TsOH/LiCl (1:1): $0.1156 \text{ kmol.m}^{-3}$; H₂O: $3.1288 \text{ kmol.m}^{-3}$; P_{CO}: 5.4 MPa; Solvent: MEK; 9.5 kmol.m^{-3} ; Temp: 388 K, Agitation: 15 Hz, Total volume: $2.5 \times 10^{-5} \text{ m}^3$

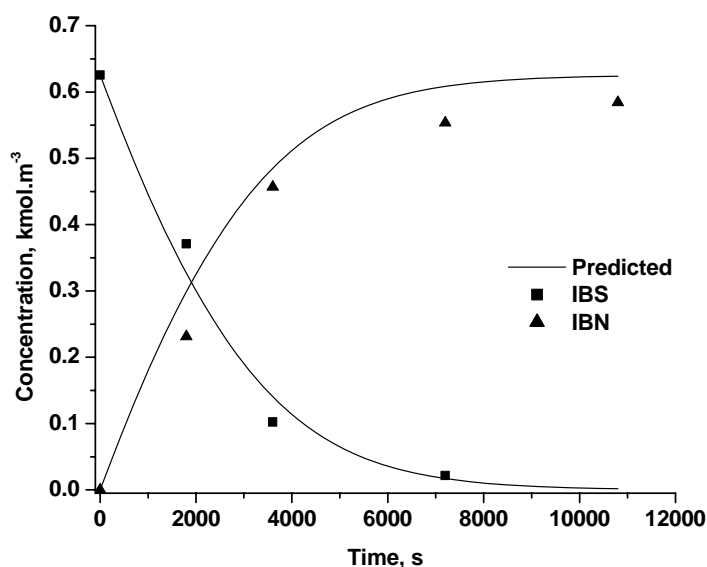


Figure 4.19: Effect of CO partial pressure at 388 K

Reaction conditions: IBS: $0.6256 \text{ kmol.m}^{-3}$; $\text{Pd}(\text{pyca})(\text{PPh}_3)(\text{OTs})$: $1.1 \times 10^{-3} \text{ kmol.m}^{-3}$; TsOH/LiCl (1:1): $0.1156 \text{ kmol.m}^{-3}$; H_2O : $1.5644 \text{ kmol.m}^{-3}$; P_{CO} : 4.08 MPa; Solvent: MEK; 9.5 kmol.m^{-3} ; Temp: 388 K, Agitation: 15 Hz, Total volume: $2.5 \times 10^{-5} \text{ m}^3$

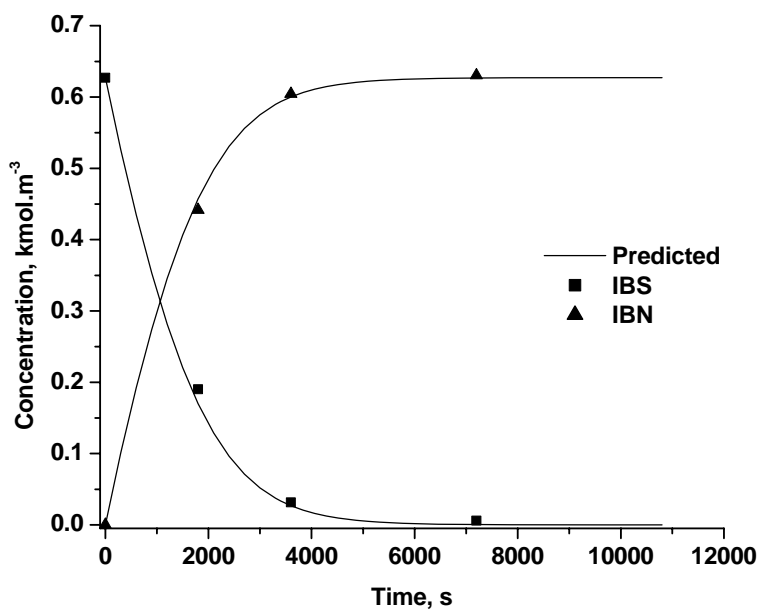


Figure 4.20: Effect of CO partial pressure at 388 K

Reaction conditions: IBS: $0.6271 \text{ kmol.m}^{-3}$; $\text{Pd}(\text{pyca})(\text{PPh}_3)(\text{OTs})$: $1.1 \times 10^{-3} \text{ kmol.m}^{-3}$; TsOH/LiCl (1:1): $0.1156 \text{ kmol.m}^{-3}$; H_2O : $1.5644 \text{ kmol.m}^{-3}$; P_{CO} : 6.80 MPa; Solvent: MEK; 9.5 kmol.m^{-3} ; Temp: 388 K, Agitation: 15 Hz, Total volume: $2.5 \times 10^{-5} \text{ m}^3$

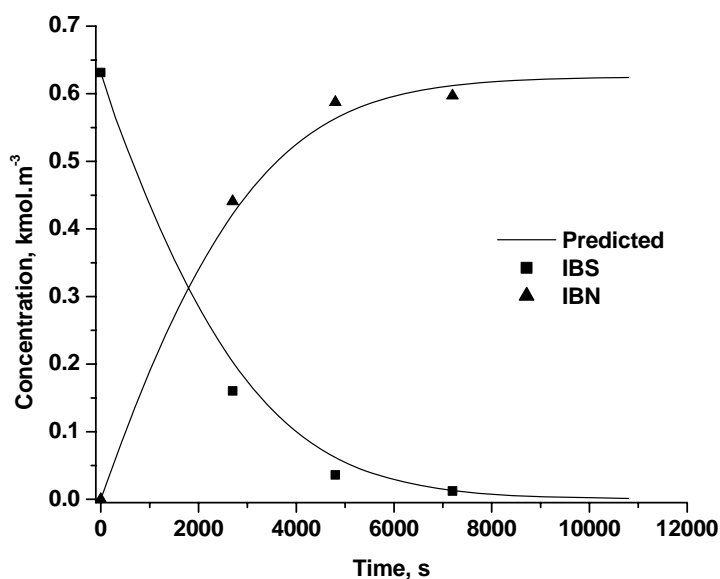


Figure 4.21: Standard carbonylation reaction at 378 K

Reaction conditions: IBS: $0.6252 \text{ kmol.m}^{-3}$; $\text{Pd}(\text{pyca})(\text{PPh}_3)(\text{OTs})$: $1.1 \times 10^{-3} \text{ kmol.m}^{-3}$; TsOH/LiCl (1:1): $0.1156 \text{ kmol.m}^{-3}$; H_2O : $1.5644 \text{ kmol.m}^{-3}$; P_{CO} : 5.4 MPa; Solvent: MEK; 9.5 kmol.m^{-3} ; Temp: 378 K, Agitation: 15 Hz, Total volume: $2.5 \times 10^{-5} \text{ m}^3$

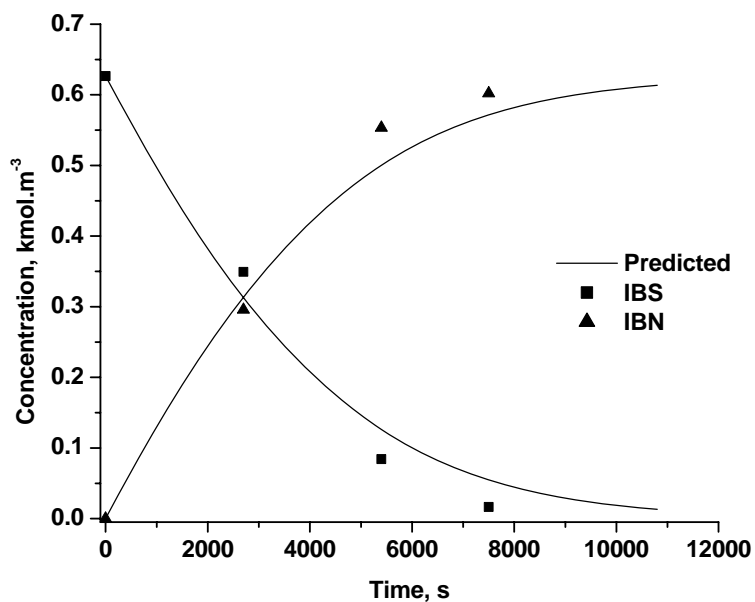


Figure 4.22: Standard carbonylation reaction at 368 K

Reaction conditions: IBS: $0.6265 \text{ kmol.m}^{-3}$; $\text{Pd}(\text{pyca})(\text{PPh}_3)(\text{OTs})$: $1.1 \times 10^{-3} \text{ kmol.m}^{-3}$; TsOH/LiCl (1:1): $0.1156 \text{ kmol.m}^{-3}$; H_2O : $1.5644 \text{ kmol.m}^{-3}$; P_{CO} : 5.4 MPa; Solvent: MEK; 9.5 kmol.m^{-3} ; Temp: 368 K, Agitation: 15 Hz, Total volume: $2.5 \times 10^{-5} \text{ m}^3$

The empirical model predicts the concentration–time profiles very efficiently for all the parametric variations. The temperature was found to have distinct effect on the rate of the carbonylation reaction. From the slope of the Arrhenius plot of the logarithm of k_1 vs $1/T$ (Figure 4.23), the activation energy of the reaction was calculated to be 43.02 $\text{kJ}\cdot\text{mol}^{-1}$.

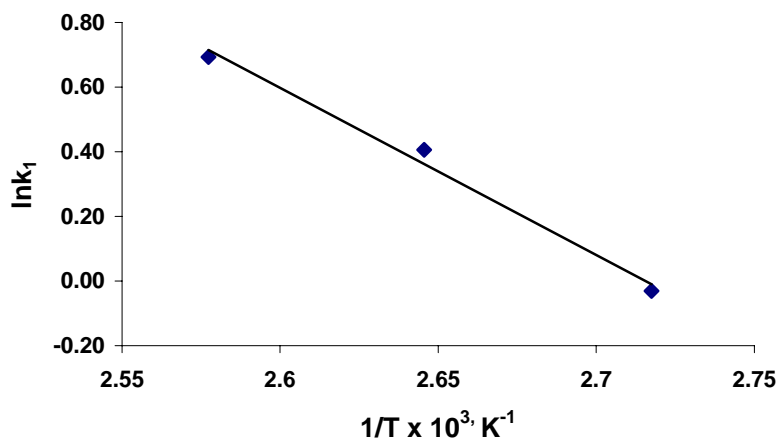


Figure 4.23: Arrhenius plot: Temperature dependence of rate constant k_1

Key observations

Even though the empirical model predicted the concentration – time profiles of the carbonylation of IBS using homogeneous Pd-complex catalyst a few important observations need mentioning.

1. Oligomerization of the olefin substrate was observed for some reactions which proceeded for longer reaction time, as the substituted styrenes are prone to oligomerization in presence of acid at high temperatures
2. Predictions were less matching to the experimental data for such cases, and also for very high substrate concentrations.

4.3.4 Kinetics of Carbonylation of IBS using Ossified Pd-complex Catalyst

4.3.4.1 Initial Rate Data

For the heterogeneous catalyzed carbonylation reaction, the initial rates were calculated for the initial period of 15 minutes from the CO-absorption data of the reactions and the empirical orders of dependence of the rates on the different reaction

parameters were calculated. The results of the variation of initial rates with different parameters are presented in the Figures 4.24 to 4.29.

Figure 4.24 represents the variation of the initial rate with the change in the substrate concentration. Here also in analogy to the homogeneous catalytic reaction, the reaction rate decreased non-linearly with the increase in the IBS concentration. Such an observation indicates substrate –inhibited kinetics. The variation of the initial rate with catalyst concentration (loading) is presented in Figure 4.25. The reaction rate increases almost linearly with respect to the catalyst concentration and hence the order of the reaction may be considered unity with respect to catalyst loading. The dependence of the initial rate of carbonylation on CO concentration is presented in Figure 4.26. The approximate order of the reaction with respect to CO-concentration was obtained as the slope of the logarithmic plot, to be three. Similar exercise was done for the promoter and water concentrations and the respective orders were calculated to be –0.1 and 0.88 respectively. The variations are presented in Figures 4.27 and 4.28 respectively. Triphenyl phosphine, PPh_3 played an important role in the heterogeneously catalyzed carbonylation, but there was no variation in initial rate with respect to its concentration, as in Figure 4.29. The order with respect to PPh_3 concentration was considered zero.

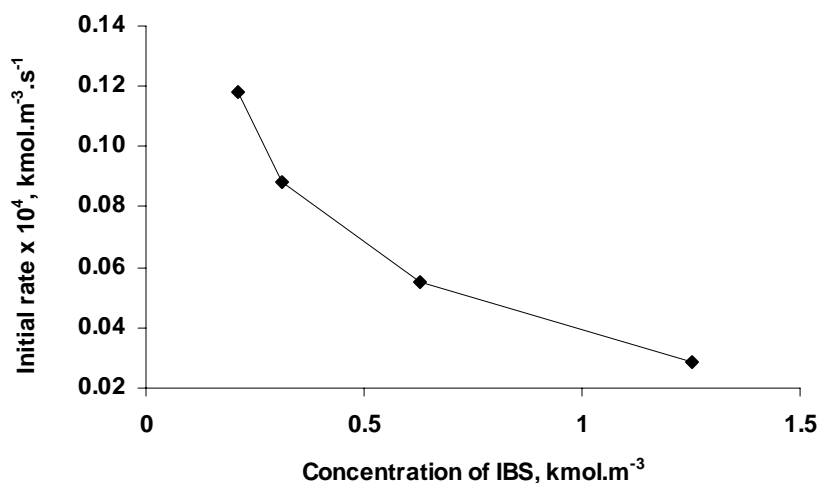


Figure 4.24: Effect of concentration of IBS on rate of carbonylation

Reaction conditions: Catalyst 1A: 0.1×10^{-3} kg; TsOH/LiCl (1:1): $0.1175 \text{ kmol.m}^{-3}$; H_2O : 1.6 kmol.m^{-3} ; PPh_3 : $3.8 \times 10^{-3} \text{ kmol.m}^{-3}$; P_{CO} : 5.4 MPa; Solvent: MEK; 9.5 kmol.m^{-3} ; Temp: 388 K, Agitation: 16.67 Hz; Total volume: $2.5 \times 10^{-5} \text{ m}^3$

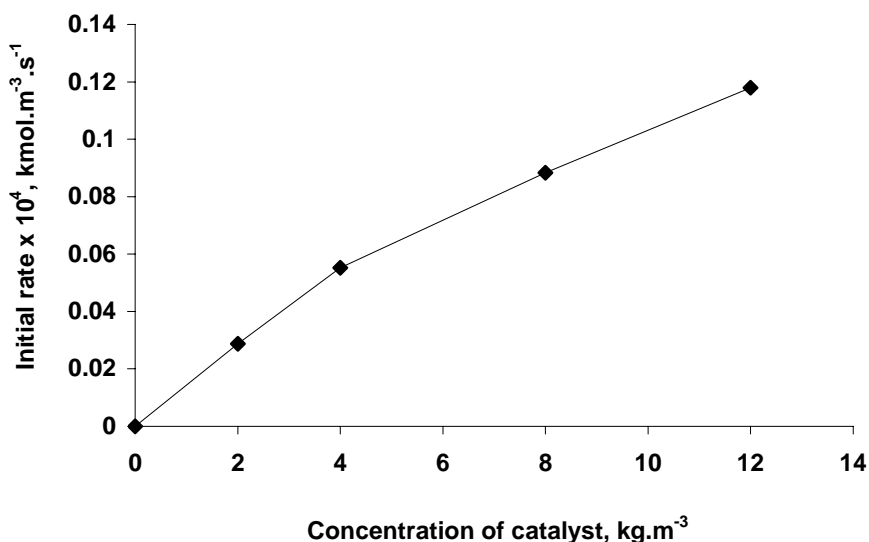


Figure 4.25: Effect of concentration of catalyst on initial rate of carbonylation

Reaction conditions: IBS: $0.625 \text{ kmol.m}^{-3}$; TsOH/LiCl (1:1): $0.1175 \text{ kmol.m}^{-3}$; H_2O : 1.6 kmol.m^{-3} ; PPh_3 : $3.8 \times 10^{-3} \text{ kmol.m}^{-3}$; P_{CO} : 5.4 MPa ; Solvent: MEK; 9.5 kmol.m^{-3} ; Temp: 388 K , Agitation: 16.67 Hz ; Total volume: $2.5 \times 10^{-5} \text{ m}^3$

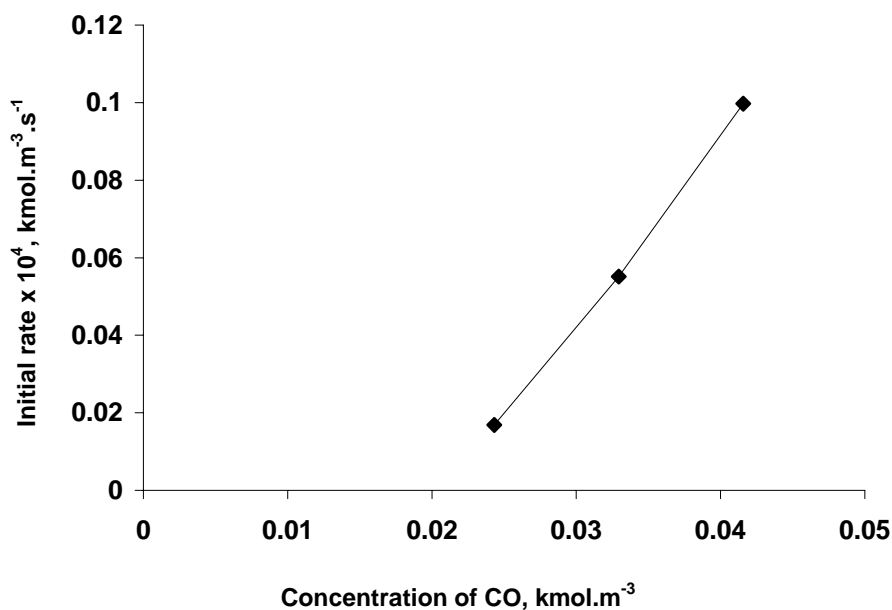


Figure 4.26: Effect of concentration of CO on initial rate of carbonylation

Reaction conditions: IBS: $0.625 \text{ kmol.m}^{-3}$; Catalyst 1A: $0.1 \times 10^{-3} \text{ kg}$; TsOH/LiCl (1:1): $0.1175 \text{ kmol.m}^{-3}$; H_2O : 1.6 kmol.m^{-3} ; PPh_3 : $3.8 \times 10^{-3} \text{ kmol.m}^{-3}$; Solvent: MEK; 9.5 kmol.m^{-3} ; Temp: 388 K , Agitation: 16.67 Hz ; Total volume: $2.5 \times 10^{-5} \text{ m}^3$

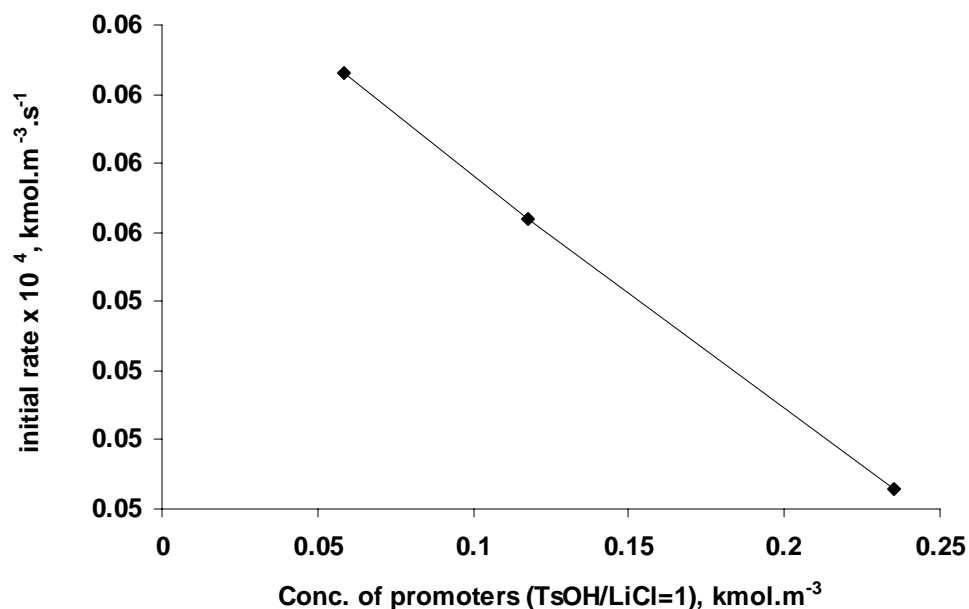


Figure 4.27: Effect of concentration of promoters on initial rate of carbonylation

Reaction conditions: IBS: $0.625 \text{ kmol.m}^{-3}$; Catalyst 1A: $0.1 \times 10^{-3} \text{ kg}$; H_2O : 1.6 kmol.m^{-3} ; PPh_3 : $3.8 \times 10^{-3} \text{ kmol.m}^{-3}$; P_{CO} : 5.4 MPa ; Solvent: MEK; 9.5 kmol.m^{-3} ; Temp: 388 K ; Agitation: 16.67 Hz ; Total volume: $2.5 \times 10^{-5} \text{ m}^3$

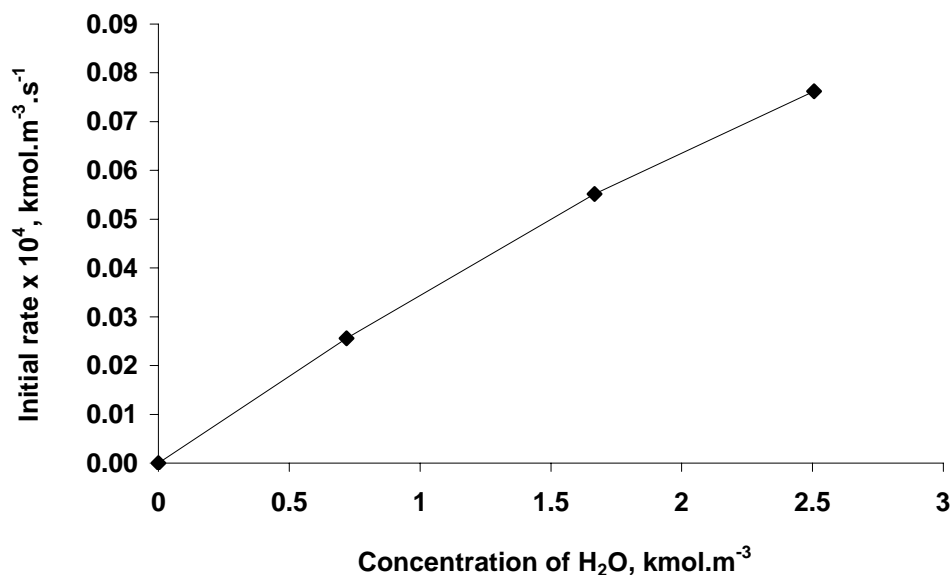


Figure 4.28: Effect of concentration of water on initial rate of carbonylation

Reaction conditions: IBS: $0.625 \text{ kmol.m}^{-3}$; Catalyst 1A: $0.1 \times 10^{-3} \text{ kg}$; TsOH/LiCl (1:1): $0.1175 \text{ kmol.m}^{-3}$; PPh_3 : $3.8 \times 10^{-3} \text{ kmol.m}^{-3}$; P_{CO} : 5.4 MPa ; Solvent: MEK; 9.5 kmol.m^{-3} ; Temp: 388 K ; Agitation: 16.67 Hz ; Total volume: $2.5 \times 10^{-5} \text{ m}^3$

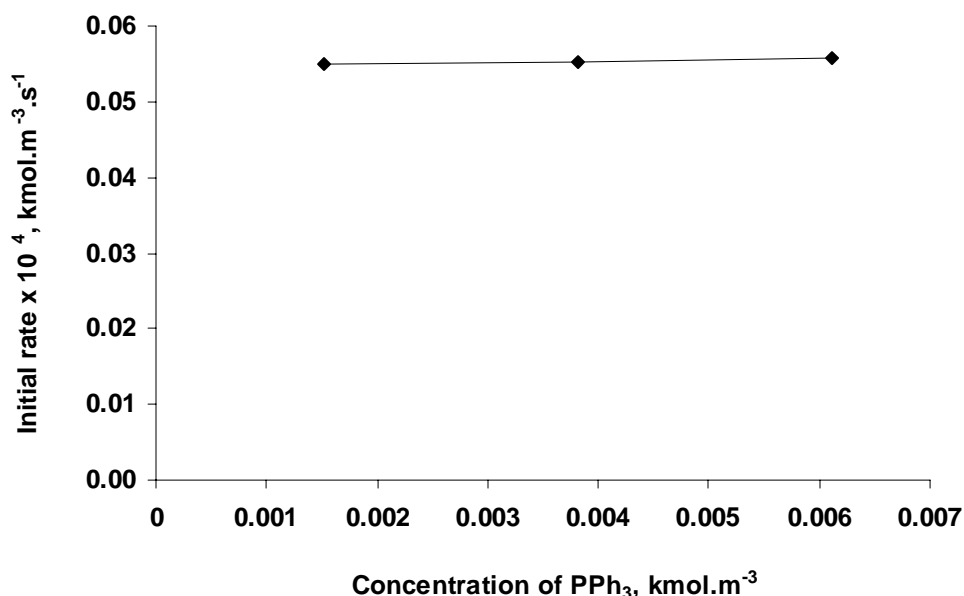


Figure 4.29: Effect of concentration of PPh₃ on initial rate of carbonylation

Reaction conditions: IBS: 0.625 kmol.m⁻³; Catalyst 1A: 0.1×10⁻³ kg; TsOH/LiCl (1:1): 0.1175 kmol.m⁻³; H₂O: 1.6 kmol.m⁻³; PPh₃: 3.8×10⁻³ kmol.m⁻³; P_{CO}: 5.4 MPa; Solvent: MEK; 9.5 kmol.m⁻³; Temp: 388 K, Agitation: 16.67 Hz; Total volume: 2.5×10⁻⁵ m³

4.3.4.2 Kinetic Modeling

Carbonylation reaction using the heterogeneous ossified Pd(pyca)(TPPTS) complex (Catalyst 1A) were performed using the similar substrate charge. Moreover, since the pattern of variation of the average initial rates of carbonylation were similar to that of the homogeneously catalyzed reaction, a similar empirical rate model was chosen. The orders of the reaction with respect to the respective reaction parameters based on the initial rate data were inserted in the rate equation, which may be represented as follows,

$$r_B = \frac{k_3 [\text{IBS}] [\text{Catalyst}] [\text{Pr omoter}]^{-0.1} [\text{H}_2\text{O}]^{0.88} [\text{CO}]^3}{1 + K_4 [\text{IBS}]} \quad (4.5)$$

Following the similar logic as that for the homogeneously catalyzed reaction, the rate of the heterogeneous reaction, r_B may be represented in the same manner as.

$$r_B = -\frac{d[\text{IBS}]}{dt} = \frac{d[\text{IBN}]}{dt} \quad (4.6)$$

Solving the equations using the experimental values gave the guess values of the rate parameter, which was similarly treated using the optimization method to generate the

theoretical concentration – time profiles. These were then matched with the experimental data. The following graphs (Figure 4.30 to 4.44) represent the fitting of the experimental data using the simulated concentration – time profile.

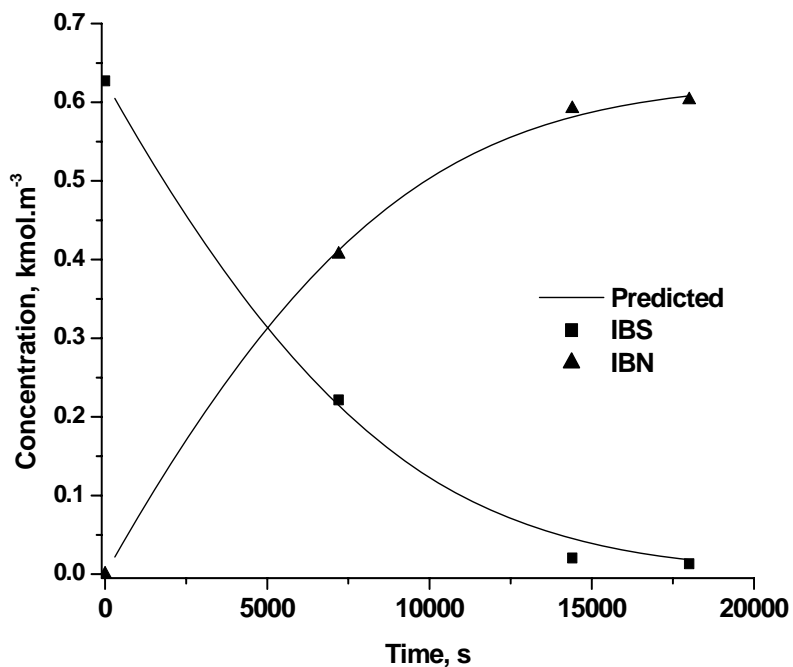


Figure 4.30: Standard carbonylation reaction at 388 K

Reaction conditions: IBS: $0.625 \text{ kmol.m}^{-3}$; Catalyst 1A: $0.1 \times 10^{-3} \text{ kg}$; TsOH/LiCl (1:1): $0.1175 \text{ kmol.m}^{-3}$; H₂O: 1.6 kmol.m^{-3} ; PPh₃: $3.8 \times 10^{-3} \text{ kmol.m}^{-3}$; P_{CO}: 5.4 MPa; Solvent: MEK; 9.5 kmol.m^{-3} ; Temp: 388 K, Agitation: 16.67 Hz; Total volume: $2.5 \times 10^{-5} \text{ m}^3$

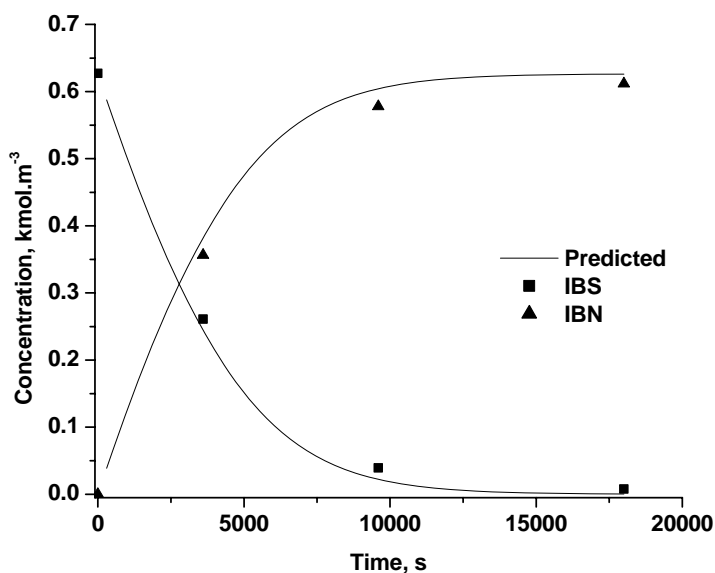


Figure 4.31: Effect of catalyst loading at 388 K

Reaction conditions: IBS: $0.625 \text{ kmol.m}^{-3}$; Catalyst 1A: $0.2 \times 10^{-3} \text{ kg}$; TsOH/LiCl (1:1): $0.1175 \text{ kmol.m}^{-3}$; H_2O : 1.6 kmol.m^{-3} ; PPh_3 : $3.8 \times 10^{-3} \text{ kmol.m}^{-3}$; P_{CO} : 5.4 MPa ; Solvent: MEK; 9.5 kmol.m^{-3} ; Temp: 388 K , Agitation: 16.67 Hz ; Total volume: $2.5 \times 10^{-5} \text{ m}^3$

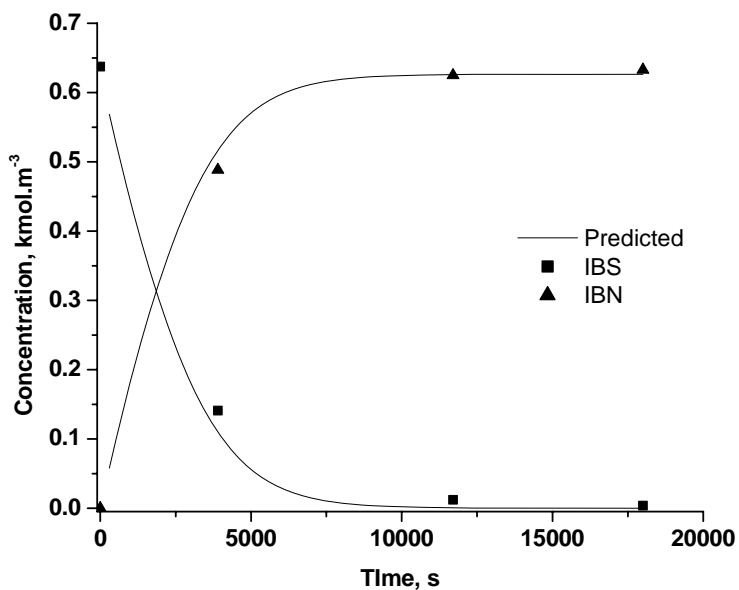


Figure 4.32: Effect of catalyst loading at 388 K

Reaction conditions: IBS: $0.625 \text{ kmol.m}^{-3}$; Catalyst 1A: $0.3 \times 10^{-3} \text{ kg}$; TsOH/LiCl (1:1): $0.1175 \text{ kmol.m}^{-3}$; H_2O : 1.6 kmol.m^{-3} ; PPh_3 : $3.8 \times 10^{-3} \text{ kmol.m}^{-3}$; P_{CO} : 5.4 MPa ; Solvent: MEK; 9.5 kmol.m^{-3} ; Temp: 388 K , Agitation: 16.67 Hz ; Total volume: $2.5 \times 10^{-5} \text{ m}^3$

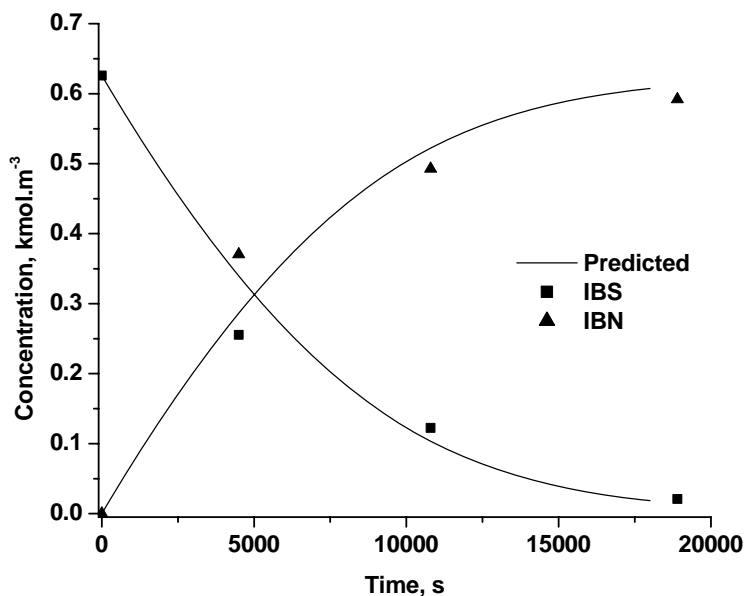


Figure 4.33: Effect of catalyst loading at 388 K

Reaction conditions: IBS: $0.625 \text{ kmol.m}^{-3}$; Catalyst 1A: $0.05 \times 10^{-3} \text{ kg}$; TsOH/LiCl (1:1): $0.1175 \text{ kmol.m}^{-3}$; H_2O : 1.6 kmol.m^{-3} ; PPh_3 : $3.8 \times 10^{-3} \text{ kmol.m}^{-3}$; P_{CO} : 5.4 MPa ; Solvent: MEK; 9.5 kmol.m^{-3} ; Temp: 388 K , Agitation: 16.67 Hz ; Total volume: $2.5 \times 10^{-5} \text{ m}^3$

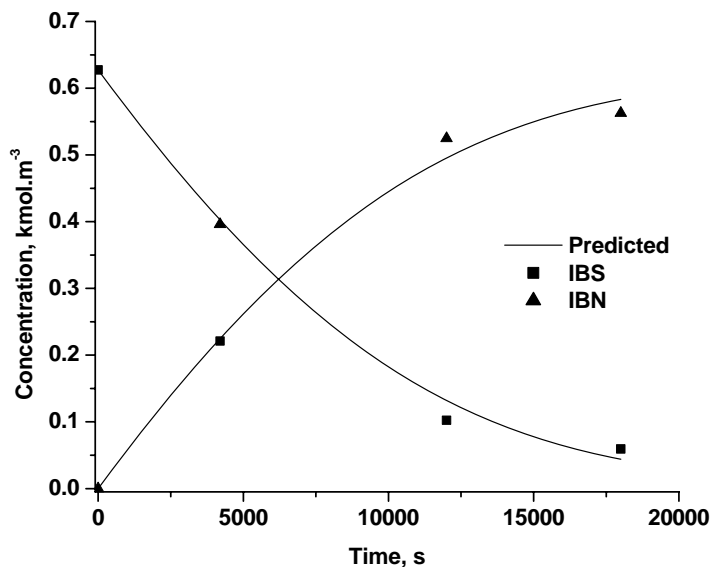


Figure 4.34: Effect of partial pressure of CO at 388 K

Reaction conditions: IBS: $0.625 \text{ kmol.m}^{-3}$; Catalyst 1A: $0.1 \times 10^{-3} \text{ kg}$; TsOH/LiCl (1:1): $0.1175 \text{ kmol.m}^{-3}$; H_2O : 1.6 kmol.m^{-3} ; PPh_3 : $3.8 \times 10^{-3} \text{ kmol.m}^{-3}$; P_{CO} : 4.08 MPa ; Solvent: MEK; 9.5 kmol.m^{-3} ; Temp: 388 K , Agitation: 16.67 Hz ; Total volume: $2.5 \times 10^{-5} \text{ m}^3$

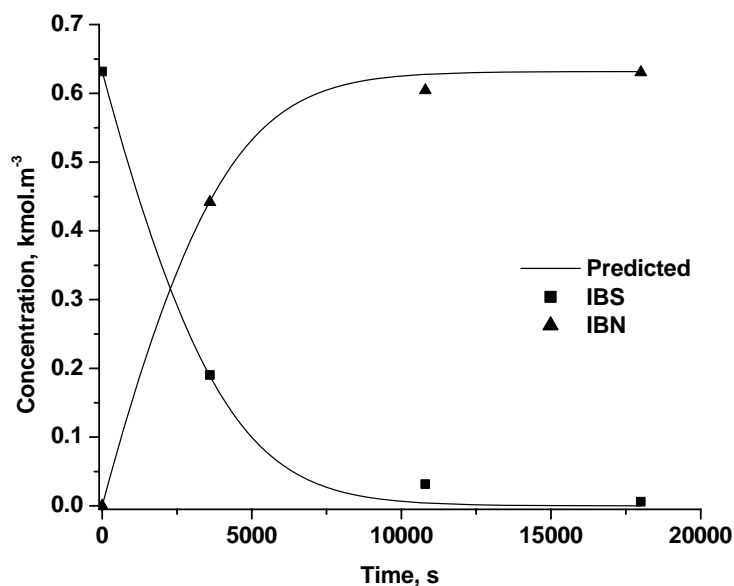


Figure 4.35: Effect of partial pressure of CO at 388 K

Reaction conditions: IBS: $0.625 \text{ kmol.m}^{-3}$; Catalyst 1A: $0.1 \times 10^{-3} \text{ kg}$; TsOH/LiCl (1:1): $0.1175 \text{ kmol.m}^{-3}$; H_2O : 1.6 kmol.m^{-3} ; PPh_3 : $3.8 \times 10^{-3} \text{ kmol.m}^{-3}$; P_{CO} : 6.8 MPa; Solvent: MEK; 9.5 kmol.m^{-3} ; Temp: 388 K, Agitation: 16.67 Hz; Total volume: $2.5 \times 10^{-5} \text{ m}^3$

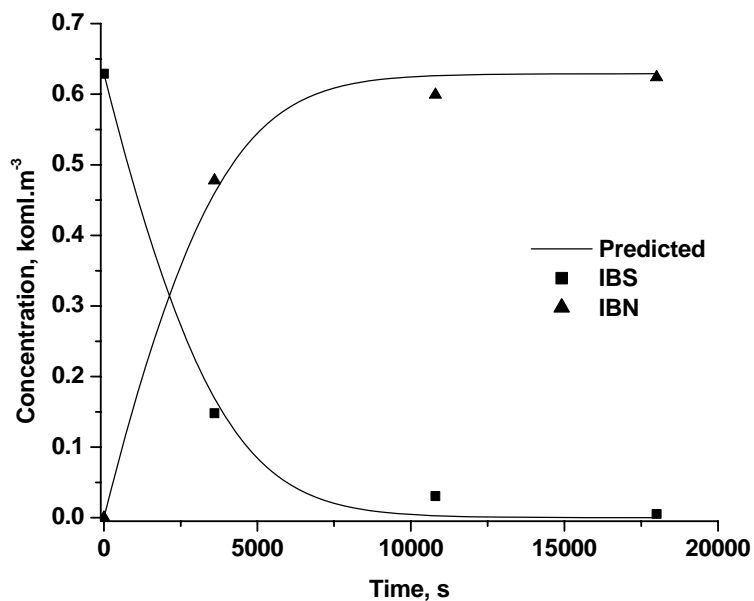


Figure 4.36: Effect of promoters at 388 K

Reaction conditions: IBS: $0.625 \text{ kmol.m}^{-3}$; Catalyst 1A: $0.1 \times 10^{-3} \text{ kg}$; TsOH/LiCl (1:1): $0.0587 \text{ kmol.m}^{-3}$; H_2O : 1.6 kmol.m^{-3} ; PPh_3 : $3.8 \times 10^{-3} \text{ kmol.m}^{-3}$; P_{CO} : 5.4 MPa; Solvent: MEK; 9.5 kmol.m^{-3} ; Temp: 388 K, Agitation: 16.67 Hz; Total volume: $2.5 \times 10^{-5} \text{ m}^3$

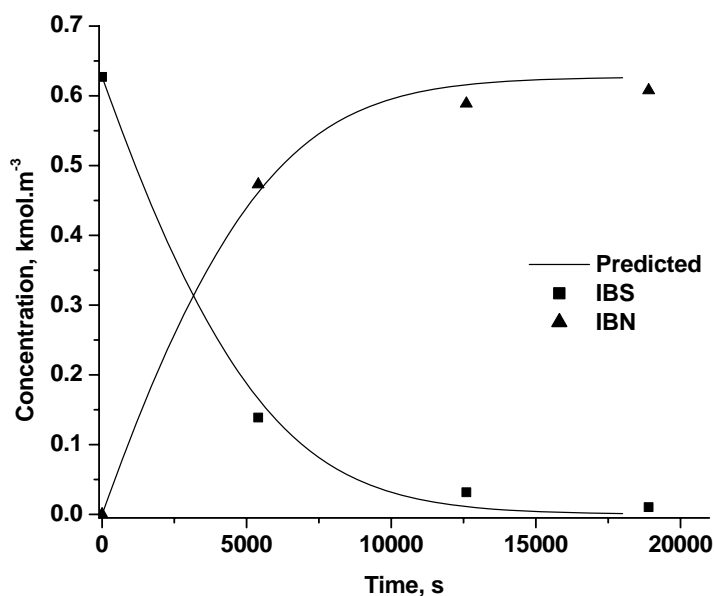


Figure 4.37: Effect of promoter concentration at 388 K

Reaction conditions: IBS: $0.625 \text{ kmol.m}^{-3}$; Catalyst 1A: $0.1 \times 10^{-3} \text{ kg}$; TsOH/LiCl (1:1): $0.2312 \text{ kmol.m}^{-3}$; H_2O : 1.6 kmol.m^{-3} ; PPh_3 : $3.8 \times 10^{-3} \text{ kmol.m}^{-3}$; P_{CO} : 5.4 MPa; Solvent: MEK; 9.5 kmol.m^{-3} ; Temp: 388 K, Agitation: 16.67 Hz; Total volume: $2.5 \times 10^{-5} \text{ m}^3$

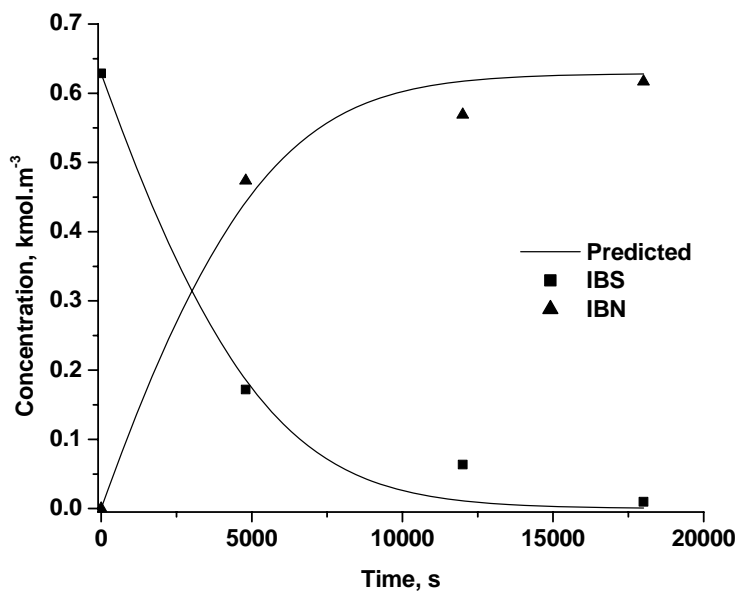


Figure 4.38: Effect of water concentration at 388 K

Reaction conditions: IBS: $0.625 \text{ kmol.m}^{-3}$; Catalyst 1A: $0.1 \times 10^{-3} \text{ kg}$; TsOH/LiCl (1:1): $0.1175 \text{ kmol.m}^{-3}$; H_2O : 2.5 kmol.m^{-3} ; PPh_3 : $3.8 \times 10^{-3} \text{ kmol.m}^{-3}$; P_{CO} : 5.4 MPa; Solvent: MEK; 9.5 kmol.m^{-3} ; Temp: 388 K, Agitation: 16.67 Hz; Total volume: $2.5 \times 10^{-5} \text{ m}^3$

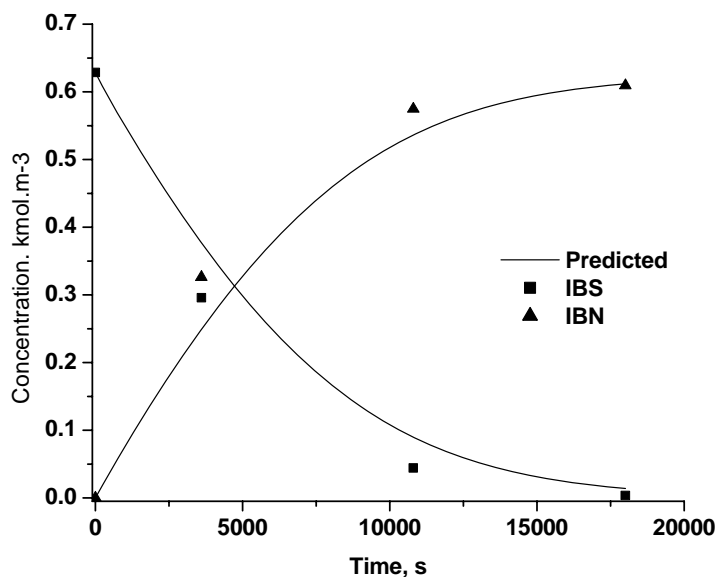


Figure 4.39: Effect of water concentration at 388 K

Reaction conditions: IBS: $0.625 \text{ kmol.m}^{-3}$; Catalyst 1A: $0.1 \times 10^{-3} \text{ kg}$; TsOH/LiCl (1:1): $0.1175 \text{ kmol.m}^{-3}$; H_2O : $0.719 \text{ kmol.m}^{-3}$; PPh_3 : $3.8 \times 10^{-3} \text{ kmol.m}^{-3}$; P_{CO} : 5.4 MPa ; Solvent: MEK; 9.5 kmol.m^{-3} ; Temp: 388 K , Agitation: 16.67 Hz ; Total volume: $2.5 \times 10^{-5} \text{ m}^3$

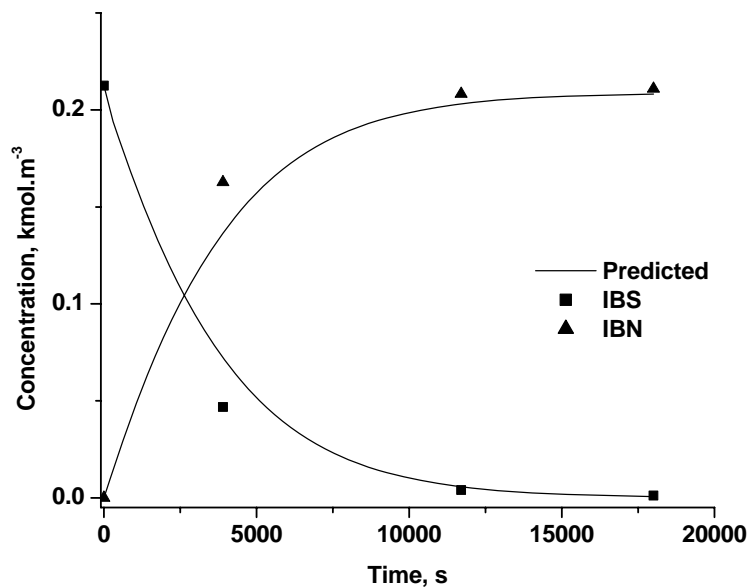


Figure 4.40: Effect of concentration of IBS at 388 K

Reaction conditions: IBS: $0.2088 \text{ kmol.m}^{-3}$; Catalyst 1A: $0.1 \times 10^{-3} \text{ kg}$; TsOH/LiCl (1:1): $0.1175 \text{ kmol.m}^{-3}$; H_2O : 1.6 kmol.m^{-3} ; PPh_3 : $3.8 \times 10^{-3} \text{ kmol.m}^{-3}$; P_{CO} : 5.4 MPa ; Solvent: MEK; 9.5 kmol.m^{-3} ; Temp: 388 K , Agitation: 16.67 Hz ; Total volume: $2.5 \times 10^{-5} \text{ m}^3$

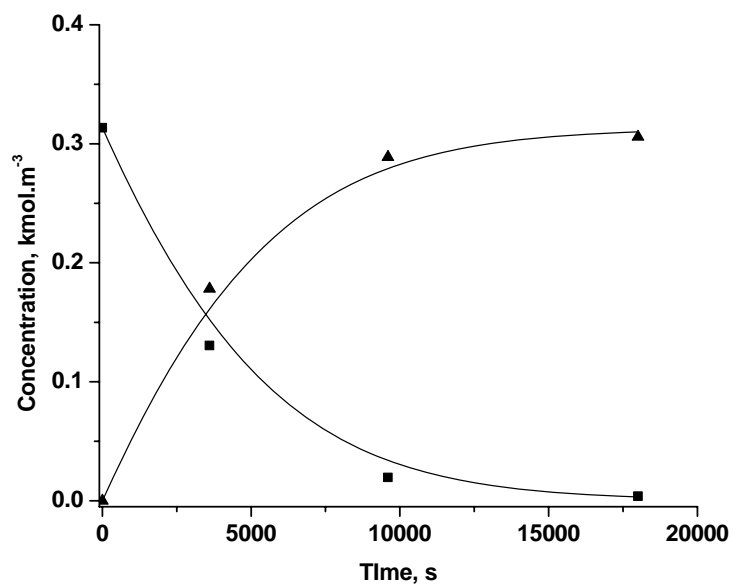


Figure 4.41: Effect of concentration of IBS at 388 K

Reaction conditions: IBS: $0.3132 \text{ kmol.m}^{-3}$; Catalyst 1A: $0.1 \times 10^{-3} \text{ kg}$; TsOH/LiCl (1:1): $0.1175 \text{ kmol.m}^{-3}$; H_2O : 1.6 kmol.m^{-3} ; PPh_3 : $3.8 \times 10^{-3} \text{ kmol.m}^{-3}$; P_{CO} : 5.4 MPa; Solvent: MEK; 9.5 kmol.m^{-3} ; Temp: 388 K, Agitation: 16.67 Hz; Total volume: $2.5 \times 10^{-5} \text{ m}^3$

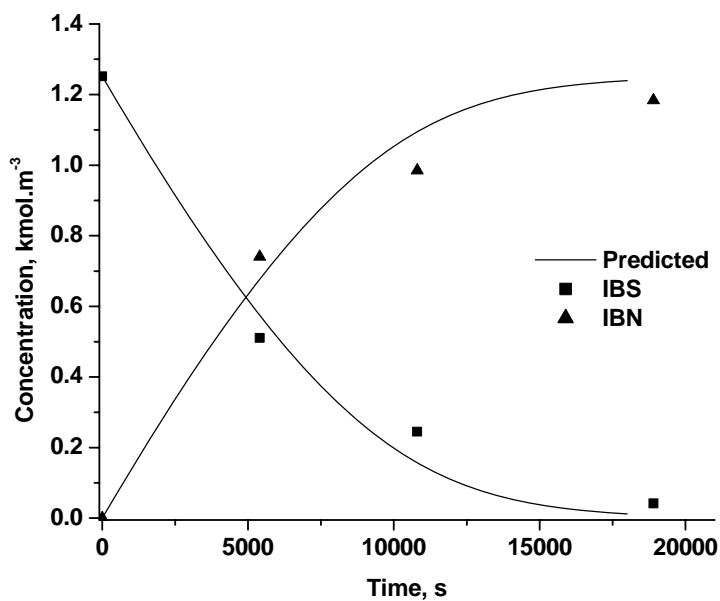


Figure 4.42: Effect of concentration of IBS at 388 K

Reaction conditions: IBS: $1.252 \text{ kmol.m}^{-3}$; Catalyst 1A: $0.1 \times 10^{-3} \text{ kg}$; TsOH/LiCl (1:1): $0.1175 \text{ kmol.m}^{-3}$; H_2O : 1.6 kmol.m^{-3} ; PPh_3 : $3.8 \times 10^{-3} \text{ kmol.m}^{-3}$; P_{CO} : 5.4 MPa; Solvent: MEK; 9.5 kmol.m^{-3} ; Temp: 388 K, Agitation: 16.67 Hz; Total volume: $2.5 \times 10^{-5} \text{ m}^3$

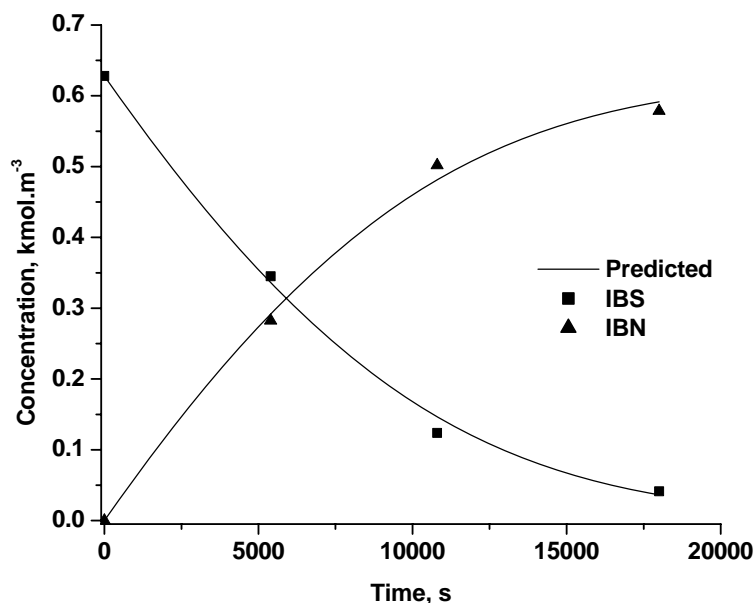


Figure 4.43: Standard reaction at 373 K

Reaction conditions: IBS: $0.625 \text{ kmol.m}^{-3}$; Catalyst 1A: $0.1 \times 10^{-3} \text{ kg}$; TsOH/LiCl (1:1): $0.1175 \text{ kmol.m}^{-3}$; H_2O : 1.6 kmol.m^{-3} ; PPh_3 : $3.8 \times 10^{-3} \text{ kmol.m}^{-3}$; P_{CO} : 5.4 MPa; Solvent: MEK; 9.5 kmol.m^{-3} ; Temp: 373 K, Agitation: 16.67 Hz; Total volume: $2.5 \times 10^{-5} \text{ m}^3$

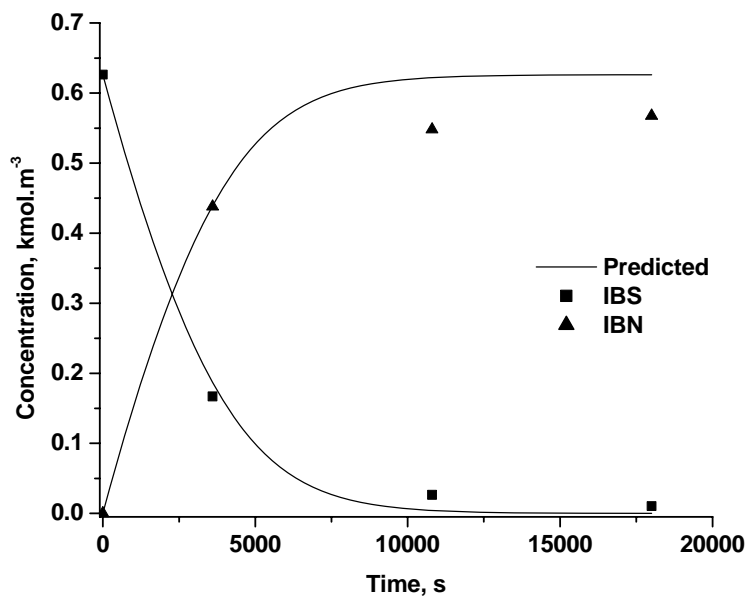


Figure 4.44: Standard reaction at 398 K

Reaction conditions: IBS: $0.625 \text{ kmol.m}^{-3}$; Catalyst 1A: $0.1 \times 10^{-3} \text{ kg}$; TsOH/LiCl (1:1): $0.1175 \text{ kmol.m}^{-3}$; H_2O : 1.6 kmol.m^{-3} ; PPh_3 : $3.8 \times 10^{-3} \text{ kmol.m}^{-3}$; P_{CO} : 5.4 MPa; Solvent: MEK; 9.5 kmol.m^{-3} ; Temp: 398 K, Agitation: 16.67 Hz; Total volume: $2.5 \times 10^{-5} \text{ m}^3$

Therefore, the empirical model successfully predicts the concentration – time profile for the carbonylation of IBS using the heterogeneous ossified Pd-complex catalyst (Catalyst 1A). The effect of temperature on the reaction rate was prominent and in analogy to the homogeneous system, the activation energy can be calculated from the slope of the plot of logarithm of k_3 vs. $1/T$ (Figure 4.45). Thus, the activation energy of the heterogeneously catalyzed carbonylation of IBS was calculated as $44.52 \text{ kJ.mol}^{-1}$.

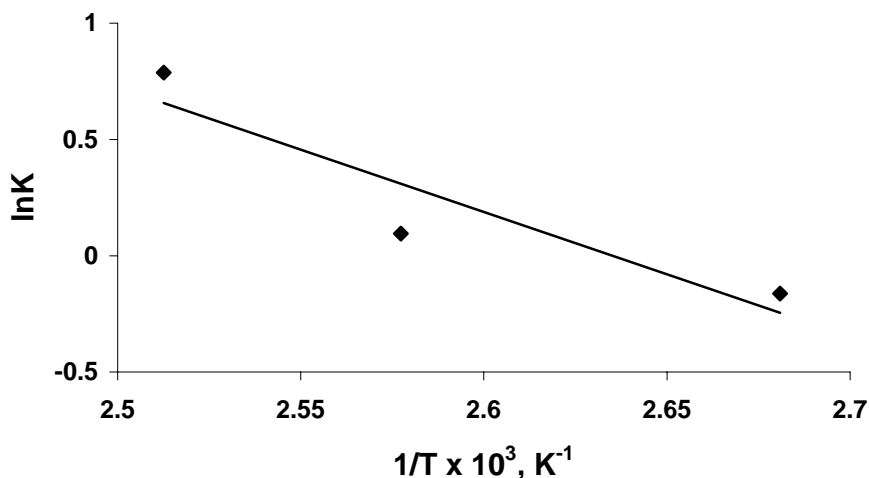


Figure 4.45: Arrhenius plot: Temperature dependence of rate constant k_3

Key Observations

1. Even though almost all of the experimental data were successfully simulated using the empirical model, a few of the effects has low matching (e.g. Figure 4.44). This again might be attributed to the oligomerization of IBS under the reaction conditions of high acidity at high temperature
2. the rates of the heterogeneously catalyzed reaction, were less compared to the homogeneous catalyzed reaction

4.4 Comparison of Homogeneous and Heterogeneous Carbonylation

The comparison of the reaction kinetics of the homogeneous and the heterogeneously catalyzed carbonylation reaction may be described as follows,

1. Both the carbonylation reactions of IBS involving the homogeneous and the heterogeneous catalysts were observed to follow a substrate inhibited kinetics

2. The homogeneously catalyzed reaction was faster than the heterogeneously catalyzed reaction. This may be due to the availability and the accessibility of the active catalytic site in the heterogeneous catalysts. The homogeneous Pd-complex catalyst is miscible in the reaction mixture, but as already described in Chapter 3, the ossified catalyst (Catalyst 1A) is in the form of microscopic lumps, thus lowering the active Pd-site count.
3. The activation energy for the homogeneous catalyzed reaction ($43.02 \text{ kJ.mol}^{-1}$) was slightly less than the heterogeneously catalyzed reaction (44.5 kJ.mol^{-1}). The exact reasoning behind this is not known under the present situation.

4.5 Conclusions

In this chapter, the detailed kinetics of the carbonylation of 4-isobutylstyrene was studied, initially using a homogeneous Pd(pyca)(PPh₃)(OTs) complex and then a heterogeneous ossified counterpart of the same catalyst, and the effect of different parameters was investigated. For the homogeneously catalyzed reaction, an empirical rate model was proposed based on the observed trends. From the temperature dependence of the rate constant the activation energy of the reaction was evaluated to be $43.02 \text{ kJ.mol}^{-1}$. The reaction was also studied using the ossified Pd-complex catalyst and it was ensured that the internal as well as the external mass transfer resistance were eliminated and the reactions were in the kinetic regime. Following the same approach as the homogeneous reaction, an empirical rate model was proposed based on the observed data. The temperature dependence of the rate constant was used to evaluate the activation energy for the heterogeneous reaction as 44.5 kJ.mol^{-1} . It was found that for both the homogeneous and the heterogeneous reactions the integral data for the concentration vs. time was predicted. It was found that agreement of the experimental and the predicted data was good.

References

- 1 Seayad A M, Jayasree S, Mills P L, Chaudhari R V, *Ind. Eng. Chem. Res.*, **2003** 42 2496
- 2 Purwanto P, Deshpande R M, Chaudhari R V, Delmas H, *J. Chem. Eng. Data*, **1997** 41 1414
- 3 Jayasree S, Seayad A, Chaudhari R V, *Org. Lett.*, **2000** 2 203

Chapter 5

Suzuki Coupling Studies Using Novel Ossified Palladium Complex Catalysts

This chapter describes the Suzuki cross coupling reactions for the synthesis of biaryls, using novel ossified palladium complex catalysts as described in Chapter 3. Under the optimized reaction conditions obtained by thorough study of the reactions parameters, the different aryl halides have been reacted with a set of different arylboronic acids to yield a series of different biaryls with a variety of functional substituents. The systematic variation of the stereo-electronic contributions of these substituents was reflected on their respective reaction rates and chemoselectivity as well. The effects of concentrations of the different components of the reaction were also investigated leading to interesting conclusions.

5.1 Introduction

Carbon-carbon bond formation reaction is one of the most well-studied and highly interesting classes of reactions leading to a wide variety of products that find applications in the fields of fine chemicals and pharmaceuticals. These commercially lucrative objectives have motivated the researchers to innovate new and improved routes to different classes of complex organic molecules using catalysis as alternative to the stoichiometric multi-step organic syntheses. Suzuki cross-coupling reaction is one of the important C-C bond-forming reactions leading to biaryl compounds with absolute flexibility of the functional groups on each of the aryl groups

Scheme 5.1: Suzuki Cross Coupling Reaction



(see Scheme 5.1). The relevant literature review on Suzuki coupling reaction from catalysis viewpoint is presented in Section 1.3, Chapter 1. Extensive work on development of novel catalysts, new target molecules, and heterogeneous catalysts has been reported on this subject with recent studies on activation of the lesser reactive chloro-arenes. A detailed review of literature on immobilized catalysts for Suzuki reactions is also discussed in Section 1.3, Chapter 1, which describes the use of different metallic and metal-complex as catalysts. Palladium catalysts have been extensively studied for the Suzuki cross coupling of aryl halides with aryl boronic acids under a wide range of reaction conditions. These palladium catalysts varied widely in nature which included Pd-metal catalysts (both nano-sized and supra-nano range) stabilized by numerous methods as well as the immobilized palladium complex catalysts.

Some recent literature reports on the use of elemental Pd-catalysts for Suzuki coupling are as follows. Sun et al¹ have reported highly dispersed Pd-C catalysts for the Suzuki coupling of alkenyl halides (e.g. α -bromostyrene) with hetero-arylboronic acids in presence of a base in aprotic solvents such as NMP. Report by Heidenreich et

al² described a specially optimized air-stable Pd-catalyst on activated charcoal for this reaction with very high TON (upto 36,000). Kim et al³ reported novel fabrication of hollow Pd spheres and their catalytic application in the Suzuki cross coupling reactions. They also demonstrated good recyclebility of the catalyst but with very low TOF. The nature of interaction of the support materials with the base required for the coupling reaction was investigated by Kabalka et al⁴. They found out while using Pd(0) supported on Al₂O₃, that the bases (e.g. NaOH, K₂CO₃, K₃PO₄, NaF, KF etc.) get adsorbed on the Al₂O₃ surface alongwith Pd for successful reaction. Conlon et al⁵ however demonstrated that while using heterogeneous Pd-C catalyst, a considerable amount of homogeneous Pd is present during reaction, which drops to < 4ppm after reaction is ceased. Corma et al⁶ described palladium containing basic zeolites as good heterogeneous catalysts for Suzuki coupling reaction having multiple recyclability. However, the authors also mentioned that depletion of catalyst activity was observed during the catalyst recycle experiments. In another recent report⁷, these authors have demonstrated the use of alkali-exchanged sepiolites (having 0.065 equivalent basic sites per 100g) containing Pd as catalysts for these reactions, and similar Pd-depletion also. Recently, Choudary et al⁸ reported nano-sized palladium clusters supported on basic layered double hydroxides as efficient catalysts for different C-C coupling reactions including Suzuki reaction. They demonstrated that the chosen basic support gave better activity than the slightly acidic supports as charcoal, SiO₂, Al₂O₃ etc. Strimbu et al⁹ illustrated the use of cyclodextrin-capped Pd-nanoparticles catalyzed Suzuki coupling reactions, whereby similar activities were observed to those obtained by using homogeneous nano-clusters. More recently, Bedford et al¹⁰ have reported Pd-nanoclusters anchored to amine-functionalized mesoporous matrices for the Suzuki coupling reactions, with practically no drop in activity during repeated recycles.

However, the uses of heterogenized Pd-complex catalysts were also reported for achieving unusually high turnovers to project the high efficiency of the catalyst systems and thereby attain advantageous impact, some recent references are as follows. A polymer supported catalytic system containing Pd-complex in it was described by Buchmeiser et al¹¹ with fairly good performance for Suzuki coupling. Mori et al¹² reported different support matrices such as hydroxyapatite for supporting the Pd(II) complexes which showed excellent performances (TON ~ 40,000). Encapsulation of Pd(II)acetate within polyurea microcapsules were demonstrated by Ley et al¹³ as

efficient catalysts for phosphine-free Suzuki coupling reactions in conventional as well as supercritical CO₂ as solvents. Phan et al¹⁴ reported Merrifield resin-supported salen-type Pd-complex for Suzuki reactions without the use of added phosphines, but with negligible metal leaching into the organic phase. Anchored oxime palladacycle complexes onto high surface area SiO₂, MCM-41, polymers etc. were reported by Baleizao et al¹⁵ as efficient catalysts with no observable Pd-leaching. The authors also mentioned that, of these previously mentioned matrices, SiO₂ and MCM-41 were shown as better than the rest. Corma et al¹⁶ also reported oxime palladacycles attached to imidazolium ionic liquids as separable catalysts, but on the ground of poor activity they further anchored the Pd-imidazolium complex to Al-MCM-41 matrix to achieve the desired activity with easy separation. Use of perovskites as supports of Pd, was reported by Andrews et al¹⁷ for Suzuki coupling but the catalyst system faced problems of high Pd-leaching, even though high turnovers were observed. Pd(II)-complexes anchored to mesoporous FSM-16 were also described as potential catalysts by Shimizu et al.¹⁸ However, of all these different results using heterogeneous Pd-catalysts for the Suzuki coupling reactions, the report by Yamada et al¹⁹ demonstrated the highest TON of 12,50,000 for the coupling of bromobenzene. However, the reaction took 36 h to completion rendering a TOF of only ~35,000 h⁻¹. This also enthused us to try out Suzuki coupling reactions to obtain higher TOFs (i.e. high activity in lesser reaction durations) using our heterogeneous Pd-catalysts.

On the basis of this background on heterogeneous Pd-catalyzed Suzuki reactions, it might be generalized that the search for a true heterogeneous catalyst for Suzuki reaction with high activity, selectivity and stability is still a good challenge to work with. Also, generation of hydrohalic acid as observed in this reaction, which requires a base to be quenched. Thus, the presence of such strong corrosive reagents damages the heterogenized catalysts leading to leaching of metal into the reaction medium. The palladium complexes immobilized previously by using the novel *ossification* technique might be visualized as potential candidates for catalyzing the Suzuki coupling reactions. Details of parametric variation of the Suzuki coupling reactions using the ossified palladium complex catalysts and subsequent applications are discussed in the following sections.

5.2 Experimental Section

5.2.1 Materials

The ossified palladium complex catalysts namely, ossified Pd(pyca)(TPPTS) complex [catalyst 1A]; ossified Pd(acpy)(TPPTS) complex [catalyst 1B]; ossified Pd(pycald)(TPPTS) complex [catalyst 1C]; and ossified Pd(bipy)(TPPTS) complex [catalyst 1D] were synthesized following procedures as described in Chapter 3, Section 3.2.2.3.6 . These catalysts were characterized properly and then used for the Suzuki coupling reactions. Phenylboronic acid, $C_6H_5B(OH)_2$, as well as all other arylboronic acids were procured from Aldrich Chemicals Limited. All the other substituted aryl halides were of analytical grade from Aldrich Chemicals Limited, and were used as obtained without any further processing. Bases such as, sodium hydroxide, NaOH; sodium carbonate, Na_2CO_3 ; sodium phosphate, Na_3PO_4 ; sodium acetate, NaOAc; potassium carbonate, K_2CO_3 , potassium *tert*-butoxide, KO*t*-Bu etc were procured from E-Merck India. Solvents such as ethanol, toluene, cyclohexane, *n*-pentane, methanol, acetone and chloroform etc. were of analytical grade and were obtained from S. D. Fine Chemicals, India and were distilled fresh before the reactions and used.

5.2.2 Reaction Methodology – Suzuki Coupling

Suzuki coupling reactions were carried out in one pot under ambient pressure conditions, a schematic of the typical reaction setup is shown in Figure 5.1. The reaction vessel was a double-necked round-bottomed flask of 25 mL capacity, fitted with a Leibig's condenser at the top, while the other neck is sealed with a septum as a provision for intermediate sampling. The whole glass apparatus is seated inside a sand-bath on a heating mantle with temperature and rotation controlling devices. In a typical reaction, the reactants and reagents in requisite amount were charged into the round-bottomed flask along with a magnetic stir bar. The apparatus is placed inside the sand-bath, already pre-heated to the desired temperature and the contents were set onto stirring magnetically. The mixture/ slurry began to reflux within 3 to 5 minutes and reaction was continued for specified period. Intermediate samples drawn at intervals by ceasing the stirring temporarily, with the help of a syringe. The reactions were stopped at definite time by stopping the stirring and removing the heat source.

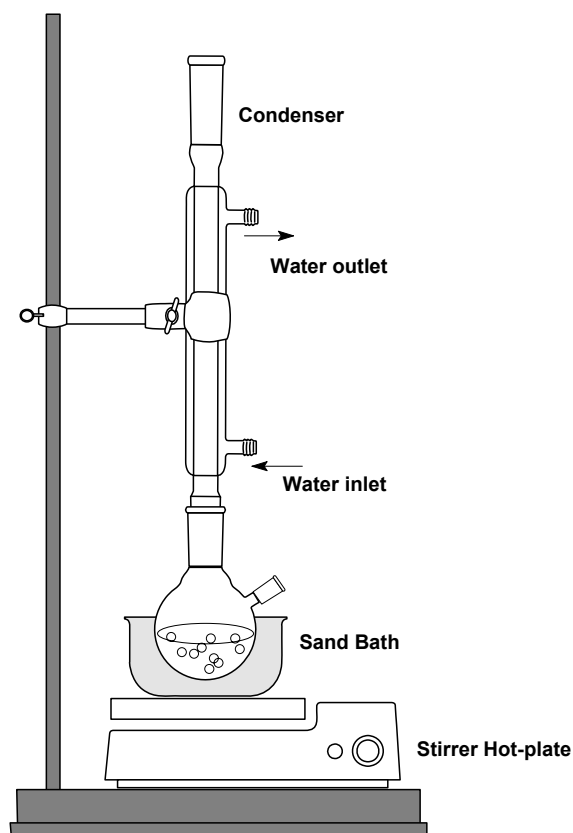


Figure 5.1: Schematic diagram setup for Suzuki coupling reaction

5.2.3 Recycle and Leaching Studies

The ossified palladium catalysts were subjected to recycle experiments in order to check the stability and reusability of them. For a typical recycle reaction, after a standard reaction was performed the reactor setup was allowed to cool down to ambient temperature and the contents were allowed to settle. Then, the supernatant was removed by decantation. The residual catalyst was given wash with 5 mL portions of EtOH by shaking and standing cycles and then was dried under vacuum. Fresh reactants and reagents were again charged to the reaction vessel and reaction done as described in Section 5.2.2. For accurate analysis of the recycle activity, the initial samples of reaction mixture were withdrawn after addition of every fresh charge, stirring with the spent catalyst and settling, before starting on the reaction. Intermediate samples of the reactions were withdrawn similar to those for the standard reactions. Analyses of the samples were performed using gas chromatography, technical details of which will be described in a later section.

For the study of stability of the ossified catalysts and their leaching behaviour under reaction conditions, leaching experiments were designed. The catalysts were mixed with the reactants (iodobenzene and phenylboronic acid) in the specified solvent and heated to the reaction temperature. Stirring and heating were ceased after ~25% conversion (<10 minutes) and the liquid were filtered hot. This hot filtrate was a very faint yellow colored liquid and was analyzed for metal content using atomic absorption spectroscopy, AAS. The detailed discussions of the results are given in a later section. A portion of the hot-filtrate was also recharged into the reaction vessel and was followed up in the same manner as a reaction without any catalyst, to look for any catalytic activity arising from the leached-out metal if any.

5.2.4 Analytical Methods

Different analytical techniques were applied for both qualitative and quantitative analysis of the reaction mixtures. For the identification of the products formed in the Suzuki coupling reactions GC-MS was primarily used. An *Agilent 6890* GC instrument attached with *Agilent 5973 N Mass Selective Detector* was use for the GC-MS analyses using a method similar to that in the GC analysis. Later, quantitative analysis of the components of the reaction was done on a HP 6890 GC using a HP-5

MS capillary column (length 30 m, diameter 0.25mm, film thickness 0.25 μ m) having 5% phenylmethylsiloxane as the stationary phase. The details of the method for GC are presented in Table 5.1. The standardization and calibration of the GC method were performed using iodobenzene in ethanol as solvent in the same range of parameters as those of the reactions.

Table 5.1: Operation parameters of the method for GC/ GC-MS analysis

Injector (split) temperature	523 K
Flame Ionization Detector temperature	Connected to MS Detector
Column (Oven) Temperature	373K (1 min); till 420K @ 3K per min; till 563K @ 10K per min
Carrier gas (He) flow rate	1 ml per min
Inlet pressure	10 psi
Split ratio	50: 1
Injection volume (auto-sampler)	1.0 μl

Based on the results of the gas chromatography, the conversion, selectivity and turnover frequency were calculated as follows,

$$\text{Conversion, \%} = \frac{\text{Initial concentration of substrate} - \text{Final concentration of substrate}}{\text{Initial concentration of substrate}} \times 100$$

$$\text{Selectivity, \%} = \frac{\text{No. of moles of the particular product formed}}{\text{No. of moles of substrate converted}} \times 100$$

$$\text{TOF, h}^{-1} = \frac{\text{No. of moles of coupling product formed}}{\text{No. of moles of catalyst used} \times \text{reaction time (in hours)}}$$

The calculations for conversion etc. were done using the calibrated area under the curve for the aryl halide (substrate) in the chromatograph, since the aryl halide was the limiting component while the other component (phenylboronic acid) was present in excess in the reaction. And also the other component was not properly quantified in GC.

The determination of the palladium content in the catalyst as well in the reaction mixture was done using Atomic Absorption Spectroscopy; the experiments were done using a Shimadzu Atomic Absorption Spectrometer.

5.3 Results and Discussions

The results of the different experiments performed to understand the applicability of the ossified Pd-complex catalysts for the Suzuki coupling reactions and hence to illustrate the versatility of the ossified Pd-complex catalysts from the applicability, stability aspects. Several reactions were carried out to obtain the optimum operating conditions for the reaction and hence, a standardized set of operating conditions were arrived at. A detailed variation of the reaction parameters is also included in this chapter.

5.3.1 The Standard Reaction

After the preliminary variations in the reaction parameters, and having known all the necessary and sufficient conditions for the Suzuki coupling reactions a set of optimized reaction parameters were achieved, which were applied for all the general

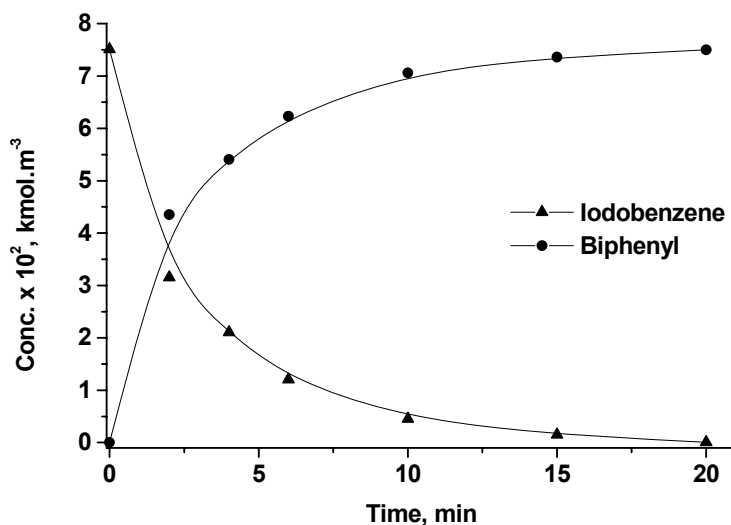


Figure 5.2: A typical Concentration – Time profile of the Suzuki coupling of iodobenzene and phenylboronic acid using ossified Pd-pyca complex catalyst
Reaction conditions: Iodobenzene, 1.5 mmol; Phenylboronic acid, 1.8 mmol; Catalyst, 25 mg; K₂CO₃, 4.5 mmol; Solvent, Ethanol, 20 ml; Reflux

reactions required for the detailed study. For this, a standard reaction of iodobenzene and phenylboronic acid were carried out and a concentration versus time profile was generated by analyzing samples at regular intervals, using gas chromatography throughout the span of the reaction. The C-T profile of the reaction may be represented in Figure 5.2. From the concentration-time profile, we can understand that the reaction is fast and runs to completion within 20 minutes (Ph-I conversion 100%). Another important observation was that the biphenyl was the only product formed and no other compound was (intermediate or by-product) detected in the intermittent samples as well as in the final reaction mixture.

5.3.2 The Parametric Variations

The Suzuki coupling reactions of the aryl halides with phenyl boronic acid were known to occur over a wider range of reaction conditions such as, solvent used, base used, relative amount of the components and operating temperature etc. Following the standard reaction conditions and the preliminary trends, a detailed parametric study was undertaken to understand the reaction more thoroughly.

5.3.2.1 Effect of the Mutual Ratio of Substrates

The effect of the relative ratio of the substrates was an important one for the understanding of the reaction conditions using the ossified catalyst. Since the aryl halide was the limiting substrate and slight excess of the phenylboronic acid was necessary, different ratios of phenyl boronic acid were tried. Considering the standard reaction conditions, two other different ratios of iodobenzene to phenylboronic acid were tested, notably, 1:1 and 1:1.5. All the three reactions were carried out for a definite duration of 0.35h and keeping all the other components of the reaction (parameters and reactants) unaltered, to understand the reaction trends. For the reaction using 1:1 ratio of the reactants 88.0% conversion was observed compared to 99.6% and 99.8% conversions for the mutual substrate ratios of 1:1.2 and 1:1.5 respectively. The results reveal that the reaction rate did not improve further beyond the substrate ratio of 1:1.2. The final reaction mixtures were subjected to GC-MS analysis to identify the by-products, if any. From the GC-MS analyses it was observed that for all the reactions no trace of the intermediate trimeric cyclic boroxine species

was remaining after the reaction, other than the regular product i.e. biphenyl. Also, the intermittent samples did not show any trace of the boroxine intermediate. However, when the reaction of substrate ratio 1:1.5 was carried in presence of Na_3PO_4 as base, similar conversion (~99.6%) of iodobenzene was obtained in 1.5h, but traces (< 1%) of the cyclic trimeric boroxine were detected in the GC-MS analysis of the final reaction mixture. This might be attributed to the self-association of the excess boronic acid over a longer reaction time required when Na_3PO_4 is used as base. The variation of the iodobenzene conversion with the variation in the ratio of iodobenzene to phenylboronic acid is presented in Figure 5.3. Hence, it was understood that when we used a molar ratio of 1:1.2 for iodobenzene to phenyl boronic acid, the reaction proceeded to near completion with no boroxine in the final reaction mixture.

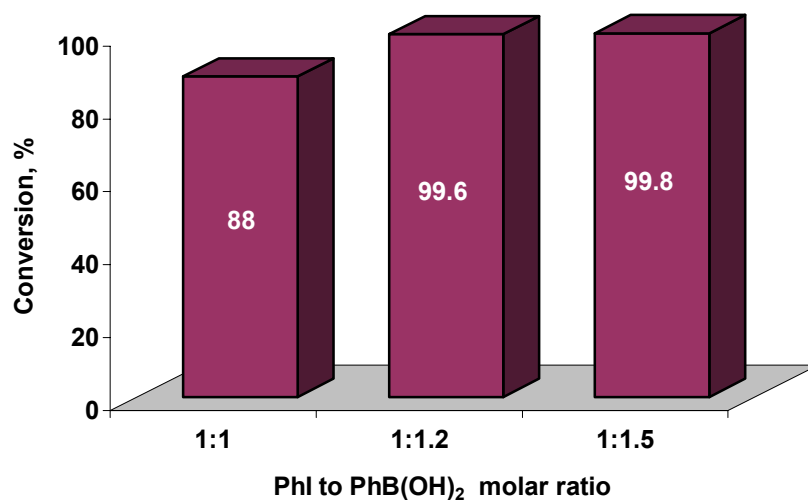


Figure 5.3: Variation of iodobenzene conversion with molar ratio of iodobenzene to phenylboronic acid in Suzuki coupling reaction

Reaction conditions: Iodobenzene, 1.5 mmol; Phenylboronic acid, as specified; Catalyst, 25 mg; K_2CO_3 , 4.5 mmol, Solvent, Ethanol, 20 ml; Reflux; Reaction time, 0.35h

5.3.2.2 Effect of Catalyst Charge

The charge of catalyst is expected to have influence on the coupling reaction. We tried to understand the effect using different catalyst charges other than the standard amount of 25 mg catalyst. The different amounts of ossified $\text{Pd}(\text{pyca})(\text{TPPTS})$ complex tried were 50 mg, 10 mg and 1 mg respectively. The variation of activity and biaryl selectivity are presented in Figure 5.4. It was observed

that the reaction rate did not change much for the 10 mg, 25 mg and 50 mg of catalyst charge. This implied that the reaction rate was independent above a certain catalyst concentration and all the applied catalyst charges were above the limiting value except for the lower catalyst charge (1 mg), where the reaction rate was slightly less. The chemoselectivity to biphenyl remained unchanged for all the different catalyst charges.

Following the observations on the variation of the reaction rate on the catalyst charge, we tried to investigate the limits of the substrate-to-catalyst (precisely, substrate-to-palladium) ratio. Expectedly, the reactions may run slow while working at extremely high substrate-to-catalyst ratios, but good conversions may illustrate the excellent activity of the ossified catalyst as compared to those in the literature. With this target, we changed the substrate to catalyst ratios and compared the conversions and selectivity patterns with few of the best-reported catalyst systems from literature. The results of which are presented in Table 5.2

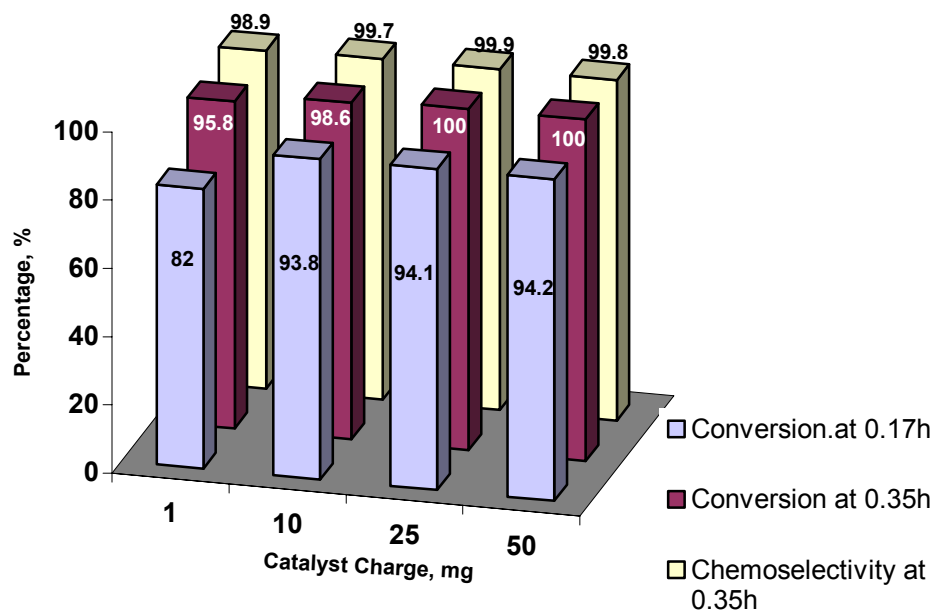


Figure 5.4: Variation of conversion and chemoselectivity with catalyst charge for Suzuki coupling of iodobenzene and phenylboronic acid

Reaction conditions: Iodobenzene, 1.5 mmol; Phenylboronic acid, 1.8 mmol; Catalyst, as specified; K_2CO_3 , 4.5 mmol; Solvent, Ethanol, 20 ml; Reflux; Reaction time, 0.35h

From the results in Table 5.2 it is clearly observed that the ossified Pd-pyca complex catalyst (Catalyst 1A) is a highly active catalyst working efficiently in the substrate-to-catalyst ratio range of ~1500 to >10,00,000 with no degradation. Even for the highest substrate-to-catalyst ratio tested, the reaction showed ~96% conversion in 3h, leading to an immensely high and *unprecedented* turnover frequency of 3,43,296 h⁻¹. This is the highest TOF obtained for Suzuki coupling reactions using any heterogeneous palladium catalyst, to the best of our knowledge. The final reaction mixture showed no sign of any leaching of palladium in the reaction mixture (after being tested negative in ICP-AES). Thus, the ossified Pd-pyca complex catalyst proved to be the most active, stable and truly heterogeneous catalyst for the Suzuki coupling reaction.

Table 5.2: Comparative study of a few heterogeneous Pd catalysts for Suzuki coupling reactions

Entry	Substrate ^a	Catalyst system ^b	S/Pd ^c	Conv., %	Sel., %	TON	Time, h	TOF, h ⁻¹	Pd-leaching	Ref.
1	Ph-I	Pd-hollows	32	99	100	31	3.0	10	Nil	3
2	Ph-Cl	NanoPd-Layered double hydroxide	100	93	-	93	10.0	9.3	Not determined	8
3	4-NO ₂ -Ph-I	Cyclodextrins capped Nano-Pd	100	98	-	96	2.0	48	Not determined	9
4	4-MeO-Ph-Br	Nano-Pd loaded on organosilicas	105	98	-	102	5.0	20	~ 50 % after 4 th recycle	10
5	Ph-Br	Pd-hydroxyapatite	50000	80	-	40000	4.0	10000	Nil	12
6	Ph-I	Pd-AS	2000	98	-	1960	24.0	82	Nil	19
7	Ph-I	Pd-AS	1250000	100	100	1250000	36.0	34722		
8	4-Cl-AcPh ^d	Palladacycle anchored to siliceous supports	25	>99	95	24	2.0	12	Present but inactive for reaction of Ar-Cl	15
9	4-Br-Ph-OH	Pd-Sepiolite	1000	99	100	990	20.0	49.5	Not determined	18
10	4-Br-Ph-OH	Pd-Sepiolite	1000000	94	100	940000	24.0	39167		
11	4-MeO-Ph-Br	Pd-perovskite	526316	75	-	399000	336.0	1187	High	17
12 ^e	Ph-I	Catalyst 1A	1445	100	99.9	1445	0.35	4128	< 0.3 ppm	-
13 ^f	Ph-I	Catalyst 1A	3614	99.8	99.9	3606	0.35	10303		-
14 ^g	Ph-I	Catalyst 1A	36137	99.4	99.9	35920	0.7	51314		-
15 ^h	Ph-I	Catalyst 1A	216818	96	100	208146	3.0	69382	Nil	-
16 ⁱ	Ph-I	Catalyst 1A	1084092	95	100	1029887	3.0	343296	Nil	-

^a Only aryl halide is mentioned, other reactant is PhB(OH)₂; ^b Reaction conditions as mentioned in the respective references and the term Pd represents either Pd-complexes or nanoclusters; ^c S/Pd = Substrate/Palladium ratio; ^d 4-Cl-AcPh = 4-Chloroacetophenone; ^e Reaction conditions - Substrate: 1.5 mmol; PhB(OH)₂: 1.8 mmol; Catalyst: 25 mg; K₂CO₃: 4.5 mmol; Solvent: EtOH, 20 ml; reflux. Pd-content in catalysts: Catalyst 1A = 0.44%; ^f Same as in Entry 12, but Catalyst: 10 mg; ^g Same as in Entry 12, but Catalyst: 1 mg; ^h Ph-I: 45 mmol; PhB(OH)₂: 54 mmol; Catalyst: 5 mg; K₂CO₃: 135 mmol; Solvent: EtOH, 150 ml; ⁱ Same as in Entry 15, but Catalyst: 1 mg.

5.3.2.3 Effect of Base

The importance of the base in the Suzuki coupling reaction is to neutralize the acidic side-products formed during the coupling reaction. The nature of the base used and the amount of the same also determines the course of the reaction and the selectivity pattern also. The proper selection of a base and its optimal quantity is a necessary and sufficient precondition for a successful reaction. Thus, the effect of base on the Suzuki coupling reactions may be discussed in details, under two heads namely, the choice of base and the quantity of it.

5.3.2.3.1 Choice of Base

Several different bases were tested for the Suzuki coupling reactions and their performances were compared with respect to the activity and selectivity of the catalyst. All the other conditions were kept constant. Generally, Brønsted bases were chosen and mostly ionic compounds of sodium or potassium, such as, NaOH, Na₂CO₃, NaOAc, K₂CO₃, KO^t-Bu etc. The standard reactions of iodobenzene and phenylboronic acid were carried out using each of these bases in presence of catalyst till only 0.35h, and conversion and chemoselectivity were observed through GC. The comparative data of these reactions is given in Table 5.3.

Table 5.3: Comparative results of Suzuki coupling of iodobenzene and phenylboronic acid using different bases in presence of ossified Pd-pyca catalyst

Entry	Base	Conv., %	Biphenyl Sel, %	Boroxine, %	Remarks
1	Na ₃ PO ₄	56	98	19	Less active, clogging observed
2	Na ₂ CO ₃	59	99	20	Less active, clogging observed
3	NaOAc	20	98	25	Least active
4	NaOH	70	98	3	Severe clogging observed
5	K ₂ CO ₃	100	100	-	Highly active, No clogging
6	KO ^t -Bu	99	99.9	-	Highly active, Clogging observed

Reaction conditions: Iodobenzene, 1.5 mmol; Phenylboronic acid, 1.8 mmol; Catalyst, 25 mg; Base, 6 mmol, Solvent, Ethanol, 20 ml; Reflux; Reaction time, 0.35h

It is clearly derived from the observations that of the different bases tested, K_2CO_3 showed the best performance with respect to activity and selectivity (Entry 5, Table 5.3). Even the intermediate cyclic trimeric boroxine was not visible in the intermediate samples and the final reaction mixture. This showed that the not only reaction was complete in the specified time, but also enhancement in rate was observed with the use of potassium carbonate. The GC results also showed that nothing else other than the desired product, i.e. biphenyl was formed, and thus a remarkable 99.9% selectivity was achieved. Also, no observable amount of the trimeric boroxine was found for this reaction in the GC-MS, and the solid residue (mostly catalyst) was freely suspended in the liquid mixture after the reaction, without any clogging. However, with all the bases having sodium cation, the presence of the trimeric cyclic boroxine in the reaction mixture in considerable amounts ($\geq 20\%$) was observed. This might be due to the longer reaction time required for completion of the coupling reaction in their presence, in comparison to K_2CO_3 . The phenylboronic acid being in excess might allow the formation of the cyclic trimer in contact with the base for a longer reaction period. Another important observation was that, the use of the Na-bases caused clogging of the solids (mainly catalysts) in the final reaction mixture into a sticky form, after the reaction was over. This made the reaction mixture difficult to separate from the catalyst by decantation/ filtration and also might lead to activity-loss during recycles due to hindered access of the substrates caused by the clogging of the catalyst. When potassium *tert*-butoxide, $KOt\text{-Bu}$ was used as the base, the reaction showed results close to those of K_2CO_3 in respect to the activity and chemoselectivity (Entry 6, Table 5.2), but with this case also, the catalyst tend to form a sticky mass after the reaction. The clogging in presence of Na-bases may be justified as that the ionic potential (Z_+/r_+) for Na^+ ion is slightly higher than that of K^+ ion, which results in bigger size of the hydrated Na^+ ion than for K^+ ion. So, being in high excess, Na^+ ion traps more of the scanty H_2O molecules (mostly from the solvent and added base) and consequently more of the catalyst ion-pairs (Ba-sulphonate) might be agglomerated into an intercalated mass along with it, since the dielectric constant of water is higher than that of ethanol ($D_{H_2O} = 80$, $D_{EtOH} = 24.3$). Hence, a feeble ionic atmosphere binds the catalyst in the form of a sticky mass. But, with $KOt\text{-Bu}$, the counter-ion $t\text{-BuO}^-$ is the key player. Compared to CO_3^{2-} it has a bigger size of the hydrated ion, and hence may play the same role as the hydrated sodium ion, attracting more water molecules and

creating the sticky-appearing residue. Thus, based on these preliminary tests, it may be inferred that potassium carbonate is best suited for the Suzuki coupling reaction of iodobenzene and phenylboronic acid under the present set of reaction conditions, and all further reactions were performed using K_2CO_3 only.

5.3.2.3.2 Quantity of Base

With the nature of the base determining the activity and selectivity profile of the ossified catalyst, the amount of the base used also has a prominent effect on the same issues. Earlier in the standard reaction three equivalents of the base with respect to the aryl halide was used for the coupling. However, to understand the role of the quantity of the base used, two different concentrations of base were used for the coupling reactions such as two and four equivalents with respect to iodobenzene. Since the reaction leads to completion in 0.35h, these test reactions were sampled at 0.17h and the overall progress and performance were observed by gas chromatography for comparative studies. The results of the reactions using different amounts of K_2CO_3 are presented in Figure 5.5. One important feature of the use of

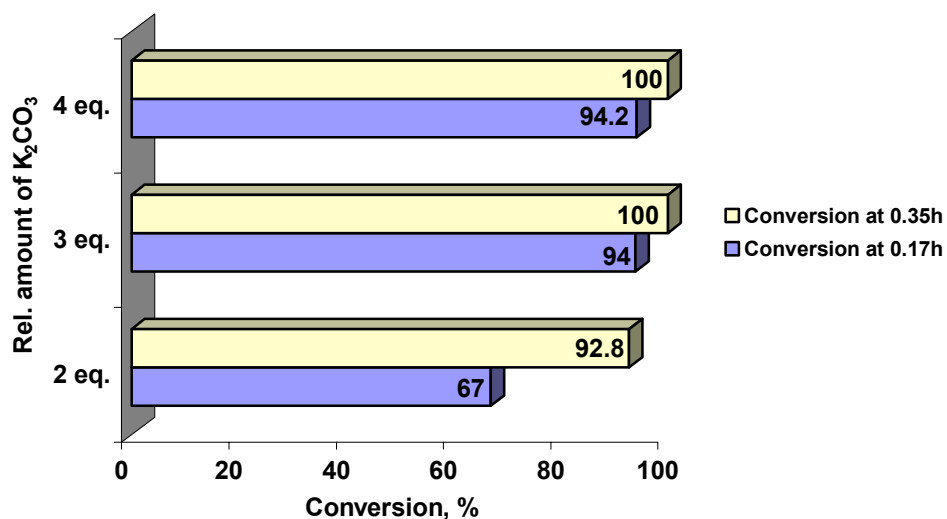


Figure 5.5: Variation of conversion with the amount of K_2CO_3 relative to iodobenzene in Suzuki coupling of iodobenzene and phenylboronic acid

Reaction conditions: Iodobenzene, 1.5 mmol; Phenylboronic acid, 1.8 mmol; Catalyst, 25 mg; K_2CO_3 , as mentioned; Solvent, Ethanol, 20 ml; Reflux; Reaction time, 0.35h

K_2CO_3 is that the reactions are clean, without the formation of any side products, so the main issue was the change in activity, if any. The Suzuki coupling reaction was carried

out in absence of the base, and the catalyst failed to have any activity without the base K_2CO_3 . So presence of a base is a necessary condition for the Suzuki coupling reaction. From the plot, it is clearly observed that when 2 equivalents of K_2CO_3 were used in the reaction, the reaction did not go to completion in 0.35h, also a slower progress was observed at the half time of the reaction (0.17h). The other two reactions, where 3 and 4 equivalents of K_2CO_3 were used with respect to moles of iodobenzene respectively, proceeded almost parallel throughout the course of reaction showing 100% conversion in 0.35h. The GC results of all the reactions however did not show any trace of the cyclic boroxine in the intermediate samples as well as in the final reaction mixtures. As the coupling of iodobenzene with phenylboronic acid occurred in the same manner and to the same extent (94% and 94.2% respectively) when either of 3 or 4 equivalents of bases was used, we may conclude that three equivalents of base was the optimal requisite amount.

5.3.2.4 Role of Solvent

The Suzuki coupling reactions are known to occur in different kinds of solvents, polar, non-polar etc. For the present studies on Suzuki coupling reactions, ethanol was used initially as solvent while using ossified Pd-pyca complex catalyst. However, a few other solvents were selected for screening based on the polarity aspect. Nonpolar solvents such as toluene, cyclohexane, *n*-pentane were tested, while among the polar contingent methanol, acetone, chloroform, tetrahydrofuran were the candidates. Since the coupling reaction performed was under refluxing conditions in ethanol (b.p. 351K), all these test reactions were performed at 351K for solvents boiling higher than ethanol (toluene, cyclohexane), and for the low boiler solvents (*n*-pentane, acetone, chloroform, methanol, tetrahydrofuran) reactions were performed under refluxing conditions. All the reactions were intermittently sampled after 0.17h and then stopped after 0.35h of start of the reaction. The comparisons of the conversions of iodobenzene at 0.17h as well as after 0.35h and the selectivity to biphenyl at the end of reactions are presented in Figure 5.6. From the results, it is clearly observed that the Suzuki coupling reaction of iodobenzene and phenylboronic acid occurred better in polar solvents than in non-polar ones. The reaction may pass through some ionic intermediate(s), which may be better stabilized in a polar media than a non-polar one.

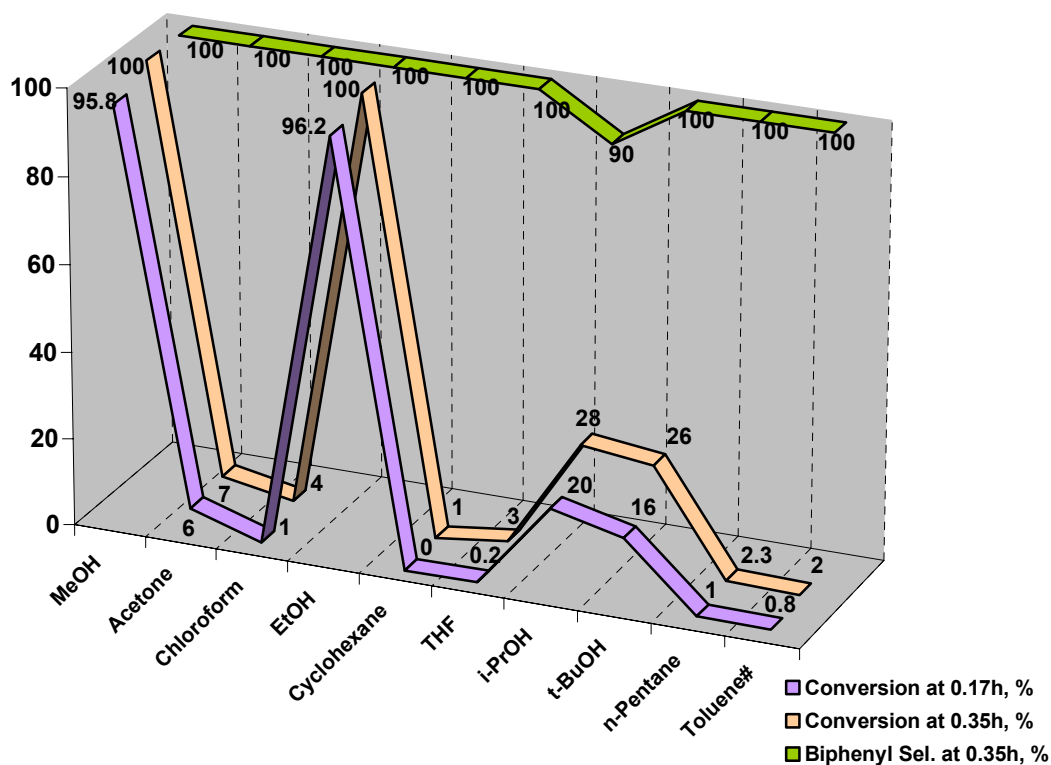


Figure 5.6: Comparison of conversions and selectivity for Suzuki coupling reaction of iodobenzene and phenylboronic acid in different solvents

Reaction conditions: Iodobenzene, 1.5 mmol; Phenylboronic acid, 1.8 mmol; Catalyst, Ossified Pd-pyca complex, 25 mg; K_2CO_3 , 4.5 mmol; Solvent, 20 ml; Reflux; Reaction time, 0.35h; # - Reaction temperature, 351 K

Thus, the reactions in polar solvents are faster and having good conversion. Among the polar media selected for the reaction, the protic solvents namely the alcohols such as methanol, ethanol etc. show better performances than the aprotic ones. The exact role of the protic solvent is not known, but a plausible explanation may be presented as follows. The base present in the reaction medium may abstract the proton from the protic solvent, which then forms the alkoxy anion as counter-ion. This counter anion being a labile but efficient ligand may help in the activation of the substrate in the catalytic cycle. In order to judge the effect of the counter-ion generated from the alcohol, the results using the different alcohols may be re-envisaged. Of the four different alcohols tested namely methanol, ethanol, iso-propanol and tertiary butyl alcohol, the order of dimension and basicity of the counter-ions is as $MeO^- \leq EtO^- < i-PrO^- < t-BuO^-$, which is exactly opposite to the reaction rates. The Suzuki coupling

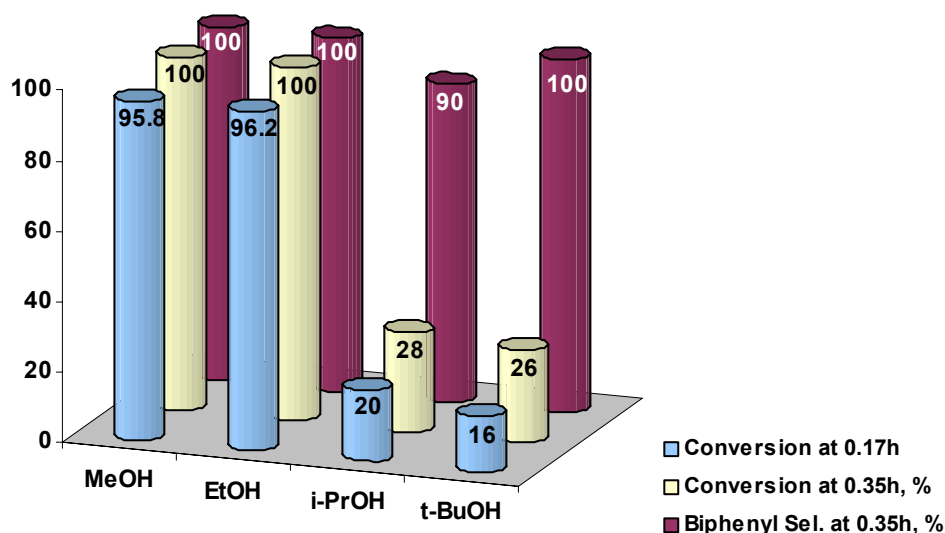


Figure 5.7: Comparison of conversions and selectivity for Suzuki coupling reaction of iodobenzene and phenylboronic acid in different alcohols as solvents
Reaction conditions: Iodobenzene, 1.5 mmol; Phenylboronic acid, 1.8 mmol; Catalyst, Ossified Pd-pyca complex, 25 mg; K_2CO_3 , 4.5 mmol; Solvent, alcohol, 20 ml; Reflux; Reaction time, 0.35h

reaction is fastest in either of methanol or ethanol, slower in iso-propanol and slowest in tertiary butanol. The variation in reaction performance may be seen in the Figure 5.7. The relatively less reactivity in iso-propanol and still lesser in tertiary butanol definitely points out some involvement of the alkoxy anions in the catalytic cycle and moreover, the stereoelectronic aspects of the different alkoxy ions tested, might lead us to the answer. The bulky and very basic *tert*-butoxy anion would definitely be slow to approach the already electron rich Pd-center than the methoxy or ethoxy anions. It is noteworthy to mention that when $KOt-Bu$ was used as the base for the reaction in presence of ethanol as solvent, the reaction went on well with high conversion (~99%). This may be explained by the fact that under those conditions the population of $t-BuO^-$ was far less than that of EtO^- derived from solvent EtOH. This EtO^- might coordinate to the Pd-center faster in competition, thus enhancing the reaction rate in ethanol solvent. But when *t*-butanol is the solvent the $t-BuO^-$ is the only alkoxy anion present in reaction mixture and hence shows the low reaction rate. However, in all the solvents tested, the chemoselectivity towards biphenyl was observed to be 100%.

Another important observation was with the use of iso-propanol as solvent. The GC-MS results of the reaction mixture revealed the formation of phenol (~10%)

alongwith the desired reaction product thus lowering the chemoselectivity towards biphenyl (~90%) Eventually, the amount of phenol formed was higher than that of biphenyl. The exact justification is still not known. So, it is understood from the aforesaid experiments that the Suzuki coupling reactions of iodobenzene and phenylboronic acid should be carried out in a polar solvent, preferably a protic one. Either of methanol or ethanol might be used as the solvent to have good performance under low temperature conditions. However, if we consider the fact that many Pd-complexes decompose to palladium black in the presence of methanol (even though there is no evidence of formation of Pd-black in the aforesaid cases discussed), we may choose ethanol as the preferred solvent for the reaction universally.

5.3.3 Different Catalysts

The ossified Pd-pyca complex catalyst (Catalyst 1A) has shown excellent performance for the Suzuki coupling reaction and has been optimized thoroughly over the wide range of reaction conditions. The other ossified Pd complex catalysts namely ossified Pd-acpy complex (Catalyst 1B), ossified Pd-pycald complex (Catalyst 1C) and ossified Pd-bipy complex (Catalyst 1D) were also tested for the Suzuki coupling reactions. The coupling of iodobenzene and phenylboronic acid was used to compare the activity of them with the ossified Pd-pyca complex catalyst. The reactions were done similar to the standard optimized reaction, only with the variation of the catalyst.

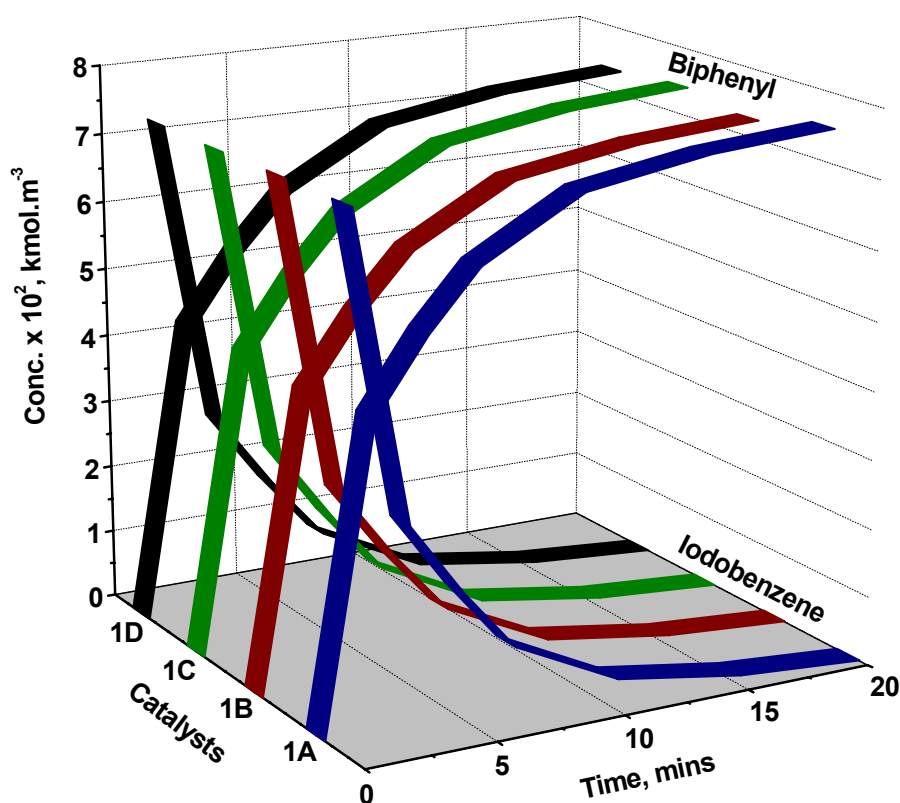


Figure 5.8: Performance of different ossified Pd-complex catalysts in Suzuki coupling reaction of iodobenzene and phenylboronic acid

Reaction conditions: Iodobenzene, 1.5 mmol; Phenylboronic acid, 1.8 mmol; Catalyst, 25 mg; K₂CO₃, 4.5 mmol; Solvent, Ethanol, 20 ml; Reflux; Reaction time, 0.35 h, Pd content of catalysts, Catalyst 1A: 0.44%, Catalyst 1B: 0.48%, Catalyst 1C: 0.45%, Catalyst 1D: 0.46%

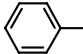
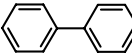
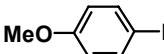
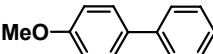
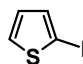
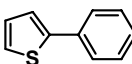
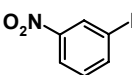
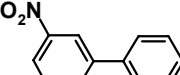
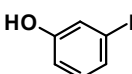
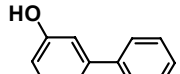
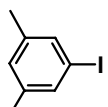
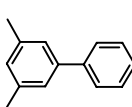
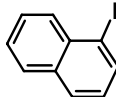
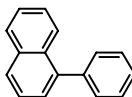
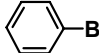
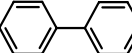
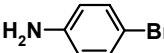
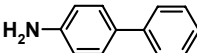
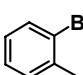
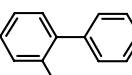
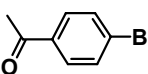
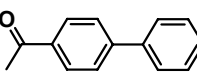
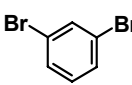
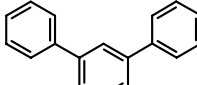
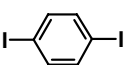
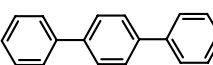
All the reactions were run for the same reaction time of 0.35h and the comparative results are presented in the Figure 5.8. From the comparative concentration-time profiles of the four catalysts, drawn over a fixed reaction time, it was observed that all the ossified Pd-complex catalysts performed almost equally well in terms of activity and selectivity. The typical conversions being 100%, 97%, 99% and 98% respectively for catalysts 1A, 1B, 1C and 1D. Excellent mass-balance was obtained for all of the runs showing 100% selectivity to the desired product i.e. biphenyl. It was very interesting to observe that no other side-products were generated during the course of the reactions for any of the catalysts. A slight variation of the activities was prominent in the reactions. Among these four ossified Pd-complex catalysts, Catalyst 1A i.e. ossified Pd-pyca complex was the superior-most showing complete conversion and 100% selectivity to biphenyl. The final reaction mixtures of all of these reactions were tested to evaluate the Pd-leaching, and the results showed that the catalysts showed absolutely zero palladium leaching during the reactions.

5.3.4 Different Substrates

After being satisfactorily applied for the extensive studies in the Suzuki coupling of iodobenzene and phenylboronic acid, the ossified Pd-pyca complex (Catalyst 1A) was tested for the coupling of two classes of substrates namely, [i] a bunch of differently substituted aryl halides to be coupled with phenylboronic acid; and [ii] different aryl boronic acids coupled with iodobenzene. From the investigations of the class [i], the study of stereoelectronic outplay of the different functional groups present on the aryl halide may be reflected as their respective performance during the coupling reaction with respect to the activity (TOF) and the selectivity aspects, while the class [ii] reactions just demonstrate the scope and extent of applicability of the ossified catalyst. The results of the reactions of class [i] are presented in Table 5.4. The identification of the products of these variedly substituted aryl halides were done using GC-MS (See Appendix I for detailed results), and quantitative results were derived from GC analysis. All the reactions were carried out using highest concentration of the catalyst as described in section 5.3.2.2, only to ensure that the reactions do not suffer due to

limiting catalyst concentrations. The examples in Table 5.4 show that most of the reactions were over within very short duration of reactions with

Table 5.4: Suzuki coupling reactions of different substituted aryl halides with phenylboronic acid using ossified Pd-pyca catalyst (Catalyst 1A)

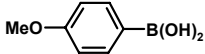
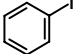
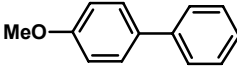
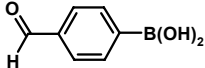
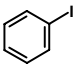
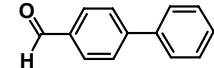
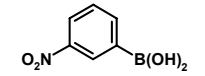
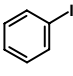
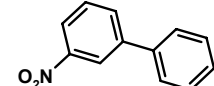
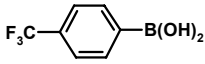
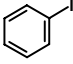
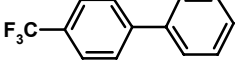
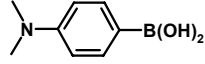
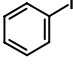
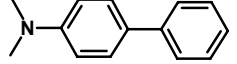
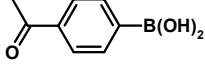
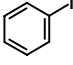
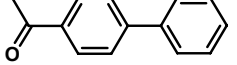
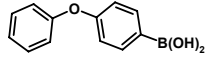
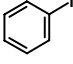
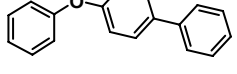
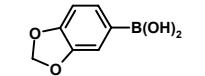
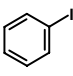
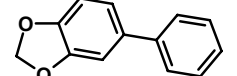
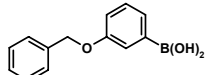
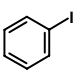
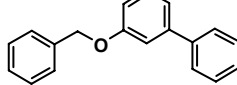
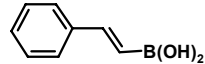
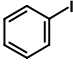
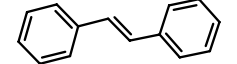
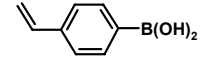
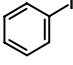
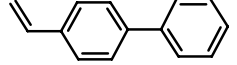
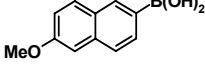
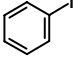
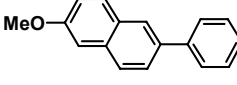
Sl. No	Substrate	Conv %	Product	Selectivity, %		TON	Time h	TOF, h ⁻¹
				Biaryl	Other			
1		100		99.9	-	1445	0.35	4126
2		98.0		99.2	0.7	1416	1.0	1416
3		99.9		99.0	0.9	1444	1.0	1444
4		100		99.9	-	1445	0.42	3440
5		99.9		99.0	0.9	1445	0.88	1642
6		99.9		99.1	0.88	1444	0.67	2155
7		99.9		99.8	0.15	1444	0.70	2065
8		89		99.8	-	1402	1.5	858
9		74		98.2	0.67	1070	4.5	238
10		83		99.1	0.8	1200	4.0	300
11		97		99.0	0.8	1401	2.5	560
12*		96		99	0.9	1387	2.0	694
13*		99.9		99.8	0.1	1443	0.8	1805

Reaction conditions: Aryl halide, 1.5 mmol; Phenylboronic acid, 1.8 mmol; Catalyst, 25mg; K₂CO₃, 4.5 mmol; Solvent, Ethanol, 20 ml; Reflux; * - 3.6 mmol PhB(OH)₂ used

excellent selectivity (> 98% for all cases) to the desired product. The difference in the activation of the aryl bromides with those of the aryl iodides was also prominently evident from the results. From these reactions, it may be observed that the aryl iodides were easier to activate and gave quantitative yields in the coupling reaction within very short reaction times. The use of ossified Pd-pyca catalyst to obtain high conversion of these substrates at a low reaction temperature of only 351K, in such a small reaction time is a remarkable achievement. Even for the di-iodide (Entry 13, Table 5.4), the reaction was complete in only 0.8h, with 99.9% conversion and negligible byproduct (0.1% biphenyl) formation. The TOF of the reactions were also very high ($\sim 2900 \text{ h}^{-1}$ for iodobenzene) and were among the best results in the literature. By studying these reactions it not only proved the wide applicability of the catalyst but also we got an idea on the role of the functional groups upon substrate activation. The nature of the substituents on the aryl iodide guided the reaction rate and conversion of the reaction. The electron-withdrawing substituents such as $-\text{NO}_2$ group etc. on the aromatic ring made the C–I bond more labile and easier activation was possible. This effect is reflected in the fast reaction of 3-nitro-iodobenzene (Entry 4, Table 5.4) – reaction got complete in only 0.42h, showing a high TOF of 3440 h^{-1} but, slower than iodobenzene, as the $-\text{NO}_2$ group was at *meta* position with respect to the iodine. While the presence of electron-donating functionalities on the aryl ring would makes the compound slightly less active for Suzuki coupling, as exactly observed in the case of 4-iodoanisole (Entry 2, Table 5.4), where the reaction took 1h for completion under similar conditions with a TOF of 1416 h^{-1} . Various other substrates also validated a similar logic during the reactions. The aryl bromides also activated under the same reaction conditions, but their duration of reaction were higher than the aryl iodides. The nature of the substituents on the aryl ring played similar role as similar to those of the iodides on the reaction rates. One more interesting observation was that the reactions with aryl bromides being slower showed the formation of the trimeric boroxine in the final reaction mixture of many such substrates. All these reactions demonstrate that the ossified Pd-pyca catalyst may be used for a large number of substrates with a wide spectrum of functional groups.

The reactions of the different substituted arylboronic acids and iodobenzene are presented in Table 5.5. Iodobenzene was used for these coupling reactions as the model substrate for most of the reactions to ensure faster reactions and good

Table 5.5: Suzuki coupling reactions of different arylboronic acids with iodobenzene using ossified Pd-pyca catalyst (Catalyst 1A)

Sl. No.	Ar-B(OH) ₂	Ar-X	Conv %	Product	Selectivity, %		Time, h	TOF, h ⁻¹
					Biaryl	Other		
1			100		96.1	3.9	0.50	2891
2			100		100	-	0.50	2891
3			100		100	-	0.50	2891
4			100		100	-	0.25	5782
6			100		100	-	0.50	2891
7			99.8		100	-	0.50	2885
8			100		100	-	0.50	2891
9			100		100	-	0.50	2891
10			100		100	-	0.50	2891
11			99		100	-	0.25	5724
12			96		100	-	0.90	1606
13			100		100	-	0.25	5782

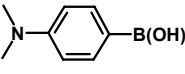
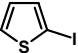
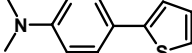
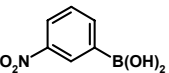
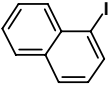
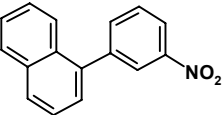
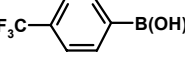
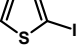
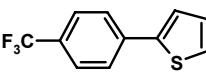
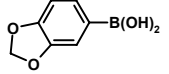
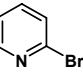
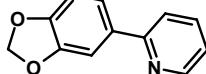
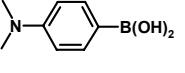
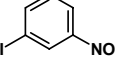
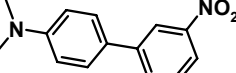
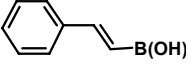
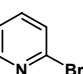
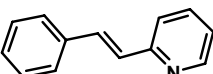
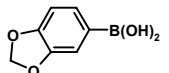
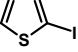
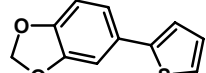
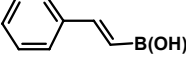
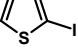
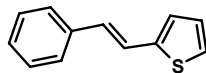
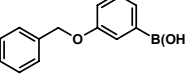
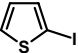
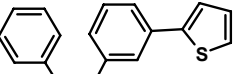
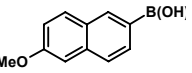
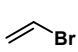
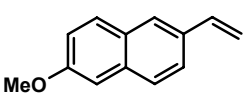
Reaction conditions: Iodobenzene, 1.5 mmol; Arylboronic acid, 1.8 mmol; Catalyst, 25mg; K₂CO₃, 4.5 mmol; Solvent, Ethanol, 20 ml; Reflux

conversions. However, different organic halides including some heterocyclic compounds were also used to obtain variedly functionalized biaryl compounds, which are presented in Table 5.6, as to extend the scope of applicability of the ossified catalyst to wide variety of functionalized substrates.

An important observation for the reactions of the almost all of the different arylboronic acids with iodobenzene was that after the reaction, these boronic acids underwent partial degradation with the removal of the boron-moiety only, yielding the corresponding aromatic compound residue as evident from the GC-MS results. But surprisingly enough, none of these affected the C-C coupling reactions in terms of the selectivities, as the boronic acids were present in slight excess with respect to the aryl halide. All the reactions went to almost quantitative (>99 %) conversions with excellent biaryl-selectivities of >99.9 %. Also, the quantity of the de-boronated aromatic species did not alter for samples of reaction mixtures drawn at different intervals during the reactions. This de-boronation might be either in the presence of base under refluxing conditions during the reaction, or due to the degradation under the pre-injection atomization process occurring inside the GC injector, at the high injector temperature of 523 K. To understand the actual fact, we injected a pure sample of 4-methoxyphenylboronic acid in GC-MS, which showed the characteristic fragments for anisole. This indicated that the detachment of the boron moiety did not occur during the reaction, and the de-boronated aromatic groups were generated from the excess arylboronic acid, present in the reaction mixture, by thermal degradation under the injection conditions of the GC. And the quantity was unchanged as the final reaction mixture contained almost same excess of the arylboronic acids over the aryl halides, for any reaction.

All the different substrates tested for the coupling reaction showed extremely high conversions and biaryl selectivities. Simple Suzuki coupling using the ossified catalyst demonstrated the syntheses of many aryl-substituted heterocyclic compounds, which were otherwise cumbersome to synthesize. The reactions involving substituted thiophene-boronic acid were typically slow and generated other byproducts other than the coupling product. These reactions being demonstrated successfully using the ossified Pd-pyca complex catalyst,

Table 5.6: Suzuki coupling reactions of different arylboronic acids with miscellaneous aryl/ alkyl halides using ossified Pd-pyca catalyst (Catalyst 1A)

Sl. No	Ar-B(OH) ₂	Ar-X	Conv %	Product	Selectivity, %		Time h	TOF, h ⁻¹
					Biary I	Other		
1			100		100	-	0.50	2891
2			100		100	-	1.00	1431
3			100		100	-	0.50	2891
4			93		100	-	2.00	672
5			100		100	-	0.25	5782
6			100		100	-	0.50	2891
7			100		100	-	0.50	2891
8			100		100	-	0.5	2891
9			100		100	-	0.35	4130
10			100		100	-	0.35	4130

Reaction conditions: Aryl/ Alkyl halide, 1.5 mmol; Arylboronic acid, 1.8 mmol; Catalyst, 25mg; K₂CO₃, 4.5 mmol; Solvent, Ethanol, 20 ml; Reflux

5.3.5 Recycle Studies

The recycle studies were performed using the procedure as described in a previous section. The ossified Pd-pyca complex (Catalyst 1A) was used as the representative catalyst and the reaction between iodobenzene and phenyl boronic acid was considered as the standard. The results of the recycle studies are presented in Figure 5.9.

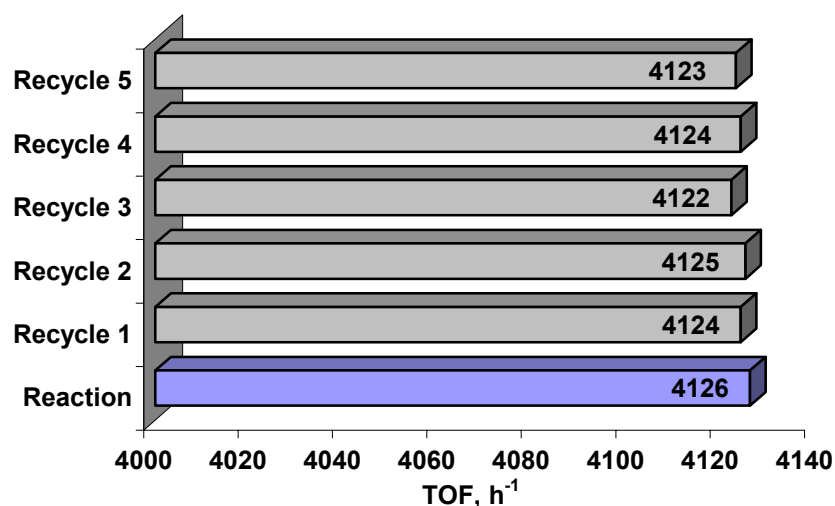


Figure 5.9: Recycle studies of Suzuki coupling of iodobenzene and phenylboronic acid using Catalyst 1A

Reaction conditions: Iodobenzene, 1.5 mmol; Phenylboronic acid, 1.8 mmol; Catalyst, 25 mg; K₂CO₃, 4.5 mmol; Solvent, Ethanol, 20 ml; Reflux; Reaction time, 0.35 h, Pd-content of Catalyst 1A: 0.44%

The recycle reactions were performed using the highest tested catalyst loading to identify any tangible catalyst degradation or leaching during the runs, which would directly be manifested in terms of the turnover frequencies and the Pd-analysis of the reaction mixtures. From the recycle studies, it was confirmed that the catalyst recycled efficiently with retention of the activity (TOF ~ 4125 h⁻¹) for at least five recycles. Since no other side products were identified in the final reaction mixture as well as the intermediate samples of any of the recycle runs, it may be concluded that the selectivity to biphenyl was also retained during the recycles. The final reaction mixtures (hot portions drawn immediately after stopping reaction) of the recycle runs were analyzed for Pd-content, which showed an extreme low leaching of 0.18×10⁻⁶ % of the total Pd-charge per run. This might be deemed negligible with respect to the

scale of the reactions; consequently, the change in the TOF of the recycle runs is very nominal. The excellent catalyst stability is also confirmed by these recycle runs.

5.4 Conclusions

The Ossified Pd-complexes have been demonstrated to have excellent performance for the Suzuki cross-coupling reactions. The very high activity and biaryl selectivity have been the crucial observations for these catalysts. The unprecedented turnover frequency of almost 3.5 million was attained, reinstating the excellent activity of the ossified catalyst. The stability of the ossified Pd-complex catalysts has been justified on the basis of the successful recycle studies involving retention of activity, selectivity and negligible leaching even at very high catalyst charge. The variation of the different reaction parameters yielded important information towards the performance of the catalysts. Later, the applications to differently substituted substrates (both for aryl halides and aryl boronic acids) led to a wide range of products, which are difficult to synthesize otherwise. Thus, the Suzuki cross-coupling reactions using the ossified Pd-complex catalysts have been a successful demonstration of the efficiency of the ossification strategy for Pd-complexes.

5.5 Scope and Future Directions

With the present state of understanding about the application of the ossified Pd-complex catalysts for the Suzuki coupling reactions in terms of their different reaction parameters and for a variety of substrates, it is important to discuss the future directions and scope of further studies in this field. A categorical description may be presented as,

- The different examples described in this chapter mostly emphasized on the reactions of different aryl-iodides and aryl-bromides, leaving ample scope of investigations using aryl-chlorides as substrates
- The ossified Pd-complexes have shown impressive performance, and following the trends of the parametric variations, detailed kinetics and mechanistic pathways need to be studied

- Applications of ossified Pd-complexes for intramolecular Suzuki coupling leading to different active pharmaceutical intermediates (API) may be interesting targets

References

- 1 Sun Y, Leblond C, Sowa J R, US Pat. Appl. No. US 20020045775 A1, Apr **2002**
- 2 Heidenreich R G, Kohler K, Krauter J G, Pietsch J, *Synlett*, **2002** 7 1118
- 3 Kim S, Kim M, Lee W Y, Hyeon T, *J. Am. Chem. Soc.*, **2002** 124(26) 7642
- 4 Kabalka G W, Pagni R M, Hair C M, Wang L, Namboodiri V, *Special Publication, Supported Catalysts and Their Applications, RSC*, **2001** 266 219
- 5 Conlon D A, Pipik B, Ferdinand S, LeBlond C R, Sowa J R Jr, Izzo B, Collins P, Ho G, Williams J M, Shi Y, Sun Y, *Adv. Synth. Catal.*, **2003** 345(8) 931
- 6 Corma A, Garcia H, Levya A, *Appl. Catal. A: Gen.*, **2002** 236(1-2) 179
- 7 Corma A, Garcia H, Levya A, Primo A, *Appl. Catal. A: Gen.*, **2004** 257(1) 77
- 8 (a) Choudary B M, Madhi S, Chowdari N S, Kantam M L, Sreedhar B, *J. Am. Chem. Soc.*, **2002** 124(47) 14127 (b) Choudary B M, Madhi S, Chowdari N S, Kantam M L, Sreedhar B, US Pat. Publ. US 2004192542 A1, Sept **2004**
- 9 Strimbu L, Liu J, Kaifer A E, *Langmuir*, **2003** 19(2) 483
- 10 Bedford R B, Singh U G, Walton R I, Williams R T, Davis S A, *Chem. Mater.*, **2005** 17(4) 701
- 11 Buchmeiser M R, Schareina T, Kempe R, Wurst K, *J. Organomet. Chem.*, **2001** 634(1) 39
- 12 Mori K, Yamaguchi K, Hara T, Mizugaki T, Ebitani K, Kaneda K, *J. Am. Chem. Soc.*, **2002** 124(39) 11572
- 13 Ley S V, Ramarao C, Gordon R S, Holmes A B, Morrison A J, McConvey I F, Shirley I M, Smith S C, Smith M D, *Chem. Commun.*, **2002** 10 1134
- 14 Phen N T S, Brown D H, Styring P, *Tetrahedron Lett.*, **2004** 45(42) 7915
- 15 Baleizao C, Corma A, Garcia H, Levya A, *J. Org. Chem.*, **2004** 69(2) 439
- 16 Corma A, Garcia H, Levya A, *Tetrahedron*, **2004** 60(38) 8553
- 17 Andrews S P, Stepan A F, Tanaka H, Ley S V, Smith M D, *Adv. Synth. Catal.*, **2005** 347 647
- 18 Shimizu K, Koizumi S, Hatamachi T, Yoshida H, Komai S, Kodama T, Kitayama Y, *J. Catal.*, **2004** 228(1) 141
- 19 Yamada Y M A, Takeda K, Takahashi H, Ikegami S, *J. Org. Chem.*, **2003** 68(20) 7733

Appendix I

Analysis of Mass-Transfer Effects

The understanding of effect of mass transfer is essential before any kinetic analysis of a multiphase reaction. In this case, the homogeneously catalyzed reaction is a *Gas-Liquid* system while; the heterogeneously catalyzed reaction involves a triphasic *Gas-Liquid-Solid* system. The aspects of gas-liquid, and gas-liquid-solid mass transfers are intricately guided by numerous system parameters, which may be evaluated in terms of the mass-transfer coefficients. The homogeneous catalyzed reactions involve one parameter (α_1), while for the heterogeneous catalyzed reactions, one gas-liquid mass transfer parameter (α_1) and a solid-liquid mass transfer parameter (α_2) are involved. The nullifying of existence of such transfer barriers is important to ascertain the regime of reaction, i.e. kinetic regime or mass transfer regime. Following the works of Ramachandran and Chaudhariⁱ, the gas-liquid and gas-liquid-solid mass transfer resistances become negligible when each of the parameters α_1 and α_2 are less than 0.1. The expression of α_1 for the homogeneous catalyzed carbonylation reaction is given as

$$\alpha_1 = \frac{R_{CO}}{K_l a_b C_{A^*}} < 0.1 \quad (i)$$

where, R_{CO} = Overall rate of carbonylation at highest temperature and catalyst concentration, $\text{kmol.m}^{-3}.\text{s}^{-1}$

K_l = Gas-liquid mass transfer coefficient, m.s^{-1}

a_b = Gas-liquid interfacial area per unit volume of reactor, m^{-1}

C_{A^*} = Saturation solubility of CO in liquid phase, kmol.m^{-3}

The expressions of α_1 and α_2 for a heterogeneous gas-liquid-solid reaction are given as

$$\alpha_1 = \frac{R_{CO}}{K_l a_b C_{A^*}} < 0.1 \quad (ii)$$

where, the variable terms are same as for (i), and

$$\alpha_2 = \frac{R_{CO}}{K_s a_p C_{A^*}} < 0.1 \quad (iii)$$

where, R_{CO} = Overall rate of carbonylation at highest temperature and catalyst concentration, $\text{kmol.m}^{-3}.\text{s}^{-1}$

K_s = Solid-liquid mass transfer coefficient, $m.s^{-1}$

a_p = Liquid-solid interfacial area, m^{-1}

C_{A^*} = Saturation solubility of CO in liquid phase, $kmol.m^{-3}$

Calculation of α_1 for homogeneous carbonylation reaction

Now, to evaluate the mass-transfer parameter α_1 for the homogeneous carbonylation reaction, we need to find the value of $K_1 a_b$ for our reaction, which is defined by Gholap et alⁱⁱ as follows,

$$K_1 a_b = 1.48 \times 10^{-3} \times (N)^{2.18} \times (V_g / V_l)^{1.88} \times (d_i / d_t)^{2.16} \times (h_1 / h_2)^{1.16} \quad (iv)$$

where, a_b : Gas liquid interfacial area per unit volume of reactor, m^2/m^3

d_i : Impeller Diameter, m

d_t : Tank Diameter, m

h_1 : Height of the impeller from the bottom, m

h_2 : Height of the liquid, m

K_1 : Liquid film mass transfer coefficient, $m.s^{-1}$

N : Speed of the agitation employed, Hz

V_g : Volume of the gas in the reactor, m^3

V_l : Volume of the liquid in the reactor, m^3

For the present case, the values of the different terms as measured, are given below.

$$d_i = 2.0 \text{ cm} \equiv 2 \times 10^{-2} \text{ m}$$

$$d_t = 3.2 \text{ cm} \equiv 3.2 \times 10^{-2} \text{ m}$$

$$V_g = 47 \text{ ml} \equiv 4.7 \times 10^{-5} \text{ m}^3$$

$$V_l = 25 \text{ ml} \equiv 2.5 \times 10^{-5} \text{ m}^3$$

$$\text{Height of the tank: } 5.7 \text{ cm} \equiv 5.7 \times 10^{-2} \text{ m}$$

$$\text{Height of the Impeller from the Head: } 4.7 \text{ cm} \equiv 4.7 \times 10^{-2} \text{ m}$$

$$h_1: \text{Height of the tank} - \text{Height of the Impeller from the head} = 5.7 - 4.7 \text{ cm} \equiv 1 \times 10^{-2} \text{ m}$$

As the volume of reactor bomb is 50 mL and our charge is of 25 mL, the height of the liquid will be 1/2 of the total height of the bomb.

$$\text{Hence, } h_2 = 5.7/2 \text{ cm.} = 2.85 \text{ cm} \equiv 2.85 \times 10^{-2} \text{ m}$$

Therefore,

$$K_1 a_b = 1.48 \times 10^{-3} \times (15)^{2.18} \times \left(\frac{47}{25}\right)^{1.88} \times \left(\frac{2}{3.2}\right)^{2.16} \times \left(\frac{1}{2.85}\right)^{1.16} \text{ s}^{-1} \quad (v)$$

$$\text{or, } K_1 a_b = 0.191 \text{ s}^{-1}$$

For calculating the value of α_1 , R_{CO} and C_{A^*} were necessary, and these were calculated as $R_{CO} = 1.15837 \times 10^{-4} \text{ kmol.m}^{-3}.\text{s}^{-1}$, and $C_{A^*} = 0.03424 \text{ kmol.m}^{-3}$

So,

$$\alpha_1 = \frac{1.15837 \times 10^{-4}}{0.191 \times 0.03424} = 0.0177 \ll 0.1$$

Therefore, it may be concluded that the gas liquid mass-transfer is negligible under the set of reaction parameters chosen for the kinetic study of carbonylation of IBS using the homogeneous catalyst.

Calculation of α_1 and α_2 for heterogeneous carbonylation reaction

In case of the heterogeneously catalyzed reaction, the calculation of α_1 involved the same terms as for the homogeneous reaction, only with a difference of the agitation speed (N) and R_{CO} values. The $K_1 a_b$ term may be calculated considering $N=16.67 \text{ Hz}$ and $R_{CO} = 3.4751 \times 10^{-5} \text{ kmol.m}^{-3}.\text{s}^{-1}$

$$K_1 a_b = 1.48 \times 10^{-3} \times (16.67)^{2.18} \times \left(\frac{47}{25}\right)^{1.88} \times \left(\frac{2}{3.2}\right)^{2.16} \times \left(\frac{1}{2.85}\right)^{1.16} \text{ s}^{-1} \quad (\text{vi})$$

$$\text{or, } K_1 a_b = 0.2337 \text{ s}^{-1}$$

Using this value of $K_1 a_b$, the value of α_1 was calculated as

$$\alpha_1 = \frac{3.4751 \times 10^{-5}}{0.2337 \times 0.03424} = 0.004681 \ll 0.1$$

Thus, the gas liquid mass-transfer was negligible for the heterogeneous catalytic carbonylation reaction.

In order to analyze the solid liquid mass transfer phenomenon, the term α_2 (expressed before) is crucial. For this calculation we needed to know the value of solid-liquid mass transfer coefficient, K_s which was calculated following Sano et al as,

$$\frac{K_s d_p}{D_m F_c} = 2 + 0.4 \left[\frac{e(d_p)^4 \rho_l^3}{\mu_l^3} \right]^{0.25} \left[\frac{\mu_l}{\rho_l D_m} \right]^{0.333} \quad (\text{vii})$$

where,

K_s : Liquid solid mass transfer coefficient, m.s^{-1}

e : Energy supplied to the liquid

F_c : Shape factor. *assumed to be unity*

d_p : Particle diameter, m

ρ_l : Density of liquid, kg.m^{-3}

μ_l : Viscosity of liquid, Poise

D_m : Molecular diffusivity, $\text{m}^2.\text{s}^{-1}$

Of these different parameters, the molecular diffusivity, D_m was obtained from the relation defined by Wilke and Chang as,

$$D_m = \frac{7.4 \times 10^{-8} T (\chi M_w)^{1/2}}{\mu_l \nu_M^{0.6}} \quad (\text{viii})$$

Where,

T: Temperature, K

χ : Association factor. = 1

M_w : Molecular weight of solvent, g.mol^{-1}

ν_M : Molar volume of solute (gas), $\text{cm}^3.\text{mol}^{-1}$

And, energy supplied, e to the liquid, is calculated using the formula by Calderbank et al as

$$e = \frac{N_p N^3 d_i^5 \psi}{\rho_l V_l} \quad (\text{ix})$$

Where, N_p : Power number.

N: Agitation speed, Hz

d_i : Diameter of agitator, m

ρ_l : Density of liquid, Kg/m^3

V_l : Volume of the liquid, m^3

ψ : Correction factor for the presence of gas bubbles

And the value of ψ is expressed by the following relation

$$\psi = 1.0 - 1.26 \left[\frac{Q_g}{N d_i^3} \right], \text{ for } \left[\frac{Q_g}{N d_i^3} \right] < 3.5 \times 10^{-2} \quad (\text{x})$$

where, Q_g is the volumetric flow of gas, and for the batch mode of reaction, this can be calculated as

$$Q_g = r_{\max} \times V_M \times V_l \quad (\text{xi})$$

Where,

r_{\max} = highest rate of carbonylation, $\text{kmol.m}^{-3}.\text{s}^{-1}$; or, $r_{\max} = 3.4751 \times 10^{-5} \text{ kmol.m}^{-3}.\text{s}^{-1}$

V_M = molar gas volume, $\text{m}^3 \cdot \text{kmol}^{-1}$

V_l = volume of liquid, m^3 , or, $V_l = 25 \times 10^{-6} \text{ m}^3$

And V_M is given by the relation $V_M = \frac{\text{volume of phase}}{\text{Moles of gas at constant pressure}} = V/n = \frac{RT}{P}$

Calculation of V_M

$$V_M = \frac{RT}{P} = \frac{8.314 \text{ N.m.mol}^{-1}\text{K}^{-1} \times 388 \text{ K}}{(800/14.7) \times 10^5 \text{ N.m}^{-2}} = 0.597376 \text{ m}^3 \cdot \text{kmol}^{-1}$$

Therefore, Q_g may be calculated as,

$$Q_g = 3.4751 \times 10^{-5} \times 0.597376 \times 25 \times 10^{-6} \text{ m}^3 \cdot \text{s}^{-1}$$

or, $Q_g = 5.1898 \times 10^{-10} \text{ m}^3 \cdot \text{s}^{-1}$

considering 20% excess value for the Q_g , $Q_g' = 6.2278 \times 10^{-10} \text{ m}^3 \cdot \text{s}^{-1}$

Calculation of ψ

$$\Psi = 1.0 - 1.26 \left[\frac{6.2278 \times 10^{-10}}{16.67 \times (2 \times 10^{-2})^3} \right]$$

$\psi = 0.999994 \approx 1$

Calculation of e

N_p : Power number = 6.3

N : Agitation speed, = 16.67 Hz

d_i : Diameter of agitator, = $2 \times 10^{-2} \text{ m}$

ρ_l : Density of liquid = 800 kg/m^3

V_l : Volume of the liquid = $25 \times 10^{-6} \text{ m}^3$

ψ : Correction factor for the presence of gas bubbles = 1

The value of e is calculated as

$$e = \frac{6.3 \times (16.67)^3 \times (2 \times 10^{-2})^5 \times 1}{800 \times 25 \times 10^{-6}} = 0.00467$$

Calculation of D_M

Following the equation viii, D_M is calculated using the following parameters.

T : Temperature, 388 K

χ : Association factor. = 1

M_w : Molecular weight of solvent, 72.11 g.mol^{-1}

v_M : Molar volume of solute (gas), $30.4 \text{ cm}^3 \cdot \text{mol}^{-1}$

Therefore,

$$D_M = \frac{7.4 \times 10^{-8} \times 388 \times (1 \times 72.11)^{0.5}}{0.43 \times (30.4)^{0.6}} = 7.602 \times 10^{-5} \text{ cm}^2 \cdot \text{s}^{-1}$$

$$= 7.602 \times 10^{-9} \text{ m}^2 \cdot \text{s}^{-1}$$

Calculation of K_S

Following the equation vii, the value of the K_S is evaluated using the following terms as,

K_S : Liquid solid mass transfer coefficient, $\text{m} \cdot \text{s}^{-1}$

e : Energy supplied to the liquid = 0.00467

F_c : Shape factor. *assumed to be unity*

d_p : Particle diameter = $450 \times 10^{-9} \text{ m}$

ρ_l : Density of liquid = $800 \text{ kg} \cdot \text{m}^{-3}$

μ_l : Viscosity of liquid = $0.043 \times 10^{-3} \text{ Pa} \cdot \text{s}$

D_m : Molecular diffusivity = $7.602 \times 10^{-9} \text{ m}^2 \cdot \text{s}^{-1}$

$$\frac{K_S \times 450 \times 10^{-9}}{7.602 \times 10^{-9} \times 1} = 2 + 0.4 \left[\frac{0.00467 \times (450 \times 10^{-9})^4 \times 800^3}{(0.043 \times 10^{-3})^3} \right]^{0.25} \times \left[\frac{0.043 \times 10^{-3}}{800 \times 7.602 \times 10^{-9}} \right]^{0.33}$$

or, $K_S = 0.0342 \text{ m} \cdot \text{s}^{-1}$

Calculations of a_p

The liquid-solid interfacial area, a_p can be obtained from the equation as follows.

$$a_p = \frac{6w}{\rho_p d_p} \quad (\text{xii})$$

where, w : weight of catalyst = $4 \text{ kg} \cdot \text{m}^{-3}$

d_p : diameter of particle = $450 \times 10^{-9} \text{ m}$

ρ_p : density of the liquid phase = $843 \text{ kg} \cdot \text{m}^{-3}$

therefore,

$$a_p = \frac{6 \times 4}{843 \times 450 \times 10^{-9}} = 63266 \text{ m}^{-1}$$

Now, to evaluate the liquid–solid resistances, the parameter α_2 needed to be calculated as in equation iii, where,

R_{CO} : Overall rate of carbonylation at highest temperature and catalyst concentration, = $3.4751 \times 10^{-5} \text{ kmol.m}^{-3}.\text{s}^{-1}$

K_s : Solid-liquid mass transfer coefficient, 0.0342 m.s^{-1}

a_p = Liquid-solid interfacial area, 63266 m^{-1}

C_{A^*} = Saturation solubility of CO in liquid phase, $0.03424 \text{ kmol.m}^{-3}$

Therefore,

$$\alpha_2 = \frac{3.4751 \times 10^{-5}}{0.0342 \times 63266 \times 0.03424} = 4.679 \times 10^{-7} \lll 0.001$$

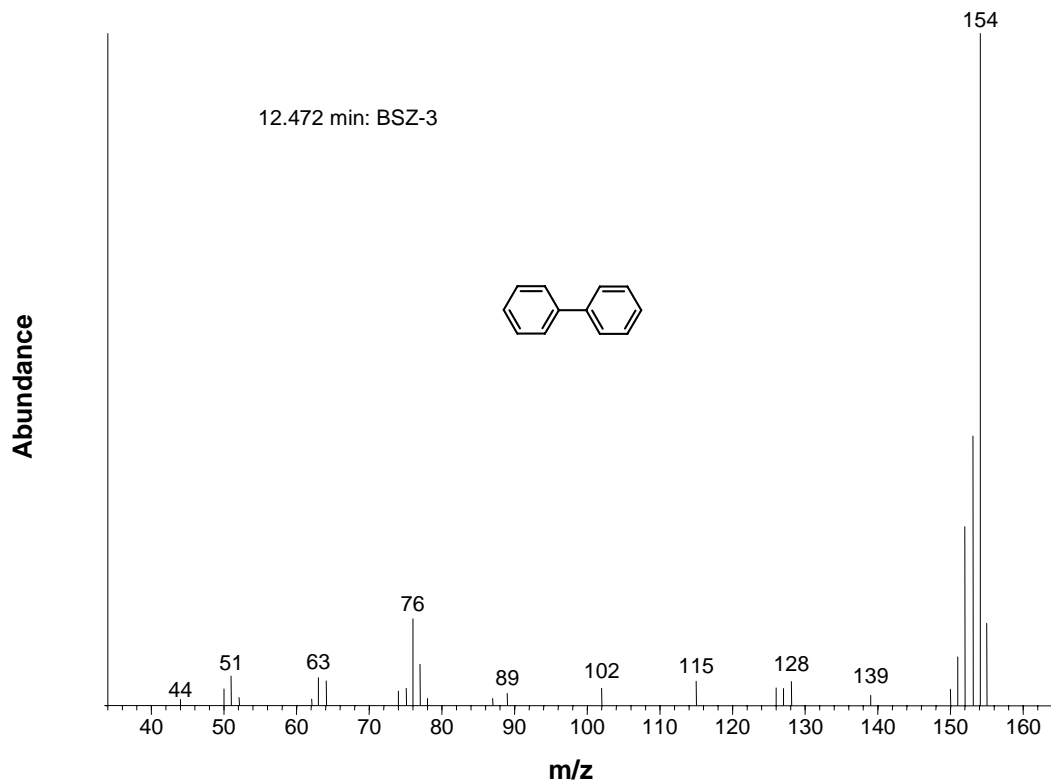
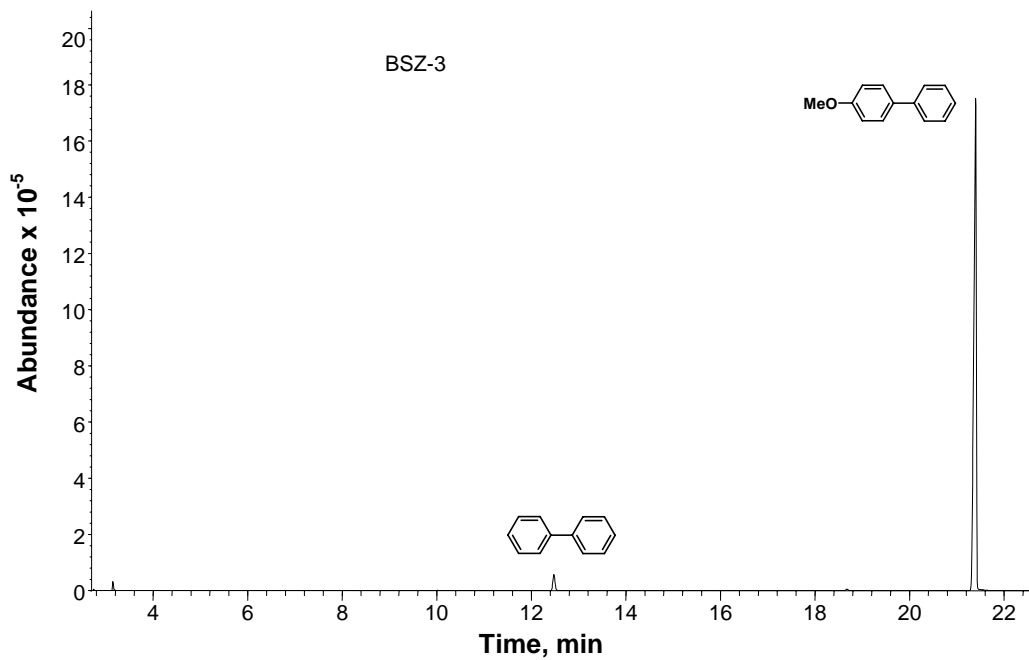
Hence, under the heterogeneous catalyst system, solid-liquid mass transfer phenomenon is negligible for the carbonylation reaction.

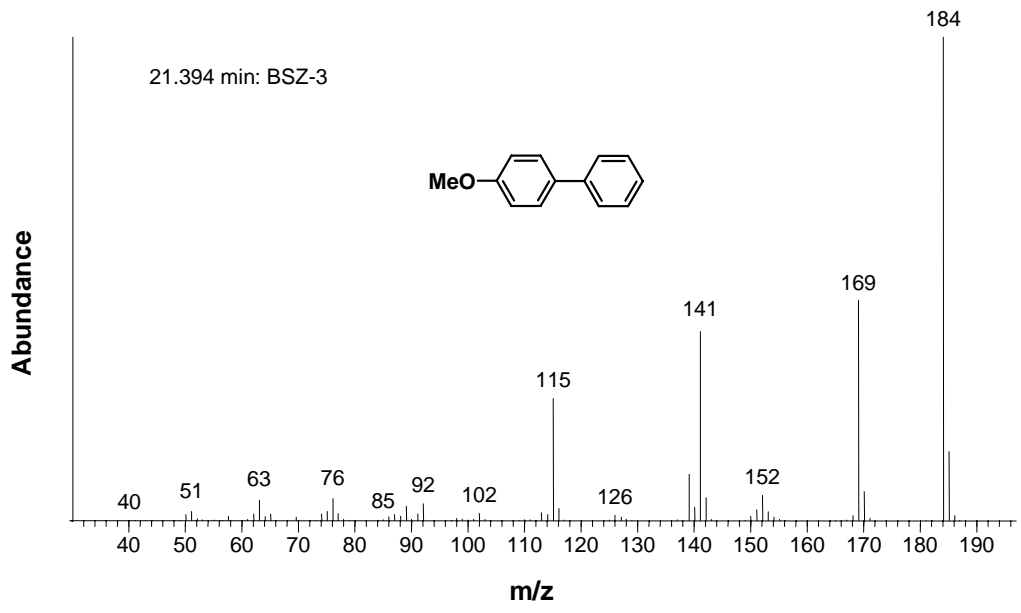
i Ramachandran P A, Chaudhari R V, *Three Phase Catalytic Reactors*, Gordon and Breach, NewYork, **1983**

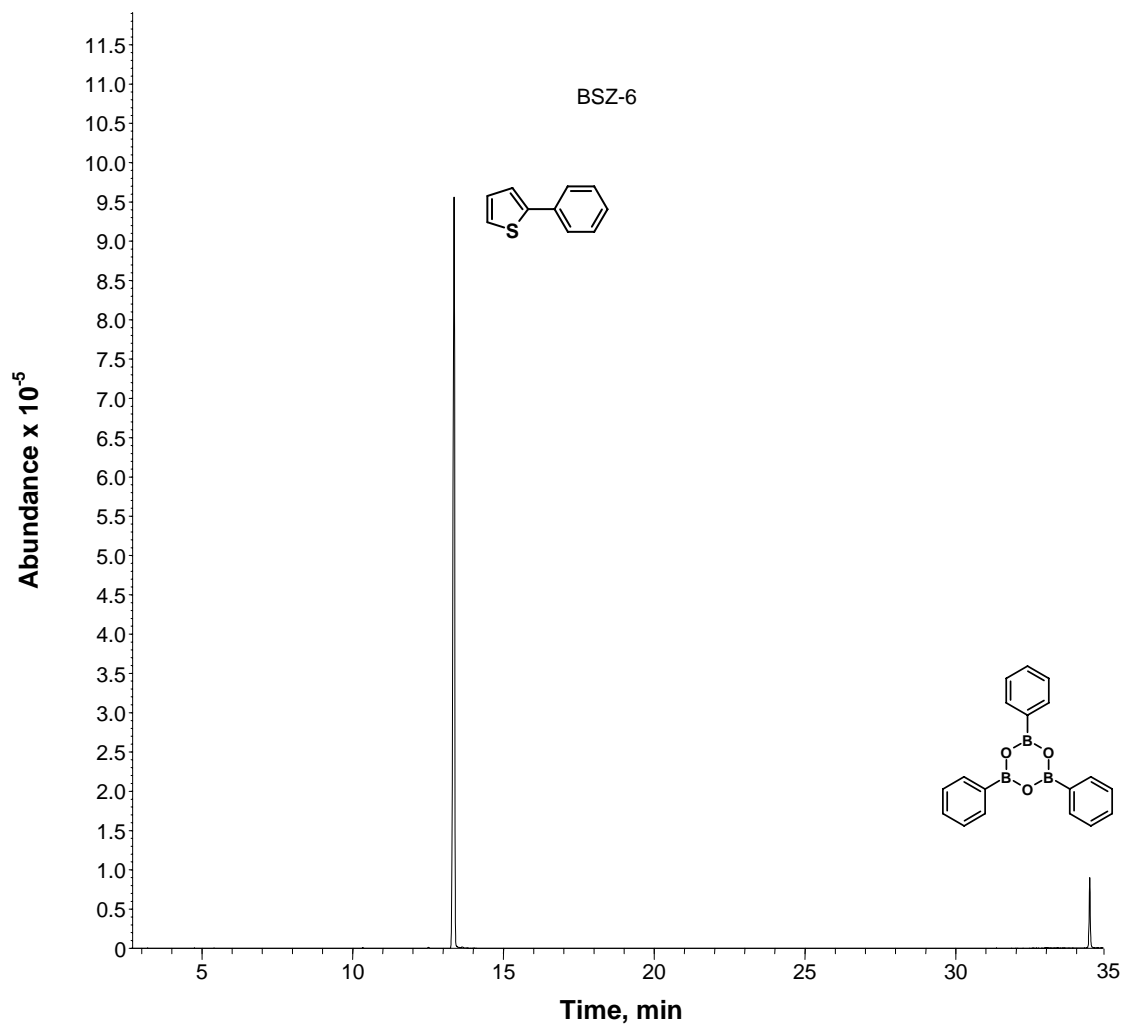
ii Chaudhari R V, Gholap R V, Emig G, Hofmann H, *Can. J. Chem. Eng.*, **1987** 65 744

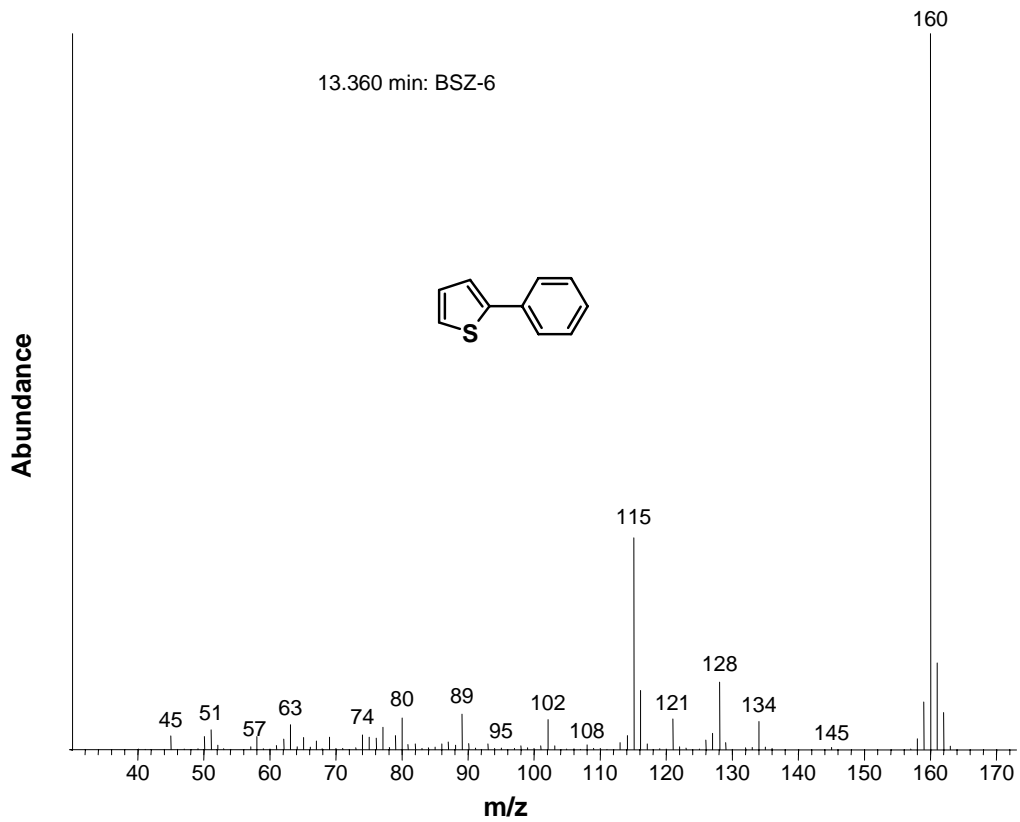
Appendix II

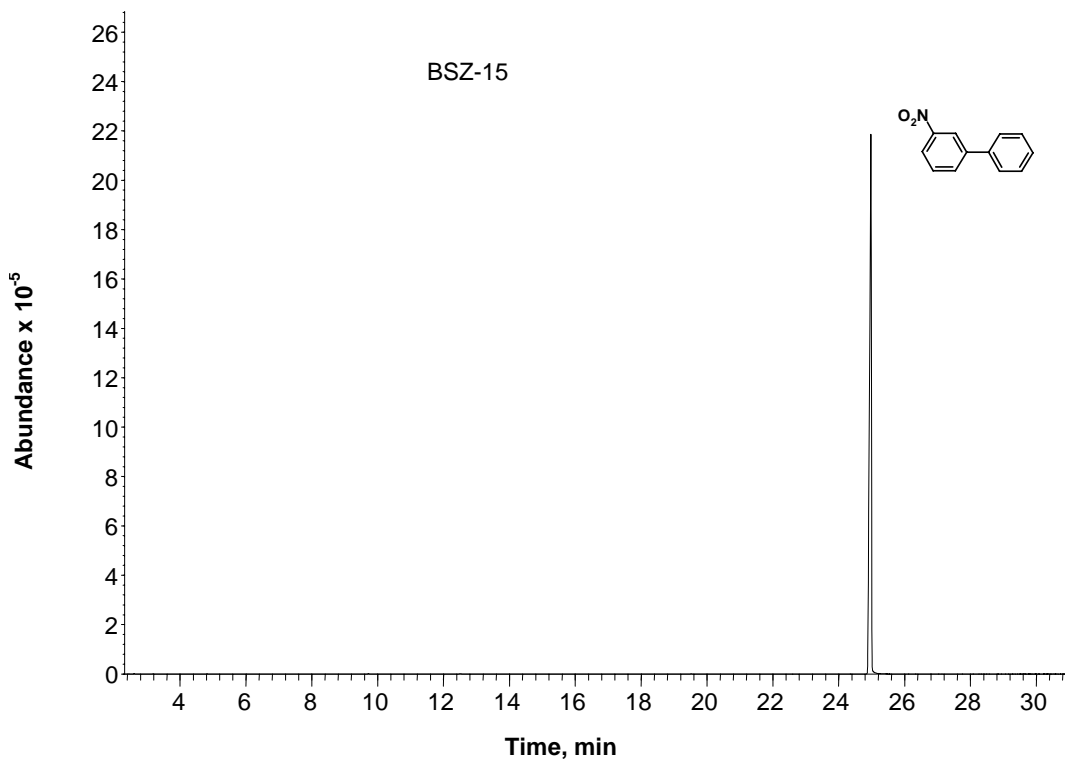
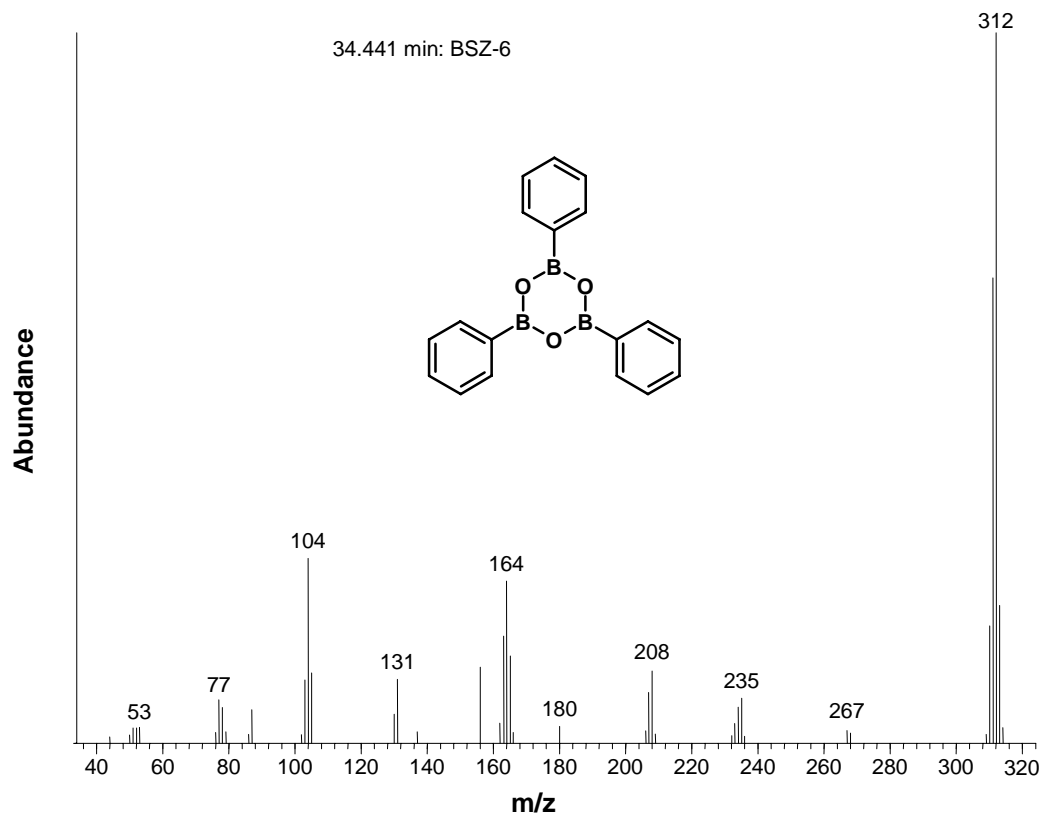
GC-MS data of the compounds of Table 5.4, in the order of their appearance

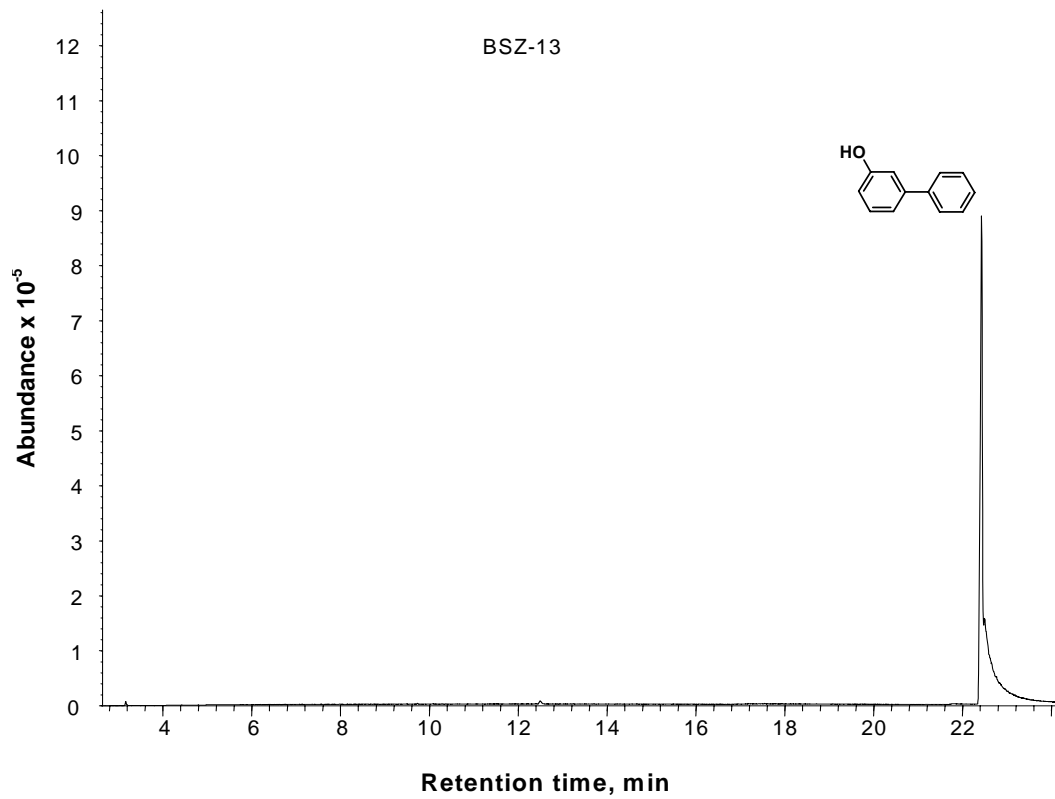
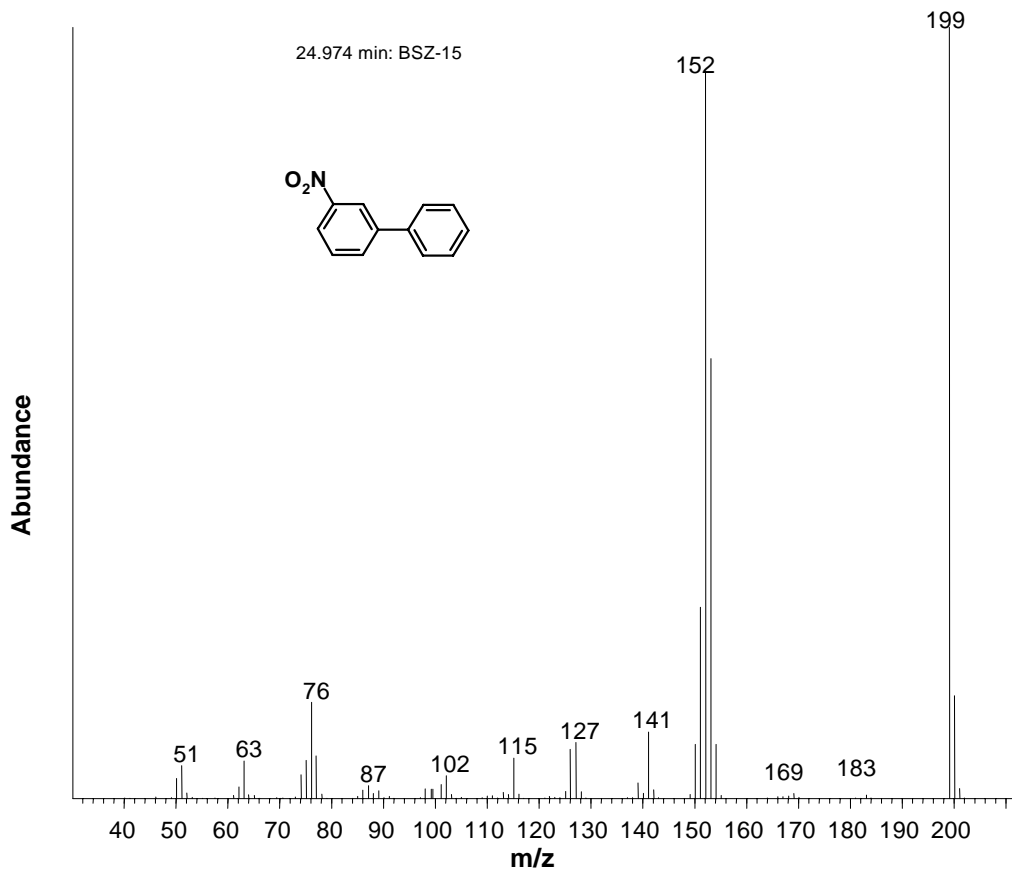


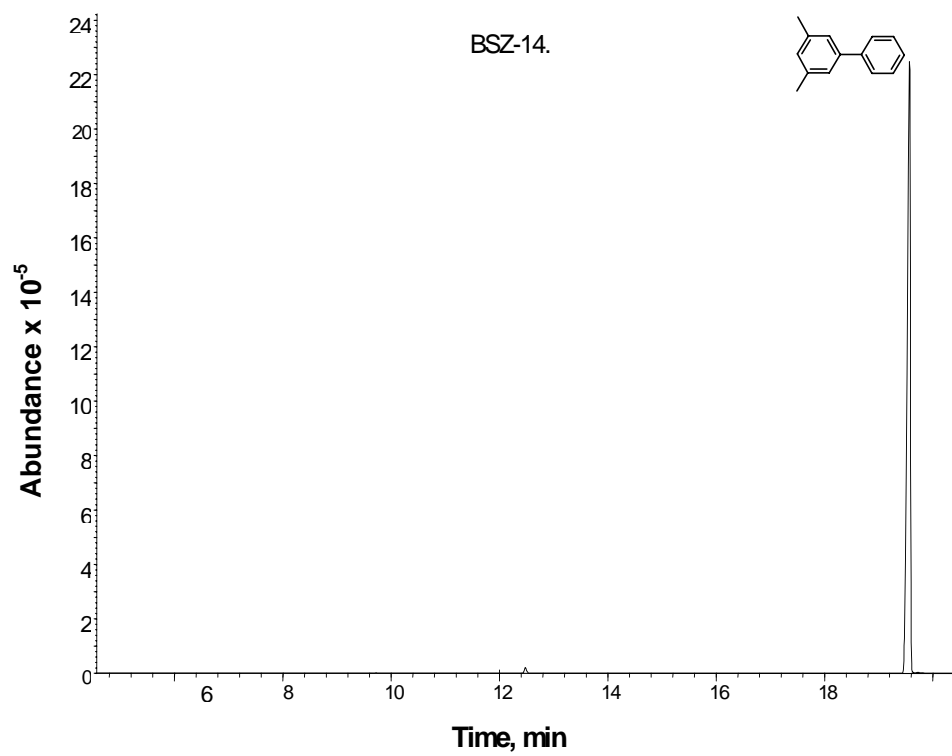
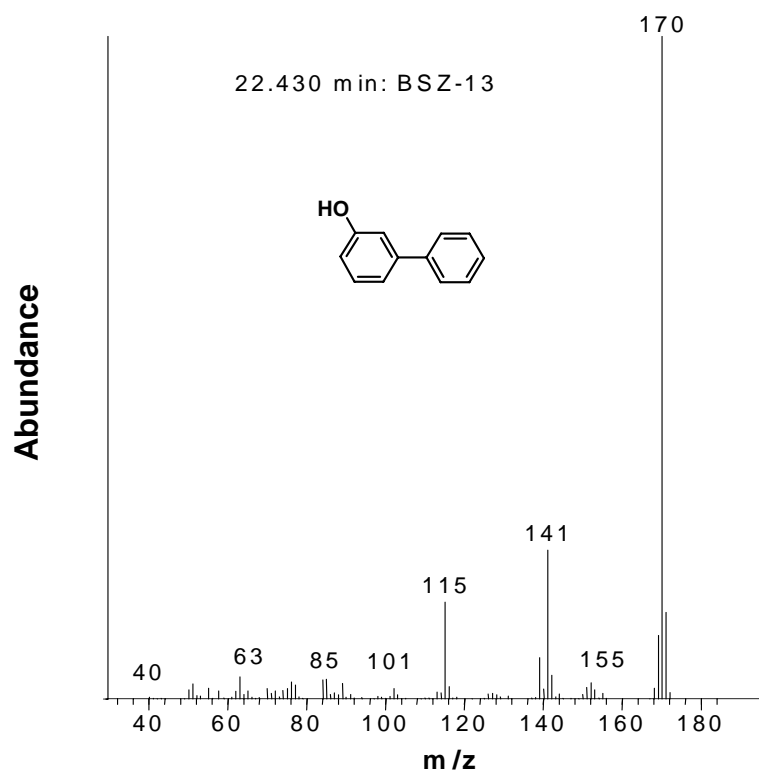


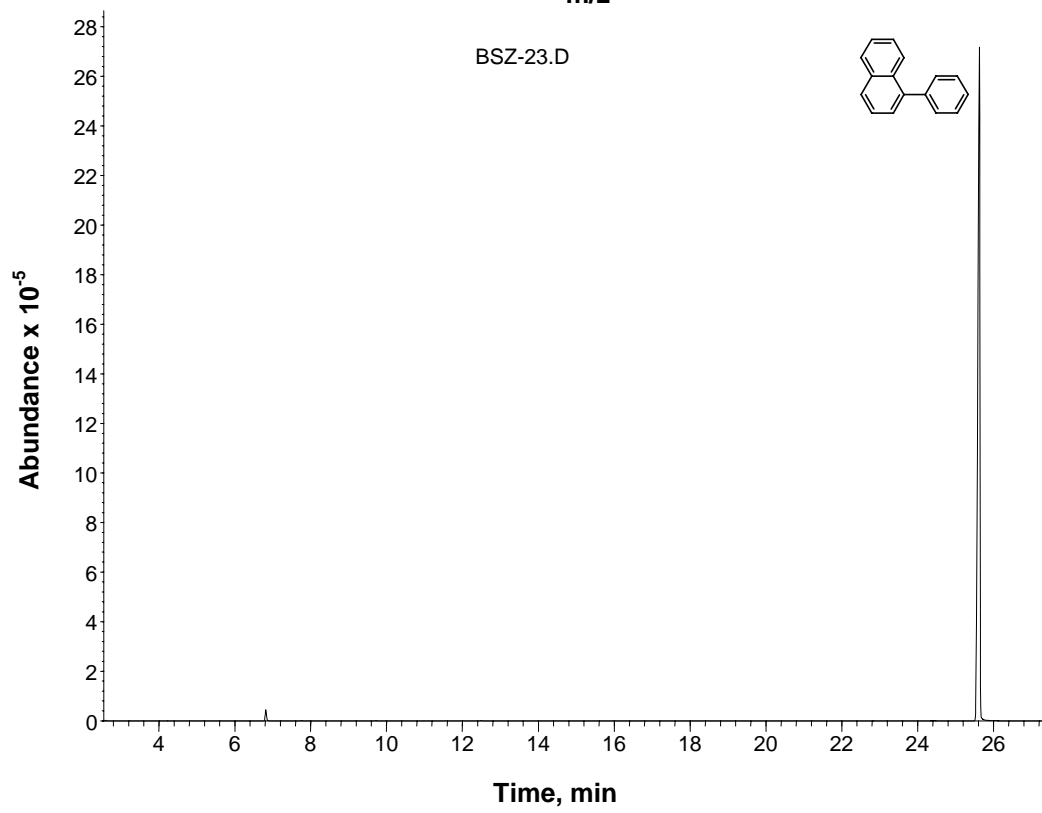
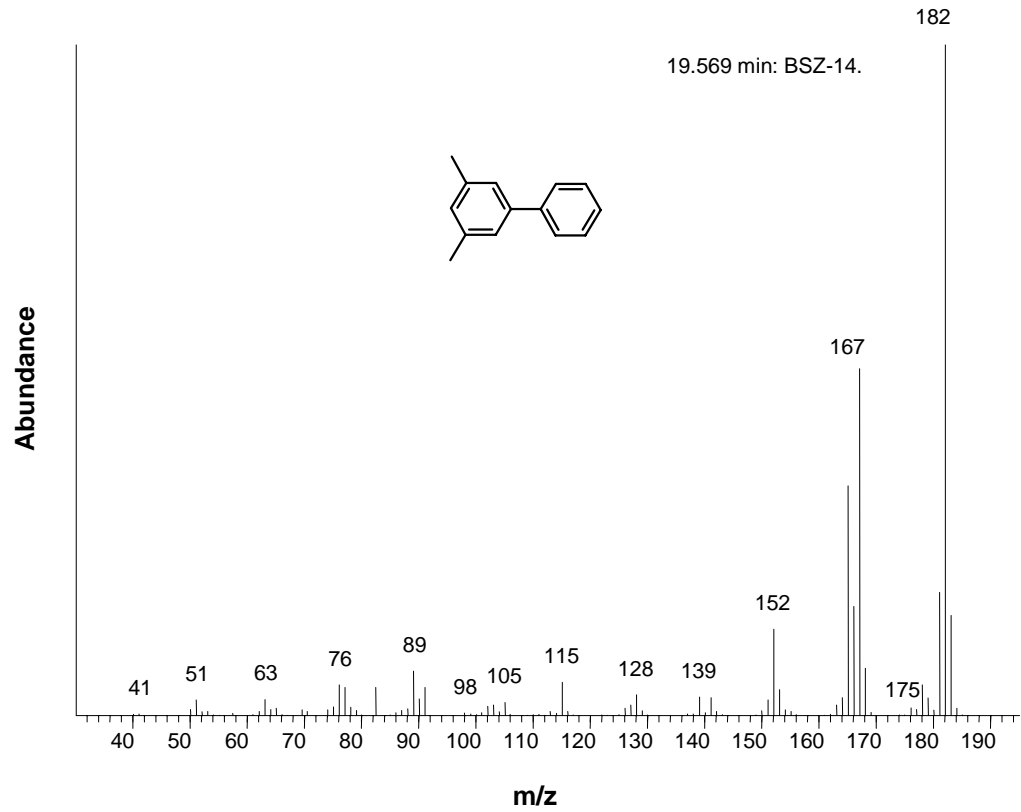


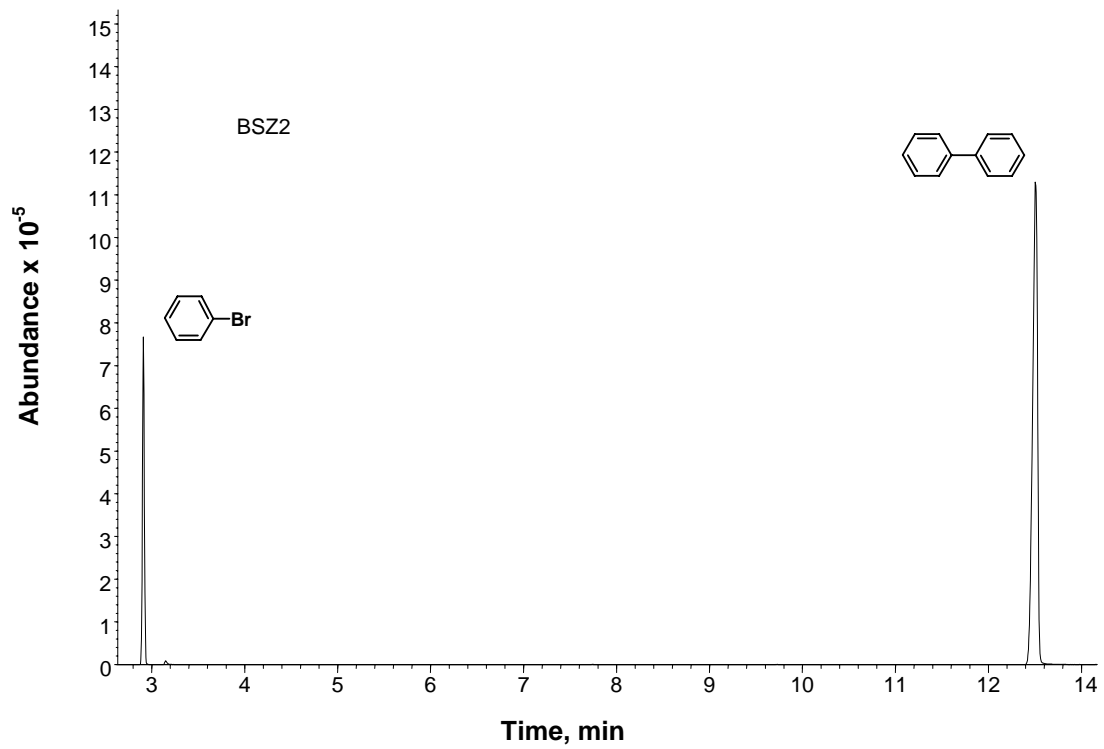
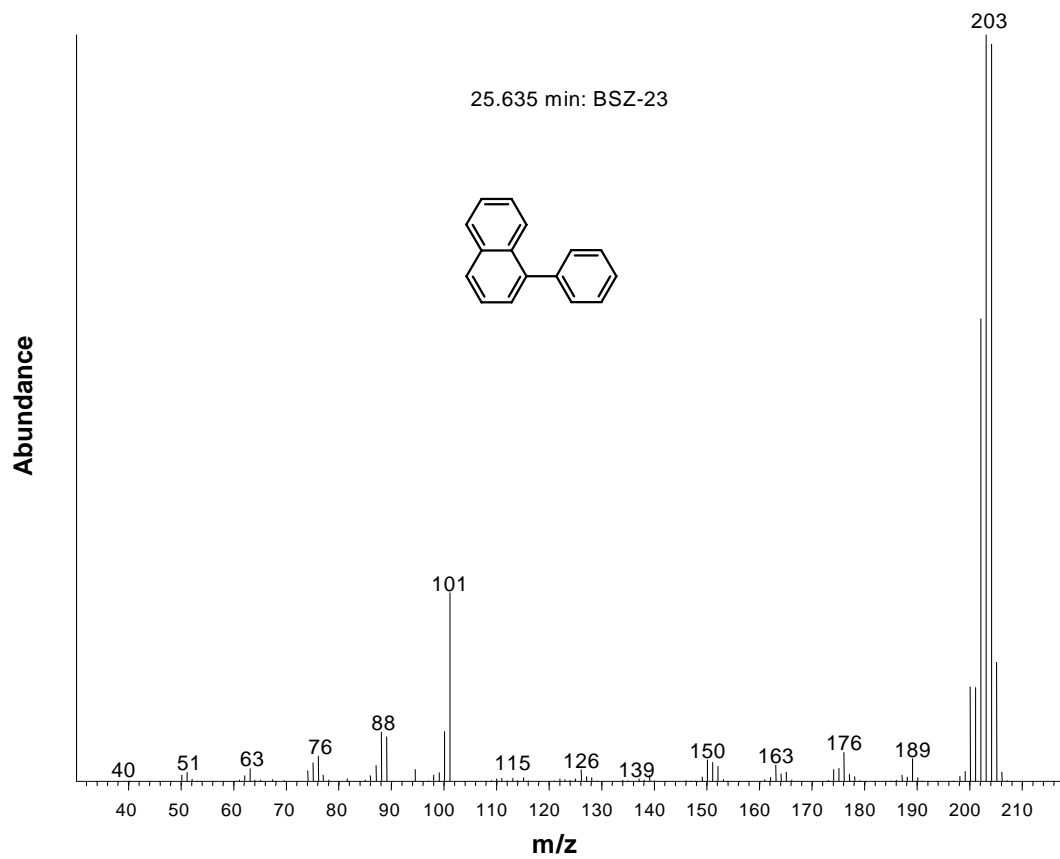


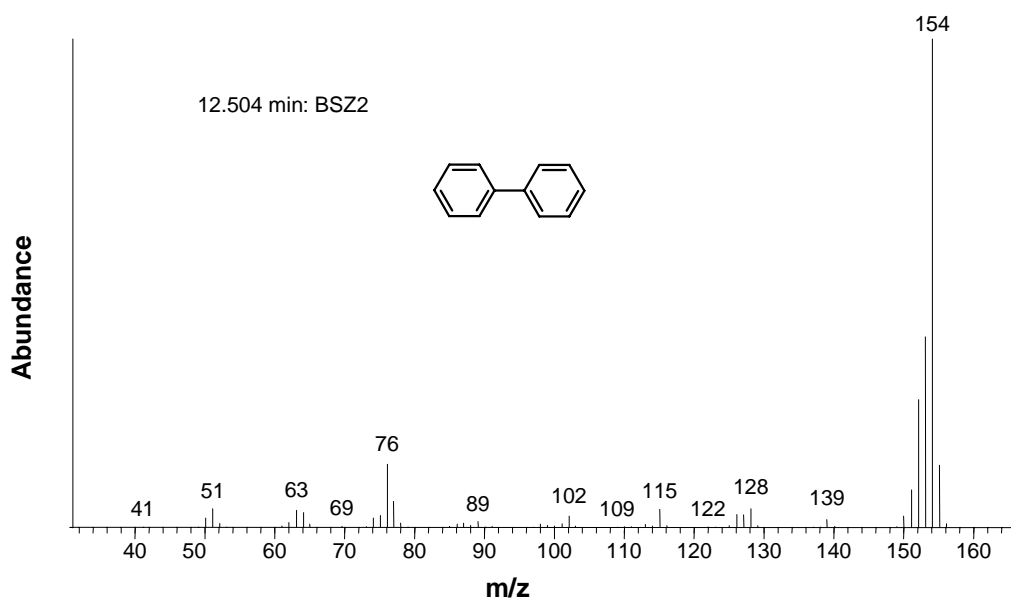
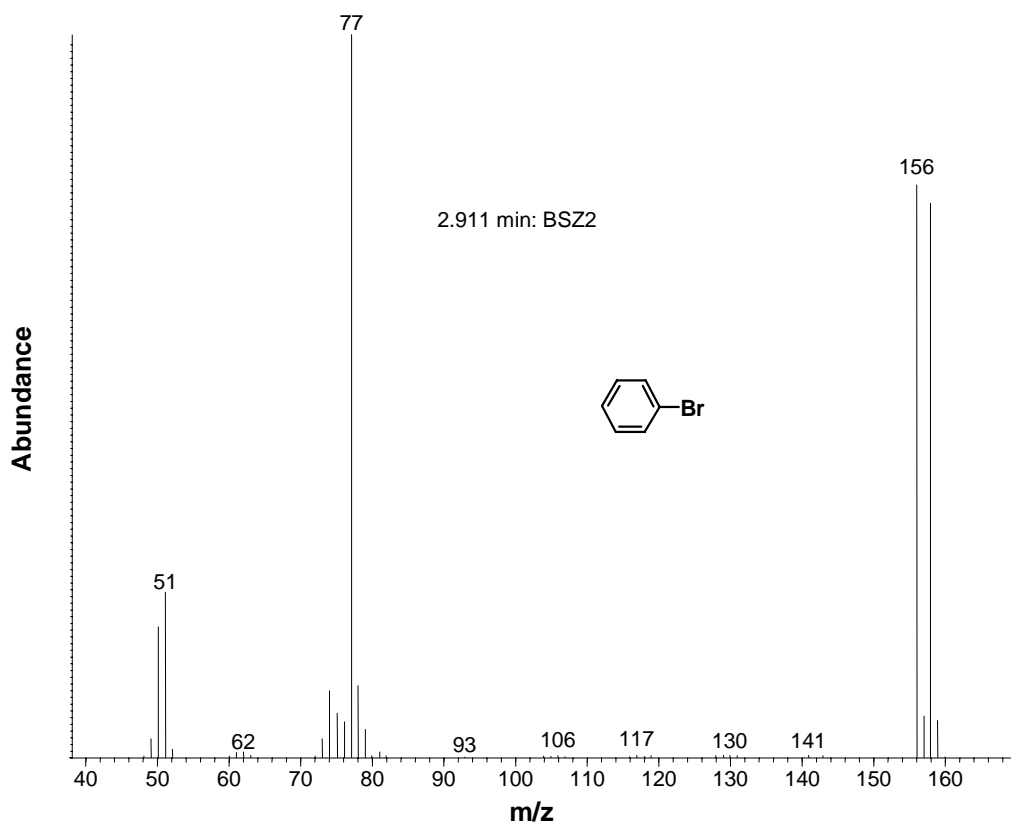


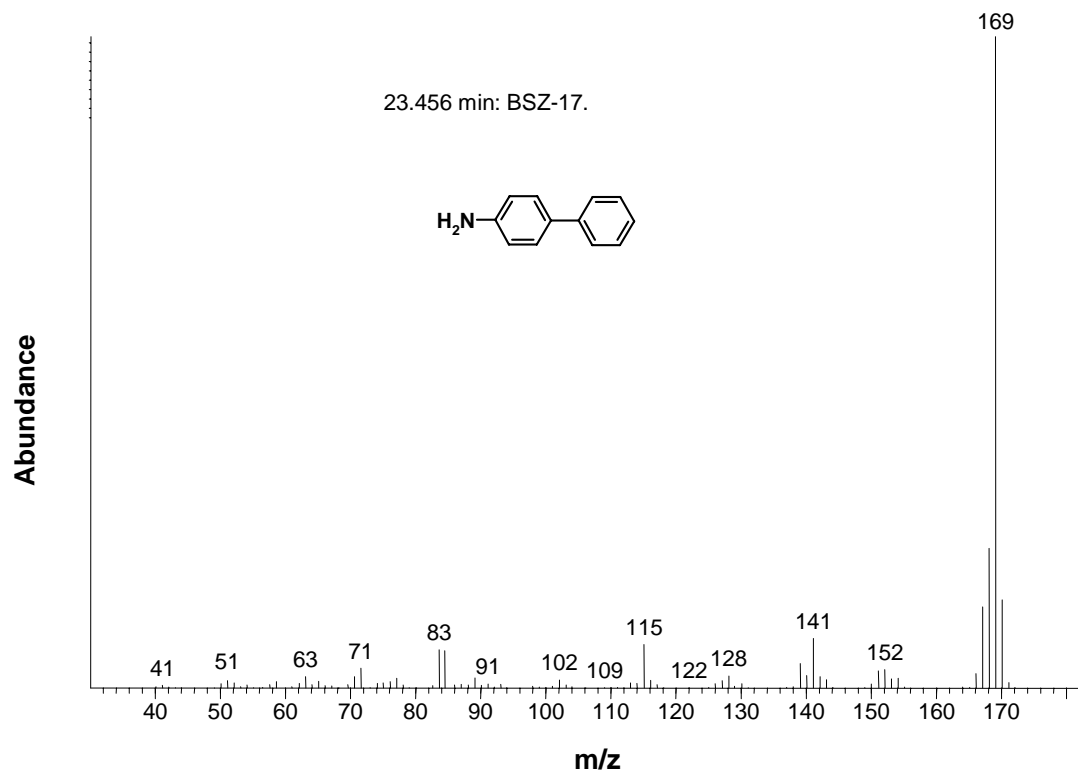
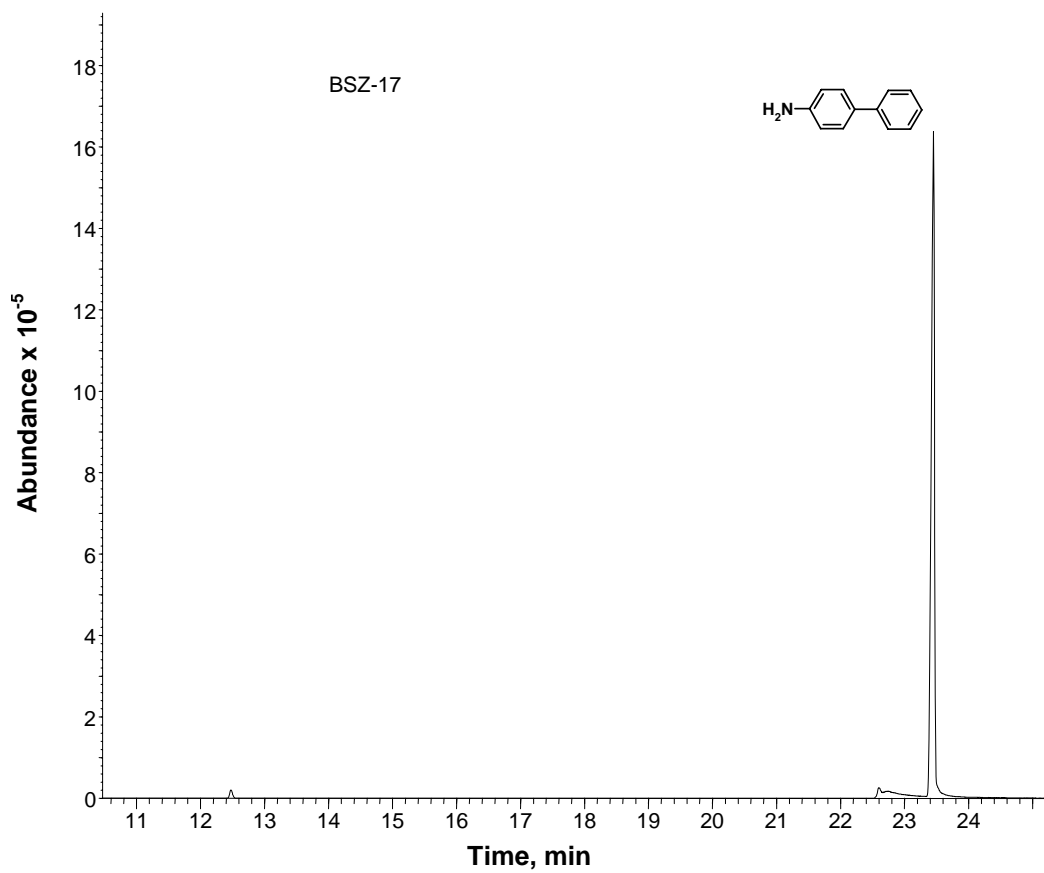


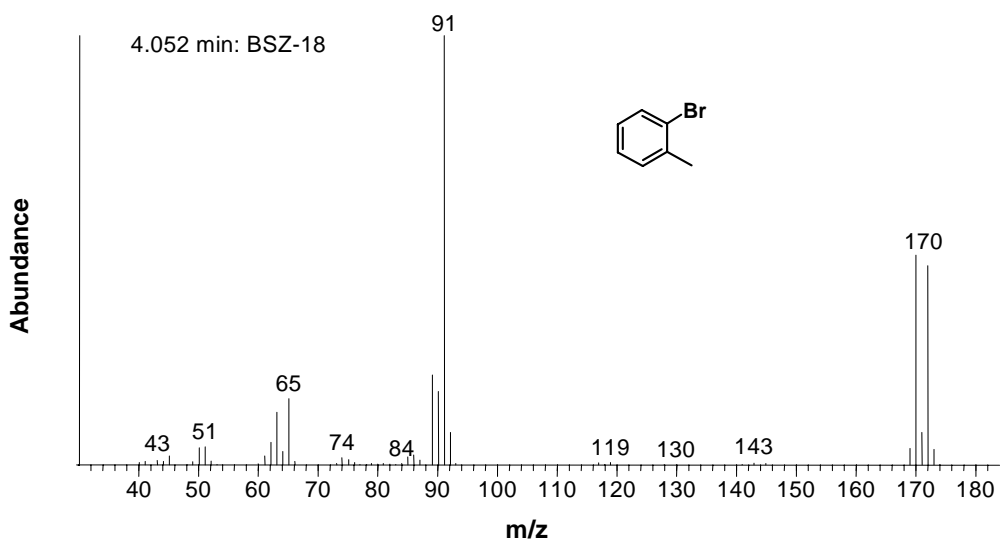
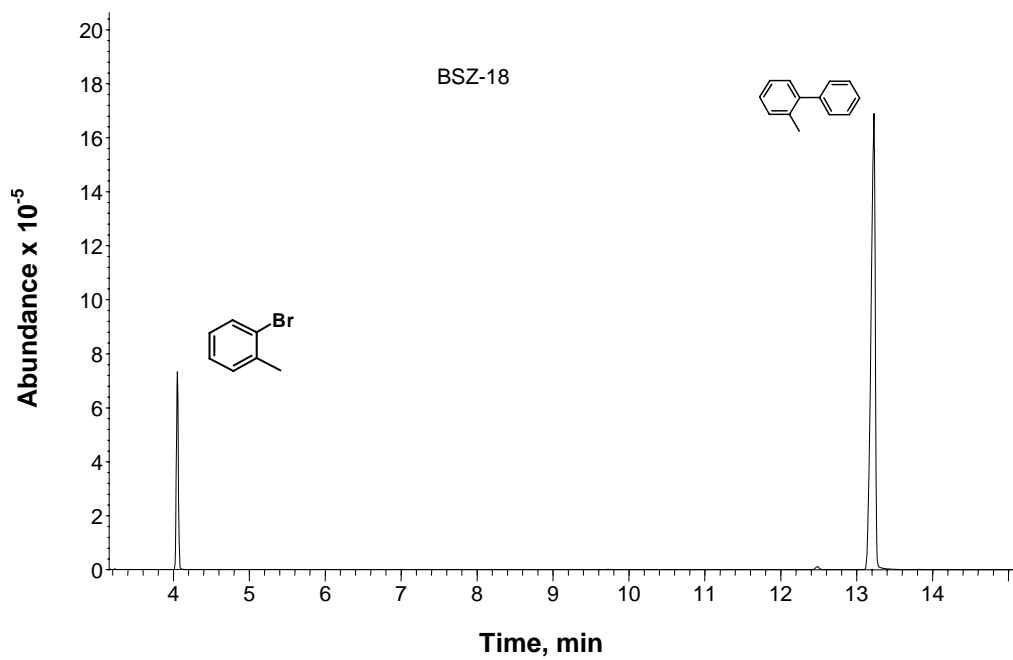


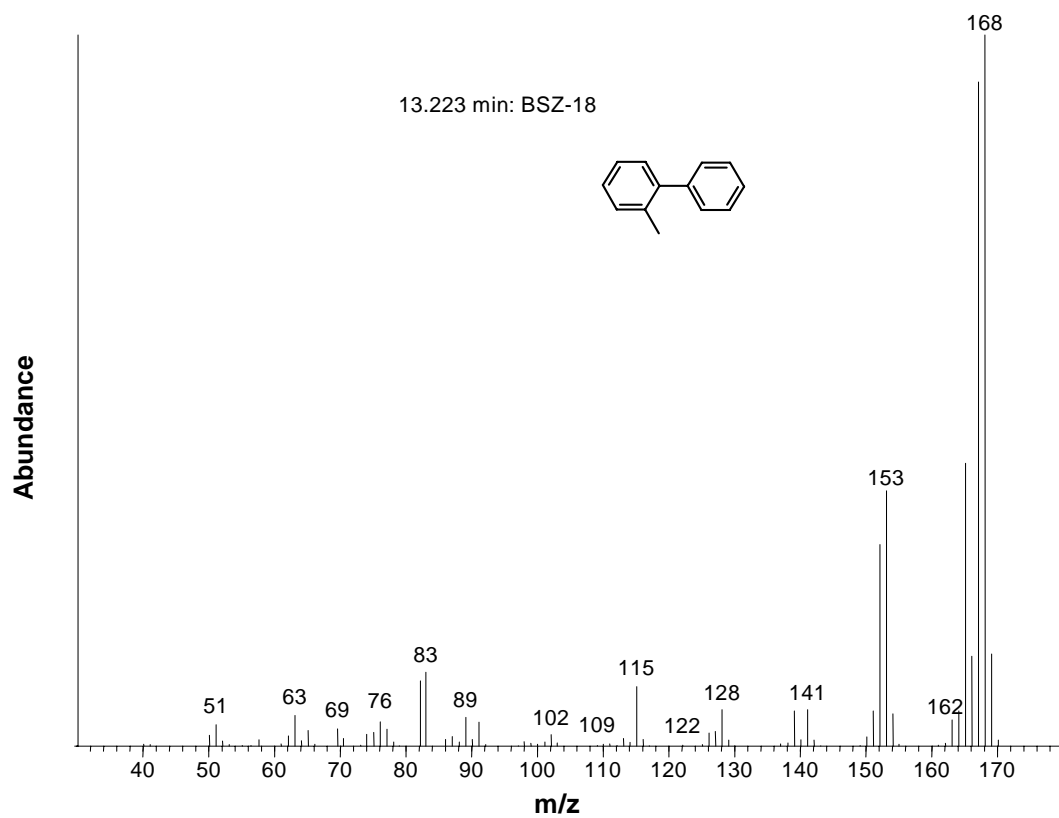


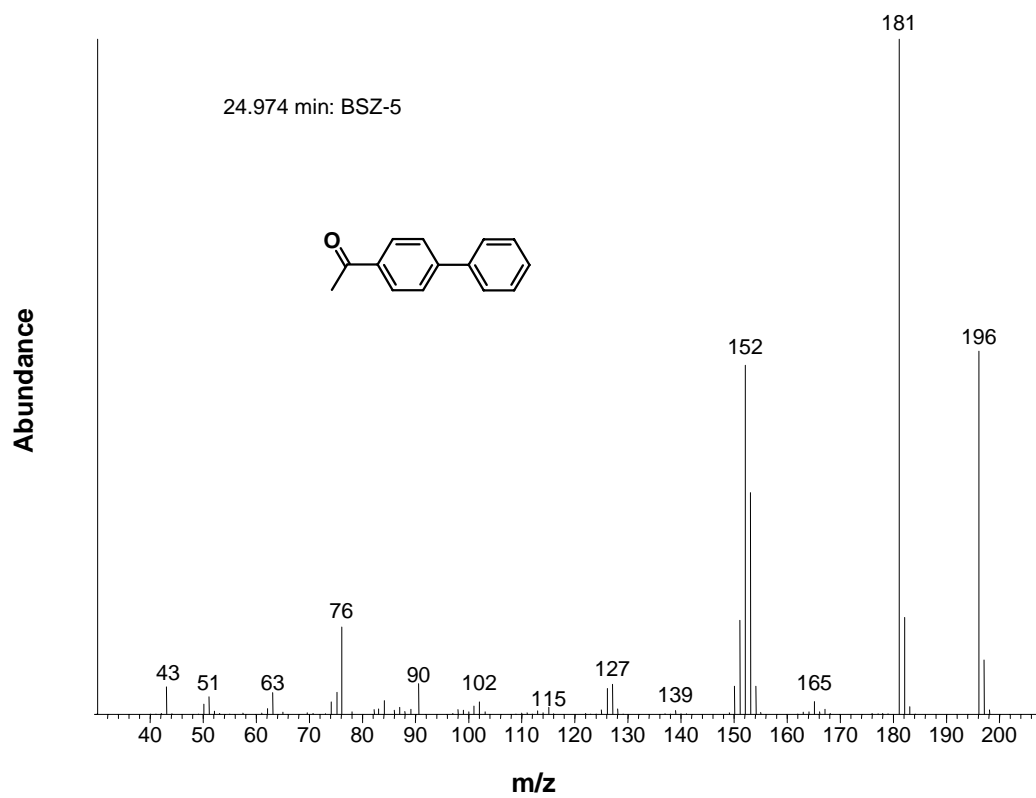
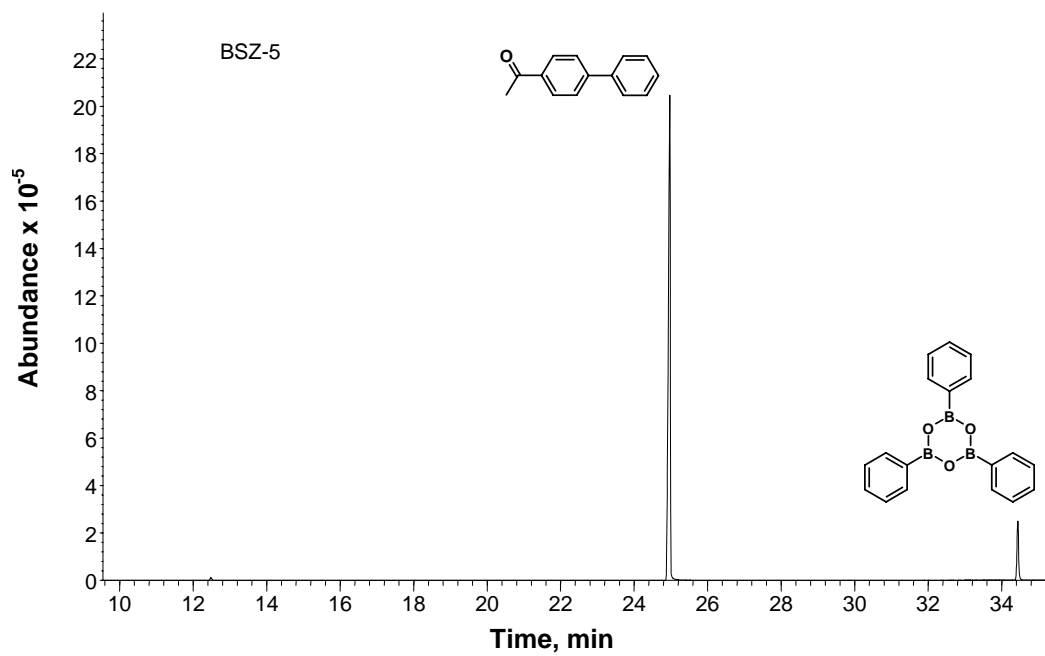


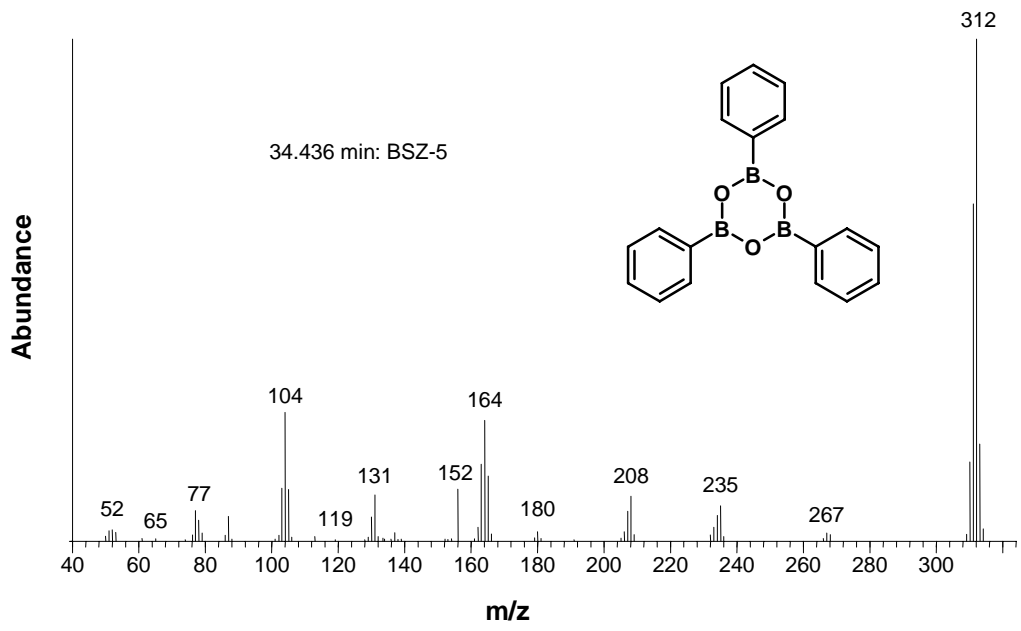


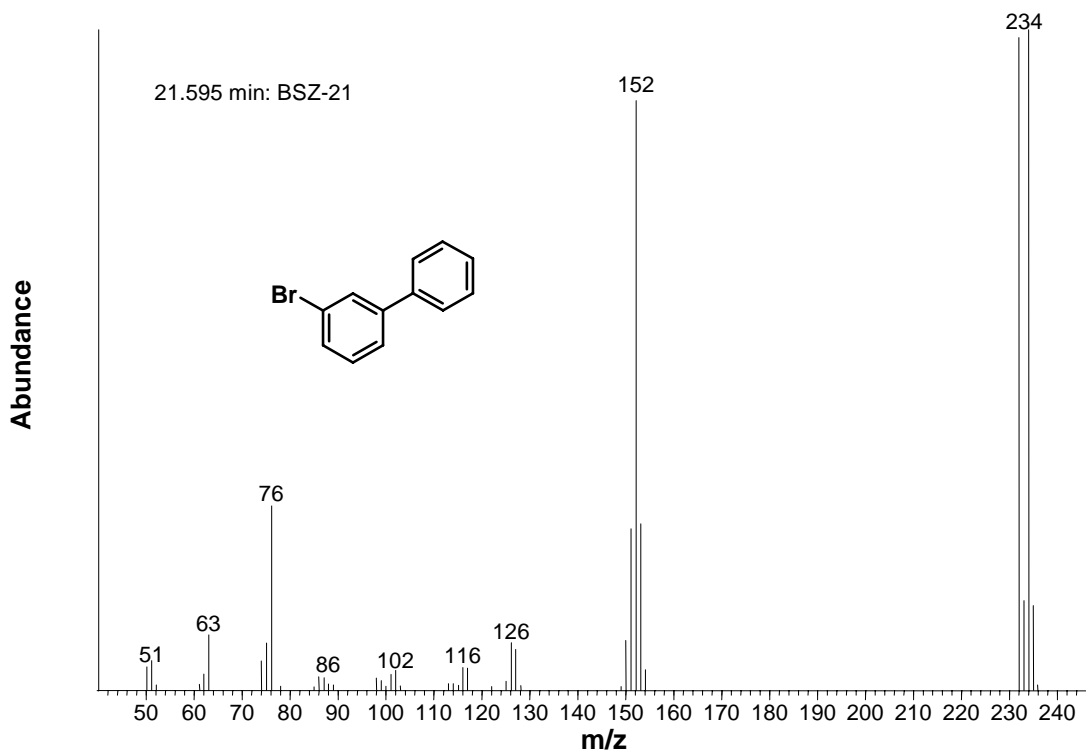
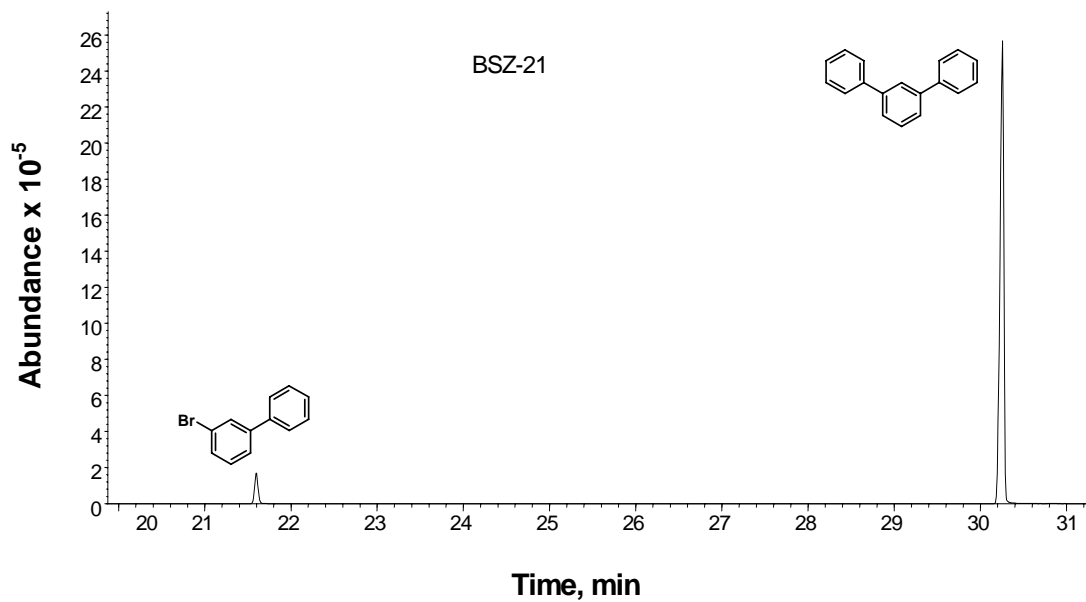


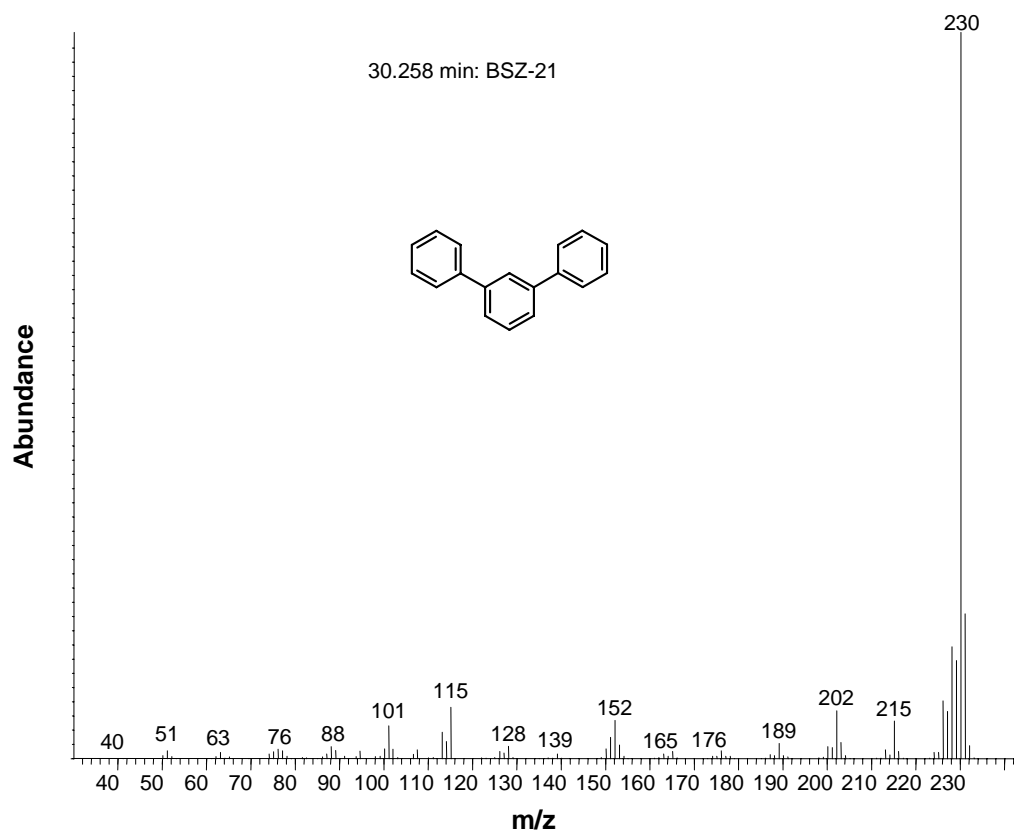


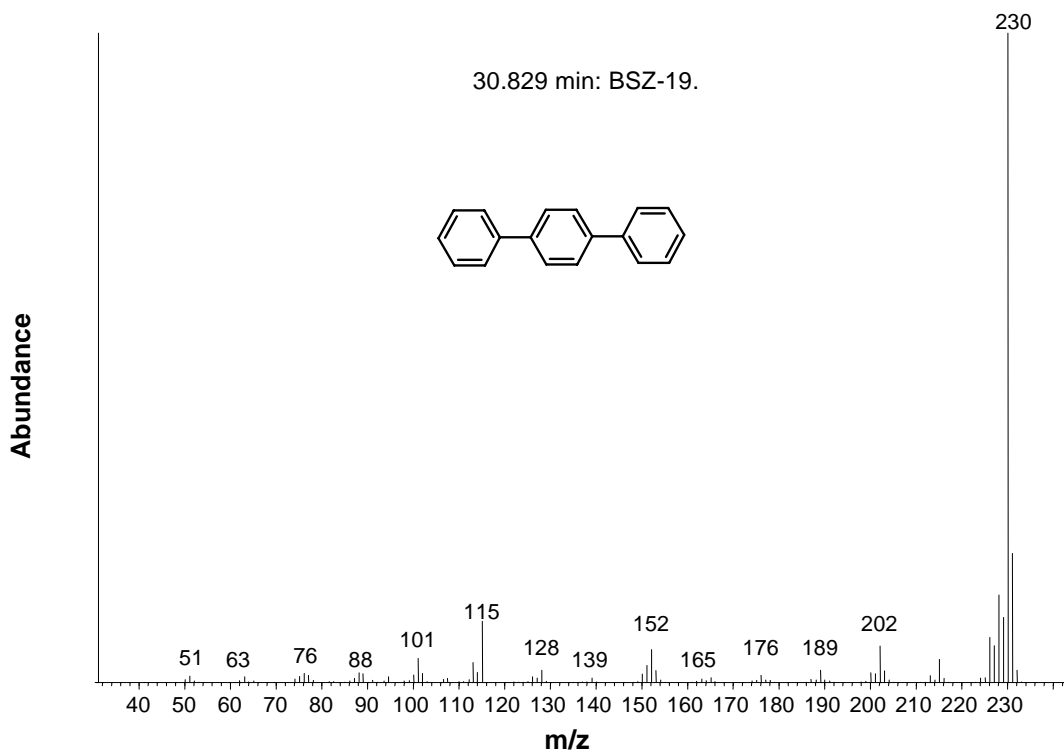
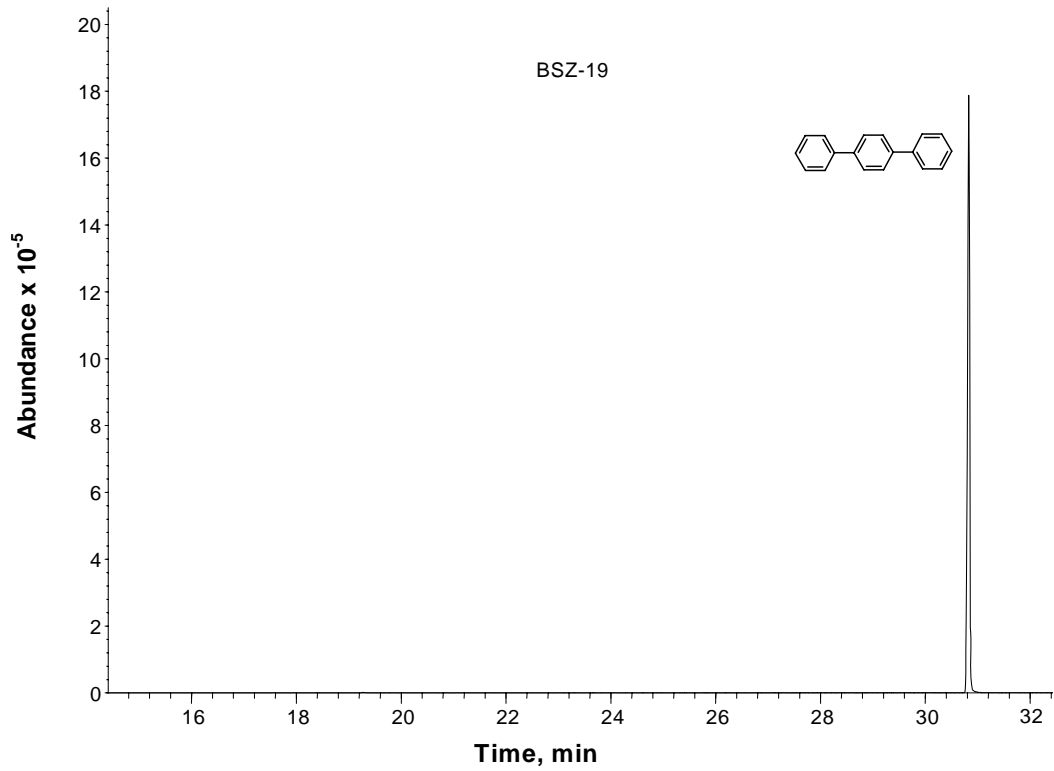




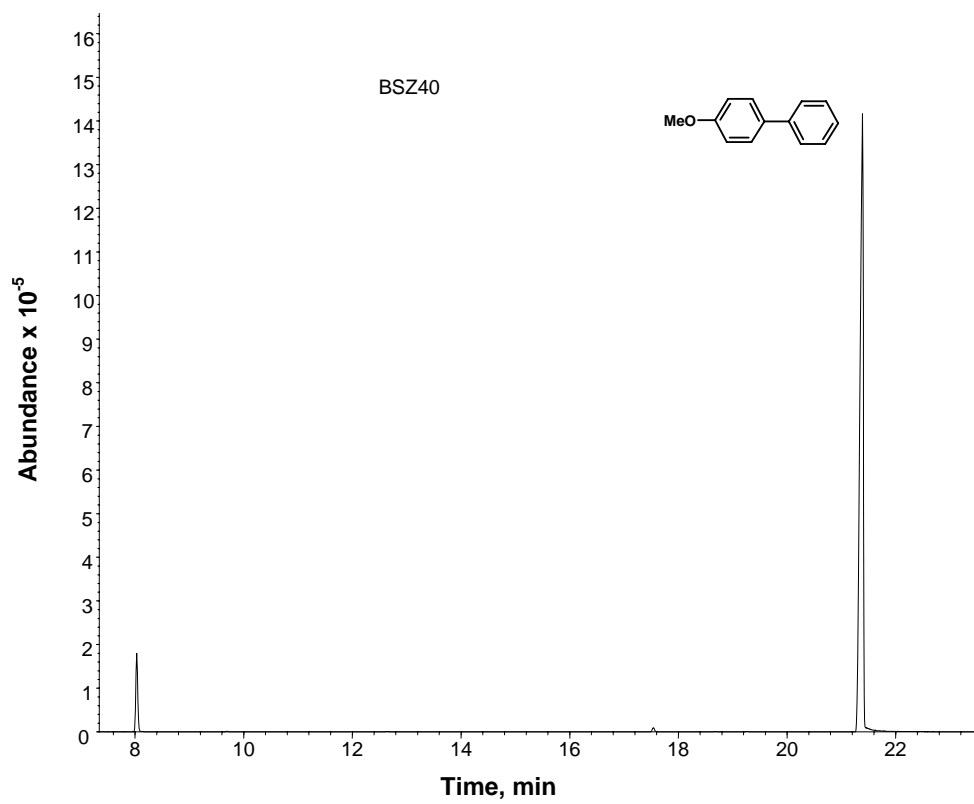


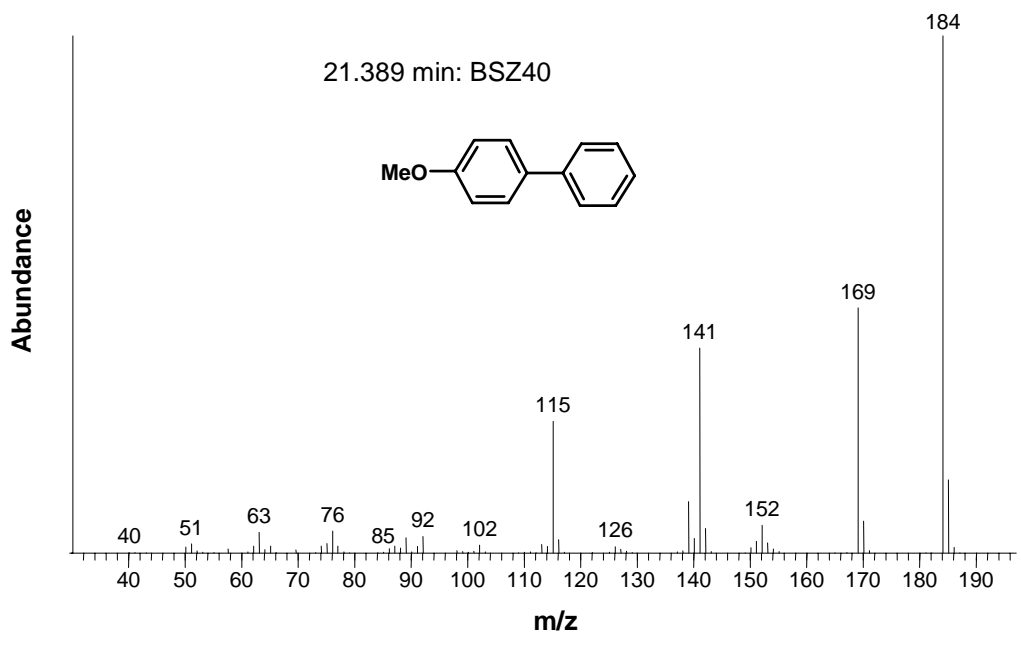
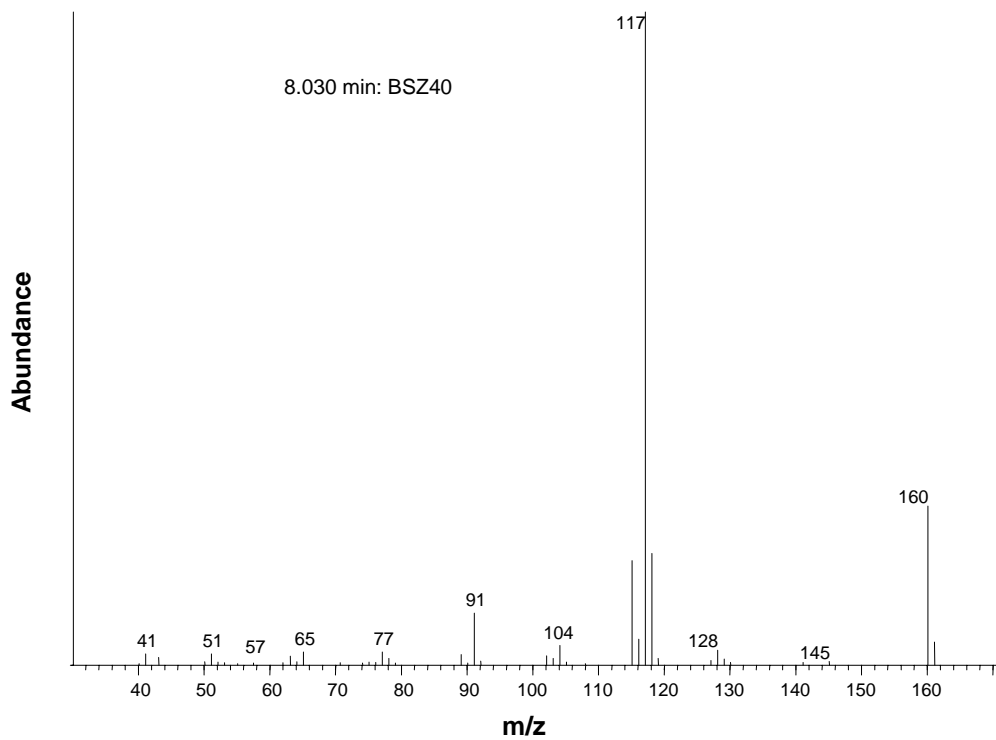


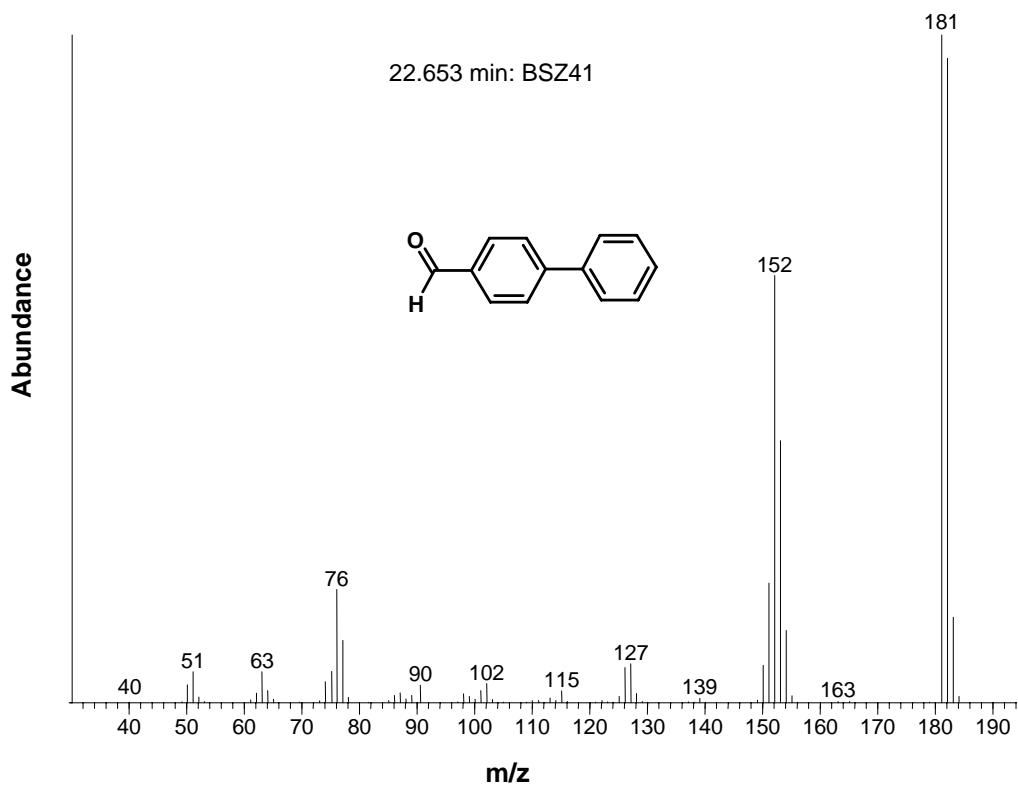
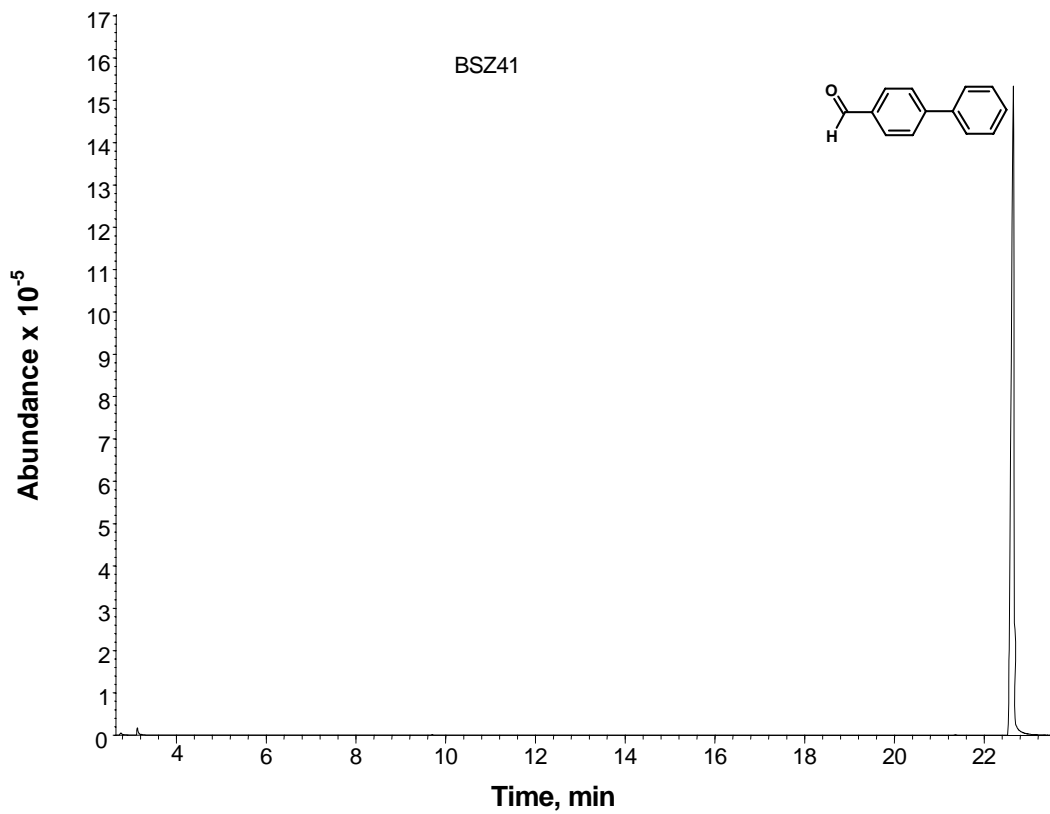


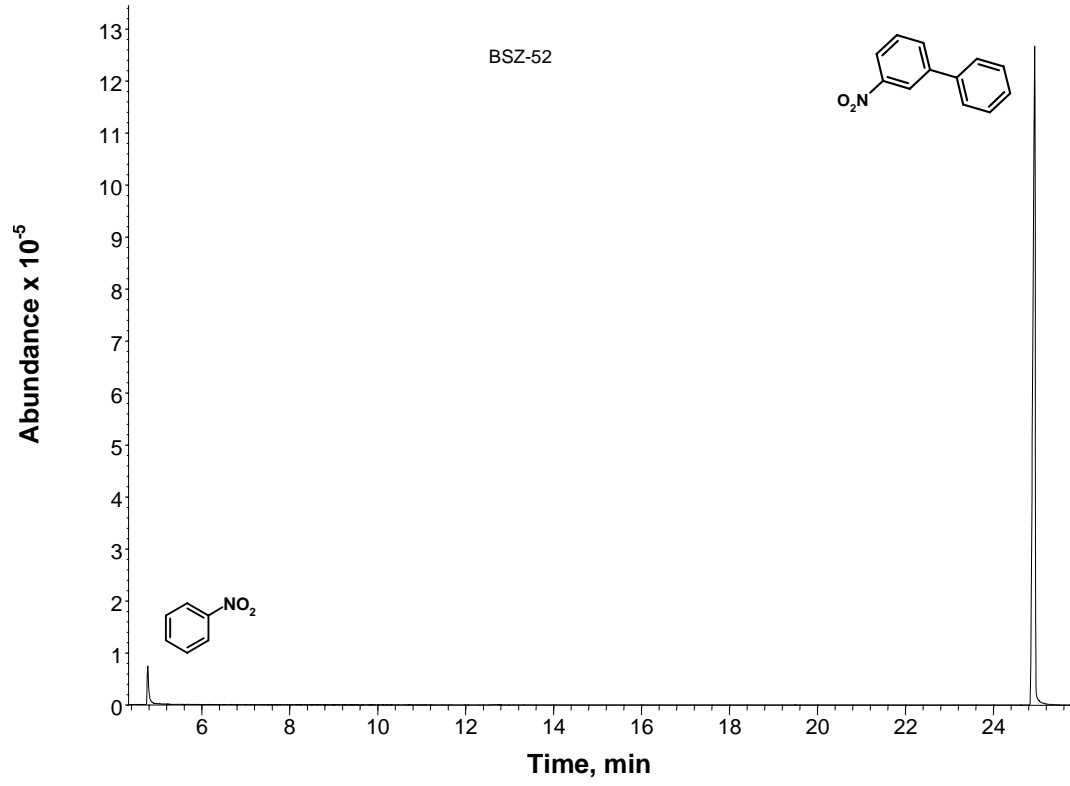


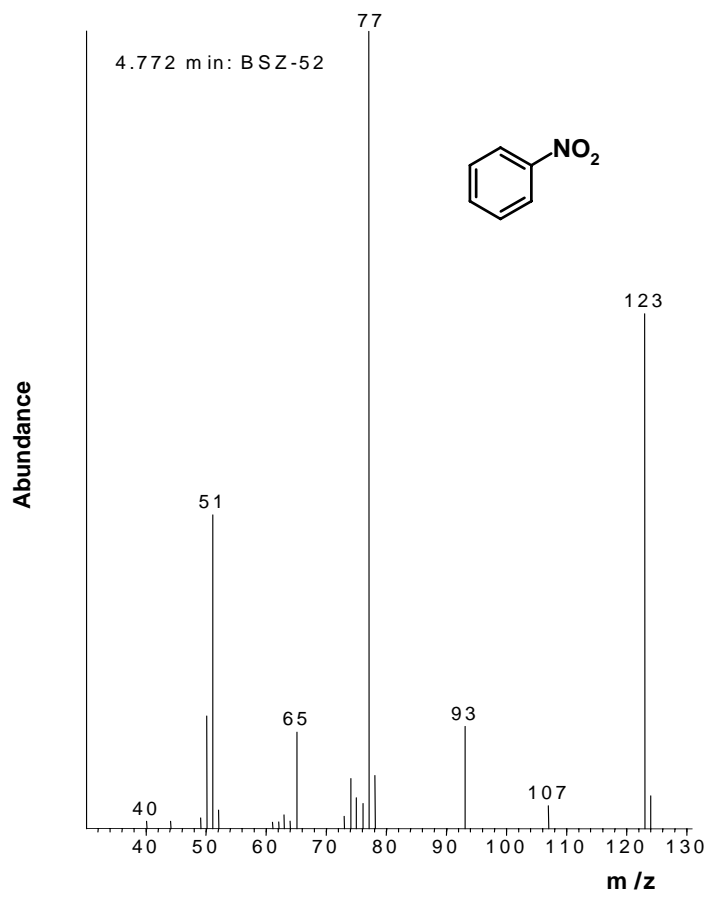
GC-MS data of the compounds of Table 5.5, in the order of their appearance

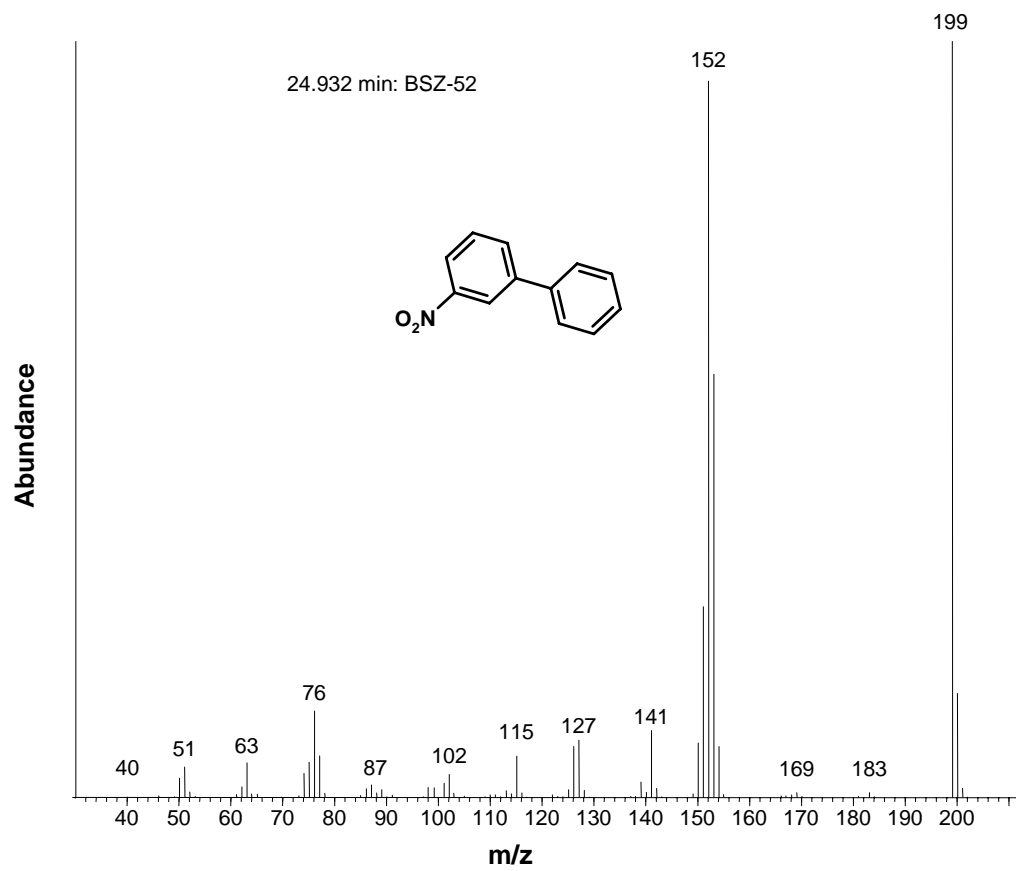


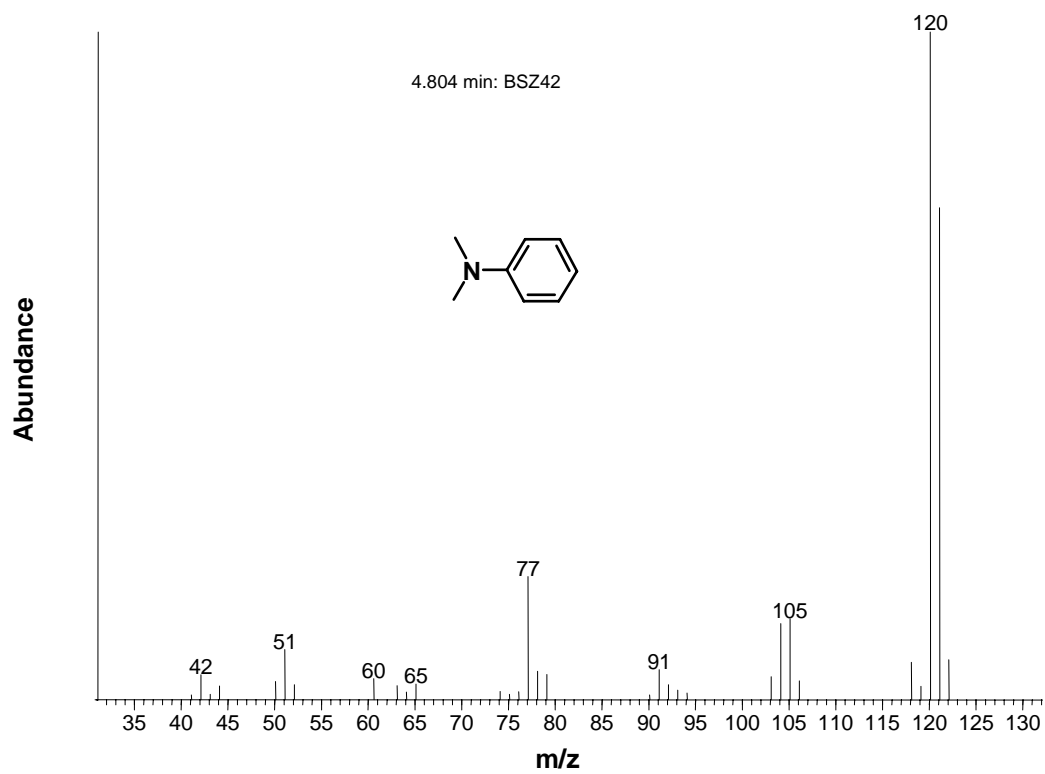
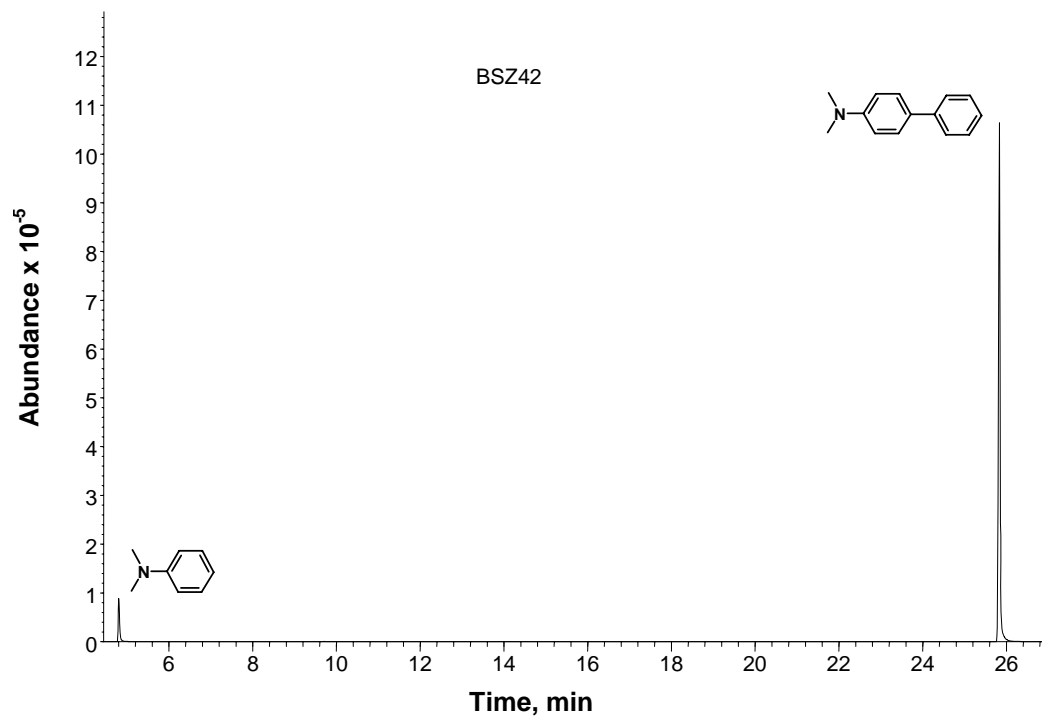


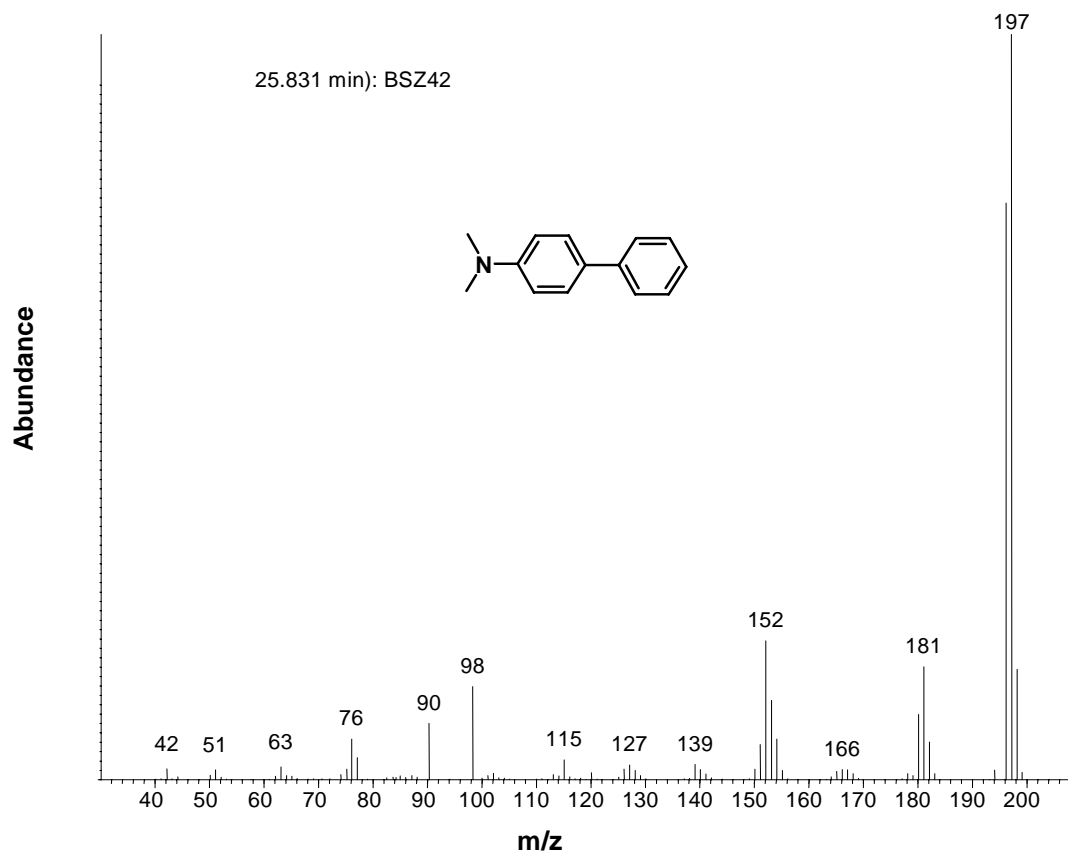


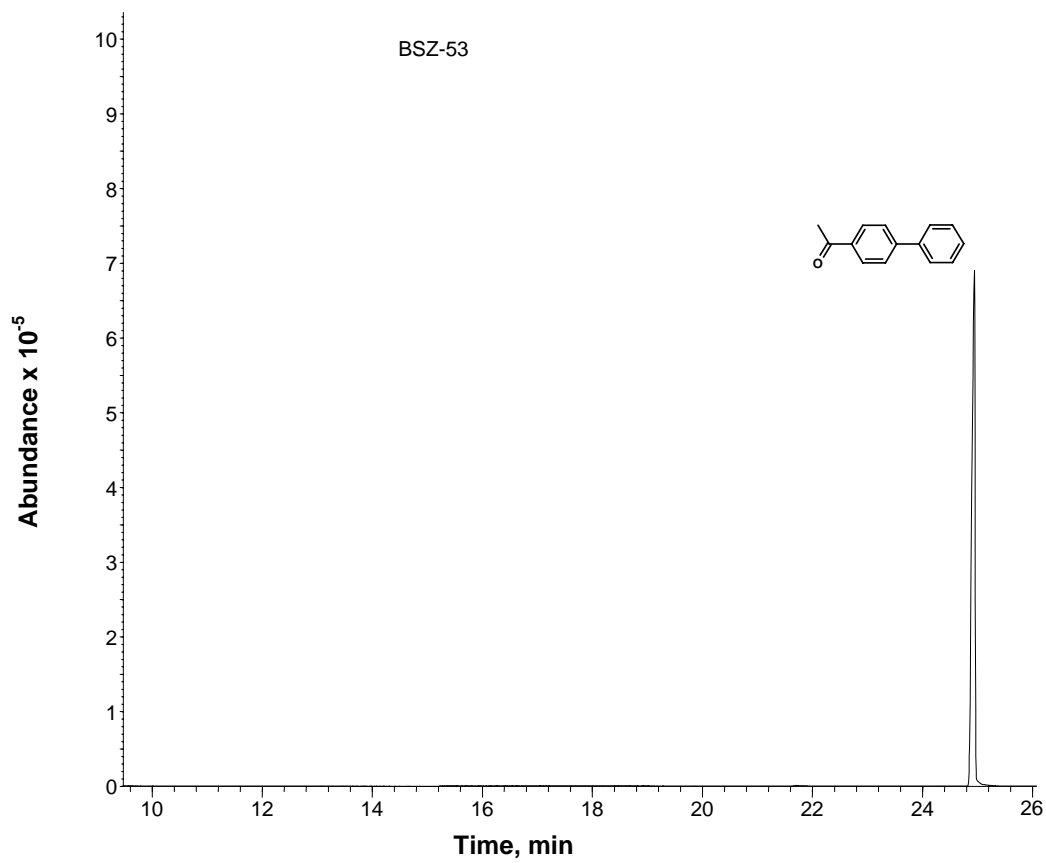


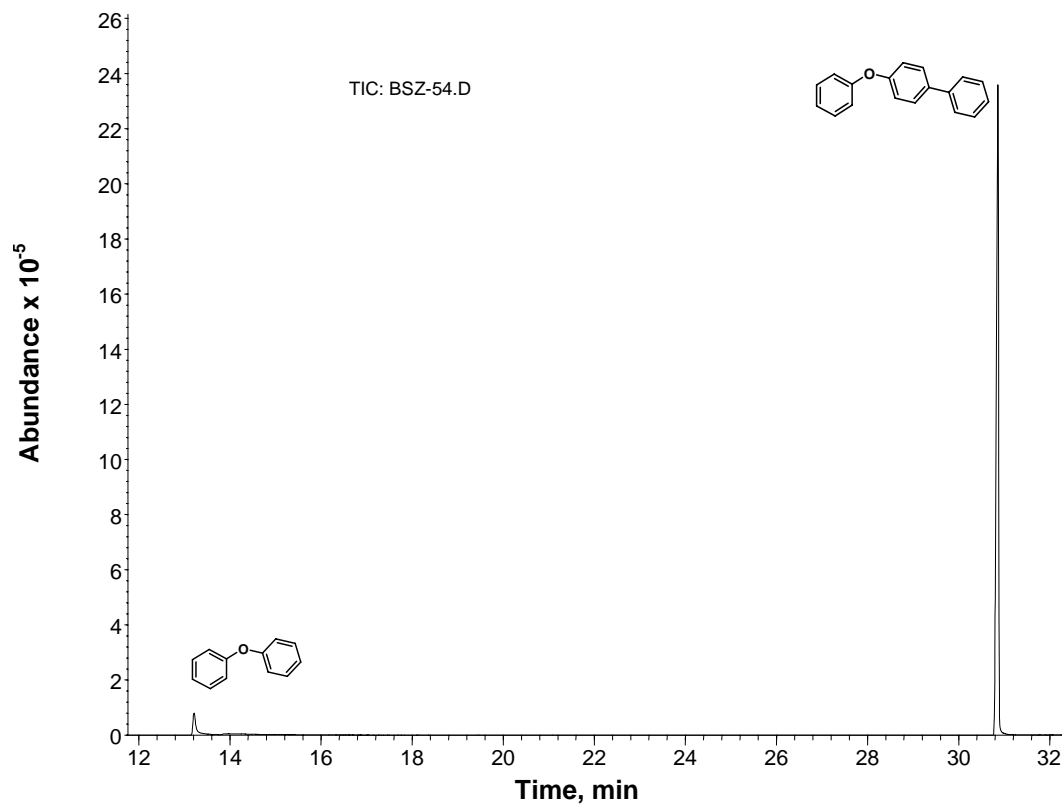
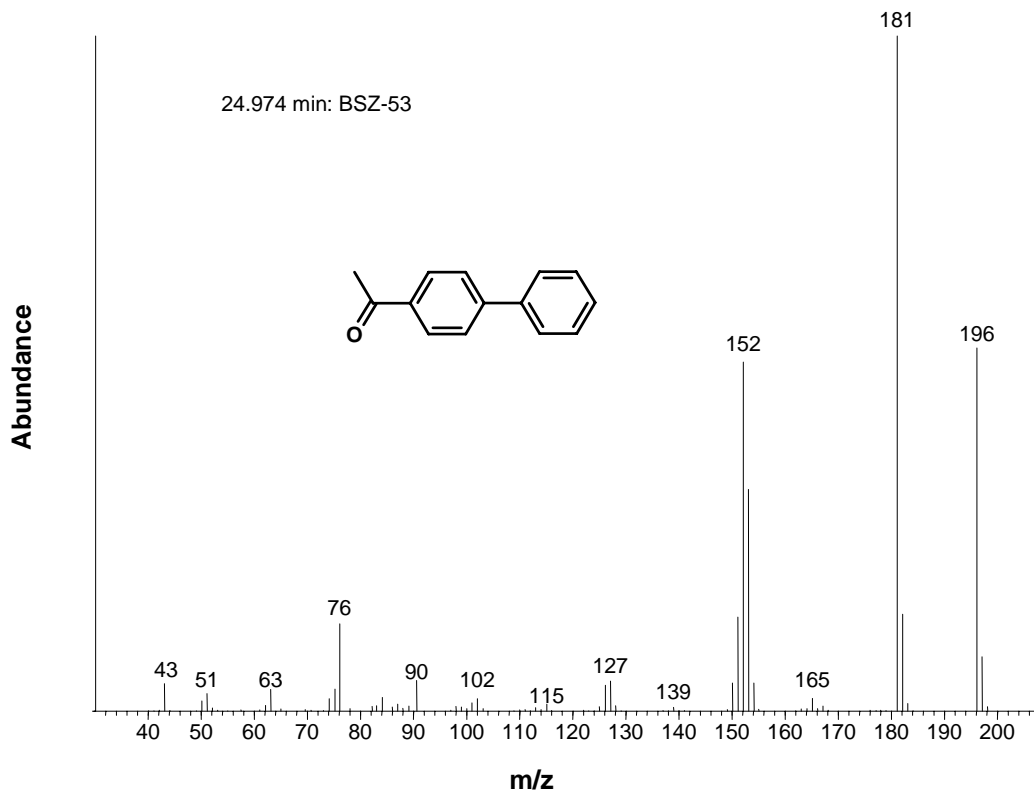


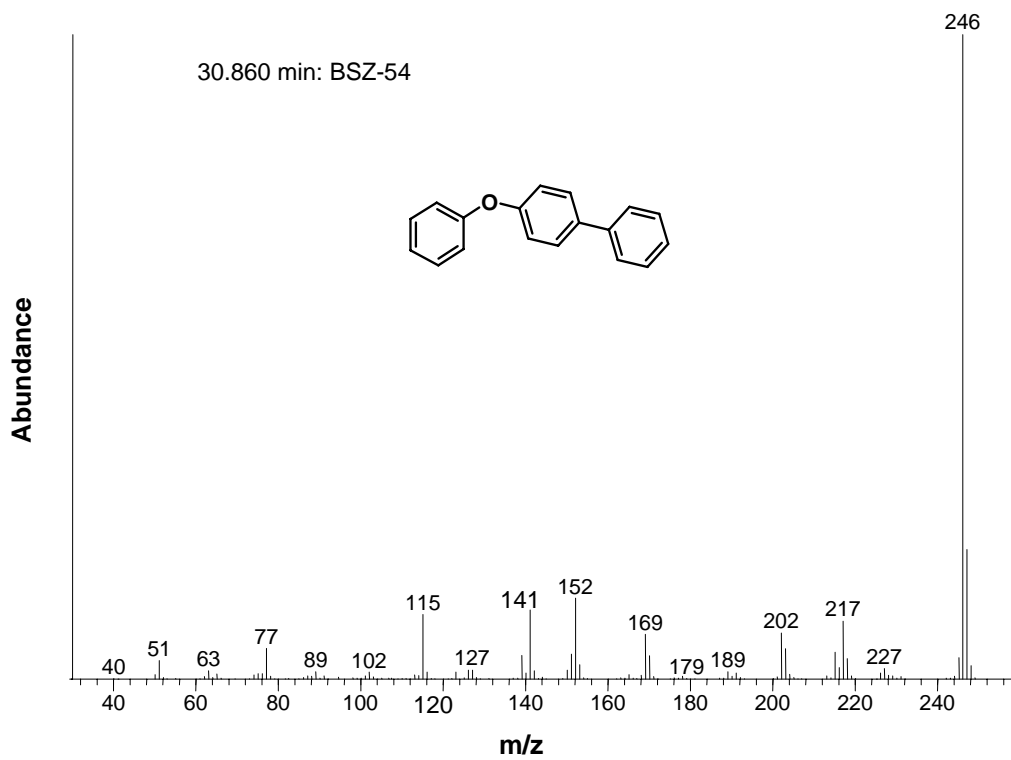
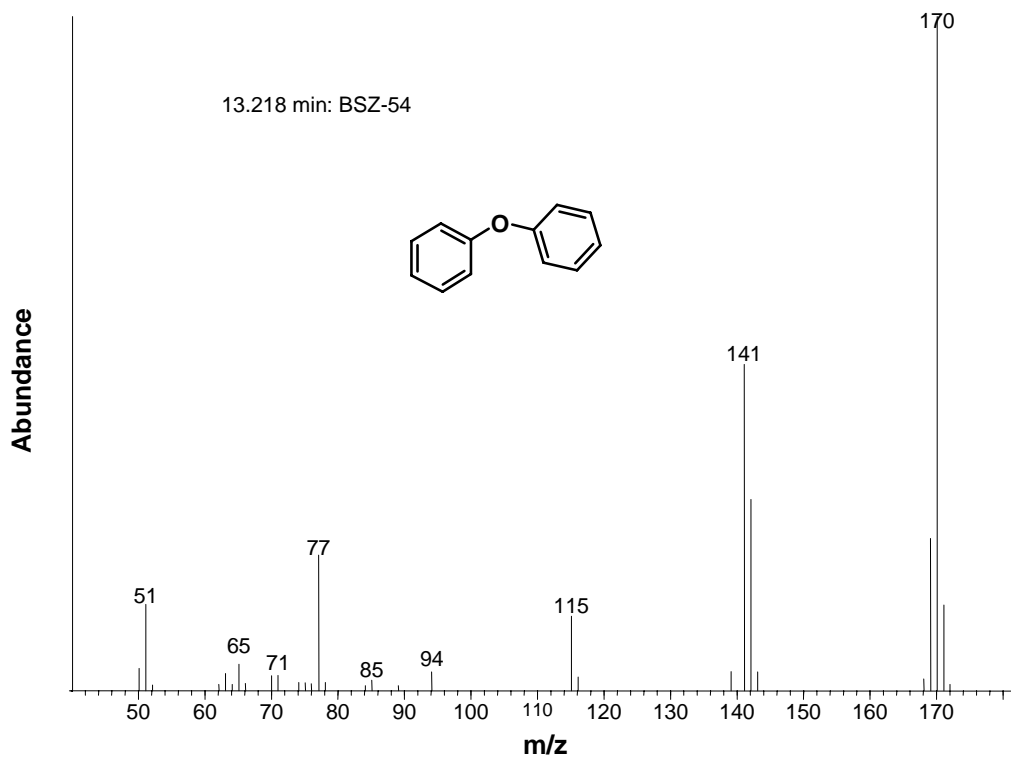


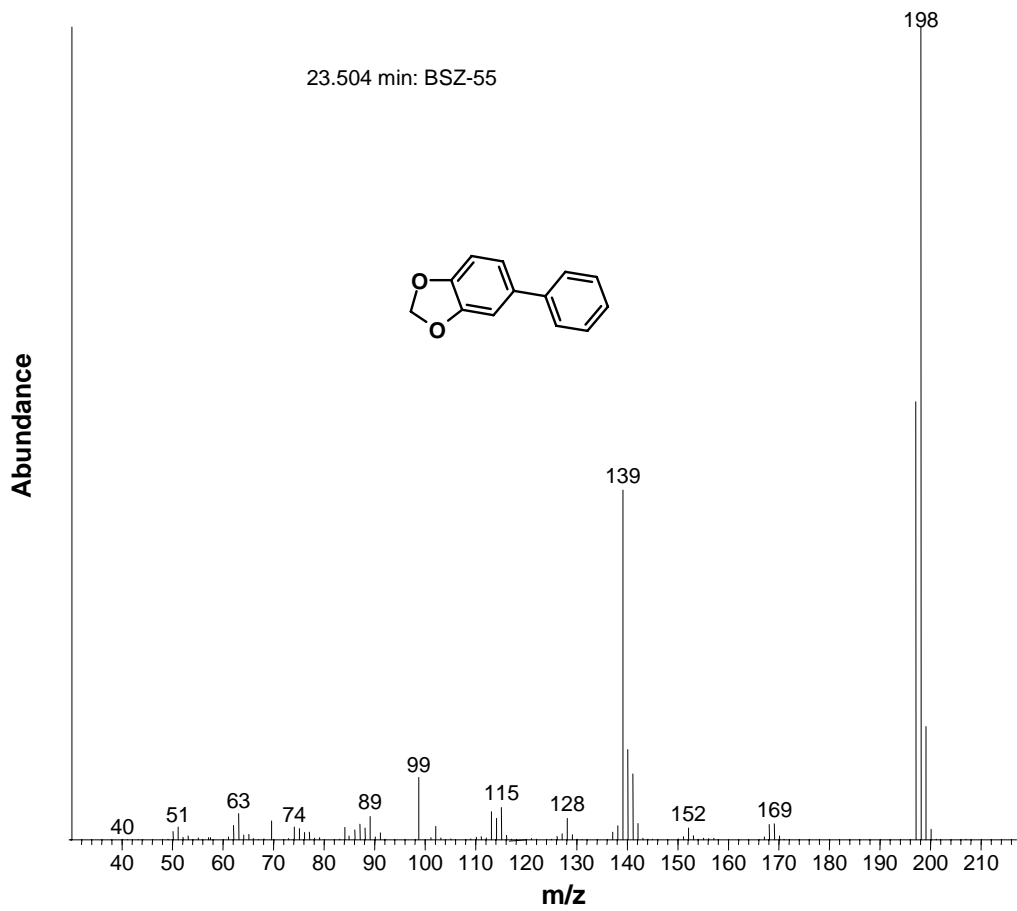


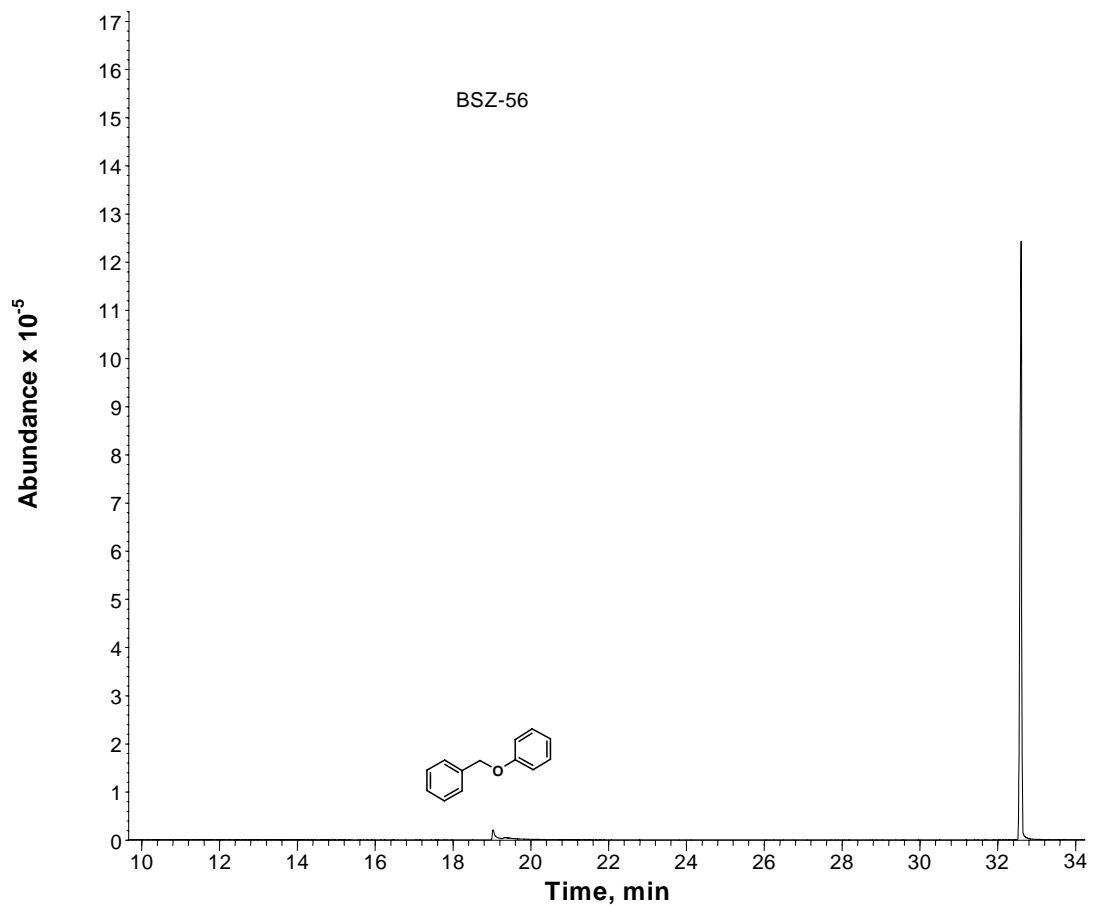


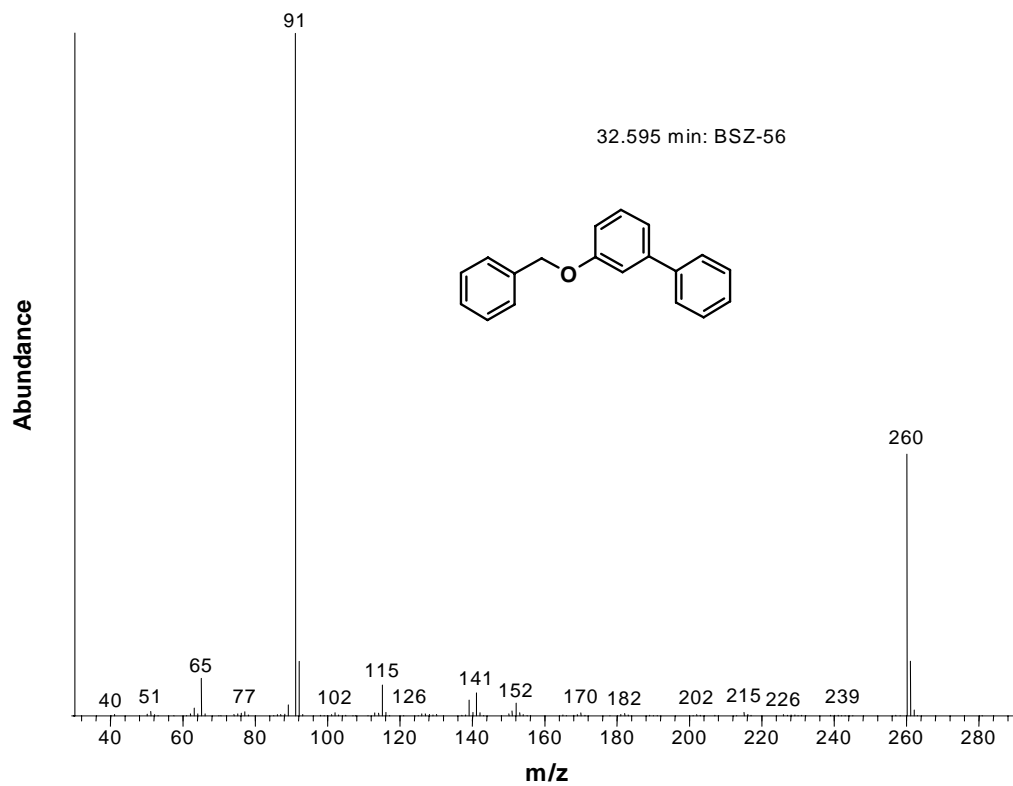


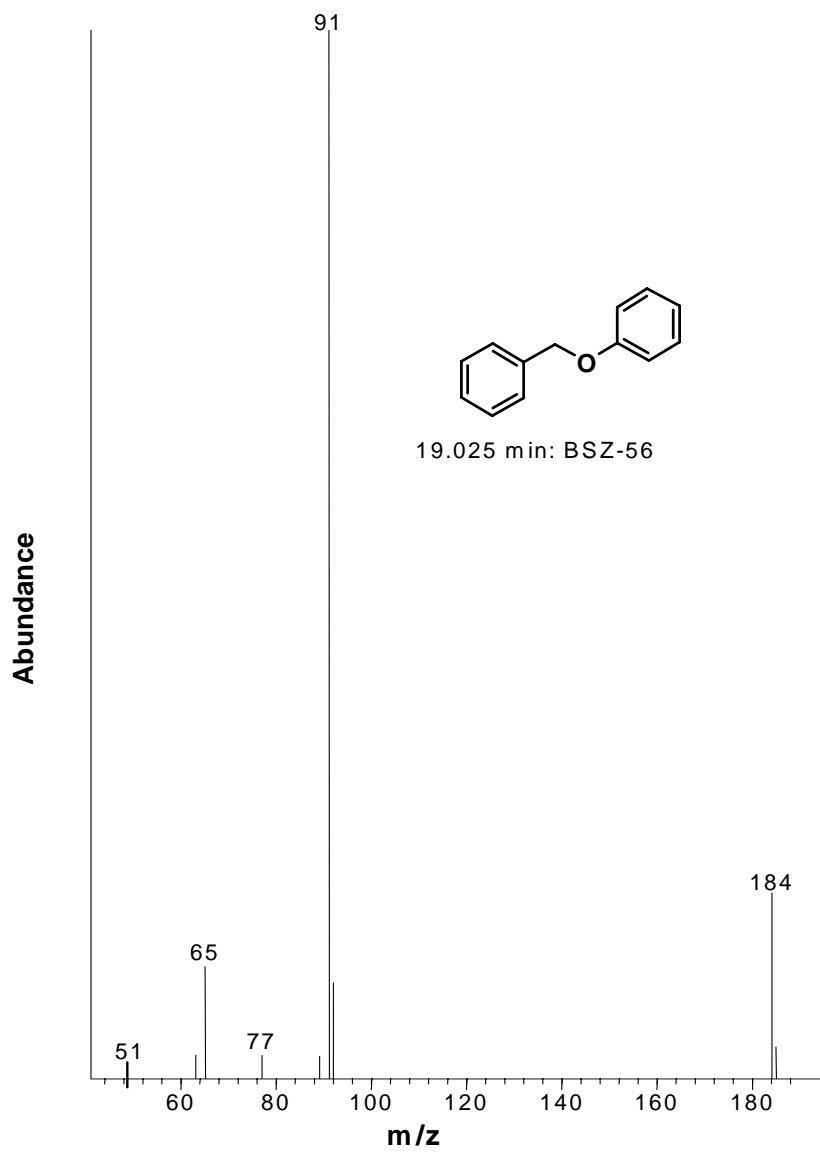


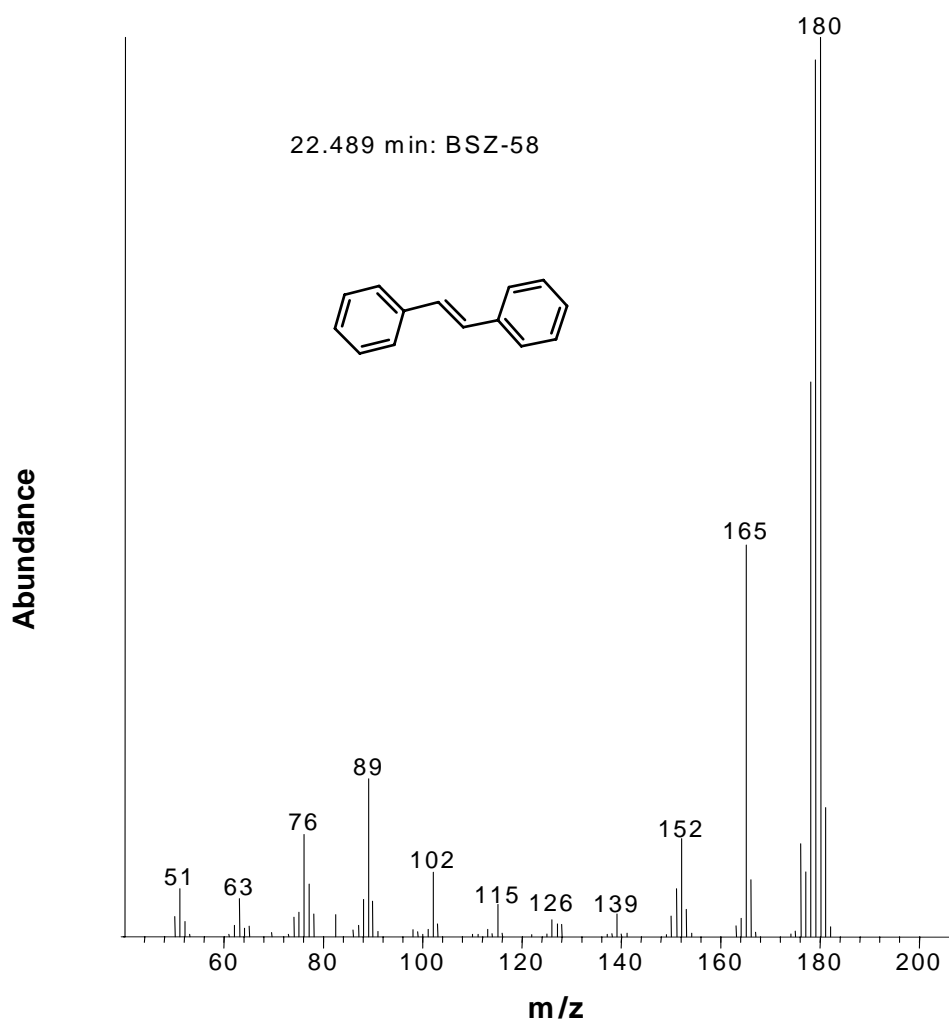
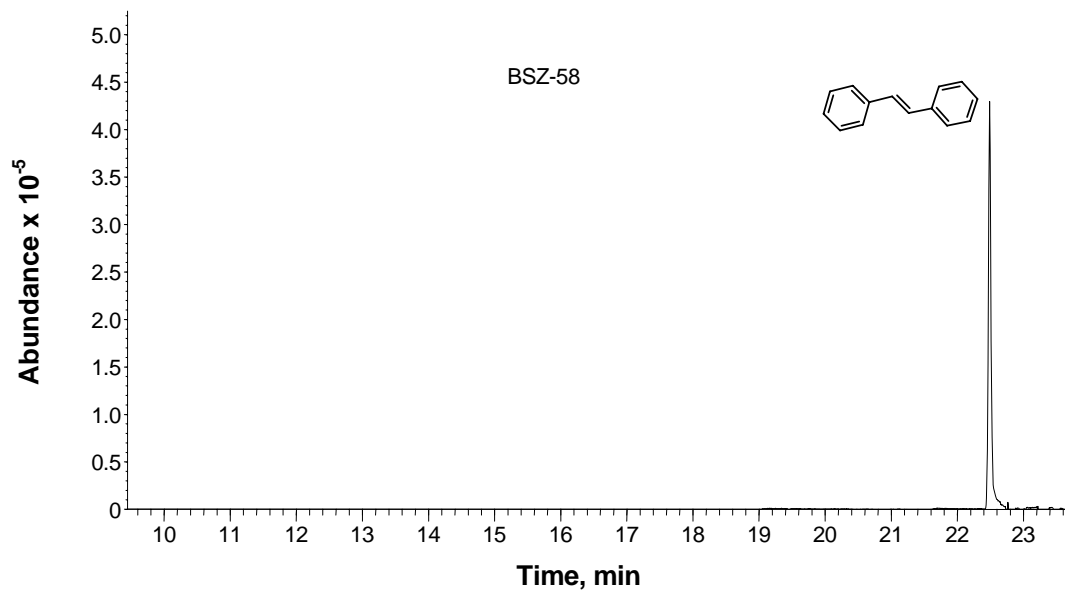


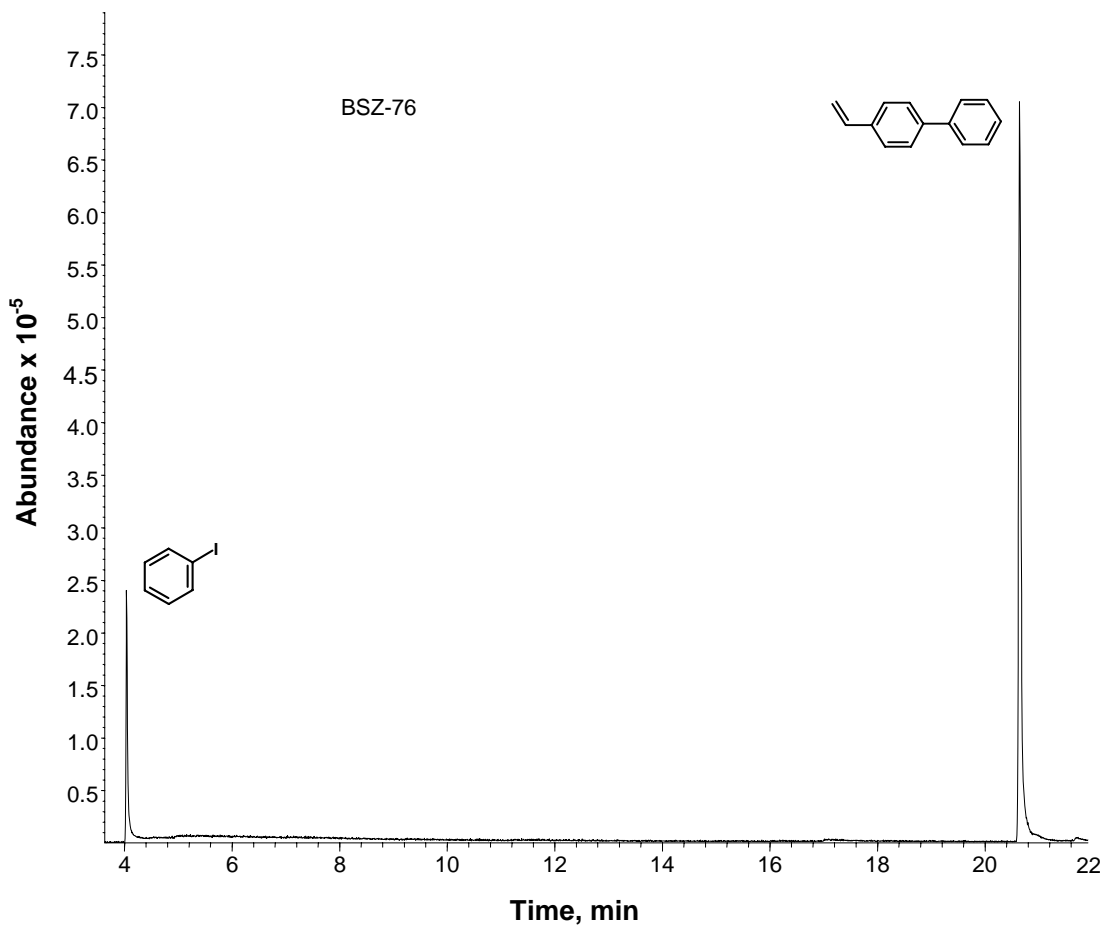


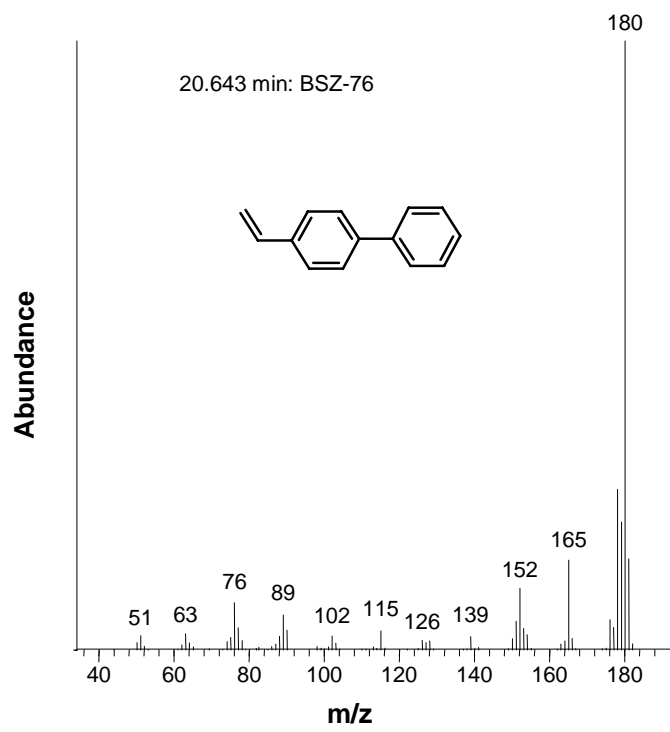
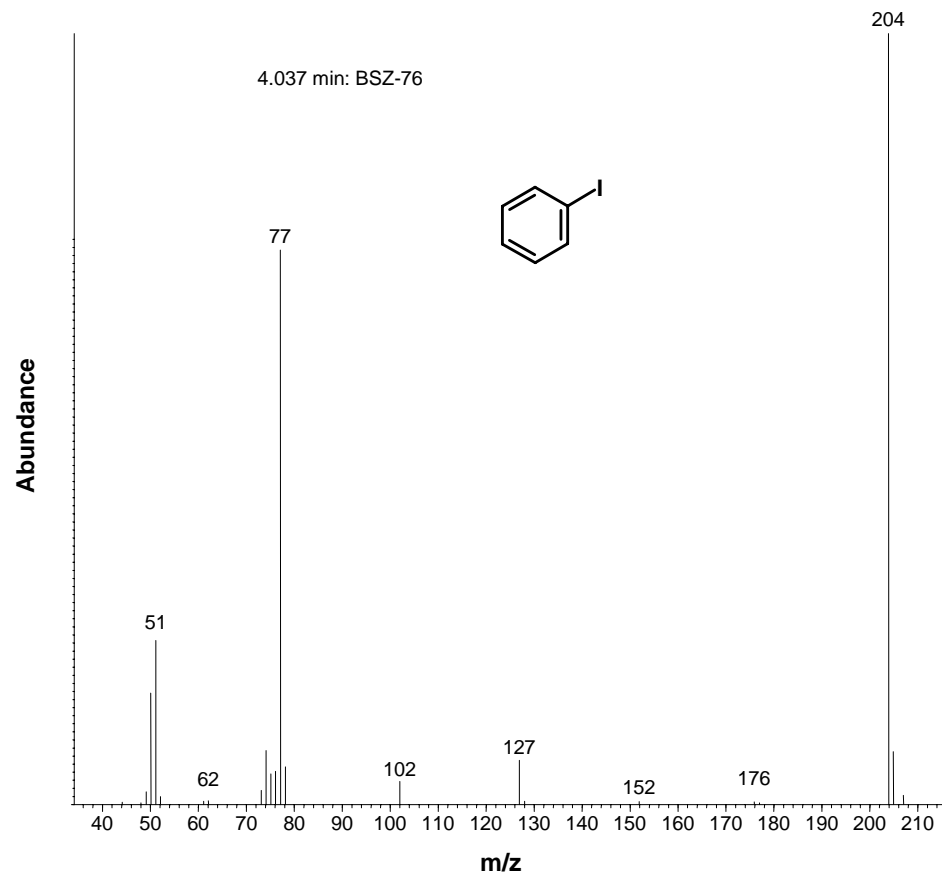


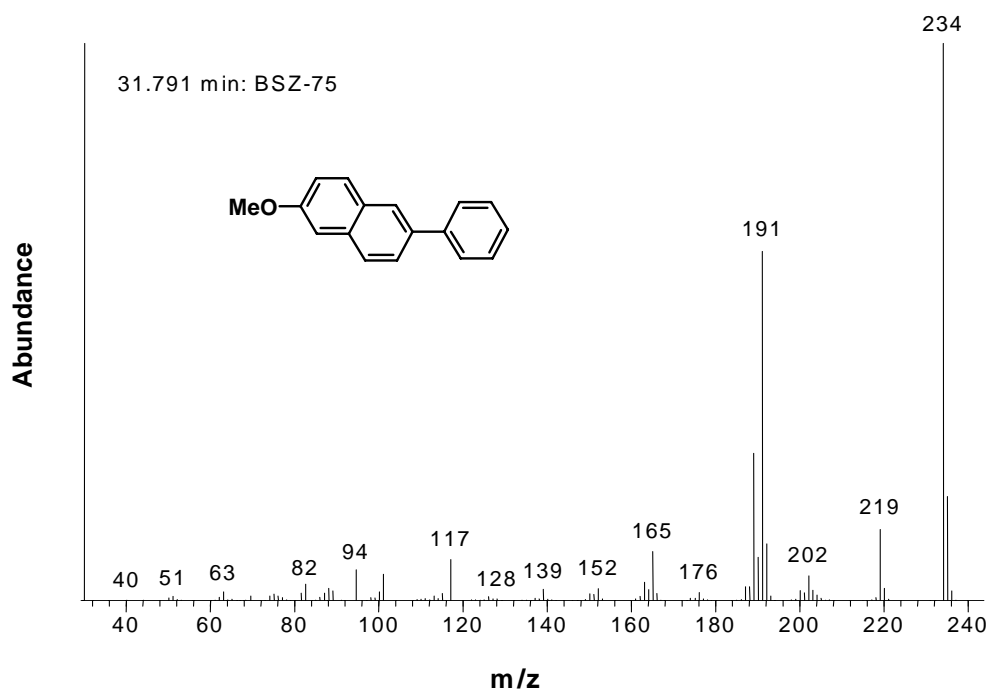
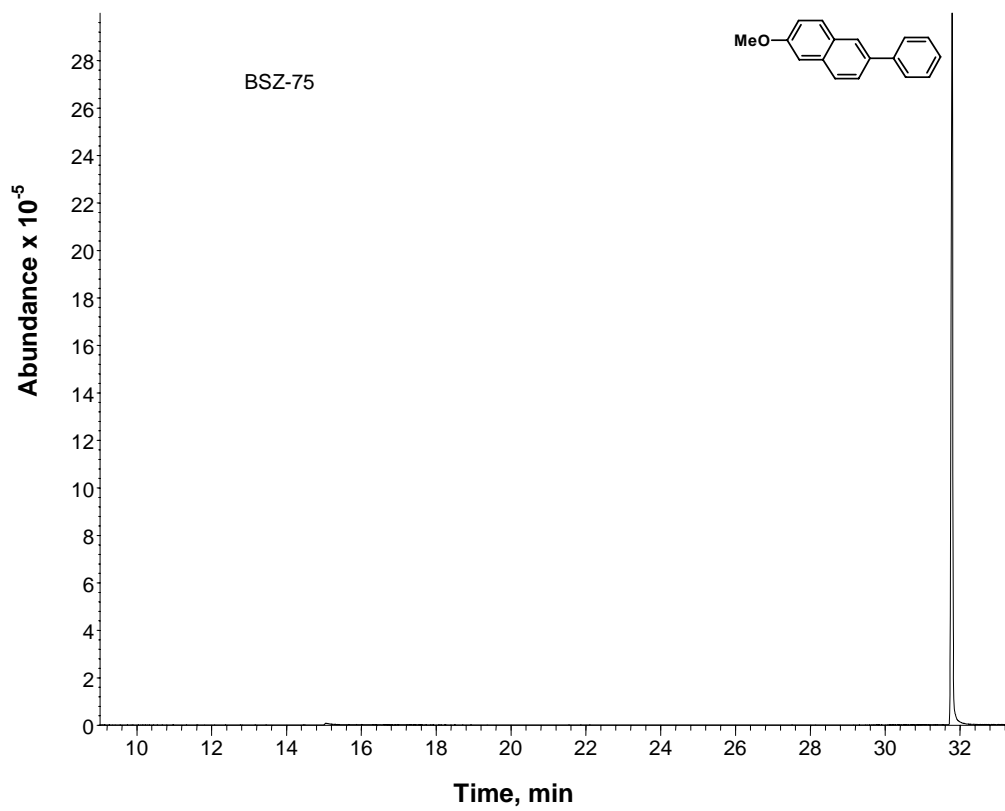




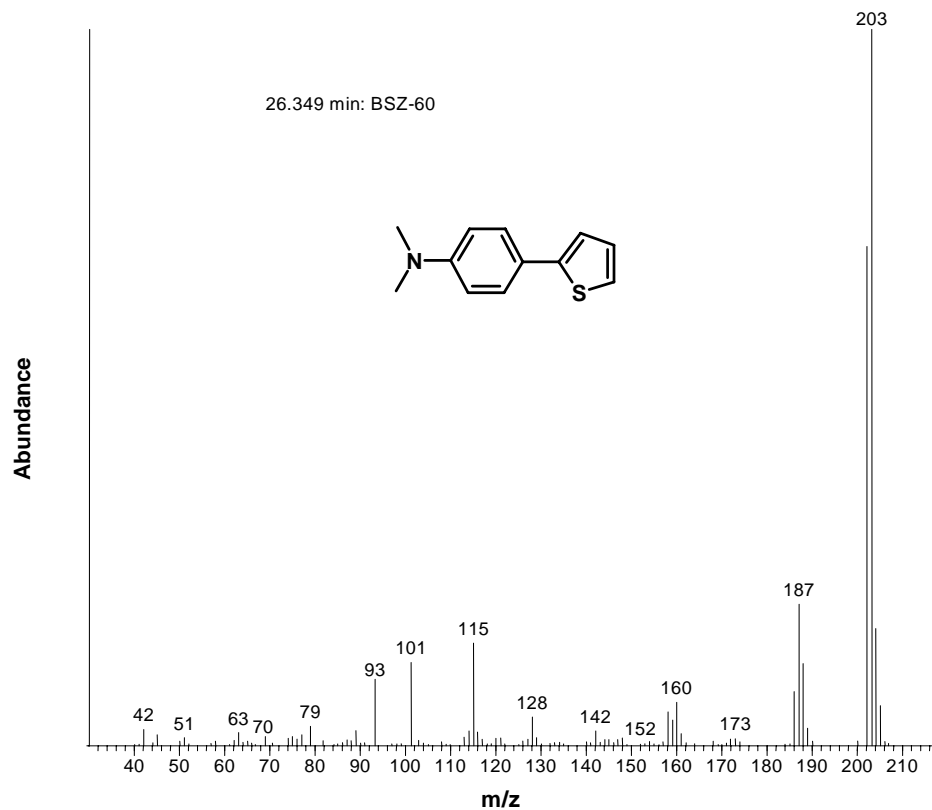
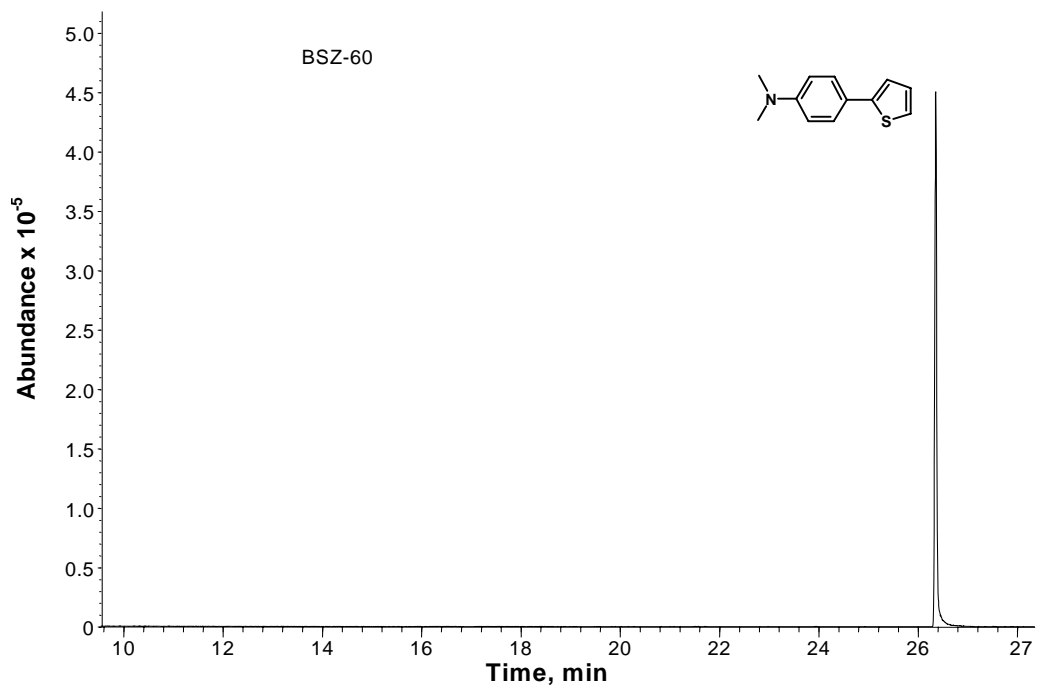


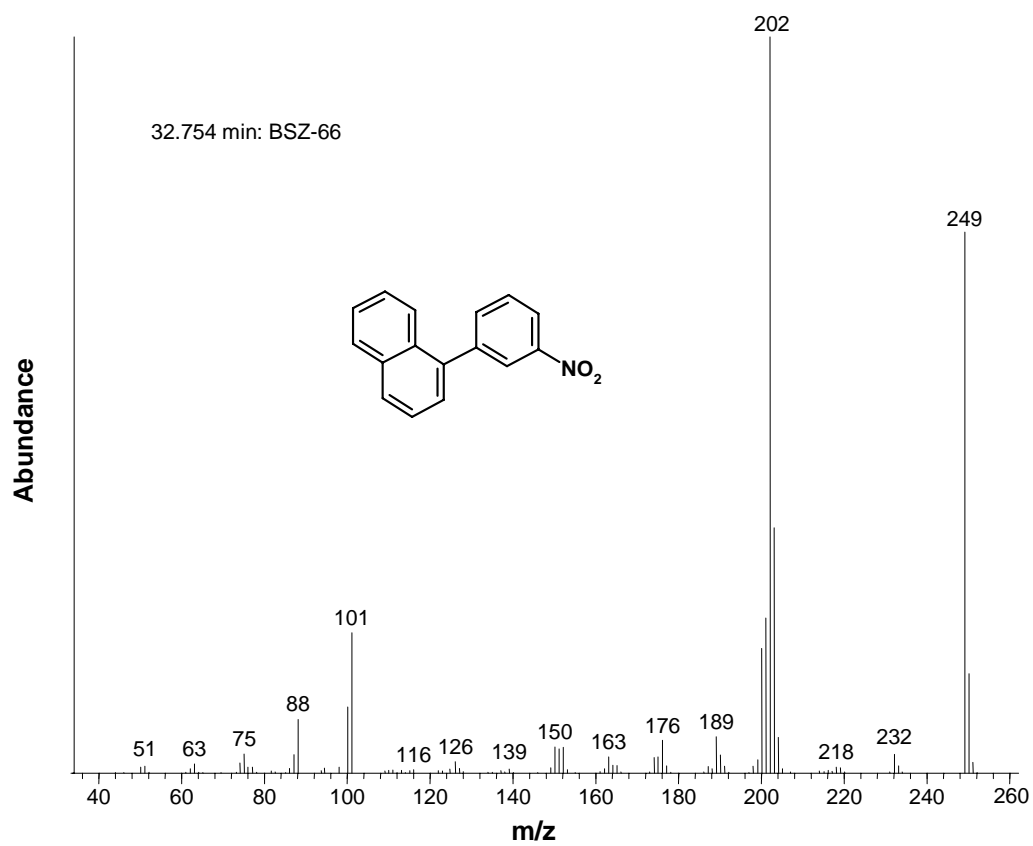
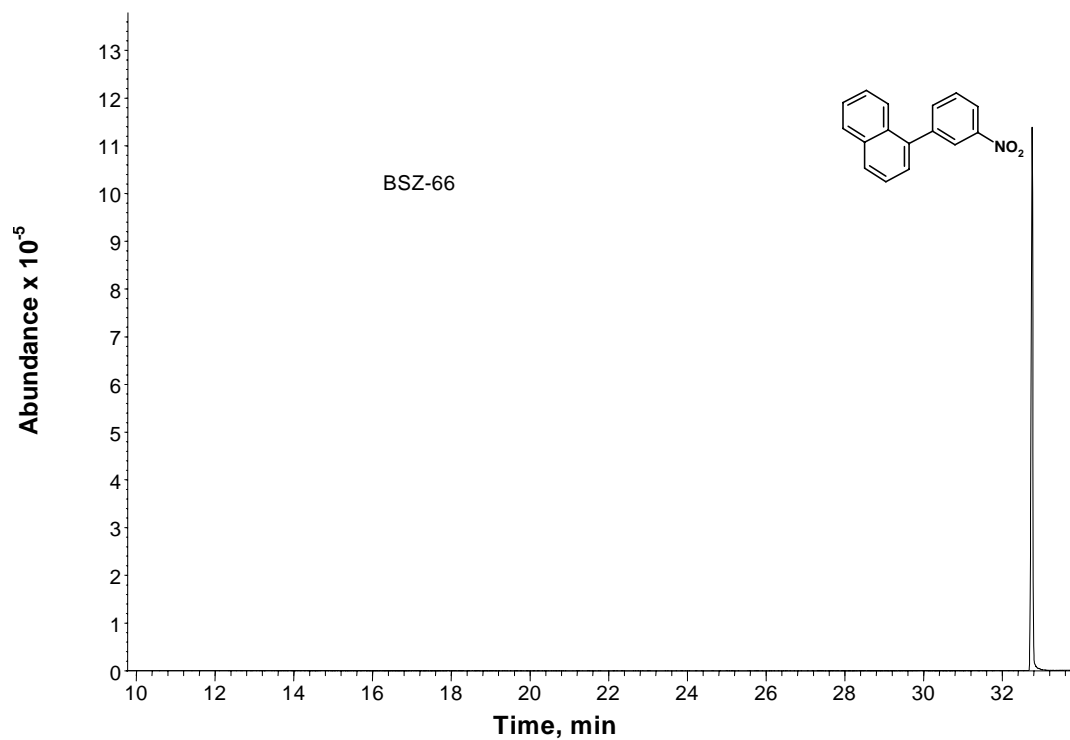


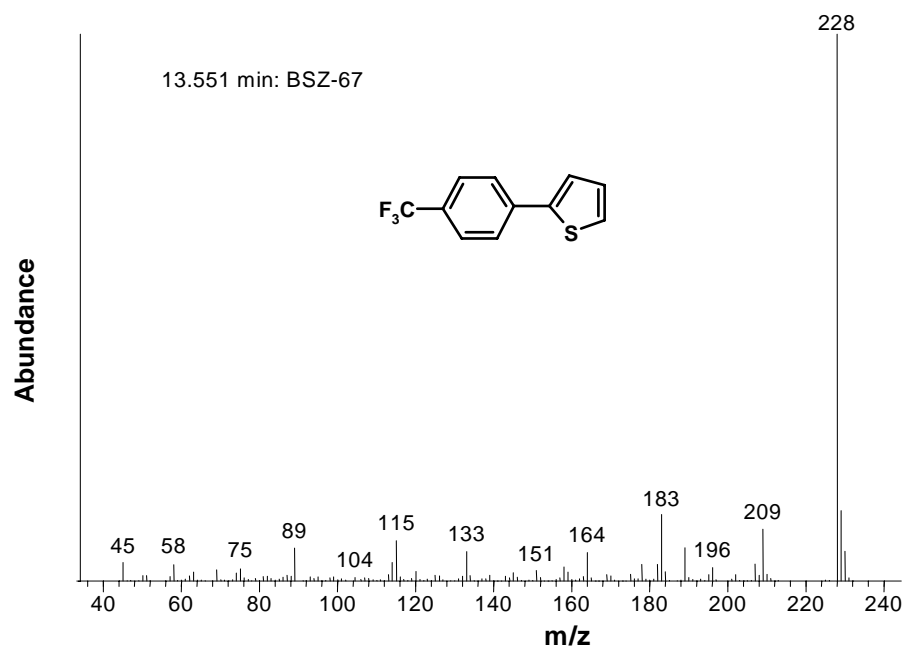
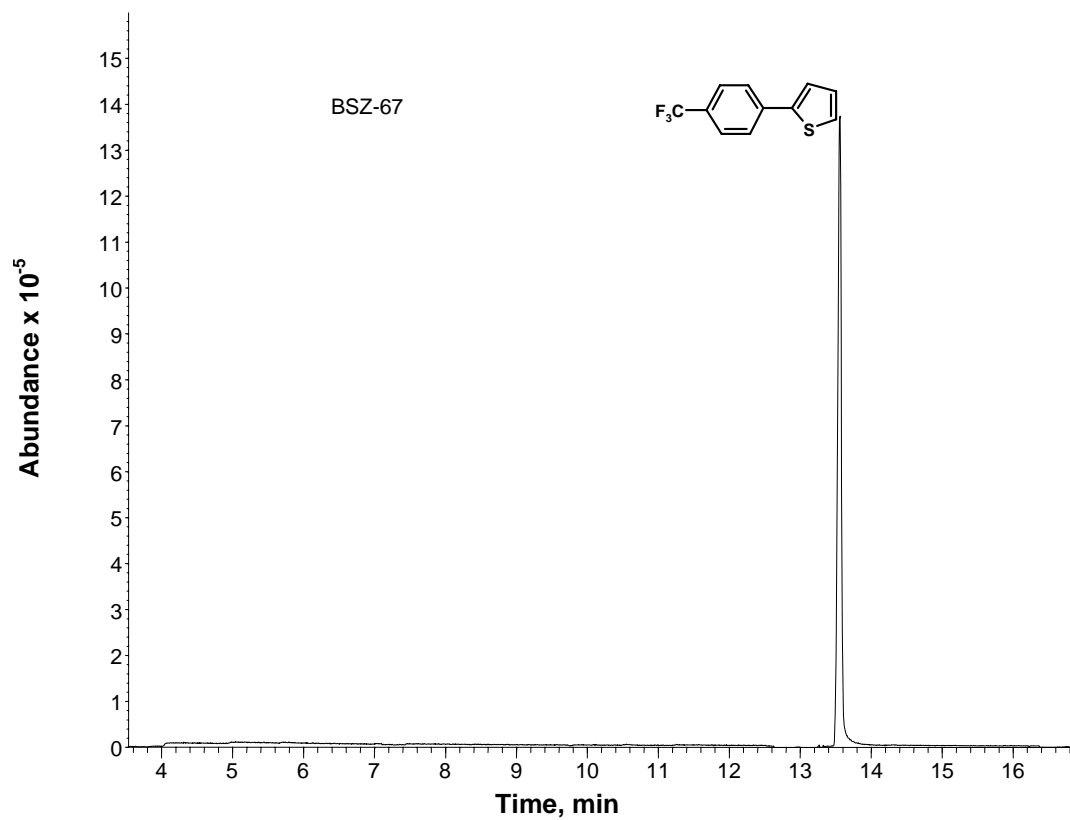


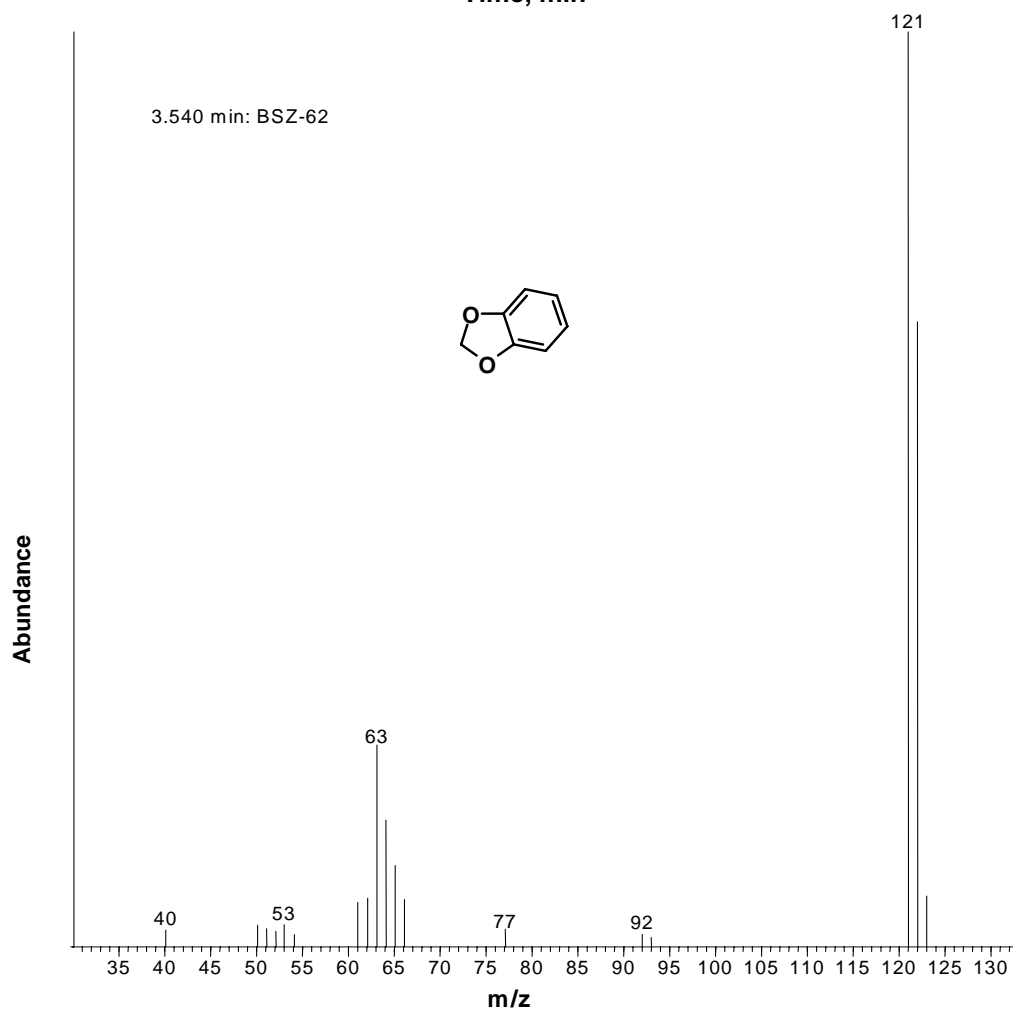
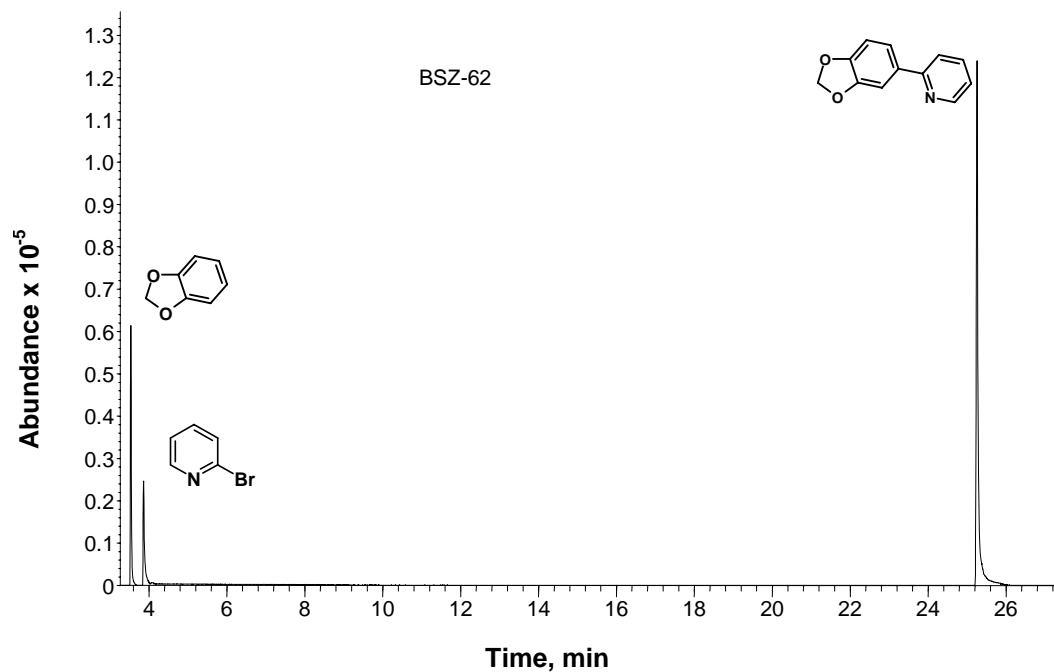


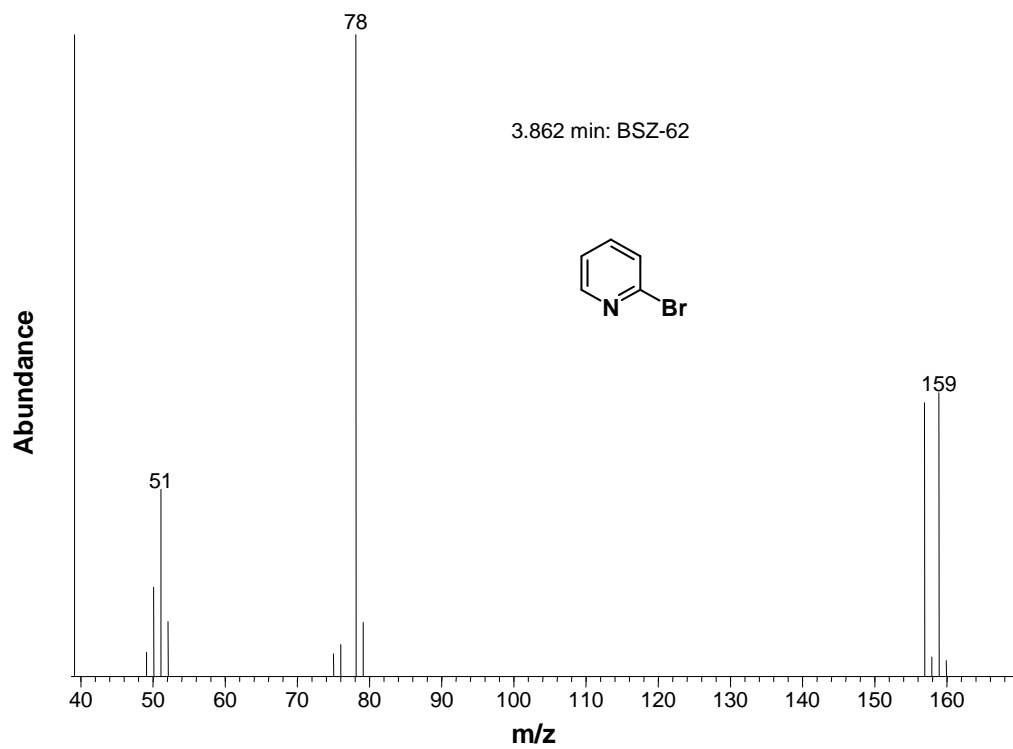
GC-MS data of the compounds of Table 5.6, in the order of their appearance

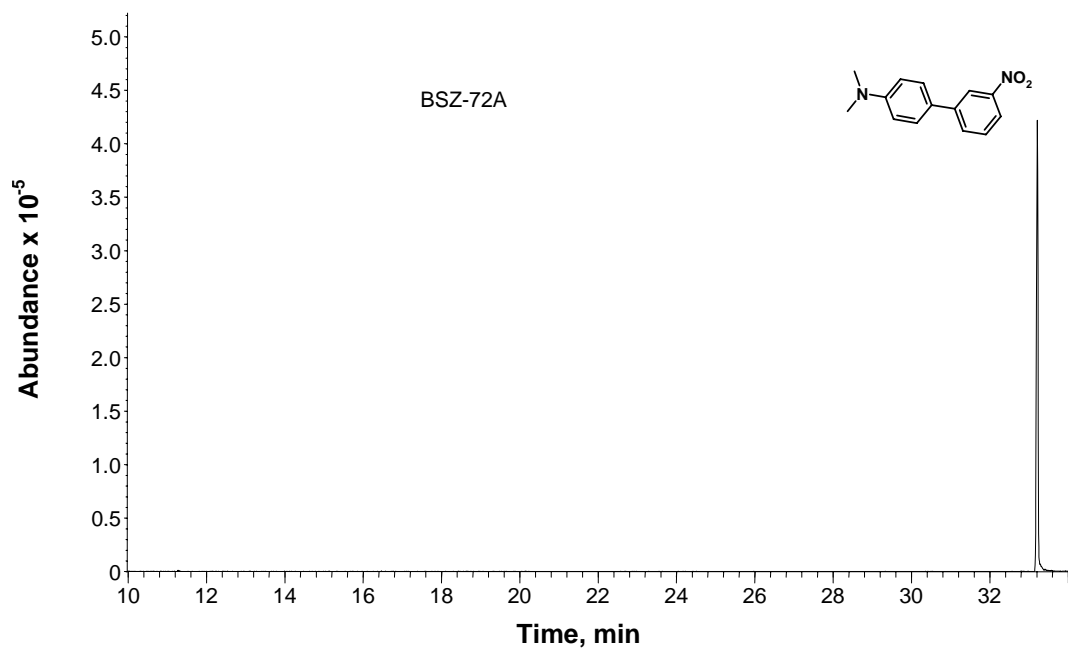
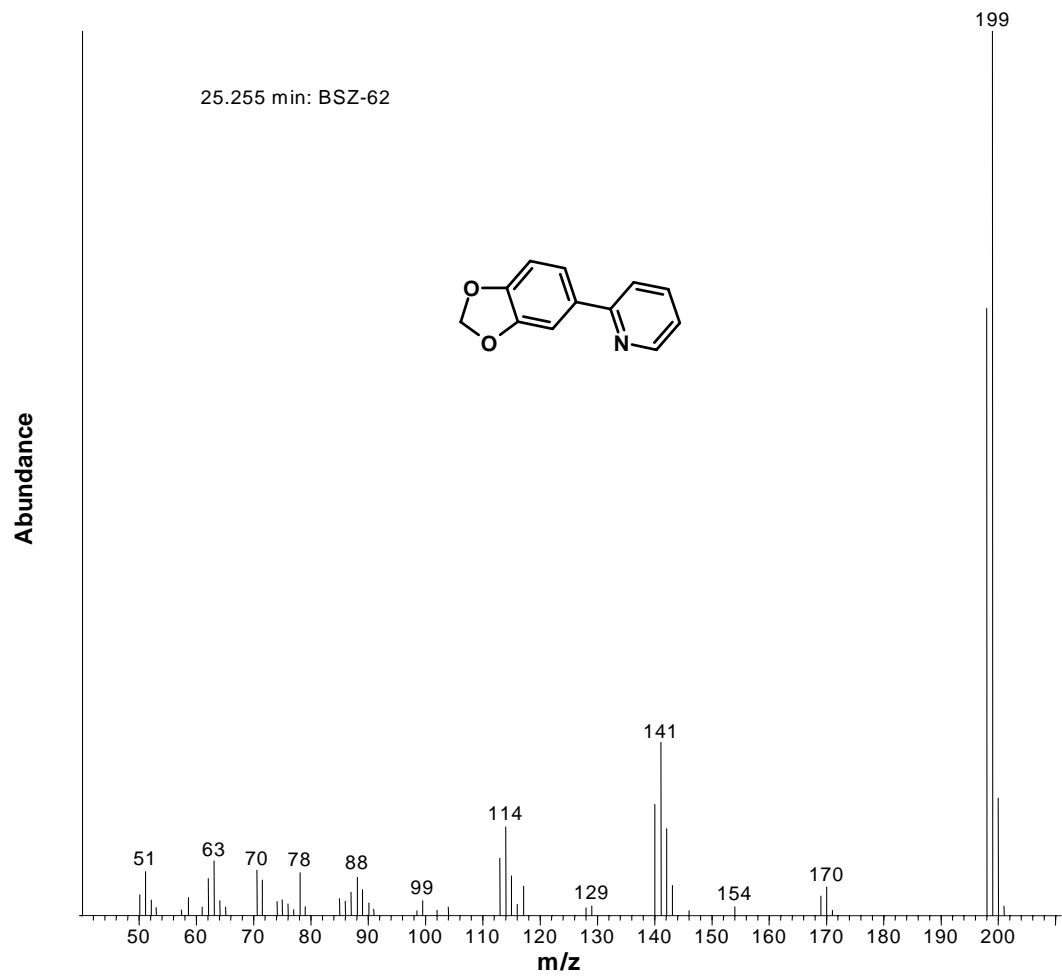


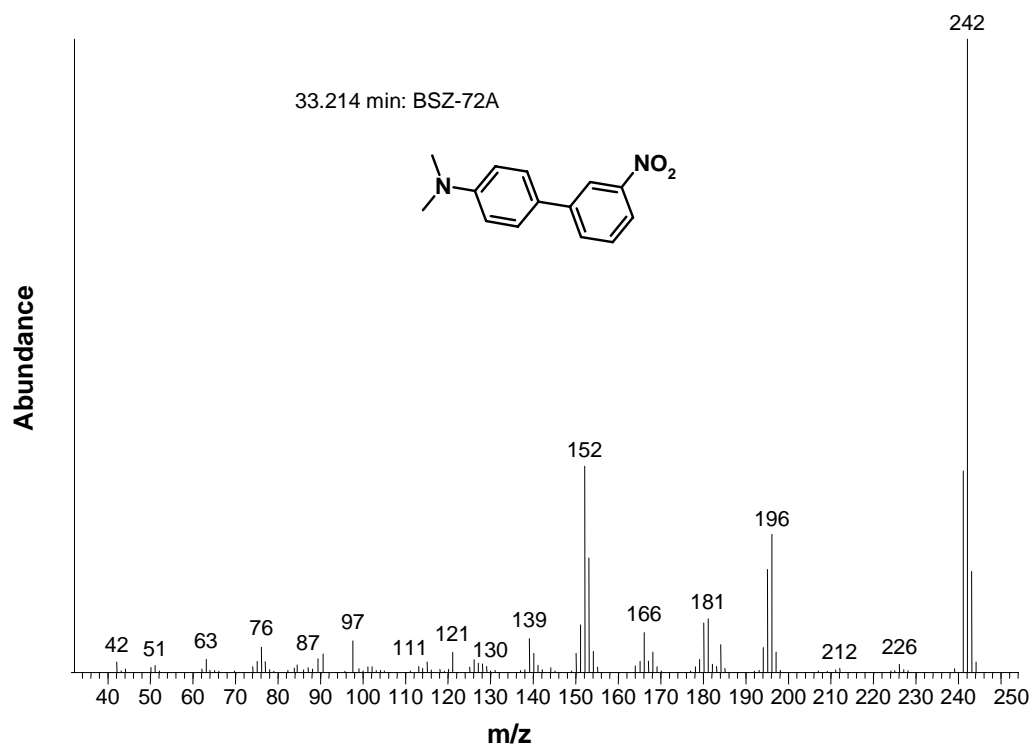


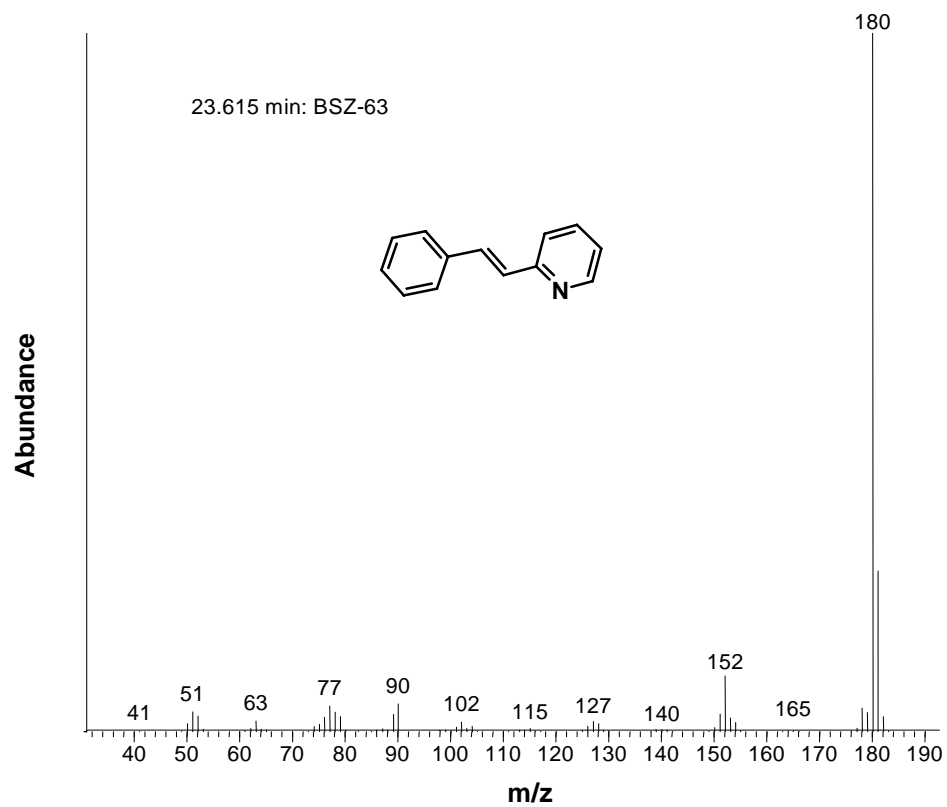
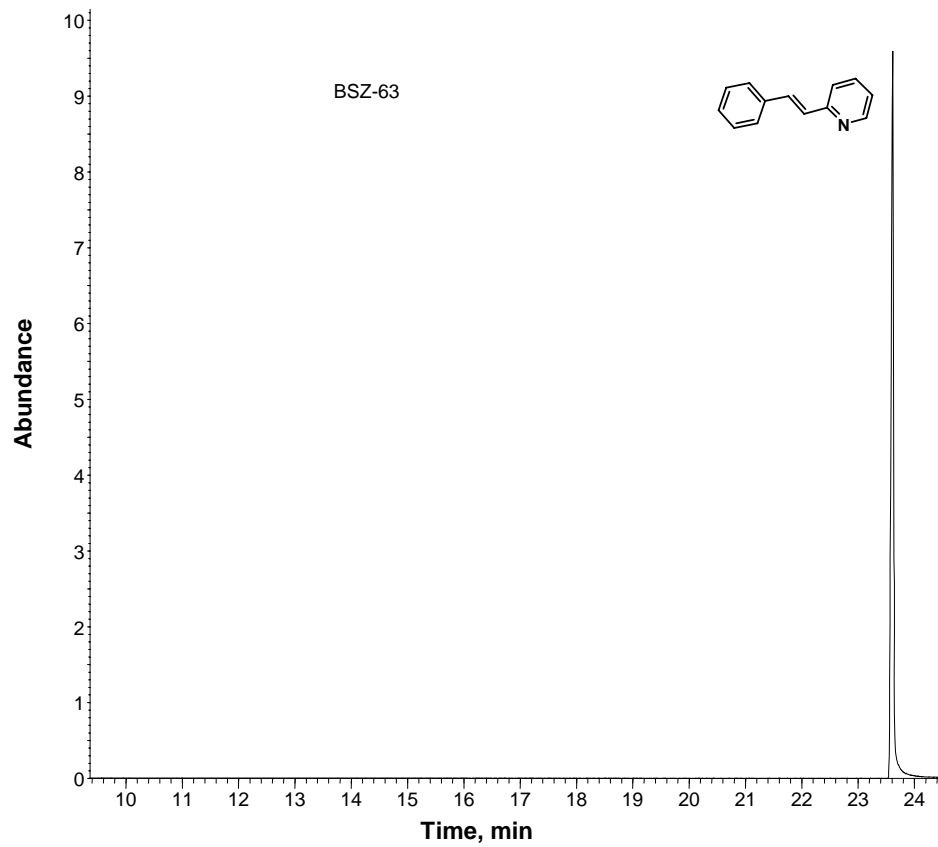


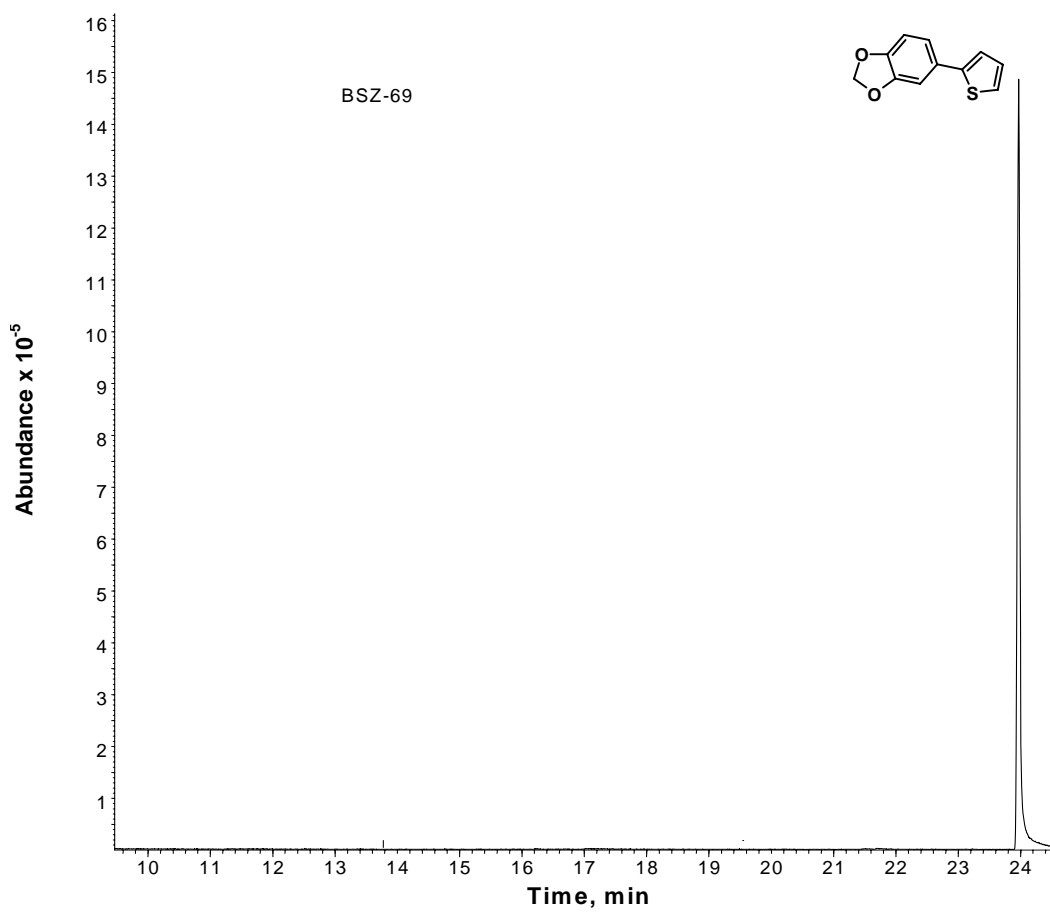


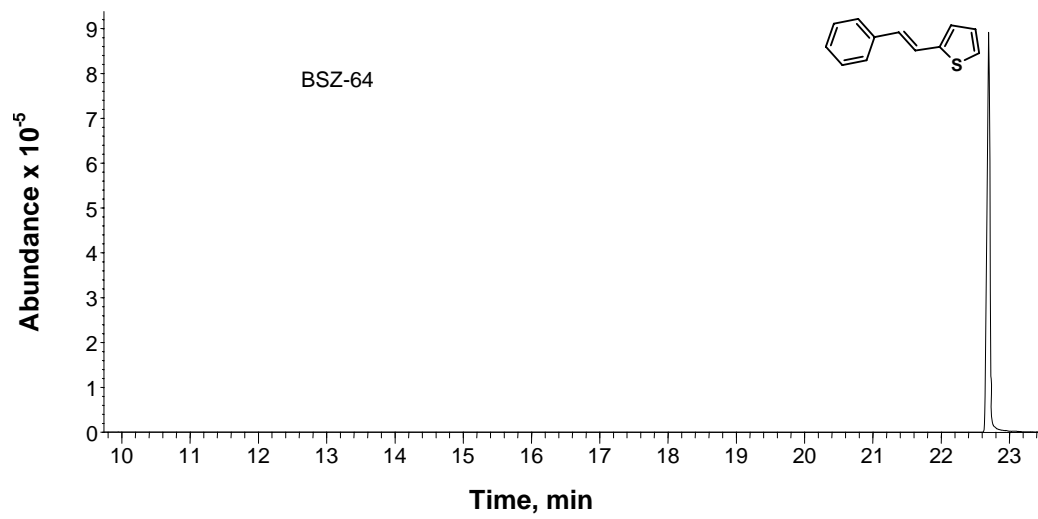
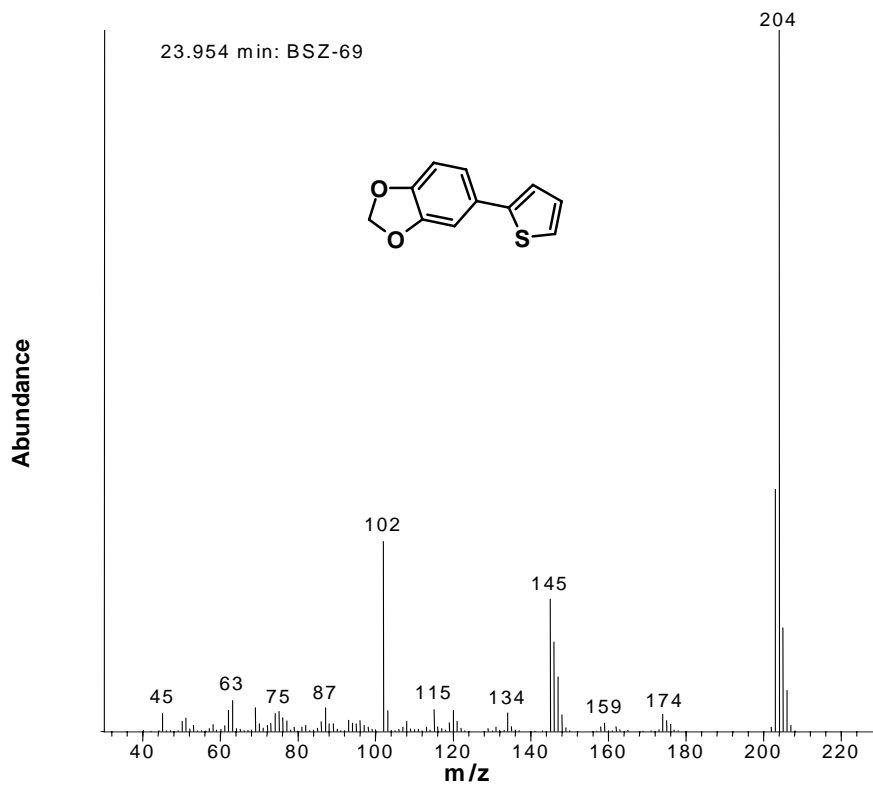


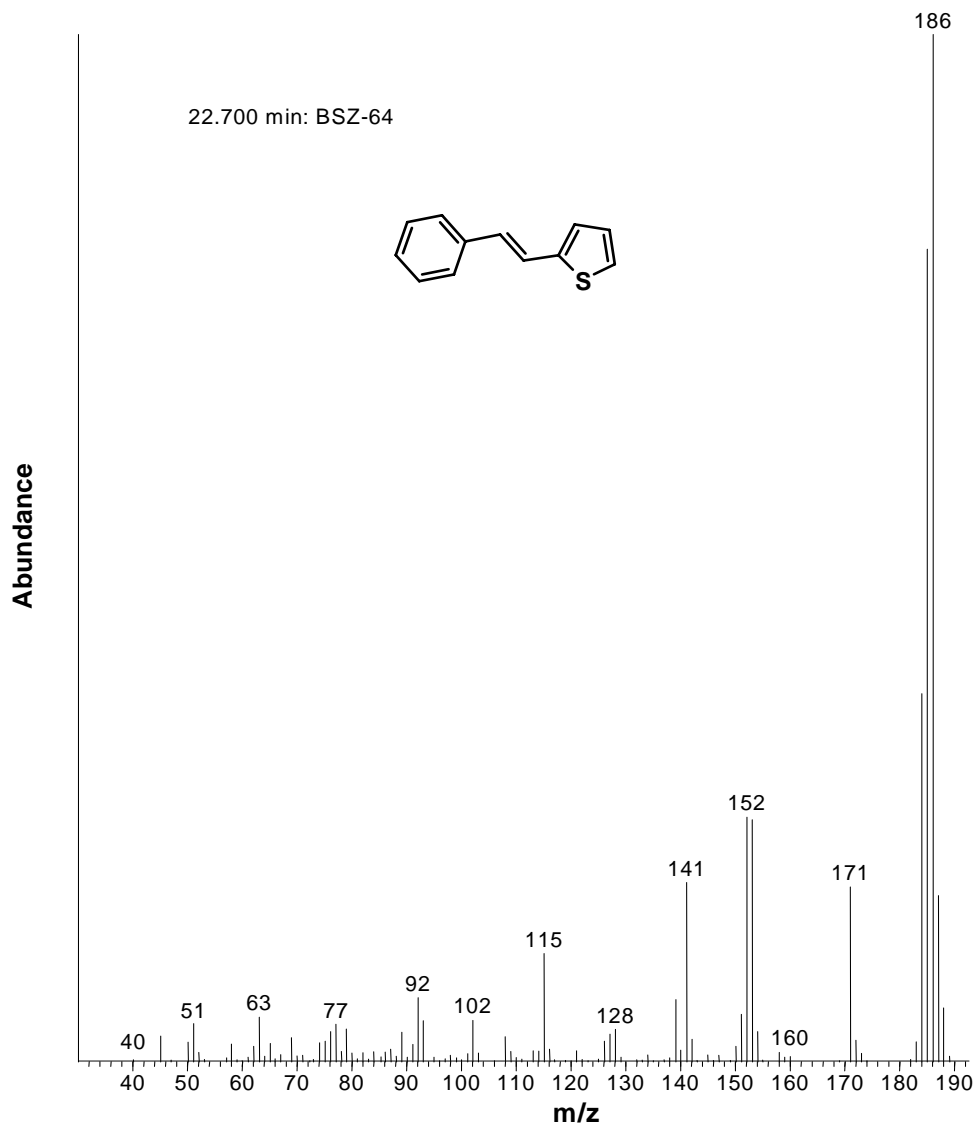


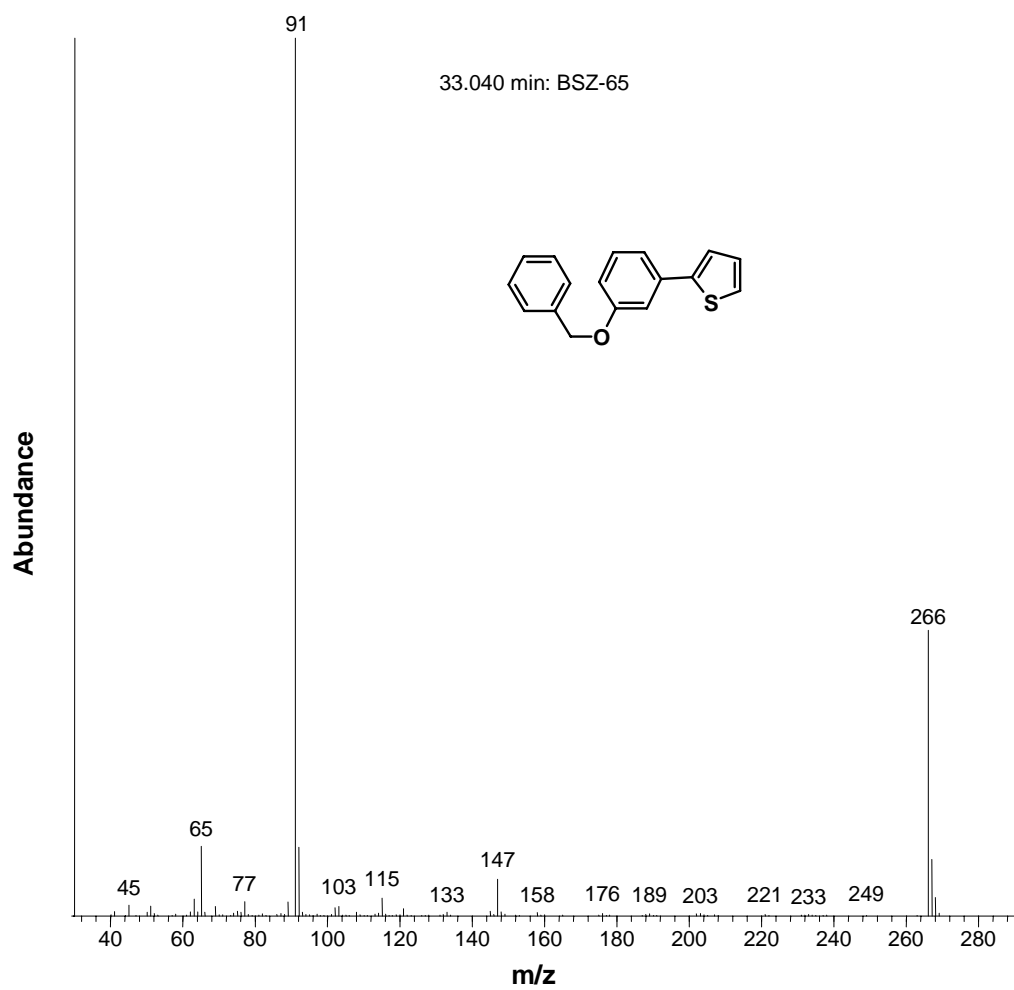
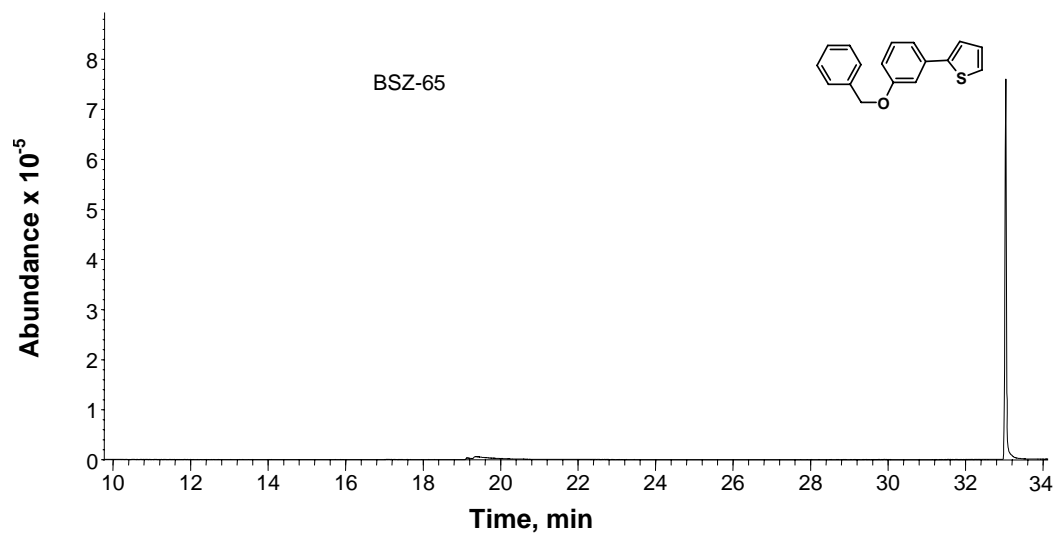












Publications and Symposia

Papers

1. Biphasic Carbonylation of Vinyl Aromatic Compounds using Novel Water-soluble Pd Catalyst: Activity, Selectivity and Mechanistic Studies
S. Jayasree, A. Seayad, **Bibhas R. Sarkar** and R. V. Chaudhari
J. Mol. Catal. A: Chem., 181, 2002, 221
2. Anchored Pd Complex in MCM-41 and MCM-48: Novel Heterogeneous Catalysts for Hydrocarboxylation of Aryl Olefins and Alcohols
K. Mukhopadhyay, **Bibhas R. Sarkar** and R. V. Chaudhari
J. Am. Chem. Soc., 124, 2002, 9692
3. Carbonylation Of Alkynes, Alkenes And Alcohols Using Metal Complex Catalysts
Bibhas R. Sarkar and Raghunath V. Chaudhari
Catal. Surv. Asia, 9(3), 2005, 193
4. Ossification: A New Approach to Immobilize Organometallic Catalysts - Applications to Carbonylation and Suzuki Coupling Reactions
Bibhas R. Sarkar and Raghunath V. Chaudhari
J. Catal., 242, 2006, 231
5. Tethered Pd-Complex on Solid Supports: Catalyst for Acid-free Carbonylation Reactions
Bibhas R. Sarkar, Kausik Mukhopadhyay and Raghunath V. Chaudhari
Catal. Commun., 2006, In Press

Patents

1. Process for Preparation of Saturated Carboxylic Acid Esters
US 6,479,693; September 2002
2. Water Soluble Palladium Complexes and Process for the Preparation thereof
US 6,469,169; October 2002
3. Process for the preparation of novel immobilized metal complex catalysts and use thereof for carbonylation reactions,
US Pat. Appl. No. 20050131252 A1, August 2005

Conference/ Course-work attended

2. ICS-UNIDO-NCL Workshop on Clean Catalytic Processes for Fine Chemicals and Pharmaceuticals, 7-13 February 2000, at NCL Pune, INDIA
3. 15th Indian National Symposium on Catalysis & 2nd Conference of Indo-Pacific Catalysis Association (IPCAT), 23-25 January 2001, at Pune, INDIA, - *Oral Presentation*
4. Orientation Program in Catalysis for Research Scholars, 28 February – 16 March 2001, at IIT-Mumbai, INDIA
5. Conference on Catalysis: Concepts to Practice, 26-27 June 2002, at NCL, Pune, INDIA
6. 13th International Congress on Catalysis (ICC), 11-16 July 2004, at Paris, FRANCE - *Oral Presentation*
7. CAMURE-6 and ISMR-4, 14-17 January 2007, at NCL Pune, INDIA – *Oral Presentation*